Réponse, acclimatation et adaptation des invertébrés marins aux changements environnementaux biotiques et abiotiques

Jeremie Vidal-Dupiol

HABILITATION A DIRIGER DES RECHERCHES

UNIVERSITE DE PERPIGNAN VIA DOMITIA

REPONSE, ACCLIMATATION ET ADAPTATION DES INVERTEBRES MARINS AUX CHANGEMENTS ENVIRONNEMENTAUX BIOTIQUES ET ABIOTIQUES

Présenté par

Jérémie VIDAL-DUPIOL

Chargé de Recherche

Soutenu le 13 Mai 2022 à l'Université de Perpignan *via domitia* devant le jury composé de :

Denis ALLEMAND	**Rapporteur**
Christine COUSTAU	**Rapporteur**
Arnaud HUVET	**Rapporteur**
Patricia GIBERT	**Examinateur**
Philippe LENFANT	**Examinateur**
Christoph GRUNAU	**Examinateur**

Laboratoire Interaction Hôtes Pathogènes Environnements

Sommaire

Annexe 11 Colour plasticity in the shells and pearls of animal graft model Pinctada margaritifera assessed by HSV colour quantification

Annexe 12 Molecular Pathways and Pigments Underlying the Colors of the Pearl Oyster *Pinctada margaritifer*a var. cumingii (Linnaeus 1758)

Annexe 13 Environmentally Driven Color Variation in the Pearl Oyster *Pinctada margaritifera* var. cumingii (Linnaeus, 1758) Is Associated With Differential Methylation of CpGs in Pigment and Biomineralization-Related Genes

Préambule

Doté d'une âme d'éleveur et passionné par tout ce qui vit dans l'eau depuis mon plus jeune âge j'ai toujours eu pour objectifs de travailler en lien avec la vie aquatique. Mauvais élève, trop peu intéressé et encore moins passionné par des matières scolaires auxquelles aucun sens n'était donné, le système m'a longtemps découragé d'accéder au métier de chercheur en biologie aquatique. J'ai cependant eu la chance d'être repêché par les filières techniques et technologiques. Hameçonné dans un premier temps par le sens qu'elles apportèrent aux choses, mes professeurs m'ont aussi montré que l'on pouvait aimer réfléchir à des sujets non choisis. C'est ainsi qu'après un bac en science et technologie de laboratoire et un BTS en aquaculture j'ai rejoint l'université de Perpignan avec pour objectif d'étudier les coraux Scléractiniaire, cet animal un peu minéral un peu végétal mais totalement fascinant. Cet objectif inespéré au début ne fut pas le plus simple à atteindre, loin s'en faut. J'ai cependant encore une fois eu la chance d'être à nouveau soutenu et aidé par les bonnes personnes, les bons encadrants, les bons directeurs de recherches devenus quelques années plus tard mes directeurs de thèses, Guillaume Mitta et Mehdi Adjeroud. Ces quelques lignes ne sont pas uniquement là pour faire état du début de mon parcours, elles le sont aussi et surtout pour souligner la conscience que j'ai du rôle majeur que joue un professeur, un maitre de stage, un directeur de thèse, un responsable d'équipe ou un directeur d'unité. La bienveillance, le juste milieu, le coaching, la psychologie et bien sûr l'éclairage scientifique sont autant de compétences et de qualités nécessaires à l'encadrement et donc à la capacité de diriger des recherches. Si la dernière de ces qualités est facilement quantifiable au travers d'un CV scientifique, les quatre premières le sont moins mais j'espère qu'en avoir conscience est le premier pas nécessaire à leur mise en application.

Jérémie Vidal-Dupiol Curriculum vitae

13 septembre 1983

jeremie.vidal.dupiol@ifremer.fr

160 rue du Massillan

34820 Teyran

A Cursus universitaire & activité de recherche

2017/aujourd'hui **Chargé de Recherche Ifremer de classe 1 :** Mécanismes d'adaptation rapide des invertébrés marins aux changements environnementaux. UMR IHPE 5244 UM-CNRS-IFREMER-UPVD, co-responsable de l'équipe Microévolution des Interactions dans l'Anthropocène, Montpellier France

2015/2017 **Chargé de Recherche Ifremer de classe 1 :** Génomique fonctionnel chez l'huître Perlière *Pinctada margatirifera* : des traits d'intérêts économique à l'adaptation aux changements globaux. UMR EIO 241 Université de la Polynésie-Ifremer-IRD-ILM, équipe Ressource Marine en Polynésie Française, Taravao, Polynésie Française

2014/2015 **Post-doctorat :** Mécanismes génétiques et épigénétiques d'une réponse efficace aux stress thermiques : variabilité inter-spécifique, inter-populationnel et intra-populationnel. Direction : Guillaume Mitta et Christoph Grunau. UMR 2EI 5244 CNRS-UPVD, Université de Perpignan.

2013/2014 **Post-doctorat :** Séquençage et assemblage du génome de *Pocillopora damicornis.* Etude des facteurs épigénétiques et génétiques dans l'augmentation de la thermo-tolérance chez les coraux. Direction: Virginia Weis et Michael Freitag. Oregon State University, Corvallis USA.

2011/2012 **Post-doctorat :** Séquençage, assemblage et annotation du transcriptome du corail constructeur de récifs *Pocillopora damicornis*. Etude de la réponse transcriptionnelle par RNA-seq (Illumina) de *Pocillopora damicornis* confronté à l'acidification des océans. Direction : Sylvie Tambutté et Denis Allemand. Centre Scientifique de Monaco.

2007/2011 **Doctorat :** de l'Ecole Pratique des Hautes Etudes, Mention très honorable avec les félicitations du jury. Direction : Mehdi Adjeroud et Guillaume Mitta. UMR BETM 5244 CNRS-EPHE-UPVD, Université de Perpignan.

Mémoire : Stress environnementaux chez le corail Scléractiniaire *Pocillopora damicornis* : du modèle expérimental à l'identification de marqueurs fonctionnels du stress.

Juillet 2007	**Ingénieur d'étude :** Taxonomie des Scléractiniaires. Direction : Michel Pichon. UMR BETM 5244 CNRS-EPHE-UPVD, Université de Perpignan.
Jan/Juin 2007	**Master 2 :** Ecologie fonctionnelle, des molécules aux populations, Université de Perpignan. Major, mention B.
	- Mémoire : Blanchissement corallien : développement d'une approche expérimentale et recherche de marqueurs fonctionnels chez le Scléractiniaire *Pocillopora damicornis*. Direction : Mehdi Adjeroud, Guillaume Mitta. UMR 5244 CNRS-EPHE-UPVD, Université de Perpignan.
Jan/Juin 2006	**Master 1 :** Ecologie fonctionnelle, des molécules aux populations, Université de Perpignan. Mention B.
	- Mémoire : Différentiation morphométrique de deux espèces du genre *Pocillopora*; *P. verrucosa* et *P. meandrina*. Direction : Michel Pichon. UMR 5244 CNRS-EPHE-UPVD, Université de Perpignan.
2003/2005	**Licence 2eme et 3eme** Biologie Ecologie Evolution, Université de Perpignan. Mention AB.
2001/2003	**BATSA** Productions aquacoles, LEGTA Lozère La Canourgue. **Major**, mention B.

B Management de la recherche

1 Encadrement :

Post-Doctorant :

- 2019-2020 Encadrement (50%) de Jennie Pistevos (Post-doc, Labex Corail). Réponse transcriptomique du lièvre de mer aux conditions de température et de pH de 2100.

- 2017-2018 Co-encadrement (50%) de Vaihiti Teaniniuraitemoana (Post-Doc, Ifremer/Délégation à la recherche de Polynésie Française). Déterminant génétique et épigénétique du sexe chez l'huître perlière.

Thèse

- 2020-2023 Co-encadrement (50%) de Louis Boismorand (Thèse, Ifremer). Comment la température et la nutrition contrôlent-elles la susceptibilité des huîtres au syndrome de mortalité des huîtres du pacifique ?

- 2018-2021 Co-encadrement (100%) de Janan Kahmo Gawra (Thèse, Université de Perpignan). Identification de marqueurs de résistance au syndrome de mortalité massive des juvéniles d'huîtres creuses, *Crassostrea gigas*, par l'étude intégrative du tryptique, transcriptome, épigénome, génome.

- 2016-2019 Co-encadrant (33%) de Pierre-Louis Stenger (Thèse, Université de la Polynésie). Plasticité et diversité chromatique de l'huître perlière *Pinctada margaritifera* var.cumingii (linnaeus, 1789) : analyse du tryptique "phénome, génome, épigénome".

- 2013-2014 Participation à l'encadrement (20%) de Kelly Brener (Thèse, Université de Perpignan). Dynamique de l'holobionte corallien et plasticité transcriptomique: variabilité inter-individuelle, inter-populationnelle et inter-spécifique.

Master

- 2017 Encadrement (100%) de Vladimir Sorodjé (Master 2 recherche, Paris Sud). Etude des efflorescences algales des lagons polynésiens en mésocosme et par meta-barcoding.

- 2016 Encadrement (100%) de Leila Chapron (Master 2 recherche, Sorbonne Université). Impacts des conditions de température et de pH prédites à l'Orée du 22eme siècle sur le métabolisme énergétique et la croissance du bénitier.

- 2012 Co-Encadrement (50%) de Rodolfo Rondon (Master 2 recherche, Université de Perpignan). Réponse transcriptomique globale du corail Scléractiniaire *Pocillopora damicornis* confronté à un stress thermique inducteur de blanchissement.

- 2010 Co-Encadrement (50%) de Marc Manetti (Master 2 recherche, Université de Perpignan). Recherche de biomarqueurs fonctionnels de l'interaction hôte/pathogène, *Pocillopora damicornis / Vibrio coralliilyticus*.

- 2010 Co-Encadrement (20%) d'Aurélie Guérécheau (Master 2 recherche, Université de Perpignan). Différentiation génétique et clonalité chez le Scléractiniaire *Pocillopora damicornis*: une analyse multi-échelle.

Autre

- 2018 Co-encadrement (70%) de Erwan Harscouet (cesure L1/M1 Université de Montpellier). Effet transcriptomique du chimérisme chez le corail *Stylophora pistillata.*

- 2018 Encadrement (100%) de Mathilde Saccas (Licence professionnel BAE, IUT Montpellier). Mise au point de l'exome capture dans le cadre de l'étude des déterminants génétiques et épigénétiques de la résistance des huîtres au syndrome de surmortalité des juvéniles

- 2013 Encadrement (100%) de Jocelyn Powell (Bachelor senior level, Oregon State University). The Knock down of RAB5 induced coral bleaching without stressful temperature.

- 2012 Encadrement (100%) module cycle de conférences, 4 étudiants en Master 2 recherche Biologie des Plantes et Microorganismes, Biotechnologies, Bioprocédés (BPMBB) spécialité Interactions Microorganismes Hôtes et Environnement (IMHE ; Université de Montpellier 2). Impacts anthropiques sur les récifs coralliens.

- 2009 Encadrement (100%) de projet tutoré, 5 lycéens en Terminale S (Lycée Arago, Perpignan). Approche expérimentale du blanchissement corallien.

2 Financement de la recherche :

- 2012 Participation à la rédaction du projet ANR blanc "Coral Integrated Evolution in a world of change (CORALIE)" Projet retenu, mais retiré par le porteur suite à l'obtention du projet ANR ADACNI (Cf. infra).

- 2012 Participation à la rédaction du projet ANR Bioadapt "Adaptative process in cnidarians: integrative study of the response to thermal stress and climate change, from genes to populations (ADACNI)", 550 k€, 2012-2016.

- 2013 Participation à la rédaction du projet Franco-Israélien Mainmonide "Experimental marine Biology: Aquaculture, Pathogens and Pollution", Collaboration avec Baruch Rinkevitch (Université de Tel Aviv, Institu National d'Océanographie), 156 k€, 2012-2014).

- 2015 Rédaction du projet Ifremer Politique de Site "Impacts des changements globaux sur la croissance, la composition GÉochimique et microstructurale de la Coquille d'Organismes d'intérêt aquacole (GECO)", 20 k€, 2015-2016 (Porteur)

- 2016 Participation à la rédaction du projet ERC consolidator "Deciphering biomineralization mechanisms through 3D explorations of mesoscale crystalline structure in calcareous biomaterials (3D-Biomat)", 1 700 k€, 2016-2021 (Responsable scientifique partenaire Ifremer)

- 2018 Rédaction du projet Ifremer Politique de Site "Génétique et Epigénétique de la résistance au syndrome de Mortalités massives des juvéniles d'huîtres creuses Crassostrea gigas", 20k€, 2018-2019 (Porteur)

- 2019 Participation à la rédaction du projet ANR blanc "Deciphering the whole complexity of the Pacific oyster mortality syndrome for modeling epidemiological risk (DECICOMP)" 690 k€, 2020-2024 (Responsable scientifique partenaire Ifremer, Leader WP2)

- 2019 Rédaction du projet Ifremer Incitation Huître "Résistance de l'huître creuse, virulence de l'herpesvirus (OsHV1-µvar) et coévolution", 250 k€, 2020-2023 (Porteur)

- 2020 Rédaction du projet FEAMP "Gestion innovante et durable des mortalités d'huîtres", 590 k€, 2021-2023 (Porteur)

- 2021 Rédaction du projet Ifremer/AFD "Signature d'Adaptation/acclimatation rapide au réchauffement climatique chez les coraux : Vers une gestion améliorée de l'Ecosystème", 200 k€, 2021-2024 (Porteur)

C Enseignement

- Ecologie et physiologie des Scléractiniaires. Cours de 12 h niveau licence 3ème année

- Techniques de culture et de maintenance des Scléractiniaires. Cours de 12 h niveau licence 3ème année

- Bases moléculaires du blanchissement corallien. Cours de 3 h niveau Master 1/2.

- Du mutualisme au parasitisme, le cas de la symbiose Cnidaires/Dinoflagellés. Cours de 3 h niveau Master 1/2.

- Recherche amont/aval en aquaculture. Cours de 8h niveau Master 2.

D Evaluation et administration de la recherche

1 Jury de thèse :

- Examinateur de la thèse de doctorat de M Thomas HUE. Impact du changement climatique sur les performances reproductives de l'étoile de mer corallivore Acanthaster sp. Le 22 avril 2021, Nouméa, Nouvelle-Calédonie

- Examinateur de la thèse de doctorat de Mlle Coralie BERNARDET. Physiologie des transports ioniques et moléculaires chez les coraux, implications environnementales. Le 8 novembre 2019, Monaco, Monaco

- Examinateur de la thèse de doctorat de Mlle Leila CHAPRON. Response of cold-water corals to global change in the Mediterranean sea: from the molecular to the reef scale. Le 10 octobre 2019, Banyuls, France

- Examinateur de la thèse de doctorat de M Antoine PUISAY. La reproduction sexuée et asexuée des coraux face aux changements environnementaux : Implications pour la conservation et la restauration des récifs coralliens. Le 23 juillet 2018, Perpignan, France

- Examinateur de la thèse de doctorat de Mlle Tepoerau MAI. Inhibiteur du qorum sensing de *Vibrio harveyi* issus d'éponges de Polynésie française. Le 25 mai 2016, Papeete, Polynésie Française

2 Comité de thèse :

- Membre du comité de thèse de Mlle Coralie BERNARDET. 2017-2019, Monaco

3 Commission de spécialistes :

- Membre nommé au conseil scientifique de l'aquarium de recherche du laboratoire Arago, Banyuls sur Mer, depuis Janvier 2019

- Membre élu au conseil scientifique du Labex TULIP (Toulouse/Perpignan) depuis Janvier 2020

4 Responsabilité d'animation/administration :

- Responsable du thème Adaptabilité des hôtes au sein de l'équipe Mécanismes d'Interactions en Milieu Marin du Laboratoire Interaction Hôte Pathogène Environnement. Novembre 2017 à Décembre 2020. Ce thème comprenait ; 1 Pr UPVD, 1 C3 Ifremer (Eq DR/Prof), 2 C2 Ifremer (Eq CR), 1 CR CNRS

- Co-responsable de l'équipe Microévolution des Interactions dans l'Anthropocène (MIA) du Laboratoire Interaction Hôte Pathogène Environnement, depuis Janvier 2021. Cette équipe comprend ; 1 Pr UPVD, 1 C3 Ifremer (Eq DR/Prof), 2 C2 Ifremer (Eq CR), 3 MCF UPVD, 1 IE CNRS

E Production Scientifique

NB : Les étudiants et Post-doctorants que j'ai encadré partiellement ou totalement et avec qui j'ai publié sont soulignés

1 Publications scientifiques :

Soumises :

1) - **Vidal-Dupiol, J***., E. Toulza, C. Grunau, O. Rey, D. Roquis, C. Chaparro, C. Cosseau, A. Picart-Picolo, P. Romans, M. Pratlong, K. Brener-Raffalli, P. Pontaroti, M. Adjeroud, and G. Mitta. Submitted. Genetic and epigenetic changes mediate rapid adaptation to global warming in a tropical coral

2) - **Vidal-Dupiol, J***., E. Harscouet, D. Shefy, E. Toulza, O. Rey, G. Mitta, and B. Rinkevich. Submitted. Coral chimera: a robust entity expressing a beforehand stress-prepared transcriptomic signature.

Publiées

2021

3) - Roquis, D., A. Picart Picolo, K. B. Raffalli, P. Romans, P. Masanet, C. Cosseau, G. Mitta, C. Grunau, and **J. Vidal-Dupiol***. Submitted. The tropical coral Pocillopora acuta has a mosaic DNA methylome, an unusual chromatin structure and shows histone H3 clipping. Wellcome Open Research

4) - Brahmi, C*., L. Chapron, G. Le Moullac, C. Soyez, B. Beliaeff, C. E. Lazareth, N. Gaertner-Mazouni, and **J. Vidal-Dupiol**. Submitted. Effects of temperature and pCO2 on the respiration, biomineralization and photophysiology of the giant clam Tridacna maxima. Conservation Physiology 9. IF=2,575

5) **-** Stenger, P.-L., C. L. Ky, C. Reisser, C. Roux, P. Durand, S. Planes, and **J. Vidal-Dupiol***. 2021. Molecular pathways and pigments underlying the colors of the pearl oyster Pinctada margaritifera var. cumingii (Linnaeus 1758). Genes 12:421. IF= 4,09

6) - Stenger, P. L., C. L. Ky, C. Reisser, C. Cosseau, C. Grunau, M. Mege, S. Planes, and **J. Vidal-Dupiol***. Submitted. Environmentally driven color variation in the pearl oyster Pinctada margaritifera var. cumingii (Linnaeus, 1758) is associated with differential methylation of CpGs in pigment- and biomineralization-related genes. Frontiers in Genetics 12. IF= 3,79

7) - Augusto, R., O. Rey, C. Cosseau, C. Chaparro, J. **Vidal-Dupiol, J**. Allienne, D. Duval, S. Pinaud, S. Tönges, R. Andriantsoa, E. Luquet, F. Aubret, M. Dia Sow, P. David, V. Thomson, D. Joly, M. Gomes Lima, D. Federico, E. Danchin, A. Minoda, and C. Grunau*. 2021. A simple ATAC-seq protocol for population epigenetics. Wellcome Open Research 5.

2020

8) - Monteiro, H. J. A., C. Brahmi, A. B. Mayfield, **J. Vidal-Dupiol,** B. Lapeyre, and J. Le Luyer*. 2020. Molecular mechanisms of acclimation to long-term elevated temperature exposure in marine symbioses. Global Change Biology 26:1271-1284. IF=8,55

9) - Horwitz, R., T. Norin, S. A. Watson, J. C. A. Pistevos, R. Beldade, S. Hacquart, J. P. Gattuso, R. Rodolfo-Metalpa, **J. Vidal-Dupiol**, S. S. Killen, and S. C. Mills*. 2020. Near-future ocean warming and acidification alter foraging behaviour, locomotion, and metabolic rate in a keystone marine mollusc. Scientific Reports 10. IF=3,99

10) - Delmotte, J., C. Chaparro, R. Galinier, J. de Lorgeril, B. Petton, P. L. Stenger, **J. Vidal-Dupiol**, D. Destoumieux-Garzon, Y. Gueguen, C. Montagnani, J. M. Escoubas*, and G. Mitta. 2020. Contribution of Viral Genomic Diversity to Oyster Susceptibility in the Pacific Oyster Mortality Syndrome. Frontiers in microbiology 11. IF=4,26

11) - Lafont, M., A. Vergnes, **J. Vidal-Dupiol**, J. de Lorgeril, Y. Gueguen, P. Haffner, B. Petton, C. Chaparro, C. Barrachina, D. Destoumieux-Garzon, G. Mitta, B. Gourbal, and C. Montagnani*. 2020. A sustained immune response supports long-term antiviraliImmune priming in the pacific oyster, Crassostrea gigas. mBio 11:e02777-02719. IF=6,78

12) - Delisle, L., M. Pauletto, **J. Vidal-Dupiol**, B. Petton, L. Bargelloni, C. Montagnani, F. Pernet, C. Corporeau, and E. Fleury*. 2020. High temperature induces transcriptomic changes in Crassostrea gigasthat hinders progress of Ostreid herpesvirus (OsHV-1) and promotes survival. The Journal of Experimental Biology jeb.226233. IF=3,01

13) - de Lorgeril, J., B. Petton, A. Lucasson, V. Perez, P.-L. Stenger, L. Dégremont, C. Montagnani, J.-M. Escoubas, P. Haffner, J.-F. Allienne, M. Leroy, F. Lagarde, **J. Vidal-Dupiol**, Y. Gueguen, and G. Mitta*. 2020. Differential basal expression of immune genes confers Crassostrea gigas resistance to Pacific oyster mortality syndrome. BMC Genomics 21:63. IF=3.59

2019

14) - Stenger, P. L., **J. Vidal-Dupiol**, C. Reisser, S. Planes, and C. L. Ky*. 2019. Colour plasticity in the shells and pearls of animal graft model Pinctada margaritifera assessed by HSV colour quantification. Scientific Reports 9. IF=3,99

15) - Lafont, M., B. Petton, J. deLorgeril, A. Vergnes, **J. Vidal-Dupiol**, Y. Gueguen, P. Haffner, G. Mitta, B. Gourbal, and C. Montagnani*. 2019. Efficient and long-lasting protection against the pacific oyster mortality syndrome through antiviral immune priming. Fish & shellfish immunology 91:461-461. IF= 3,30

16) - Rubio, T., D. Oyanedel, Y. Labreuche, E. Toulza, X. Luo, M. Bruto, C. Chaparro, M. Torres, J. de Lorgeril, P. Haffner, **J. Vidal-Dupiol**, A. Lagorce, B. Petton, G. Mitta, A. Jacq, F. Le Roux, G. M. Charrière, and D. Destoumieux-Garzón*. 2019. Species-specific mechanisms of cytotoxicity toward immune cells determine the successful outcome of Vibrio infections. Proceedings of the National Academy of Sciences 116:14238-14247. IF=9,42

17) - Le Luyer, J*., P. Auffret, V. Quillien, N. Leclerc, C. Reisser, **J. Vidal-Dupiol**, and C. L. Ky. 2019. Whole transcriptome sequencing and biomineralization gene architecture associated with cultured pearl quality traits in the pearl oyster, Pinctada margaritifera. BMC Genomics 20:111. IF=3.59

18) - Brener-Raffalli, K., **J. Vidal-Dupiol**, M. Adjeroud, O. Rey, P. Romans, F. Bonhomme, M. Pratlong, A. Haguenauer, R. Pillot, L. Feuillassier, M. Claereboudt, H. Magalon, P. Gélin, P. Pontarotti, D. Aurelle, G. Mitta, and E. Toulza*. 2019. Gene expression plasticity and frontloading promote thermotolerance in Pocillopora corals. PCI Ecology:398602. IF= non indexed journal

2018

19) - de Lorgeril, J., A. Lucasson, B. Petton, E. Toulza, C. Montagnani, C. Clerissi, **J. Vidal-Dupiol**, C. Chaparro, R. Galinier, J.-M. Escoubas, P. Haffner, L. Dégremont, G. M. Charrière, M. Lafont, A. Delort, A. Vergnes, M. Chiarello, N. Faury, T. Rubio, M. A. Leroy, A. Pérignon, D. Régler, B. Morga, M. Alunno-Bruscia, P. Boudry, F. Le Roux, D. Destoumieux-Garzón, Y. Gueguen*, and G. Mitta*. 2018. Immune-suppression by OsHV-1 viral infection causes fatal bacteraemia in Pacific oysters. Nature Communications 9:4215. IF=11,88

20) - Clerissi, C*., S. Brunet, **J. Vidal-Dupiol**, M. Adjeroud, P. Lepage, L. Guillou, J.-M. Escoubas, and E. Toulza. 2018. Protists Within Corals: The Hidden Diversity. Frontiers in microbiology 9. IF=4,26

21) - Brener-Raffalli, K., C. Clerissi, **J. Vidal-Dupiol**, M. Adjeroud, F. Bonhomme, M. Pratlong, D. Aurelle, G. Mitta, and E. Toulza*. 2018. Thermal regime and host clade, rather than geography, drive Symbiodinium and bacterial assemblages in the scleractinian coral Pocillopora damicornis sensu lato. Microbiome 6:39. IF=10,47

2017

22) - Torda, G., J. M. Donelson, M. Aranda, D. J. Barshis, L. Bay, M. L. Berumen, D. G. Bourne, N. Cantin, S. Foret, M. Matz, D. J. Miller, A. Moya, H. M. Putnam, T. Ravasi, M. J. H. van Oppen, R. V. Thurber, **J. Vidal-Dupiol**, C. R. Voolstra, S.-A. Watson, E. Whitelaw, B. L. Willis*, and P. L. Munday*. 2017. Rapid adaptive responses to climate change in corals. Nature Climate Change 7:627. IF=19.18

2016

23) - Le Moullac, G*., C. Soyez, **J. Vidal-Dupiol**, C. Belliard, J. Fievet, M. Sham Koua, A. Lo-Yat, D. Saulnier, N. Gaertner-Mazouni, and Y. Gueguen. 2016. Impact of pCO2 on the energy, reproduction and growth of the shell of the pearl oyster Pinctada margaritifera. Estuarine, Coastal and Shelf Science 182, Part B:274-282. IF=2,18

24) - Le Moullac, G., C. Soyez, O. Latchere, **J. Vidal-Dupiol***, J. Fremery, D. Saulnier, A. Lo Yat, C. Belliard, N. Mazouni-Gaertner, and Y. Gueguen. 2016. Pinctada margaritifera responses to temperature and pH: Acclimation capabilities and physiological limits. Estuarine, Coastal and Shelf Science 182, Part B:261-269. IF=2,18

25) - Destoumieux-Garzón, D*., R. D. Rosa, P. Schmitt, C. Barreto, **J. Vidal-Dupiol**, G. Mitta, Y. Gueguen, and E. Bachère. 2016. Antimicrobial peptides in marine invertebrate health and disease. Philosophical Transactions of the Royal Society B: Biological Sciences 371. IF= 5,85

2015

26) - **Vidal-Dupiol, J***. Dheilly. NM, Rondon, R. Grunau, C. Cosseau, C. Smith, KM. Freitag, M. Adjeroud, M. Mitta, G (2014). Thermal stress triggers profound *Pocillopora damicornis* transcriptome remodeling favoring infection, but virulent *Vibrio coralliilyticus* induced immuno-suppression. Plos One, 9.9: e107672 IF = 3,73

27) - Adjeroud, M*. Guérécheau, A. **Vidal-Dupiol, J**. J-F Flot, Arnaud-Haond, S. Bonhomme, F (2014). Genetic diversity, clonality and connectivity in the scleractinian coral *Pocillopora damicornis*: a multi-scale analysis in an insular, fragmented reef system. Marine Biology, 161, 3, 531-541. IF = 2,47

2014

28) - Ladrière, O. Penin, L*. Van Lierde, E. **Vidal-Dupiol, J**. Roberty, S. Poulicek, M. Adjeroud, M. (2014). Natural spatial variability of algal endosymbiont density in the coral *Acropora globiceps*: a small-scale approach along environmental gradients around Moorea (French Polynesia). Journal of the Marine Biological Association of the United Kingdom, 94, 1, 65-74. IF = 1,02

2013

29) - Vidal-Dupiol, J*. Zoccola, D. Tambutté, E. Grunau, C. Cosseau, C. Smith, KM. Freitag, M. Dheilly, NM. Allemand, D. Tambutté, S. (2013). Genes related to ion-transport and energy production are upregulated in response to CO_2-driven pH decrease in corals: new insights from transcriptome analysis. PloS One, 8 (3), doi:10.1371/journal.pone.0058652. IF = 3,73

2012

30) - Penin, L*. **Vidal-Dupiol, J**. Adjeroud, M. (2012). Response of coral assemblages to thermal stress: Are bleaching intensity and spatial patterns consistent between events? Environmental Monitoring and Assessment, DOI 10.1007/s10661-012-2923-3 IF = 1,59

2011

31) - Vidal-Dupiol, J. Ladrière, O. Meiztercheim, A.L. Destoumieux, D. Tambutté, E. Tambutté, S. Adjeroud, M. Mitta, G*. (2011). Innate immune responses of a scleractinian coral to vibriosis. *The Journal of Biological Chemistry*, 286, 25, 22688-22698. IF = 5,33

32) - **Vidal-Dupiol, J**. Ladrière, O. Meiztercheim, A.L. Adjeroud, M. Mitta, G*. (2011). Physiological responses of the scleractinian coral *Pocillopora damicornis* to bacterial stress from *Vibrio coralliilyticus*. *The Journal of Experimental Biology*, 214, 1533-1545. IF = 3,04

2009

33) - Vidal-Dupiol, J. Adjeroud, M. Roger, E. Foure, L. Duval, D. Moné, Y. Ferrier-Pagès, C. Tambutté, E. Tambutté, S. Zoccola, D. Allemand, D. Mitta, G*. (2009). Coral bleaching under thermal stress: putative involvement of host/symbiont recognition mechanisms. *BMC Physiology,* 9 : 14. IF = non indexé par Thomson reuters

34) - Adjeroud, M*. Michonneau, F. Edmunds, P.J. Chancerelle, Y. Lison de Loma, T. Penin, L. Thibaut, L. **Vidal-Dupiol, J**. Salvat, B. Galzin, R. (2009). Recurrent disturbances, recovery trajectories, and resilience of coral assemblages on a South Central Pacific reef. *Coral Reefs,* 28 : 775-780. IF = 3,78

2 Organisation d'évènements scientifiques :

1) - Membre du comité d'organisation du congrès international EPIMAR EPIgenetic in MARin biology. 6-9 octobre 2020, Covid-free Online event, France
2) - Chairman de la session What role does phenotypic plasticity play in acclimatization or adaptation to environmental change? 14th International Coral Reef Symposium, 18-23 Juillet 2021, Bremen, Allemagne.

3 Présentations orales en congrès internationaux :

2021

1) Vidal-Dupiol J., Harscouet E., Shefy D., Toulza E., Rey O., Allienne J-F.; Mitta G., Rinkevich B. 2021 Coral chimeras: when a loose of transcriptomic plasticity increase robustness. 13th International Coral Reef Symposium (13th ICRS), July 2021, Bremen, Germany

2019

2) -Teaniniuraitemoana V., Reisser C., **Vidal-Dupiol J**., Le Moullac G. 2019 Genomic Factors Involved in Sex Determination and Differentiation in a Protandrous Hermaphrodite Bivalve, the Pearl Oyster Pinctada margaritifera. 2019. World Congress of Malacology (WCM 2019), July 2019, Pacific Grove, California, USA.
3) - Reisser C., **Vidal-Dupiol J**., Le Luyer J., Planes S., Ky C.L. 2019. Genome Assembly of the Pearl Oyster Pinctada margaritifera : a Tool for Environmental and Evolutionary Research. World Congress of Malacology (WCM 2019), July 2019, Pacific Grove, California, USA.
4) **-** Stenger PL., Ky CL., Reisser C., Planes S., **Vidal-Dupiol J**. 2019. Deciphering shell color pigmentation pathways in the pearl oyster Pinctada margaritifera (Linnaeus, 1758) through whole transcriptome sequencing and fine gene expression tuning. World Congress of Malacology (WCM 2019), July 2019, Pacific Grove, California, USA.

2018

5) - Montagnani C., Lafont M., Petton B., de Lorgeril J., Fallet M., Vergnes A., **Vidal-Dupiol J**., Gueguen Y., Chaparro C., Toulza E., Grunau C., Gourbal B., Mitta G. and Cosseau C. How to strain your oyster ? A story of immune shaping and priming in the pacific oyster, Crassostrea gigas. Aqua 2018 XIV International Symposium on Aquaculture Nutrition, World Aquaculture Society, Aout 2018, Montpellier, France.
6) - Mitta G., de Lorgeril J., Lucasson A., Petton B., Toulza E., Montagnani C., Clerissi C., **Vidal-Dupiol J**., Chaparro C., Galinier R., Escoubas J.-M., Haffner P., Dégremont L., Charrière G.M., Lafont M., Delort A., Vergnes A., Chiarello M., Rubio T., Leroy M., Pérignon A., Régler D., Alunno-Bruscia M., Boudry P., Le Roux F., Destoumieux-Garzón D. and Gueguen Y. 2018. Cracking the code of Pacific oyster mortality syndrom. Aqua 2018 XIV International Symposium on Aquaculture Nutrition, World Aquaculture Society, Aout 2018, Montpellier, France.

2017

7) - De Lorgeril J, Lucasson A, Petton B, Toulza E, Haffner P, Destoumieux-Garzón D, Chaparro C, Galinier R, Clerissi C, Montagnani C, Escoubas J.M., Vergnes A., Leroy M., Degrémont L., **Vidal-Dupiol J**., Chiarello M., Pérignon A., Alunno-Bruscia M., Boudry P., Le Roux F., Gueguen Y., Mitta G. 2017. An integrative approach to decipher the mortality syndrome affecting juvenile Pacific oysters. International Conference on Holobionts, Avril 2017, Paris, France

2016

8) - Le Moullac, G., Soyez, C., **Vidal-Dupiol, J**., Latchère, O., Belliard, C., Fievet, J., Sham-Koua, M., Gueguen, Y., (2016) High pCO2 and warming are threats for the pearl oyster *Pinctada margaritifera* and the pearl farming 13th International Coral Reefs Symposium, Juillet 2016, Honolulu, Hawai'i. Abstract ID: 28220
9) **- Vidal-Dupiol, J**., Toulza, E., Grunau, C., Chaparro, C., Roquis, D., Picart-Picolo, A., Brener, K., Mitta, G., (2016) Recurrent bleaching inducing thermotolerance increases: a dive into the holobiont adaptability through (meta)genomic and epigenomic mechanisms. 13th International Coral Reefs Symposium, Juillet 20016, Honolulu, Hawai'i. (Abstract ID: 28242)

10) - Brener Raffalli, K., Pratlong, M., **Vidal-Dupiol, J**., Adjeroud, M., Romans, P., Pillot, R., Feuillassier, L., Aurelle, D., Pontarotti, P., Haguenauer, A., Mitta, G., Toulza, E., Coral plasticity and holobiont dynamics under thermal stress: intrapopulational, interpopulational, and interspecific variability 13th International Coral Reefs Symposium, Juillet 20016, Honolulu, Hawai'i. (Abstract ID: 29194)

2013

11) - **Vidal-Dupiol J** (2013). Coral stress responses to global changes, from transcriptome to epigenome. Zoo-Biol seminar circle at Oregon State University, Octobre 2013, Corvallis, Orateur invité.
12) - Aurelle D., **Vidal-Dupiol J**.,Haguenauer A., Grunau C., Forcioli D., Toulza E., Mitta G (2013). The puzzle of cnidarians adaptation: an integrative approach. XIV Congress of the European Society for Evolutionary Biology, August 2013, Lisbon, Portugal, Abstract volume p 1330.

2012

13) **- Vidal-Dupiol J**., ZoccolaD., Tambutté E., Grunau C., Cosseau C., Freitag M., Adjeroud M., Dheilly N., Allemand D., Mitta G & Tambutté S (2012). Global coral transcriptomic responses to ocean acidification.12th International Coral Reefs Symposium, Juillet 2012, Cairns, Australia. Abstract volume p 140.
14) **- Vidal-Dupiol J**., Ladrière O., Dheilly N., Destoumieux-Garzon D., Tambutté S., Grunau C., Cosseau C., Freitag M., Adjeroud Me &Mitta G (2012). The immune response of *Pocillopora damicornis* confronted to *Vibrio coralliilyticus*. 12th International Coral Reefs Symposium, Juillet 2012, Cairns, Australia. Abstract volume p 396.

2009

15) **- Vidal-Dupiol J**., Mitta G., Roger E., Allemand D., Ferrier-Pagès C., Furla P., Grover R., Merle P.-L., Tambutté E., Tambutté S., Zoccola D., Ladrière O., Poulicek M., Fouré L. &Adjeroud M (2009).Potential implication of host/symbiont recognition mechanisms during coral bleaching. Advancing the Science of Limnology and Oceanography, Janvier 2009, Nice, France. Abstract volume p 278.
16) - Penin L., **Vidal-Dupiol J** & Adjeroud M (2009). Bleaching events: are spatial and taxonomic patterns consistent among year? A case study around Moorea, French Polynesia.11th Pacific Science Inter-Congres, Mars 2009, Papeete, Polynésie Française. Abstract volume p 200.
17) - Adjeroud M., Michonneau F., Edmunds PJ., Chancerelle Y., Penin L., Thibaut L., **Vidal-Dupiol J**., Salvat B &Galzin R (2009). Recurrent large-scale disturbances, recovery trajectories, and resilience of coral assemblage on a coral reef in the south-central pacific. 11th Pacific Science Inter-Congres, Mars 2009, Papeete, Polynésie Française. Abstract volume p 198.

2008

18) - Adjeroud M., Michonneau F., Edmunds PJ., Chancerelle Y., Penin L., Thibaut L., **Vidal-Dupiol J**., Salvat B &Galzin R (2008). Recurrent large-scale disturbances, recovery trajectories, and resilience of coral assemblage on a coral reef in the south-central pacific. 11th International Coral Reefs Symposium, Juillet 2008, Fort Lauderdale, USA. Abstract volume p 161.

4 Présentations orales en congrès nationaux :

2017

1) **-** de Lorgeril J, Lucasson A. Petton B, Toulza E, Haffner P, Destoumieux-Garzón D, Chaparro C, Galinier R, Clerissi C, Montagnani C, **Vidal-Dupiol J**, Escoubas J.M., Vergnes A, Leroy M,

Degrémont L, Pérignon A, Le Grand J, Ratiskol D, Alunno-Bruscia M, Boudry P, Le Roux F, Gueguen Y, and Mitta G. An integrative approach to decipher the summer mortality syndrome affecting Pacific oysters. Immuninv 2017, 7-9 juin 2017, Lyon, France.

2013

2) - Roquis D., **Vidal-Dupiol J**., Cosseau C., Mitta G., Grunau C (2013). Possible epigenetic origin of thermal stress adaptation of the tropical coral *Pocillopora damicornis*. Epigénétique en Ecologie et Evolution, Décembre 2013, Gif-sur-Yvette, France.
3) - **Vidal-Dupiol J**., Grunau C., Cosseau C., Freitag M., &Mitta G (2013). Stratégies et méthodes de RNA-seq appliquées aux questions écologiques sur organismes non modèles. Journée Séquençage nouvelle génération, May 2013, Marseille, France, Orateur invité.

2012

4) **- Vidal-Dupiol J**., Ladrière O., Dheilly N.M., Destoumieux-Garzon D., Tambutté S., Grunau C., Cosseau C., Freitag M., Adjeroud M &Mitta G (2012). The immune response of *Pocillopora damicornis* confronted to *Vibrio coralliilyticus*. Imuninv, October 2012, Perpignan, France. Abstract volume p 22, Talk.
5) **- Vidal-Dupiol J**., Ladrière O., Dheilly N., Destoumieux-Garzon D., Tambutté S., Grunau C., Cosseau C., Freitag M., Adjeroud M & Mitta G (2012). The immune response of *Pocillopora damicornis* confronted to *Vibrio coralliilyticus*. Immuninv, octobre 2012, Perpignan, France. Abstract volume p 26.
6) **- Vidal-Dupiol J**., Ladrière O.,Destoumieux-Garzon D.,Sautière P-E.,Meistertzheim A-L.,Tambutté E.,Tambutté S., Duval D.,Fouré L., Adjeroud M.,Mitta G (2012). Damicornin, the first AMP from a scleractinian coral: characterization and expression disturbance during vibriosis. Réseau Ecologie des Interactions Durables, Fevrier 2012, Rennes, France.

2011

7) **- Vidal-Dupiol J**., Dheilly N., Grunau C., Cosseau C., Freitag M., Mitta G (2011). The immune response of *Pocillopora damicornis* confronted to *Vibrio coralliilyticus*: a RNA-seq approach. Journée Interactions Hôtes/Microorganismes, Novembre 2011, Montpellier, France. Orateur invité.

5 Présentations affichées :

2020

1) - Gawra Gawra J.K., Lamy J.B., Saccas M., De Lorgeril J., Gueguen Y., Escoubas J.M., Destoumieux-Garzon D., Leroy M.A., Haffner P., Morga B., Dégremont L., Petton B., Cosseau C., Grunau C., Mitta G., **Vidal-Dupiol J** (2020). Integrative approach of the resistance mechanisms to the mass mortality syndrome affecting the juvenile of the oyster *Crassostrea gigas* (POMS). First Epigenetic In Marine Biology Congress, October 2020, Montpellier, France

2018

2) **- Vidal-Dupiol, J**., E. Toulza, C. Grunau, O. Rey, D. Roquis, C. Chaparro, C. Cosseau, A. Picart-Picolo, P. Romans, M. Pratlong, K. Brener-Raffalli, P. Pontaroti, M. Adjeroud, and G. Mitta (2018). Epigenetic and genetic mechanisms of trained adaptation to global warming in corals. II Joint congress on Evolutionary Biology, Montpellier 2018, France. Poster ID: P-0524

2016

3) - **Vidal-Dupiol, J**., Soyez, C., Le Moullac, G., Chapron, L., Beliaeff, B., Gaertner-Mazouni, N., Brahmi, C., (2016) Impact of temperature and pH predicted for the 22th century on energy metabolisms and shell growth of the giant clams *Tridacna* 13th International Coral Reefs Symposium, Juillet 20016, Honolulu, Hawai'i. Abstract ID: 28237

2010

4) **- Vidal-Dupiol J**., Ladrière O., Meistertzheim, A-L., Destoumieux-Garzon, D., Tambutté E., Tambutté S., Zoccola D., Adjeroud M &Mitta G (2010). Antimicrobial response of the scleractinian coral *Pocillopora damicornis* to bacterial stress from *Vibrio coralliilyticus*.11th European Coral Reefs Symposium, December 2010, Wageningen, Netherland. Abstract volume p 153. Poster.

2008

5) **- Vidal-Dupiol J**., Mitta G., Roger E., Allemand D., Ferrier-Pagès C., Furla P., Grover R., Merle P.-L., Tambutté E., Tambutté S., Zoccola D., Ladrière O., Poulicek M., Fouré L. &Adjeroud M (2008). Potential implication of host/symbiont recognition mechanisms during coral bleaching.11th International Coral Reefs Symposium, Juillet 2008, Fort Lauderdale, USA. Abstract volume p 298. Poster.
6) **- Vidal-Dupiol J** & Pichon M (2008).*Pocillopora verrucosa* and *Pocillopora meandrina* are distinct species: Morphometric evidences. 11th International Coral Reefs Symposium, Juillet 2008, Fort Lauderdale, USA. Abstract volume p 561. Poster.
7) **- Vidal-Dupiol J**., Mitta G., Roger E., Allemand D., Ferrier-Pagès C., Furla P., Grover R., Merle P.-L., Tambutté E., Tambutté S., Zoccola D., Ladrière O., Poulicek M., Fouré L. &Adjeroud M (2008). Potential implication of host/symbiont recognition mechanisms during coral bleaching.13th France-Japan oceanography symposium, September 2008, Marseille, France. Abstract volume p 109. Poster.

2007

8) **- Vidal-Dupiol** (2007). Le réchauffement climatique sonne-t-il le glas des récifs coralliens ? Exposition du CNRS Explorateurs des Mers, Juillet 2007, Paris, France. Poster.

Introduction générale

Les changements environnementaux se révèlent d'année en année de plus en plus prégnants et affectent directement ou indirectement l'ensemble du système terre. Le rôle des populations humaines dans la genèse de ces phénomènes est de moins en moins discuté et les impacts cumulés sont aujourd'hui tels, qu'ils signent une nouvelle aire géologique l'Anthropocène (Zalasiewicz et al. 2011). Très nombreux dans leurs origines et diversifiés dans leurs impacts je me suis plus particulièrement intéressé aux phénomènes biologiques liés au réchauffement climatique, à l'acidification des océans et plus récemment à l'émergence de maladies infectieuses.

Depuis la révolution industrielle et la généralisation de l'utilisation des énergies fossiles, les taux de gaz à effet de serre dans l'atmosphère sont en augmentation constante (Pachauri 2007). Leur forçage radiatif a déjà induit une augmentation moyenne des températures des eaux océaniques de plus de 0,6°C conduisant de surcroit à une stratification accrue de la colonne d'eau (Polovina *et al.* 2008) et une diminution de la disponibilité en O_2 des eaux les plus profondes (Matear et al. 2000, Diaz and Rosenberg 2008). Ce réchauffement généralisé augmenterait également en fréquence et en intensité l'occurrence de phénomènes climatiques extrêmes tels que les cyclones (Knutson *et al.* 2010).

Outre cet impact sur le climat mondial, le CO_2 influe également directement le pH des océans. En effet, plus de 25% du CO_2 émis est absorbé par les océans ou il a déjà conduit à une diminution de plus de 0,1 unité pH depuis l'ère préindustrielle (Doney *et al.* 2009). Bien qu'apparemment minime cette chute représente une déviation majeure par rapport aux conditions physico-chimiques de l'eau de mer prévalant depuis plusieurs millions d'années (Petit et al. 1999, Pelejero et al. 2010).

Les effets des changements environnementaux abiotiques combinés à la mondialisation des échanges et à l'intensification des élevages a en outre favorisé l'émergence de maladies infectieuses (Harvell et al. 1999, Harvell et al. 2002). Ces maladies touchent des espèces d'intérêt écologique aussi bien qu'économique. Bien souvent polymicrobiennes et plurifactorielles, elles peuvent avoir des impacts significatifs pouvant stopper l'exploitation d'une espèce (Lafferty et al. 2015) ou dégrader profondément un écosystème (Harvell et al. 2007).

J'ai pu au fil de mon parcours étudier les effets de ces changements sur différentes espèces d'invertébrés marins : i) les coraux Scleractiniaires notamment *Pocillopora acuta* (Fig. 1a et b ; thèse, post doc, recherche en cours) ; ii) le bénitier *Tridacna maxima* (Fig. 1c et d ; début de carrière Ifremer), iii) l'huître perlière *Pinctada margaritifera* (Fig. 1e ; début de

carrière Ifremer et recherche actuelle) ; et iv) l'huître creuse *Crassostrea gigas* (Fig. 1f ; recherche en cours). Depuis quelques années maintenant ce sont les questions en lien à l'adaptation et l'acclimatation de ces espèces à ces changements environnementaux qui m'animent. Ces études m'ont permis d'appréhender différentes méthodologies (biologie moléculaire, séquençage NGS, bioinformatique, écologie…) et échelle d'intégration (de la molécule jusqu'aux aspects écologiques) qui me permettent aujourd'hui de bénéficier d'une bonne culture scientifique dans ces domaines.

Dans un premier chapitre je ferai une brève présentation des modèles biologiques étudiés, en mettant l'accent sur les caractéristiques particulières de leur biologie ou écologie qui ont fait leur attrait dans mes recherches. Dans un deuxième chapitre je présenterai une synthèse des effets induits par l'acidification des océans. Les troisième et quatrième chapitres seront dédiés respectivement aux effets du réchauffement climatique et aux mécanismes d'adaptation et d'acclimatation des coraux au stress thermique. Le chapitre 5 présentera un aparté coloré dans le monde des perles de Polynésie. Pour finir, le chapitre 6 présentera les projets que je souhaite développer dans les cinq à six prochaines années.

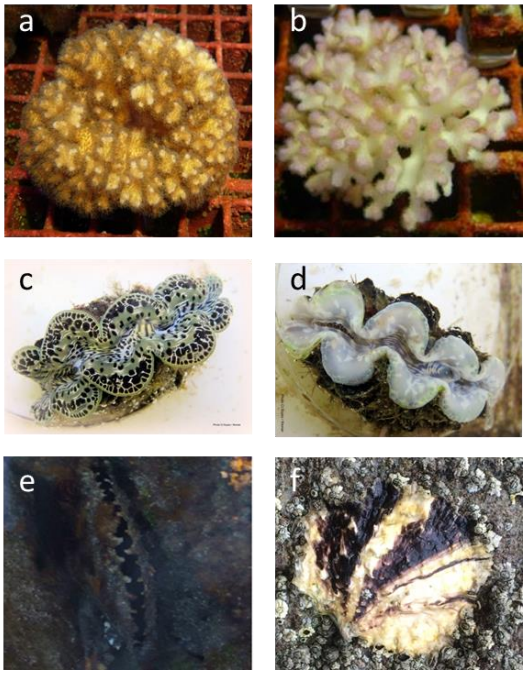

Figure 1: Principaux modèles biologiques étudiés.
a) Corail *Pocillopora acuta* en pleine santé en aquarium ; b) Corail *Pocillopora acuta* blanchi *;* c) Bénitier *Tridacna maxima* en pleine santé ; d) Bénitier *Tridacna maxima* blanchi ; e) Huître perlière *Pinctada maxima* ; f) Naissain (juvenile) d'huître creuse, *Crassostrea gigas*

Chapitre I Des modèles biologiques d'intérêt écologique et économique

A Les récifs coralliens, les coraux Scleractiniares et *Pocillopora acuta*

Les récifs coralliens sont la structure bioconstruite la plus grande au monde et la seule à être visible de l'espace. Ils constituent l'un des plus vastes écosystèmes de notre planète. Inféodés à la zone intertropicale, (35° N - 32° S) les récifs coralliens se développent dans des eaux chaudes (18-35°C) et oligotrophes (D'Elia and Wiebe 1990, Birkeland 1997). D'une superficie estimée à environ 600 000 km^2 (0,17% de la surface des océans) (Birkeland 1997) cet écosystème abriterait plus de 950 000 espèces dont environ 600 espèces de coraux Scléractiniaires, 2000 espèces de poissons et 5000 de mollusques (Reaka-Kudla 1997, Veron 2000). Touchés de plein fouet par les changements environnementaux notamment le réchauffement climatique, les récifs coralliens sont significativement dégradés et leur avenir menacé (Hughes et al. 2017). Comprendre les réponses des coraux à ces perturbations et décortiquer les processus moléculaires d'acclimatation et d'adaptation de ces organismes constituent un enjeu fort des 20 dernières années.

Les récifs coralliens reposent biologiquement et physiquement sur un groupe d'organismes les Scléractiniaires. Ces coraux présentent une biologie particulière expliquant leur réussite dans cet environnement oligotrophe. En effet, il forme une endosymbiose mutualiste phototrophe avec des microalgues de la famille des dinoflagellés et de l'ordre des Symbiodiniaceae (couramment appelé zooxanthelles). Cette symbiose permet au corail d'être mixotrophe et donc d'utiliser des sources de carbone aussi bien organique qu'inorganique. Cette complémentarité trophique lui permet de produire avec une relative rapidité un exosquelette d'aragonite qui est la bio-brique du récif corallien (Allemand et al. 2011).

D'un point de vue évolutif les Scléractiniaires présentent l'intérêt d'être à la base des eumétazoaires (Miller *et al.* 2007). Principalement sessile et coloniale, l'unité soumise à la sélection n'est pas l'individu mais la colonie. La colonie corallienne est quant à elle l'image même du concept d'holobionte puisque composée du cnidaire hôte, de symbiotes mutualistes (microalgues mais aussi bactéries) et d'une grande diversité microbienne associée (Brener-Raffalli et al. 2018, Clerissi et al. 2018).

Pocillopora acuta appartient à la famille des Pocilloporidae (Fig. 1a). De forme branchue, les colonies peuvent atteindre des tailles remarquables allant jusqu'au mètre. Cette espèce se trouve plutôt à faible profondeur, le plus souvent inféodée aux récifs frangeants de faible hydrodynamisme. Son aire de répartition est très large, et couvre la quasi-totalité des récifs de l'Indo-Pacifique (Veron 2000).

Le cycle de vie de *P. acuta* peut reposer sur de la reproduction asexuée aussi bien que sexuée. Cette dernière passe par l'émission de gamètes ou de larves planulas issus d'une fécondation interne. Ces larves constituent la phase pélagique du cycle de vie, puis vont se fixer au substrat et se métamorphoser, pour débuter leur phase benthique sessile. Trois à quatre ans sont généralement nécessaires pour passer du stade juvénile au stade adulte. Outre la reproduction sexuée, *P. damicornis* peut également se reproduire de façon asexuée ; par fragmentation, par bourgeonnement ou par émission de larves parthénogénétiques (Harrison and Wallace 1990, Yeoh and Dai 2010). Cette clonalité fait des coraux un modèle de tout premier choix pour l'étude des effets de l'environnement sur la plasticité de la réponse au stress et les mécanismes d'acclimatations et d'adaptations sous-jacents (Torda et al. 2017). Par ailleurs, il est intéressant de noter que *P. acuta* peut former des chimères issues de la fusion de deux (ou plus) colonies génétiquement différentes (Huffmyer et al. 2021).

Comme la plupart des Pocilloporidae, *P. acuta* est sensible au blanchissement (e.g. la dissociation de la symbiose entre l'hôte et la zooxanthelle en réponse à un stress environnemental notamment thermique ; Fig. 1b). Lors d'un épisode de blanchissement c'est l'une des premières espèces à être affectée (Glynn 1983, Fisk and Done 1985, Salvat 1992, Drollet et al. 1994, Loya et al. 2001). Très souvent utilisée comme espèce modèle les connaissances sur *P. acuta* sont nombreuses, de même que les ressources génomiques à disposition. J'ai au fil de mon parcours participé à l'enrichissement de ces données au travers de l'assemblage, de l'annotation et de la publication de son transcriptome de référence (Vidal-Dupiol et al. 2014) mais aussi de son génome de référence (Vidal-Dupiol et al. 2019).

B Les bivalves tropicaux, l'huître perlière *Pinctada margaritifera* et le bénitier *Tridacna maxima*

Les bénitiers (Fig. 1c) et les huîtres perlières (Fig. 1e) sont des organismes emblématiques jouant un rôle fonctionnel important dans les écosystèmes coralliens. Ils sont notamment d'une grande importance économique et vivrière pour les populations locales de nombreuses îles du Pacifique tel qu'en Polynésie française. Dans le cas du bénitier, l'exploitation de sa chair dans les îles des archipels des Tuamotu-Est et des Australes représente un chiffre d'affaire annuel non négligeable pour les pêcheurs de ces îles peu peuplées. L'huître perlière, quant à elle, est utilisée dans la production des perles noires de Polynésie, production représentant à ce jour la seconde ressource économique et le premier produit d'exportation de Polynésie Française.

Ces activités d'aquaculture et de perliculture font face aux changements environnementaux en cours. Ces changements impactent déjà négativement les cheptels de bénitiers en induisant des phénomènes de mortalité massive comme en 2009 ou près de 90% des bénitiers sont morts dans certaines zones du lagon de Tatakoto suite à un événement de stress thermique (Andréfouët et al. 2013). Mieux comprendre les risques encourus par ces ressources biologiques essentielles est un enjeu fort pour maximiser l'adaptabilité des sociétés humaines des pays insulaires océaniens aux changements globaux.

Tout comme les coraux, bénitiers et huîtres perlières sont des organismes biomineralisateurs participant tout de même mais de façon moindre à la construction du récif. Cette fonction de bio minéralisation est toutefois assez couteuse en énergie. Ces deux espèces ont donc acquis des adaptations différentes mais poursuivant le même objectif celui d'acquérir suffisamment de carbone dans un milieu oligotrophe. Dans le cas des bénitiers cette capacité repose tout comme pour les coraux sur une symbiose phototrophique grâce aux mêmes microalgues de la famille des Symbiodiniaceae. Les zooxanthelles sont ici localisées hors des cellules, au sein du manteau (tissu exposé à la lumière et dont le bourrelet externe est minéralisateur) dans un système tubulaire en Z directement connecté à l'estomac (Norton *et al.*, 1992; Holt *et al.*, 2014). Cette symbiose permet au bénitier d'être mixotrophe et de se nourrir de carbone inorganique issu de la photosynthèse des zooxanthelles et de carbone organique issu de son activité de filtration (microalgues essentiellement). Tout comme le corail, le bénitier peu souffrir de blanchissement (Fig. 1d). La capacité de l'huître perlière à vivre dans un milieu oligotrophe repose quant à elle sur une capacité de filtration hors du commun avec des débits de filtration de près 25,8 L/h/W (g de poids sec) contre 4.8 L/h/W chez l'huître creuse *Crassostrea gigas* ou 7,4 L/h/W chez la moule *Mytilus edulis* (Pouvreau et al. 1999). *P. margaritifera* sera en outre rencontrée essentiellement dans le lagon, partie de l'écosystème récifal plus riche en nutriment que les pentes externes.

Les connaissances sur ces deux modèles biologiques sont assez mal équilibrées. L'huître perlière dispose d'une base de connaissance nettement plus développée grâce au très fort intérêt économique qu'elle revêt mais aussi pour son rôle d'espèce modèle dans l'étude des processus de biomineralisation chez les bivalves (Marie et al. 2012, Stenger et al. 2021a). Du point de vue des ressources génomiques, nous disposons de plusieurs transcriptomes de référence (Joubert et al. 2010, Teaniniuraitemoana et al. 2014, Le Luyer et al. 2019) et d'un génome de référence que j'ai eu la chance de séquencer et d'assembler et qui est en cours de finalisation. Le bénitier *T. maxima* a quant à lui été plus étudié sur un aspect écologique et

écophysiologie. Les données moléculaires sont encore peu développées mais un transcriptome de référence de manteau est aujourd'hui disponible (Monteiro et al. 2020).

C L'huître de bouche *Crassostrea gigas*

L'ostréiculture occupe une place prépondérante dans le paysage français métropolitain tant d'un point de vue culturel et géographique que socio-économique. Au niveau mondial, la France occupe, en 2012, le 5ème rang en volume, loin derrière la Chine qui concentre 83 % de la production, et le 2nd rang en valeur (Remongin 2019). La production ostréicole française constitue, de loin, la première production communautaire (85 % des volumes en 2012) et se répartit sur toutes les côtes françaises. Dans l'hexagone, elle est la principale production conchylicole et représente, en 2013, 50 % des quantités et 72 % du chiffre d'affaire de la filière conchylicole. En 2012, 950 entreprises ostréicoles employaient 17 800 salariés (Le Brech 2012). Cette activité constitue la première ressource aquacole française avec une production atteignant son maximum en 2008 pour 120 000 tonnes de coquillages. Sous la pression des maladies récurrentes l'affectant (POMS et *V. aestuarianus*), la production nationale a baissé jusqu'en 2011 avant de se stabiliser autour des 80 000 tonnes.

L'histoire de la filière ostréicole est jalonnée de crises infectieuses ayant impactées plus ou moins profondément et durablement la profession. Ainsi, l'espèce originelle, *Ostrea edulis*, élevée jusqu'au milieu du XIXème siècle a quasiment disparu sous les pressions conjointes de la surpêche et de l'introduction des parasites *Marteilia refringens* et *Bonamia ostreae*. Dans les années 60, *O. edulis* fut remplacée par l'huître portugaise *Crassostrea angulata*. Cette dernière a connu, en 1967, un début de crise infectieuse, dont la maladie est caractérisée par des lésions branchiales. Cette maladie, causée par un iridovirus-like, a décimé les cultures en quelques années. En 1973, la culture de *C. angulata* a été stoppée, près de 5000 ostréiculteurs ont vu leurs activités arrêtées avec une perte économique évaluée à plus de 8 millions d'euros. C'est l'introduction de *Crassostrea gigas* (Fig. 1f), en provenance du Japon et de Colombie Britannique qui a sauvé et relancé durablement l'ostréiculture en France. Cette espèce, bien que particulièrement robuste et présentant de fortes capacités adaptatives, est aujourd'hui régulièrement confrontée à des maladies infectieuses de plus en plus sévères.

Depuis 2008 les naissains de *C. gigas* sont impactés par des mortalités massives (jusqu'à 80% de pertes) sur l'ensemble des bassins de production français et depuis 2012, des mortalités d'adultes sont régulièrement relevées et impactent de plus en plus significativement les élevages. Ces deux épizooties constituent des pathogénèses très

différentes. Les mortalités affectant les naissains (POMS, pour Pacific Oyster Mortality Syndrome) ont été associées à une maladie polymicrobienne où l'herpès virus OsHV-1 infecte les cellules immunitaires de l'huître induisant une immuno-suppression conduisant ensuite à une septicémie mortelle causé par un core pathobiome (de Lorgeril et al. 2018, Rubio et al. 2019). La maladie des adultes est quant à elle mono-microbienne et implique une bactérie du genre vibrio, *Vibrio aestuarianus*, qui après infection tue son hôte (Travers et al. 2014).

Chapitre 2 : Impact de l'acidification des océans sur les biomineralisateurs tropicaux

Contexte et problématique

Les coraux Scléractiniaires, les bénitiers ou encore les huîtres perlières sont des organismes biomineralisateurs ; tous sécrètent des structures à base de carbonate de calcium ($CaCO_3$). Que ce soit le squelette des coraux ou la coquille des bivalves les processus généraux de biominéralisation sont les mêmes (Tambutté et al. 2011, Clark 2020). Le tissu biominéralisateur, l'ectoderme calicoblastique chez les coraux et l'épithélium externe du manteau chez les bivalves, vont apporter/secréter de façon active et/ou passive des ions HCO_3^- / CO_3^{2-} et Ca^{2+} ainsi que des protéines enzymatiques ou non mais dites de matrice organique à l'interface tissu/biomineral. L'action couplée de ces apports en ions et de certaines activités enzymatiques telles que celles des anhydrases carboniques va induire une augmentation locale du pH du milieu calcifiant. Cette augmentation de pH, combinée à la présence des protéines de matrice et de la sursaturation du milieu calcifiant en CO_3^{2-} et Ca^{2+} va permettre la précipitation du $CaCO_3$ (carbonate de calcium). Cette première étape, dite de nucléation, est suivie d'une phase de croissance du cristal de $CaCO_3$ dont la forme et la taille seraient contrôlées par les protéines de la matrice organique grâce aux interactions protéine/protéine et protéine/$CaCO_3$ qu'elles forment (Tambutté et al. 2011, Clark 2020). Ce processus biochimique en lien avec la composition de la matrice organique va permettre la formation d'une diversité de cristaux dont la brique est le $CaCO_3$. Ainsi, les coraux forment des cristaux d'aragonite s'associant en structure de type fibreux (Tambutté et al. 2011), le bénitier des cristaux d'aragonite avec une structure de type prismatique sur la face interne de la coquille et lamellaire croisé sur la face externe (Brahmi et al. 2021) et l'huître perlière des prismes de calcite en face externe et des tablettes d'aragonite (la nacre des perles) en face interne (Marie et al. 2012). Contrairement aux coraux, les bivalves produisent une couche externe organique servant probablement de support aux premiers dépôts minéraux le périostracum (Clark 2020).

Les processus de biominéralisation et le devenir des structures de carbonate de calcium biogénique sont plus ou moins dépendants des caractéristiques physico-chimiques de l'eau de mer (Kleypas and Langdon 2006). C'est notamment le cas de la concentration en ions Ca^{2+} et CO_3^{2-}. Ce dernier est largement impliqué dans le maintien du pH de l'eau de mer et est lié à la concentration en CO_2 atmosphérique (Hoegh-Guldberg et al. 2007, Hoegh-Guldberg and Bruno 2010). Les liens chimiques entre la formation du CaCO3 et la concentration en Ca^{2+} et en ions CO_3^{2-} dans l'eau de mer peuvent être explicités au travers de la saturation en aragonite notée $\Omega_{aragonite}$ ($\Omega_{aragonite} = ([Ca^{2+}] \times [CO_3^{2-}]) / Ksp_{aragonite}$; ou $Ksp_{aragonite}$ est le produit de

solubilité de l'aragonite ; (Hoegh-Guldberg et al. 2007). A la valeur actuelle de la concentration en CO_2 atmosphérique (380 ppm), l'$\Omega_{aragonite}$ des océans est de 3,3 ; mais l'augmentation du CO_2 atmosphérique conduit à une consommation des ions CO_3^{2-} et, par conséquent, à une baisse de l'$\Omega_{aragonite}$ et du pH (Hoegh-Guldberg *et al.* 2007). Cette diminution de $\Omega_{aragonite}$ et du pH des océans a questionné et questionne toujours la communauté scientifique sur le devenir des organismes biomineralisateurs dans des conditions d'acidification des océans. C'est bien souvent en se basant sur les projections du GIEC (Fig. 2) que la communauté scientifique a cherché à répondre à ces questionnements au travers d'approches expérimentales permettant la manipulation fine des paramètres chimiques de l'eau de mer ou en étudiant des sites particuliers enrichis naturellement en CO_2.

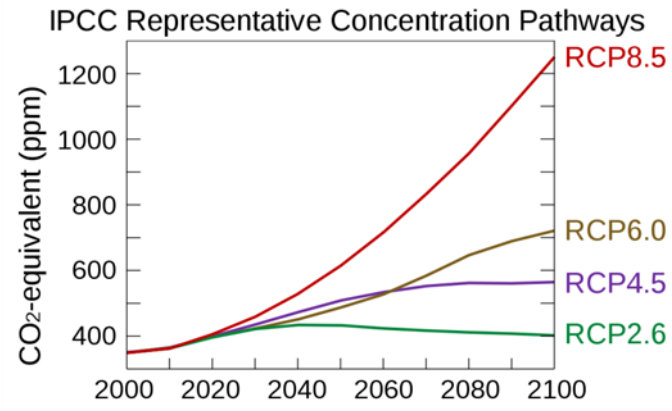

Figure 2: Prévision de l'évolution de la concentration en CO2 .
RCP2.6) Scénario très optimiste impliquant une maîtrise importante et rapide des émissions des gaz à effet de serre avec une réduction des émissions dès 2020. L'augmentation de la température des océans ne serait que de 1°C en moyenne en 2100 et le CO2 dissous dans l'eau de mer de 400µatm ; **RCP4.5)** Scénario médian impliquant une maitrise importante des émissions des gaz à effet de serre et une réduction des émissions dès 2050. L'augmentation de la température des océans serait de 1.5°C en moyenne en 2100 et le CO2 dissous dans l'eau de mer de 580µatm) ; **RCP6.0)** Scénario médian impliquant une maitrise des émissions des gaz à effet de serre puis une réduction de leur émission dès 2060. L'augmentation de la température des océans serait de 2°C en moyenne en 2100 et le CO2 dissous dans l'eau de mer de 760 µatm ; **RCP8.5)** Scénario pessimiste où aucune gestion de l'émission des gaz à effet de serre ne serait mise en œuvre. L'augmentation de la température des océans serait de 4°C en moyenne en 2100 et le CO2 dissous dans l'eau de mer de 1250 µatm. A ce jour les objectifs des accords de Paris nous positionnent entre les RCP4.5 et 6.0.

C'est dans ce contexte que j'ai pu étudier la réponse transcriptomique globale de *Pocillopora acuta* (Vidal-Dupiol et al. 2013) (Annexe 1) , la réponse transcriptomique (ciblée) et écophysiologique de *Pinctada margaritifera* (Le Moullac et al. 2016a, Le Moullac

et al. 2016b) (Annexe 2 et 3) et la réponse écophysiologie de *Tridacna maxima* (Brahmi et al. 2021) (Annexe 4).

Méthodologies mises en œuvre

Approches expérimentales

Méthodologiquement ces différentes études étaient basées sur des approches expérimentales similaires dans leur philosophie (exposer les animaux à un pH[1] plus bas qu'actuel) mais qui différaient dans les valeurs d'acidification induites et les temps d'expositions. Ainsi le corail *Pocilloppora acuta* fut exposé 21 jours à des équivalents en pression partielle de CO_2 de 400 µatm (actuel pH_{tot}=8.1), 850 µatm (pH_{tot}=7.8), 2200 µatm (pH_{tot}=7.4) et 3900 µatm (pH_{tot}=7.2). L'huître perlière *Pinctada margaritifera* a été exposée sept ou 100 jours à des équivalents en pression partielle de CO_2 de 430 µatm (actuel pH_{NBS}=8.1), 1200 µatm (pH_{NBS}=7.8), et 3660 µatm (pH_{NBS}=7.4). Le bénitier *Tridacna maxima* a quant à lui été exposé 65 jours à des équivalents en pression partielle de CO_2 de 430 µatm (actuel pH_{NBS}=8.1) et 1200 µatm (pH_{NBS}=7.8).

Mesures écophysiologiques

Des expérimentations d'écophysiologies ont pu être menées sur deux des trois modèles biologiques étudiés, l'huître perlière *P. margaritifera* et le bénitier *T. maxima.* Ces mesures ont été faites sur banc écophysiologique et par des observations au microscope électronique à balayage. Pour les deux espèces ; la consommation d'oxygène, la croissance, la microstructure de la coquille, le periostracum et les faces internes et externes de la coquille ont été étudiés. Pour l'huître perlière ces paramètres ont été complétés par des mesures de bioénergie au travers de la caractérisation du taux d'ingestion, de l'efficacité d'assimilation, de l'efficacité de croissance (scope for growth) et de la gamétogénèse. La physiologie du bénitier a quant à elle été complétée par des mesures de production photosynthétique et de densité en symbiote dans le manteau.

Mesure transcriptomique

Les effets de l'exposition aux différentes conditions d'acidification ont également été appréhendés au niveau de l'expression des gènes. Ainsi, l'intégralité du transcriptome du

[1] Le pH peut être exprimé selon différentes calibrations, l'échelle totale (pH_{tot}) ou l'échelle NBS (pH_{NBS} ; est celle classiquement utilisée en laboratoire). Ces calibrations induisent que pour une même valeur de pH la concentration en CO_2 dissous est différente. Afin de simplifier la compréhension j'ai fait le choix d'exprimer la valeur d'acidification induite expérimentalement en donnant la concentration de CO_2 atteinte en µatm.

corail *P. acuta* a pu être étudiée aux valeurs de pCO_2 de 400 et 2200 µatm par une approche de RNA-seq, ce qui à l'époque (2011-2013) était extrêmement novateur. Ces données ont ensuite été complétées par des approches ciblées par RT-PCR-quantitative visant à quantifier aux autres valeurs de pH l'expression des gènes impliqués dans : le transport du Ca^{2+} et de l'HCO_3^-, la conversion de l'HCO_3^- en CO_3^{2-}, la production de matrice organique, la photosynthèse, le métabolisme énergétique de l'hôte (glycolyse, cycle de krebbs, phosphorilation oxidative, lipolyse et beta-oxidation). Ce même type d'approche ciblée a été développé chez l'huître perlière en ciblant des gènes de la matrice organique spécifiques des primes de calcite ou des tablettes d'aragonite.

Principaux résultats

Bioénergie

Que ce soit sur l'huître perlière ou le bénitier la baisse de pH de l'eau de mer n'a eu aucun effet sur les paramètres physiologiques liés à la production d'énergie ou la reproduction (consommation d'oxygène, taux d'ingestion, de l'efficacité d'assimilation, de l'efficacité de croissance (scope for growth) et de la gamétogénèse). L'efficacité de la photosynthèse de même que la densité en symbiote dans le manteau de *T. maxima* a été négativement impactée à partir du 53^{eme} jour d'exposition pour le premier et du 29^{eme} pour le second.

Croissance et microstructure des coquilles

Bénitiers et huitres perlières ont vu leurs croissances diminuer en réponse à la baisse de pH. Cette réduction de croissance n'est devenue significative qu'à une concentration en CO_2 de 3660 µatm ce qui équivaut à un pH de $7,4_{NBS}$. Chez le bénitier cette réduction de croissance est significative dès le 29^{eme} jour d'exposition à une pCO_2 de 1200 µatm (pH_{NBS}=7.8). Elle s'est ensuite intensifiée au 53^{eme} jour. La microstructure des cristaux d'aragonite ou de calcite formée durant la phase d'exposition n'a pas montré de différence avec celle formée avant cette phase chez l'huitre perlière. Chez le bénitier, des différences sont observables dès le 41^{eme} jour d'exposition à une pCO_2 de 1200 µatm. Des signes de dissolution des minéraux et de la matrice organique ont été observés chez l'huitre perlière (Fig. 3a). Cette dissolution n'est visible que chez les échantillons ayant subi le traitement le plus long (100j) et elle semble proportionnelle à l'intensité de l'acidification induite. Ainsi, le periostracum des huitres exposées au pH le plus bas présente une dépigmentation très importante avec une coquille gris clair contrastant avec le noir habituel. La face interne de la coquille présente quant à elle des stigmates de dissolution très poussés au pH le plus bas. Ces

stigmates sont caractérisés par une disparition de la structure des minéraux normalement formée ainsi que celle de la matière organique.

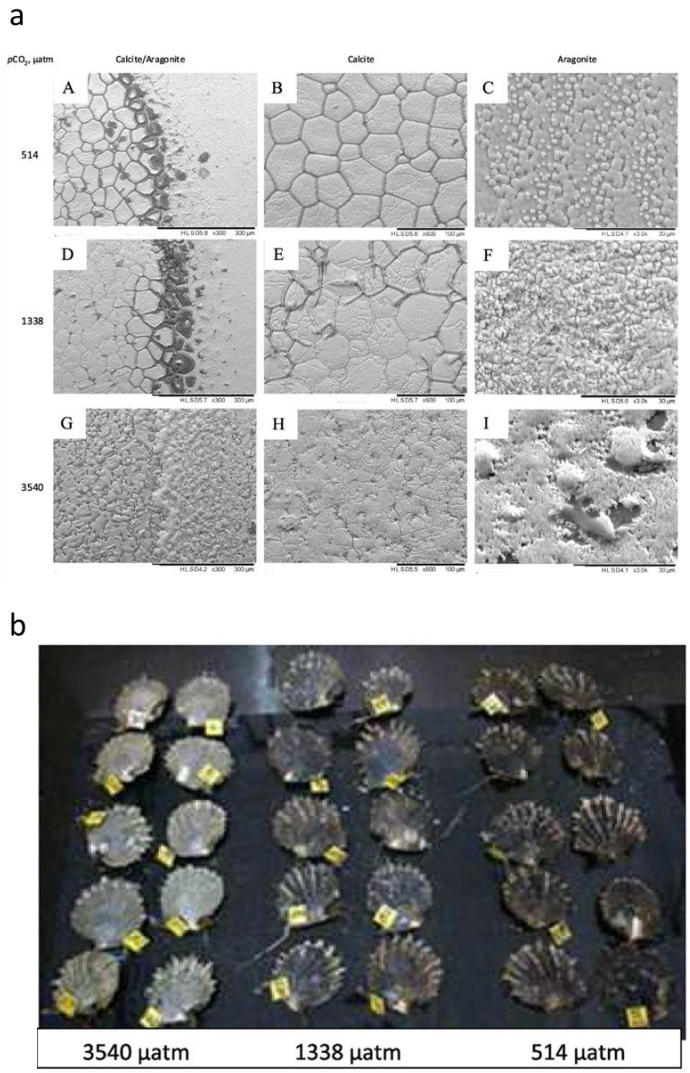

Figure 2: Effet des pH bas sur la face interne et externe de coquille de *Pinctada margaritifera*.
a) Face interne de la coquille, avec la transition calcite/aragonite (colonne de gauche) la partie calcite au milieu et aragonite à droite. **b)** Illustration de la dépigmentation du periostracum en fonction du niveau d'acidification.

Expression génique

Chez l'huitre perlière, les approches par RT-PCR-quantitatives ciblant les gènes de la matrice organique n'ont pas montré de différences significatives.

L'approche RNA-seq développée chez le corail *P. acuta* a montré l'expression différentielle de 16% des gènes du transcriptome (10% sous-exprimés et 6% sur-exprimés) en réponse à 21 jours d'exposition à une pCO_2 de 2200 µatm. L'analyse par enrichissement des GO term à l'échelle des processus biologiques avait montré une sur-représentation des

fonctions associées au transport d'ions et de protéines ainsi qu'à la production d'énergie, qu'elle soit issue d'une source de carbone organique ou inorganique. Nous avons ainsi montré qu'à une pCO_2 de 850 µatm (pH_{tot}=7.8) les gènes codant pour des protéines clefs de la biominéralisation (transport du Ca^{2+} et de l'HCO_3^-, conversion de l'HCO_3^- en CO_3^{2-}, matrice organique) étaient tous significativement sur-représentés. A une pCO_2 de 2200 µatm (pH_{tot}=7.4) ce pattern était maintenu mais l'intensité du différentiel d'expression était atténuée. A 3900 µatm de CO_2 (pH_{tot}=7.2) les gènes codant pour les transporteurs ou les convertisseurs ioniques présentaient des sous-expressions et seuls les gènes codant pour des protéines de matrice organique étaient encore significativement sur-exprimés. Le métabolisme énergétique associé à l'utilisation d'une source de carbone organique a présenté le même pattern que celui des transporteurs d'ions avec des sur-expressions au pH les moins stressants pour finir par être sous-exprimés au pH le plus faible. Le métabolisme associé à la photosynthèse a quant à lui été sur-exprimé au 3 pH bas.

Implication de ces résultats pour la communauté

Ces expériences et les résultats en ayant découlé ont selon moi apporté un éclairage sur la problématique de l'impact de l'acidification des océans sur les organismes biominéralisateurs à deux niveaux. Tout d'abord sur le fait que dans la gamme de pH qui devrait être atteinte dans le contexte et l'évolution actuelle des émissions de CO_2, il ne semble pas que ce changement environnemental puisse à lui seul être un danger de premier ordre sur les stades adultes ou sub-adultes. Dans un deuxième temps, je pense que ces résultats montrent également qu'il existe une différence extrêmement significative entre organisme à « endosquelette » tel que les coraux scléractiniaires et ceux à exosquelette comme les bivalves. Les premiers étant à mon sens moins à risque que les seconds. Ce sont de ces deux points que je discuterai dans les paragraphes suivants.

La recherche sur l'impact de l'acidification des océans sur les organismes calcifiants a « débuté » vers la fin des années 90 et le début des années 2000 (Gattuso and Buddemeier 2000). Cette thématique scientifique a par la suite bénéficié d'un très fort engouement avec l'implication de très nombreuses équipes travaillant sur de nombreux modèles biologiques marins. Cette thématique très en vogue dans les années 2010 a je pense été dopée par une forme d'alarmisme peut être un peu exagérée et prédisant la fin ou presque des organismes calcifiants dans les décennies à venir (Hoegh-Guldberg et al. 2007). Avec 10 années de recul en plus il me semble qu'aujourd'hui les prévisions sont plus tempérées ou du moins, plus documentées. Ainsi l'article intitulé Genes related to ion-transport and energy production are

upregulated in response to CO2-driven pH decrease in corals: New insights from transcriptome analysis et publié en 2013 (Vidal-Dupiol et al. 2013) participe à la vague d'articles ayant tempéré ces conclusions alarmistes. Dans cet article nous présentons des résultats soutenant l'hypothèse que les coraux disposeraient des ressources physiologiques permettant de contrebalancer la baisse de pH induite par l'augmentation de la concentration en CO_2 atmosphérique (Fig 4). En effet nous proposons que la sur-expression des gènes impliqués dans le transport des ions Ca2+ et CO_3^{2-} ou de la conversion de l'HCO_3^- en CO_3^{2-} permettrait de maintenir les conditions chimiques nécessaires à la biomineralisation. Parallèlement à ce mécanisme de compensation biochimique, l'augmentation de l'activité de transcription des protéines de matrice organique suggérait de possible modification du ratio matière organique/matière minérale au sein du squelette. Cela nous a conduit à proposer qu'une augmentation de la fraction organique, moins sensible à l'acidification, permettrait de contrebalancer les effets néfastes de cette dernière. En parallèle de l'activation de ces mécanismes une augmentation de l'activité métabolique permettrait de compenser leur coût énergétique. Ces hypothèses ont d'ailleurs toutes été confirmées quelques années plus tard. Ainsi, il fut démontré en 2013 que sous des conditions d'acidification réalistes les coraux été capables de compenser la baisse de pH environnante et de maintenir un pH adéquat à la biominéralisation au site de calcification (Venn et al. 2013). Quelques années plus tard c'est l'hypothèse de l'enrichissement du squelette en matrice organique qui fut confirmée (Tambutté et al. 2015). En 2019 et 2021 c'est l'augmentation de la production d'énergie par la photosynthèse des symbiotes et par les mitochondries de l'hôte qui fut confirmée (Biscéré et al. 2019, Agostini et al. 2021). S'il est aujourd'hui indiscutable que l'acidification des océans est une réelle problématique pour les organismes calcifiants elle n'est plus présentée comme un danger de mort quasi immédiat. Ainsi ce sont plutôt les capacités et les mécanismes d'adaptation à ce phénomène qui sont aujourd'hui « en haut de l'affiche » (Liew et al. 2018) et qui portent un message un peu plus optimiste à l'image des coraux capables de se développer proche des sources hydrothermales riches en CO_2 (Camp et al. 2017).

L'une des différences majeures observée entre coraux scléractiniaires et mollusques bivalves réside dans la présence de phénomène de dissolution du biominéral chez ces derniers. Contrairement aux coraux où le squelette se trouve protégé du milieu extérieur par les tissus de l'animal, la coquille des bivalves est quant à elle directement exposée à l'eau de mer. Cette exposition directe est très certainement l'explication sous-jacente à ces dissolutions (Rodolfo-Metalpa et al. 2011). Si aux pH de demain les plus écologiquement réalistes, ces dissolutions sont considérées d'un impact minime ; il faut rappeler que ces études sont faites

sur les huitres perlières et les bénitiers adultes et bénéficiant donc d'une coquille déjà largement consolidée. Une analyse de l'impact de cette dissolution sur les plus jeunes stades vie me semble aujourd'hui manquer pour pouvoir préciser les risques encourus par la perliculture ou les tridacni-cultures. En effet, les animaux présentant les coquilles les plus fines tels que les ptéropodes ont montré une grande vulnérabilité à ces phénomènes de dissolution (McClintock et al. 2009, Bednaršek et al. 2012). Les études menées chez des larves de mollusque montrent par contre des résultats très contrastés d'une espèce à l'autre (Barros et al. 2013, Frieder et al. 2014, Campanati et al. 2018) démontrant que des généralités sont difficilement déterminables vis-à-vis de cette question (Gazeau et al. 2013).

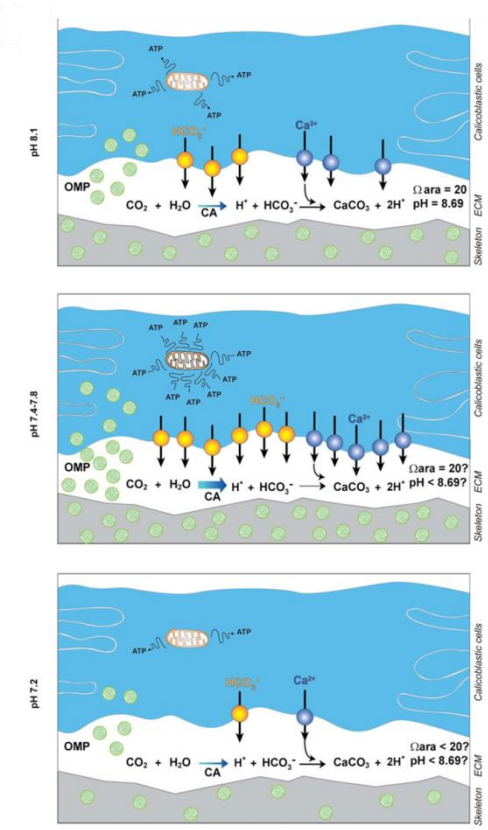

Figure 4: Illustration des processus mis en œuvre pour compenser l'acidification.
OMP = Organic Matrix Proteins

Chapitre 3 : Réponse des coraux et bivalves tropicaux au réchauffement climatique

Contexte et problématique

Par comparaison aux mers et océans tempérés, les eaux marines tropicales sont en partie caractérisées par leur stabilité thermique accrue. Cette stabilité a conduit la sélection d'organisme sténotherme vivant de fait très proche de leur limite de tolérance thermique (Tewksbury et al. 2008, Dahlke et al. 2020). La température étant un facteur contrôlant nombre de processus tant chimiques que biologiques l'augmentation des températures subit ces dernières décennies n'est pas sans impact sur les populations d'invertébrés marins tropicaux.

Les coraux scléractiniaires furent parmi les premiers organismes ayant été affectés par le réchauffement climatique. Ainsi, quelques semaines d'une augmentation de quelques dixièmes de degrés au moyennes habituelles suffisent à induire un phénomène appelé blanchissement corallien (Jokiel & Coles 1977; Glynn & D'croz 1990; Jokiel & Coles 1990). Ce phénomène correspond à la dissociation de la symbiose entre l'hôte cnidaire et le symbiote dinoflagellé. Les coraux apparaissent alors blancs, leur squelette calcaire devenant visible au travers des tissus devenus transparents ou presque (Fig. 1b). Si le stress thermique n'est que de courte durée les coraux pourront survivre, être recolonisés par les zooxanthelles et reconstituer leurs réserves énergétiques en 6 à 12 mois selon les espèces (Grottoli et al. 2004; Grottoli et al. 2006; Rodrigues et al. 2008a; Rodrigues et al. 2008b). A contrario, si le stress est maintenu trop longtemps l'hôte corallien finira par mourir. Ces évènements de blanchissement peuvent être très localisés mais aussi s'étendre sur de très larges aires, nous parlons alors de blanchissement de masse pouvant avoir des répercutions significatives pour l'ensemble de l'écosystème (Hughes et al. 2017). Les questionnements scientifiques développés ces 15-20 dernières années sur le blanchissement corallien ont dans un premier temps porté sur la compréhension des facteurs environnementaux inducteurs de blanchissement (Brown 1997), puis sur la caractérisation des mécanismes cellulaires et moléculaires du blanchissement (Weis 2008) pour enfin aborder les aspects d'acclimatation et d'adaptation à la température (Torda et al. 2017).

Les phénomènes de blanchissement corallien induits par des augmentations de température sont aujourd'hui très documentés. Cette « hyper connaissance » fut dopée par le rôle majeur que jouent les coraux dans le fonctionnement des récifs coralliens mais aussi car ce phénomène est très spectaculaire. Comment ne pas voir qu'un récif entier a changé de couleur en quelques jours. Or, des phénomènes de mortalité ont également été rapportés chez d'autres organismes sessiles du récif tels que les bivalves. Ce fut notamment le cas des

bénitiers comme en 2009 ou près de 90% sont morts dans certaines zones du lagon de Tatakoto suite à un événement de stress thermique (Andréfouët et al. 2013) ou encore en 2016 lors d'un phénomène El niño ayant fortement touché la Polynésie (Andréfouët et al. 2015). Moins essentielle au fonctionnement de l'écosystème que les coraux, la problématique de l'impact du réchauffement climatique sur les bivalves tropicaux n'en est pas moins essentielle particulièrement au regard de leur rôle économique et social fondamental. Comme pour les coraux un peu avant il est aujourd'hui question de comprendre comment ces animaux répondent à ce stress, quelles sont les limites physiologiques qui les caractérisent et quels sont les mécanismes d'acclimatation et d'adaptation possiblement mis en jeux.

C'est dans ce contexte que j'ai pu étudier la réponse transcriptomique au stress thermique de *Pocillopora acuta* (Vidal-Dupiol et al. 2009, Vidal-Dupiol et al. 2014) (Annexe 5 et 6), la réponse transcriptomique (ciblée) et écophysiologique de *Tridacna maxima* (Monteiro et al. 2020, Brahmi et al. 2021) (Annexe 4 et 7) et la réponse écophysiologique de *Pinctada margaritifera* (Le Moullac et al. 2016a) (Annexe 2). L'objectif de ces travaux était de comprendre les mécanismes moléculaires précocement initiés lors d'un stress thermique chez les coraux. Chez les bivalves l'objectif était d'apporter les toutes premières réponses aux questions du risque encouru par les ressources biologiques que sont l'huître perlière et le bénitier.

Méthodologies mises en œuvre

Approches expérimentales

Un des points clefs de ma recherche en milieu contrôlé sur le stress thermique a résidé dans le développement de protocoles expérimentaux "écologiquement réalistes" à savoir, reproduisant le plus fidèlement possible ce qui est subit par les animaux en milieu naturel. L'idée peut sembler simpliste mais nombre d'études visant à étudier le blanchissement corallien ont utilisé des "chocs" thermiques (augmentations de plusieurs °C en quelques heures) pour étudier un phénomène de stress étant par définition de faible amplitude mais de longue durée. Ainsi, c'est grâce à l'analyse de séries temporelles issues de données satellitaires et complétées par la bibliographie à disposition pour chaque population étudiée que les protocoles de stress thermiques ont été définis (Fig. 5). Pour les coraux ils commencent à une température dite contrôle représentant la moyenne des 3 mois les plus chauds sur les 15 dernières années. Après 15 jours d'acclimatation à cette température contrôle, les coraux sont soumis à une augmentation graduelle de la température de un degré par pas de temps (tous les 3 jours ou tous les 7 jours) jusqu'à l'expression de symptôme de

stress (e.g. la fermeture des polypes). Une fois ce seuil de stress atteint la température est ensuite maintenue à cette valeur jusqu'à la dissociation de la symbiose (Vidal-Dupiol et al. 2009, Vidal-Dupiol et al. 2014).

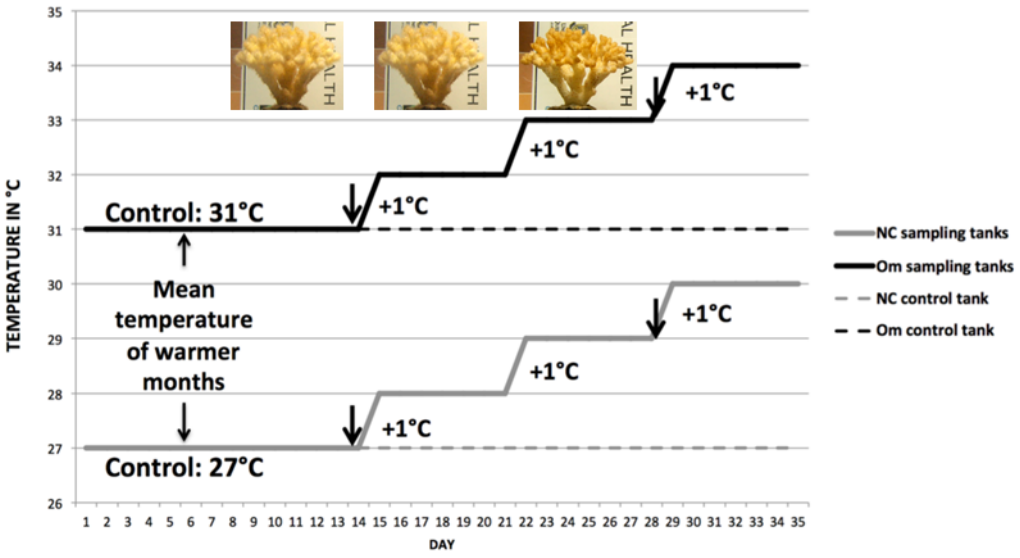

Figure 4: Protocole de stress écologiquement réaliste. Illustration des protocoles de stress écologiquement réalistes utilisés et représentant dans cet exemple la cinétique appliquée aux coraux d'Oman et de Nouvelle-Calédonie. Les photos illustrent la fermeture des polypes attestant de l'état de stress de la colonie mais de l'absence de blanchissement.

Chez le bénitier une approche philosophiquement proche de celle développée chez les coraux a été mise en œuvre. La différence ici réside dans l'absence de montée graduelle en température avec un positionnement en terme de contrôle à la température stressante actuelle pour les populations d'invertébrés polynésiens (29,2°C) et de 30,7°C pour ce qui serait les températures stressantes de demain selon le modèle du GIEC RCP4.5 (réchauffement climatique modéré). Ces températures ont été maintenues 65 jours (Monteiro et al. 2020, Brahmi et al. 2021). Pour l'huitre perlière les protocoles ont consisté en une première étape d'acclimatation à une température contrôle puis en une montée ou une descente lente mais continue à une température seuil qui sera par la suite maintenue 7 jours. Ce design, non réaliste permet cependant de déterminer la température optimale de vie (Le Moullac et al. 2016a).

Mesures écophysiologiques

Des expérimentations d'écophysiologie ont pu être menées sur deux des trois modèles biologiques étudiés, l'huitre perlière *P. margaritifera* et le bénitier *T. maxima*. Pour la

première nous avions mesuré à l'aide d'un banc d'écophysiologie : la consommation d'oxygène, le taux d'ingestion, l'efficacité d'assimilation et l'efficacité de croissance et de reproduction (scope for growth). La physiologie du bénitier a quant à elle été étudiée par des mesures de : bilan oxygène, de production photosynthétique de densité en symbiote dans le manteau et de croissance. Ceci a été complété par des observations au microscope électronique à balayage de la microstructure de la coquille, du periostracum et des faces internes et externes de la coquille. Chez le corail des mesures de densité en zooxanthelle ont été effectuées à certaines occasions.

Mesures transcriptomiques

Ces travaux s'étendent sur la période 2007-2020 et incluent donc une certaine diversité d'approches transcriptomiques. Ainsi ma première étude des mécanismes de dissociation de la symbiose chez le corail *P. acuta* a été réalisée par une approche par banque soustractive couplée au séquençage d'EST par méthode Sanger ainsi qu'une quantification du différentiel d'expression par RT-PCR-quantitative (Vidal-Dupiol et al. 2009). En 2011 j'ai développé pour la première fois du RNA-seq (Illumina) permettant de caractériser et de quantifier les différences transcriptomiques entre coraux maintenus à une température contrôle et coraux stressés. Cette approche RNA-seq avait été complétée par de la RT-PCR-quantitative (Vidal-Dupiol et al. 2014). En 2017 c'est du RNA-seq dernière génération qui a permis l'étude des différences transcriptomiques caractérisant l'holobionte bénitiers exposés aux températures de 29,2°C et de 30,7°C. Pour l'huitre perlière la partie transcriptomique a été limitée à l'étude ciblée de certains gènes de la matrice organique spécifique des primes de calcite ou des tablettes d'aragonite.

Biologie fonctionnelle

Afin de compléter les informations sur le rôle potentiel de certains gènes candidats, des approches de RACE-PCR, de modélisation protéique et d'immunohistochimie ont été réalisées.

Principaux résultats

Ecophysiologie

Sur l'huitre perlière les mesures écophysiologiques ont mis en lumière un effet positif d'une augmentation de température jusqu'à un seuil de 30 degrés au-delà duquel une dégradation rapide de l'état de santé de l'animal se fait sentir. La modélisation polynomiale de

ces paramètres, notamment du scope for growth intégrant l'ensemble des mesures faites montre que la température optimale de croissance et de reproduction de l'huitre perlière est de 28,7°C.

Chez le bénitier l'exposition à la température la plus haute a induit un blanchissement partiel des individus dès le 41eme jour d'exposition. Cette baisse de la densité en zooxanthelle est associée à une diminution de la production photosynthétique (*Fv/Fm*) preuve que les symbiotes souffrent de photoinhibition. En parallèle de ce phénomène le bilan O_2 de l'holobionte a logiquement diminué. Si la microstructure du squelette présente des signes d'altération en lien avec le stress thermique, la croissance n'est pas affectée de façon significative.

Chez les coraux les mesures de densité en zooxanthelle effectuées au cours des augmentations de température ont montré que le stress était effectif à 31°C sans qu'il y ait eu activation des mécanismes de dissociation de la symbiose. Ces derniers sont intervenus à 32°C (seuil maximal de température atteint) après 6 jours d'exposition et ont conduit à une perte de 80% des symbiotes.

Expression génique et localisation tissulaire

Chez l'huitre perlière les mesures d'expression de gènes impliqués dans la biominéralisation présentent, pour quatre des neufs candidats, un pattern de transcription avec un maximum d'expression à 26°C. Aucune différence n'a été identifiée pour les cinq autres gènes.

Chez le corail *P. acuta*, le couplage de l'approche par banque soustractive et q-RT-PCR a permis de mettre en évidence deux gènes précocement (six jours avant le blanchissement) et significativement réprimés (entre 10 et 100 fois) par rapport au contrôle. Ces gènes étudiés par RACE-PCR présentent pour le premier un peptide signal suivi d'un domaine lectin de type C (DC-SIGN) où l'ensemble des acides aminés essentiel au fonctionnement de la protéine est présent. Ce gène fut nommé PdC-lectin. Le deuxième gène présente également un peptide signal et un domaine riche en cysteine caractéristique des toxines de serpent et des interactions protéine/protéine (uPAR/Ly6/CD59/Snake toxin super familly). Ce gène fut nommé Pdcyst-rich. Les résultats d'immunohistochimie ont démontré que PdC-Lectin était produit dans les cellules de l'endoderme oral (siège de la symbiose) puis sécrété dans le cœlenteron où la protéine servirait de molécules de reconnaissances des symbiotes et d'opsonine permettant la phagocytose des zooxanthelles. Le deuxième gène, Pdcyst-rich est exprimé dans l'ectoderme aboral siège de la biominéralisation. La protéine est

localisée dans les granules des desmocytes, des cellules d'ancrage des tissus au squelette. L'approche RNAseq développée ultérieurement a confirmé la forte baisse d'expression de ces deux gènes six jours avant l'expression des symptômes. Cette approche RNA-seq a en outre montré la surexpression de gènes anti-oxydants et de gène de la famille des heat shock protein incluant leur facteur de transcription HSF. Une régulation des gènes codant les protéines de type Rab au moment de la dissociation de la symbiose a également été observée (sous expression des Rab 4 et 5 et sur-expression des Rab 7 et 11). Il a aussi été montré qu'au moment où le stress devenait effectif de nombreux gènes de biominéralisation étaient réprimés de même que beaucoup (plusieurs milliers) d'autres sans qu'un lien fonctionnel entre eux puisse être identifié.

Chez le bénitier les résultats obtenus ont tout d'abord pu être reliés aux données d'écophysiologie produites lors de la même expérience. Cette approche basée sur le package WGCNA permet d'identifier des clusters de gènes coexprimés et corrélés positivement ou négativement à des valeurs physiologiques ou à des paramètres environnementaux. Cette approche a permis d'identifier deux clusters de gènes, l'un positivement corrélé avec la température et négativement corrélé à la densité en symbiote et à l'efficacité de la photosynthèse ; l'autre corrélé positivement à l'efficacité de la photosynthèse seulement. Chez le premier était retrouvé des gènes impliqués dans des processus liés au développement, au métabolisme de l'acide ascorbique et du tryptophane, à la régulation de l'apoptose, à l'efflux du cholestérol et au mouvement ciliaire. Le second cluster contenait des gènes liés au fonctionnement du système nerveux, au métabolisme énergétique et au métabolisme des espèces réactives de l'oxygène.

Implication de ces résultats pour la communauté

Ces travaux de recherche ont permis d'étudier pour la toute première fois les limites de tolérance thermique de l'huitre perlière. Ainsi nous avons pu montrer que la température optimale pour la croissance et la reproduction doit être proche de 28,7 °C pour la population étudiée. Une fois cet optimum dépassé les capacités physiologiques de l'animal sont rapidement diminuées jusqu'à chuter drastiquement. Ce seuil thermique repositionné dans le contexte des cycles thermiques annuels d'aujourd'hui montre que les huitres perlières passent déjà plus de 121 jours au-dessus de cet optimum (Fig 6). Repositionnées cette fois dans le contexte de demain selon les trois modèles prédits par le GIEC il apparait que les huitres perlières passeraient 210 jours au-dessus de ce seuil dans le scenario le plus optimiste (RCP2.6), 252 jours au-dessus de ce seuil dans le scénario médian (RCP4.5) et l'intégralité de

l'année au-dessus de ce seuil dans le scenario le plus pessimiste (RCP8.5). Bien que la ressource biologique que représente l'huitre perlière semble ne pas être significativement affectée par le réchauffement climatique aujourd'hui, cette contextualisation montre que des problèmes pourraient intervenir prochainement. De nouvelles études ont d'ailleurs été initiées depuis au centre Ifremer du Pacifique afin de confirmer et/ou de préciser le seuil précédemment défini. Ainsi de nouvelles approches d'écophysiologie basées sur l'identification des points de basculement seront prochainement menées. Des travaux de génétique et de transcriptomique comparative entre population supposée thermotolérante et thermosensible sont en cours de finalisation et cette notion de thermorésistante est maintenant prise en compte dans les programmes d'amélioration génétique de l'espèce (Le Luyer et al. 2021).

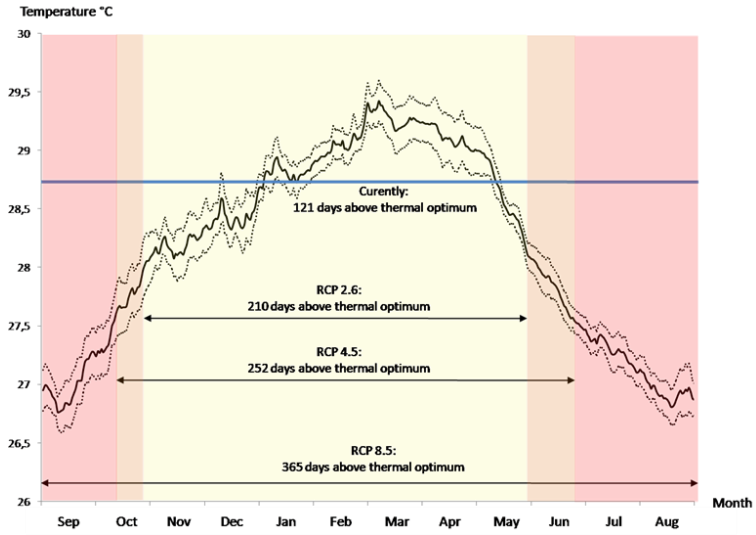

Figure 6 : Prévision du temps passé au- dessus de son optimum thermique pour l'huitre perlière selon les RCP 2.5 à 8.5.

La ligne bleue représente le seuil d'optimum thermique.

Les symbioses à zooxanthelles sont nombreuses et diversifiées. La famille des Symbiodiniaceae est d'ailleurs 100% symbiotique. Si cette symbiose est indispensable à la réussite des coraux et bénitiers au sein d'un environnement aussi pauvre en nutriment elle semble aussi en être le talon d'Achille comme le montre les similitudes de réponses entre coraux et bénitiers. Chez les coraux il a été montré à de nombreuses reprises que la première fonction altérée lors d'un stress thermique est la photosynthèse, *via* un phénomène de photoinhibition caractérisé entre autre par une chute de la production photosynthétique

(Lesser 2006, Venn et al. 2008, Weis 2008). Ce dysfonctionnement de la photosynthèse va conduire à la production d'une grande quantité des radicaux libres oxygénés, les ROS (Lesser 2006, Venn et al. 2008, Weis 2008). En réponse à cette production des gènes codant des protéines détoxifiant les ROS (superoxydes dismutases, des catalases et autres glutathions) vont être surexprimées de même que des protéines de type Heat Shock Protein (Lesser 1996, Downs et al. 2002, Franklin et al. 2004, Plantivaux et al. 2004, Richier et al. 2006, Merle et al. 2007, Desalvo et al. 2008, Richier et al. 2008, Rodriguez-Lanetty et al. 2009, Vidal-Dupiol et al. 2014). Si le stress thermique est prolongé et/ou gagne en intensité, ces mécanismes de détoxification et de réparation finissent par être dépassés. Les zooxanthelles étant la source première de ce stress oxydant intense elles ne seraient donc plus considérées comme symbiote mais comme un pathogène à éliminer induisant dès lors les mécanismes du blanchissement. Dans le cas des bénitiers les connaissances sur les liens symbiotiques formés avec la zooxanthelle sont bien moins connus de même que les mécanismes de réponse au stress thermique. Les travaux menés entre 2015 et 2020 sur ce modèle ont montré, qu'ici aussi, un phénomène de photoinhibition thermiquement induit chez la zooxanthelle, précédait la dissociation de la symbiose (Brahmi et al. 2021). Les expériences complémentaires menées en transcriptomique ont d'ailleurs mis en évidence l'activation de voie moléculaire liée à la réponse au stress oxydant (Monteiro et al. 2020). Il ressort ainsi de ces travaux et de la bibliographie que la réponse au stress thermique chez les coraux et les bénitiers pourrait être un cas intéressant d'évolution convergente vis-à-vis du facteur commun que représente la symbiose à zooxanthelle.

Les interactions hôte symbiote sont par définition des interactions durables et intimes. Cela suggère que les deux protagonistes échangent moléculairement des informations pour se reconnaitre se tolérer et éventuellement se séparer. Mes travaux menés sur la réponse au stress thermique des coraux m'ont permis de participer à l'établissement de ces connaissances à différents niveaux. Ainsi il ressort que les coraux et les zooxanthelles se reconnaissent au travers d'une interaction lectin/glycan (Wood-Charlson et al. 2006) où les sucres sont localisés à la surface des zooxanthelles et où les lectins sont produites par les coraux. Parmi ces sucres il a été montré que le mannose est essentiel (Wood-Charlson et al. 2006). Le corail quant à lui exprime des lectins de type C (reconnaissant spécifiquement le mannose) dans les cellules de l'endoderme oral. Elles y sont alors stockées dans des granules et secrétées dans le cœlenteron ou elles vont pouvoir interagir avec les sucres présents à la surface des zooxanthelles (Vidal-Dupiol et al. 2009). Ces lectins ont été identifiées chez d'autre espèces

de cnidaire (Kvennefors et al. 2008, Wood-Charlson and Weis 2009) et participent à l'établissement d'au moins une autre symbiose marine (Bulgheresi et al. 2006). Une fois l'interaction et la reconnaissance établies la lectin servirait d'opsonine et permettrait à la zooxanthelle d'être phagocytée. Une fois le phagosome formé ce dernier stoppe sa maturation et devient le symbiosome. L'arrêt de cette maturation serait le fruit du recrutement et du maintien à la surface du symbiosome de protéines de la famille des Roh GTPase (Rab4 et Rab5) qui sont impliquées dans la régulation du trafic des vésicules intracellulaires (Chen et al. 2004, Vidal-Dupiol et al. 2014). Rab4 et Rab5 sont des protéines qui maintiennent le phagosome dans un stade immature. Elles sont également antagonistes à Rab7 et Rab11, qui, lorsqu'elles sont présentes à la surface du phagosome induisent sa maturation et sa fusion avec les vésicules de lysosomes (Chen et al. 2003, Chen et al. 2004, Chen et al. 2005). De façon intéressante, en période de stress thermique lorsque le symbiote devient plus toxique que bénéfique les gènes de reconnaissance et d'initiation de la symbiose sont réprimés (Vidal-Dupiol et al. 2009). Dans le même temps les gènes permettant le maintien du phagosome dans un stade immature (Rab4 et Rab5) sont également réprimés alors que ceux induisant la maturation et donc l'élimination du symbiote sont induits (Rab7 et Rab11) (Vidal-Dupiol et al. 2014). Ainsi il apparait à la lumière de ces résultats que les mécanismes d'initiation et de dissociation de la symbiose seraient *quasi* les mêmes mais avec des régulations géniques inversées.

Nota bene **sur les cumuls de stress**

Afin de bien comprendre les effets que peut avoir une modification environnementale sur la physiologie d'un organisme il est essentiel de simplifier les choses et de travailler tout autres paramètres constants. Cette approche de simplification est nécessaire mais présente l'inconvénient de ne pas permettre une évaluation des potentiels effets d'addition, de synergie voire d'antagonisme que le cumul de différents stress peut avoir sur l'organisme. Ainsi, réchauffement climatique et acidification des océans vont à l'avenir se cumuler. C'est dans l'objectif d'appréhender ce type de phénomène que j'ai pu étudier les effets conjoints de ces deux facteurs de stress sur la physiologie de l'huitre perlière et du bénitier (Le Moullac et al. 2016a, Brahmi et al. 2021). Le seul paramètre physiologique ayant présenté une interaction significative entre température haute et acidification fut le taux d'extension de la coquille du bénitier. Il ressort cependant qu'à des valeurs écologiquement réalistes le facteur température

était très largement dominant dans ses effets néfastes par rapport au facteur acidification des océans.

Chapitre 4 : Acclimatation et adaptation au réchauffement climatique chez les coraux

Contexte et problématique

La théorie synthétique de l'évolution a proposé que les organismes vivent et évoluent dans l'espace et le temps, sous des pressions environnementales constantes qui sélectionnent le génotype le mieux adapté (adaptation génétique). Bien qu'ancienne, cette question fondamentale est toujours ouverte et des avancées nouvelles tant technologiques que conceptuelles sont intervenues en conjonction avec les changements globaux et ont ouvert de nouvelles perspectives de recherche. En effet, les populations vivantes confrontées à ces dérèglements climatiques peuvent survivre par différents moyens tels qu'un changement de leur répartition suivant l'hypothèse de conservation de niche (Martínez-Meyer et al. 2004) ou encore au travers de phénomènes de sauvetage génétique également liés à la migration (Whiteley et al. 2015). Elles peuvent également s'acclimater et/ou s'adapter localement (Kawecki and Ebert 2004, Charmantier et al. 2008). Ces dernières années, un nouveau pan émerge dans le domaine de l'évolution, le rôle potentiel des mécanismes non-génétiques dans les processus adaptatifs notamment au travers du rôle de l'épigénétique dans la plasticité phénotypique et l'expression de phénotype cryptique (Jablonka et al. 2005, Bossdorf et al. 2008, Danchin 2013). La plasticité phénotypique peut être sous contrôle génétique et épigénétique, mais le poids de ces deux mécanismes n'est pas encore quantifié. La plasticité transgénérationnelle encodée épigénétiquement pourrait donc être une condition préalable et un moteur pour le processus d'adaptation génétique en permettant une correspondance rapide entre le phénotype et les nouvelles conditions environnementales (Pal and Miklos 1999, Ghalambor et al. 2007, Cosseau et al. 2010, Danchin et al. 2011). Un tel phénomène peut en effet permettre une réponse efficace et transitoire offrant le temps nécessaire à l'adaptation génétique de s'établir par assimilation génétique par exemple (Pigliucci et al. 2006, Draghi and Whitlock 2012).

Compte tenu du caractère sessile et longé vive des coraux, les mécanismes d'acclimatation et d'adaptation reposant sur la plasticité phénotypique apparaissent comme très pertinents pour produire une réponse adaptative rapide aux changements globaux. Des signes d'adaptation ou d'acclimatation en milieu naturel commencent d'ailleurs à être de plus en plus fréquemment reportés. Ainsi, si l'effet des premiers stress thermiques ont conduit à des mortalités massives, les stress suivants, même de plus forte intensité, ont démontré une augmentation de la thermotolérance des coraux (Adjeroud et al. 2009, Thompson and Woesik 2009, Penin et al. 2012, Coles et al. 2018, DeCarlo et al. 2019).

C’est dans ce contexte que j’ai développé une recherche sur les mécanismes d’adaptation rapide au réchauffement climatique chez les coraux avec un positionnement central de la plasticité phénotypique et de ce qui la contrôle. Cette recherche s’est appuyée sur un article d’opinion (Torda et al. 2017) (Annexe 8), un article sur les liens entre plasticité phénotypique et variation des températures (Brener-Raffalli et al. 2019) (Annexe 9) et un article sur l’impact des stress récurrents sur la plasticité phénotypique et ses déterminants (Vidal-Dupiol et al. submitted) (Annexe 10). Ces travaux peuvent être structurés en deux hypothèses : i) Un environnement thermique très variable sélectionne une forte plasticité (Brener-Raffalli et al. 2019), ii) Des stress récurrents affectant une même colonie vont induire un changement de plasticité adaptatif au travers de modifications épigénétiques (Vidal-Dupiol et al. submitted).

Méthodologies mises en œuvre

Matériel biologique et approches expérimentales

Afin de répondre à la première hypothèse la stratégie employée fut d’échantillonner deux populations de *Pocillopora acuta sensus lato* issues de zone géographique au régime thermique très contrasté. Ainsi nous avons échantillonné et rapatrié vivant à l’aquarium de Banyuls sur Mer des coraux du sultanat d’Oman et des coraux de Nouvelle-Calédonie. Les populations omanaises sont confrontées à des températures annuelles moyennes de 27,9°C, des maxima de 33, 2°C et des minima de 22,1°C ; la variance annuelle de la température y est de 9.5. Les populations néo-calédoniennes sont confrontées à des températures annuelles moyennes de 24.8°C, des maxima de 27,1°C et des minima de 22,6°C; la variance annuelle de la température y est de 2,7. Ces coraux une fois ramenés en France furent acclimatés aux conditions de maintien en aquarium puis soumis à un stress thermique écologiquement réaliste (température contrôle correspondant à la moyenne des 3 mois les plus chauds puis augmentation graduelle d’un degré par semaine jusqu’à l’expression des symptômes de stress e.g. la fermeture des polypes). Cette approche permet la comparaison des réponses de ces deux populations très différentes à des états physiologiques identiques (Fig. 5). Faire ce comparatif à une même température n’aurait eu aucun sens.

Afin de répondre à la deuxième hypothèse, une colonie de *P. acuta* a été bouturée de façon à produire deux « populations » de coraux identiques au départ. L’une de ces population, appelée naïve, a été maintenue à une température contrôle oscillant entre 26 et 28 degrés durant les deux années de l’expérience. La deuxième, dite entrainée, a été confrontée à un stress thermique inducteur de blanchissement au début de l’année une et au début de

l'année deux. Au début de l'année trois les populations naïves et entrainées ont été confrontées à un même stress thermique inducteur de blanchissement. Durant ce stress la thermotolérance de chacune des populations a été quantifiée. Comme précédemment les stress thermiques ont consisté en une montée graduelle (1°C/semaine) de la moyenne des 3 mois les plus chauds jusqu'à la fermeture des polypes. Une fois ce stade atteint la température était maintenue jusqu'au blanchissement puis redescendue à une température contrôle pour permettre aux coraux de récupérer durant une année, temps minimum séparant deux évènement de blanchissement (Fig. 7).

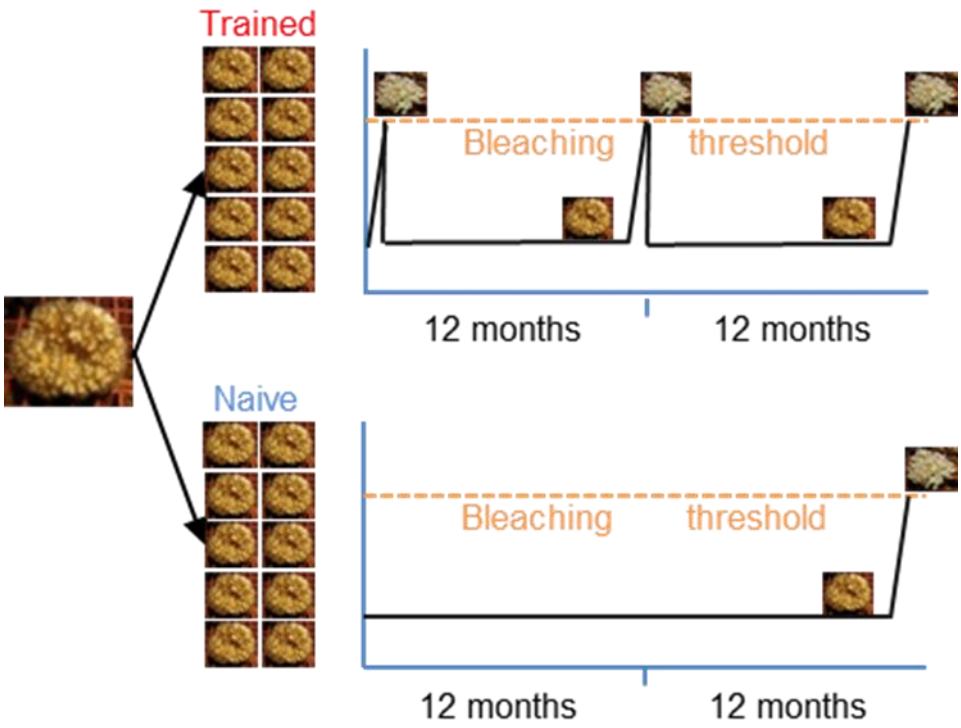

Figure 7: Protocole de stress récurrent écologiquement réaliste.
Coraux naïfs et entrainés proviennent de la même colonie mère.

Omic integrative

Afin d'appréhender un maximum de la plasticité exprimée, des approches d'Omic intégratives ont été développées.

Ainsi, des expérimentations de RNA-seq ont été mises en œuvre pour caractériser la plasticité transcriptomique exprimée entre condition contrôle et condition stressée au sein des populations étudiées (Oman, Nouvelle-Calédonie, coraux naïfs et entrainés).

Pour comprendre les modifications de plasticité induites par les stress récurrents, des expérimentations de Whole Génome Bisulfite Sequencing (étude de la méthylation de l'ADN) et de Whole Genome Sequencing ont été menées pour caractériser respectivement, les variations de méthylation de l'ADN et les variations de séquence d'ADN.

Une caractérisation des populations de zooxanthelles a également été menée par metabarcoding ITS2. Les résultats étant peu concluant ils ne seront pas présentés ci-dessous.

Principaux résultats

Phénotypage et thermotolérance

Les expérimentations de stress thermiques développées afin de répondre à l'hypothèse une ont montré des patterns de réponse au stress très similaires entre les populations d'Oman et de Nouvelle-Calédonie. Ainsi toutes deux ont montré des symptômes de stress à partir du 30^{eme} jour d'expérience ce qui correspond à une température de 34°C et de 30°c pour Oman et Nouvelle-Calédonie respectivement.

Dans les expériences menées pour répondre à l'hypothèse deux, les coraux entrainés ont comme attendu exprimé une thermotolérance significativement plus forte que les coraux naïfs. Ainsi, pour une température maximale de 32°C, les coraux entrainés ont blanchi, présentés des mortalités partielles ou des mortalités totales avec respectivement sept, sept et 11 jours de décalage par rapport aux coraux naïfs.

Plasticité transcriptomique

Dans une première approche visant à caractériser la plasticité transcriptomique entre population Omanaise et Néo-Calédonienne ou coraux naïfs et entrainés une analyse DAPC (Discriminant Analysis of Principal Component) a été menée. Elle a démontré une plasticité plus forte chez les coraux d'Oman. L'analyse des normes de réaction a permis de montrer que les coraux Omanais cumulent deux types de plasticité transcriptomique précédemment identifiés chez des coraux plus résistants aux variations environnementales : i) le frontloading ; un niveau d'expression basal de certains gènes plus élevé que chez les coraux thermosensibles mais une réponse au stress moins intense (Barshis et al. 2013) et ii) la résilience transcriptomique ; une très grande capacité de réponse au stress permise par de forte amplitude d'expression (Kenkel and Matz 2016).

Dans le cadre de l'expérience de stress récurrent la même analyse de DAPC montre que ce sont ici les coraux naïfs qui ont présentés la plasticité transcriptomique la plus

importante. Les normes de réaction ont montré que les coraux entrainés ont très clairement évolué vers le frontlaoding.

Lien entre plasticité et fonction biologique

Les résultats des analyses RNA-seq entre coraux Omanais et Néo-Calédoniens ont logiquement montré un plus grand nombre de gènes différentiellement exprimés en réponse au stress thermique chez les premiers (5287 gènes) que chez les deuxièmes (1460 gènes). Les fonctions biologiques impliquées dans ces réponses montrent que ces deux populations sur-expriment des gènes de la réponse au stress thermique tel que des ROS scavengers, de Heat Shock Protein, de gènes immunitaires, des voies de l'apoptose et de la mort cellulaire programmée. Cette expression est cependant plus efficace chez les coraux omanais car ces gènes sont exprimés à des niveaux plus élevés en condition contrôle et atteignent des taux de sur expression également plus important.

Les résultats de l'analyse RNAseq menée sur les coraux naïfs et entrainés ont montré un pattern différent avec ici, un plus grand nombre de gènes différentiellement exprimés chez les coraux les plus sensibles à la température (2508 gènes chez les naïfs et 949 chez les entrainés). Paradoxalement la réponse typique des coraux au stress thermique n'a été retrouvée que chez les coraux naïfs. Une analyse plus fine, focalisée sur les gènes frontloadés et donc non différentiellement exprimés entre condition contrôle et stressée a permis de montrer que c'est dans cette catégorie qu'étaient retrouvés les gènes de la réponse aux stress thermiques des coraux.

Variation génétique et épigénétique

Dans le but de comprendre par quels mécanismes les coraux entrainés avaient pu passer d'une réponse plastique à une réponse de type frontloading des analyses de la variation épigénétique (méthylation de l'ADN) et de la variation génétique (SNP et variation du nombre de copies) ont été entreprises.

Du point de vue génétique et contrairement à ce qui été attendu, de nombreuses différences ont été identifiées et reflètent probablement un cas de chimerisme non identifié au départ de l'expérience. Ainsi les coraux entrainés présentaient plus de SNP et plus de variation dans le nombre de copie d'une même séquence au sein du génome. Afin de lier ces variations à la thermotolérance les gènes portant dans leur séquence des différences génétiques significatives ont été étudiés. Parmi eux seuls ceux présentant une variation dans le nombre de copie ont montré un lien avec la thermotolérance. De façon très intéressante, sur

les 22 gènes présentant un lien connu avec la thermotolérance, 20 appartiennent à la famille des tnf/tnf receptor associated factors. Ces gènes sont connus pour être clefs dans la thermotolérance des coraux sans que leur fonction dans ce processus soit réellement comprise (Palumbi et al. 2014).

Au niveau épigénétique coraux naïfs et entrainés présentaient 10 648 régions de 500 pb différentiellement méthylées. Parmi elles, 8708 étaient hypométhylées et 1940 hypermethylées chez les coraux entrainés par rapport aux naïfs. Une analyse d'enrichissement au sein des gènes contenant des régions différentiellement méthylées a montré que de nombreux gènes essentiels à la réponse au stress présentaient des régions hyper ou hypométhylées sans qu'aucune corrélation avec un différentiel d'expression ne puisse être trouvée. Si ce dernier résultat n'est pas surprenant pour un invertébré il est aujourd'hui de plus en plus admis que les liens entre transcription et méthylation présentent une courbe en cloche, où les gènes exprimés en réponse à des modifications environnementales sont faiblement méthylés alors que les gènes exprimés constitutivement sont fortement méthylés, les gènes les plus méthylés étant exprimés à des taux constitutifs de plus en plus faibles. Il ressort ainsi qu'un maximum d'expression constitutive correspondrait à une fourchette de méthylation donnée. Dans le cas de notre étude ce pattern fut confirmé et le maximum de transcription correspondait à un taux de méthylation avoisinant les 20%. Nous avons donc testé si les gènes frontloadés présentaient des gains ou des pertes de méthylation permettant de maximiser leur expression constitutive en approchant leur taux de méthylation des 20%. Le résultat montre en effet que ces modifications ont permis d'augmenter le nombre des gènes de la réponse au stress positionné dans la fenêtre de méthylation correspondant au maximum d'expression.

Implication de ces résultats pour la communauté

Les études sur la plasticité phénotypique, notamment transcriptomique, ont permis ces dernières années des avancées majeures de la compréhension que nous avons de la thermotolérance des coraux. Ces approches ont été essentiellement développées à partir de transplantation réciproque et de jardin commun. Les populations thermotolérantes étant parfois localisées dans des micro-habitats très particuliers et donc non génétiquement différentes de celles thermosensibles et situées juste à côté. Dans d'autres situations le gradient de distance entre populations est plus important et est sous tendu par des différences génétiques entre thermosensibles et thermotolérants. Ces études ont mis en lumière quatre types de plasticité transcriptomique par comparaison à une réponse plastique normale et

représentant une population thermosensible (Fig 8). Le dampening est caractérisé par une norme de réaction atténuée en réponse à une courte période d'acclimatation à de forte températures préalablement au stress thermique (Bay and Palumbi 2015). Le frontloading est caractérisé par une norme de réaction de faible amplitude mais avec des niveaux d'expression constitutifs plus élevés que chez la population sensible (Barshis et al. 2013). Ce frontloading a été identifié chez des coraux acclimatés à des stress récurrents. La résilience transcriptomique caractérisée par une réponse plastique de plus grande amplitude est rencontrée dans le cas de population adaptée à un environnement très variable (Kenkel and Matz 2016). Ainsi il ressort que le dampening et le frontloading seraient plutôt de type acclimatatif et non fixé génétiquement alors que la transcriptomique résilience serait de type adaptatif au sens génétiquement fixé. Les résultats obtenus dans les études auxquelles j'ai participé sur la plasticité transcriptomique présente un cas typique de frontloading en réponse à un stress récurrent (Vidal-Dupiol et al. submitted) et un mélange entre frontloading et transcriptomique résilience (Brener-Raffalli et al. 2019). Cette dernière étude est particulièrement parlante puisqu'elle s'intéresse à la population d'Oman, une des populations de coraux les plus thermotolérantes au monde, adaptée de longue date à un environnement très variable et hyperthermique (Fig. 8). La présence de frontlaoding chez ces « super coraux » (adaptés) mis en parallèle du fait que ce frontloading est encodé épigénétique chez des coraux entrainés (acclimatés) suggère que ce type de plasticité transcriptomique puisse être transmise aux générations suivantes (Torda et al. 2017). Ainsi, on peut proposer que cette population d'Oman a dans un premier temps intégré génétiquement le frontloading par assimilation génétique (Danchin et al. 2019). Cette première étape d'évolution vers une thermotolérance accrue pourrait être suivie d'une deuxième phase permettant un retour vers plus de plasticité allant jusqu'à de la transcriptomique résilience telle qu'observée chez ces coraux (Fig 8).

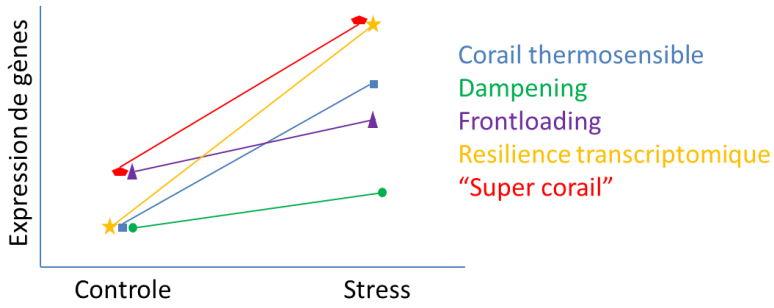

Figure 8: Différents types de plasticité phénotypique caractérisant des coraux thermotolérants.

Frontloading et dampening sont issus de processus d'acclimatation. La résilience transcriptomique et le profil super corail seraient issus de processus d'adaptation.

Outre cet aspect plasticité transcriptomique, les résultats de ce chapitre sont intéressants pour la communauté scientifique en termes d'analyse et d'interprétation de la méthylation de l'ADN chez les invertébrés. En effet les résultats obtenus et les méthodes utilisées pour interpréter les changements de méthylation de l'ADN permettent de renforcer et d'approfondir la compréhension émergente du rôle de la méthylation de l'ADN dans l'écologie et l'évolution des invertébrés. Il a été proposé que les changements de méthylation de l'ADN reflètent un équilibre changeant entre l'expression de gènes sensibles à l'environnement et de gènes de ménage (Dixon et al. 2018), soulignant son rôle pour l'acclimatation intragénérationnelle. La récente démonstration que la méthylation de l'ADN est transmise des adultes à leurs spermatozoïdes et à leurs larves au niveau des CpG confirme en outre le rôle de la méthylation des CpG dans l'acclimatation intergénérationnelle des invertébrés (Liew et al. 2020). Bien que les conséquences des changements de méthylation de l'ADN intragénique soient encore mal comprises, les résultats produits dans Vidal-Dupiol et al (submitted) apportent de nouveaux éléments : i) la notion de maximum d'expression correspondant à une fenêtre de méthylation donnée et ii) le fait que des modifications de méthylation opposées (hyper *vs.* hypométhylation) puissent donc induire le phénotype transcriptionnel (Fig. 9). Ainsi, les preuves d'un lien entre le frontloading et les modifications de méthylation renforcent ainsi l'hypothèse récemment proposée que « la transcription et le taux de méthylation intra génique peuvent s'influencer mutuellement au travers d'une boucle de rétroaction où une transcription croissante induirait la méthylation du gène tandis qu'une méthylation trop importante en réduirait sa transcription » (Dixon et al. 2018). Ce modèle prédit que les gènes qui nécessitent une expression élevée et constitutive devraient afficher un taux de méthylation proche de la valeur associée au maximum de transcription. Cette prédiction est en effet confirmée dans notre expérience ou la principale force environnementale induisant l'acclimatation est la récurrence des stress thermiques et que cette récurrence a conduit à l'expression en continu des gènes de réponse au stress qui sont caractérisés par un taux de méthylation plus proche du maximum d'expression constitutive qu'avant cette récurrence de stress.

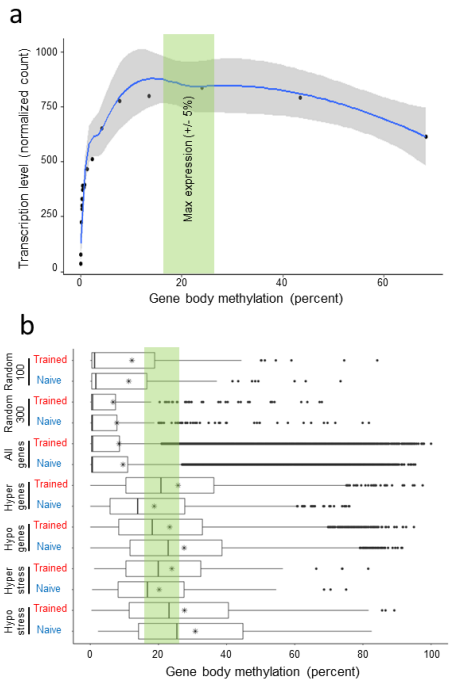

Figure 9 : Lien entre méthylation et différentiel de méthylation des gènes et transcription

a) niveau de transcription (axe Y) en fonction du taux de méthylation du gène (axe des X). Le carré vert met en évidence le taux de méthylation (+/-5%) associé au maximum d'abondance de transcrits (calculé à partir des 1000 transcrits les plus abondants). **b)** boxplot du taux de méthylation des gènes chez les coraux entraînés et naïfs pour : les gènes significativement hyper ou hypométhylés qui appartiennent au GO terme lié au stress ; l'ensemble des gènes montrant une hyper ou une hypométhylation significative ; tous les gènes du génome et une sélection aléatoire de 100 ou 300 gènes comme référence. La case verte met en évidence le taux de méthylation (+/-5%) associé au maximum d'abondance de transcrits (calculé à partir des 1000 transcrits les plus abondants).

Chapitre 5 : Un peu de couleur

Je ne développerai pas ce chapitre de façon importante mais il me semblait indispensable de le présenter étant donné qu'il est constitué des travaux de thèse de Pierre-louis Stenger, le premier étudiant en thèse que j'ai officiellement encadré et ayant aujourd'hui soutenu. Voici un résumé des travaux entrepris et ayant conduit à la publication de trois articles (Stenger et al. 2019, Stenger et al. 2021a, Stenger et al. 2021b) (Annexe 11 et 12 et 13).

Les couleurs de la coquille des mollusques ont attiré les naturalistes et les collectionneurs depuis des centaines d'années et de nombreux bijoux sont issus de ces biominéraux. L'un des plus emblématique de ces biominéraux est la perle, notamment de Polynésie car possédant un panel de couleur quasi infini. Bien que cette industrie représente la deuxième ressource économique du pays peu de chose sont connus sur les facteurs contrôlant les couleurs de la perle. Ainsi, les voies moléculaires régulant la production de pigments et les pigments eux-mêmes restent mal décrits. Dans cette première étude, notre objectif était d'identifier les principaux pigments et les voies moléculaires produisant ces pigments chez l'huître perlière *Pinctada margaritifera* (Stenger et al. 2021a). Afin de répondre à cet objectif nous nous sommes focalisés sur les trois couleurs principales de la coquille interne ; le rouge, le jaune et le vert. Afin de maximiser l'homogénéité phénotypique des individus étudiés nous avons développé une approche où la diversité génétique était contrôlée, combinée à une normalisation physiologique des individus par un conditionnement en jardin commun. L'analyse comparative des transcriptomes (RNA-seq) de *P. margaritifera* avec différentes couleurs de coquille a révélé le rôle central de la voie de l'hème, qui est impliquée dans la production de pigments rouge (uroporphyrine et dérivés ; Fig. 10), jaune (bilirubine ; Fig. 10) et verts (biliverdine et formes de cobalamine ; Fig. 10). De plus, il a été démontré que les voies métaboliques du cycle de Raper-Mason et des purines produisent les pigments jaunes (phéomélanine et xanthine ; Fig. 10) et noirs eumélanine (Fig. 10). La présence de tous ces pigments dans la coquille a été validée par spectroscopie Raman. Cette méthode a également mis en évidence que toutes les voies et pigments identifiés sont en fait exprimés de manière ubiquitaire et que la couleur dominante de la coquille n'est due qu'à l'expression préférentielle d'une voie par rapport aux autres.

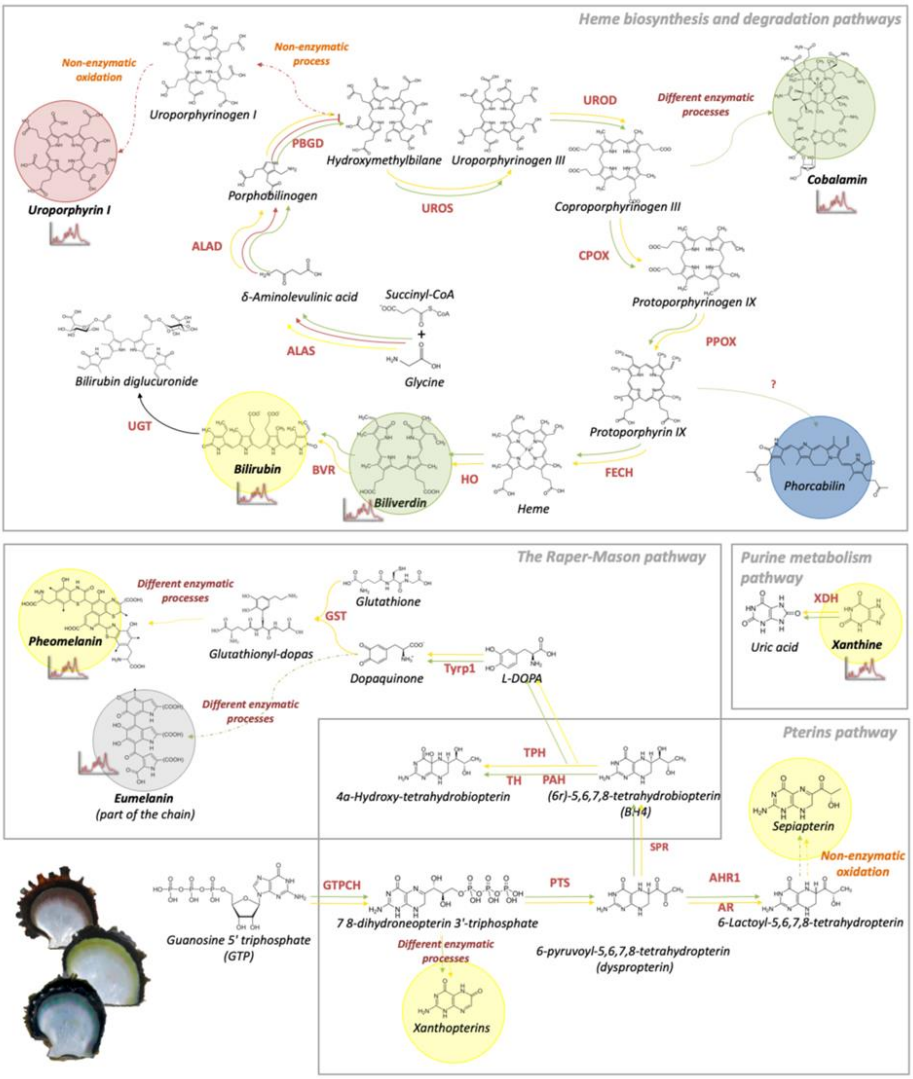

Figure 10 : Les voies de biosynthèse de la couleur chez l'huître :
Les voies de biosynthèse et de dégradation de l'hème; la voie des ptérines ; la voie Raper-Mason ; la voie du métabolisme des purines. Les pigments potentiels sont représentés par des cercles colorés ; ceux ayant été validés par spectroscopie Raman ont un symbole de diagramme Raman. Les flèches rouges, jaunes et vertes font respectivement référence à la synthèse des pigments rouges, jaunes et verts. ALAS : acide aminolévuliniquesynthase; ALAD : acide delta-aminolévulinique déshydratase ; PBGD : porphibilinogène désaminase ; UROS : uroporphyrinogèneIII synthase; UROD : uroporphyrinogène décarboxylase ; CPOX : coproporphyrinogène oxydase ; PPOX : protoporphyrinogèneoxydase; FECH : ferrochélatase ; HO : hème oxygénase ; BVR : biliverdine réductase ; UGT : UDP-glucuronyltransférase ; GTPH :GTP cyclohydrolyase I; PTS : 6-pyruvoyltétrahydroptérine/6-carboxytétrahydroptérine synthase ; AR : aldose réductase ; AHR1 :aldéhyde réductase 1; SPR : sépiaptérine réductase ; HAP : phénylalanine-4-hydroxylase ; TPH : tryptophane 5-monooxygénase ;TH : tyrosine 3-monooxygénase ; Tyrp1 : protéine liée à la tyrosinase 1 ; GST : glutathion-S-transférase ; XDH : xanthinedéshydrogénase.

Dans ces deuxième et troisième articles nous avons étudié si les facteurs environnementaux peuvent modifier l'intensité de la couleur des huîtres (Stenger et al. 2019) et si des mécanismes épigénétiques pouvaient expliquer ce changement (Stenger et al. 2021b).

Dans un premier temps nous avions montré que l'intensité de la couleur était un trait plastique répondant à des variations de la profondeur notamment au travers d'un assombrissement généralisé de la nacre à une plus grande profondeur. Afin de tester l'implication possible de facteurs épigénétiques dans le contrôle de la plasticité de ce trait, une expérience de variation de profondeur associée à une étude de méthylation de l'ADN par Whole Genome Bisulfite Sequencing a été réalisée. Nos résultats ont révélé à génotype constant, la présence de six gènes présentant des CpG méthylés de manière différentielle en réponse au changement environnemental. Parmi ces gènes quatre sont liés à des processus de régulations de la pigmentation (GART, ABCC1, MAPKAP1, GRL101), et plus particulièrement à un assombrissement. Fait intéressant, les gènes perlucines et MGAT1, tous deux impliqués dans le processus de biominéralisation (dépôt de cristaux d'aragonite et de calcite), ont également montré une méthylation différentielle, suggérant qu'une éventuelle différence dans l'organisation physique et/ou spatiale des cristaux pourrait aussi être à l'origine de cet assombrissement (irisation ou modification de la transparence du biominéral).

Que ce soit les voies moléculaires et les pigments responsables de la couleur des huîtres ou encore le rôle de l'environnement et de l'épigénome dans leur variation, ces données sont d'intérêts pour l'industrie perlicole. En effet, des perles entièrement noires, ou à l'inverse de perles les plus pâles et pastel possible ont une valeur marchande plus élevée selon le marché économique considéré. Par ailleurs, une meilleure connaissance des mécanismes régulant la couleur des perles est aussi un premier pas vers l'amélioration assistée par marqueur.

Chapitre 6 : Projet de recherche

Comme signalé en introduction, l'Anthropocène est la période géologique actuelle au cours de laquelle les activités humaines sont les principaux moteurs des changements géologiques et écosystémiques à l'échelle du globe. Les profonds changements environnementaux qui la caractérise s'accélèrent depuis la révolution industrielle et s'imposent à une vitesse sans précédent à toutes les espèces contemporaines. La recherche que je souhaite développer dans les années à venir se concentrera sur ces changements rapides ayant lieux à l'échelle de la durée de vie de l'individu ou à celle d'un petit nombre de générations. Mes objectifs généraux seront: i) de comprendre les réponses adaptatives rapides (*sensu lato*) des populations naturelles à ces changements environnementaux; et ii) d'utiliser ses connaissances pour développer de nouveaux outils de gestion des problématiques sociétales adossées à ces phénomènes.

Ces recherches seront développées aussi bien en populations naturelles qu'en milieu contrôlé. C'est au travers de collaborations au sein du laboratoire IHPE mais aussi nationales et internationales que j'ambitionne d'étudier les modifications pouvant être déclenchées par ces changements environnementaux et permettant des adaptations rapides : variations génomiques (mutations, variations du nombre de copies, introgression, etc.), variations épigénomiques (modifications des histones, méthylation, etc.) et variations fonctionnelles du microbiote au sein des holobiontes.

Ces questionnements seront abordés au sein de deux modèles biologiques complémentaires, les coraux Scléractiniaires face au réchauffement climatique et l'huître de bouche *Crassostrea gigas* face à l'émergence de pathogènes.

A. Signature d'Adaptation et d'acclimatation rapide au réchauffement climatique chez les coraux : Vers une gestion améliorée de l'Ecosystème (Projet SAVE financement AFD 2021-2025 200k€)

Contexte et problématique

Pour s'adapter rapidement au réchauffement climatique en cours les coraux Scléractiniaires peuvent bénéficier d'une large diversité de mécanisme. Bien qu'apparemment limités, des phénomènes de sauvetage génétique peuvent venir enrichir en allèle de thermotolérance des populations thermosensibles (Matz et al. 2018). Les coraux peuvent également bénéficier d'une modification de leur contenu en symbiote au profit de zooxanthelle plus thermotolérante (Buddemeier et al. 2004, Chakravarti et al. 2017). La variabilité génétique intra-coloniale, qu'elle soit d'origine chimérique (cohabitation de plusieurs génotypes au sein d'une colonie) ou mosaïque (genèse de diversité génétique par mutation somatique au sein de la colonie) peut également entrer en jeux (Van Oppen et al. 2012, Rinkevich 2019). Pour finir des modifications adaptatives de l'épigénome pourraient conduire à l'expression de phénotype plus thermotolérant (Torda et al. 2017). Identifier et comprendre ces processus adaptatifs permettraient le développement de biomarqueurs d'adaptation permettant de mieux assister la gestion des écosystèmes et la biologie de la conservation (Rey et al. 2019).

En plus de constituer un trésor de biodiversité les récifs coralliens fournissent des services écosystémiques essentiels à de nombreux pays. Ainsi, des actions de gestion des écosystèmes ont été entrepris depuis de nombreuses années et visent directement (restauration des récifs par évolution assistée ou non (van Oppen et al. 2015)) ou indirectement (aires marines protégées (Hoegh-Guldberg et al. 2018)) à améliorer les capacités de tolérance thermique et de résilience des coraux. Cependant, quelle que soit la stratégie à laquelle on s'adresse, plusieurs questions restent sans réponse : i) quelle est la répartition spatiale des coraux thermotolérants ? ; ii) dans quelle mesure sont-ils thermotolérants ? ; iii) quels sont les mécanismes qui sous-tendent cette thermotolérance (Mumby et al. 2011) ?. Même si ces mécanismes sont examinés attentivement depuis plusieurs années, les déterminants moléculaires de l'hôte codant pour la tolérance thermique sont encore largement méconnus. Il est donc impossible de distinguer les populations thermotolérantes des autres avec un niveau de confiance élevée. Pour contourner ce manque, des approches corrélatives basées sur le suivi des températures passées et l'historique des blanchissements sont classiquement utilisées (Fig. 11A) mais peuvent inférer des hypothèses erronées conduisant à la protection de

populations mal adaptées (Fig. 11B). À titre d'exemple, avant le blanchissement mondial de 2016, les coraux de Nouvelle-Calédonie étaient considérés par beaucoup comme thermotolérants puisqu' aucun blanchissement n'y avait été signalé. En réalité, les facteurs d'atténuations locaux qui sont habituellement présents pendant la saison chaude étaient absents en 2016 ce qui a conduit à un blanchissement de plus de 80% des coraux (Adjeroud et al. 2009). Le développement de biomarqueurs fonctionnels d'acclimatation et ou d'adaptation apparait donc comme crucial pour mieux identifier les entités fonctionnelles qui doivent être prises en compte pour améliorer les stratégies de gestion et de conservation actuelles (Fig. 11C et D).

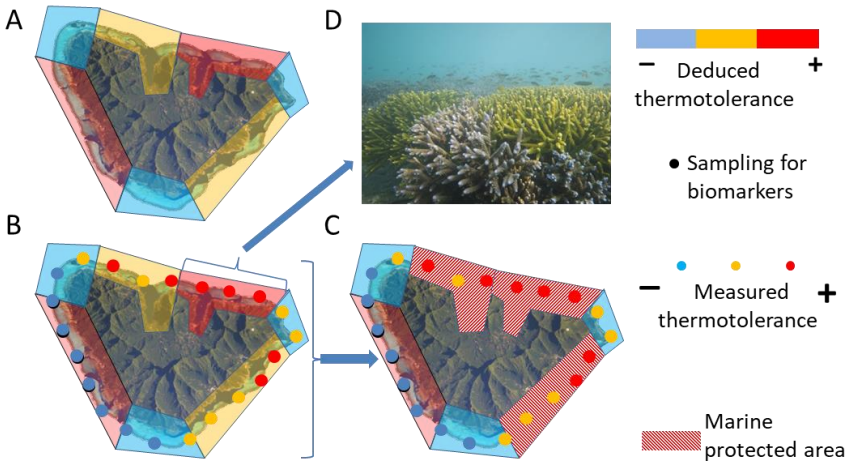

Figure 11 : Biomarqueurs d'adaptation/acclimatation des coraux et gestion de l'écosystème. Les méthodes actuelles de cartographie de la thermotolérance des coraux et donc en partie de la gestion des récifs sont essentiellement basées sur des approches corrélatives (B). Ces approches peuvent conduire à l'identification erronée de zones hébergeant des populations mal adaptées ce qui pourrait être évité grâce à l'emploi de biomarqueurs (B). Cette nouvelle cartographie permettrait une optimisation des pratiques de gestions que ce soit pour le design d'aires marines protégées (C) ou des approches de restauration (D).

Objectifs

L'objectif principal de ce projet sera donc d'identifier des variations génétiques ou de méthylation de l'ADN spécifiquement associés au corail thermotolérant pour aider à la gestion et à la conservation des écosystèmes.

Afin d'atteindre cet objectif je propose d'étudier les populations naturelles de coraux dans différentes zones géographiques et à différentes échelles de temps (de l'échelle saisonnière au siècle). Deux espèces appartenant à des groupes fonctionnels distincts et présentant des intérêts complémentaires pour la gestion des écosystèmes seront utilisées ; *Pocillopora acuta*, espèce compétitive mais sensible au stress, et *Porites lobata* espèce à croissance lente mais tolérante au stress (Darling et al. 2019). La première aura une réponse basée sur la plasticité et permettra d'explorer la variation transcriptomique en lien avec la variation génétique et épigénétique à une échelle temporelle courte. La seconde aura une réponse basée sur la robustesse et permettra d'étudier les modifications épigénétiques et génétiques mises en œuvre à plus long terme (étude paléoépigénomique, variation décennale : Fig. 11). Ces colonies proviendront de trois zones génétiquement connectées (Adjeroud et al. 2014) mais caractérisées par des histoires de stress thermique contrastées ; Polynésie française (stress récurrent (Adjeroud et al. 2009)), Fiji (stress récurrents) et Nouvelle-Calédonie (stress rare (Adjeroud et al. 2019)). Dans les environnements où les stress sont récurrents et donc prévisibles, nous nous attendons à ce que des changements soient localisés spécifiquement dans ou proches des gènes de réponse au stress (gènes induits par l'environnement, stress prévisible). Dans l'environnement non stressant, nous nous attendons à des variations développementales stochastiques liées à une stratégie de betedging permettant l'exploration phénotypique en réponse à un stress rare (imprévisible).

Méthodologies

Échantillonnage et caractérisation environnementale

P. acuta et *P. lobata* sont des espèces ubiquistes trouvées dans les récifs frangeants et les lagons de l'Indo-Pacifique. Nous nous concentrerons sur 3 sites et affichant différents niveaux de pression anthropique en Polynésie Française aux Fiji et en Nouvelle-Calédonie. *P. acuta* et *P. lobata* seront échantillonnés sur le même site. Pour l'étude d'(épi)génomique des populations, 60 colonies génétiquement distinctes de *P. acuta* seront échantillonnées par site pendant deux années successives ; à la fin de la saison estivale et hivernale (n individu=540*4). Ce plan d'échantillonnage permettra de démêler la variabilité saisonnière de la diversité adaptative. Pour l'étude paléoépigénétique, trois carottes de *P. lobata* seront échantillonnées sur chaque site (n individu=27). Ces prélèvements permettront de cibler les changements (épi)génétiques intervenant dans le temps (échelle de l'année sur 100 ans) et chez un même individu (n années=20 incluant le tissu vivant correspondant à l'année de prélèvement). Ces carottes seront également utilisées pour caractériser l'histoire thermique

passée de chaque site par des approches de paléo reconstruction basées sur les signatures de δ18O, δ13C et le rapport Sr/Ca et Li/Mg (Wu et al. 2018)

Thermotolérance et phénotype moléculaire

Afin de pouvoir associer le phénotype à l'histoire thermique des individus et aux variations (épi)génétiques, le phénotype moléculaire (transcriptome) et la thermotolérance de chaque colonie seront évalués expérimentalement en condition contrôlée et selon les protocoles de stress validés antérieurement (Brener-Raffalli et al. 2018). Pour la caractérisation du phénotype moléculaire (analyse Quant-seq) les prélèvements seront effectués à la fermeture des polypes (Brener-Raffalli et al. 2018) tandis que pour la quantification de la thermotolérance, les échantillons seront exposés au stress jusqu'à la mort ce qui permettra un suivi de l'apparition successive du blanchissement, des mortalités partielles puis totales (Vidal-Dupiol et al. submitted).

Caractérisation (epi)génétique

Parmi les porteurs d'informations épigénétiques, nous nous concentrerons sur la méthylation de l'ADN qui est connue pour être impliquée dans la réponse des coraux aux changements environnementaux (Dixon et al. 2018, Liew et al. 2018). C'est aussi le seul porteur qui peut être étudié à l'aide d'ADN ancien. Pour *P. acuta* et *P. lobata*, une méthode récente basée sur la conversion enzymatique des cytosines sera utilisée. Pour *P. lobata,* une approche par CT SCAN 3D permettra dans un premier temps d'identifier les périodes d'intérêt qui seront ensuite échantillonnées sous guidage CT SCAN.

Bioinformatique et biostatistique

Le génome de référence de *P. acuta* a été récemment assemblé et annoté (Vidal-Dupiol et al. 2019). Pour *P. lobata,* le génome de référence est en cours d'assemblage et d'annotation. Les approches de bioinformatique tels que le contrôle qualité des reads et leur filtration, l'analyse différentielle de l'expression des gènes, l'enrichissement des fonctions biologiques, le méthylation calling et l'analyse des différentiels de méthylation, le SNP calling l'analyse du nombre de copies et l'appel de variant sont des outils disponibles et maitrisés au laboratoire. Une fois les matrices de thermotolérance, de transcriptomique, de diversité génétique et épigénétique construites, nous pourrons utiliser différentes méthodes de détection des signatures d'adaptation. Cela comprendra par exemple des approches telles que la détection de QTL d'expression (Kliebenstein 2009), la détection de QTL par des modèles

linéaires mixtes (Wang et al. 1999) ou encore celle de methQTL (Cortijo et al. 2014). Des approches populationnelles de type GWAS et EWAS seront également envisagées (Korte and Farlow 2013, Flanagan 2015).

Validation de la signature identifiée

Une fois les signatures d'acclimatation ou d'adaptation identifiées, elles seront validées à l'aide d'(épi)génotypage ciblé et de reconstruction d'historique thermique par télédétection. Cette validation se fera sur *P. acuta* sur une large collection d'échantillon déjà disponible et couvrant plusieurs régions de l'océan Indo/Pacifique (déjà disponible Polynésie française, Nouvelle-Calédonie, La Réunion, Madagascar, Mayotte, Djibouti, Maurice, Oman, archipel des Ryukyu).

B. Signature génétique et epigénétique d'adaptation rapide au virus OsHv1 chez l'huitre creuse *Crassostrea gigas* : vers une gestion des maladies en ostréiculture (Projets GT huitre financement Ifremer 2020-2025 200k€ et GestInnov financement FEAMP 2021-2023 600k€)

Contexte et problématique

Les interactions hôtes pathogènes sont caractérisées par une très forte dynamique coévolutive au travers de laquelle les deux protagonistes s'infligent mutuellement de fortes pressions sélectives. Ainsi, les populations de pathogènes vont au gré de la sélection naturelle acquérir de nouveaux mécanismes leur permettant de contrer les stratégies de défenses des hôtes qui subissent elles-mêmes de perpétuelles évolutions. Parmi les mécanismes en jeu, seuls ceux qui étaient codés par le génome ont très longtemps été considérés. Des études récentes ont montré que cette vision devait évoluer et que l'épigénotype devait également être pris en compte au même titre que le génotype comme un moteur de la variation phénotypique (Deng et al. 2017). Ainsi, il faut désormais considérer que le phénotype de l'hôte, codé par le génotype et l'épigénotype (sous influence environnementale), est le matériel sur lequel la sélection par le pathogène agit (et vice-versa) et qui sera transmis à la descendance (Cosseau et al. 2010). Des études récentes menées en milieu contrôlé ont pris en compte les facteurs génétiques et épigénétiques ; elles ont pu expliquer des phénomènes jusqu'alors incompris, notamment chez les invertébrés, comme l'induction d'une résistance au cours de la vie d'un génotype initialement sensible puis, la transmission de ce trait aux générations suivantes (priming/shaping transgénérationnel ; (Galindo-Villegas et al. 2012, Mukherjee et al. 2017)). L'implication de la combinaison de ces mécanismes génétiques/épigénétiques doit maintenant être appréhendée en populations naturelles afin d'en déterminer la validité dans un contexte écologique. Ceci représente un prérequis nécessaire pour déterminer l'importance du couple génétique/épigénétique dans l'adaptabilité des espèces et les émergences de maladies, un phénomène de plus en plus fréquent et problématique à l'aire anthropocène (Harvell et al. 1999).

Pour appréhender ces questionnements le phénomène du POMS (Pacific Oyster Mortality Syndrom) apparait comme particulièrement adapté et pourrait s'apparenter à une expérience d'évolution expérimentale grandeur nature et en temps réel. En effet, depuis 2008, des évènements de mortalité massive (jusqu'à 80% de mortalité) de juvéniles d'huître creuse, *Crassostrea gigas,* sont observés annuellement dans les bassins de production français. L'accroissement de ces mortalités a été corrélé à l'émergence en 2008 d'un variant du virus Ostreid Herpes-1 (OsHV-1) nommé µvar, lequel est systématiquement associé aux huîtres

lors des épisodes de mortalité massive (Segarra et al. 2010). De façon intéressante, il est possible d'accéder à des populations d'huîtres sauvages soumises à des pressions de sélection variable et donc présentant des phénotypes de résistance contrastée. Des populations issues de zones proches des grands bassins de production ostréicole surdensitaire présentent une résistance élevée alors que des populations recrutées loin de ces zones présentent des phénotypes très largement sensibles. Il a ainsi été possible dans le cadre de l'ANR DECIPHER de produire des familles 100% sensibles à 100% résistantes grâce à des croisements biparentaux d'individus sauvages échantillonnés dans de telles zones aussi bien en Atlantique qu'en Méditerranée (de Lorgeril et al. 2018).

Le POMS, est une maladie d'étiologie complexe. Récemment, notre laboratoire a développé une approche holistique pour en caractériser la pathogenèse. Cette étude a démontré que cette maladie est polymicrobienne. Le processus débute par une infection virale causée par l'herpès virus OsHV-1 µvar. Cette infection touchant en partie les cellules immunitaires de l'huître induit l'immuno-dépression de l'hôte ouvrant la voie à une infection bactérienne secondaire conduisant à la mort par septicémie (de Lorgeril et al. 2018). Dans cette même étude nous avons démontré qu'au niveau du phénotype moléculaire les familles d'huîtres résistantes développaient une réponse antivirale plus rapide et plus intense que les sensibles (de Lorgeril et al. 2018). Par ailleurs, le niveau de transcription basale de certains gènes semble pouvoir prédire la résistance ou la sensibilité d'un individu (Rosa et al. 2012, Azéma et al. 2015, de Lorgeril et al. 2018, de Lorgeril et al. 2020).

Si cette maladie est polymicrobienne, les déterminants de la résistance sont eux aussi multifactoriels (Fig. 12). Certains sont directement associés à l'huître et des études de génétique quantitative ont montré que la résistance est un trait héritable (Azéma et al. 2017), reposant en partie sur des bases génétiques (Fig. 3a), associée à l'identification de QTL (Sauvage et al. 2010, Gutierrez et al. 2018). D'autres études, en lien avec le microbiote, montrent que certains microorganismes (et notamment une espèce de cyanobactérie) sont spécifiquement associés aux huîtres résistantes ou sensibles et peuvent être utilisés comme prédicteurs des mortalités (Clerissi et al. 2020). De façon intéressante, une exposition au cours du développement embryonnaire à une flore microbienne diversifiée permet d'améliorer le taux de résistance de la cohorte exposée de 50% (Fig. 3b) grâce à un effet immuno-modulateur (Fallet 2019). Ce trait phénotypique étant transmis transgénérationnellement cela suggère l'implication de base épigénétique (Fig 3c) (Fallet 2019). Cette dernière hypothèse a récemment été renforcée en milieu naturel où des populations sauvages d'huîtres génétiquement non différenciées présentaient des contrastes de résistance importants bien que

séparées de seulement quelques centaines de mètres (Fig. 3d, (Khamo Gawra Gawra et al. 2020)).

Objectifs

L'ensemble de ces résultats met en évidence que la résistance des huîtres à OsHV-1 µvar repose sur plusieurs mécanismes moléculaires héréditaires et non-exclusifs impliquant des bases génétiques et non-génétiques (épigénétiques et microbiote). L'objectif de ce projet est de les identifier afin de permettre le développement d'une sélection assistée par marqueur où des conditionnements environnementaux inducteurs des modifications épigénétiques propres à la résistance (Yáñez et al. 2014, Gavery and Roberts 2017, Eirin-Lopez and Putnam 2019).

Méthodologie

Echantillonnage des populations d'huître et d'isolat d'OsHV-1µvar

L'objectif de cet échantillonnage est d'obtenir le matériel biologique (huîtres creuses, virus OsHV-1µvar) ayant été confronté à un historique environnemental contrasté et présentant des phénotypes contrastés.

Des populations d'huîtres sauvages seront échantillonnées dans 5 bassins de production (Bretagne, Marennes-Oléron, Bassin d'Arcachon, étang de Leucate, étang de Thau). Au sein de ces bassins, deux populations (une issue de zones à forte pression infectieuse, une exempte de maladie) seront échantillonnées. Les huîtres adultes prélevées seront utilisées pour effectuer le plan de croisement présenté ci-dessous.

Sur chacun des sites exposés aux pressions infectieuses, deux lots de 1000 huîtres *specific pathogen free* seront déployés. L'un en amont du déclenchement des mortalités afin de quantifier la pression infectieuse opérée et l'autre au moment des maladies pour « capter et cryoconserver » les populations virales vivant en sympathie avec les populations d'huîtres échantillonnées. Les populations virales seront isolées à partir d'huîtres moribondes collectées sur les différents sites.

Production des lots/populations

Pour chaque bassin de production, et chaque population prélevée, des croisements intra-populations seront réalisés (10 males croisé avec 10 femelles). Deux lignées résistantes ROsHV1 et ROsHV1Va seront également produites pour servir de témoin, ainsi qu'une lignée n'ayant jamais été confrontée à OsHV-1µvar (conservée en zone biosécurisée depuis 2007).

Tous les parents utilisés seront sacrifiés après la reproduction afin de permettre la caractérisation du patrimoine potentiellement transmis à leurs descendants (génétique, épigénétique, microbien).

Infection expérimentale en interaction allopatrique et sympatrique

Cette tâche a pour objectif de caractériser de façon standardisée la résistance des hôtes dans le cas d'interactions sympatriques (hôte et virus/bactérie issus de la même localisation géographique) et allopatriques (hôte et virus/bactérie issus de localisations géographiques différentes). Cette expérimentation produira également les échantillons qui seront utilisés pour la caractérisation des phénotypes moléculaires ((méta)transcriptome) de résistance et de leurs déterminants (génétique / épigénétique / microbiotique). Le design expérimental est basé sur un plan d'interaction complet permettant d'exposer tous les lots produits à tous les isolats viraux échantillonnés. Deux types d'échantillonnage seront menés : i) des échantillonnages au cours de l'infection de façon à avoir accès à la réponse des hôtes et aux processus infectieux ; ii) un échantillonnage en point final, juste avant la mort pour les individus sensibles et en fin d'expérience pour les résistants afin de pouvoir associer phénotypes de résistance et déterminants moléculaires (génétique/épigénétique/microbiotique).

Phénotypages moléculaires

La caractérisation du phénotype moléculaire en condition « naïve » et au cours de la réponse immunitaire des hôtes (temps précoces) sera menée par des approches RNAseq (SE 75 pb 25M reads/échantillons) sur 320 échantillons (160 individus naïfs et 160 individus 6h après exposition, 6 réplicas par lot). Elle permettra de quantifier l'expression des gènes de l'huître.

(Epi)génotypage

La caractérisation du génotype et de l'épigénotype des huîtres d'intérêt sera faite par une approche de séquençage de l'ADN sur lesquelles les cytosines non méthylées auront été converties enzymatiquement.

Bioinformatique et biostatistique

Différentes versions du génome de l'huitre creuse sont disponibles et présentent des qualité d'assemblage avec un ancrage chromosomique (Peñaloza et al. 2021). Les approches de bioinformatique telles que le contrôle qualité des reads et leur filtration, l'analyse

différentielle de l'expression des gènes, l'enrichissement des fonctions biologiques, le méthylation calling et l'analyse des différentiels de méthylation, le SNP calling l'analyse du nombre de copies et l'appel de variant sont des outils disponibles au laboratoire. Une fois les matrices de thermotolérance, de transcriptomique, de diversité génétique et épigénétique construites nous pourrons utiliser différentes méthodes de détection des signatures d'adaptation. Cela comprendra par exemple des approches telles que la détection de QTL d'expression (Kliebenstein 2009), la détection de QTL par des modèles linéaires mixtes (Wang et al. 1999) ou encore celle de methQTL (Cortijo et al. 2014). Nous pourrons prendre en compte la structure du lot en utilisant des modèles de type nested GLM. Des approches populationnelles de type GWAS et EWAS seront également envisagées (Korte and Farlow 2013, Flanagan 2015).

Chapitre 7 : Références bibliographiques

Adjeroud, M., A. Guérécheau, J. Vidal-Dupiol, J.-F. Flot, S. Arnaud-Haond, and F. Bonhomme. 2014. Genetic diversity, clonality and connectivity in the scleractinian coral *Pocillopora damicornis*: a multi-scale analysis in an insular, fragmented reef system. Marine Biology **161**:531-541.

Adjeroud, M., F. Michonneau, P. Edmunds, Y. Chancerelle, T. de Loma, L. Penin, L. Thibaut, J. Vidal-Dupiol, B. Salvat, and R. Galzin. 2009. Recurrent disturbances, recovery trajectories, and resilience of coral assemblages on a South Central Pacific reef. Coral reefs **28**:775-780.

Adjeroud, M., E. Poisson, C. Peignon, L. Penin, and M. Kayal. 2019. Spatial Patterns and Short-term Changes of Coral Assemblages Along a Cross-shelf Gradient in the Southwestern Lagoon of New Caledonia. Diversity **11**:21.

Agostini, S., F. Houlbrèque, T. Biscéré, B. P. Harvey, J. M. Heitzman, R. Takimoto, W. Yamazaki, M. Milazzo, and R. Rodolfo-Metalpa. 2021. Greater Mitochondrial Energy Production Provides Resistance to Ocean Acidification in "Winning" Hermatypic Corals. Frontiers in Marine Science **7**.

Allemand, D., E. Tambutté, D. Zoccola, and S. Tambutté. 2011. Coral calcification, cells to reefs. Pages 119-150 *in* Z. Dubinsky and N. Stambler, editors. Coral reefs: an ecosystem in transition. Springer, New York.

Andréfouët, S., C. Dutheil, C. E. Menkes, M. Bador, and M. Lengaigne. 2015. Mass mortality events in atoll lagoons: environmental control and increased future vulnerability. Global Change Biology **21**:195-205.

Andréfouët, S., S. Van Wynsberge, N. Gaertner-Mazouni, C. Menkes, A. Gilbert, and G. Remoissenet. 2013. Climate variability and massive mortalities challenge giant clam conservation and management efforts in French Polynesia atolls. Biological conservation **160**:190-199.

Azéma, P., J.-B. Lamy, P. Boudry, T. Renault, M.-A. Travers, and L. Dégremont. 2017. Genetic parameters of resistance to *Vibrio aestuarianus*, and OsHV-1 infections in the Pacific oyster, *Crassostrea gigas*, at three different life stages. Genetics Selection Evolution **49**:23.

Azéma, P., M.-A. Travers, J. Lorgeril, D. Tourbiez, and L. Dégremont. 2015. Can selection for resistance to OsHV-1 infection modify susceptibility to Vibrio aestuarianus infection in Crassostrea gigas? First insights from experimental challenges using primary and successive exposures. Veterinary research **46**:139.

Barros, P., P. Sobral, P. Range, L. Chícharo, and D. Matias. 2013. Effects of sea-water acidification on fertilization and larval development of the oyster Crassostrea gigas. Journal of Experimental Marine Biology and Ecology **440**:200-206.

Barshis, D. J., J. T. Ladner, T. A. Oliver, F. o. O. Seneca, N. Traylor-Knowles, and S. R. Palumbi. 2013. Genomic basis for coral resilience to climate change. Proceeding of the Nationnal Acedemy of Science of the United States of America **110**:1387-1392.

Bay, R. A. and S. R. Palumbi. 2015. Rapid Acclimation Ability Mediated by Transcriptome Changes in Reef-Building Corals. Genome Biology and Evolution **7**:1602-1612.

Bednaršek, N., G. A. Tarling, D. C. Bakker, S. Fielding, A. Cohen, A. Kuzirian, D. McCorkle, B. Lézé, and R. Montagna. 2012. Description and quantification of pteropod shell dissolution: a sensitive bioindicator of ocean acidification. Global Change Biology **18**:2378-2388.

Birkeland, C. 1997. Introduction. Pages 1-13 *in* C. Birkeland, editor. Life and death of coral reef. Chapman and Hall, New-York.

Biscéré, T., M. Zampighi, A. Lorrain, S. Jurriaans, A. Foggo, F. Houlbrèque, and R. Rodolfo-Metalpa. 2019. High pCO2 promotes coral primary production. Biology Letters **15**:20180777.

Bossdorf, O., C. L. Richards, and M. Pigliucci. 2008. Epigenetics for ecologists. Ecology Letters **11**:106-115.

Brahmi, C., L. Chapron, G. Le Moullac, C. Soyez, B. Beliaeff, C. E. Lazareth, N. Gaertner-Mazouni, and J. Vidal-Dupiol. 2021. Effects of elevated temperature and pCO2 on the respiration,

biomineralization and photophysiology of the giant clam Tridacna maxima. Conservation Physiology **9**.

Brener-Raffalli, K., C. Clerissi, J. Vidal-Dupiol, M. Adjeroud, F. Bonhomme, M. Pratlong, D. Aurelle, G. Mitta, and E. Toulza. 2018. Thermal regime and host clade, rather than geography, drive Symbiodinium and bacterial assemblages in the scleractinian coral Pocillopora damicornis sensu lato. Microbiome **6**:39.

Brener-Raffalli, K., J. Vidal-Dupiol, M. Adjeroud, O. Rey, P. Romans, F. Bonhomme, M. Pratlong, A. Haguenauer, R. Pillot, L. Feuillassier, M. Claereboudt, H. Magalon, P. Gélin, P. Pontarotti, D. Aurelle, G. Mitta, and E. Toulza. 2019. Gene expression plasticity and frontloading promote thermotolerance in *Pocillopora* corals. PCI Ecology:398602.

Brown, B. E. 1997. Coral bleaching: Causes and consequences. Coral reefs **16 (supplement)**:129-138.

Buddemeier, R. W., A. C. Baker, D. G. Fautin, and J. R. Jacobs. 2004. The adaptative hypothesis of bleaching. Pages 427-444 *in* E. Rosenberg and Y. Loya, editors. Coral Health and Diseases. Springer-Verlag, Berlin Heidelberg.

Bulgheresi, S., I. Schabussova, T. Chen, N. P. Mullin, R. M. Maizels, and J. A. Ott. 2006. A new C-Type Lectin similar to the human immunoreceptor DC-SIGN mediates symbiont acquisition by a marine nematode. Applied and Environmental Microbiology **72**:2950-2956.

Camp, E. F., M. R. Nitschke, R. Rodolfo-Metalpa, F. Houlbreque, S. G. Gardner, D. J. Smith, M. Zampighi, and D. J. Suggett. 2017. Reef-building corals thrive within hot-acidified and deoxygenated waters. Scientific Reports **7**:2434.

Campanati, C., S. Dupont, G. A. Williams, and V. Thiyagarajan. 2018. Differential sensitivity of larvae to ocean acidification in two interacting mollusc species. Marine Environmental Research **141**:66-74.

Chakravarti, L. J., V. H. Beltran, and M. J. H. van Oppen. 2017. Rapid thermal adaptation in photosymbionts of reef-building corals. Global Change Biology **23**:4675-4688.

Charmantier, A., R. H. McCleery, L. R. Cole, C. Perrins, L. E. B. Kruuk, and B. C. Sheldon. 2008. Adaptive phenotypic plasticity in response to climate change in a wild bird population. Science **320**:800-803.

Chen, M.-C., Y.-M. Cheng, M.-C. Hong, and L.-S. Fang. 2004. Molecular cloning of Rab5 (ApRab5) in *Aiptasia pulchella* and its retention in phagosomes harboring live zooxanthellae. Biochemical and biophysical research communications **324**:1024-1033.

Chen, M.-C., Y.-M. Cheng, P.-J. Sung, C.-E. Kuo, and L.-S. Fang. 2003. Molecular identification of Rab7 (ApRab7) in *Aiptasia pulchella* and its exclusion from phagosomes harboring zooxanthellae. Biochemical and biophysical research communications **308**:586-595.

Chen, M.-C., M.-C. Hong, Y.-S. Huang, M.-C. Liu, Y.-M. Cheng, and L.-S. Fang. 2005. ApRab11, a cnidarian homologue of the recycling regulatory protein Rab11, is involved in the establishment and maintenance of the *Aiptasia-Symbiodinium* endosymbiosis. Biochemical and biophysical research communications **338**:1607-1616.

Clark, M. S. 2020. Molecular mechanisms of biomineralization in marine invertebrates. Journal of Experimental Biology **223**.

Clerissi, C., S. Brunet, J. Vidal-Dupiol, M. Adjeroud, P. Lepage, L. Guillou, J.-M. Escoubas, and E. Toulza. 2018. Protists Within Corals: The Hidden Diversity. Frontiers in microbiology **9**.

Clerissi, C., J. de Lorgeril, B. Petton, A. Lucasson, J.-M. Escoubas, Y. Gueguen, L. Dégremont, G. Mitta, and E. Toulza. 2020. Microbiota Composition and Evenness Predict Survival Rate of Oysters Confronted to Pacific Oyster Mortality Syndrome. Frontiers in microbiology **11**.

Coles, S. L., K. D. Bahr, K. u. S. Rodgers, S. L. May, A. E. McGowan, A. Tsang, J. Bumgarner, and J. H. Han. 2018. Evidence of acclimatization or adaptation in Hawaiian corals to higher ocean temperatures. PeerJ **6**:e5347.

Cortijo, S., R. Wardenaar, M. Colomé-Tatché, A. Gilly, M. Etcheverry, K. Labadie, E. Caillieux, F. Hospital, J.-M. Aury, P. Wincker, F. Roudier, R. C. Jansen, V. Colot, and F. Johannes. 2014. Mapping the epigenetic basis of complex traits. Science **343**:1145-1148.

Cosseau, C., A. Azzi, A. Rognon, J. Boissier, S. Gourbière, E. Roger, G. Mitta, and C. Grunau. 2010. Epigenetic and phenotypic variability in populations of *Schistosoma mansoni* a possible kick off for adaptive host/parasite evolution. Oikos **119**:669-678.

D'Elia, C. F. and W. J. Wiebe 1990. Biogeochemical nutrient cycles in coral reef ecosystem. Pages 49-74 *in* Z. Dubinsky editor. Ecosystem of the world: Coral reefs. Elsevier Science publisher B.V., Amsderdam.

Dahlke, F. T., S. Wohlrab, M. Butzin, and H.-O. Pörtner. 2020. Thermal bottlenecks in the life cycle define climate vulnerability of fish. Science **369**:65-70.

Danchin, E. 2013. Avatars of information: Towards an inclusive evolutionary synthesis. Trends in ecology & evolution **28**:351-358.

Danchin, É., A. Charmantier, F. A. Champagne, A. Mesoudi, B. Pujol, and S. Blanchet. 2011. Beyond DNA: integrating inclusive inheritance into an extended theory of evolution. Nature Reviews Genetics **12**:475-486.

Danchin, E., A. Pocheville, O. Rey, B. Pujol, and S. Blanchet. 2019. Epigenetically facilitated mutational assimilation: epigenetics as a hub within the inclusive evolutionary synthesis. Biological Reviews **94**:259-282.

Darling, E. S., T. R. McClanahan, J. Maina, G. G. Gurney, N. A. J. Graham, F. Januchowski-Hartley, J. E. Cinner, C. Mora, C. C. Hicks, E. Maire, M. Puotinen, W. J. Skirving, M. Adjeroud, G. Ahmadia, R. Arthur, A. G. Bauman, M. Beger, M. L. Berumen, L. Bigot, J. Bouwmeester, A. Brenier, T. C. L. Bridge, E. Brown, S. J. Campbell, S. Cannon, B. Cauvin, C. A. Chen, J. Claudet, V. Denis, S. Donner, Estradivari, N. Fadli, D. A. Feary, D. Fenner, H. Fox, E. C. Franklin, A. Friedlander, J. Gilmour, C. Goiran, J. Guest, J.-P. A. Hobbs, A. S. Hoey, P. Houk, S. Johnson, S. D. Jupiter, M. Kayal, C.-y. Kuo, J. Lamb, M. A. C. Lee, J. Low, N. Muthiga, E. Muttaqin, Y. Nand, K. L. Nash, O. Nedlic, J. M. Pandolfi, S. Pardede, V. Patankar, L. Penin, L. Ribas-Deulofeu, Z. Richards, T. E. Roberts, K. u. S. Rodgers, C. D. M. Safuan, E. Sala, G. Shedrawi, T. M. Sin, P. Smallhorn-West, J. E. Smith, B. Sommer, P. D. Steinberg, M. Sutthacheep, C. H. J. Tan, G. J. Williams, S. Wilson, T. Yeemin, J. F. Bruno, M.-J. Fortin, M. Krkosek, and D. Mouillot. 2019. Social–environmental drivers inform strategic management of coral reefs in the Anthropocene. Nature Ecology & Evolution **3**:1341-1350.

de Lorgeril, J., A. Lucasson, B. Petton, E. Toulza, C. Montagnani, C. Clerissi, J. Vidal-Dupiol, C. Chaparro, R. Galinier, J.-M. Escoubas, P. Haffner, L. Dégremont, G. M. Charrière, M. Lafont, A. Delort, A. Vergnes, M. Chiarello, N. Faury, T. Rubio, M. A. Leroy, A. Pérignon, D. Régler, B. Morga, M. Alunno-Bruscia, P. Boudry, F. Le Roux, D. Destoumieux-Garzón, Y. Gueguen, and G. Mitta. 2018. Immune-suppression by OsHV-1 viral infection causes fatal bacteraemia in Pacific oysters. Nature Communications **9**:4215.

de Lorgeril, J., B. Petton, A. Lucasson, V. Perez, P.-L. Stenger, L. Dégremont, C. Montagnani, J.-M. Escoubas, P. Haffner, J.-F. Allienne, M. Leroy, F. Lagarde, J. Vidal-Dupiol, Y. Gueguen, and G. Mitta. 2020. Differential basal expression of immune genes confers Crassostrea gigas resistance to Pacific oyster mortality syndrome. BMC Genomics **21**:63.

DeCarlo, T. M., H. B. Harrison, L. Gajdzik, D. Alaguarda, R. Rodolfo-Metalpa, J. D'Olivo, G. Liu, D. Patalwala, and M. T. McCulloch. 2019. Acclimatization of massive reef-building corals to consecutive heatwaves. Proceedings of the Royal Society B: Biological Sciences **286**:20190235.

Deng, Y., K. Zhai, Z. Xie, D. Yang, X. Zhu, J. Liu, X. Wang, P. Qin, Y. Yang, and G. Zhang. 2017. Epigenetic regulation of antagonistic receptors confers rice blast resistance with yield balance. Science:eaai8898.

Desalvo, M. K., C. R. Voolstra, S. Sunagawa, J. A. Schwarz, J. H. Stillman, M. A. Coffroth, A. M. Szmant, and M. Medina. 2008. Differential gene expression during thermal stress and bleaching in the Caribbean coral *Montastraea faveolata*. Molecular Ecology **17**:3952-3971.

Diaz, R. J. and R. Rosenberg. 2008. Spreading dead zones and consequences for marine ecosystems. Science **321**:926-929.

Dixon, G., Y. Liao, L. K. Bay, and M. V. Matz. 2018. Role of gene body methylation in acclimatization and adaptation in a basal metazoan. Proceedings of the National Academy of Sciences of The United States Of America **115**:13342-13346.

Doney, S. C., V. J. Fabry, R. A. Feely, and J. A. Kleypas. 2009. Ocean acidification: The other CO2 problem. Annual Reviews of Marine Science **1**:169-192.

Downs, C. A., J. E. Fauth, J. C. Halas, P. Dustan, J. Bemiss, and C. M. Woodley. 2002. Oxidative stress and seasonal coral bleaching. Free Radical Biology and Medicine **33**:533-543.

Draghi, J. A. and M. C. Whitlock. 2012. Phenotypic plasticity facilitates mutational variance, genetic variance and evolvability along the major axis of environmental variation. Evolution **66**:2891-2902.

Drollet, J. H., M. Faucon, S. Maritorena, and P. M. V. Martin. 1994. A survey of environmental physico-chemical parameters during a minor mass bleaching event in Tahiti in 1993. Australian Journal of Marine and Freshwater research **45**:1149-1156.

Eirin-Lopez, J. M. and H. M. Putnam. 2019. Marine Environmental Epigenetics. Annual Review of Marine Science **11**:335-368.

Fallet, M. 2019. Etude de la réponse environnementale et transgénérationnelle chez l'huitre creuse Crassostrea gigas : focus sur les mécanismes épigénétiques. Université de Perpignan Via Domitia, Perpignan.

Fisk, D. A. and T. J. Done. 1985. Taxonomic and bathymetric patterns of bleaching in corals, Myrmidon Reef. Pages 149-154 *in* Proceedings of the 5th International Coral Reef Congress, Tahiti.

Flanagan, J. M. 2015. Epigenome-wide association studies (EWAS): past, present, and future. Pages 51-63 Cancer Epigenetics. Springer.

Franklin, D. J., O. Hoegh-Guldberg, R. J. Jones, and J. A. Berges. 2004. Cell death and degeneration in the symbiotic dinoflagellates of the coral *Stylophora pistillata* during bleaching. Marine Ecology Progress Series **272**:117-130.

Frieder, C. A., J. P. Gonzalez, E. E. Bockmon, M. O. Navarro, and L. A. Levin. 2014. Can variable pH and low oxygen moderate ocean acidification outcomes for mussel larvae? Global Change Biology **20**:754-764.

Galindo-Villegas, J., D. García-Moreno, S. de Oliveira, J. Meseguer, and V. Mulero. 2012. Regulation of immunity and disease resistance by commensal microbes and chromatin modifications during zebrafish development. Proceedings of the National Academy of Sciences **109**:E2605-E2614.

Gattuso, J.-P. and R. W. Buddemeier. 2000. Calcification and CO2. Nature **407**:311-313.

Gavery, M. R. and S. B. Roberts. 2017. Epigenetic considerations in aquaculture. PeerJ **5**:e4147-e4147.

Gazeau, F., L. M. Parker, S. Comeau, J.-P. Gattuso, W. A. O'Connor, S. Martin, H.-O. Pörtner, and P. M. Ross. 2013. Impacts of ocean acidification on marine shelled molluscs. Marine Biology **160**:2207-2245.

Ghalambor, C. K., J. K. McKay, S. P. Carroll, and D. N. Reznick. 2007. Adaptive versus non-adaptive phenotypic plasticity and the potential for contemporary adaptation in new environments. Functional Ecology **21**:394-407.

Glynn, P. W. 1983. Extensive 'bleaching' and death of reef corals on the Pacific coast of Panama. Environmental Conservation **10**:149-154.

Gutierrez, A. P., T. P. Bean, C. Hooper, C. A. Stenton, M. B. Sanders, R. K. Paley, P. Rastas, M. Bryrom, O. Matika, and R. D. Houston. 2018. A Genome-Wide Association Study for Host Resistance to Ostreid Herpesvirus in Pacific Oysters (Crassostrea gigas). G3: Genes|Genomes|Genetics **8**:1273-1280.

Harrison, P. L. and C. C. Wallace. 1990. Reproduction, dispersal and recruitment of scleractinian corals. Pages 133-196 *in* Z. Dubinsky editor. Ecosystem of the world: Coral reefs. Elsevier Science publisher B.V., Amsderdam.

Harvell, C. D., K. Kim, J. M. Burkholder, R. R. Colwell, P. R. Epstein, D. J. Grimes, E. E. Hofmann, E. K. Lipp, A. Osterhaus, and R. M. Overstreet. 1999. Emerging marine diseases--climate links and anthropogenic factors. Science **285**:1505-1510.

Harvell, C. D., C. E. Mitchell, J. R. Ward, S. Altizer, A. P. Dobson, R. S. Ostfeld, and M. D. Samuel. 2002. Climate warming and disease risks for terrestrial and marine biota. Science **296**:2158-2162.

Harvell, D., E. Jordán-Dahlgren, S. Merkel, E. Rosenberg, L. Raymundo, G. Smith, E. Weil, and B. Willis. 2007. Coral disease, environmental drivers, and the balance between coral and microbial associates. Oceanography **20**:172-195.

Hoegh-Guldberg, O. and J. F. Bruno. 2010. The impact of climate change on the world's marine ecosystems. Science **328**:1523-1528.

Hoegh-Guldberg, O., E. V. Kennedy, H. L. Beyer, C. McClennen, and H. P. Possingham. 2018. Securing a Long-term Future for Coral Reefs. Trends in ecology & evolution **33**:936-944.

Hoegh-Guldberg, O., P. J. Mumby, A. J. Hooten, R. S. Steneck, P. Greenfield, E. Gomez, C. D. Harvell, P. F. Sale, A. J. Edwards, K. Caldeira, N. Knowlton, C. M. Eakin, R. Iglesias-Prieto, N. Muthiga, R. H. Bradbury, A. Dubi, and M. E. Hatziolos. 2007. Coral reefs under rapid climate change and ocean acidification. Science **318**:1737-1742.

Huffmyer, A. S., C. Drury, E. Majerová, J. D. Lemus, and R. D. Gates. 2021. Tissue fusion and enhanced genotypic diversity support the survival of Pocillopora acuta coral recruits under thermal stress. Coral reefs **40**:447-458.

Hughes, T. P., J. T. Kerry, M. Álvarez-Noriega, J. G. Álvarez-Romero, K. D. Anderson, A. H. Baird, R. C. Babcock, M. Beger, D. R. Bellwood, R. Berkelmans, T. C. Bridge, I. R. Butler, M. Byrne, N. E. Cantin, S. Comeau, S. R. Connolly, G. S. Cumming, S. J. Dalton, G. Diaz-Pulido, C. M. Eakin, W. F. Figueira, J. P. Gilmour, H. B. Harrison, S. F. Heron, A. S. Hoey, J.-P. A. Hobbs, M. O. Hoogenboom, E. V. Kennedy, C.-y. Kuo, J. M. Lough, R. J. Lowe, G. Liu, M. T. McCulloch, H. A. Malcolm, M. J. McWilliam, J. M. Pandolfi, R. J. Pears, M. S. Pratchett, V. Schoepf, T. Simpson, W. J. Skirving, B. Sommer, G. Torda, D. R. Wachenfeld, B. L. Willis, and S. K. Wilson. 2017. Global warming and recurrent mass bleaching of corals. Nature **543**:373.

Jablonka, E., M. J. Lamb, and A. Zeligowski. 2005. Evolution in four dimensions. MIT, Cambridge.

Joubert, C., D. Piquemal, B. Marie, L. Manchon, F. Pierrat, I. Zanella-Cléon, N. Cochennec-Laureau, Y. Gueguen, and C. Montagnani. 2010. Transcriptome and proteome analysis of *Pinctada margaritifera* calcifying mantle and shell: focus on biomineralization. BMC Genomics **11**:613.

Kawecki, T. J. and D. Ebert. 2004. Conceptual issues in local adaptation. Ecology Letters **7**:1225-1241.

Kenkel, C. D. and M. V. Matz. 2016. Gene expression plasticity as a mechanism of coral adaptation to a variable environment. Nature Ecology & Evolution **1**:0014.

Khamo Gawra Gawra, J., J.-B. Lamy, M. Saccas, J. de Lorgeril, Y. Gueguen, J.-M. Escoubas, D. Destoumieux-Garzón, M. Leroy, P. Haffner, B. Morga, L. Dégremont, B. Petton, C. Grunau, G. Mitta, and J. Vidal-Dupiol. 2020. Genetic and Epigenetic determinants of resistance in the Pacific oyster Crassostrea gigas : A case study in natural population.*in* Epigenetic in Marine Biology.

Kleypas, J. A. and C. Langdon. 2006. Coral reefs and changing seawater carbonate chemistry. Coastal and Estuarine Studies **61**:73-110.

Kliebenstein, D. 2009. Quantitative genomics: analyzing intraspecific variation using global gene expression polymorphisms or eQTLs. Plant Biology **60**:93.

Knutson, T. R., J. L. McBride, J. Chan, K. Emanuel, G. Holland, C. Landsea, I. Held, J. P. Kossin, A. K. Srivastava, and M. Sugi. 2010. Tropical cyclones and climate change. Nature Geoscience **3**:157-163.

Korte, A. and A. Farlow. 2013. The advantages and limitations of trait analysis with GWAS: a review. Plant methods **9**:1-9.

Kvennefors, E. C. E., W. Leggat, O. Hoegh-Guldberg, B. M. Degnan, and A. C. Barnes. 2008. An ancient and variable mannose-binding lectin from the coral *Acropora millepora* binds both pathogens and symbionts. Developmental and Comparative Immunology **32**:1582-1592.

Lafferty, K. D., C. D. Harvell, J. M. Conrad, C. S. Friedman, M. L. Kent, A. M. Kuris, E. N. Powell, D. Rondeau, and S. M. Saksida. 2015. Infectious Diseases Affect Marine Fisheries and Aquaculture Economics. Annual Review of Marine Science **7**:471-496.

Le Brech, C. 2012. Requiem pour une huître. France TV.

Le Luyer, J., P. Auffret, V. Quillien, N. Leclerc, C. Reisser, J. Vidal-Dupiol, and C. L. Ky. 2019. Whole transcriptome sequencing and biomineralization gene architecture associated with cultured pearl quality traits in the pearl oyster, Pinctada margaritifera. BMC Genomics **20**:111.

Le Luyer, J., L. Milhade, C. Reisser, C. Soyez, C. J. Monaco, C. Belliard, G. Le Moullac, C.-L. Ky, and F. Pernet. 2021. Gene expression plasticity, genetic variation and fatty acid remodelling in divergent populations of a tropical bivalve species. bioRxiv:2021.2002.2008.429829.

Le Moullac, G., C. Soyez, O. Latchere, J. Vidal-Dupiol, J. Fremery, D. Saulnier, A. Lo Yat, C. Belliard, N. Mazouni-Gaertner, and Y. Gueguen. 2016a. Pinctada margaritifera responses to temperature and pH: Acclimation capabilities and physiological limits. Estuarine, Coastal and Shelf Science **182, Part B**:261-269.

Le Moullac, G., C. Soyez, J. Vidal-Dupiol, C. Belliard, J. Fievet, M. Sham Koua, A. Lo-Yat, D. Saulnier, N. Gaertner-Mazouni, and Y. Gueguen. 2016b. Impact of pCO2 on the energy, reproduction and growth of the shell of the pearl oyster *Pinctada margaritifera*. Estuarine, Coastal and Shelf Science.

Lesser, M. P. 1996. Exposure of symbiotic dynoflagellates to elevated temperatures and ultraviolet radiation causes oxidatives stress and inhibits photosynthesis. Limnology and oceanography **41**:271-283.

Lesser, M. P. 2006. Oxidative stress in marine environments: Biochemistry and physiological ecology. Annual Review of Physiology **68**:253-278.

Liew, Y. J., E. J. Howells, X. Wang, C. T. Michell, J. A. Burt, Y. Idaghdour, and M. Aranda. 2020. Intergenerational epigenetic inheritance in reef-building corals. Nature Climate Change **10**:254-259.

Liew, Y. J., D. Zoccola, Y. Li, E. Tambutté, A. A. Venn, C. T. Michell, G. Cui, E. S. Deutekom, J. A. Kaandorp, C. R. Voolstra, S. Forêt, D. Allemand, S. Tambutté, and M. Aranda. 2018. Epigenome-associated phenotypic acclimatization to ocean acidification in a reef-building coral. Science Advances **4**:eaar8028.

Loya, Y., K. Sakai, K. Yamazato, Y. Nakano, R. Sambali, and R. V. Van Woesik. 2001. Coral bleaching: the winners and the losers. Ecology Letters **4**:122-131.

Marie, B., C. Joubert, A. Tayalé, I. Zanella-Cléon, C. Belliard, D. Piquemal, N. Cochennec-Laureau, F. Marin, Y. Gueguen, and C. Montagnani. 2012. Different secretory repertoires control the biomineralization processes of prism and nacre deposition of the pearl oyster shell. Proceedings of the National Academy of Sciences of The United States Of America **109**:20986-20991.

Martínez-Meyer, E., A. Townsend Peterson, and W. W. Hargrove. 2004. Ecological niches as stable distributional constraints on mammal species, with implications for Pleistocene extinctions and climate change projections for biodiversity. Global Ecology and Biogeography **13**:305-314.

Matear, R. J., A. C. Hirst, and B. I. McNeil. 2000. Changes in dissolved oxygen in the Southern Ocean with climate change. Geochemistry Geophysic Geosystem **1**.

Matz, M. V., E. A. Treml, G. V. Aglyamova, and L. K. Bay. 2018. Potential and limits for rapid genetic adaptation to warming in a Great Barrier Reef coral. PLoS genetics **14**:e1007220.

McClintock, J. B., R. A. Angus, M. R. McDonald, C. D. Amsler, S. A. Catledge, and Y. K. Vohra. 2009. Rapid dissolution of shells of weakly calcified Antarctic benthic macroorganisms indicates high vulnerability to ocean acidification. Antarctic Science **21**:449-456.

Merle, P. L., C. Sabourault, S. Richier, D. Allemand, and P. Furla. 2007. Catalase characterization and implication in bleaching of a symbiotic sea anemone. Free Radical Biology and Medicine **42**:236-246.

Miller, D., G. Hemmrich, E. Ball, D. Hayward, K. Khalturin, N. Funayama, K. Agata, and T. Bosch. 2007. The innate immune repertoire in Cnidaria - ancestral complexity and stochastic gene loss. Genome biology **8**:R59.

Monteiro, H. J. A., C. Brahmi, A. B. Mayfield, J. Vidal-Dupiol, B. Lapeyre, and J. Le Luyer. 2020. Molecular mechanisms of acclimation to long-term elevated temperature exposure in marine symbioses. Global Change Biology **26**:1271-1284.

Mukherjee, K., E. Grizanova, E. Chertkova, R. Lehmann, I. Dubovskiy, and A. Vilcinskas. 2017. Experimental evolution of resistance against Bacillus thuringiensis in the insect model host Galleria mellonella results in epigenetic modifications. Virulence:00-00.

Mumby, P. J., I. A. Elliott, C. M. Eakin, W. Skirving, C. B. Paris, H. J. Edwards, S. Enríquez, R. Iglesias Prieto, L. M. Cherubin, and J. R. Stevens. 2011. Reserve design for uncertain responses of coral reefs to climate change. Ecology Letters **14**:132-140.

Pachauri, R. K. 2007. Climate change 2007: Synthesis report. IPCC Secreteria, Geneva.

Pal, C. and I. Miklos. 1999. Epigenetic inheritance, genetic assimilation and speciation. Journal of theoretical biology **200**:19-37.

Palumbi, S. R., D. J. Barshis, N. Traylor-Knowles, and R. A. Bay. 2014. Mechanisms of reef coral resistance to future climate change. Science **344**:895-898.

Pelejero, C., E. Calvo, and O. Hoegh-Guldberg. 2010. Paleo-perspectives on ocean acidification. Trends in ecology & evolution **25**:332-344.

Peñaloza, C., A. P. Gutierrez, L. Eöry, S. Wang, X. Guo, A. L. Archibald, T. P. Bean, and R. D. Houston. 2021. A chromosome-level genome assembly for the Pacific oyster Crassostrea gigas. GigaScience **10**.

Penin, L., J. Vidal-Dupiol, and M. Adjeroud. 2012. Response of coral assemblages to thermal stress: are bleaching intensity and spatial patterns consistent between events? Environmental Monitoring and Assessment:1-12.

Petit, J. R., J. Jouzel, D. Raynaud, N. I. Barkov, J. M. Barnola, I. Basile, M. Bender, J. Chappellaz, M. Davis, G. Delaygue, M. Delmotte, V. M. Kotlyakov, M. Legrand, V. Y. Lipenkov, C. Lorius, L. Pepin, C. Ritz, E. Saltzman, and M. Stievenard. 1999. Climate and atmospheric history of the past 420,000 years from the Vostok ice core, Antarctica. Nature **399**:429-436.

Pigliucci, M., C. J. Murren, and C. D. Schlichting. 2006. Phenotypic plasticity and evolution by genetic assimilation. Journal of Experimental Biology **209**:2362-2367.

Plantivaux, A., P. Furla, D. Zoccola, G. Garello, D. Forcioli, S. Richier, P.-L. Merle, E. Tambutte, S. Tambutte, and D. Allemand. 2004. Molecular characterization of two CuZn-superoxide dismutases in a sea anemone. Free Radical Biology and Medicine **37**:1170-1181.

Polovina, J. J., E. A. Howell, and M. Abecassis. 2008. Ocean's least productive waters are expanding. Geophysical Research Letter **35**:L03618.

Pouvreau, S., G. Jonquières, and D. Buestel. 1999. Filtration by the pearl oyster, Pinctada margaritifera, under conditions of low seston load and small particle size in a tropical lagoon habitat. Aquaculture **176**:295-314.

Reaka-Kudla, M. L. 1997. The global biodiversity of coral reefs: A comparison with rain forests. Pages 83-104 *in* M. L. Reaka-Kudla, D. E. Wilson, and E. O. Wilson, editors. Biodiversity II Understanding and protecting our biological resources. Joseph Henry Press, Washington.

Remongin, X. 2019. La conchyliculture : production et élevages. Ministère de l'Agriculture et de l'Alimentation.

Rey, O., C. Eizaguirre, B. Angers, M. Baltazar-Soares, K. Sagonas, J. G. Prunier, and S. Blanchet. 2019. Linking epigenetics and biological conservation: Towards a conservation epigenetics perspective. Functional Ecology **0**:1-14.

Richier, S., J.-M. Cottalorda, M. M. M. Guillaume, C. Fernandez, D. Allemand, and P. Furla. 2008. Depth-dependant response to light of the reef building coral, *Pocillopora verrucosa*: Implication of oxidative stress. Journal of Experimental Marine Biology and Ecology **357**:48-56.

Richier, S., C. Sabourault, J. Courtiade, N. Zucchini, D. Allemand, and P. Furla. 2006. Oxidative stress and apoptotic events during thermal stress in the symbiotic sea anemone, *Anemonia viridis*. FEBS Journal **273**:4186-4198.

Rinkevich, B. 2019. Coral chimerism as an evolutionary rescue mechanism to mitigate global climate change impacts. Global Change Biology **25**:1198-1206.

Rodolfo-Metalpa, R., F. Houlbrèque, E. Tambuttè, F. Boisson, C. Baggini, F. P. Patti, R. Jeffree, M. Fine, A. Foggo, and J. P. Gattuso. 2011. Coral and mollusc resistance to ocean acidification adversely affected by warming. Nature Climate Change **1**:308-312.

Rodriguez-Lanetty, M., S. Harii, and O. Hoegh-Guldberg. 2009. Early molecular responses of coral larvae to hyperthermal stress. Molecular Ecology **18**:5101-5114.

Rosa, R. D., J. De Lorgeril, P. Tailliez, R. Bruno, D. Piquemal, and E. Bachère. 2012. A hemocyte gene expression signature correlated with predictive capacity of oysters to survive Vibrio infections. BMC Genomics **13**:252.

Rubio, T., D. Oyanedel, Y. Labreuche, E. Toulza, X. Luo, M. Bruto, C. Chaparro, M. Torres, J. de Lorgeril, P. Haffner, J. Vidal-Dupiol, A. Lagorce, B. Petton, G. Mitta, A. Jacq, F. Le Roux, G. M. Charrière, and D. Destoumieux-Garzón. 2019. Species-specific mechanisms of cytotoxicity toward immune cells determine the successful outcome of Vibrio infections. Proceedings of the National Academy of Sciences **116**:14238-14247.

Salvat, B. 1992. Natural bleaching and mortality of scleractinian corals on Moorea Reefs (Society Archipelago) in 1991. Comptes rendus de l'Académie des sciences. Série 3, Sciences de la vie **314**:105-111.

Sauvage, C., P. Boudry, D. J. De Koning, C. S. Haley, S. Heurtebise, and S. Lapègue. 2010. QTL for resistance to summer mortality and OsHV-1 load in the Pacific oyster (Crassostrea gigas). Animal genetics **41**:390-399.

Segarra, A., J.-F. Pepin, I. Arzul, B. Morga, N. Faury, and T. Renault. 2010. Detection and description of a particular Ostreid herpesvirus 1 genotype associated with massive mortality outbreaks of Pacific oysters, Crassostrea gigas, in France in 2008. Virus Research **153**:92-99.

Stenger, P.-L., C.-L. Ky, C. Reisser, J. Duboisset, H. Dicko, P. Durand, L. Quintric, S. Planes, and J. Vidal-Dupiol. 2021a. Molecular Pathways and Pigments Underlying the Colors of the Pearl Oyster Pinctada margaritifera var. cumingii (Linnaeus 1758). Genes **12**:421.

Stenger, P.-L., C.-L. Ky, C. M. O. Reisser, C. Cosseau, C. Grunau, M. Mege, S. Planes, and J. Vidal-Dupiol. 2021b. Environmentally Driven Color Variation in the Pearl Oyster Pinctada margaritifera var. cumingii (Linnaeus, 1758) Is Associated With Differential Methylation of CpGs in Pigment- and Biomineralization-Related Genes. Frontiers in Genetics **12**.

Stenger, P. L., J. Vidal-Dupior, C. Reisser, S. Planes, and C. L. Ky. 2019. Colour plasticity in the shells and pearls of animal graft model Pinctada margaritifera assessed by HSV colour quantification. Scientific Reports **9**.

Tambutté, E., A. A. Venn, M. Holcomb, N. Segonds, N. Techer, D. Zoccola, D. Allemand, and S. Tambutté. 2015. Morphological plasticity of the coral skeleton under CO2-driven seawater acidification. Nature Communications **6**:7368.

Tambutté, S., M. Holcomb, C. Ferrier-Pagès, S. Reynaud, E. Tambutté, D. Zoccola, and D. Allemand. 2011. Coral biomineralization: from the gene to the environment. Journal of Experimental Marine Biology and Ecology **408**:58-78.

Teaniniuraitemoana, V., A. Huvet, P. Levy, C. Klopp, E. Lhuillier, N. Gaertner-Mazouni, Y. Gueguen, and G. Le Moullac. 2014. Gonad transcriptome analysis of pearl oyster *Pinctada margaritifera*: identification of potential sex differentiation and sex determining genes. BMC Genomics **15**:491.

Tewksbury, J. J., R. B. Huey, and C. A. Deutsch. 2008. Putting the Heat on Tropical Animals. Science **320**:1296-1297.

Thompson, D. M. and R. v. Woesik. 2009. Corals escape bleaching in regions that recently and historically experienced frequent thermal stress. Proceedings of the Royal Society B: Biological Sciences **276**:2893-2901.

Torda, G., J. M. Donelson, M. Aranda, D. J. Barshis, L. Bay, M. L. Berumen, D. G. Bourne, N. Cantin, S. Foret, M. Matz, D. J. Miller, A. Moya, H. M. Putnam, T. Ravasi, M. J. H. van Oppen, R. V. Thurber, J. Vidal-Dupiol, C. R. Voolstra, S.-A. Watson, E. Whitelaw, B. L. Willis, and P. L. Munday. 2017. Rapid adaptive responses to climate change in corals. Nature Climate Change **7**:627.

Travers, M.-A., L. Degremont, J. De Lorgeril, P. Azema, C. Montagnani, A. Benabdelmouna, J.-L. Nicolas, and F. Le Roux. 2014. Mortalités d'huîtres creuses adultes (Crassostrea gigas) et infection à Vibrio aestuarianus-AESTU.

van Oppen, M. J. H., R. D. Gates, L. L. Blackall, N. Cantin, L. J. Chakravarti, W. Y. Chan, C. Cormick, A. Crean, K. Damjanovic, H. Epstein, P. L. Harrison, T. A. Jones, M. Miller, R. J. Pears, L. M. Peplow, D. A. Raftos, B. Schaffelke, K. Stewart, G. Torda, D. Wachenfeld, A. R. Weeks, and H. M. Putnam. 2017. Shifting paradigms in restoration of the world's coral reefs. Global Change Biology **23**:3437-3448.

van Oppen, M. J. H., J. K. Oliver, H. M. Putnam, and R. D. Gates. 2015. Building coral reef resilience through assisted evolution. Proceedings of the National Academy of Sciences of The United States Of America **112**:2307-2313.

Van Oppen, M. J. H., P. Souter, E. J. Howells, A. Heyward, and R. Berkelmans. 2012. Novel genetic diversity through somatic mutations: fuel for adaptation of reef corals? Diversity **3**:405-423.

Venn, A. A., J. E. Loram, and A. E. Douglas. 2008. Photosynthetic symbioses in animals. Journal of Experimental Botany **59**:1069-1080.

Venn, A. A., E. Tambutté, M. Holcomb, J. Laurent, D. Allemand, and S. Tambutté. 2013. Impact of seawater acidification on pH at the tissue–skeleton interface and calcification in reef corals. Proceedings of the National Academy of Sciences **110**:1634-1639.

Veron, J. E. N. 2000. Corals of the World. Australian Institute of Marine Science, Townsville.

Vidal-Dupiol, J., M. Adjeroud, E. Roger, L. Foure, D. Duval, Y. Mone, C. Ferrier-Pages, E. Tambutte, S. Tambutte, D. Zoccola, D. Allemand, and G. Mitta. 2009. Coral bleaching under thermal stress: putative involvement of host/symbiont recognition mechanisms. BMC Physiology **9**:14.

Vidal-Dupiol, J., C. Chaparro, M. Pratlong, P. Pontarotti, C. Grunau, and G. Mitta. 2019. Sequencing, *de novo* assembly and annotation of the genome of the scleractinian coral, *Pocillopora acuta*. bioRxiv:698688.

Vidal-Dupiol, J., N. M. Dheilly, R. Rondon, C. Grunau, C. Cosseau, K. M. Smith, M. Freitag, M. Adjeroud, and G. Mitta. 2014. Thermal stress triggers broad Pocillopora damicornis transcriptomic remodeling, while Vibrio coralliilyticus infection induces a more targeted immuno-suppression response. PLoS ONE **9**:e107672.

Vidal-Dupiol, J., E. Toulza, C. Grunau, O. Rey, D. Roquis, C. Chaparro, C. Cosseau, A. Picart-Picolo, P. Romans, M. Pratlong, K. Brener-Raffalli, P. Pontaroti, M. Adjeroud, and G. Mitta. submitted. Genetic and epigenetic changes can mediate rapid acclimatization of tropical corals to global warming.

Vidal-Dupiol, J., D. Zoccola, E. Tambutté, C. Grunau, C. Cosseau, K. M. Smith, M. Freitag, N. M. Dheilly, D. Allemand, and S. Tambutté. 2013. Genes related to ion-transport and energy production are upregulated in response to CO_2-driven pH decrease in corals: New insights from transcriptome analysis. PLoS ONE **8**:e58652.

Wang, D., J. Zhu, Z. Li, and A. Paterson. 1999. Mapping QTLs with epistatic effects and QTL× environment interactions by mixed linear model approaches. TAG Theoretical and Applied Genetics **99**:1255-1264.

Weis, V. M. 2008. Cellular mechanisms of Cnidarian bleaching: stress causes the collapse of symbiosis. The Journal of Experimental Biology **211**:3059-3066.

Whiteley, A. R., S. W. Fitzpatrick, W. C. Funk, and D. A. Tallmon. 2015. Genetic rescue to the rescue. Trends in ecology & evolution **30**:42-49.

Wood-Charlson, E. M., L. L. Hollingsworth, D. A. Krupp, and V. M. Weis. 2006. Lectin/glycan interactions play a role in recognition in a coral/dinoflagellate symbiosis. Cellular Microbiology **8**:1985-1993.

Wood-Charlson, E. M. and V. M. Weis. 2009. The diversity of C-type lectins in the genome of a basal metazoan, *Nematostella vectensis*. Developmental & Comparative Immunology **33**:881-889.

Wu, H. C., D. Dissard, E. Douville, D. Blamart, L. Bordier, A. Tribollet, F. Le Cornec, E. Pons-Branchu, A. Dapoigny, and C. E. Lazareth. 2018. Surface ocean pH variations since 1689 CE and recent ocean acidification in the tropical South Pacific. Nature Communications **9**:2543.

Yáñez, J. M., R. D. Houston, and S. Newman. 2014. Genetics and genomics of disease resistance in salmonid species. Frontiers in Genetics **5**.

Yeoh, S.-R. and C.-F. Dai. 2010. The production of sexual and asexual larvae within single broods of the scleractinian coral, *Pocillopora damicornis*. Marine Biology **157**:351-359.

Zalasiewicz, J., M. Williams, A. Haywood, and M. Ellis. 2011. The Anthropocene: a new epoch of geological time? Philosophical Transactions of the Royal Society A **369**:835-841.

ANNEXE 1

ANNEXE 2

ANNEXE 3

ANNEXE 4

ANNEXE 5

ANNEXE 6

ANNEXE 7

ANNEXE 8

ANNEXE 9

ANNEXE 10

ANNEXE 11

ANNEXE 12

ANNEXE 13

ANNEXE 1

OPEN ACCESS Freely available online

PLOS ONE

Genes Related to Ion-Transport and Energy Production Are Upregulated in Response to CO_2-Driven pH Decrease in Corals: New Insights from Transcriptome Analysis

Jeremie Vidal-Dupiol[1]*, Didier Zoccola[1], Eric Tambutté[1], Christoph Grunau[2,3], Céline Cosseau[2,3], Kristina M. Smith[4], Michael Freitag[4], Nolwenn M. Dheilly[2,3], Denis Allemand[1], Sylvie Tambutté[1]

1 Centre Scientifique de Monaco, Monaco, Monaco, **2** Univ. Perpignan Via Domitia, Ecologie et Evolution des Interactions, UMR 5244, Perpignan, France, **3** CNRS, Ecologie et Evolution des Interactions, UMR 5244, Perpignan, France, **4** Department of Biochemistry and Biophysics, Center for Genome Research and Biocomputing, Oregon State University, Corvallis, Oregon, United States of America

Abstract

Since the preindustrial era, the average surface ocean pH has declined by 0.1 pH units and is predicted to decline by an additional 0.3 units by the year 2100. Although subtle, this decreasing pH has profound effects on the seawater saturation state of carbonate minerals and is thus predicted to impact on calcifying organisms. Among these are the scleractinian corals, which are the main builders of tropical coral reefs. Several recent studies have evaluated the physiological impact of low pH, particularly in relation to coral growth and calcification. However, very few studies have focused on the impact of low pH at the global molecular level. In this context we investigated global transcriptomic modifications in a scleractinian coral (*Pocillopora damicornis*) exposed to pH 7.4 compared to pH 8.1during a 3-week period. The RNAseq approach shows that 16% of our transcriptome was affected by the treatment with 6% of upregulations and 10% of downregulations. A more detailed analysis suggests that the downregulations are less coordinated than the upregulations and allowed the identification of several biological functions of interest. In order to better understand the links between these functions and the pH, transcript abundance of 48 candidate genes was quantified by q-RT-PCR (corals exposed at pH 7.2 and 7.8 for 3 weeks). The combined results of these two approaches suggest that pH≥7.4 induces an upregulation of genes coding for proteins involved in calcium and carbonate transport, conversion of CO_2 into HCO_3^- and organic matrix that may sustain calcification. Concomitantly, genes coding for heterotrophic and autotrophic related proteins are upregulated. This can reflect that low pH may increase the coral energy requirements, leading to an increase of energetic metabolism with the mobilization of energy reserves. In addition, the uncoordinated downregulations measured can reflect a general trade-off mechanism that may enable energy reallocation.

Citation: Vidal-Dupiol J, Zoccola D, Tambutté E, Grunau C, Cosseau C, et al. (2013) Genes Related to Ion-Transport and Energy Production Are Upregulated in Response to CO_2-Driven pH Decrease in Corals: New Insights from Transcriptome Analysis. PLoS ONE 8(3): e58652. doi:10.1371/journal.pone.0058652

Editor: Sam Dupont, University of Gothenburg, Sweden

Received August 30, 2012; **Accepted** February 7, 2013; **Published** March 27, 2013

Funding: This work was supported by funds from the American Cancer Society (RSG-08-030-01-CCG) and start-up funds from the OSU Computational and Genome Biology Initiative. JV-D's postdoctoral fellowship was supported by the Centre Scientifique de Monaco (CSM). The funders had no role in study design, data collection and analysis, decision to publish, or preparation of the manuscript.

Competing Interests: To note, one of the authors of this manuscript, Michael Freitag, is a PLOS ONE editorial board member. This does not alter the authors' adherence to all the PLOS ONE policies on sharing data and materials.

* E-mail: jeremie.vidal-dupiol@univ-perp.fr

Introduction

Coral reefs are key ecosystems characterized by a high level of biodiversity, ecological complexity and primary productivity. Reef-building corals are key species in coral reefs, providing physical and biological foundations for the ecosystem. The ability of corals to build reefs in oligotrophic tropical oceans is mainly explained by the mutualistic association they form with zooxanthellae (photosynthetic dinoflagellates of the genus S*ymbiodinium*), which produce autotrophically most of the energy required for the calcification process [1].

Global climate change is impacting on coral reefs, with approximately 19% of reefs worldwide being permanently degraded, 15% showing symptoms of imminent collapse, and another 20% at risk of becoming critically affected in the next few decades [2]. This alarming level of reef degradation is mainly due to an increase in frequency and intensity of natural and anthropogenic disturbances affecting reefs [3]. Among, these disturbances is ocean pH decrease, also termed "ocean acidification" [4,5].

Several experimental studies have shown that low pH decreases the net calcification rate and skeletal growth of various coral species [6–15]. However, in other studies no effects on gross calcification (or an increase) have been reported [16–18]. In ecosystems naturally subject to low pH conditions (e.g. CO_2 vents), coral net calcification has been reported to not decrease, or to decrease only slightly [19,20], but at the ecosystem level low pH induces marked community changes [19]. In addition to its impact on calcification rates, low pH has been shown to: (i) modify the composition, size, shape and orientation of aragonite crystals in primary polyps [7]; and (ii) increase the coral tissue biomass [11,21]. Contradictory findings have been reported in relation to the effects of low pH on the symbiont component of the coral holobiont. These include findings of a decrease in the density of

zooxanthellae [17,22], and effects on their chlorophyll concentration [11] and photosynthetic efficiency [9]. On the other hand, these results have been challenged in recent studies [9,14,16]. To date only 2 recent works have explored the transcriptomic response of corals exposed to low pH: a whole transcriptomic analysis on early life history stages [23] and a cDNA microarrays analysis on adults [17]. Both of these studies were performed on the coral *Acropora millepora* which phylogenetically belongs to the coral "complex" clade which has a less heavily calcified skeletons, and a more porous construction of corallite walls than corals belonging to the "robust" clade [24,25].

The aim of the present study was to initiate a whole-transcriptome analysis in the adult scleractinian tropical coral *Pocillopora damicornis* exposed to low pH. Such whole-transcriptome analysis has already successfully been used in studies on the impact of global climate change on coastal organisms [23,26–28]. It is also an interesting prerequisite for studies that will target specific biological functions or phenotypic plasticity across populations facing different pH conditions. Finally, RNAseq experiments offer the possibility to highlight unexpected physiological pathways. In the present study we choose to work on the scleractinian tropical coral *P. damicornis* for several reasons: i) it is a major reef-building coral widely distributed in the Indo-Pacific ocean [29]; ii) it is naturally confronted to diverse values of ocean pH, ranging from 7.8 in the particular case of volcanic CO_2 vents, to 7.9–8.0 in the Eastern tropical Pacific and to 8.1 in other locations [19,30]; iii) it is known to be highly sensitive to a wide range of natural and anthropogenic disturbances [31–33]; iv) it belongs to the "robust" clade which has not yet been studied by transcriptomic approaches [24,25]. This "robust" clade is characterized by a highly calcified and low porous skeleton compared to corals belonging to the "complex" clade. Taking into account the impact of low pH on calcifying organisms, these last characteristics can lead to different responses to low pH conditions between clades. To address our aims we first assembled the transcriptomes of *P. damicornis* using the result of several RNAseq experiments. In order to maximize the amplitude of the transcriptomic response, an exposure of three weeks to an extreme value of today (volcanic CO_2 vents) or near future natural variability (lower value on the daily variation scale) of pH (7.4) was used and the transcriptome obtained was compared to the control transcriptome (nubbins maintained for three weeks at a current seawater pH of 8.1). After the identification of the biological functions of interest responding to this low pH, a candidate gene approach (by q-RT-PCR) was performed on mRNA from nubbins exposed to a predicted pH of 7.8 and to a very low pH of 7.2 (3 weeks of exposure).

Methods

Coral collection, maintenance, and experimental stress

The *Pocillopora damicornis* (Linnaeus, 1758) isolate used in this study was collected in Lombok, Indonesia (CITES Management Authority, CITES number 06832/VI/SATS/LN/2001-E; Direction de l'Environnement, CITES number 06832/VI/SATS/LN/2001-I). The site of collection corresponds to an usual fringing-reef subjected to the usual day/night pH variation (8.3/7.85) observed on such reefs [34,35]. *P. damicornis* colonies were then maintained since the year 2001 in an open water aquarium system where pH fluctuates between day and night due to photosynthesis and respiration between maxima and minima values of 8.3 and 7.9 respectively for day and night. For experiments, coral explants (3 cm height, 3 cm diameter) from the same parent colony were left to allow tissues to grow over skeleton (recover) for a period of 1 month prior to use in experiments.

Following recovery, coral nubbins were incubated during 3 weeks into experimental tanks. Temperature ($25\pm0.5^{\circ}C$) was kept constant in each tank using heaters connected to electronic controllers (IKS, Karlsbad, Germany), and seawater was mixed using 2 submersible pumps. Corals received a constant saturating irradiance of 175 ± 10 µmol photons m^{-2} s^{-1} (photoperiod was 12 h:12 h light/dark) using HQI-10000K metal halide lamps (BLV-Nepturion). They were fed twice a week with *Artemia salina* nauplii in order to reach a natural heterotrophic rate. Tanks, pumps, sensors and electrodes were rigorously cleaned every week to prevent the growth of epiphytic algae and fouling communities or the accumulation of detritus. Water renewal rate in each tank was 60% per hour (continuous water flow).

Carbonate chemistry was manipulated in 3 of 4 tanks by bubbling with CO_2 to reduce pH to target values and the fourth tank (control tank) was not bubbled with CO_2 (see values below). pH electrodes and temperature sensors installed in each tank were connected to a pH-stat system (IKS, Karlsbad) that continuously monitored pH (calibrated to NBS scale), temperature and controlled CO_2 bubbling. On a daily basis, additional pH checks were carried with a Plastogel-Ponsel pH probe (Ponsel), calibrated to pH total scale (pH_T). Moreover biweekly pH_T measurements were made using the indicator dye m-cresol purple (mCP Acros 199250050) adapted from Dickson *et al.* [36]; the absorbance was measured using spectrophotometer ($UVmc^2$, Safas, Monaco). According to these results, the pH-stat system was adjusted. The control tank was maintained at ambient pH_T: 8.07 ± 0.07 (396 µatm pCO_2), the other tanks at pH_T: 7.75 ± 0.12, (856 µatm pCO_2), pH_T: 7.42 ± 0.21 (2181 µatm pCO_2), pH_T: 7.19 ± 0.18 (3880 µatm pCO_2). For easier reading, throughout the manuscript, these four values of pH_T will be respectively indicated as pH 8.1 (control tank), pH 7.8, pH 7.4 and pH 7.2. After 3 weeks of exposure, 3 nubbins in each treatment tank were sampled at the same time and stored in liquid nitrogen until analyzed.

Water samples were collected in scintillation vials (Wheaton) and stored refrigerated no more than 1 week prior to measurement. Biweekly total alkalinity (TA) was measured via titration with 0.01 N HCl containing 40.7 g NaCl l^{-1} using a Metrohm Titrando 888 dosimat controlled by Tiamo software to perform automated normalized Gran titrations of 1 ml samples. For each sample run, certified seawater reference material supplied by the lab of A.G. Dickson (Scripps Institution of Oceanography) was used to check quality of measurements.

Parameters of carbonate seawater chemistry were calculated from pH_T, mean AT, temperature, and salinity using the free access CO_2 Systat package [37] using constants from Mehrbach *et al.* [38] as refit by Dickson and Millero [39]. Parameters of carbonate seawater chemistry are given in Table 1 and 2.

cDNA library construction and high-throughput sequencing

We assembled a transcriptome *de novo* from 80-nucleotide paired-end short sequence reads (SSRs) based on 6 lanes of Illumina sequencing. To maximize the coverage of potential transcriptomes, the cDNA from corals exposed to various environmental conditions (pH 7.4 and its dedicated control (see above), thermal stress, bacterial challenge, bacterial infection and a dedicated control for these last conditions [40]) were sequenced (one illumina lane per condition). Despite the recent publication of a reference transcriptome for *P. damicornis* [41] we preferred to assemble *de novo* a reference transcriptome with the SSRs

generated by our RNAseq approach rather than map our reads on the one previously published. Indeed, this reference transcriptome (Roche 454 data) was obtained from Hawaiian *P. damicornis*, a population that is geographically very distant from the one we studied (Lombok, Indonesia). Such a distance may lead to a high number of single nucleotide polymorphisms that can skew the mapping step. In addition, the Hawaiian study did not use specimens exposed to low pH, thatpH that could lead to the absence of transcripts or spliced transcripts specifically expressed under such environmental condition.

Total RNA from 3 nubbins per condition was extracted, purified using TRIzol reagent (Invitrogen), and pooled together (one pool per condition) to reach a sufficient amount of biological material for the RNAseq procedure, as described previously [42]. A cDNA library was subsequently constructed following a published protocol [43]. A minimum of 1 µg of cDNA was used to generate each of the paired-end Illumina sequencing libraries. The libraries were prepared using Illumina adapter and PCR primers according to previously published protocols [44,45]. Libraries with an average insert size of 400–500 bp were isolated and the concentration was adjusted to 10 nM. The samples (7 pM per sample) were loaded into separate channels of an Illumina GAIIx sequencer, and sequenced at the Oregon State University Center for Genome Research and Biocomputing.

Reference transcriptome assembly and annotation

The SSRs obtained were processed using an Illumina pipeline (RTA1.6_CASAVA1.6), and SSRs from 'sequence.txt' files were filtered to select only those SSRs that matched high quality standards. Velvet software version 1.1.04 was subsequently used, evoking velveth with parameters *[k-mer] – fasta – shortPaired*, and velvetg with parameter *-read_trkg yes* [46]. The k-mer value was tested between 31 and 61 and optimized using a subset of data for maximum size of longest contig, average contig length, contig number, n50 value and total transcriptome length. Optima were obtained at k-mer 55 and 57, and we decided for k-mer 55 based on the higher number of included reads. Using the above parameters, 45,596,723 of 131,859,606 SSRs were incorporated into the assembly, producing 102,571 contigs. These served as the input for the *de novo* transcriptome assembler software Oases 0.1.21 [47], using the input parameter *-ins_length 400* and *default parameters -cov_cutoff 3 -min_pair_cov 4 -paired_cutoff 0.1* and with or without *-scaffolding*. This assembly generated 84,511 contigs. The scaffolding had no effect. Since oases 0.1.x was known to generate a number of exactly identical sequences (duplicates), a reassembly was performed using TIGR assembler [48] based on the default parameters in the original *run_TA* script (ftp://ftp.jcvi.org/pub/software/assembler/), which reduced the number of contigs to 72,924. The remaining exact duplicates and reverse complement exact duplicates were removed using *prinseq-lite.pl* (http://prinseq.sourceforge.net; parameter -derep 14), yielding a total of 72,890 transcript contigs.

Functional annotation of this reference transcriptome was performed using Blast2GO version 2.4.2 [49], which enabled a semi-automated functional annotation of all contigs using a set of similarity search tools. The default parameters was used and included: i) an initial annotation with BLASTX (against the nonredundant NCBI database; e-value at 1×10^{-3}); ii) a protein domain search using InterProscan; iii) an enzyme annotation using the Kyoto Encyclopedia of Genes and Genomes (KEGG); and iv) assignment of a Gene Ontology term (GO; http://www.geneontology.org/).

The taxonomic assignment of contigs (sequences from the coral host or zooxanthellae symbiont) were predicted using 3 approaches: i) top hit species from the BLASTX results (the species with the best/first sequence alignment for a given BLASTX result); ii) the percentage of GC bases, GC content of corals is approximately 42%, and 54% for zooxanthellae [50]; and iii) species specific sequence signatures based on CLaMS analysis [51].

Differential gene expression analysis

To assess changes in gene expression regulated by low pH, SSRs from both low pH and control libraries were mapped against the reference transcriptome and counted using BWA [52]. Because RNAseq data are functions of both the molar concentration and the transcript length, the results of the mapping step were corrected and expressed as reads per kilobase per million mapped reads (RPKM; [53]). This enabled comparison of SSRs counts between transcripts and from samples derived from differing conditions [53]. To identify significantly different gene expression among conditions, the MARS method (MA plot-based methods using a random sampling model) of the R package in DEGseq was used [54]. Differences in transcripts levels between low pH and control conditions were considered statistically significant at $p<0.0001$.

q-RT-PCR

Quantitative real-time PCR (q-RT-PCR) was used to validate expression profiles obtained from the MARS DEGseq analysis of the RNAseq data [27]. It was also used to measure expression levels of selected 48 candidate genes in *P. damicornis* subjected to complementary pH conditions (7.8 and 7.2). Total RNA was extracted, treated with DNase, and the poly(A) RNA was purified as described above. Approximately 50 ng of purified poly(A) RNA were reverse transcribed with hexamer random primers using ReverTAid H Minus Reverse Transcriptase (Fermentas). The q-RT-PCR experiments were performed on cDNAs obtained from 3 nubbins per treatments as described previously [40]. For each candidate gene the level of transcription was normalized using the mean geometric transcription rate of 3 reference sequences encoding ribosomal protein genes from *P. damicornis* (60S ribosomal protein L22, GenBank accession numbers HO112261, 60S ribosomal protein L40A, HO112283 and 60S acidic ribosomal phosphoprotein P0, HO112666). These housekeeping genes had <10% variation in expression between control and low pH conditions and were previously shown to be stable in *P. damicornis* subjected to different environmental conditions [40]. The primers used for amplification are provided in File S1.

Results

Assembly of the reference transcriptome

To quantify changes in gene expression between the pH 7.4 treatment and the control, we assembled a reference transcriptome *de novo*. To maximize the diversity of transcripts, the cDNA samples derived from corals exposed to various environmental conditions (pH 7.4 and its dedicated control, thermal stress, bacterial challenge, bacterial infection and a dedicated control for these last conditions) were sequenced and assembled together. After the assemble work flow, a total of 72,890 transcript contigs were generated. The functional annotation performed using Blast2GO produced the following result: i) 22,419 contigs had significant similarities to proteins of known function; ii) GO term was assigned to 23,170 contigs; iii) KEGG enzymatic codes were found for 2,837 contigs; and vi) 46,295 conserved protein domains were detected by InterProScan. Using a combination of BlastX top hit species results, GC% calculation of each contig (perl script)

Table 1. Seawater chemistry (Total alkalinity, pH, TC and pCO_2) obtained from continuously monitored pH.

	Total alkalinity (μmol/kg-SW)		pH		TC (μmol/kg-SW)		pCO_2 (μatm)	
	Mean	SD	Mean	SD	Mean	SD	Mean	SD
Tank 8.1	2515.0	18.0	8.07	0.07	2155.33	33.96	396.24	57.2
Tank 7.8	2557.0	22.0	7.79	0.08	2319.10	39.82	856.97	182.38
Tank 7.4	2498.0	17.0	7.42	0.06	2457.13	22.15	2180.86	323.17
Tank 7.2	2542.0	13.0	7.19	0.07	2587.85	27.91	3879.69	654.28

doi:10.1371/journal.pone.0058652.t001

and sequence signature analysis (CLaMS program; [51], 27.7% and 69.8% of the contigs were predicted to belong to the symbiont and the host transcriptome, respectively. The remaining contigs could not be taxonomically attributed. The assembled and annotated reference transcriptome is publicly available at http://2ei.univ-perp.fr/telechargement/transcriptomes/blast2go_fasta_Pdamv2.zip. The raw data (untreated SSRs) for the pH treatment and its corresponding control are publicly available at http://www.ncbi.nlm.nih.gov/sra (study accession number SRP011059.1).

Expression in 16% of the genes changes after exposure to low pH

The RNAseq approach resulted in the sequencing of 25.2 and 22.3 million Short Sequence Reads (SSRs) for the pH 8.1 and the pH 7.4 conditions, respectively. A total of approximately 10 and 9 million SSRs (~40%) passed the quality filter and were successfully mapped on the reference transcriptome for the control and the low pH conditions, respectively. Nearly 80% (57,259 contigs) of the reference transcripts were mapped by at least one SSR from either 1 of the 2 experimental conditions.

To highlight the genes significantly up or downregulated by the pH 7.4 treatment, the mapped results (RPKM) were analyzed using the MARS method in the DEGseq R package. In response to pH 7.4, 6.0% (3,204) of the transcripts were significantly upregulated and 10.0% (5,758) were downregulated ($p<0.0001$; Figure 1). Among the upregulated genes, 60.4% showed no significant similarity to known proteins, 2.7% showed significant similarity to proteins of unknown function, and 36.9% showed significant similarity to proteins of known function (Significant similarity: *e*value $<1\times10^{-3}$). Among the downregulated genes, 69.5% of their products showed no significant similarity to known proteins, 3.5% showed significant similarity to proteins of unknown function, and 27.0% showed significant similarity to proteins of known function.

To assess the accuracy of the quantification analysis a validation step involving an alternative method of quantification (q-RT-PCR) was conducted on 25 transcripts arbitrarily selected along the gradient of expression (from highly upregulated to highly downregulated gene) obtained from the RNAseq data. There was a significant correlation ($r^2=0.86$; $p<0.0001$; Figure 2) between the $\log_2$ fold change in expression (relative to the control) of the RNAseq and the q-RT-PCR data which confirmed the accuracy of the results obtained with the RNAseq data.

Specific biological processes are altered after exposure to pH 7.4 for three weeks

To study the transcriptomic changes resulting from exposure to pH 7.4 for 3 weeks, a GO term enrichment analysis (Figure 3) was performed [55]. It showed that 32 biological process categories were enriched in the subset of sequences associated with significant upregulation (Fig. 3A). Several of the functions involved were of particular interest in the context of this study, including transport, photosynthesis, gluconeogenesis, generation of precursor metabolites and energy and pyruvate metabolic process. Analysis of the subset of transcripts of significantly downregulated genes showed that only those for the GO term 'cellular macromolecule metabolic process' were represented at a higher rate than expected by chance ($p<0.01$; Fig. 3B). The GO terms 'post-translational protein modification' and 'cellular protein metabolism' were more significantly represented ($p<0.05$) among the downregulated set than in the reference sequence set. The numbers of genes belonging to each biological process are indicated in File S2.

Response of some biological functions to an exposure to pH 7.8, 7.4 or 7.2 for 3 weeks

Based on GO term enrichment analysis and DEGseq results (Figure 3), 48 candidate genes significantly regulated ($p<0.0001$) were identified as corresponding to biological functions of interest in the context of our study and were selected (see File S1) and investigated further. Their transcript abundance was measured

Table 2. Seawater chemistry (CO_2, HCO_3^-, CO_3^-, Ω Ca^{2-} and Ω Aragonite) obtained from continuously monitored pH.

	CO_2 (μmol/kg-SW)		HCO_3^- (μmol/kg-SW)		CO_3^{2-} (μmol/kg-SW)		Ω Ca^{2-}		Ω Aragonite	
	Mean	SD	Mean	SD	Mean	SD	Mean	SD	Mean	SD
Tank 8.1	11.04	1.59	1887.31	54.52	256.98	22.15	6.03	0.52	3.99	0.34
Tank 7.8	23.88	5.08	2142.15	58.77	153.07	24.03	3.59	0.56	2.38	0.37
Tank 7.4	60.77	9.00	2325.48	22.27	70.89	9.13	1.66	0.21	1.10	0.14
Tank 7.2	108.10	18.23	2436.02	16.46	43.72	6.78	1.03	0.16	0.68	0.11

doi:10.1371/journal.pone.0058652.t002

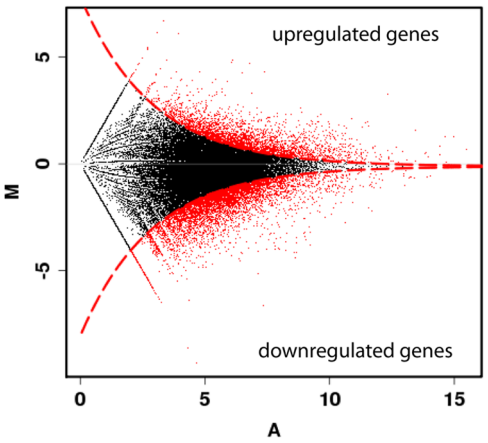

Figure 1. Differential gene expression between control samples and samples exposed to pH 7.4 for three weeks. The detection of genes differentially expressed in the two conditions was performed using the DEGseq R package and plotted as a MA plot. The M axis is the log2 fold change for the pH-treated sample compared with the control sample (log2 fold change = log2 [RPKM acid stress/RPKM control]), and the A axis is the average log2 normalized counts in both samples. Each point represents a single contig of the reference transcriptome. The red points correspond to contigs significantly differentially represented between the two conditions ($p<0.0001$). Among the 57,259 contigs analyzed, 5758 were significantly downregulated (10%) and 3204 (6%) were upregulated.
doi:10.1371/journal.pone.0058652.g001

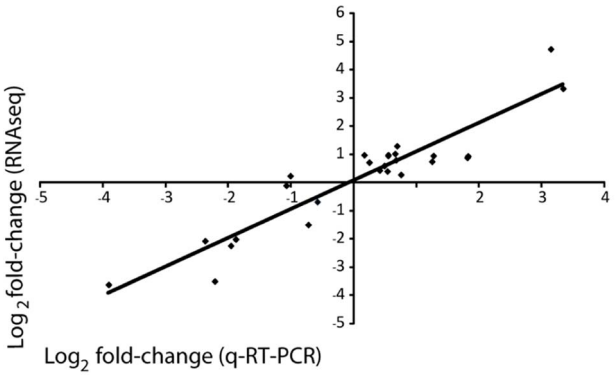

Figure 2. Validation of the RNAseq approach using q-RT-PCR. Twenty-five genes that whose expression was significantly different in the control and treatment conditions were arbitrary selected from highly upregulated to highly downregulated contig. Their levels of expression were quantified by q-RT-PCR, and the results were compared with those obtained using the RNAseq approach. The log2 change in expression of q-RT-PCR and RNAseq was closely correlated ($r^2 = 0.86$; $p<0.0001$), indicating the accuracy of the RNAseq approach for quantification.
doi:10.1371/journal.pone.0058652.g002

on corals exposed for 3 weeks at pH 8.1, 7.8, 7.4 and 7.2. This transcript abundance was obtained by q-RT-PCR for the pH 7.8 and 7.2 whereas the RNAseq results were used for the pH 7.4 treatment. All changes in transcript abundance were expressed relative to the control (pH 8.1). All these results are presented in Figure 4 and the numerical values are detailed in File S3.

Briefly, the GO term enrichment analysis (Figure 3) showed a significant increase in gene expression involved in the biological processes 'transport', which includes transport of ions and proteins. As calcification involves Ca^{2+} and inorganic carbon [56] we investigated genes encoding proteins involved in the transcellular transport of Ca^{2+} and HCO_3^- ions, and carbonic anhydrases involved in converting CO_2 into HCO_3^-. Among these candidates: i) The six HCO_3^- transporters were upregulated at pH 7.8 and 7.4 (between 17.75 and 1.52 fold increase) and were downregulated at pH 7.2 (between 3.81 and 1.57 fold decrease); ii) a Ca^{2+} plasma membrane ATPase was upregulated at pH 7.8 and 7.4 (1.47 and 1.43 fold increase, respectively), but was downregulated at pH 7.2 (3.01 fold decrease); iii) an extracellular (upregulated at all pH between 2.51 and 3.34 fold increase) and a cytosolic carbonic anhydrase (upregulated at pH 7.8 and 7.4, 2.51 and 1.85 fold increase respectively). The Ca^{2+} plasma membrane ATPase and the two carbonic anhydrase present significant similarities with proteins that were previously shown to be involved in *Stylophora pistillata* calcification [57–59]. In addition to $CaCO_3$, the skeleton of scleractinian corals contains organic matrix proteins [56], and their production was affected by low pH treatment. Indeed, seven genes encoding skeleton organic matrix proteins were identified in the present study. One of these genes regulated at pH 7.4 (3.5 fold increase) presents significant similarities to galaxin from *Galaxea fascicularis* [60], and the four other transcripts to the galaxin-like (only 2 of them were subjected to q-RT-PCR experiment, and were upregulated at all pH between 70.03 and 4.11 fold increase) proteins family from *Acropora millepora* [61]. The remaining two genes had significant similarities to the bone morphogenetic protein superfamily [62] and were upregulated at pH 7.8 and 7.4 (between 2.91 and 1.93 fold increase), but downregulated at pH 7.2 (between 2.68 and 1.56 fold decrease). For a complete description of candidate genes expression see Figure 4 and File S3.

Biological functions involved in energy production (photosynthesis, glycolysis, Krebbs cycle, oxidative phosphorylation, lipolysis and beta oxidation; Figure 4) were also significantly enriched in the set of up-regulated genes (GO term enrichment analysis, Figure 3). As calcification represents approximately 13–30% of the daily coral energy demand [1], we also investigated the regulation of these metabolic related genes by q-RT-PCR for the 3 pH treatments. Among the eight candidates genes involved in photosynthesis, seven were upregulated (between 1.15 and 5.54 fold increase) and one, the PS I p700 chlorophyll a apoprotein a2-like was downregulated at pH 7.4 (1.96 fold decrease). Three of the four candidate genes involved in glycolysis were upregulated at pH 7.8 and 7.4 (between 6.68 and 1.22 fold increase) and two were downregulated at pH 7.2 (between 2.11 and 1.22 fold decrease). Among the eight the candidates genes involved in the Krebs cycle six shows upregulations at pH 7.8 and/or 7.4 (between 3.36 and 1.33 fold increase) and five were downregulated at pH 7.2 (between 2.36 to 1.1 fold decrease). Four of the genes involved in oxidative phosphorylation were upregulated at pH 7.8 and 7.4 (between 10.85 and 1.28 fold increase), but one become downregulated at pH 7.2 (1.89 fold decrease). One of the genes involved in lipolysis was upregulated at pH 7.8 and 7.4 (1.15 and 1.95 fold increase respectively) but was downregulated by a factor of 2 in the pH 7.2 treatment. Finally, the three candidate genes involved in beta oxidation were upregulated at all pH (between 5.98 and 1.37 fold increase), except the Acyl-CoA dehydrogenase-like that was downregulated by a factor of 2.17 at pH 7.2. For a complete description of candidate genes expression see the Figure 4 and File S3.

Finally, very few biological processes were significantly enriched in the genes downregulated at pH 7.4 (GO term enrichment analysis, Figure 3). However, these included the category 'post-translational protein modification' (GO term enrichment analysis; $p<0.05$), which contains genes encoding kinases. Because of their important role in signal transduction, four of those were selected,

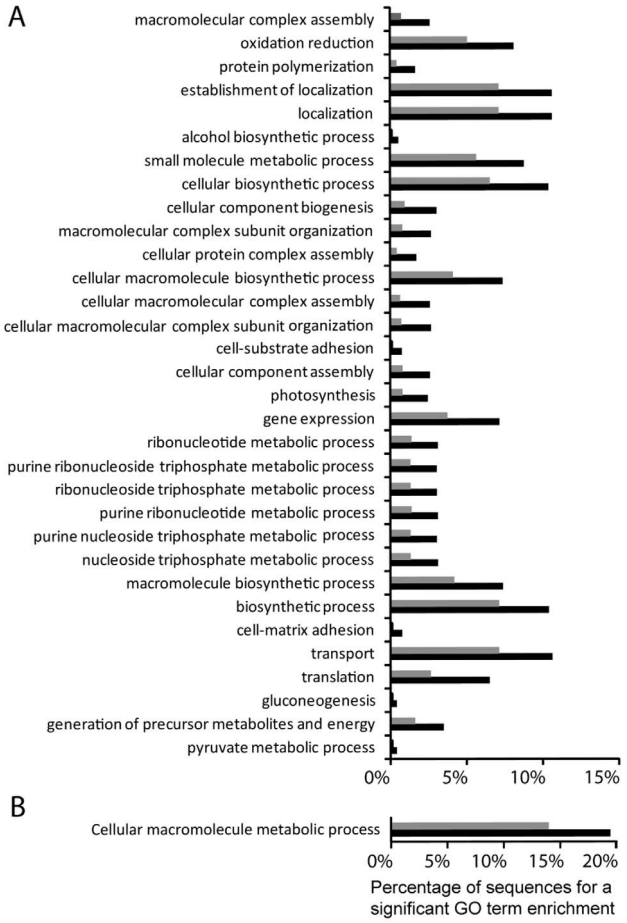

Figure 3. Biological functions involved in the response to pH 7.4 treatment, GO term enrichment analysis. The enrichment analysis (x axis) is expressed as the percentage of sequences at both, test (black bars) and reference (grey bars) set, for GO terms having a *p*value A) Enrichment analysis performed with the set of induced genes (''test set'', state condition, black bars) compared with genes detected in the RNAseq experiment (''reference set'', grey bars). B) Enrichment analysis performed with the set of repressed genes (''test set'', black bars) compared with all genes detected in the RNAseq experiment (reference set, grey bars). Black bars represent the percentage of induced gene (A) or repressed gene (B) in the test set, for a given GO terms. The grey bars represent the percentage of gene for a given GO terms in the reference set. The statistical test was considered significant at the 1% error level.
doi:10.1371/journal.pone.0058652.g003

two encoded tyrosine protein kinase while the other two genes encoded serine/threonine protein kinases. These four genes were downregulated at pH 7.4 and 7.2 (between 22.01 and 1.82 fold decrease). For a complete description of candidate genes expression see the Figure 4 and File S3.

Discussion

Validation of the RNAseq approach to the study of coral responses to low pH

An RNAseq approach was used to compare the transcriptomes of corals maintained under seawater pH conditions with those of corals exposed to pH 7.4 (an extreme value of today or near future natural variability) for a 3-weeks period. Based on our reference transcriptome, the constant expression of 84% of the genes evidenced that *Pocillopora damicornis* transcriptome is not completely disturbed by the treatment and that its response to pH 7.4 is mediated by the modification of 16% of its transcriptome. Complementary analysis of these 16% of genes allowed us to identity several molecular pathways and candidate genes putatively involved in the response to low pH. In order to better understand the response of these affected biological functions at a pH 7.8 and 7.2, we measured the transcript abundance of genes belonging to these affected functions by q-RT-PCR method.

The quantification of gene expression by RNAseq requires a reference genome/transcriptome for the mapping step [53]. However, such molecular data are scarce, especially for non-model species. This explains why few global transcriptomic analyses have been undertaken using non-model species. Among scleractinian corals such analyses were only possible for a few species such as *Acropora millepora* and *A. digitifera* because their transcriptome or genome data were available [27,63,64]. Recent progress in the development of next generation sequencing made it possible to deal with this problem. In a two-step process, the sequences obtained under different physiological conditions were first used to assemble the transcriptome. Secondly, the sequences for each condition were used for quantification of gene expression. The use of transcripts from different environmental conditions allowed us also to cover the largest possible range of mRNAs resulting from differential transcription and alternative splicing [65,66]. Comparison of the quantitative data obtained using the RNAseq and the q-RT-PCR approaches (the latter performed on 25 arbitrarily selected genes) showed a significant correlation between these two methods of quantification. The correlation obtained ($r^2 = 0.86$) is comparable to those reported in other studies by Oliver and collaborators [67], $r^2 = 0.83$; Wang and collaborators [68], $r^2 = 0.83$; Castruita and collaborators [69], $r^2 = 0.95$; and Meyer and collaborators [27] $r^2 = 0.74$). This confirms that the two-step RNAseq approach we used is suitable for measuring gene expression in corals exposed to various environmental conditions.

Specific upregulation of biological functions under low pH

The overall pattern of gene expression showed that 6% of the genes were significantly upregulated during exposure to pH 7.4 compared to pH 8.1. One important finding is that genes coding for organic matrix proteins and proteins involved in the transport of Ca^{2+} and HCO_3^- are modulated under low pH conditions, suggesting that low pH affects the calcification process at the transcriptomic level. We showed that genes coding for HCO_3^- and Ca^{2+} transporters and carbonic anhydrases were upregulated at low pH values (7.8 and 7.4) but downregulated at the extreme level of pH 7.2 (Figure 4). A similar effect was observed for genes encoding skeletal organic matrix proteins (similar to BMP1 and BMP7 of the bone morphogenic protein superfamily, and the galaxin superfamily).

These results contrasts with some of those obtained in two recent works: one studying by RNAseq the short term (3 days exposure) response of *Acropora millepora* primary polyps to pH 7.96 and 7.86 compared to pH 8.16 [23], and the second one studying by microarray the short and midterm (1 day and 28 days) responses of adults *A. millepora* to pH 7.85 and 7.65 compared to pH 8.1 [17]. Among these three studies, if the two using *A. millepora* as a model species are the most realistic in terms of pH exposure (pH~7.9), ours offer the opportunity to study the response to pH below 7.6 (7.4 and 7.2), which can exacerbate the transcriptomic response. Concerning the comparison with the study of Moya and collaborators [23], in condition where pH

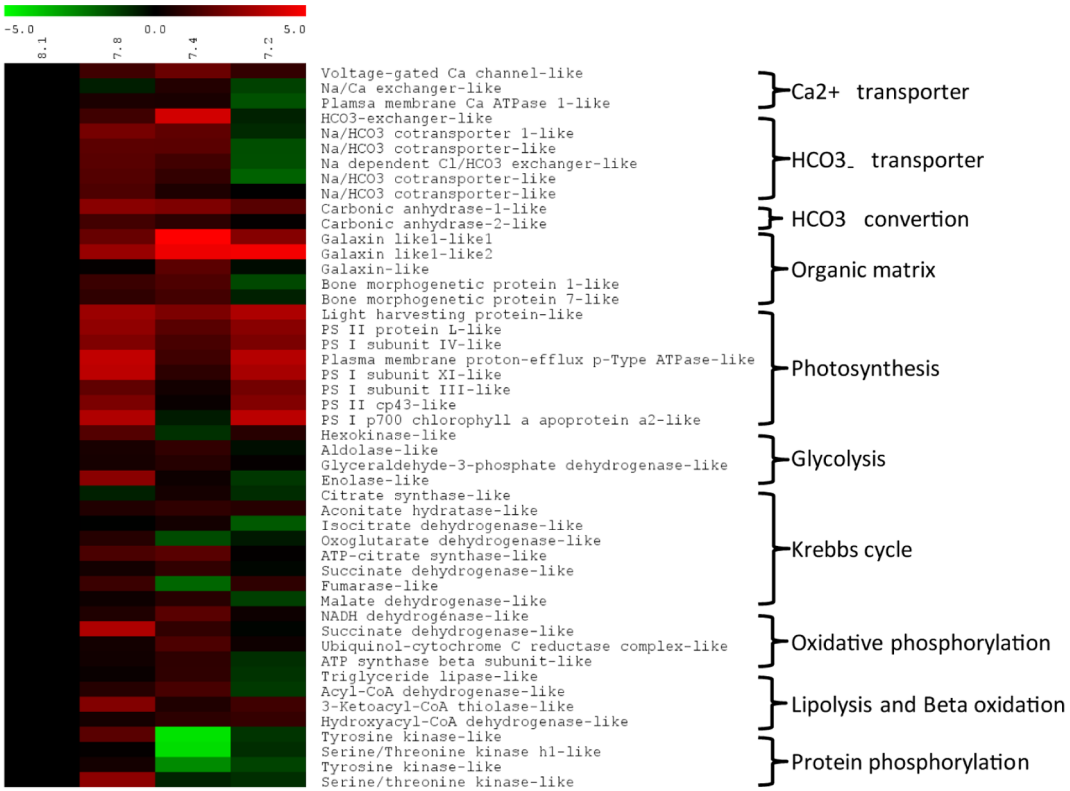

Figure 4. Gene expression for key biological functions following exposure to various pH levels for three weeks. The data included q-RT-PCR results for samples exposed to pH 7.8 and 7.2, and RNAseq results for samples exposed to pH 7.4. Quantification was normalized by comparison with results for exposure to pH 8.1 (present seawater pH); the results are presented as a log2 fold change in expression.
doi:10.1371/journal.pone.0058652.g004

between studies is the closest (7.8), their results are in agreement with ours for the genes coding for Ca^{2+} transporters and Galaxin-like protein. However, carbonic anhydrase and some organic matrix encoding genes are downregulated in their experiment while it is the contrary in ours. These contradictions are not surprising since we worked at a different time-scale, on a different species and on adult corals whereas they worked on early aposymbiotic life stages. However, even when considering the same species *A. millepora*, Moya and collaborators [23] have obtained results different from the ones obtained by Kaniewska and collaborators [17]. For example, the genes coding for organic matrix proteins (such as galaxin) clearly shows that effect of pCO_2 is dependent on the life stage. Then differences obtained between our study and the study of Kaniewska and collaborators [17] mainly concern the opposite pattern of expression for the metabolic related genes. Indeed, we measured upregulation while they highlight downregulation. In this last case the contradiction reported may be the results of i) phylogenetic differences (*Acropora* belongs to the "complex" coral clade whereas *Pocillopora* belongs to the "robust" coral clade; [24,25]), ii) and/or experimental protocol differences (light and nutrition were different in the two studies) iii) and/or differences in previous life history (corals are from different geographical origin). Such differences in the response of marine invertebrates belonging to the same phyla were also previously described. In the sea urchin group, *Paracentrotus lividus* and *Strongylocentrotus purpuratus* larvae showed mixed transcriptomic responses for ortholog genes when larvae are submitted to a comparable exposition to low pH. In *S.purpuratus* the genes involved in calcification processes msp130 and SM30 were down-regulated at pH 7.7 [70], while the same gene in *P. lividus* were not at pH 7.7, but up-regulated at pH 7.0 [71]. In coccolithophores, a decreasing calcification between ancient (past 400 years) and actual specimens was shown [72]. However they also discovered a heavily calcified coccolithophore in modern water with low pH, *Emiliana* huxleyi morphotype evidencing variation in responses of phyla to environmental forcing factors [72]. In the case of marine mollusks, low pH induced mainly a decrease of calcification both at the transcriptomic and the animal level, but some exceptions were reported [73–77]. These data highlight the difficulties to extrapolate the results obtained from one species to the whole phylum.

In our study, we hypothesize that the upregulation of genes encoding proteins involved in ion transport counteract the negative effect of low pH on the calcification process (Figure 5). If the aragonite saturation state (Ω_{arag}) decreased in the extracellular calcifying medium (ECM) due to a decreasing pH in the ECM [78,79], the upregulation of ion transporters would allow to increase ion concentration and to maintain the same calcification efficiency in a less favorable pH conditions (Figure 5). Upregulation of genes involved in ion transport could indeed help to increase the saturation state of aragonite, which depends on the concentration of Ca^{2+} and CO_3^{2-} (Figure 5). The increase in expression of genes coding for organic matrix proteins needs to be further investigated. However, we postulate that they may modify nucleation, crystal growth inhibition and orientation, and because of their negative charge help to locally increase Ω_{arag} by trapping Ca^{2+} ions [1,56]. It is also possible that the relative composition of the skeleton (inorganic versus organic matrix) could change under low pH; an increase in the organic matrix proportion could help sustain coral growth (Figure 5). In

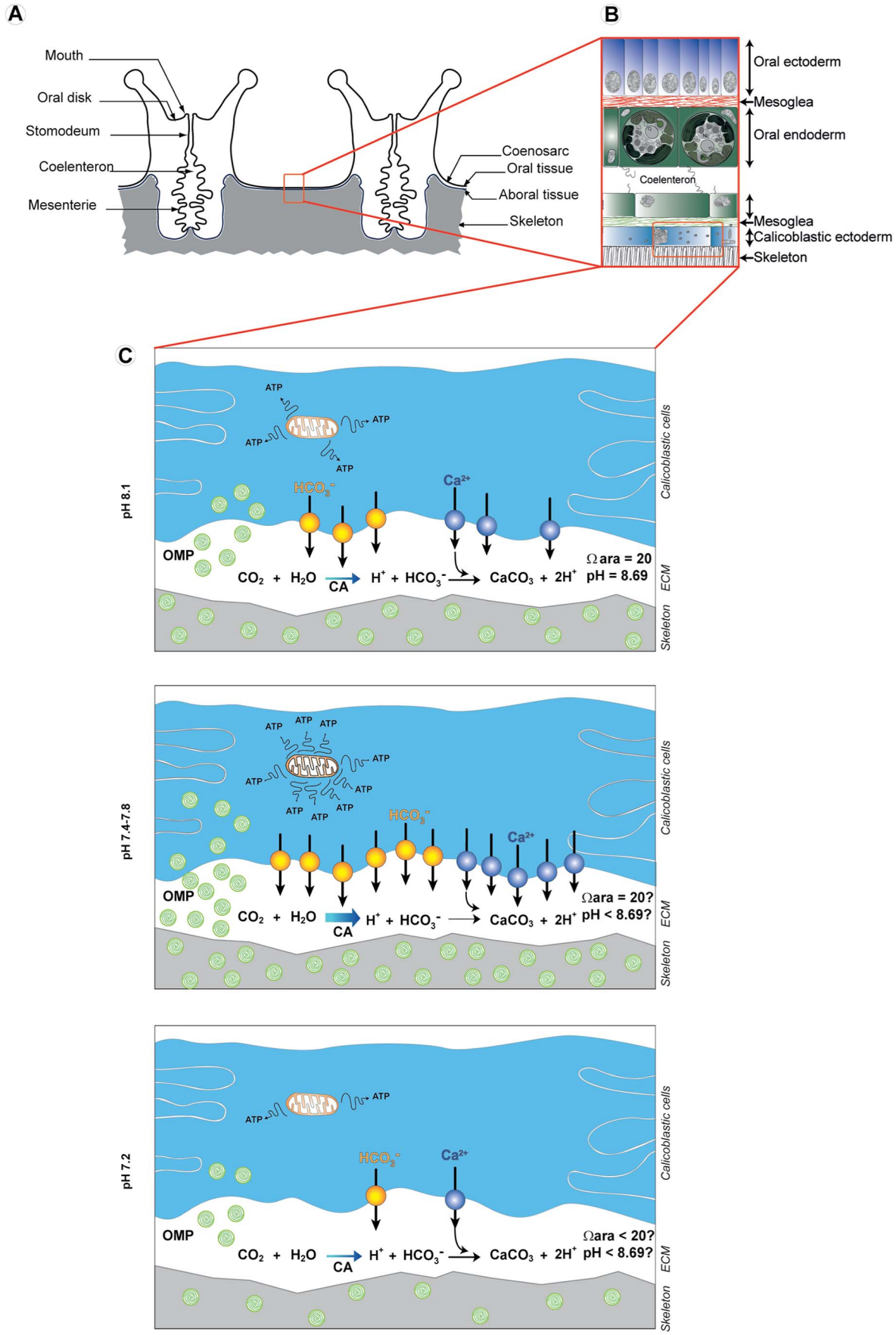
A
Mouth
Oral disk
Stomodeum
Coelenteron
Mesenterie
Coenosarc
Oral tissue
Aboral tissue
Skeleton
B
Oral ectoderm
Mesoglea
Oral endoderm
Coelenteron
Mesoglea
Calicoblastic ectoderm
Skeleton
C
pH 8.1
ATP
HCO3-
Ca2+
OMP
CO2 + H2O
CA
H+ + HCO3-
CaCO3 + 2H+
Ωara = 20
pH = 8.69
Calicoblastic cells
ECM
Skeleton
pH 7.4-7.8
Ωara = 20?
pH < 8.69?
pH 7.2
Ωara < 20?
pH < 8.69?

Figure 5. Schematic representation of key biological processes regulated under different levels of low pH. A) Anatomy of two polyps of a coral colony. B) Representation of the coenosarc composed of the oral and aboral tissues. C) Magnification of the calicoblastic ectoderm showing the calicoblastic cells with the up and downregulation of the key biological processes at different pH. At pH 7.8 or 7.4, Ca^{2+} and HCO_3^- transport to the extracellular calcifying medium (ECM) increase through an increasing number of Ca^{2+} and HCO_3^- transporters. The rate of CO_2 conversion to HCO_3^- increases through an upregulation of carbonic anhydrase (CA). Production and secretion of organic matrix protein (OMP round green shape) also increase. This process may help to maintain a sufficient aragonite saturation state (Ω_{arag}) despite a decrease in pH, enabling to maintain the same calcification in less favorable pH conditions. This process is energetically costly and need an increase in energy production (ATP) through an increasing metabolic activity and a general trade off mechanism. Finally, at a pH 7.2, the coral cannot cope anymore with such a low pH and there could be a physiological collapse of the colony. Values of omega aragonite (Ω) and pH in the ECM at pH 8.1 are from [97].
doi:10.1371/journal.pone.0058652.g005

summary, the concomitant and putative additive effect of the increase in ion transport and deposition of organic matrix proteins may help *P. damicornis* to cope with low pH exposure (Figure 5). This hypothesis is supported by recent studies performed on marine calcifying invertebrates at several levels of organization. In larvae of the sea urchin *P. lividus*, there was no effect of low pH on the calcification rate at the organism level with an upregulation of biomineralization related genes at the transcriptomic level [71]. In the mollusk *Mytilus edulis* exposed to low pH, gene transcription of a tyrosinase putatively involved in the periostracum formation was strongly upregulated and organic matrix protein coding gene remained expressed at a high level. Both mechanisms were associated to the protection and the maintenance of shell formation [74]. In the red abalone *Haliothis rufescens*, organic matrix protein coding genes remained expressed at a high level during exposure to low pH [80]. At the organism level examples of calcification increase were reported in several organisms such as *Crepidula fornicata*, *Arbacia punctulata* [77]. Finally, a recent work on the coral *Stylophora pistillata* has shown that between pH 8.1 and pH 7.4, the animal controls sufficiently the pH in the ECM to allow the maintenance of calcification [81]. Even if all these examples strengthen our hypothesis, it should be confirmed in *P. damicornis* further by direct quantification of skeletal Ca_2^+ incorporation, organic matrix skeletal content, and measurements of pH in the ECM.

In tropical corals energy is supplied by prey capture (heterotrophic nutrition) and translocation of photosynthates from symbionts to their host [82]. The upregulation of genes involved in heterotrophic and autotrophic pathways may reflect an increase in coral energetic requirements under low pH stress. In this context, it is known that calcification is an energetically costly process consuming up to 30% of the daily energy budget [1]; the need to maintain calcification under stress conditions could in part explain the increase in energetic needs and energy production (Figure 5). In this context, the upregulation of lipolysis and beta-oxidation metabolic pathways shows that corals may use their fatty acid reserves under low pH conditions. However, these reserves are not inexhaustible and should be replenished, whereas global climate change is predicted to cause a decrease in ocean primary production [5,83,84]. Thus, it is uncertain whether corals can maintain their energy production from heterotrophic and autotrophic resources when primary production is predicted to decrease.

Usually high CO_2 concentration driving seawater pH decrease is known to induce bleaching of photosymbiotic organisms such as reef-building coral and foraminifera [17,22,85], even if the photophysiology of the phototrophic symbiont shows mixed responses to this treatment (see introduction section). Our study is the first to show the upregulation of several photosynthetic related genes at pH<8.1. The lack of photophysiological data in the present study makes it difficult to interpret such upregulations but argue in favor of an increasing photosynthetic capability of the holobiont *P. damicornis* under pH of 7.8, 7.4 and 7.2. Such a positive effect of high CO_2 concentration on photosymbiotic species just begins to be revealed in the literature. Indeed, the acoel worm *Symsagittifera roscoffensis* entering in symbiosis with the microalgae *Tetraselmis convolutae* shows a remarkable symbiosis stability even at a very low pH level (up to pH 6) [86]. In a second example, the sea anemone *Anthopleura elegantissima*/*Symbiodinium muscatinei* photosymbiosis, high pCO_2 level (pH 8.08 and pH 7.35) induces a higher rate of photosynthesis and mitotic index of the algae compared to pH 8.1 [87]. Under such conditions the cnidarian host received more of their respiratory carbon from the symbiont that under the actual pH condition [87]. These results taking together confirmed the hypothesis that photosymbiosis could be resistant to high pCO_2, and that the negative effect of this high pCO_2 could be the results of indirect impact at other levels (hypothesis proposed in [86]).

Uncoordinated downregulation of biological functions under low pH

During exposure to pH 7.4 compared to 8.1, 10% of genes were downregulated and 6% were upregulated. Although more genes were downregulated, the enrichment analysis shows that the upregulation of genes was more readily explained and informative. A total of 32 biological functions were upregulated under low pH conditions ($p>0.01$), while only 1, the 'cellular macromolecule metabolic process' was downregulated (Fig. 3; $p>0.01$) despite a comparable number of contigs with a Gene Ontology term (1696 for the downregulated set, 1495 for the upregulated set). Such a results may reflect that the downregulation measured are un or less coordinated than the upregulation. This kind of uncoordinated downregulation of genes has been reported in several other animal species exposed to stress [88–90]. A similar response was also observed in the coral *Montastraea faveolata* subject to thermal stress [91]. Downregulation could reflect a trade-off mechanism induced by the low pH treatment, providing energy savings necessary for efficient stress responses (Figure 5). This hypothesis is supported by the results of the q-RT-PCR experiments performed on selected host genes. Indeed, the level of downregulation increased concomitantly with the pH level. At pH 7.2 the downregulation was maximal and, as it has been observed and hypothesized in other species subjected to extreme physiological stress conditions, this may reflect a trade-off mechanism [89,91–94].

Post-translational protein modification was one of the biological functions downregulated (GO term enrichment analysis, $p<0.05$) during low pH treatment, as evidenced by the substantial downregulation of several genes encoding protein kinases (serine/threonine kinase and tyrosine kinase). Protein kinases phosphorylate proteins to modulate their activity, and play key roles in signal transduction pathways [95]. The four protein kinases selected for q-RT-PCR analysis showed similar patterns of expression, with upregulation occurring at pH 7.8 and downregulation occurring at pH 7.4 and 7.2. This variable pattern of transcription could reflect the disturbance or molecular plasticity of signaling in coral cells under stress. Such results are strengthened by a proteomic study of the barnacle *Balanus amphitrite* exposed to low pH. Indeed, under low pH condition

the phosphoproteome is modified revealing a regulation of kinase activity and/or synthesis [96]. The biological effects of all these downregulation events were difficult to resolve because of the very large number of pathways in which kinases are involved, and this will require further study.

Supporting Information

File S1 Biological function, annotation, BlastX top hit species, BlastX evalue, contig number and primer sequence of the selected candidate genes.
(DOCX)

File S2 Table results of the GO term enrichment analysis.
(DOCX)

File S3 Numerical value corresponding to the qRT-PCR. Quantification was normalized by comparison with results for exposure to pH 8.1 (present seawater pH); the results are presented as a log2 fold change in expression.
(DOCX)

Acknowledgments

We thank Mark Dasenko, Chris Sullivan, and Matthew Peterson at the OSU CGRB core facility for assistance with Illumina sequencing. The authors thank Julie Lepesant for her help with R. We thank Michael Holcomb for helping in carbonate seawater chemistry. We thank anonymous reviewers for their very helpful comments.

Author Contributions

Conceived and designed the experiments: JV-D DZ ET CG CC KMS MF DA ST. Performed the experiments: JV-D DZ ET CG CC KMS MF NMD. Analyzed the data: JV-D DZ CG CC KMS MF NMD DA ST. Contributed reagents/materials/analysis tools: ET CG CC KMS MF. Wrote the paper: JV-D DA ST.

References

1. Allemand D, Tambutté E, Zoccola D, Tambutté S (2011) Coral calcification, cells to reefs. In: Dubinsky Z, Stambler N, editors. Coral reefs: an ecosystem in transition. New York: Springer. 119–150.
2. Wilkinson C (2008) Status of coral reefs of the world. In: Wilkinson C, editor. Status of Coral Reefs of the World. Townsville: Global Coral Reef Monitoring Network and Reef and Rainforest Research Center. 296.
3. Bellwood DR, Hughes TP, Folke C, Nyström M (2004) Confronting the coral reef crisis. Nature 429: 827–833.
4. De'ath G, Lough JM, Fabricius KE (2009) Declining coral calcification on the Great Barrier reef. Science 323(5910): 116–119.
5. Hoegh-Guldberg O, Bruno JF (2010) The impact of climate change on the world's marine ecosystems. Science 328(5985): 1523–1528.
6. Albright R, Mason B, Miller M, Langdon C (2011) Ocean acidification compromises recruitment success of the threatened Caribbean coral *Acropora palmata*. Proc Natl Acad Sci USA 107(47): 20400.
7. Cohen AL, McCorkle DC, de Putron S, Gaetani GA, Rose KA (2009) Morphological and compositional changes in the skeletons of new coral recruits reared in acidified seawater: Insights into the biomineralization response to ocean acidification. Geochem Geophys Geosyst 10(7).
8. Erez J, Reynaud S, Silverman J, Schneider K, Allemand D (2011) Coral calcification under ocean acidification and global change. In: Dubinsky Z, Stambler N, editors. Coral Reefs: An Ecosystem in Transition. New York: Springer. 151–176.
9. Iguchi A, Ozaki S, Nakamura T, Inoue M, Tanaka Y, et al. (2012) Effects of acidified seawater on coral calcification and symbiotic algae on the massive coral *Porites australiensis*. Mar Environ Res 73: 32–36.
10. Inoue M, Suwa R, Suzuki A, Sakai K, Kawahata H (2011) Effects of seawater pH on growth and skeletal U/Ca ratios of *Acropora digitifera* coral polyps. Geophysical Research Letters 38(12): L12809.
11. Krief S, Hendy EJ, Fine M, Yam R, Meibom A, et al. (2010) Physiological and isotopic responses of scleractinian corals to ocean acidification. Geochim Cosmochim Acta 74(17): 4988–5001.
12. Langdon C, Atkinson MJ (2005) Effect of elevated pCO_2 on photosynthesis and calcification of corals and interactions with seasonal change in temperature/irradiance and nutrient enrichment. J Geophys Res 110(C9): C09S07.
13. Leclercq N, Gattuso JP, Jaubert J (2002) Primary production, respiration, and calcification of a coral reef mesocosm under increased CO_2 partial pressure. Limnol Oceanogr 47(2): 558–564.
14. Marubini F, Ferrier-Pages C, Furla P, Allemand D (2008) Coral calcification responds to seawater acidification: a working hypothesis towards a physiological mechanism. Coral Reefs 27(3): 491–499.
15. Ries JB, Cohen AL, McCorkle DC (2009) Marine calcifiers exhibit mixed responses to CO2-induced ocean acidification. Geology 37(12): 1131.
16. Houlbrèque F, Rodolfo-Metalpa R, Jeffree R, Oberhänsli F, Teyssiè JL, et al. (2012) Effects of increased pCO_2 on zinc uptake and calcification in the tropical coral *Stylophora pistillata*. Coral Reefs 31(1): 1–9.
17. Kaniewska P, Campbell PR, Kline DI, Rodriguez-Lanetty M, Miller DJ, et al. (2012) Major cellular and physiological impacts of ocean acidification on a reef-building coral. PLoS ONE 7(4): e34659.
18. Reynaud S, Leclercq N, Romaine-Lioud S, Ferrier-Pagès C, Jaubert J, et al. (2003) Interacting effects of CO_2 partial pressure and temperature on photosynthesis and calcification in a scleractinian coral. Glob chang biol 9(11): 1660–1668.
19. Fabricius KE, Langdon C, Uthicke S, Humphrey C, Noonan S, et al. (2011) Losers and winners in coral reefs acclimatized to elevated carbon dioxide concentrations. Nat Clim Chang 1(3): 165–169.
20. Rodolfo-Metalpa R, Houlbrèque F, Tambuttè E, Boisson F, Baggini C, et al. (2011) Coral and mollusc resistance to ocean acidification adversely affected by warming. Nat Clim Chang 1(6): 308–312.
21. Fine M, Tchernov D (2007) Scleractinian coral species survive and recover from decalcification. Science 315(5820): 1811.
22. Anthony KRN, Kline DI, Diaz-Pulido G, Dove S, Hoegh-Guldberg O (2008) Ocean acidification causes bleaching and productivity loss in coral reef builders. Proc Natl Acad Sci USA 105(45): 17442–17446.
23. Moya A, Huisman L, Ball EE, Hayward DC, Grasso LC, et al. (2012) Whole transcriptome analysis of the coral *Acropora millepora* reveals complex responses to CO_2-driven acidification during the initiation of calcification. Mol Ecol 21(10): 2440–2454.
24. Kitahara MV, Cairns SD, Stolarski J, Blair D, Miller DJ (2010) A comprehensive phylogenetic analysis of the Scleractinia (Cnidaria, Anthozoa) based on mitochondrial CO1 sequence data. PloS ONE 5(7): e11490.
25. Romano SL, Cairns SD (2000) Molecular phylogenetic hypotheses for the evolution of scleractinian corals. Bull Mar Sci 67(3): 1043–1068.
26. Franssen SU, Gu J, Bergmann N, Winters G, Klostermeier UC, et al. (2011) Transcriptomic resilience to global warming in the seagrass *Zostera marina*, a marine foundation species. Proc Natl Acad Sci USA 108(48): 19276–19281.
27. Meyer E, Aglyamova GV, Matz MV (2011) Profiling gene expression responses of coral larvae (*Acropora millepora*) to elevated temperature and settlement inducers using a novel RNA-Seq procedure. Mol Ecol 20(17): 3599–3616.
28. Runcie DE, Garfield DA, Babbitt CC, Wygoda JA, Mukherjee S, et al. (2012) Genetics of gene expression responses to temperature stress in a sea urchin gene network. Mol Ecol 21(18): 4547–4562.
29. Veron JEN (2000) Corals of the World; Stafford-Smith M, editor. Townsville: Australian Institute of Marine Science. 463 p.
30. Manzello DP (2010) Ocean acidification hot spots: Spatio-temporal dynamics of the seawater $C0_2$ system of eastern Pacific coral reefs. Limnol Oceanogr 55(1): 239.
31. Ben-Haim Y, Rosenberg E (2002) A novel *Vibrio* sp. pathogen of the coral *Pocillopora damicornis*. Mar Biol 141: 47–55.
32. Hashimoto K, Shibuno T, Murayama-Kayano E, Tanaka H, Kayano T (2004) Isolation and characterization of stress-responsive genes from the scleractinian coral *Pocillopora damicornis*. Coral Reefs 23: 485–491.
33. Loya Y, Sakai K, Yamazato K, Nakano Y, Sambali R, et al. (2001) Coral bleaching: the winners and the losers. Ecol Lett 4(2): 122–131.
34. Gagliano M, McCormick M, Moore J, Depczynski M (2010) The basics of acidification: baseline variability of pH on Australian coral reefs. Mar Biol 157(8): 1849–1856.
35. Santos IR, Glud RN, Maher D, Erler D, Eyre BD (2011) Diel coral reef acidification driven by porewater advection in permeable carbonate sands, Heron Island, Great Barrier Reef. Geophysical Research Letters 38(3): L03604.
36. Dickson AG, Sabine CL, Christian JR (2007) Guide to best practices for ocean CO_2 measurements. PICES Special Publication 3: 191.
37. van Heuven S, Pierrot D, Lewis E, Wallace DWR (2009) MATLAB Program developed for CO_2 system calculations.
38. Mehrbach C, Culberson CH, Hawley JE, Pytkowicz RM (1973) Measurement of the apparent dissociation constants of carbonic acid in seawater at atmospheric pressure. Limnol Oceanogr 18: 897–907.
39. Dickson AG, Millero FJ (1987) A comparison of the equilibrium constants for the dissociation of carbonic acid in seawater media. Deep-Sea Res 34(1733–1743).
40. Vidal-Dupiol J, Ladrière O, Meistertzheim AL, Fouré L, Adjeroud M, et al. (2011) Physiological responses of the scleractinian coral *Pocillopora damicornis* to bacterial stress from *Vibrio coralliilyticus*. J Exp Biol 214: 1533–1545.

41. Traylor-Knowles N, Granger B, Lubinski T, Parikh J, Garamszegi S, et al. (2011) Production of a reference transcriptome and a transcriptomic database (PocilloporaBase) for the cauliflower coral, *Pocillopora damicornis*. BMC Genomics 12(1): 585.
42. Moya A, Tambutté S, Bertucci A, Tambutté E, Lotto S, et al. (2008) Carbonic anhydrase in the scleractinian coral *Stylophora pistillata*. J Biol Chem 283(37): 25475–25484.
43. Fox S, Sergei F, Mockler TC (2010) Applications of ultra-hignt-throughput sequencing. In: Belostotky DA, editor. Plant systems Biology. New York: Humana Press. 79–108.
44. Pomraning KR, Smith KM, Bredeweg EL, Phatale PA, Connolly LR, et al. (2012) Paired-end library preparation for rapid genome sequencing. Fungal Secondary Metabolism. New York: Humana Press.
45. Pomraning KR, Smith KM, Freitag M (2009) Genome-wide high throughput analysis of DNA methylation in eukaryotes. Methods 47: 142–150.
46. Zerbino DR (2010) Using the Velvet de novo Assembler for Short-Read Sequencing Technologies: John Wiley & Sons, Inc. 1–12 p.
47. Schulz MH, Zerbino DR, Vingron M, Birney E (2012) Oases: Robust de novo RNA-seq assembly across the dynamic range of expression levels. Bioinformatics.
48. Sutton GG, White O, Adams MD, Kerlavage AR (1995) TIGR Assembler: A new tool for assembling large shotgun sequencing projects. Genom Sci Tech 1(1): 9–19.
49. Conesa A, Götz S, Garcia-Gomez JM, Terol J, Talon M, et al. (2005) Blast2GO: a universal tool for annotation, visualization and analysis in functional genomics research. Bioinformatics 21(18): 3674–3676.
50. Sabourault C, Ganot P, Deleury E, Allemand D, Furla P (2009) Comprehensive EST analysis of the symbiotic sea anemone *Anemonia viridis*. BMC Genomics 10(1): 333.
51. Pati A, Heath LS, Kyrpides NC, Ivanova N (2011) ClaMS: A Classifier for Metagenomic Sequences. Stand Genom Sci 5(2): 248.
52. Li H, Durbin R (2009) Fast and accurate short read alignment with Burrows-Wheeler transform. Bioinformatics 25(14): 1754–1760.
53. Mortazavi A, Williams BA, McCue K, Schaeffer L, Wold B (2008) Mapping and quantifying mammalian transcriptomes by RNA-Seq. Nat Methods 5(7): 621–628.
54. Wang L, Feng Z, Wang X, Wang X, Zhang X (2010) DEGseq: an R package for identifying differentially expressed genes from RNA-seq data. Bioinformatics 26(1): 136–138.
55. Bluthgen N, Brand K, Cajavec B, Swat M, Herzel H, et al. (2004) Biological profiling of gene groups utilizing Gene Ontology. Arxiv preprint q-bio/0407034.
56. Tambutté S, Holcomb M, Ferrier-Pagès C, Reynaud S, Tambutté E, et al. (2011) Coral biomineralization: from the gene to the environment. J Exp Mar Biol Ecol 408(1): 58–78.
57. Bertucci A, Tambutté S, Supuran C, Allemand D, Zoccola D (2011) A new coral carbonic anhydrase in *Stylophora pistillata*. Mar Biotechnol 13(5): 992–1002.
58. Moya A, Ferrier-Pagès C, Furla P, Richier S, Tambutté E, et al. (2008) Calcification and associated physiological parameters during a stress event in the scleractinian coral *Stylophora pistillata*. Comp Biochem Physiol A-Mol Integr Physiol 151(1): 29–36.
59. Zoccola D, Tambutte E, Kulhanek E, Puverel S, Scimeca JC, et al. (2004) Molecular cloning and localization of a PMCA P-type calcium ATPase from the coral *Stylophora pistillata*. Biochim Biophys Acta 1663: 117–126.
60. Fukuda I, Ooki S, Fujita T, Murayama E, Nagasawa H, et al. (2003) Molecular cloning of a cDNA encoding a soluble protein in the coral exoskeleton. Biochem Biophys Res Commun 304(1): 11–17.
61. Reyes-Bermudez A, Lin Z, Hayward D, Miller D, Ball E (2009) Differential expression of three galaxin-related genes during settlement and metamorphosis in the scleractinian coral *Acropora millepora*. BMC Evol Biol 9(1): 178.
62. Zoccola D, Moya A, Béranger G, Tambutté E, Allemand D, et al. (2009) Specific expression of BMP2/4 ortholog in biomineralizing tissues of corals and action on mouse BMP receptor. Mar Biotechnol 11(2): 260–269.
63. Meyer E, Aglyamova G, Wang S, Buchanan-Carter J, Abrego D, et al. (2009) Sequencing and de novo analysis of a coral larval transcriptome using 454 GSFlx. BMC Genomics 10(1): 219.
64. Shinzato C, Shoguchi E, Kawashima T, Hamada M, Hisata K, et al. (2011) Using the *Acropora digitifera* genome to understand coral responses to environmental change. Nature 476: 320–323.
65. Robinson JL, Hall JR, Charman M, Ewart KV, Driedzic WR (2011) Molecular analysis, tissue profiles, and seasonal patterns of cytosolic and mitochondrial GPDH in freeze-resistant rainbow smelt (*Osmerus mordax*). Physiol Biochem Zool 84(4): 363–376.
66. Zhu J, Dong C-H, Zhu J-K (2007) Interplay between cold-responsive gene regulation, metabolism and RNA processing during plant cold acclimation. Curr Opin Plant Biol 10(3): 290–295.
67. Oliver H, Orsi R, Ponnala L, Keich U, Wang W, et al. (2009) Deep RNA sequencing of L. monocytogenes reveals overlapping and extensive stationary phase and sigma B-dependent transcriptomes, including multiple highly transcribed noncoding RNAs. BMC Genomics 10(1): 641.
68. Wang Z, Kadouri D, Wu M (2011) Genomic insights into an obligate epibiotic bacterial predator: *Micavibrio aeruginosavorus* ARL-13. BMC Genomics 12(1): 453.
69. Castruita M, Casero D, Karpowicz SJ, Kropat J, Vieler A, et al. (2011) Systems biology approach in chlamydomonas reveals connections between copper nutrition and multiple metabolic steps. Plant Cell Onl 23(4): 1273–1292.
70. Stumpp M, Dupont S, Thorndyke MC, Melzner F (2011) CO_2 induced seawater acidification impacts sea urchin larval development II: Gene expression patterns in pluteus larvae. Comparative Biochemistry and Physiology-Part A: Molecular & Integrative Physiology 160(3): 320–330.
71. Martin S, Richier S, Pedrotti ML, Dupont S, Castejon C, et al. (2011) Early development and molecular plasticity in the Mediterranean sea urchin *Paracentrotus lividus* exposed to CO_2-driven acidification. J Exp Biol 214(8): 1357–1368.
72. Beaufort L, Probert I, de Garidel-Thoron T, Bendif EM, Ruiz-Pino D, et al. (2011) Sensitivity of coccolithophores to carbonate chemistry and ocean acidification. Nature 476(7358): 80–83.
73. Dickinson GH, Ivanina AV, Matoo OB, Pörtner HO, Lannig G, et al. (2012) Interactive effects of salinity and elevated CO_2 levels on juvenile eastern oysters, *Crassostrea virginica*. J Exp Biol 215(1): 29–43.
74. Hüning AK, Melzner F, Thomsen J, Gutowska MA, Krämer L, et al. (2012) Impacts of seawater acidification on mantle gene expression patterns of the Baltic Sea blue mussel: implications for shell formation and energy metabolism. Mar Biol: 1–17.
75. Liu W, Huang X, Lin J, He M (2012) Seawater acidification and elevated temperature affect gene expression patterns of the pearl oyster *Pinctada fucata*. PloS ONE 7(3): e33679.
76. Melzner F, Stange P, Trübenbach K, Thomsen J, Casties I, et al. (2011) Food supply and seawater pCO2 impact calcification and internal shell dissolution in the blue mussel *Mytilus edulis*. PloS ONE 6(9): e24223.
77. Ries JB, Cohen AL, McCorkle DC (2009) Marine calcifiers exhibit mixed responses to CO_2-induced ocean acidification. Geology 37(12): 1131–1134.
78. McCulloch M, Falter J, Trotter J, Montagna P (2012) Coral resilience to ocean acidification and global warming through pH up-regulation. Nat Clim Chang advance online publication.
79. McCulloch M, Trotter J, Montagna P, Falter J, Dunbar R, et al. (2012) Resilience of cold-water scleractinian corals to ocean acidification: Boron isotopic systematics of pH and saturation state up-regulation. Geochim Cosmochim Acta 87: 21–34.
80. Zippay MKL, Hofmann GE (2010) Effect of pH on gene expression and thermal tolerance of early life history stages of red abalone (*Haliotis rufescens*). J Shellfish Res 29(2): 429–439.
81. Venn A, Tambutté E, Holcomb M, Laurent J, Allemand D, et al. (in press) Impact of seawater acidification on pH at the tissue-skeleton interface and calcification in reef corals. Proc Natl Acad Sci U S A.
82. Houlbrèque F, Ferrier-Pagès C (2009) Heterotrophy in tropical scleractinian corals. Biol Rev 84(1): 1–17.
83. Doney SC, Fabry VJ, Feely RA, Kleypas JA (2009) Ocean acidification: The other CO2 problem. Annu Rev Mar Sci 1(1): 169–192.
84. Polovina JJ, Howell EA, Abecassis M (2008) Ocean's least productive waters are expanding. Geophys Res Lett 35(3): L03618.
85. Stoecker DK, Johnson MD, de Vargas C, Not F (2009) Acquired phototrophy in aquatic protists. Aquat Microb Ecol 57: 279–310.
86. Dupont S, Moya A, Bailly X (2012) Stable photosymbiotic relationship under CO_2-induced acidification in the acoel worm *Symsagittifera roscoffensis*. PloS ONE 7(1): e29568.
87. Towanda T, Thuesen EV (2012) Prolonged exposure to elevated CO_2 promotes growth of the algal symbiont *Symbiodinium muscatinei* in the intertidal sea anemone *Anthopleura elegantissima*. Biology Open 1(7): 615–621.
88. Eisen MB, Spellman PT, Brown PO, Botstein D (1998) Cluster analysis and display of genome-wide expression patterns. Proc Natl Acad Sci U S A 95(25): 14863–14868.
89. Gasch AP, Spellman PT, Kao CM, Carmel-Harel O, Eisen MB, et al. (2000) Genomic expression programs in the response of yeast cells to environmental changes. Mol Biol Cell 11(12): 4241–4257.
90. Warner JR (1999) The economics of ribosome biosynthesis in yeast. Trends Biochem Sci 24(11): 437–440.
91. Edge SE, Morgan MB, Gleason DF, Snell TW (2005) Development of a coral cDNA array to examine gene expression profiles in *Montastraea faveolata* exposed to environmental stress. Mar Pollut Bull 51(5–7): 507–523.
92. Brulle F, Mitta G, Leroux R, Lemière S, Leprêtre A, et al. (2007) The strong induction of metallothionein gene following cadmium exposure transiently affects the expression of many genes in *Eisenia fetida*: A trade-off mechanism? Comp Biochem Physiol C-Toxicol Pharmacol 144(4): 334–341.
93. Su J, Yang C, Xiong F, Wang Y, Zhu Z (2009) Toll-like receptor 4 signaling pathway can be triggered by grass carp reovirus and *Aeromonas hydrophila* infection in rare minnow *Gobiocypris rarus*. Fish Shellfish Immunol 27(1): 33–39.
94. Wang B, Li F, Dong B, Zhang X, Zhang C, et al. (2006) Discovery of the genes in response to White Spot Syndrome Virus (WSSV) infection in *Fenneropenaeus chinensis* through cDNA microarray. Mar Biotechnol 8(5): 491–500.
95. Seo J, Lee KJ (2004) Post-translational modifications and their biological functions: proteomic analysis and systematic approaches. J Biochem Mol Biol 37(1): 35–44.
96. Wong KKW, Lane AC, Leung PTY, Thiyagarajan V (2011) Response of larval barnacle proteome to CO_2-driven seawater acidification. Comp Biochem Physiol D-Genomics Proteomics 6(3): 310–321.
97. Venn A, Tambutté E, Holcomb M, Allemand D, Tambutté S (2011) Live tissue imaging shows reef corals elevate pH under their calcifying tissue relative to seawater. PloS ONE 6(5): e20013.

ANNEXE 2

Estuarine, Coastal and Shelf Science xxx (2016) 1–9

Contents lists available at ScienceDirect

Estuarine, Coastal and Shelf Science

journal homepage: www.elsevier.com/locate/ecss

Pinctada margaritifera responses to temperature and pH: Acclimation capabilities and physiological limits

Gilles Le Moullac [a], Claude Soyez [a], Oihana Latchere [a], Jeremie Vidal-Dupiol [a, *], Juliette Fremery [a], Denis Saulnier [a], Alain Lo Yat [a], Corinne Belliard [a], Nabila Mazouni-Gaertner [b], Yannick Gueguen [a, c]

[a] Ifremer, UMR 241 EIO, LabexCorail, BP 7004, 98719 Taravao, Tahiti, French Polynesia
[b] Université de la Polynésie Française, UMR 241 EIO, Campus d'Outumaoro, BP 6570, 98702 Faa'a, French Polynesia
[c] Ifremer, UMR 5244 IHPE, UPVD, CNRS, Université de Montpellier, CC 80, F-34095 Montpellier, France

ARTICLE INFO

Article history:
Received 9 July 2015
Received in revised form
16 January 2016
Accepted 15 April 2016
Available online xxx

Keywords and regional index terms:
Global change
Pearl oyster
Bioenergetic
Biomineralization
Pacific ocean
French Polynesia

ABSTRACT

The pearl culture is one of the most lucrative aquacultures worldwide. In many South Pacific areas, it depends on the exploitation of the pearl oyster *Pinctada margaritifera* and relies entirely on the environmental conditions encountered in the lagoon. In this context, assessing the impact of climatic stressors, such as global warming and ocean acidification, on the functionality of the resource in terms of renewal and exploitation is fundamental. In this study, we experimentally addressed the impact of temperature (22, 26, 30 and 34 °C) and partial pressure of carbon dioxide pCO_2 (294, 763 and 2485 μatm) on the biomineralization and metabolic capabilities of pearl oysters. While the energy metabolism was strongly dependent on temperature, results showed its independence from pCO_2 levels; no interaction between temperature and pCO_2 was revealed. The energy metabolism, ingestion, oxygen consumption and, hence, the scope for growth (SFG) were maximised at 30 °C and dramatically fell at 34 °C. Biomineralization was examined through the expression measurement of nine mantle's genes coding for shell matrix proteins involved in the formation of calcitic prisms and/or nacreous shell structures; significant changes were recorded for four of the nine (*Pmarg*-Nacrein *A1*, *Pmarg*-MRNP34, *Pmarg*-Prismalin 14 and *Pmarg*-Aspein). These changes showed that the maximum and minimum expression of these genes was at 26 and 34 °C, respectively. Surprisingly, the modelled thermal optimum for biomineralization (ranging between 21.5 and 26.5 °C) and somatic growth and reproduction (28.7 °C) appeared to be significantly different. Finally, the responses to high temperatures were contextualised with the Intergovernmental Panel on Climate Change (IPCC) projections, which highlighted that pearl oyster stocks and cultures would be severely threatened in the next decade.

1. Introduction

Since the industrial revolution, the use of fossil energy has been constantly increasing, and has already led to the emission of gigatons of greenhouse gases into the atmosphere, inducing global climate changes. This phenomenon drives significant environmental pressures through global warming and ocean acidification. The former has already been materialised by a global ocean temperature increase of 0.7 °C, and the second through the loss of 0.1 pH units (Hoegh-Guldberg et al., 2007). The latest Intergovernmental Panel on Climate Change (IPCC) report highlights that, under all scenarios of greenhouse gas emission for the next century, the sea surface temperature will continue to increase from about +1 °C to +2.5 °C by the horizon 2081–2100 in tropical areas (IPCC, 2014). Concomitantly to the worsening of global warming, ocean surface water will lose an additional 0.1 pH units under the most optimistic scenario and 0.4 pH units under the most pessimistic one (IPCC, 2014).

The main scientific concerns about the effect of ocean acidification were about its putative negative effect on the ability of marine calcifiers to maintain the processes of biomineralization. Indeed, several experimental, ecophysiological and molecular

* Corresponding author. Address: Ifremer, BP 7004, 98719 Taravao, Tahiti, French Polynesia.
E-mail address: jeremie.vidal.dupiol@ifremer.fr (J. Vidal-Dupiol).

http://dx.doi.org/10.1016/j.ecss.2016.04.011
0272-7714/

studies have shown that a low pH can decrease the calcification rate and skeletal growth of these organisms (Kroeker et al., 2010; Ries et al., 2009). However, others have reported the absence of effects, or even an increase in biomineralization activity (Kroeker et al., 2010; Ries et al., 2009). These contrasting results were also confirmed in ecosystems naturally subjected to low pH levels because of CO_2 vents (Fabricius et al., 2011; Rodolfo-Metalpa et al., 2011). Another important concern linked to the increase of partial pressure of carbon dioxide (pCO_2) is the induction of hypercapnia and its subsequent metabolic deregulation. While its effects on marine vertebrates have been studied to some extent (Ishimatsu et al., 2005; Pörtner et al., 2005), little is known about the ecophysiological impacts of pCO_2 increase on invertebrates. Some recent studies suggest that ocean acidification exerts a negative effect on the energetic balance of marine invertebrates (Stumpp et al., 2011; Zhang et al., 2015), which would directly affect populations through various biological and ecological processes such as a the reduction of reproduction efficiency (Kurihara, 2008). However, counter examples exist (Thomsen et al., 2013; Zhang et al., 2015). Addressed from various methodologies and organisation scales, the main answer to the question resulting from ocean acidification was that the physiological and molecular responses could not be generalised to all phyla or functional groups, and thus, were species-and even life stage-specific.

In ectotherms, many biological processes, such as development and survival, are subject to temperature. All species have an optimal thermal window with both upper and lower limits of tolerance, which allows them to acquire energy for growth and reproduction. Beyond this thermal window, the conditions are not met for proper development. At low temperatures, the energy acquisition is low; at high temperatures, energy consumption is higher than the energy gained. Temperature directly regulates the metabolism of ectotherms, with increasing growth rates as temperatures rises; however, warming directly affects individuals that struggle to maintain cardiac function and respiration in the face of increased metabolic demand (Neuheimer et al., 2011; Pörtner et al., 2007).

In this environmental context, many human activities supported by marine calcifiers could be considered endangered. Among these marine calcifiers is the pearl oyster *Pinctada margaritifera*. This marine bivalve has a significant aesthetic, patrimonial and commercial value, particularly in relation to pearl production, tourism and international standing. In this context, the aim of the present study is to characterise, at the bioenergetic and biomineralization levels, the impacts of climate change (global warming and ocean acidification) on the pearl oyster (*P. margaritifera*). To address this aim, oysters were subjected to an acidification (pH 8.2, 7.8 and 7.4) cross-temperature (22, 26, 30 and 34 °C) experiment. The impacts of treatments were quantified at the bioenergetic and the biomineralization levels. Finally, the results obtained were contextualised with the prediction of environmental changes to lay the foundation for the first projection of the future of *P. margaritifera* in the northern lagoons of French Polynesia.

2. Material and methods

2.1. Rearing system, temperature and pH control

The rearing system was set up in an experimental bivalve hatchery operated by Ifremer in Vairao, Tahiti, French Polynesia. The facility is supplied with filtered seawater from the Vairao lagoon. The pearl oysters were placed in 500 L tanks with controlled flow-through. Seawater was renewed at the rate of 100 L h^{-1} for all the experiments. The pearl oysters were fed with the microalgae *Isochrysis galbana* supplied continuously using Blackstone dosing pumps (Hanna). A constant concentration of 25,000-cell mL^{-1} was maintained throughout the experiment. Temperature and algae concentration were controlled continuously by a fluorescence probe (Seapoint Sensor Inc.) and a temperature sensor (PT 100). Seawater was heated by an electric heater or cooled with a heat exchanger (calorie exchange with cold freshwater) plugged into a sensor. Both apparatuses were operated by a temperature controller. The pH was manipulated in flow-through tanks by bubbling CO_2 until the pH target was reached. This was operated by pH electrodes and temperature sensors connected to a pH-stat system (Dennerle) that continuously monitored pH (calibrated to NIST scale) and temperature to control CO_2 bubbling.

2.2. Carbonate chemistry

Total alkalinity (TA) was measured via titration with 0.01 N of HCl containing 40.7 g NaCl L^{-1} using a Titrator (Schott Titroline Easy). Parameters of carbonate seawater chemistry were calculated from pH, mean TA, temperature, and salinity using the free access CO_2 Systat package (van Heuven et al., 2009). Targeted values were pH 7.4 (3667 μatm CO_2), pH 7.8 (1198 μatm CO_2) and the control at pH 8.2 (426 μatm CO_2). Parameters of carbonate seawater chemistry are given in Table 1.

2.3. Experimental designs and biological material

The pearl oysters used in this experiment were reared at the Ifremer hatchery. They were obtained from a hatchery batch constituted by 8 wild parents originated from Takaroa atoll (North Tuamotu archipelago). Twelve experimental conditions were tested by applying four temperatures (22, 26, 30 and 34 °C) and three different pH levels (pH 8.2, 426 μatm pCO_2; pH 7.8, 1198 μatm pCO_2; pH 7.4, 3667 μatm pCO_2). First, 48 individuals (110.3 ± 9.3 mm shell height) were randomly distributed in the 12 tanks one week before starting the experimental exposure period. During this acclimatization step to the controlled conditions, temperature and pH were linearly modified in order to reach the attended value for the beginning of the experimental exposure. After seven days of exposure to the targeted conditions, four pearl oysters were subjected to metabolic measurements for an additional 48 h exposure to the treatments. They were then dissected to withdraw a piece of mantle for the gene expression analysis.

2.4. Bioenergetic measurements of P. margaritifera

Once the exposures were finished, four oysters from each treatment were transferred to the ecophysiological measurement system (EMS) where they were individually placed in a metabolic chamber to monitor ingestion and respiration rates (RRs). During these 48hs period, the pearl oysters were placed on biodeposition collectors to quantify the assimilation of organic matter (OM). The EMS consisted of five open-flow chambers. For each treatment, each of the four oysters was placed, simultaneously, in one of the chambers, and the fifth chamber remained empty as a control (Chávez-Villalba et al., 2013). The experimental conditions applied during treatments (temperature, pH) were replicated in the EMS during measurements.

Ingestion rate (IR, cell. h^{-1}), an indicator of feeding activity, was defined as the quantity of microalgae cleared per unit of time. IR was estimated using fluorescence measurements and calculated as: $IR = V(C1 - C2)$, where C1 is the fluorescence level of the control chamber, C2 is the fluorescence of the experimental chamber containing an oyster, and V is the constant water flow rate (10 L h^{-1}).

Respiration rate (RR, mg O_2 h^{-1}) was calculated using differences in oxygen concentrations between the control and

Please cite this article in press as: Le Moullac, G., et al., *Pinctada margaritifera* responses to temperature and pH: Acclimation capabilities and physiological limits, Estuarine, Coastal and Shelf Science (2016), http://dx.doi.org/10.1016/j.ecss.2016.04.011

Table 1
Water parameters calculated from samples taken from all experimental trays. The carbonate parameters were calculated using CO_2systat software.

Temperature (°C)	pH	Salinity (‰)	Alkalinity (μmol/kg-SW)	pCO_2 (μatm)	Ωca.	Ωar.
34	7.4	35	2660	3712	1.78	1.21
34	7.8	35	1980	996	3.01	2.05
34	8.2	35	2950	489	9.32	6.33
30	7.4	35	2760	3767	1.62	1.09
30	7.8	35	2730	1366	3.72	2.49
30	8.2	35	1940	317	5.43	3.64
26	7.4	35	2770	3679	1.43	0.94
26	7.8	35	2340	1326	3.25	2.15
26	8.2	36	2870	473	7.44	4.93
22	7.4	35	2730	3510	1.23	0.80
22	7.8	35	2310	1105	2.44	1.60
22	8.2	35	2600	426	6.00	3.92

experimental chambers. RR = V(O1 − O2), where O1 is the oxygen concentration in the control chamber, O2 is the oxygen concentration in the experimental chamber, and V is the water flow rate.

To compare ingestion and RRs, it was necessary to correct for differences in specimen weights. Values of the ecophysiological activities were converted to a standard animal basis (1 g, dry weight), using the formula: Ys = (Ws/We)b × Ye, where Ys is the physiological activity of a standard oyster, Ws is the dry weight of a standard oyster (1 g), We is the dry weight of the specimen, Ye is the measured physiological activity, and b is the allometric coefficient of a given activity. The average b allometric coefficients were 0.66 for IR and 0.75 for oxygen consumption rate (Savina and Pouvreau, 2004).

Assimilation efficiency (AE) of OM was assessed by analysing microalgae, faeces and pseudofaeces according to Conover (1966) and described by Chávez-Villalba et al. (2013). The pearl oysters were laid out in a collector, in which the deposits were collected on a 10-μm sieve. Biodeposits were centrifuged for 15 min at 4500 t min^{-1}. The supernatant was removed, and the pellet was washed twice with ammonium formate (37% in distilled water). The pellet was then put in a pre-weighed aluminium cup to be dried at 70 °C for 36 h before being burnt at 450 °C for 4 h. Microalgae OM was obtained by the centrifugation of 5 L of the microalgae mixture, and the pellet was treated with the same procedure used for the biodeposits. The AE was then calculated according to the following equation:

$$AE = \frac{\%OM\mu alg - \%OMbiodeposit}{(100 - \%OMbiodeposit) \times \%OM\mu alg}$$

Ecophysiological data were converted into energetic values to define the Scope For Growth (SFG) for each oyster: SFG = (IR × AE) − RR, where IR is the ingestion rate, AE is the assimilation efficiency, and RR is the respiration rate. We used 20.3 J for 1 mg of particulate OM (Bayne et al., 1987) and 14.1 J for 1 mg O_2 (Bayne and Newell, 1983; Gnaiger, 1983).

In order to model the optimal temperature for somatic growth and reproduction, RR was used according to the following polynomial equation:

$$RR = -0.02615T^2 + 1.49875T - 18.84308$$

where RR is oxygen consumption and T is temperature. The temperature corresponding to the maximum value of RR is given by the following equation:

$$ToptRR = \frac{-b}{2a}$$

where T_{optRR} is the optimal temperature, a = −0.02615 and b = 1.49875.

2.5. Gene expression in mantle of P. margaritifera

Once the ecophysiological measures were complete, the pearl oysters were sacrificed, and a strip of mantle tissue, measuring approximately 0.5 cm in width, was dissected from the mantle edge to the adductor muscle. The mantle strip was dissected on the right valve along the maximum shell height. Gene expression in the calcifying mantle of four individuals per temperature treatment were analysed (n = 16 *P. margaritifera*). Total RNA was extracted from each sample using TRIZOL®Reagent (Life Technologies), according to the manufacturer's recommendations. RNA was quantified using a NanoDrop®ND-1000 spectrophotometer (NanoDrop®TechnologiesInc). Three thousand ng of total RNA were treated for each sample with DNAse (Ambion) to degrade any potential contaminating DNA in the samples. First strand cDNA was synthesised from 500 ng of total RNA using the Transcriptor First Strand cDNA Synthesis Kit (Roche), using 2 μL of anchored-oligo (dT) and 1 μL of random hexamer primers.

The expression levels of nine genes, four encoding proteins specific to the nacreous layer (*Pmarg-Pif 177, MSI60, Pmarg-Pearlin* and *Pmarg-MRNP34*), four encoding proteins of the prismatic layers (*Pmarg-Shematrin 9, Pmarg-Prismalin14, Pmarg-PUSP6* and *Pmarg-Aspein*) and one involved in the organic matrix of both layers (*Pmarg-Nacrein A1*) (Marie et al., 2012a, 2012b; Montagnani et al., 2011), were quantified to characterise the response of pearl oysters to treatments at the biomineralization level. These expressions were analysed by quantitative RT-PCR analysis using a set of forward and reverse primers provided in Table 2. Three genes, commonly used as reference genes for the comparison of gene expression data, were chosen based on their ubiquitous and constitutive expression pattern in bivalves: universal primers for the 18S rRNA gene (Larsen et al., 2005), GAPDH (Dheilly et al., 2011) and specific to *P. margaritifera* tissue: REF1 (Joubert et al., 2014). Quantitative-RT-PCR amplifications were carried out on a Stratagene MX3000P (Agilent Technologies) using 12.5 μL of Brilliant II SYBR® Green QPCR Master Mix (Stratagene) with 400 nM of each primer and 10 μL of a 1:100 cDNA template.

The following amplification protocol was used: initial denaturation at 95 °C for 10 min followed by 40 cycles of denaturation at 95 °C for 30 s, primers annealing at 60 °C for 30 s and extension at 72 °C for 1 min. Lastly, to verify the specificity of the product, a melting curve analysis was performed from 55 to 95 °C increasing at increments of 0.5 °C. All q-RT-PCR reactions were made in duplicate. The comparative Ct (threshold cycle) method was used to analyse the expression levels of the candidate's genes. The relative expression ratio was calculated based on the delta-delta method, normalised with three reference genes to compare the relative

Please cite this article in press as: Le Moullac, G., et al., *Pinctada margaritifera* responses to temperature and pH: Acclimation capabilities and physiological limits, Estuarine, Coastal and Shelf Science (2016), http://dx.doi.org/10.1016/j.ecss.2016.04.011

Table 2
Set of forward and reverse primers used for the gene expression analysis.

Gene	GenBank Accession number	Forward primer	Reverse primer
Pmarg-PIF 177	HE610401	5′-AGATTGAGGGCATAGCATGG-3′	5′-TGAGGCCGACTTTCTTGG-3′
Pmarg-Pearlin	DQ665305	5′-TACCGGCTGTGTTGCTACTG-3′	5′-CACAGGGTGTAATATCTGGAACC-3′
Pmarg-MRNP34	HQ625028	5′-GTATGATGGGAGGCTTTGGA-3′	5′-TTGTGCGTACAGCTGAGGAG-3′
Pmarg-MSI60	SRX022139[a]	5′-TCAAGAGCAATGGTGCTAGG-3′	5′-GCAGAGCCCTTCAATAGACC-3′
Pmarg-Shematrin 9	ABO92761	5′-TGGTGGCGTAAGTACAGGTG-3′	5′-GGAAACTAAGGCACGTCCAC-3′
Pmarg-Prismalin 14	HE610393	5′-CCGATACTTCCCTATCTACAATCG-3′	5′-CCTCCATAACCGAAAATTGG-3′
Pmarg-PUSP6	SRX022139[a]	5′-TTCATTTTGGTGGTTATGGAATG-3′	5′-CCGTTTCCACCTCCGTTAC-3′
Pmarg-Aspein	SRX022139[a]	5′- TGAAGGGGATAGCCATTCTTC -3′	5′- ACTCGGTTCGGAAACAACTG -3′
Pmarg-Nacrein A1	HQ654770	5′-CTCCATGCACAGACATGACC-3′	5′-GCCAGTAATACGGACCTTGG-3′

[a] SRA accession number; EST library published in Joubert et al., (2014).

expression results, which is defined as: ratio $= 2^{-[\Delta Ct\ sample - \Delta Ct\ calibrator]} = 2^{-\Delta\Delta Ct}$ (Livak and Schmittgen, 2001). Here, the ΔCt calibrator represents the mean of the ΔCt values obtained for all tested genes in all conditions.

2.6. Temperature data

In order to contextualise the results obtained for the different thermal treatments with the current and predicted temperatures, data measured in 10 lagoons located in the north of the Tuamotu Archipelago were used. The current temperatures correspond to daily mean temperatures recorded from 1 January 1999 to 31 December 2007 in the lagoons of Ahe, Apataki, Arutua, Fakarava, Manihi, Rangiroa, Raroia, Takapoto, Takaroa and Takume (Bissery and Nicet, 2008). Natural temperature variations were estimated by the calculation of the confidence interval at the 5% level. The temperatures predicted for 2081–2100 were calculated according to the geographic localisation of the Tuamotu combined with the IPCC scenarios (IPCC, 2014); RCP 2.6 (+1 °C), RCP 4.5 (+1.5 °C) and RCP 8.5 (+2.5 °C).

2.7. Statistical analysis

Normality of data distribution and homogeneity of variance were tested using the Shapiro-Wilk test and the Bartlett test, respectively. RR data followed the conditions of application of parametric tests, but IR and SFG data were subjected to the Box-Cox transformation to satisfy these conditions. AE was analysed using the arcsine square root AE/100 value. The impact of temperature and the pCO_2 level was tested using a two-way ANOVA followed by PLSD Fisher post hoc tests. Alpha was set at 0.05 for all analyses. The expression values of the nine candidate genes met the condition for a parametric ANOVA after normalisation by the Box-Cox transformation. PLSD Fisher tests were used to determine significant differences.

3. Results

The aim of the present study was to characterise, at the bioenergetic and biomineralization levels, the impact of a seven-day exposure to an acidification (pH 8.2, 7.8 and 7.4) cross temperature (22, 26, 30 and 34 °C) experiment.

3.1. Bioenergetics

The two-way ANOVA did not reveal significant differences between AE in response to the temperature ($p = 0.94$; Table 3) or the pCO_2 ($p = 0.20$; Table 3); nor did it reveal an interaction between both treatments ($p = 0.10$; Table 3). Conversely, the same analysis showed that the IRs were significantly different between temperature treatments ($p < 0.0001$; Table 3) but not according to the pCO_2 ($p = 0.83$; Table 3). No significant interaction was revealed ($p = 0.28$; Table 3). The PLSD Fisher test showed that the IR increased significantly with the temperature until it reached a maximum at 30 °C; finally, at 34 °C, it significantly dropped to the value measured at 22 °C (Fig. 1A). The oxygen consumption rate (OC) was significantly affected by temperature ($p < 0.0001$; Table 3), but not by pCO_2 ($p = 0.52$; Table 3), and no significant interaction between treatments was revealed ($p = 0.94$; Table 3). The PLSD Fisher test showed that OC was lowest at 22 °C, highest at 26 °C and 30 °C, and started to decrease at 34 °C (Fig. 1B). SFG increased significantly with temperature ($p = 0.0003$; Table 3), but it was not affected by the pCO_2 level ($p = 0.38$; Table 3), and no significant interaction was revealed ($p = 0.59$; Table 3). The PLSD Fisher test showed a significant increase at 30 °C in comparison to the three other temperatures tested (Fig. 1C). According to the polynomial equation provided above, the optimal temperature for somatic growth and reproduction was $T_{optRR} = 28.7$ °C.

3.2. Mantle gene expression

Gene expression measurements were focused on the effect of temperature because of the absence of a pCO_2 effect at the bioenergetic level. Among the nine candidate genes tested, the expression of four were significantly affected by temperature treatments (Fig. 2). *Pmarg-MRNP34* gene expression decreased significantly at 30 and 34 °C in comparison to 26 °C ($p = 0.05$; Table 4, Fig. 2D). A significant change of the *Pmarg-Prismalin14* gene expression was recorded ($p = 0.01$; Table 4, Fig. 2F) between 26 and 30 °C. *Pmarg-Aspein* expression was significantly higher at 26 °C and decreased significantly at 30 °C and 34 °C ($p = 0.01$; Table 4, Fig. 2G). *Pmarg-Nacrein A1* gene expression was maximal at 26 °C and decreased significantly at 30 and 34 °C ($p = 0.01$; Table 4, Fig. 2I). According to the polynomial equation provided above, the optimal temperatures for *Pmarg-Nacrein A1*, *Pmarg-MRNP34*, *Pmarg-Prismalin14* and *Pmarg-Aspein* expression were 24.8 °C, 24.6 °C, 21.5 °C and 26.5 °C, respectively.

3.3. Actual and predicted temperature in the lagoon of the north Tuamotu Archipelago

The temperature data measured in 10 lagoons of the North Tuamotu Archipelago and the downstream descriptive statistical analysis showed that the annual average temperature between 1999 and 2007 was 27.88 °C (±1.00 °C). The warmest month was March (29.14 ± 0.05 °C), and the coldest was August (26.35 ± 0.05 °C). With this regime, pearl oysters were experiencing temperatures above their physiological optimal temperature threshold 121 days per year. In perspective with the IPCC scenarios (RCP 2.6, RCP 4.5 and RCP 8.5), this threshold would be exceeded, 210, 252 and 365 days per year, respectively (Fig. 3).

Please cite this article in press as: Le Moullac, G., et al., *Pinctada margaritifera* responses to temperature and pH: Acclimation capabilities and physiological limits, Estuarine, Coastal and Shelf Science (2016), http://dx.doi.org/10.1016/j.ecss.2016.04.011

Table 3
Two-way ANOVA results for bioenergetic values of seven day exposure to temperature and pCO_2 level (absorption efficiency (AE), ingestion rate (IR), respiration rate (RR), scope for growth (SFG)). Value in bold indicate significant differences.

Sources of variation	ddl	AE (arcsinsqr)		IR (Box Cox)		RR		SFG (Box Cox)	
		F	*p*	*F*	*p*	*F*	*p*	*F*	*p*
Temperature	3	0.14	0.94	11.03	**<0.0001**	16.21	**<0.0001**	8.13	**0.0003**
pCO_2	2	1.68	0.20	0.18	0.83	0.67	0.52	0.98	0.38
Temperature × pCO_2	6	3.40	0.10	1.31	0.28	0.28	0.94	0.78	0.59

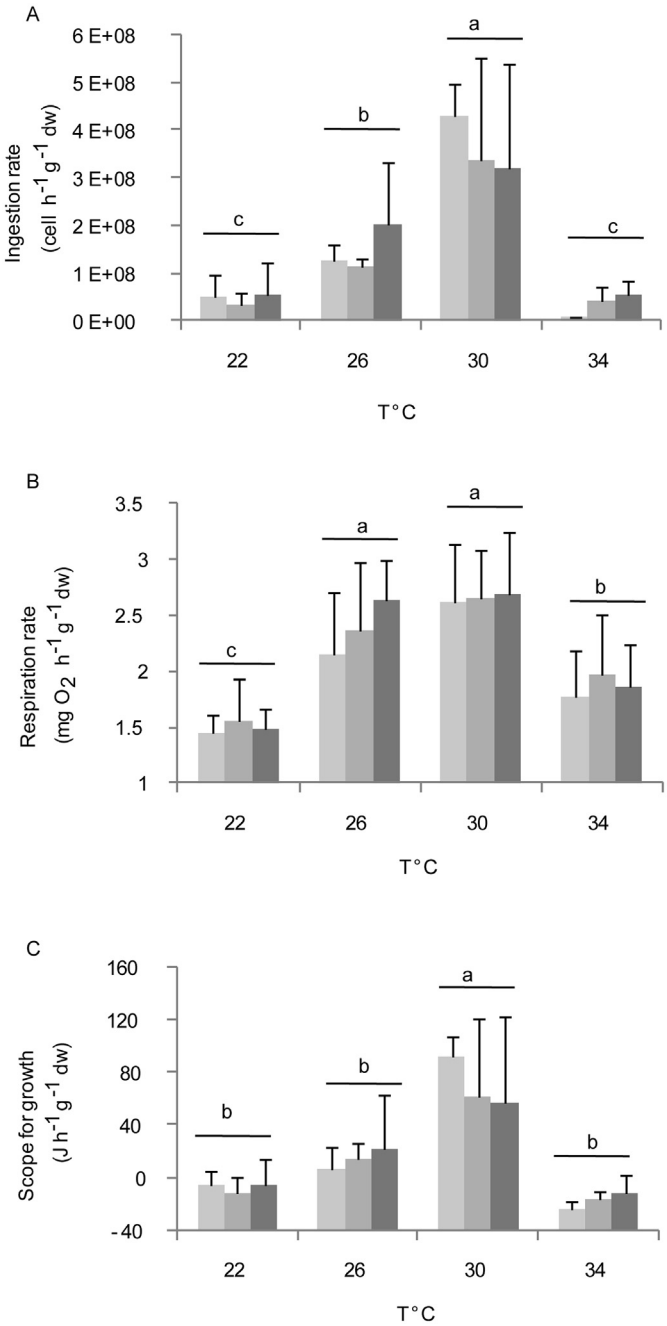

Fig. 1. Bioenergetic responses. Bioenergetic behaviour after one week exposure to temperature (22, 26, 30 and 34 °C) and pCO_2 level (3667 µatm (light grey), 1198 µatm (grey), 426 µatm (dark grey); (A) ingestion rate (IR), (B) respiration rate (RR) (C) scope for growth (SFG)) of the black-lip pearl oyster *Pinctada margaritifera*. Means are presented with standard error (n = 4). Lowercases illustrate significant differences between temperatures.

4. Discussion

Bivalve growth is known to be strongly influenced by environmental conditions such as food supply and water temperature. The aim of this study was to simultaneously evaluate *P. margaritifera's* bioenergetic and biomineralization abilities as a function of environmental conditions, temperature and pCO_2 in the context of global warming and ocean acidification.

4.1. Acidification did not influence energy management in Pinctada margaritifera

This first study on the impact of acidification on energy metabolism of *P. margaritifera* indicated that, after a short-term exposure (9 days), no significant change occurred; *P. margaritifera* seems tolerant to acidification given that the metabolic index did not vary. This is not the case for other species of bivalves living in temperate areas where different levels of metabolic adaptation have been observed. The energy input is reduced in the clam *Ruditapes decussatus* when exposed to high pCO_2 levels, due to a general metabolic depression (Fernández-Reiriz et al., 2011). When the mussel *Mytilus galloprovincialis* was exposed to high pCO_2, the SFG was better, thus promoting better growth and reproduction; this is based on better absorption efficiency and a lower ammonium excretion rate (Fernández-Reiriz et al., 2012). The metabolic rate of the wild oyster *Saccostrea glomerata* was not impacted by low pCO_2, while, for selected oysters (for growth and disease resistance) it increased oxygen needs (Parker et al., 2012). In addition, the response to acidification seems sometimes contradictory. Indeed, within the same species, *Ruditapes decussatus*, at similar sizes and in similar experimental conditions, conclusions on the impacts of acidification are not the same. At the metabolic level, Fernández-Reiriz et al. (2011) observed a depression, while Range et al. (2011) measured no difference in terms of net calcification, size or weight. They argue that the local response was not extrapolated to the overall response of the species. In any case, the accumulation of data obtained from an intraspecific to an interspecific level in bivalves over several years argues in favour of a high genetic and phylogenetic effect on the response to ocean acidification.

In this study, we used a short term exposure to the high pCO_2 treatments. This short-term period did not aim to induce a response of an adaptive type but to study the acclimation stage. In Le Moullac et al. (in this ECSS issue) authors have shown that, after 100 days of exposure, the metabolic response did not vary regardless of the tested level of pCO_2. This suggests that in response to high pCO_2, the adjustment of the energy metabolism in the pearl oyster is fast which confirms that this species seems to be tolerant to such a disturbance.

4.2. The effects of temperature on Pinctada margaritifera

As previously shown in numerous bivalves (Aldridge et al., 1995; Hicks and McMahon, 2002; Le Moullac et al., 2007; Marsden and Weatherhead, 1998) including sister species of the genus *Pinctada*

Please cite this article in press as: Le Moullac, G., et al., *Pinctada margaritifera* responses to temperature and pH: Acclimation capabilities and physiological limits, Estuarine, Coastal and Shelf Science (2016), http://dx.doi.org/10.1016/j.ecss.2016.04.011

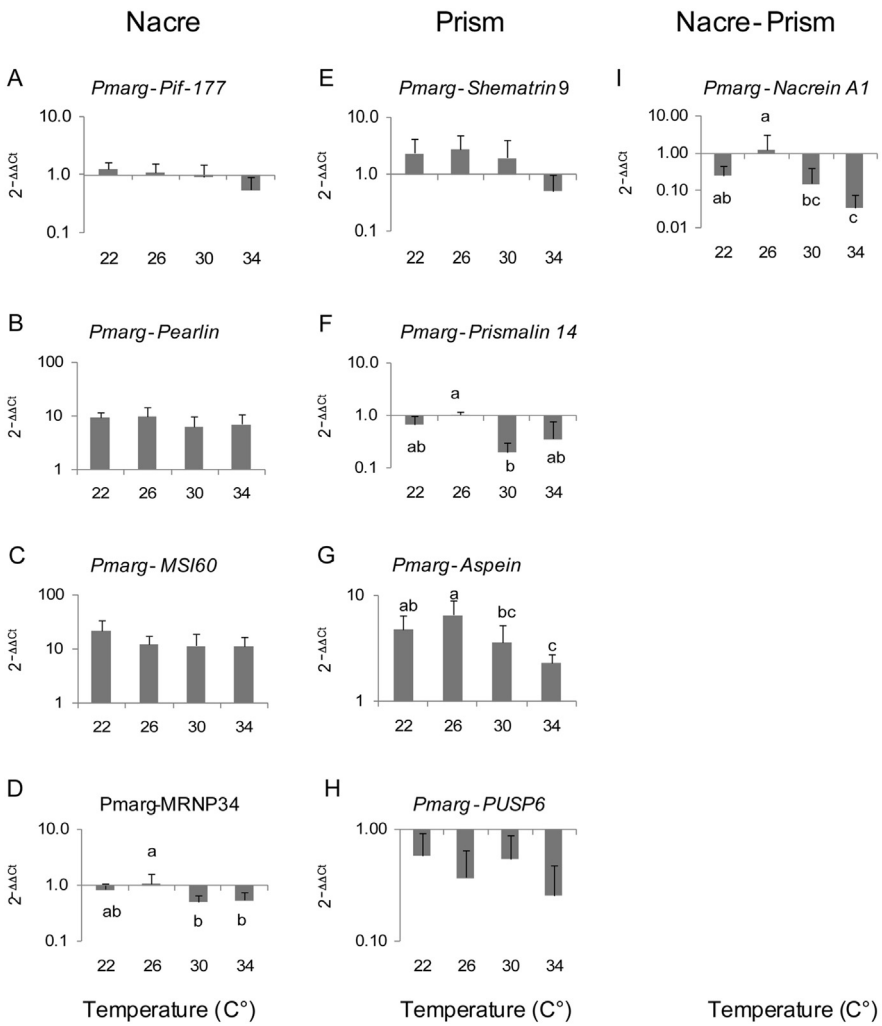

Fig. 2. Biomineralization response. Effects of seven days exposure to 22, 26, 30 and 34 °C on the expression of nine candidate genes involved in biomineralization. *Pmar-Pif-177*, *Pmar-pearlin*, *Pmar-MS160* and *Pmar-MRNP34* are involved in nacre. *Pmar-Shematrin 9*, *Pmar-Prismalin14*, *Pmar-Aspein,* and *Pmar-PUSP6* are involved in prism. *Pmar-Nacrein A1* is involved in both minerals.

Table 4
Significance level of ANOVA and Kruskal Wallis test of biomineralization related gene expression levels according to temperature levels. Value in bold indicate significant differences.

	Pmarg-PIF-177		*Pmarg-Nacrein A1*		*Pmarg-PUSP6*		*Pmarg-Pearlin*		*Pmarg-MRNP34*		*Pmarg-MSI60*		*Pmarg-Shematrin 9*		*Pmarg-Primalin 14*		*Pmarg-Aspein*	
	F	*p*	F	*p*	F	*p*	F	*p*	F	*p*	F	*p*	F	*p*	F	*p*	F	*p*
T°C	1.79	*0.19*	5.15	***0.01***	1.00	*0.42*	0.85	*0.49*	3.16	***0.05***	1.36	*0.29*	1.27	*0.32*	7.28	***0.003***	5.31	***0.01***

sp. (Saucedo et al., 2004; Yukihira et al., 2000), our study confirms that temperature influences metabolic rates (MR) in the pearl oyster *P. margaritifera*. Indeed, the linear relationship between temperature and MR shows an increase of energy gain from 22 to 30 °C, which is the temperature where MRs were maximised.

Otherwise, our study revealed a non-lethal thermal-maximum, at 34 °C, that caused a severe metabolic depression where the individual could no longer acquire energy. Indeed, the RR at 34 °C still represent 70% of the RR at 30 °C, which represent a high-energy expenditure, while the concomitant food intake represent a lack of energy acquisition. This metabolic situation is akin to fasting, and may not last for a long time since pearl oysters would rely on their energy reserves which will lead to an energy deficit and thus, to the death by exhaustion (Patterson et al., 1999). To date, this is the first evidence about the putative consequences of warming on the physiology of the pearl oyster. This phenomenon must be studied further given that it would result in a strong population disorder induced by an energy depletion and/or a decrease of the reproduction capacity.

The general metabolism of an organism can be evaluated by measuring RR, which is a good biomarker of health and energetic balance. Experimental approaches had confirmed in many bivalves that RR increases with increasing temperatures (Bougrier et al., 1995). However, the relationship between RR and the temperature is only valid in a range of temperatures corresponding to the thermal limits of the species. Concerning *P. margaritifera*, the RR is

Please cite this article in press as: Le Moullac, G., et al., *Pinctada margaritifera* responses to temperature and pH: Acclimation capabilities and physiological limits, Estuarine, Coastal and Shelf Science (2016), http://dx.doi.org/10.1016/j.ecss.2016.04.011

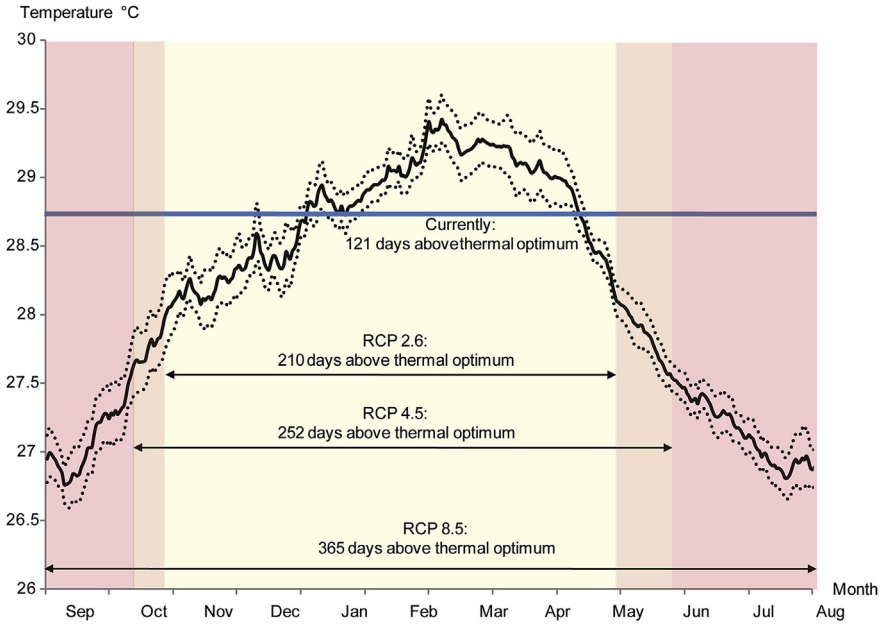

Fig. 3. Thermal optimum and future temperature at the horizon of 22nd century. Under the current temperature regime (black line; dotted line is the confidence interval at 5%), the pearl oyster spends 121 days above its thermal optimum (blue line). Under the RCP scenarios 2.6 (+1 °C), this would be 210 days (yellow), 252 days under the RCP4.5 (+1.5 °C; orange) and 365 days under the RCP8.5 (+2.5 °C; red). (For interpretation of the references to colour in this figure legend, the reader is referred to the web version of this article.)

maximal at 30 °C. However, the polynomial modelling of the relationship with the temperature highlights 28.7 °C as the thermal optimum. This value can be considered as a reference value for *P. margaritifera* pointing out the temperature threshold where above the organism is stressed by the temperature inducing an energy deficit.

In molluscs, the biomineralization of the shell is a costly function (Palmer, 1992), which suggests an intimate link between the bioenergetic balance and temperature. To address these links over the range of temperatures that *P. margaritifera* can experience, the expression levels of nine gene-encoding proteins of the shell organic matrix were quantified on mantle samples taken off at 22, 26, 30 and 34 °C. Among these genes were four encoded for proteins specific to the nacreous layer (*Pmarg-Pif 177, Pmarg-MSI60, Pmarg-Pearlin* and *Pmarg-MRNP34*), four encoded for proteins of the prismatic layer (*Pmarg-Shematrin 9, Pmarg-Prismalin14, Pmarg-PUSP6* and *Pmarg-Aspein*) and one involved in the organic matrix of both layers (*Nacrein A1*) (Marie et al., 2012a, 2012b; Montagnani et al., 2011). Among these genes, four were significantly regulated by temperature (*Pmarg-Prismalin14*, *Pmarg-Aspein*, *Pmarg-MRNP34* and *Pmarg-Nacrein A1*) and displayed a maximum expression between 21.5 and 26.5 °C. Surprisingly, these maximums were all below the optimal temperature for somatic growth and reproduction. However, these regulations are in agreement with those previously reported for *P. margaritifera* (Joubert et al., 2014) and a closely related species, *Pinctada fucata* (Liu et al., 2012).

The differences observed between the bioenergetic thermal optimum and the one calculated for the biomineralization argue in favour of the presence of an antagonistic biological function that is highly thermal-dependent. Among these processes, reproduction in bivalves is well known to be highly correlated with temperature (Moal et al., 2007). This function requires much energy to ensure an optimal gametogenesis resulting in the so-called trade-off mechanism, "the reproductive cost" (Calow, 1979). In *P. margaritifera,* reproduction occurs throughout the year, but presents maximal activity during the warm season (Pouvreau et al., 2000a); the season where shells grow at the slowest rate (Pouvreau et al., 2000b). This correlation would explain the differences observed between the optimum temperature for somatic growth/reproduction and the optimum temperature for biomineralization. Further works will be needed to disentangle all putative confounding effects and to confirm this hypothesis.

4.3. The pearl oyster in front of global warming

One of the most direct effects of global change is the sea surface temperature increase. Indeed, since the beginning of the 20th century, the global ocean temperature has already increased by 0.7 °C (Hoegh-Guldberg et al., 2007). The last IPPC report highlighted that, under all scenarios of greenhouse gas emissions for the next century, temperatures will continue to increase, with a higher intensity for tropical areas (IPCC, 2014). The results of our work show that the optimal temperature for *P. margaritifera* somatic growth and reproduction is 28.7 °C under our experimental conditions. This result is in agreement with previous work highlighting an optimal temperature range for growth between 23–28 °C and 26–29 °C for adult and larvae of Australian population of *P. margaritifera,* respectively (Doroudi et al., 1999; Yukihira et al., 2000). The threshold of 28.7 °C is already exceeded annually during the warmer months (121 days per year), during which the growth rate of *P. margaritifera* was shown to decrease (Pouvreau et al., 2000b). Indeed, it is well documented that thermal optimums of tropical marine ectotherms are usually very close to their critical thermal maximums, which explains how close to the edge they are in front of global warming (Somero, 2012). All these data taken together let us hypothesize that major biological functions, such as somatic growth, reproduction and biomineralization, will be annually compromised, or at least significantly slowed, during the next decades. Under the optimistic scenario, RCP2.6 (+1 °C), and the medium scenario, RCP4.2 (+1.5 °C), pearl oysters in the lagoons of the North Tuamotu archipelago will be confronted to temperatures above their thermal optimum for 210 and 252 days per year, respectively. Alarmingly, this threshold will be exceeded throughout the year in the most pessimistic scenario, the RCP8.5

Please cite this article in press as: Le Moullac, G., et al., *Pinctada margaritifera* responses to temperature and pH: Acclimation capabilities and physiological limits, Estuarine, Coastal and Shelf Science (2016), http://dx.doi.org/10.1016/j.ecss.2016.04.011

(+2.5 °C).

In the socio-economical context of French Polynesia, these hypotheses and predictions suggest that major scientific works will be needed to sustain pearl production. Future research should be developed to better calibrate the critical thermal maximums of different pearl oyster populations. The battery of "Omics" and physiological tools in association with the power of next-generation sequencing will be useful to characterise and quantify pearl oyster adaptability throughout the Polynesian archipelago. All these fundamental approaches would enable the identification of the mechanisms of thermotolerance in *P. margaritifera.* This research would provide new management tools such as biomarkers of thermal tolerance that would be used in the emerging genetic selection plan (Ky et al., 2013). In parallel some actions should be undertaken to significantly enhance the chances of natural adaptation in *P. margaritifera* populations. As an example among others, we can mention the needs in management effort aiming to conserve the genetic diversity of *P. margaritifera*, a diversity that had already suffered from the pearl culture activity (Arnaud-Haond et al., 2004; Lemer and Planes, 2012). In every instance, the Austral archipelago, an area identified as a temporary thermal refuge in French Polynesia (Van Hooidonk et al., 2013) would be used to maintain this activity if the temperature becomes a too strong environmental pressure.

Acknowledgments

This work was financially supported by the ANR funding POLYPERL project (reference ANR-11-AGRO-006-01-POLYPERL).

References

Aldridge, D.W., Payne, B.S., Miller, A.C., 1995. Oxygen consumption, nitrogenous excretion, and filtration rates of *Dreissena polymorpha* at acclimation temperatures between 20 and 32 C. Can. J. Fish. Aquatic Sci. 52, 1761–1767.

Arnaud-Haond, S., Vonau, V., Bonhomme, F., Boudry, P., Blanc, F., Prou, J., Seaman, T., Goyard, E., 2004. Spatio-temporal variation in the genetic composition of wild populations of pearl oyster (*Pinctada margaritifera cumingii*) in French Polynesia following 10 years of juvenile translocation. Mol. Ecol. 13, 2001–2007.

Bayne, B., Hawkins, A., Navarro, E., 1987. Feeding and digestion by the mussel *Mytilus edulis* L. (Bivalvia: Mollusca) in mixtures of silt and algal cells at low concentrations. J. Exp. Mar. Biol. Ecol. 111, 1–22.

Bayne, B., Newell, R., 1983. Physiological energetics of marine molluscs. In: Saleuddin, A., Wilbur, K. (Eds.), The Mollusca. Academic Press, New York, pp. 407–515.

Bissery, C., Nicet, J.-B., 2008. In: Ecoconsult, P. (Ed.), Suivi de la température marine de sub-surface en Polynésie Française de 1998 à 2008. Service de la pêche, Papeete, pp. 1–26.

Bougrier, S., Geairon, P., Deslous-Paoli, J., Bacher, C., Jonquières, G., 1995. Allometric relationships and effects of temperature on clearance and oxygen consumption rates of *Crassostrea gigas* (Thunberg). Aquaculture 134, 143–154.

Calow, P., 1979. The cost of reproduction – a physiological approach. Biol. Rev. 54, 23–40.

Chávez-Villalba, J., Soyez, C., Aurentz, H., Le Moullac, G., 2013. Physiological responses of female and male black-lip pearl oysters (*Pinctada margaritifera*) to different temperatures and concentrations of food. Aquat. Living Resour. 26, 263–271.

Conover, R.J., 1966. Assimilation of organic matter by zooplankton. Limnol. Oceanogr. 11, 338–345.

Dheilly, N.M., Lelong, C., Huvet, A., Favrel, P., 2011. Development of a Pacific oyster (*Crassostrea gigas*) 31,918-feature microarray: identification of reference genes and tissue-enriched expression patterns. BMC Genomics 12, 468.

Doroudi, M.S., Southgate, P.C., Mayer, R.J., 1999. The combined effects of temperature and salinity on embryos and larvae of the black-lip pearl oyster, *Pinctada margaritifera* (L.). Aquac. Res. 30, 271–277.

Fabricius, K.E., Langdon, C., Uthicke, S., Humphrey, C., Noonan, S., De'ath, G., Okazaki, R., Muehllehner, N., Glas, M.S., Lough, J.M., 2011. Losers and winners in coral reefs acclimatized to elevated carbon dioxide concentrations. Nat. Clim. Change 1, 165–169.

Fernández-Reiriz, M.J., Range, P., Álvarez-Salgado, X.A., Espinosa, J., Labarta, U., 2012. Tolerance of juvenile *Mytilus galloprovincialis* to experimental seawater acidification. Mar. Ecol. Prog. Ser. 454, 65–74.

Fernández-Reiriz, M.J., Range, P., Álvarez-Salgado, X.A., Labarta, U., 2011. Physiological energetics of juvenile clams *Ruditapes decussatus* in a high CO_2 coastal ocean. Mar. Ecol. Prog. Ser. 433, 97–105.

Gnaiger, E., 1983. Heat dissipation and energetic efficiency in animal anoxibiosis: economy contra power. J. Exp. Zool. 228, 471–490.

Hicks, D.W., McMahon, R.F., 2002. Respiratory responses to temperature and hypoxia in the nonindigenous brown mussel, *Perna perna* (Bivalvia: Mytilidae), from the Gulf of Mexico. J. Exp. Mar. Biol. Ecol. 277, 61–78.

Hoegh-Guldberg, O., Mumby, P.J., Hooten, A.J., Steneck, R.S., Greenfield, P., Gomez, E., Harvell, C.D., Sale, P.F., Edwards, A.J., Caldeira, K., Knowlton, N., Eakin, C.M., Iglesias-Prieto, R., Muthiga, N., Bradbury, R.H., Dubi, A., Hatziolos, M.E., 2007. Coral reefs under rapid climate change and ocean acidification. Science 318, 1737–1742.

IPCC, 2014. Climate change 2014: synthesis report. In: Team C.W., Pachaury, R.K., L.A M. (Eds.), Contribution of Working Groups I, II and II to the Fifth Assessment Report of the Intergovernmental Panel on Climate Change. IPCC, Geneva, p. 151.

Ishimatsu, A., Hayashi, M., Lee, K. Seon, Kikkawa, T., Kita, J., 2005. Physiological effects on fishes in a high pCO2 world. J. Geophys. Res. 110, 1–8.

Joubert, C., Linard, C., Le Moullac, G., Soyez, C., Saulnier, D., Teaniniuraitemoana, V., Ky, C.L., Gueguen, Y., 2014. Temperature and food influence shell growth and mantle gene expression of shell matrix proteins in the pearl pyster *Pinctada margaritifera*. PLoS One 9, e103944.

Kroeker, K.J., Kordas, R.L., Crim, R.N., Singh, G.G., 2010. Meta-analysis reveals negative yet variable effects of ocean acidification on marine organisms. Ecol. Lett. 13, 1419–1434.

Kurihara, H., 2008. Effects of CO2-driven ocean acidification on the early developmental stages of invertebrates. Mar. Ecol. Prog. Ser. 373, 275–284.

Ky, C.-L., Blay, C., Sham-Koua, M., Vanaa, V., Lo, C., Cabral, P., 2013. Family effect on cultured pearl quality in black-lipped pearl oyster *Pinctada margaritifera* and insights for genetic improvement. Aquat. Living Resour. 26, 133–145.

Larsen, J.B., Frischer, M.E., Rasmussen, L.J., Hansen, B.W., 2005. Single-step nested multiplex PCR to differentiate between various bivalve larvae. Mar. Biol. 146, 1119–1129.

Le Moullac, G., Quéau, I., Le Souchu, P., Pouvreau, S., Moal, J., René Le Coz, J., François Samain, J., 2007. Metabolic adjustments in the oyster *Crassostrea gigas* according to oxygen level and temperature. Mar. Biol. Res. 3, 357–366.

Lemer, S., Planes, S., 2012. Translocation of wild populations: conservation implications for the genetic diversity of the black-lipped pearl oyster *Pinctada margaritifera*. Mol. Ecol. 21, 2949–2962.

Liu, W., Huang, X., Lin, J., He, M., 2012. Seawater acidification and elevated temperature affect gene expression patterns of the pearl oyster *Pinctada fucata*. PLoS One 7, e33679.

Livak, K., Schmittgen, T., 2001. Analysis of relative gene expression data using real-time quantitative PCR and the 2(-Delta Delta C(T)) method. Methods 25, 402–408.

Marie, B., Joubert, C., Belliard, C., Tayale, A., Zanella-Cléon, I., Marin, F., Gueguen, Y., Montagnani, C., 2012a. Characterization of MRNP34, a novel methionine-rich nacre protein from the pearl oysters. Amino Acids 42, 2009–2017.

Marie, B., Joubert, C., Tayalé, A., Zanella-Cléon, I., Belliard, C., Piquemal, D., Cochennec-Laureau, N., Marin, F., Gueguen, Y., Montagnani, C., 2012b. Different secretory repertoires control the biomineralization processes of prism and nacre deposition of the pearl oyster shell. Proc. Natl. Acad. Sci. U. S. A. 109, 20986–20991.

Marsden, I.D., Weatherhead, M.A., 1998. Effects of aerial exposure on oxygen consumption by the New Zealand mussel *Perna canaliculus* (Gmelin, 1791) from an intertidal habitat. J. Exp. Mar. Biol. Ecol. 230, 15–29.

Moal, J., Lambert, M., Pouvreau, S., Le Moullac, G., Samain, J., 2007. Temperature as a risk factor in oyster summer mortality. In: Samain, J. (Ed.), Summer Mortality of the Pacific Oyster Crassostrea gigas: the Morest Project. Edition Quae, Versailles, pp. 289–306.

Montagnani, C., Marie, B., Marin, F., Belliard, C., Riquet, F., Tayalé, A., Zanella-Cléon, I., Fleury, E., Gueguen, Y., Piquemal, D., 2011. Pmarg-Pearlin is a matrix protein involved in nacre framework formation in the pearl oyster *Pinctada margaritifera*. Chembiochem 12, 2033–2043.

Neuheimer, A., Thresher, R., Lyle, J., Semmens, J., 2011. Tolerance limit for fish growth exceeded by warming waters. Nat. Clim. Change 1, 110–113.

Palmer, A.R., 1992. Calcification in marine molluscs: how costly is it? Proc. Natl. Acad. Sci. U. S. A. 89, 1379–1382.

Parker, L.M., Ross, P.M., O'Connor, W.A., Borysko, L., Raftos, D.A., Pörtner, H.O., 2012. Adult exposure influences offspring response to ocean acidification in oysters. Glob. Change Biol. 18, 82–92.

Patterson, M.A., Parker, B.C., Neves, R.J., 1999. Glycogen concentration in the mantle tissue of freshwater mussels (Bivalvia: Unionidae) during starvation and controlled feeding. Am. Malacol. Bull. 15, 47–50.

Pörtner, H.O., Langenbuch, M., Michaelidis, B., 2005. Synergistic effects of temperature extremes, hypoxia, and increases in CO_2 on marine animals: from earth history to global change. J. Geophys. Res. Oceans 110, C09S10.

Pörtner, H.O., Peck, L., Somero, G., 2007. Thermal limits and adaptation in marine Antarctic ectotherms: an integrative view. Philos. Trans. R. Soc. B Biol. Sci. 362, 2233–2258.

Pouvreau, S., Gangnery, A., Tiapari, J., Lagarde, F., Garnier, M., Bodoy, A., 2000a. Gametogenic cycle and reproductive effort of the tropical blacklip pearl oyster, *Pinctada margaritifera* (Bivalvia: Pteriidae), cultivated in Takapoto atoll (French Polynesia). Aquat. Living Resour. 13, 37–48.

Pouvreau, S., Tiapari, J., Gangnery, A., Lagarde, F., Garnier, M., Teissier, H., Haumani, G., Buestel, D., Bodoy, A., 2000b. Growth of the black-lip pearl oyster, *Pinctada margaritifera*, in suspended culture under hydrobiological conditions of Takapoto lagoon (French Polynesia). Aquaculture 184, 133–154.

Please cite this article in press as: Le Moullac, G., et al., *Pinctada margaritifera* responses to temperature and pH: Acclimation capabilities and physiological limits, Estuarine, Coastal and Shelf Science (2016), http://dx.doi.org/10.1016/j.ecss.2016.04.011

Range, P., Chícharo, M., Ben-Hamadou, R., Piló, D., Matias, D., Joaquim, S., Oliveira, A., Chícharo, L., 2011. Calcification, growth and mortality of juvenile clams *Ruditapes decussatus* under increased pCO_2 and reduced pH: variable responses to ocean acidification at local scales? J. Exp. Mar. Biol. Ecol. 396, 177–184.

Ries, J.B., Cohen, A.L., McCorkle, D.C., 2009. Marine calcifiers exhibit mixed responses to CO_2-induced ocean acidification. Geology 37, 1131–1134.

Rodolfo-Metalpa, R., Houlbrèque, F., Tambuttè, E., Boisson, F., Baggini, C., Patti, F.P., Jeffree, R., Fine, M., Foggo, A., Gattuso, J.P., 2011. Coral and mollusc resistance to ocean acidification adversely affected by warming. Nat. Clim. Change 1, 308–312.

Saucedo, P.E., Ocampo, L., Monteforte, M., Bervera, H., 2004. Effect of temperature on oxygen consumption and ammonia excretion in the Calafia mother-of-pearl oyster, *Pinctada mazatlanica* (Hanley, 1856). Aquaculture 229, 377–387.

Savina, M., Pouvreau, S., 2004. A comparative ecophysiological study of two infaunal filter-feeding bivalves: *Paphia rhomboïdes* and *Glycymeris glycymeris*. Aquaculture 239, 289–306.

Somero, G.N., 2012. The physiology of global change: linking patterns to mechanisms. Annu. Rev. Mar. Sci. 4, 39–61.

Stumpp, M., Dupont, S., Thorndyke, M.C., Melzner, F., 2011. CO_2 induced seawater acidification impacts sea urchin larval development II: gene expression patterns in pluteus larvae. Comp. Biochem. Physiol-Part A Mol. Integr. Physiol. 160, 320–330.

Thomsen, J., Casties, I., Pansch, C., Körtzinger, A., Melzner, F., 2013. Food availability outweighs ocean acidification effects in juvenile *Mytilus edulis*: laboratory and field experiments. Glob. Change Biol. 19, 1017–1027.

van Heuven, S., Pierrot, D., Lewis, E., Wallace, D.W.R., 2009. MATLAB Program Developed for CO_2 System Calculations, ORNL/CDIAC-105b, Carbon Dioxide Information Analysis Center, Oak Ridge National Laboratory, US Department of Energy, Oak Ridge, Tennessee.

Van Hooidonk, R., Maynard, J., Planes, S., 2013. Temporary refugia for coral reefs in a warming world. Nat. Clim. Change 3, 508–511.

Yukihira, H., Lucas, J.S., Klumpp, D.W., 2000. Comparative effects of temperature on suspension feeding and energy budgets of the pearl oysters *Pinctada margaritifera* and *P. maxima*. Mar. Ecol. Prog. Ser. 195, 179–188.

Zhang, H., Shin, P.K.S., Cheung, S.G., 2015. Physiological responses and scope for growth upon medium-term exposure to the combined effects of ocean acidification and temperature in a subtidal scavenger *Nassarius conoidalis*. Mar. Environ. Res. 106, 51–60.

Please cite this article in press as: Le Moullac, G., et al., *Pinctada margaritifera* responses to temperature and pH: Acclimation capabilities and physiological limits, Estuarine, Coastal and Shelf Science (2016), http://dx.doi.org/10.1016/j.ecss.2016.04.011

ANNEXE 3

Estuarine, Coastal and Shelf Science xxx (2016) 1–9

Contents lists available at ScienceDirect

Estuarine, Coastal and Shelf Science

journal homepage: www.elsevier.com/locate/ecss

Impact of pCO_2 on the energy, reproduction and growth of the shell of the pearl oyster *Pinctada margaritifera*

Le Moullac Gilles [a, *], Soyez Claude [a], Vidal-Dupiol Jérémie [a], Belliard Corinne [a], Fievet Julie [a], Sham Koua Manaarii [a], Lo-Yat Alain [a], Saulnier Denis [a], Gaertner-Mazouni Nabila [b], Gueguen Yannick [c]

[a] Ifremer, UMR 241 Ecosystèmes Insulaires Océaniens (EIO), Labex Corail, Centre du Pacifique, BP 49, 98719 Taravao, Tahiti, French Polynesia
[b] Université de la Polynésie Française, UMR 241 Ecosystèmes Insulaires Océaniens (EIO), Labex Corail, BP 6570, 98702 Faa'a, Tahiti, French Polynesia
[c] Ifremer, UMR 5244 IHPE, UPVD, CNRS, Université de Montpellier, CC 80, F-34095 Montpellier, France

ARTICLE INFO

Article history:
Received 8 July 2015
Received in revised form
24 February 2016
Accepted 20 March 2016
Available online xxx

Keywords:
Global change
Pearl oyster
Bioenergetic
Biomineralization
Pacific Ocean
French Polynesia

ABSTRACT

The possible consequences of acidification on pearl farming are disruption of oyster metabolism and change in growth. In the laboratory, we studied the impact of pCO_2 (3540, 1338 and 541 μatm) on the physiology of pearl oysters exposed for 100 days. This experiment was repeated after an interval of one year. Several physiological compartments were examined in pearl oysters: the scope for growth by measuring ingestion, assimilation and oxygen consumption, gametogenesis by means of histological observations, shell growth by measurement and observation by optical and electronic microscopy, and at molecular level by measuring the expression of nine genes of mantle cells implied in the biomineralisation process. Results from both experiments showed that high pCO_2 had no effect on scope for growth and gametogenesis. High pCO_2 (3540 μatm) significantly slowed down the shell deposit rate at the ventral side and SEM observations of the inside of the shell found signs of chemical dissolution. Of the nine examined genes high pCO_2significantly decreased the expression level of one gene (*Pmarg*-PUSP 6). This study showed that shell growth of the pearl oyster would be slowed down without threatening the species since the management of energy and reproduction functions appeared to be preserved. Further investigations should be conducted on the response of offspring to acidification.

1. Introduction

Global climate change is a major concern caused by mainly two factors, temperature and the atmospheric CO_2 level. In the marine world, this translates into the elevation of the temperature of the oceans and a tendency to acidification of sea water. Some marine ecosystems may suffer from this global change, including the tropical coral reef ecosystems and all the communities who live there. It is accepted that the pH in the global ocean has already fallen by 0.1 units and is likely to fall a further 0.3 units by 2050 and 0.5 units by 2100 (Caldeira and Wickett, 2005; Orr et al., 2005). Some recent studies suggest that ocean acidification would directly affect the population of calcifiers (Kurihara and Ishimatsu, 2008) and have negative impacts on invertebrate reproduction (Siikavuopio et al., 2007; Kurihara et al., 2008). The potential effects of the decline in pH, however, on marine organisms and ecosystems are disturbances affecting growth (Berge et al., 2006), calcification (Ross et al., 2011; Gazeau et al., 2013) and metabolic rates (Thomsen and Melzner, 2010; Fernández-Reiriz et al., 2011; Wang et al., 2015). Nevertheless, some species are positively affected by high CO_2 such as the sea urchin *Echinometra* sp., and show strong resistance to high pCO_2 after about one year exposure (Hazan et al., 2014). Similarly the brittlestar *Amphiura filiformis* shows an increase in metabolism and calcification when exposed to pH 7.3 (Wood et al., 2008). In the mussel *Mytilus galloprovincialis* exposed to high pCO_2, the scope for growth is better, promoting reproduction; this is due to better absorption efficiency and a lower ammonium excretion rate (Fernández-Reiriz et al., 2012). Lastly, the metabolic rate of the wild oyster *Saccostrea glomerata* is not impacted by low pCO_2 (Parker et al., 2012). This literature review shows that the responses of organisms can be very different. The present challenge is to understand the potential impact of acidification of the aquatic

* Corresponding author.
E-mail address: Gilles.Le.Moullac@ifremer.fr (L.M. Gilles).

http://dx.doi.org/10.1016/j.ecss.2016.03.011
0272-7714/

environment on the physiology of the pearl oyster, which is a valuable resource in French Polynesia. Pearl culture there depends on the exploitation of a single species, the pearl oyster *Pinctada margaritifera*, and relies entirely on the supply of wild juveniles collected on artificial substrates (Thomas et al., 2012). Cultured pearls are the product of grafting *P. margaritifera* and then rearing these oysters in their natural environment (Cochennec-Laureau et al., 2010). Considering that the pearl oyster *P. margaritifera* is an emblematic bivalve of the South Pacific atoll, especially French Polynesia, it is important to assess if climatic stressors impact its physiology, in terms of energy management and biomineralization process. Scope for growth (SFG) is a physiological index commonly used in the strategy of energy management (Bayne and Newell, 1983). Acquisition of energy in bivalves is described by the ingestion rate (IR), the concentration of microalgae being used as a marker (Yukihira et al., 1998) which is a saturating function of microalgae concentration in *P. margaritifera* (Le Moullac et al., 2013). Assimilation efficiency (AE) can then be derived by considering the residual organic matter content in the animal's faeces and pseudofaeces. Assimilation of organic matter by a bivalve varies according to the quantity and quality of suspended particulate matter (Saraiva et al., 2011). Energy losses involve oxygen consumption and excretion (Pouvreau et al., 2000) and are mainly related to temperature and food level (Chavez-Villalba et al., 2013). The scope for growth (SFG), resulting in energy gained or lost, is the difference between the energy acquired by feeding and that lost by respiration and excretion (Pouvreau et al., 2000). So, knowing the impact of pCO_2 on energy management could help us to evaluate the threshold of risk for survival of the species.

The proper functioning of the process of biomineralisation is a challenge in terms of growing pearl oysters and pearl culture. Mantle edge cells are the headquarters of the molecular processes involved in the production of calcite and aragonite (Joubert et al., 2010; Kinoshita et al., 2011). The molecular processes that control shell growth are subject to environmental conditions. Joubert et al. (2014) have shown that the deposition rate of nacre at the ventral edge of the shells of *P margaritifera* depends on environmental conditions and some genes are specifically regulated by the level of food whereas others are controlled by the seawater temperature. Previous studies show that acidification could deregulate the expression of some genes associated with calcification (Liu et al., 2012). The question is how these molecular deregulations will impact on the biomineralisation of shell structures.

We studied the impact of acidification (pH 7.8 and 7.4) compared with an actual pH of 8.2 on the physiology of pearl oysters at a bioenergetic level by measuring metabolic flux, reproduction and shell biomineralisation at microscopic, microstructural and molecular levels. The effects of these changes will be studied across the organism (individuals, population) by means of an experimental approach designed to simulate environmental conditions.

2. Material and methods

2.1. Ethical statement

The authorisation (No. 542) for pearl oysters' translocation from Takaroa atoll (14°26′59.12″S, 144°58′19.91″W, Tuamotu Archipelago, French Polynesia) to the lagoon of Vairao (Ifremer marine concession No. 8120/MLD: 17°48′26.0″S, 149°18′14.4″W, Tahiti, French Polynesia) was issued by the Ministry of Marine Resources on 2 February 2012. After collection from Takaroa atoll, 400 pearl oysters of an average height of 80 mm were packed in isothermal boxes for shipment (by air). Upon their arrival at Vairao, pearl oysters were immersed for 30 min in a hyper-saline water bath (Salinity 120) following the prophylactic recommendations supplied with the transfer authorisation. Then, the pearl oysters were stored in the lagoon of Vairao for four months to enable complete physiological recovery and to avoid any bias caused by the shipment and/or the hyper-saline water treatment. This study did not involve protected or endangered species.

2.2. Experimental design

Three different pH levels, 8.2, 7.8 and 7.4, were maintained for 100 days by means of the experimental system described below. This experiment was conducted twice, first from 24 May 2012 and then, after the interval of one year, from 17 June 2013, with different pearl oysters of the same set. The individuals used had an average height of 98.1 ± 6.5 mm and 117 ± 12.6 mm for the first and the second experiment, respectively. In total, and for each experiment, 60 oysters were randomly distributed in the three tanks. In order to measure the impact of each treatment on the oysters' growth rate their shells were marked with calcein (Sigma Aldrich, France) one day before the beginning of each experiment. The stain powder was dissolved over 12 h at 24 °C in filtered seawater (0.1 μm) with a magnetic stirrer. Pearl oyster shells were marked by immersion of the pearl oysters in 150 mg L^{-1} calcein solution for 12 h, as described in Linard et al. (2011).

2.3. Rearing system and pH control

The rearing system was set up in an experimental bivalve hatchery operated by Ifremer in Vairao, Tahiti, French Polynesia. The facility is supplied with filtered (25 μm) seawater from the Vairao lagoon. The pearl oysters were placed in 500-L tanks with controlled flow-through. Seawater was renewed at the rate of 100 L h^{-1} in all the experiments. The pearl oysters were fed with microalgae *Isochrysis galbana* (T-Iso) supplied continuously by means of Blackstone dosing pumps (Hanna). A constant concentration of 25,000 cell mL^{-1} was maintained throughout the experiments. Temperature and algae concentration were controlled continuously by a fluorescent probe (Seapoint Sensor Inc.) and a temperature sensor (PT 100). The pH was manipulated in flow-through tanks by bubbling CO_2 until the target pH was reached. This was operated by pH electrodes and temperature sensors connected to a pH-stat system (Dennerle) that continuously monitored pH (calibrated to the NIST scale).

2.4. Carbonate chemistry

Total alkalinity (TA) was measured weekly via titration with 0.01 N HCl containing 40.7 g NaCl L^{-1} and using a titrator (Schott Titroline Easy). Parameters of carbonate seawater chemistry were calculated from pH, mean TA, temperature, and salinity with the free access CO_2 Systat package. Average pCO_2 corresponding to pH 7.4, 7.8 and 8.2 was respectively of 3540, 1338 and 514 μatm. Other parameters of carbonate seawater chemistry are given in Table 1.

2.5. Bioenergetic measurements

During the last 48 h of each treatment, the pearl oysters were placed on biodeposit collectors to quantify the assimilation of organic matter. Once the exposures were finished, four oysters from each treatment were transferred to the ecophysiological measurement system (EMS), where they were individually placed in a metabolic chamber to monitor clearance rate and oxygen consumption. The EMS consists of five open-flow chambers. For each treatment, each of the four oysters was placed, successively, in one of the chambers and the fifth chamber remained empty for use as a

Please cite this article in press as: Gilles, L.M., et al., Impact of pCO_2 on the energy, reproduction and growth of the shell of the pearl oyster *Pinctada margaritifera*, Estuarine, Coastal and Shelf Science (2016), http://dx.doi.org/10.1016/j.ecss.2016.03.011

Table 1
Water parameters calculated from samples taken from all experimental trays across the experimental period. Measurements were made once a week. The carbonate parameters were calculated using CO2sys software.

pH	Temperature (°C)	Salinity	Alcalinity (μmol/kg)	pCO_2 (μatm)	Ωca.	Ωar.
7.4	26.1 ± 0.6	35	2768 ± 231	3540 ± 402	1.32 ± 0.20	0.88 ± 0.13
7.8	26.2 ± 0.7	35	2753 ± 77	1338 ± 172	3.03 ± 0.26	2.01 ± 0.17
8.2	26.1 ± 0.7	35	2673 ± 198	514 ± 67	5.74 ± 0.57	3.80 ± 0.37

control (Chavez-Villalba et al., 2013). The experimental conditions applied during the adaptation period were replicated in the EMS during measurements.

Ingestion rate, an indicator of feeding activity, is defined as the quantity of microalgae cleared per unit of time. Ingestion rate (IR) was estimated by means of fluorescence measurements and calculated as: IR = V(C1−C2), where C1 is the fluorescence level of the control chamber, C2 is the fluorescence of the experimental chamber containing an oyster, and V is the constant water flow rate (10 L h^{-1}).

Respiration rate (RR mg O_2 h^{-1}) was calculated from differences in oxygen concentration between the control and experimental chambers where by RR = V(O1 − O2), where O1 is the oxygen concentration in the control chamber, O2 is the oxygen concentration in the experimental chamber, and V is the water flow rate.

To compare ingestion and respiration rates, it was necessary to correct for differences in specimen weight. Values of the ecophysiological activities were converted to a standard animal basis (1 g, dry weight) by using the formula Ys = (Ws/We)b × Ye, where Ys is the physiological activity of a standard oyster, Ws is the dry weight of a standard oyster (1 g), We is the dry weight of the specimen, Ye is the measured physiological activity, and b is the allometric coefficient of a given activity. The average b allometric coefficients were 0.66 for ingestion rate and 0.75 for oxygen consumption rate (Savina and Pouvreau, 2004).

Assimilation efficiency (AE) of organic matter was assessed by analysing microalgae, faeces and pseudofaeces according to Conover's method (1966). The pearl oysters were laid out in a collector, in which the deposits were collected on a 10-μm sieve. Biodeposits were centrifuged for 15 min at 4500 t min^{-1}. The supernatant was removed and the pellet was washed twice with ammonium formate (37g L^{-1} in distilled water). The pellet was then put in a pre-weighed aluminium cup to be dried at 60 °C for 48 h before being burnt at 450 °C for 4 h. Microalgae OM was obtained by the centrifugation of 5 L of the microalgae mixture and treatment of the pellet according to the same procedure as for the biodeposits. The absorption efficiency (AE) was then calculated according to the following equation:

$$AE = \frac{\%OM\mu alg - \%OMbiodeposit}{(100 - \%OMbiodeposit)x\ \%OM\mu alg}$$

Ecophysiological data were converted into energetic values to define the scope for growth (SFG) for each oyster: SFG = (IR × AE)− RR, where IR is the ingestion rate, AE is the assimilation efficiency, and RR is oxygen consumption. We used 20.3 J for 1 mg of particulate organic matter (Bayne et al., 1987) and 14.1 J for 1 mg O_2 (Bayne and Newell, 1983; Gnaiger, 1983).

2.6. Gonad histological analysis

Gonad development stages were determined by histological methods and samples were classified according to the different categories of gonadic tissues previously described in Teaniniuraitemoana et al. (2014). In order to simplify analysis, certain stages were grouped according to the dynamic of gametogenesis. Gonads in early, intermediate and mature stages were grouped in one group, and gonads in regression and undetermined constituted the two other groups.

2.7. Shell growth rate and nacremicrostructure

To investigate shell growth, the shells were sawn with a 'Swap Top' Trim Saw machine (Inland, Middlesex, UK), which included a diamond Trim Saw Blade (Thin Cut) IC-40961. Shell edges were then polished for 5 s with various grades of water sandpaper sheets. The shell sections were then examined under a Leitz Dialux 22 compound fluorescence microscope equipped with a I3-filter block and an optical micrometer. Shell growth was measured by evaluating the thickness of deposits at the ventral side of the shell and the calcein marks with an optical micrometer (Linard et al., 2011). Shell deposit rate (SDR) was calculated by dividing the thickness of deposits by the time which had elapsed since the marking. SDR was expressed in μm.d^{-1} (Linard et al., 2011; Joubert et al., 2014).

Electron Microscopy was performed on the electron microscopy platform (Université de la Polynésie Française). The structure of the shell deposit was observed by scanning electron microscopy (SEM) with a Hitachi Analytical Table Top SEM TM3030. The aragonitic tablets and the growing edge of nacre lining the shells were examined. Before observation, the sawn shells were treated by formic acid (1%), sonicated and dried. Observations relied on pictures, taken at the internal side of the shell (magnification 9000, accelerating voltage 15 KV). The thickness of aragonitic tablets was measured with post-acquisition image tools.

2.8. Gene expression in mantle

At the end of the 100 days exposure at different pCO_2, mantle samples from each pearl oyster were withdrawn and grouped randomly in fours, thus constituting five pools to limit the variability of individual responses for gene expression. Total RNA was extracted from each sample with TRIZOL®Reagent (Life Technologies) according to the manufacturer's recommendations. RNA was quantified with a NanoDrop®ND-1000 spectrophotometer (NanoDrop®Technologies Inc.); 3000 ng of total RNA were treated for each sample with DNAse (Ambion) to degrade any potentially contaminating DNA in the samples. First-strand cDNA was synthesised from 500 ng of total RNA with the Transcriptor First Strand cDNA Synthesis Kit (Roche), using 2 μL of anchored-oligo(dT) and 1 μL of random hexamer primers. The expression levels of nine genes were analysed by quantitative RT-PCR analysis with a set of forward and reverse primers (Table 2). Three genes, commonly used as reference genes for comparisons of gene expression data, were chosen because of their ubiquitous and constitutive expression pattern: 18S rRNA gene (Larsen et al., 2005), GAPDH (Dheilly et al., 2011) and SAGE. Quantitative-RT-PCR amplifications were carried out on a Stratagene MX3000P (Agilent Technologies), using 12.5 μL of Brilliant II SYBR® Green QPCR Master Mix (Stratagene) with 400 nM of each primer and 10 μL of 1:100 cDNA template. The following amplification protocol was used: initial denaturation at 95 °C for 10 min followed by 40 cycles of denaturation at 95 °C for 30 s, primer annealing at 60 °C for 30 s and extension at 72 °C for

Please cite this article in press as: Gilles, L.M., et al., Impact of pCO_2 on the energy, reproduction and growth of the shell of the pearl oyster *Pinctada margaritifera*, Estuarine, Coastal and Shelf Science (2016), http://dx.doi.org/10.1016/j.ecss.2016.03.011

Table 2
Set of forward and reverse primers used for the gene expression analysis (*SRA accession number of EST library published in Joubert et al., 2010).

Gene	GenBank Accession number	Forward primer	Reverse primer
Pmarg-PIF 177	HE610401	5′-AGATTGAGGGCATAGCATGG-3′	5′-TGAGGCCGACTTTCTTGG-3′
Pmarg-Pearlin	DQ665305	5′-TACCGGCTGTGTTGCTACTG-3′	5′-CACAGGGTGTAATATCTGGAACC-3′
Pmarg-MRNP34	HQ625028	5′-GTATGATGGGAGGCTTTGGA-3′	5′-TTGTGCGTACAGCTGAGGAG-3′
Pmarg-MSI60	SRX022139*	5′-TCAAGAGCAATGGTGCTAGG-3′	5′-GCAGAGCCCTTCAATAGACC-3′
Pmarg-Shematrin 9	ABO92761	5′-TGGTGGCGTAAGTACAGGTG-3′	5′-GGAAACTAAGGCACGTCCAC-3′
Pmarg-Prismalin 14	HE610393	5′-CCGATACTTCCCTATCTACAATCG-3′	5′-CCTCCATAACCGAAAATTGG-3′
Pmarg-PUSP6	SRX022139*	5′-TTCATTTTGGTGGTTATGGAATG-3′	5′-CCGTTTCCACCTCCGTTAC-3′
Pmarg-Aspein	SRX022139*	5′-TGGAGGTGGAGGTATCGTTC-3′	5′-ACACCTGATACCCTGCTTGG-3′
Pmarg-Nacrein A1	HQ654770	5′-CTCCATGCACAGACATGACC-3′	5′-GCCAGTAATACGGACCTTGG-3′

1 min. Lastly, to verify the specificity of the product, a melting curve analysis was performed from 55 to 95 °C increasing by 0.5 °C. All q-RT-PCR reactions were duplicated. The comparative Ct (threshold cycle) method was used to analyse the expression levels of the candidate genes. The relative expression ratio of each analysed cDNA was based on the delta-delta method normalised with three reference genes for comparing the relative expression results, which is defined as: ratio $= 2^{-[\Delta Ct\ sample - \Delta Ct\ calibrator]} = 2^{-\Delta\Delta Ct}$ (Livak and Schmittgen, 2001). Here the ΔCt calibrator represented the mean of the ΔCt values obtained for all tested genes in all conditions.

2.9. Statistical analysis

Normality of data distribution and homogeneity of variance were tested with the Shapiro-Wilk test and the Bartlett test, respectively. Respiration rate data followed the conditions of application of parametric tests, but Ingestion rate and SFG data were subjected to the Box Cox transformation to satisfy these conditions. AE was analysed by using arcsine square root AE/100 values. Comparison of energy values and SDR after 100 days of exposure to different pCO_2 levels was done by using a two-way ANOVA where factors were the experimental series (one-year interval between the two experiments) and the pCO_2 level. Post hoc comparison was done with the unilateral test of Dunnet using the lowest pCO_2 levels as a control for comparison with the highest one. α was set at 0.05 for all analyses. Impact of pCO_2 levels on gametogenesis was analysed with the Chi-square test. The expression values of the nine candidate genes met the condition for parametric ANOVA after normalization with the BoxCox transformation. Post hoc comparison was done with the unilateral test of Dunnet using the lowest pCO_2 levels as a control for comparison with the highest one α was set at 0.05 for all analyses.

3. Results

3.1. Bioenergetics

The 100-day exposure to various pCO_2 levels did not induce modifications of the bioenergetics descriptors (Table 3). The assimilation efficiency (AE; F = 0.134, $p = 0.87$), ingestion rate (IR; F = 0.22, $p = 0.8$), respiration rate (RR; F = 1.35, $p = 0.26$) and SFG (F = 0.02, p = 0.98) were not significantly changed by any of the treatments in either of the two experiments (Fig. 1a–c). However, the comparison between the two experiments highlights that all bioenergetics descriptors increased significantly with oyster size; AE (F = 59.86, $p < 0.0001$), IR (F = 7.14, $p = 0.01$), RR (F = 7.56, $p = 0.01$) and SFG (F = 12.82, $p = 0.001$).

3.2. Reproduction

It was necessary to do groupings since the sample sizes for certain classes was insufficient to meet the conditions for the application of the Chi-square test. Therefore, the impact of pCO_2 level on gametogenesis was analysed for three gonadic stages and the two experimental series were grouped (Fig. 2). With this data set, the Chi-square test did not show any significant effect of the pCO_2 level on the gametogenic process (chi2 = 4.81, $p = 0.31$).

3.3. Shell integrity, growth and microstructural organisation

The external side of the shells whitened during the 100 days of exposure to acidification. Fig. 3 shows the three lots of pearl oysters grouped by level of pCO_2 exposure. We observed a gradient in the bleaching of the outer surface of the shell depending on the level of exposure to pCO_2. The shells of pearl oysters exposed to pCO_2 of 3540 atm had blanched considerably, and those exposed to pCO_2 1338 atm were an intermediate shade.

Shell deposition rate (SDR) measurement was done with calcein marking in order to analyse the effect of environmental pCO_2level on shell growth. Two-way ANOVA showed a significant effect of pCO_2 level on SDR (F = 3.208, p = 0.045) but also an age effect (F = 61.11, p < 0.0001). The unilateral test of Dunnett highlighted that the SDR decreased significantly between the control treatment and pH 7.4 (Fig. 4a). At microstructural scale, MEB observation and measurement showed that the thickness of aragonite tablets did not change with pCO_2 level. The mean value of aragonite thickness tablets remained an average size of 0.4 nm (Fig. 4b).

Observation of the growing edge of nacre lining the shells showed that shells exposed to acidified conditions (pCO_2 of 1338

Table 3
Two-way ANOVA results for bioenergetic values of 100 day exposure to the pCO_2 level in two separated experiments at one year interval (absorption efficiency (AE), ingestion rate (IR), respiration rate (RR), scope for growth (SFG).

Sources of variation	ddl	AE (arcsinsqr)		IR (Box Cox)		RR		SFG (Box Cox)	
		F	p	F	p	F	p	F	p
pCO_2	2	0.13	0.87	0.22	0.80	1.35	0.26	0.02	0.98
Experiment	1	59.86	**<0.0001**	7.14	**0.01**	7.56	**0.01**	12.82	**0.001**
pCO_2 × experiment	2	1.32	0.27	0.13	0.88	0.13	0.88	0.35	0.70

The p values under 0.05 are in bold.

Please cite this article in press as: Gilles, L.M., et al., Impact of pCO_2 on the energy, reproduction and growth of the shell of the pearl oyster *Pinctada margaritifera*, Estuarine, Coastal and Shelf Science (2016), http://dx.doi.org/10.1016/j.ecss.2016.03.011

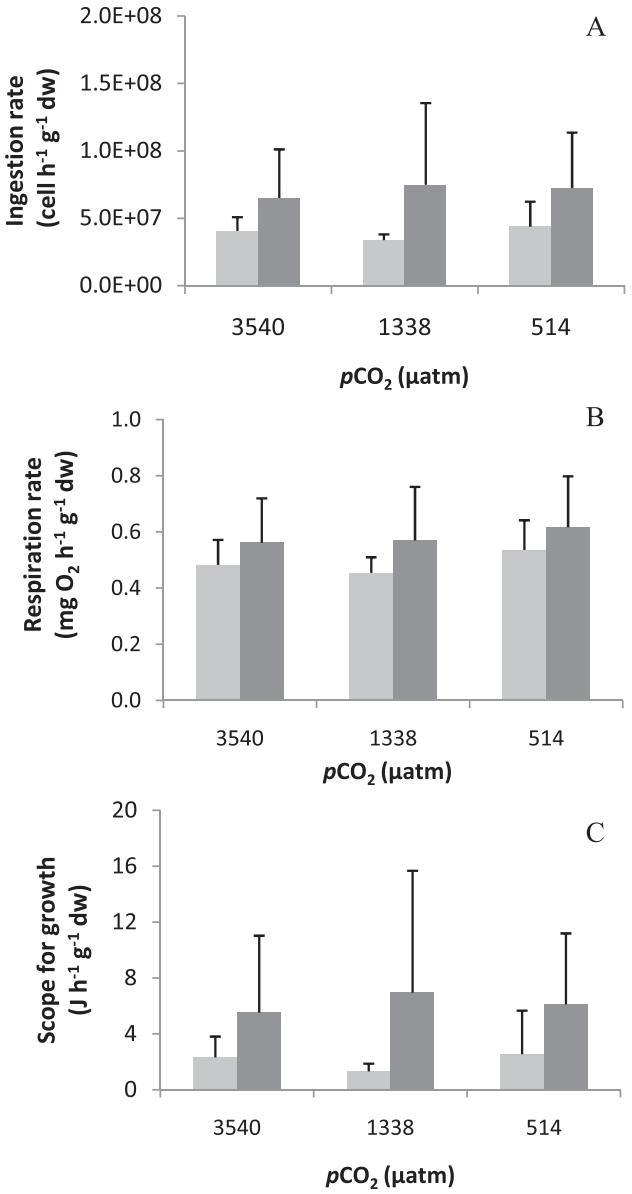

Fig. 1. Bioenergetic behavior after one hundred days exposure to pCO_2 level at one year interval (1st experiment (grey), 2nd experiment (dark grey)); (A) ingestion rate (IR), (B) respiration rate (RR) (C) scope for growth (SFG)) of the black-lip pearl oyster *Pinctada margaritifera*. Means are presented with standard error ($12 < n < 16$).

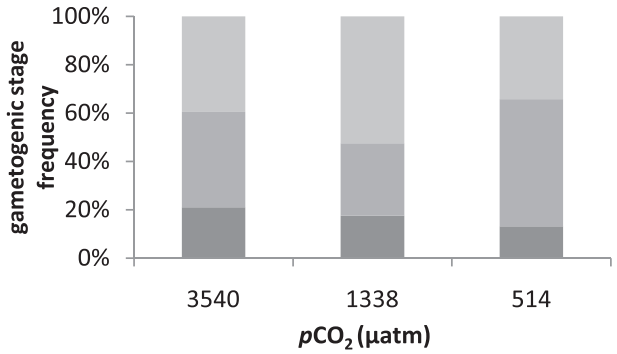

Fig. 2. Effect of the pCO_2 level on gametogenesis of pearl oyster exposed for one hundred days ($38 < n < 41$).

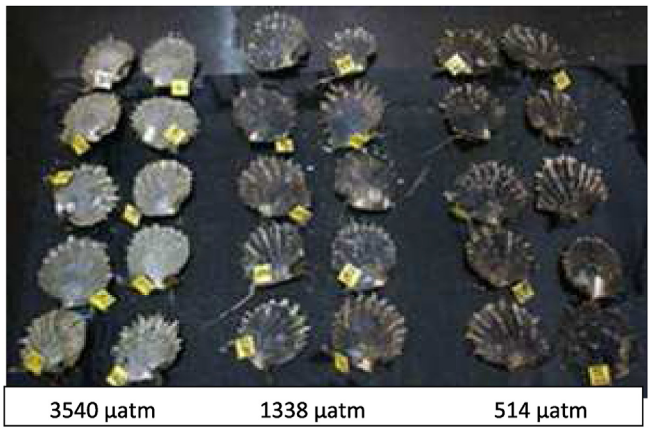

Fig. 3. Effect of the pCO_2 level on bleaching of external side of shells of pearl oyster exposed for one hundred days.

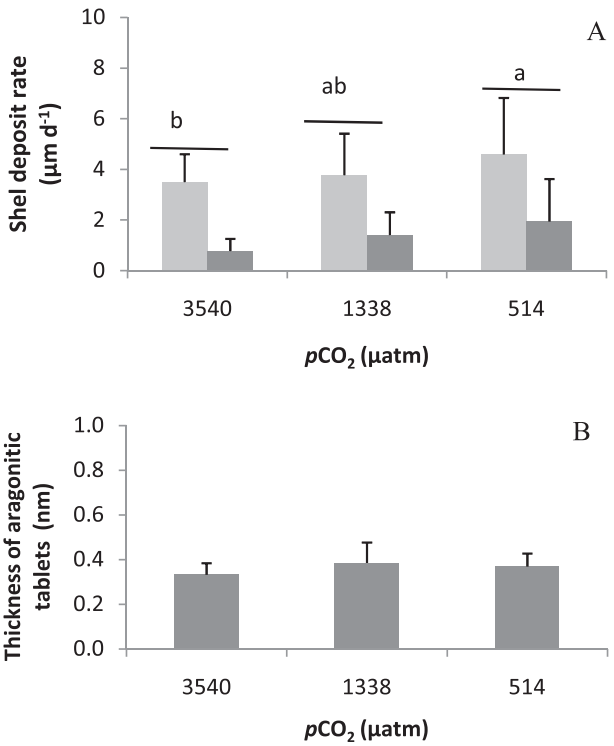

Fig. 4. Effect of the pCO_2 level on shell growth (A) shell deposit rate, (1srt experiment (grey), 2nd experiment (dark grey), (B) thickness of aragonite tablet, 2nd experiment. ($n = 8–9$).

and 3540 µatm) showed signs of malformation and/or dissolution compared with controls. This study found notable differences in the appearance of the growing edge of the nacreous layer of *P. margaritifera* kept at high pCO_2. Oysters from the control (pCO_2 514 µatm) had nacre that showed a distinct boundary between the fully formed and developing nacre tablets (Fig. 5a), the organic matrix was intact (Fig. 5b) and growth of nacre also showed a clear wave-like pattern and nacre tablets forming within an extensive organic matrix (Fig. 5c). Inspection of nacre from oysters held at pCO_2 of 1338 µatm still showed a distinct boundary between calcite and aragonite (Fig. 5d), although the organic matrix disappeared in places (Fig. 5e) and the wave-like pattern became anarchic (Fig. 5f). At pCO_2 of 3540 µatm the boundary was visible (Fig. 5g), but the

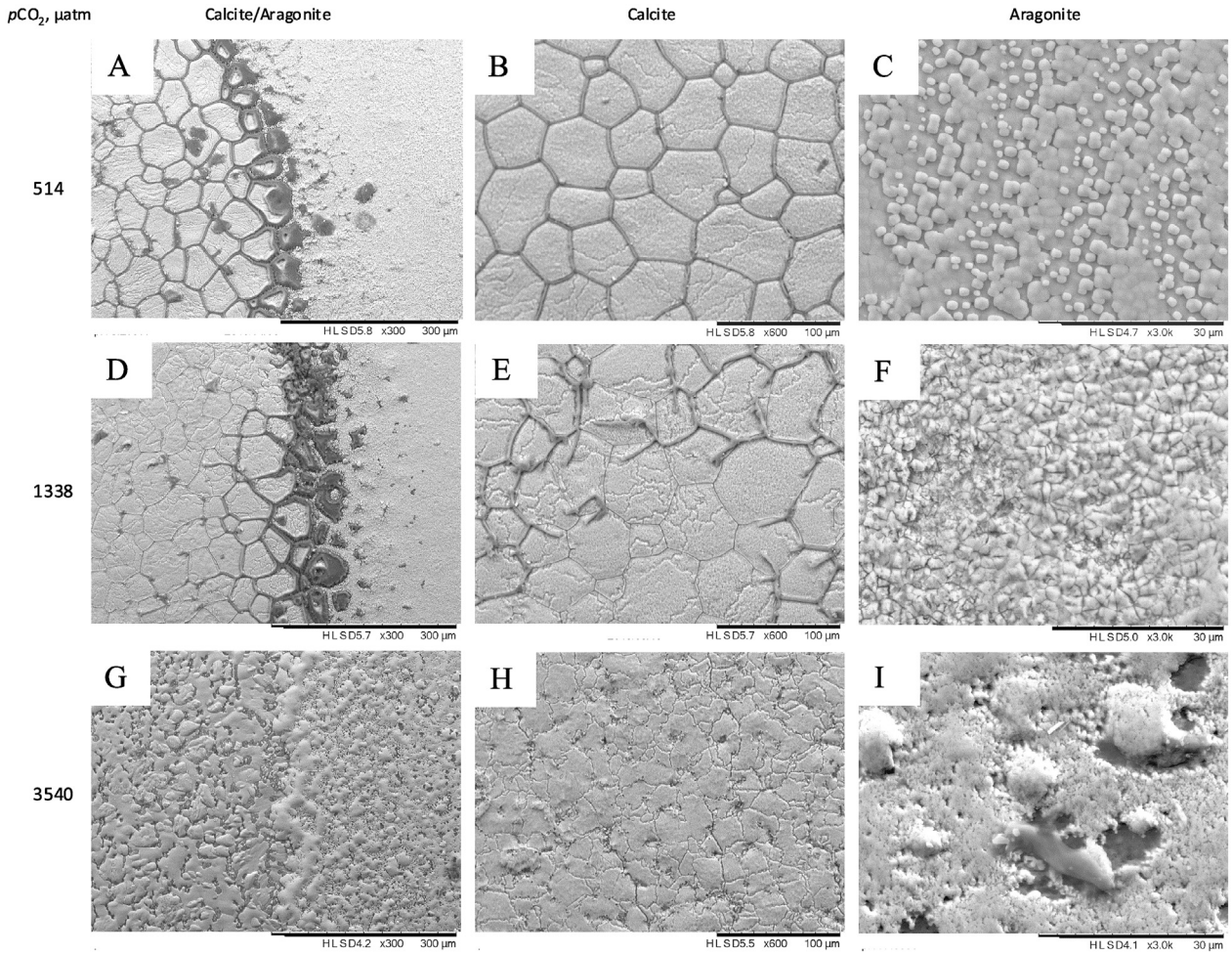

Fig. 5. SEM of growing edge of the nacre layer within shells of *Pinctada margaritifera* (A, D, G), calcite formation (B, E, H), aragonite (C, F, I) after one hundred days exposure to pCO_2 level (514, 1338, 3540 µatm).

organic matrix disappeared completely (Fig. 5h), the aragonite tablets also disappeared leaving space for a kind of nacre where the shelves were merged (Fig. 5i).

3.4. Mantle gene expression

Among the nine candidate genes tested, the expression of eight of them was not modulated by the experimental treatments. The one affected was the *Pmarg*-PUSP6 gene. Its expression significantly decreased at the highest pCO_2 level compared with the lowest (Table 4, Fig. 6).

4. Discussion

Bivalve growth is known to be strongly influenced by environmental conditions such as food supply and water temperature. The aim of this study was simultaneously to evaluate *P. margaritifera* bioenergetics and biomineralisation ability depending on pCO_2 level. We acclimatised pearl oysters for 100 days at three levels of pCO_2 in two identical experiments with a one-year interval between them. We determined that acidification does not impact on the pearl oyster at the energy management level; hence gametogenesis is not affected. Our observations showed that the shell growth slowdown could result from active chemical dissolution of shell and/or from a deregulation of some genes since we found that the functioning of one of them altered amongst the nine tested.

4.1. pCO_2 did not influence energy management and reproduction

The other main result of this study was that high pCO_2 did not change bioenergetics in *P margaritifera* exposed for 100 days. This has already been found for the mussel *Mytilus galloprovincialis*, for which the acidified seawater did not change clearance, ingestion and respiration rates. However, SFG increases significantly under more efficient assimilation of organic matter (Fernández-Reiriz et al., 2012). The same group (Fernández-Reiriz et al., 2011) revealed a consistent effect of high pCO_2 as shown by the reduction of ingestion rate by 60% in the clam *Ruditapes decussatus* and slow growth as a result of acidification. Other studies have shown no effect of low pH on SFG in the mussel *Mytilus coruscus* exposed for 14 days (Wang et al., 2015). Similarly, in the gastropod *Nassarius conoidalis*, 31-day exposure to acidification has no effect on the energetics of the species (Zhang et al., 2015). These results show that bivalves can adapt immediately without suffering any impact on their physiology or in the longer term with an impact on growth. For *P. margaritifera*, in the short and medium term, our results showed no impact on energy management and gametogenesis. Histological observations of gonads have shown that the cellular process is not affected by pCO_2. Often, when stress or a nutritional problem occurs, the germinal process will stop at the level of

Please cite this article in press as: Gilles, L.M., et al., Impact of pCO_2 on the energy, reproduction and growth of the shell of the pearl oyster *Pinctada margaritifera*, Estuarine, Coastal and Shelf Science (2016), http://dx.doi.org/10.1016/j.ecss.2016.03.011

Table 4
Significance level of ANOVA test of calcifying genes expression level according to pCO_2 level in two separated experiments at one year interval.

Sources of variation	Pmarg-PIF177		Pmarg-Nacrein		Pmarg-PUSP6		Pmarg-Pearlin		Pmarg-MRNP34		Pmarg-MSI60		Pmarg-Shematrin9 9		Pmarg-Prismalin14		Pmarg-Aspein	
	F	p	F	p	F	p	F	p	F	p	F	p	F	p	F	p	F	p
pCO_2	1.16	*0.34*	0.63	*0.54*	4.62	***0.02***	0.56	*0.58*	1.95	*0.17*	1.73	*0.21*	2.10	*0.16*	1.45	*0.26*	0.49	*0.62*
Experiment	*14.29*	***0.001***	*7.06*	***0.02***	*0.535*	*0.47*	*0.002*	*0.97*	*2.94*	*0.10*	*38.63*	***0.0001***	*14.07*	***0.001***	*2.84*	*0.11*	*7.35*	***0.01***
pCO_2 × experiment	*1.45*	*0.26*	*1.65*	*0.22*	*0.55*	*0.59*	*2.65*	*0.10*	*2.08*	*0.15*	*2.23*	*0.14*	*1.39*	*0.28*	*1.37*	*0.28*	*0.094*	*0.91*

The p values under 0.05 are in bold.

differentiation of germinal stem cells (Bishop and Watt, 1994; Le Moullac et al., 2013). Gametogenesis of pearl oysters subject to acidification of their environment is not changed.

This suggests that *P margaritifera* appears to be resistant at short term to pCO_2 increase at energy management level implying hence reproduction.

4.2. pCO_2 influences shell integrity, growth rate and molecular process

A high pCO_2 level acted on *P. margaritifera*'s shell and biomineralisation process. First, the external side of the shell was highly blanched at pCO_2 of 3540 µatm. Bleaching of the external side of the shell is the consequence of periostracum dissolution,

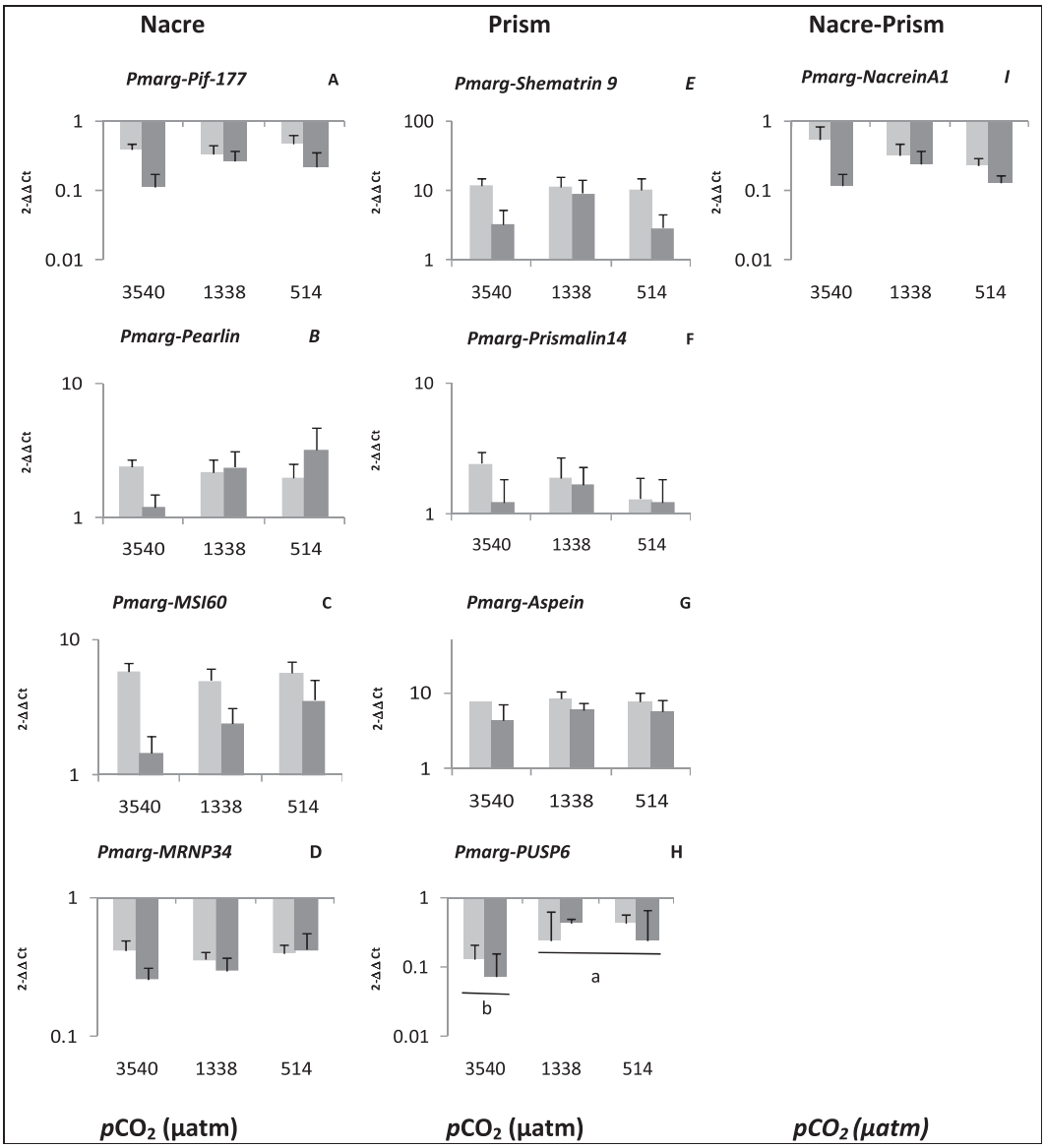

Fig. 6. Effect of the pCO_2 level on mantle gene expression in pearl oyster exposed one hundred days shell deposit rate, (1srt experiment (grey), 2nd experiment (dark grey)) (a) *Pmarg*-Pif-177, (b) *Pmarg*-Pearlin, (c) *Pmarg*-MSI 60, (d) *Pmarg*-MRNP34, (e) *Pmarg*-Shematrin 9, (F) *Pmarg*-Prismalin 14, (g) *Pmarg*-Aspein, (h) *Pmarg*-PUSP6, (i) N*Pmarg*-Nacrein A1(n = 5).

Please cite this article in press as: Gilles, L.M., et al., Impact of pCO_2 on the energy, reproduction and growth of the shell of the pearl oyster *Pinctada margaritifera*, Estuarine, Coastal and Shelf Science (2016), http://dx.doi.org/10.1016/j.ecss.2016.03.011

and hence could render pearl oysters more sensitive to shell parasites. Parasitism of the shell of *P. margaritifera* results in biodegradation by shell-boring organisms, especially sponges, and the shells become brittle (Mao Che et al., 1996).

At high pCO_2 of 3540 μatm, the shell deposit rate was reduced and the inside of the shell showed signs of active chemical dissolution. Aragonite and calcite were unstructured, appearing as fade. This appearance coincided with the total absence of the organic matrix. At pCO_2 of 1338 μatm, part of the organic matrix remained intact while in other part, the organic matrix was lacking. Therefore, the structural integrity of the shells of *P margaritifera* seems compromised as has already been shown in tropical as well as in arctic bivalves (McClintock et al., 2009; Welladsen et al., 2010).

In parallel, high pCO_2 of 3540 μatm reduced the expression level of certain genes implied in biomineralisation. One gene (*Pmarg*-PUSP6) coding for a matrix protein among the nine tested showed down-regulation with high pCO_2. The expression of the *Pmarg*-PUSP6 gene decreased about five fold under the effect of the higher pCO_2 compared with controls. *P fucata* seems more sensitive to low pH, since aspein and nacrein expression decreased by 30 and 60% at pH 8.1 and 7.7 respectively after short-term exposure (Liu et al., 2012), whereas expression of these genes (*Pmarg*-Aspein and *Pmarg*-Nacrein A1) in *P margaritifera* did not change in the present study; that could be an adaptive response after an eventual acute response. Little is known of *Pmarg*-PUSP6 activity; this gene expressed in the mantle edge and in the mantle pallium is involved in the production of calcite (Marie et al., 2012). This study details the role of *Pmarg*-PUSP6 as a direct link can be made with shell growth, whose expression is regulated by pCO_2.

5. Conclusions

However, is this a purely chemical reaction or a coping strategy that favours the vital processes? In our study, energy management was not changed under pCO_2 treatment, and reproduction was apparently maintained, although biomineralisation and the integrity of the shells were affected, giving weight to the hypothesis of Melzner et al. (2011) who observed in the mussel *Mytilus edu*lis that pCO_2 decreased shell length growth, suggested that energy is allocated to more vital processes (somatic mass maintenance) instead of shell conservation.

It would be useful to determine the impact of acidification on ability of gametes for fertilisation and finally on the development of larvae. The shells of larvae, primarily formed of aragonite, could be weakened by low pH, which may alter development until fixation, which is crucial for the bivalves. Changes in *Pmarg*-PUSP6 expression suggest that other genes are deregulated; only a differential transcriptomic approach could analyse more accurately the effect and consequence of acidification.

Acknowledgment

This study is a part of the research project "Management and adaptation of pearl culture in French Polynesia in the context of global change: an environmental, economic and social approach" (POLYPERL) funded by the French National Research Agency within the framework of the program AGROBIOSHERE (ANR-11-AGRO-006). The authors greatly acknowledge the electron microscopy platform of the University of French Polynesia and its personnel. The authors wish to thank the staff of the laboratory of studies and environmental monitoring (LESE) for his help in the realization of chemical measurements of sea water.

References

Bayne, B.L., Hawkins, A.J.S., Navarro, E., 1987. Feeding and digestion by the mussel *Mytilus edulis* L. (Bivalvia: Mollusca) in mixtures of silt and algal cells at low concentrations. J. Exp. Mar. Biol. Ecol. 111, 1–22.

Bayne, B.L., Newell, R.C., 1983. Physiological energetics of marine molluscs. In: Saleuddin, A.S.M., Wilbur, K.M. (Eds.), The Mollusca, vol. 4. Academic Press, New York, NY, pp. 407–515.

Berge, J.A., Bjerkeng, B., Pettersen, O., Schaanning, T., Oxnevad, S., 2006. Effects of increased seawater concentration of CO_2 on growth of the bivalve *Mytilus edulis* L. Chemosphere 62, 681–687.

Bishop, C.D., Watt, S.A., 1994. Two-stage recovery of gametogenic activity following starvation in *Lytechinusvariegatus* Lamarck (Echinodermata: Echinoidea). J. Exp. Mar. Biol. Ecol. 177, 27–36.

Caldeira, K., Wickett, M.E., 2005. Ocean model predictions of chemistry changes from carbon dioxide emissions to the atmosphere and ocean. J. Geophys. Res. 110, C09S04. http://dx.doi.org/10.1029/2004JC002671.

Chavez-Villalba, J., Soyez, C., Aurentz, H., Le Moullac, G., 2013. Physiological responses of female and male black-lip pearl oysters (*Pinctadamargaritifera*) to different temperatures and concentrations of food. Aquat. Living Resour. 26, 263–271. http://dx.doi.org/10.1051/alr/2013059. Publisher's official version. http://archimer.ifremer.fr/doc/00157/26855/. Open Access version.

Cochennec-Laureau, N., Montagnani, C., Saulnier, D., Fougerouse, A., Levy, P., Lo, C., 2010. A histological examination of grafting success in pearl oyster *Pinctada-margaritifera* in French Polynesia. Aquat. Living Resour. 23, 131–140. http://dx.doi.org/10.1051/alr/2010006. Publisher's official version.

Conover, R., 1966. Assimilation of organic matter by zooplankton. Limnol. Oceanogr. 11, 338–345.

Dheilly, N., Lelong, C., Huvet, A., Favrel, P., 2011. Development of a Pacific oyster (*Crassostrea gigas*) 31,918-feature microarray: identification of reference genes and tissue-enriched expression patterns. BMC Genom. 2011 (12), 468. http://dx.doi.org/10.1186/1471-2164-12-468.

Fernández-Reiriz, M.J., Range, P., Álvarez-Salgado, X.A., Esponisa, J., Labarta, U., 2012. Tolerance of juvenile *Mytilus galloprovencialis* to experimental seawater acidification. Mar. Ecol. Prog. Ser. 454, 65–74.

Fernández-Reiriz, M.J., Range, P., Álvarez-Salgado, X.A., Labarta, U., 2011. Physiological energetics of juvenile clams *Ruditapes decussatus* in a high CO_2 coastal ocean. Mar. Ecol. Prog. Ser. 433, 97–105.

Gazeau, F., Parker, L.M., Comeau, S., Gattuso, J.-P., O'Connor, W.A., Martin, S., Pörtner, H.-O., Ross, P.M., 2013. Impacts of ocean acidification on marine shelled molluscs. Mar. Biol. 160, 2207–2245. http://dx.doi.org/10.1007/s00227-013-2219-3.

Gnaiger, E., 1983. Heat dissipation and energetic efficiency in animal anoxibiosis. Economy contra power. J. Exp. Zool. 228, 471–490.

Hazan, Y., Wangensteen, O.S., Fine, M., 2014. Tough as a rock-boring urchin: adult *Echinometra* sp. EE from the Red Sea show high resistance to ocean acidification over long-term exposures. Mar. Biol. 161, 2531–2545. http://dx.doi.org/10.1007/s00227-014-2525-4.

Joubert, C., Linard, C., Le Moullac, G., Soyez, C., Saulnier, D., Teaniniuraitemoana, V., Ky, C.L., Gueguen, Y., 2014. Temperature and food influence shell growth and mantle gene expression of shell matrix proteins in the pearl oyster *Pinctada margaritifera*. PLoS One 9 (8), e103944. http://dx.doi.org/10.1371/journal.pone.0103944.

Joubert, C., Piquemal, D., Marie, B., Manchon, L., Pierrat, F., Zanella-Cleon, I., Cochennec-Laureau, N., Gueguen, Y., Montagnani, C., 2010. Transcriptome and proteome analysis of *Pinctada margaritifera* calcifying mantle and shell: focus on biomineralization. BMC Genom. 11, 1–13. Publisher's official version. http://dx.doi.org/10.1186/1471-2164-11-613.

Kinoshita, S., Wang, N., Inoue, H., Maeyama, K., Okamoto, K., Nagai, K., Kondo, H., Hirono, I., Asakawa, S., Watabe, S., 2011. Deep sequencing of ESTs from nacreous and prismatic layer producing tissues and a screen for novel shell formation-related genes in the pearl oyster. PLoS One 6 (6), e21238. http://dx.doi.org/10.1371/journal.pone.0021238.

Kurihara, H., Asai, T., Kato, S., Ishimatsu, A., 2008. Effects of elevated pCO_2 on early development in the mussel *Mytilus galloprovincialis*. Aquat. Biol. 4, 225–233. http://dx.doi.org/10.3354/ab00109.

Kurihara, H., Ishimatsu, A., 2008. Effects of high CO2 seawater on the copepod (*Acartia tsuensis*) through all life stages and subsequent generations. Mar. Pollut. Bull. 56, 1086–1090. http://dx.doi.org/10.1016/j.marpolbul.2008.03.023.

Larsen, J.B., Frischer, M.E., Rasmussen, L.J., Hansen, B.W., 2005. Single-step nested multiplex PCR to differentiate between various bivalve larvae. Mar. Biol. 146, 1119–1129.

Le Moullac, G., Soyez, C., Sham-Koua, M., Levy, P., Moriceau, J., Vonau, V., Maihota, M., Cochard, J.C., 2013. Feeding the pearl oyster *Pinctada margaritifera* during reproductive conditioning. Aquac. Res. 44, 404–411.

Linard, C., Gueguen, Y., Moriceau, J., Soyez, C., Hui, B., Raoux, A., Cuif, J.-P., Cochard, J.-C., Le Pennec, M., Le Moullac, G., 2011. Calcein staining of calcified structures in pearl oyster *Pinctada margaritifera* and the effect of food resource level on shell growth. Aquaculture 313, 149–155. http://dx.doi.org/10.1016/j.aquaculture.2011.01.008. Publisher's official version.

Liu, W., Huang, X., Lin, J., He, M., 2012. Seawater acidification and elevated temperature affect gene expression patterns of the pearl oyster *Pinctada fucata*. PLoS One 7 (3), e33679. http://dx.doi.org/10.1371/journal.pone.0033679.

Livak, K.J., Schmittgen, T.D., 2001. Analysis of relative gene expression data using

Please cite this article in press as: Gilles, L.M., et al., Impact of pCO_2 on the energy, reproduction and growth of the shell of the pearl oyster *Pinctada margaritifera*, Estuarine, Coastal and Shelf Science (2016), http://dx.doi.org/10.1016/j.ecss.2016.03.011

real-time quantitative PCR and the 2(-Delta Delta C(T)) method. Methods 25, 402–408.
McClintock, J.B., Angus, R.A., McDonald, M.R., Amsler, C.D., Catledge, S.A., Vohra, Y.K., 2009. Rapid dissolution of shells of weakly calcified Antarctic benthic macroorganisms indicates high vulnerability to ocean acidification. Antarct. Sci. 21, 449–456.
Mao Che, L., Le Campion-Alsumard, T., Boury-Esnault, N., Payri, C., Golubic, S., Bézac, C., 1996. Biodegradation of shells of the black pearl oyster, *Pinctada margaritifera* var. cumingii, by microborers and sponges of French Polynesia. Mar. Biol. 126, 509–519.
Marie, B., Joubert, C., Tayale, A., Zanella-Cleon, I., Belliard, C., Piquemal, D., Cochennec-Laureau, N., Marin, F., Gueguen, Y., Montagnani, C., 2012. Different secretory repertoires control the biomineralization processes of prism and nacre deposition of the pearl oyster shell. Proc. Natl. Acad. Sci. U. S. A. 109 (51), 20986–20991. Publisher's official version. http://dx.doi.org/10.1073/pnas.1210552109.
Melzner, F., Stange, P., Trübenbach, K., Thomsen, J., Casties, I., Panknin, U., Gorb, S.N., Gutowska, M.A., 2011. Food supply and seawater pCO2 impact calcification and internal shell dissolution in the blue mussel *Mytilus edulis*. Plos One 6, e24223. http://dx.doi.org/10.1371/journalpone.0024223.
Orr, J.C., Fabry, V.J., Aumont, O., Bopp, L., Doney, S.C., Feely, R.A., Gnanadesikan, A., Gruber, N., Ishida, A., Joos, F., Key, R.M., Lindsay, K., Maier-Reimer, E., Matear, R., Monfray, P., Mouchet, A., Najjar, R.G., Plattner, G.K., Rodgers, K.B., Sabine, C.L., Sarmiento, J.L., Schlitzer, R., Slater, R.D., Totterdell, I.J., Weirig, M.F., Yamanaka, Y., Yool, A., 2005. Anthropogenic ocean acidification over the twenty-first century and its impact on calcifying organisms. Nature 437 (7059), 681–686.
Parker, L.M., Ross, P.M., O'Connor, W.A., Borysko, L., Raftos, D.A., Pörtner, H.-O., 2012. Adult exposure influences offspring response to ocean acidification in oysters. Glob. Change Biol. 18, 82–92. http://dx.doi.org/10.1111/j.1365-2486.2011.02520.x.
Pouvreau, S., Tiapari, J., Gangnery, A., Lagarde, F., Garnier, M., Teissier, H., Haumani, G., Buestel, D., Bodoy, A., 2000. Growth of the black-lip pearl oyster, *Pinctada margaritifera*, in suspended culture under hydrobiological conditions of Takapoto lagoon (French Polynesia). Aquaculture 184, 133–154.
Ross, P.M., Parker, L., O'Connor, W.A., Bailey, E.A., 2011. The impact of ocean acidification on reproduction, early development and settlement of marine organisms. Water 3, 1005–1030.
Saraiva, S., van der Meer, J., Kooijman, S.A.L.M., Sousa, T., 2011. Modelling feeding processes in bivalves: a mechanistic approach. Ecol. Model. 222, 514–523.
Savina, M., Pouvreau, S., 2004. A comparative ecophysiological study of two infaunal filter-feeding bivalves: *Paphia rhomboides* and *Glycymeris glycymeris*. Aquaculture 239, 289–306. http://dx.doi.org/10.1016/j.aquaculture.2004.05.029. Publisher's official version.
Siikavuopio, S.I., Mortensen, A., Dale, T., Foss, A., 2007. Effects of carbon dioxide exposure on feed intake and gonad growth in green sea urchin, *Strongylocentrotus droebachiensis*. Aquaculture 266, 97–101.
Teaniniuraitemoana, V., Huvet, A., Levy, P., Klopp, C., Lhuillier, E., Gaertner-Mazouni, N., Gueguen, Y., Le Moullac, G., 2014. Gonad transcriptome analysis of pearl oyster *Pinctada margaritifera*: identification of potential sex differentiation and sex determining genes. BMC Genom. 15, 1–20. http://dx.doi.org/10.1186/1471-2164-15-491. Publisher's official version.
Thomas, Y., Garen, P., Bennett, A., Le Pennec, M., Clavier, J., 2012. Multi-scale distribution and dynamics of bivalve larvae in a deep atoll lagoon (Ahe, French Polynesia). Mar. Pollut. Bull. 65, 453–462. http://dx.doi.org/10.1016/j.marpolbul.2011.12.028. Publisher's official version.
Thomsen, J., Melzner, F., 2010. Moderate seawater acidification does not elicit long-term metabolic depression in the blue mussel *Mytilus edulis*. Mar. Biol. 157, 2667–2676. http://dx.doi.org/10.1007/s00227-010-1527-0.
Wang, Y., Li, L., Hu, M., Lu, W., 2015. Physiological energetics of the thick shell mussel *Mytilus coruscus* exposed to seawater acidification and thermal stress. Sci. Total Environ. 514, 261–272. http://dx.doi.org/10.1016/j.scitotenv.2015.01.092.
Welladsen, H.M., Southgate, P.C., Heimann, K., 2010. The effects of exposure to near-future levels of ocean acidification on shell characteristics of *Pinctada fucata* (Bivalvia: Pteriidae). Molluscan Res. 30, 125–130.
Wood, H.L., Spicer, J.I., Widdicombe, S., 2008. Ocean acidification may increase calcification rates, but at a cost. Proc. R. Soc. B Biol. Sci. 275 (1644), 1767–1773. http://dx.doi.org/10.1098/rspb.2008.0343.
Yukihira, H., Klumpp, D.W., Lucas, J.S., 1998. Effects of body size on suspension feeding and energy budgets of the pearl oysters *Pinctada margaritifera* and *P. maxima*. Mar. Ecol. Prog. Ser. 170, 120–130.
Zhang, H., Shin, P.K.S., Cheung, S.G., 2015. Physiological responses and scope for growth upon medium-term exposure to the combined effects of ocean acidification and temperature in a subtidal scavenger *Nassarius conoidalis*. Mar. Environ. Res. 106, 51–60.

Please cite this article in press as: Gilles, L.M., et al., Impact of pCO_2 on the energy, reproduction and growth of the shell of the pearl oyster *Pinctada margaritifera*, Estuarine, Coastal and Shelf Science (2016), http://dx.doi.org/10.1016/j.ecss.2016.03.011

ANNEXE 4

Conservation Physiology

Volume 9 • 2021 10.1093/conphys/coab041

SEB SOCIETY FOR EXPERIMENTAL BIOLOGY

Research article

Effects of elevated temperature and pCO_2 on the respiration, biomineralization and photophysiology of the giant clam *Tridacna maxima*

Chloé Brahmi[1,*], Leila Chapron[2], Gilles Le Moullac[3], Claude Soyez[3], Benoît Beliaeff[3], Claire E. Lazareth[4], Nabila Gaertner-Mazouni[1] and Jeremie Vidal-Dupiol[3,5]

[1]Univ. Polynésie française, IFREMER, ILM, IRD, EIO UMR 241, F-98702 Faa'a, Tahiti, Polynésie française
[2]School of Earth Sciences, The Ohio State University, Columbus, OH 43210, USA
[3]IFREMER, IRD, Institut Louis-Malardé, Univ. Polynésie française, EIO, F-98719 Taravao, Tahiti, Polynésie française, France
[4]Laboratoire de Biologie des Organismes et Ecosystèmes Aquatiques (BOREA) MNHN, CNRS, IRD, SU, UCN, UA, Muséum National d'Histoire Naturelle, 61 Rue Buffon, CP53, 75231, Paris Cedex 05, France
[5]IHPE, Univ. Montpellier, CNRS, Ifremer, Univ. Perpignan Via Domitia, Montpellier France

*Corresponding author: Univ. Polynésie française, EIO UMR 241, BP 6570, F-98702 Faa'a, Tahiti, French Polynesia. Tel: +689 40 866 479. Email: chloe.brahmi@upf.pf

Many reef organisms, such as the giant clams, are confronted with global change effects. Abnormally high seawater temperatures can lead to mass bleaching events and subsequent mortality, while ocean acidification may impact biomineralization processes. Despite its strong ecological and socio-economic importance, its responses to these threats still need to be explored. We investigated physiological responses of 4-year-old *Tridacna maxima* to realistic levels of temperature (+1.5°C) and partial pressure of carbon dioxide (pCO_2) (+800 µatm of CO_2) predicted for 2100 in French Polynesian lagoons during the warmer season. During a 65-day crossed-factorial experiment, individuals were exposed to two temperatures (29.2°C, 30.7°C) and two pCO_2 (430 µatm, 1212 µatm) conditions. The impact of each environmental parameter and their potential synergetic effect were evaluated based on respiration, biomineralization and photophysiology. Kinetics of thermal and/or acidification stress were evaluated by performing measurements at different times of exposure (29, 41, 53, 65 days). At 30.7°C, the holobiont O_2 production, symbiont photosynthetic yield and density were negatively impacted. High pCO_2 had a significant negative effect on shell growth rate, symbiont photosynthetic yield and density. No significant differences of the shell microstructure were observed between control and experimental conditions in the first 29 days; however, modifications (i.e. less-cohesive lamellae) appeared from 41 days in all temperature and pCO_2 conditions. No significant synergetic effect was found. Present thermal conditions (29.2°C) appeared to be sufficiently stressful to induce a host acclimatization response. All these observations indicate that temperature and pCO_2 are both forcing variables affecting *T. maxima*'s physiology and jeopardize its survival under environmental conditions predicted for the end of this century.

Key words: Giant clams, ocean acidification, photosynthetic yield, respiration, symbionts, thermal stress

Editor: Steven Cooke

Received 7 July 2020; Revised 18 January 2021; Editorial Decision 17 May 2021; Accepted 22 May 2021

Cite as: Brahmi C, Chapron L, Le Moullac G, Soyez C, Beliaeff B, Lazareth CE, Gaertner-Mazouni N, Vidal-Dupiol J (2021) Effects of elevated temperature and pCO_2 on the respiration, biomineralization and photophysiology of the giant clam *Tridacna maxima*. *Conserv Physiol* 9(1): coab041; doi:10.1093/conphys/coab041.

Introduction

Anthropocene era is characterized by human activities releasing gigatons of CO_2 in the atmosphere and contributing to induce global climate change (Broeker *et al.*, 1979; Caldeira and Wickett, 2003; Sabine *et al.*, 2004; Zeebe *et al.*, 2008; IPCC, 2014). The transfer of CO_2 from the atmosphere to the ocean results consequently to the increase of dissolved CO_2 in the seawater inducing significant pH decreases. On the other hand, due to the 'greenhouse gas' property of CO_2, terrestrial and sea surface temperature rise constantly (i.e. global warming). According to the last Intergovernmental Panel on Climate Change report (IPCC, 2019), warming had already reached +1°C by comparison to the pre-industrial period and may reach +1.5°C around 2040 if the current rate of emission is maintained. Enrichment of dissolved CO_2 in the ocean modifies the carbonate chemistry by decreasing carbonate ion concentration ($[CO_3^{2-}]$) and releasing protons that respectively decrease calcium carbonate saturation state (Ω) and seawater pH, i.e. ocean acidification (Kleypas *et al.*, 1999; Caldeira and Wickett, 2003). Indeed, pH had already decreased by 0.1 pH unit and this drop may reach −0.3 by 2100 (according to the RCP (Representative Concentration Pathway) 8.5 scenario; IPCC, 2019).

CO_3^{2-} is a carbonate ion form involved in biologically controlled calcification process, i.e. biomineralization (Orr *et al.*, 2005) of many marine organisms such as scleractinian corals and molluscs constructing calcium carbonate structures (e.g. exoskeleton, shell, test, spicule). This characteristic of their physiology make them highly sensitive to ocean acidification (Hoegh-Guldberg *et al.*, 2007; Ries *et al.*, 2009; Kroeker *et al.*, 2013; Gazeau *et al.*, 2013; Parker *et al.*, 2013), especially when this skeleton is made of aragonite, which is more sensitive to dissolution than calcite (Morse *et al.*, 2007). Among marine calcifying molluscs (e.g. oysters, mussels, giant clams, abalones, limpets) negative impacts of temperature and pCO_2 have been demonstrated on the survival, growth, biomineralization processes and other key physiological functions on different stages of their life cycle (Bougrier *et al.*, 1995; Kurihara, 2008; McClintock *et al.*, 2009; Gazeau *et al.*, 2010; Welladsen *et al.*, 2010; Melzner *et al.*, 2011; Rodolfo-Metalpa *et al.*, 2011; Schwartzmann *et al.*, 2011; Talmage and Gobler, 2011; Liu *et al.*, 2012; Watson *et al.*, 2012; Kurihara *et al.*, 2013; Fitzer *et al.*, 2014; Le Moullac *et al.*, 2016a, b; Meng *et al.*, 2018; Wessel *et al.*, 2018; Avignon *et al.*, 2020). However, effects of each stressor and their potential synergetic effect on giant clam's physiology are still poorly understood.

Giant clams produce an aragonitic shell composed of a prismatic inner layer and a crossed-lamellar outer layer (Pätzold *et al.*, 1991; Faylona *et al.*, 2011; Agbaje *et al.*, 2017; Gannon *et al.*, 2017). These organisms form an extracellular phototrophic mutualistic symbiosis with dinoflagellates of the Symbiodiniaceae family (Holt *et al.*, 2014; LaJeunesse *et al.*, 2018). The symbionts are hosted in the mantle part exposed to the light, in a tubular system (Z-tubules) directly connected to the stomach (Norton *et al.*, 1992; Holt *et al.*, 2014). The resulting mixotrophic organisms therefore acquire nutrients from heterotrophic (seawater filtration) and photoautotrophic pathways (Klumpp *et al.*, 1992; Hawkins and Klumpp, 1995). Nutrients provided by symbionts (such as glucose; Ishikura *et al.*, 1999) may account for a major part of the giant clam's energy needs (Klumpp *et al.*, 1992; Klumpp and Griffiths, 1994; Klumpp and Lucas, 1994; Hawkins and Klumpp, 1995; Elfwing *et al.*, 2002; Yau and Fan, 2012; Holt *et al.*, 2014; Soo and Todd, 2014).

Despite their ecological and socio-economic importance, effects of thermal stress and acidification on giant clams still need to be investigated. Thermal stress has shown to decrease fertilization success in *T. maxima* (Armstrong *et al.*, 2020), decrease oxygen production in *Tridacna derasa* and *Tridacna gigas* as well as respiration rates in *T. derasa* species (Blidberg *et al.*, 2000). In contrast, an increase of respiration with a high photosynthetic rate in the holobiont was reported for *Tridacna squamosa* (Elfwing *et al.*, 2001). Thermal stress also reduces the abundance of symbionts in *T. gigas* (Leggat *et al.*, 2003) and *Tridacna crocea* (Zhou *et al.*, 2019) and a decrease of photosynthate export from symbionts to the host (Leggat *et al.*, 2003). In *T. maxima*, heat stress was shown to induce changes in the fatty acid composition, lipid pathways and the overexpression of genes encoding reactive oxygen species (ROS) scavengers (Dubousquet *et al.*, 2016). In symbionts hosted in *T. gigas*, high-light levels and heat stress caused a decrease of symbiont density, cell size and chlorophyll content (Buck *et al.*, 2002). Toonen *et al.* (2012) demonstrated that low pH combined with high nutrient concentration have different impacts on shell growth rate depending on the *Tridacna* species. Moreover, Watson (2015) showed that high-light irradiance condition (i.e. high photosynthetically active radiation level) may limit the impact of pCO_2 on shell growth and total animal mass gain. Regarding the potential synergetic effect of temperature and pCO_2 parameters, the only study carried out showed that the survival of *T. squamosa* juveniles may decrease by ocean warming and acidification (Watson *et al.*, 2012). To our knowledge, no study had investigated the impacts of both parameters, and their potential synergetic effect, on several key physiological parameters of both *T. maxima* host and its symbionts. To fill this gap, our experimental approach was designed to better understand the physiological mechanisms underlying the response of giant clams to global climate changes.

In French Polynesia, *T. maxima* (Röding, 1798) is one of the most emblematic and patrimonial species. It represents an important food resource for inhabitants of remote atolls and giant clam fishery and aquaculture activities generate substantial incomes for local fishermen and farmers (Van Wynsberge *et al.*, 2016; Andréfouët *et al.*, 2017). However, wild and cultivated giant clam stocks are largely threatened by environmental disturbances such as abnormally high sea surface temperature inducing mass mortality events as reported in Tuamotu atolls by Addessi (2001) and Andréfouët *et al.* (2013). Like the symbiotic coral species, bleaching events (e.g. the symbiosis dissociation) affecting giant clam have been

Table 1: Measured and calculated parameters of seawater for all treatments

Treatments	Temperature (°C)	pCO_2 (μatm)	pH_{NBS}	Salinity (‰)	A_T (µmol/kg SW)	DIC (µmol/kg SW)	$\Omega_{aragonite}$
Control	29.2 (±0.1)	428 (±21)	8.19 (±0.01)	35	2422 (±170)	2071 (±85)	4.17
Thermal stress	30.7 (±0.1)	431(±25)	8.19 (±0.01)	35	2409 (±157)	2051 (±89)	4.14
Acidification stress	29.2 (±0.1)	1210 (±41)	7.81 (±0.03)	35	2466 (±90)	2306 (±34)	1.99
Acidification and thermal stress	30.7 (±0.1)	1213 (±29)	7.81 (±0.03)	35	2423 (±110)	2252 (±58)	2.02

Total alkalinity (A_T) is given in mean (±SD) based on weekly measurements for each experimental tank and for each condition. pCO_2, $\Omega_{aragonite}$ and dissolved inorganic carbon (DIC) were calculated using the CO_2SYS software.

recorded several times in the Indo-Pacific Region (Addessi, 2001; Buck *et al.*, 2002; Leggat *et al.*, 2003; Andréfouët *et al.*, 2013, 2015; Junchompoo *et al.*, 2013) in association to seawater temperature increase by a few degrees above the seasonal maximum (Addessi, 2001; Andréfouët *et al.*, 2013). More recently, two mass bleaching events of giant clams occurring in Reao and Tatakoto (Tuamotu islands) were linked to a prolonged exposure to high temperature (≥30°C over several weeks) (Andréfouët *et al.*, 2017; see Supplementary Fig. S1).

Based on a 65-day crossed-factorial experiment, we investigated physiological responses of 4-year-old *T. maxima* to temperature and pCO_2 conditions in the French Polynesian lagoons during the present warmer season and those predicted for 2100 by the IPCC 2014: +1.5°C (RCP 4.5 scenario) and +800 μatm of CO_2 (RCP 8.5 scenario). The effect of each parameter and their potential synergetic effect were evaluated based on respiration, biomineralization and photophysiology by analyzing the holobiont O_2 production and respiration, growth rate, ultrastructure of the shell, symbiont density and photosynthetic yield. In addition, the kinetics of thermal and acidification stress were assessed by performing analyses at different time of exposure (i.e. 29, 41, 53, 65 days).

Materials and methods

Biological material

Two hundred juvenile *T. maxima* (4-year-old, ∼5–6 cm height), with brownish/dark-green colour, were collected from the cultivated stock in Reao lagoon (Tuamotu islands). Then, they were exported to the Centre Ifremer du Pacifique in Tahiti where they were acclimatized in outdoor tank continuously renewed with natural, unfiltered, lagoonal seawater providing a constant input of microflora and fauna at natural concentration. Each individual was placed onto a petri dish on which byssal gland further developed for attachment. All individuals directly opened up right after their transfer into the outdoor tank. No visual sign of stress was observed during the acclimation period except for 4 individuals that died within the first 3 days (corresponding to a 2% mortality rate). Specimens used in this study were collected and held under a special permit (MEI #284) delivered by the French Polynesian government.

Experimental design and rearing system

To study the impact of temperature, pCO_2, and their synergetic effect on the physiology of the giant clams and their symbionts, 4 experimental conditions were set up by applying 2 temperatures (29.2°C and 30.7°C) and 2 levels of pCO_2 (430 ± 22 μatm and 1212 ± 35 μatm). The tested conditions were as follows: (i) control: 29.2°C, 430 μatm; (ii) acidification stress: 29.2°C, 1212 μatm; (iii) thermal stress: 30.7°C, 430 μatm; and (iv) acidification and thermal stress: 30.7°C, 1212 μatm (Table 1). Temperature was set and maintained with an electronic controller (Hobby Biotherm Professional) connected to an aquarium heater (Shego). The pH was manipulated by bubbling CO_2 in water tanks. This was controlled by a pH-stat system (Dennerle) that continuously monitored pH (calibrated to NIST scale) and temperature to control the quantity of CO_2 to maintain the desired pH. The light was set to obtain a photosynthetically active radiation of 200 ± 20 µmol of photons $m^{-2}.s^{-1}$ on a 12:12 h light/dark photoperiod.

After a 3-week acclimation period in an outdoor tank, 96 clams were randomly distributed in the experimental tanks 1 week before starting the experiment. For each condition, we used a 500-l tank containing 4 tanks of 30 l (ecological replicates) renewed with natural unfiltered lagoonal seawater at a flow rate of 50 l/h providing a constant input of microflora and fauna at natural concentration. Each 30-l tank contained 6 clams (biological replicates). To avoid physiological shock, targeted temperature and pCO_2 were linearly achieved over 7 days. To evaluate the kinetics of the thermal and/or acidification stress, analyses were performed at 4 different times of exposure, i.e. 29, 41, 53 and 65 days. In total, 64 clams were used for data acquisition corresponding to 4 individuals per condition (1 individual per 30-l tank) and per time of exposure.

Monitoring of temperature, pH and water quality

To insure the stability of experimental conditions, temperature and pH parameters were measured twice a day for each tank at 8:00 am and 4:00 pm using a mercury thermometer certified ISO 9001 (±0.1°C accuracy) and a pH-meter Consort P603 (±0.01 accuracy). Total alkalinity (TA) was weekly titrated using a 0.01-N HCl solution and a titrator (Schott Titroline Easy). Levels of pCO_2 and aragonite saturation state were calculated from temperature, pH (NBS scale), salinity and mean TA using the CO_2SYS software (van Heuven *et al.*, 2009). All parameters including seawater carbonate chemistry are reported in Table 1.

Holobiont O_2 consumption and production measurements

Giant clams were placed in an ecophysiological measurement system (EMS) to monitor O_2 consumption and production. The EMS consisted of five open-flow chambers. Four giant clams were individually placed into four chambers, while an empty shell was placed into a fifth chamber used as a control. EMS chambers contained water at the same temperature and pCO_2 conditions as in the experimental tanks. The light energy and photoperiod conditions were the same as for the acclimation tanks. Flow rate in all chambers was constantly maintained at 12 $l.h^{-1}$. Each chamber was equipped with a two-way electromagnetic valve activated by an automaton (FieldPoint National Instruments). When the electro-valve was opened, the water released from the chamber was analyzed for 3 min using an oxygen sensor (OXI 538, Cellox 325, WTW, Weilheim, Germany) to quantify dissolved oxygen. Oxygen measurements were performed over 48 h. The first 8 h of measurement were discarded due to the animal acclimatization to the chamber. In each chamber, the cycle was completed within 3 min: the first 2 min served to stabilize the measurement and an average of oxygen data was performed on the last minute of acquisition. This cycle was followed by another time frame of 3 min in the control chamber following the sequence specimen #1, control, specimen #2, control, specimen #3, control, specimen #4, control.

Respiration rate (RR) and production rate (PR) were calculated from the data obtained during night time and day time, respectively, using differences in oxygen concentrations between the control and experimental chambers. RR and PR = V(O1 − O2), where O1 is the oxygen concentration in the control chamber, O2 is the oxygen concentration in the experimental chamber and V is the water flow rate. RR and PR data were normalized to tissue dry weight. Once normalized, the terminology becomes O_2 consumption for RR and O_2 production for PR; both expressed in mg $O_2.h^{-1}.g^{-1}$ dry weight.

After O_2 production and O_2 consumption analyses were completed, a piece of the mantle was dissected for further symbiont fluorescence and density analyses (see Section Fluorescence and density measurements of symbionts). The remaining soft tissues were frozen and lyophilized for RR and PR data normalization.

Fluorescence and density measurements of symbionts

Potential effect of temperature and pCO_2 conditions on the photophysiology of the symbionts was studied by comparing fluorescence yield of photosystem II (PSII) between all experimental conditions. After clams were sacrificed, a 1 × 2-cm mantle fragment was dissected. The tissue fragment was gently swiped using tissue paper to remove excess mucus and symbionts were collected by doing 5 smears using a sterilized razor blade. Collected symbionts were diluted into 5-ml of 0.2-µm filtered seawater and placed at the obscurity for 10 min to inactive the PSII before light excitation. Samples were homogenized and 3 ml of the homogenate were collected, placed into a quartz-glass cuvette and analyzed with AquaPen fluorometer (APC-100, Photon System Instruments®, Czech Republic) at a 450-nm wavelength. The minimal fluorescence (F_0) and the maximal fluorescence (F_m) were measured. The quantum yield of photosynthesis was calculated as F_v/F_m where F_v is the variable fluorescence ($F_v = F_m – F_0$).

In addition, symbiont densities were evaluated from mantle fragments. For each individual, a circular (5 mm in diameter) piece of mantle was collected using a punch. The piece was weighed, grounded in 0.2-µm filtered seawater and homogenized. Then, 20 µl of the tissue extract were immediately collected and placed into Malassez cells for symbiont counting under optical microscope. For each sample, counting was performed on 4 replicates (3 columns per replicate). Data are expressed in number of symbionts/mg of mantle tissue.

Calcein labelling for evaluating daily shell extension rate

To study the impact of temperature and pCO_2 on shell growth rate, the mineralization front of giant clams was marked using calcein fluorochrome, which is irreversibly precipitated at the $CaCO_3$ mineralization site. Before the experiment starts, giant clams were immersed in a 100-$mg.l^{-1}$ calcein solution (Sigma Aldrich) (calcein diluted in 1-µm filtered-seawater) for 8 h in the dark. During the labelling procedure, the bath of calcein solution was aerated using bubblers and water current was created via pumps. Calcein-labelled specimens were then placed into the experimental tanks. At the end of the experiment, for each individual, a 5-mm thick section was cut along the maximal shell growth axis through the right valve using a Swap Top Inland® diamond saw. All sections obtained were polished and observed under epifluorescence with a Leitz Dialux® 22 microscope. The distance between the fluorescent calcein mark and the edge of the shell formed during the experiment was measured following the maximal

growth direction. Daily shell extension rate (expressed in $\mu m.day^{-1}$) was obtained by dividing the measured distance by the number of days of incubation in experimental conditions.

Shell scanning electron microscopy study

To characterize temperature and pCO_2 effect on the shell ultrastructure, a scanning electron microscopy (SEM) study was carried out. For each individual, a 10-mm thick shell section was cut facing the section used for calcein observations. The section was then fractured along the width, 2 cm below the growing part of the shell (marginal part), using a small chisel and a hammer. Then, the apical fragment was longitudinally fractured and one piece was sonicated in tap water for 10 s, air dried and an additional drying was done overnight at 35°C. Sample was placed on a stub covered with carbon tape, gold-coated and observed at 15 kV using a Hitachi TM3030 SEM at the Université de la Polynésie française. For each condition, and for each time of exposure, two samples were selected based on their daily shell extension rate, i.e. samples showing the lowest and the highest rate. To evaluate the impact of temperature and/or pCO_2 on the shell ultrastructure, SEM observations were performed for each specimen in two different zones of the crossed-lamellar outer layer. Zone 1 corresponds to the shell formed *in situ* (i.e. in the shell region located before the calcein mark), while zone 2 corresponds to the shell formed during the experiment. Observations were made at the ultrastructural level and focused on the aspect and integrity of the lamellae of the crossed-lamellar outer layer. In addition, to check the potential effect of temperature and pCO_2 on the external shell surface, the periostracum (i.e. the organic layer covering the shell external surface) of two individuals per experimental condition (65 days of exposure) was observed.

Statistical analyses and data processing

Normality of data distribution and homogeneity of variance were tested with the Shapiro–Wilk test and the Bartlett test, respectively. Production and consumption of O_2 data followed the conditions of application of parametric tests, but photosynthetic yields and symbiont densities were transformed using Box Cox transformation while shell extension rates were square root transformed to meet these conditions. Comparisons were done using a three-way ANOVA with interactions (fixed factors: time of exposure, temperature and pCO_2). Tukey post hoc comparisons were done at $\alpha = 0.05$ for all analyses. Correlations between physiological parameters were tested using Pearson method with a threshold of $r = 0.25$ ($\alpha = 0.05$).

For all physiological parameters, i.e. O_2 respiration, O_2 consumption, symbiont photosynthetic yield and density, means (±SD) were calculated based on the four biological replicates for each condition and each time of exposure. For the daily shell extension rate, means (±SD) were calculated for each condition and each time of exposure based on the number of biological replicates displaying a detectable calcein mark.

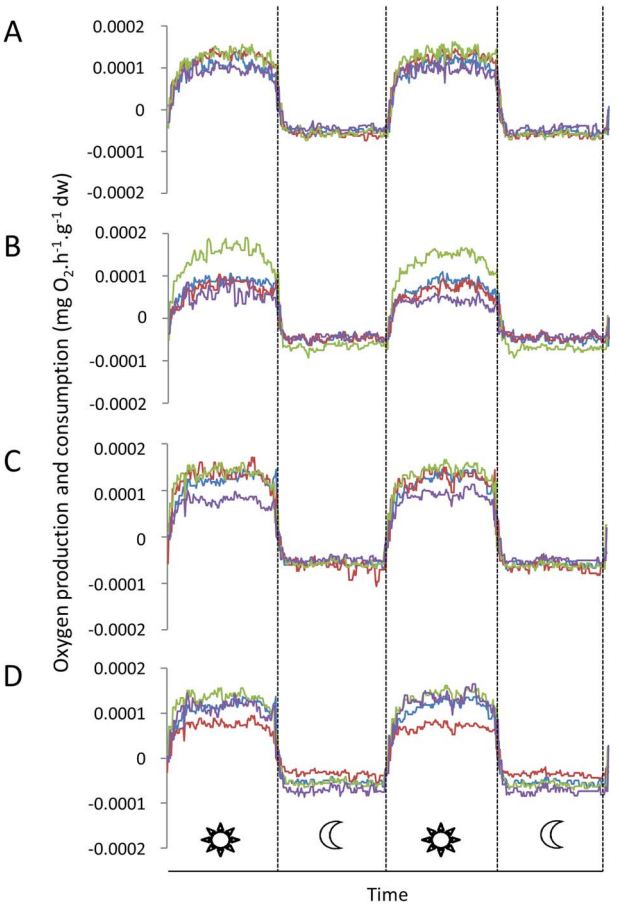

Figure 1: Variations of O_2 production and O_2 consumption acquired over a 48-h period after 29 days of exposure to different temperature/pCO_2 conditions: (**A**) 29.2°C, 430 μatm of CO_2; (**B**) 30.7°C, 430 μatm of CO_2; (**C**) 29.2°C, 1212 μatm of CO_2; and (**D**) 30.7°C, 1212 μatm of CO_2. Data are expressed in mg $O_2.h^{-1}.g^{-1}$ tissue dry weight (dw) and correspond to day-time and night-time acquisitions for four replicates per condition (each color line represents one replicate).

Results

Effect of temperature and pCO_2 on the holobiont oxygen balance

For all sampling time (i.e. 29, 41, 53, 65 days), a cyclic pattern of O_2 production and consumption was observed following the circadian cycle (Fig. 1). This pattern corresponds to oxygen photosynthetically produced and heterotrophically consumed by the holobiont during the day and the night, respectively. No mortality was observed in all tested temperature/pCO_2 conditions during the whole experiment.

Mean values of normalized O_2 production and consumption are shown in Fig. 2. Tukey post hoc test results are

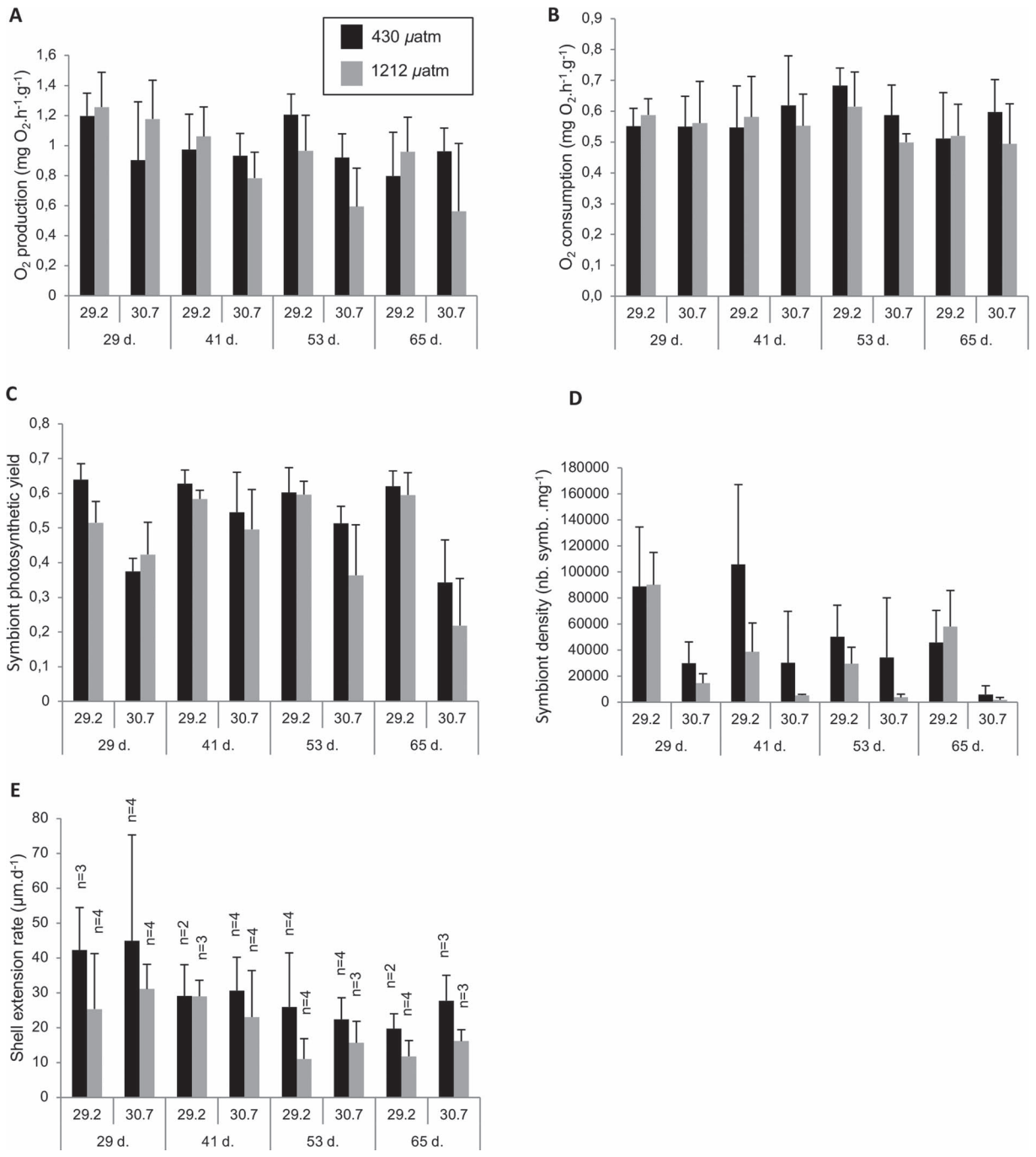

Figure 2: Graphs reporting data of (**A**) oxygen production, (**B**) oxygen consumption, (**C**) symbiont photosynthethic yield, (**D**) symbiont density and (**E**) daily shell extension rate obtained for each temperature/pCO_2 experimental condition and time of exposure (black and grey columns correspond to 430 μatm and 1212 μatm, respectively). Data are given in mean (+SD) calculated from four replicates for all physiological parameters except for daily shell extension rate for which numbers of replicates are specified.

reported in Table 3. The ANOVA has indicated that oxygen production of the holobiont during day time was significantly altered at 30.7°C ($P = 0.009$) but not at 1212 μatm of CO_2 ($P = 0.362$) (Table 2). In addition, O_2 production was higher at 29.2°C than at 30.7°C for all times of exposure (Fig. 2A) and decreased over time ($P = 0.030$, Table 2). The night-time O_2 consumption, however, was not significantly influenced by temperature ($P = 0.590$) neither by pCO_2 ($P = 0.361$) nor

Table 2: Results from the three-way ANOVA performed on holobiont O_2 production and consumption data, symbiont photosynthetic yield, symbiont density and giant clam shell extension rate

		O_2 production ($n = 64$)	O_2 consumption ($n = 64$)	Photosynthetic yield ($n = 64$)	Symbiont density ($n = 64$)	Shell extension rate ($n = 55$)
Time	*F*	3.264	0.740	3.566	6.035	4.695
	P	0.030*	0.533	0.021*	0.001***	0.007**
Temperature	*F*	7.551	0.294	65.200	79.158	0.466
	P	0.009**	0.590	<0.0001***	<0.0001***	0.499
pCO_2	*F*	0.846	0.851	6.125	8.665	7.409
	P	0.362	0.361	0.017*	0.005**	0.010**
Time × temperature	*F*	0.413	0.965	3.393	1.528	0.319
	P	0.744	0.417	0.025*	0.219	0.812
Time × pCO_2	*F*	1.765	0.476	0.024	1.033	0.251
	P	0.167	0.700	0.995	0.386	0.860
Temperature × pCO_2	*F*	1.334	1.029	0.100	1.989	0.026
	P	0.254	0.315	0.753	0.165	0.872
Time × temperature x pCO_2	*F*	1.216	0.148	2.153	0.474	0.336
	P	0.314	0.930	0.106	0.702	0.799

The three fixed factors are pCO_2, temperature and time of exposure. Asterisks denote significant differences ($^*P \leq 0.05$, $^{**}P \leq 0.01$, $^{***}P \leq 0.001$).

by time of exposure ($P = 0.533$) and remained stable throughout the whole experiment (Fig. 2B). No interaction effect between the three tested factors was found to affect the holobiont oxygen balance (Table 2).

Symbiont density and photosynthesis under different temperature/pCO_2 conditions

After 2 months of exposure, the symbiont photosynthetic yield and density were significantly impacted at 30.7°C ($P < 0.0001$), high pCO_2 (1212 μatm) ($P = 0.017$ and $P = 0.005$, respectively) and by the time of exposure ($P = 0.021$ and $P = 0.001$, respectively). During the whole experiment and for both pCO_2 conditions, the means of photosynthetic yield (Fig. 2C) and symbiont density (Fig. 2D) tended to be higher at 29.2°C than at 30.7°C. However, an inter-individual variability was observed.

Concerning the interaction parameters, only interaction between temperature and time of exposure parameters had a significant effect on the symbiont photosynthetic yield ($P = 0.025$) (Table 2). No parameter interaction was found to affect the symbiont density (Table 2).

Effect of pCO_2 on daily shell extension rate

Calcein mark was detectable in 55 over 64 shell sections. Statistical analyses on shell extension rate showed that pCO_2 and the time of exposure had a significant effect on the shell extension rate ($P = 0.010$ and $P = 0.007$, respectively, Table 2). As shown in Fig. 2E, the mean values of shell extension rates tended to be lower at high pCO_2.

Effect of long-term exposure to temperature and pCO_2 on the periostracum and the shell microstructure

As a first approach, SEM observations of the periostracum (external shell surface) were made in order to evaluate potential effect of the treatments. These observations were performed at two different places of the shell: (i) the ventral extremity part and (ii) a lower part of the shell. Two individuals per experimental condition (65 days of exposure) were studied. For all the samples, the periostracum was of the same colour (based on visual observations). Under SEM, at the ventral extremity in control condition (29.2°C, 430 μatm), the periostracum did not appear altered (Supplementary Fig. S2A, C; Table 4), in the lower part it displayed a 'mushy' aspect with numerous micro-borer galleries (Supplementary Fig. S2B, D). These features were observed in all the other experimental conditions (i.e. 29.2°C, 1212 μatm; 30.7°C, 430 μatm; 30.7°C, 1212 μatm; Fig. S2) and for all the samples studied, which may signify that the treatments did not significantly affect the periostracum.

To strengthen the results above ultrastructural observations of shell fractures were done in two zones: zone 1 corresponding to the shell formed *in situ* (i.e. before the experiment) and zone 2 corresponding to the shell formed during the experimental conditions. In the control condition

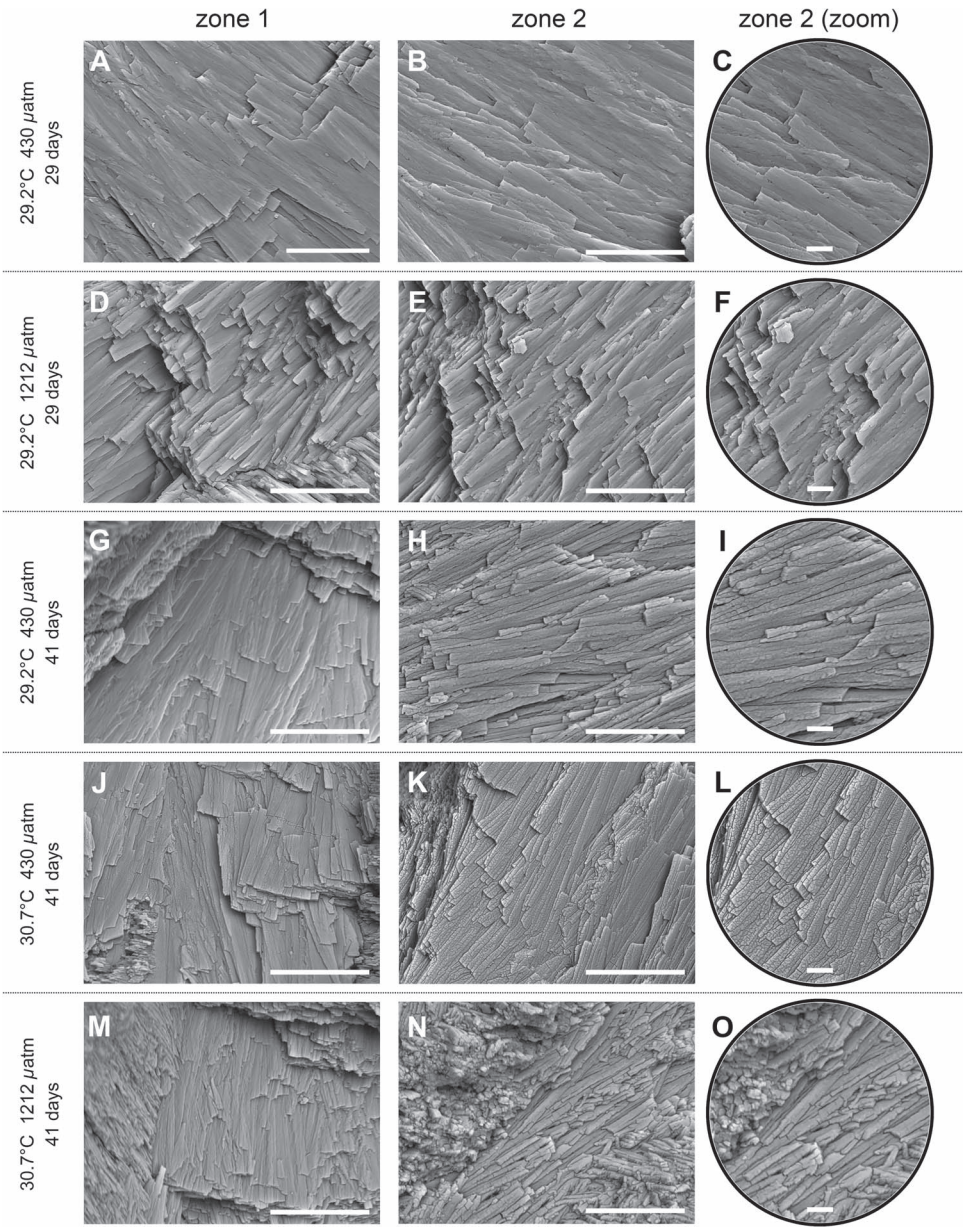

Figure 3: Effects of experimental conditions on the ultrastructure of the *T. maxima* shell outer layer investigated via SEM. (**A**, **B**, **D**, **E**, **G**, **H**, **J**, **K**, **M**, **N**: scale bar, 10 µm; **C**, **F**, **I**, **L**, **O**: scale bar, 2 µm). Zone 1 and zone 2 correspond to the shell formed *in situ* (i.e. before the experiment) and in the experimental conditions, respectively. At 29 days, no significant differences between zones 1 and 2 are observed (A–C: 29.2°C, 430 μatm; D–F: 29.2°C, 1212 μatm). In both zones, lamellae are well cohesive, displaying elongated shape with a smooth surface and slightly rounded outlines. This latter microstructural feature is observed in all shells formed *in situ* (zone 1), for all temperature/pCO_2 conditions and all time of exposure (A, D, G, J, M). At 41 days, lamellae in zone 2 are less cohesive with or without pronounced granular aspect (H, I: 29.2°C, 430 μatm; K, L: 30.7°C, 430 μatm; N, O: 30.7°C, 1212 μatm).

(i.e. 29.2°C, 430 μatm), after 29 days of exposure, the lamellae formed before the experiment (zone 1) and during the experiment (zone 2) were well cohesive and displayed an elongated shape, a smooth surface and sharp or slightly rounded outlines (Fig. 3A–C). At 29 days, no difference was observed between both zones for all temperature/pCO_2 conditions (example given for 29.2°C, 1212 μatm in Fig. 3D–F; Table 4). From 41 days and after, and for all temperature/pCO_2 experimental conditions, the shell formed before the experiment (zone 1) displayed the same microstructural features like the ones described above (example given for 29.2°C, 430 μatm; 30.7°C, 430 μatm; and 30.7°C, 1212 μatm at 41 days in Fig. 3G, J, M; Table 4). At 41 days, the lamellae observed in the majority of shells formed during the experiment (zone 2),

Table 3: Results from Tukey post hoc tests following the three-way ANOVA performed on analyzed physiological parameters

		O_2 production	Photosynthetic yield	Symbiont density	Shell extension rate
Time	29 days	a	a	a	a
	41 days	ab	ab	ab	ab
	53 days	ab	ab	b	b
	65 days	b	b	b	b
Temperature	29.2 °C	a	a	a	-
	30.7 °C	b	b	b	-
pCO_2	430 μatm	-	a	a	a
	1212 μatm	-	b	b	b
Time × temperature	29 days × 29.2°C	-	ab	-	-
	41 days × 29.2°C	-	a	-	-
	53 days × 29.2°C	-	a	-	-
	65 days × 29.2°C	-	a	-	-
	29 days × 30.7°C	-	cd	-	-
	41 days × 30.7°C	-	abc	-	-
	53 days × 30.7°C	-	bcd	-	-
	65 days × 30.7°C	-	d	-	-

The effects of significant parameters were tested as time of exposure alone and combined to the temperature. The letter annotations correspond to the significances between conditions ($P < 0.05$).

in all temperature/pCO_2 conditions, appeared less cohesive (Fig. 3N, O showing shell formed at 30.7°C, 1212 μatm; Table 4) and some of them additionally displayed a pronounced granular aspect of the surface even in the control condition (Fig. 3H, I and Fig. 3K, L showing shell formed at 29.2°C, 430 μatm and 30.7°C, 430 μatm, respectively; Table 4). These modifications were observed for the majority of shells formed in all temperature/pCO_2 conditions, at 53 and 65 days (Table 4). Two states classifying ultrastructural differences between the shell formed before and during the experiment were defined as follows: (i) ND, no difference observed between zones 1 and 2; and (ii) D, difference observed between zones 1 and 2 meaning that the lamellae were less cohesive in zone 2 compared to zone 1 (see Table 4). In total, 19 samples over 32 displayed differences in lamellae aspect between both zones.

Effect of time of exposure on oxygen balance, biomineralization and symbiont photophysiology

Time of exposure to thermal and acidification stress was shown to have a significant impact on O_2 production ($P = 0.030$), photosynthetic yield ($P = 0.021$), symbiont density ($P = 0.001$) and shell growth rate ($P = 0.007$) (Table 2). Post hoc tests showed that the kinetics of thermal or acidification stress varies depending on the physiological parameter measured: O_2 production and photosynthetic yield were significantly different between 29 and 65 days while symbiont density and shell growth rate were both impacted from 53 days of exposure (Table 3).

Relationship between physiological parameters

To establish if relationships exist between the various physiological parameters measured, a correlation matrix was generated (Table 5). The photosynthetic yield of symbionts was strongly correlated to their density ($r = 0.667$). O_2 production was also strongly correlated to symbiont density ($r = 0.492$) and photosynthetic yield ($r = 0.331$). Concerning the circadian functioning of the holobiont, its nocturnal oxygen need was strongly correlated to the diurnal O_2 production ($r = 0.629$). No significant correlation was found between shell extension rate and other physiological parameters.

Discussion

In the present study, we investigated the physiological responses of *T. maxima* (i.e. 4-year-old specimens) to temperature and pCO_2 conditions in the French Polynesian lagoons under current warmer season conditions and those predicted for 2100 by the IPCC 2014 (+1.5°C and +800 μatm of CO_2). Present thermal conditions were stressful enough to induce an acclimatization process characterized

Table 4: Compilation of ultrastructural observations of lamellae of the shell outer layer and the periostracum using SEM

Time of exposure	Temperature (°C)	pCO_2 (μatm)	Sample	Lamellae of outer shell layer	Periostracum
29 days	29.2	430	A	ND	
			B	ND	
	30.7	430	A	ND	
			B	ND	
	29.2	1212	A	ND	
			B	ND	
	30.7	1212	A	ND	
			B	ND	
41 days	29.2	430	A	D	
			B	D	
	30.7	430	A	D	
			B	D	
	29.2	1212	A	D	
			B	D	
	30.7	1212	A	D	
			B	ND	
53 days	29.2	430	A	D	
			B	D	
	30.7	430	A	D	
			B	D	
	29.2	1212	A	ND	
			B	D	
	30.7	1212	A	D	
			B	ND	
65 days	29.2	430	A	D	No alteration
			B	D	No alteration
	30.7	430	A	D	No alteration
			B	ND	No alteration
	29.2	1212	A	D	No alteration
			B	D	No alteration
	30.7	1212	A	ND	No alteration
			B	D	No alteration

'A' and 'B' represent the two samples observed for each treatment and time of exposure; 'ND' means that no significant difference is observed between the shell formed before and during the experiment for the lamellae of the outer shell layer; 'D' means that a notable difference is observed between both parts of the shell (i.e. the lamellae are less cohesive). For the periostracum, 'no alteration' means that the periostracum covering the ventral extremity part of the shell is well preserved.

by a slight regulation of the symbiont density without the collapse of the photosynthesis. However, the predicted thermal and pCO_2 conditions were much more stressful and induced strong disturbances of the processes linked to the phototrophic symbiosis and the biomineralization.

Indeed, the 30.7°C treatments have significantly impacted the holobiont by inducing a strong bleaching response illustrated by the reduction of its O_2 production, symbiont density and photosynthetic yield. High pCO_2 (+800 μatm of CO_2) was shown to alter the symbiont photosynthetic yield and

Table 5: Correlation matrix integrating the different physiological parameters monitored, i.e. O_2 production and consumption, shell extension rate and symbiont photosynthetic yield and density

	Photosynthetic yield ($n = 64$)	Symbiont density ($n = 64$)	Shell extension rate ($n = 55$)	O_2 production ($n = 64$)
Symbiont density	0.667*			
Shell extension rate	−0.032	0.168		
O_2 production	0.331*	0.492*	0.221	
O_2 consumption	0.163	0.226	0.129	0.629*

Correlation was tested using the Pearson method (threshold of $r = 0.250$, $\alpha = 0.05$) and significant relationships between parameters are indicated by an asterisk (*).

density and affect its biomineralization process by decreasing the shell growth rate.

No synergetic effect between temperature and pCO_2 on giant clam and symbiont physiological parameters

Increase in atmospheric CO_2 impacts both the seawater temperature and pH inducing ocean warming and acidification (Sabine *et al.*, 2004; IPCC, 2014). Therefore, the analysis of the synergetic effect of both stressors on marine bivalve's physiology is crucial. Watson *et al.* (2012) reported in *T. squamosa* juveniles a decrease of giant clam's survival rate induced by exposure to high-temperature or high-pCO_2 conditions. The lowest survival rate (i.e. <20%) was observed under the highest pCO_2 condition (+600 μatm of CO_2) at +1.5°C and +3°C, after 60 days of exposure.

In our study, no synergetic effect was detected for all measured physiological parameters. Moreover, no mortality was observed in all tested temperature/pCO_2 conditions during the whole experiment which leads us to suggest that a temperature of 30.7°C and a pCO_2 of 1212 μatm seem to be non-lethal, at least over 65 days of exposure. However, we cannot exclude that some specimens, especially the bleached individuals, may have died after longer exposure to the experimental conditions.

Effect of temperature on holobiont oxygen balance, symbiont photophysiology and shell ultrastructure

Temperature is one of the most important parameters driving bivalve physiology (Aldridge *et al.*, 1995; Bougrier *et al.*, 1995; Watson *et al.*, 2012; Gazeau *et al.*, 2013; Le Moullac *et al.*, 2016a; Latchère *et al.*, 2017). However, since giant clams live in symbiosis with photosynthetic symbionts (Klumpp *et al.*, 1992; Klumpp and Griffiths, 1994; Soo and Todd, 2014), the comparison at the metabolic level with non-symbiotic bivalves can be misleading. Discussion on elevated temperature effect on the holobiont oxygen balance should therefore integrate the effect on both giant clam and its symbionts (Jones and Hoegh-Guldberg, 2001). Even though physiological and molecular responses to thermal stress may differ, the comparison with scleractinian corals, which are also symbiotic and calcifying organisms, makes sense to better understand the impact of temperature on the holobiont physiology.

We observed that high temperature (+1.5°C) significantly reduced the holobiont O_2 production, the density and the photosynthetic yield of symbionts from 29 days of exposure. Additionally, partial or total bleaching was observed for the majority of individuals exposed to 30.7°C (at both ambient and high pCO_2, see Supplementary Fig. S3). This suggests that thermal stress has a significant impact on the holobiont photophysiology. The reduction of the symbiont photosynthetic yield could reflect photoinhibition. Photoinhibition was previously linked to the degradation of the D1 protein of the reaction center of the PSII altering the photosynthetic apparatus functioning in symbiotic corals and sea anemone subjected to thermal stress (Warner *et al.*, 1999; Smith *et al.*, 2005; Richier *et al.*, 2006; Ferrier-Pagès *et al.*, 2007). Decrease of photosynthetic activity reduced the symbiont O_2 production and consequently, impacted the holobiont O_2 production. Comparable results were obtained from a 24-h experiment showing that an increase of 3°C affected the oxygen production of *T. gigas* and *T. derasa* (Blidberg *et al.*, 2000). Photoinhibition led to the production of ROS by symbionts, which are known to pass through cellular membranes, cause oxidative damages (Lesser *et al.*, 1990; Lesser, 1996; Downs *et al.*, 2002) and impact the PSII (Richter *et al.*, 1990). In corals, Downs *et al.* (2002) showed that high levels of oxidative damage associated with coral bleaching. Indeed, ROS such as hydrogen peroxide (H_2O_2) may play a role in signalling molecule activating the symbiosis dissociation (Fitt *et al.*, 2001; Smith *et al.*, 2005; Perez and Weis, 2006). Expulsion of symbionts by the host may be a strategy to limit oxidative stress and damage to ultimately survive environmental stress (Downs *et al.*, 2002; Perez and Weis, 2006). Two recent works support this hypothesis. Firstly, Zhou *et al.* (2019) related a decrease in symbiont density in response to an excess of oxidative stress in thermally stressed *T. crocea*. Secondly, Dubousquet *et al.* (2016) showed that *T. maxima* overexpressed genes encoding ROS scavengers in response to thermal stress. Interestingly, the cellular and molecular mechanisms enhanced before the bleaching response (e.g. the loose of the symbionts) seem similar between giant clams and corals and conduct to

the same phenomenon of symbiosis dissociation. However, since giant clams and corals display an extra- and an intracellular symbiosis, respectively, the mechanisms of symbiosis dissociation may differ. This constitutes an interesting example of evolutionary convergence of a stress response in two very distant organisms. In this context, it would be interesting to test if the bleaching response in giant clam can be adaptive as it was proposed for corals (Fautin and Buddemeier, 2004) and if variations in giant clam thermotolerance are correlated to the composition of the symbiotic population (Baker, 2003).

Concerning the effect of temperature on the ultrastructure of the crossed-lamellar structure, the lamellae formed in all experimental conditions in the first 29 days were well cohesive with elongated shape and a slight granular aspect, which is consistent with the description made by Faylona *et al.* (2011) in *T. maxima*, Belda *et al.* (1993) in *T. gigas* and Agbaje *et al.* (2017) in *T. derasa*. However, after 29 days, the lamellae observed in the majority of the shells formed in both temperature conditions (whatever the pCO_2 condition) appeared to be less cohesive with pronounced granular aspect. We suggest that these features are due to a lack of organic matrix between the lamellae (i.e. inter-lamellar organic matrix) and embedding the nano-grains forming the lamellae in the crossed-lamellar structure. Indeed, the biomineralization of calcium carbonate structures involves the transport of ions to the mineralization site and the synthesis of macromolecules referred to as 'organic matrix' (Allemand *et al.*, 2004). The organic matrix, consisting of 0.9 wt% and 1.83 wt% in *T. derasa* and *T. gigas* shell, respectively (Agbaje *et al.*, 2017, 2019), is mainly composed of macromolecules commonly found in molluscan shell organic matrix such as lipids, polysaccharides and proteins displaying various levels of glycosylation (Marin *et al.* 2012; Agbaje *et al.*, 2017). The formation of these macromolecules may be energetically costly for molluscs such as marine gastropods (Palmer, 1992). We suggest that in our tested experimental temperature, while oxygen balance is significantly altered, less energy may be available and allocated to the synthesis of macromolecules involved in biomineralization, which may explain the lack of organic matrix embedded into the giant clam shell.

Effect of pCO_2 on giant clam biomineralization and symbiont photophysiology

Results of the present study have indicated that in *T. maxima* high-pCO_2 condition (+800 μatm) induced a significant decrease of the shell extension rate. This observation is in accordance with those obtained for giant clams in three different experiments using various CO_2 enrichment levels and exposure durations. Watson (2015) has exposed juveniles *T. squamosa* to +250 and +550 μatm of CO_2 for 8 weeks under various light levels. Under mid-light level, the author has reported a reduced survival and growth while under high-light levels the growth only was affected. Kurihara and Shikota (2018) also reported a negative effect of pCO_2 on shell growth (i.e. shell height) in juveniles *T. crocea* when exposed to +600 μatm and +1600 μatm for 4 weeks. Toonen *et al.* (2012) demonstrated that young specimens of *T. maxima* and *T. squamosa* had lower shell growth rates, compared to those reported in the literature under natural pCO_2/pH conditions, when kept 1 year in +350 to +1000 μatm pCO_2 conditions.

As mentioned above, high-pCO_2 condition (+800 μatm) affected giant clam's shell growth rate and also photosynthetic yield and density of symbionts. Negative effect of pCO_2 on the shell growth rate may be linked to two non-exclusive hypotheses: (i) the physiological adjustment needed to thrive with a seawater at 1212 μatm of CO_2 instead of 430 μatm and/or (ii) an alteration of symbiont photophysiology leading to a potential reduction of the 'light-enhanced calcification' (LEC) phenomenon. Concerning the former, the increase of CO_2 dissolution in the water column leads to the modification of the carbonate chemistry equilibrium and to the increase of H^+ concentration (Cyronak *et al.*, 2016). These strong environmental changes affect the whole organism's homeostasis, but more particularly physiological functions, such as biomineralization, where the control of carbonate concentration and pH are the most essential. To form their mineralized structures, calcifying organisms modify the carbonate composition at the mineralization site to promote $CaCO_3$ precipitation. These modifications are performed by several enzymatic reactions, including the removal of H^+ to locally increase the pH at the mineralization site for maintaining chemical conditions to enhance $CaCO_3$ precipitation (Allemand *et al.*, 2011; Taylor *et al.*, 2012). Corals are known to regulate the pH at their mineralization site (Venn *et al.*, 2013; Holcomb *et al.*, 2014) but a decrease of coral calcification was also linked to a decline in pH in the calcifying fluid (Ries, 2011; McCulloch *et al.*, 2012). The maintenance of biomineralization under these non-optimal environmental conditions are therefore energetically costly, which may result in a general decrease of growth (Vidal-Dupiol *et al.*, 2013). In our case, we suggest that giant clam *T. maxima* exposed to high pCO_2 may allocate more energy to maintain a proper pH of the extrapallial fluid for nucleation and deposition of aragonite. Regarding the LEC (Vandermeulen *et al.*, 1972), this phenomenon observed in Symbiodiniaceae-host symbiosis has been extensively described in corals and represents the capacity of symbionts to stimulate the host calcification (Allemand *et al.*, 2004). The symbionts stimulate the host metabolism and calcification by providing energy resources and/or O_2 (Chalker and Taylor, 1975). Moreover, symbionts may promote the aragonite precipitation by providing inorganic carbon, nitrogen and phosphorus and by synthetizing molecules used as precursor for the synthesis of skeletal organic matrix (Pearse and Muscatine, 1971; Cuif *et al.*, 1999; Furla *et al.*, 2000; Muscatine *et al.*, 2005). They also facilitate $CaCO_3$ precipitation by influencing the dissolved inorganic carbon (DIC) equilibrium by removing the CO_2 via photosynthesis (Goreau, 1959). Such phenomenon

has been also described in giant clams (Ip *et al*., 2006; Ip *et al*., 2017). In *T. squamosa*, LEC increased the pH and reduced the ammonia concentration at the interface between the inner mantle and the shell in the extrapallial fluid, where the biomineralization occurs (Ip *et al*., 2006). Recently, Chew *et al*. (2019) reported a light-enhanced expression of carbonic anhydrase, i.e. CA4-like, in the inner mantle of *T. squamosa* and suggested that this enzyme is involved in giant clam biomineralization by catalyzing the conversion of HCO_3^- to CO_2. In this context, an altered photophysiology of the symbionts can rationally alter LEC and consequently results in a decrease of the shell growth rate. Finally, one can suggest that under acidification stress, giant clam may reduce some physiological functions such as biomineralization and allocate more energy to essential functions for its survival. In our study, temperature also altered photophysiology and holobiont O_2 production, but did not significantly affect shell growth rate. Therefore, the most plausible hypothesis explaining the negative effect of pCO_2 on shell growth rate may be related to the low aragonite saturation state at high pCO_2.

Concerning the effect of pCO_2 on the shell microstructural integrity, in the temperate bivalve *Mytilus edulis*, an exposure to +150, +350 and +600 μatm of CO_2 for 6 months induced disorientation in the shell of the newly formed calcite crystals of the prismatic layer (Fitzer *et al*., 2014). In the giant clam *T. maxima*, high pCO_2 had no significant effect on the integrity of the aragonitic lamellae of the crossed-lamellar layer during the first 29 days of exposure. From 41 days of exposure, its potential impact remains unresolved as differences were noticed in the shells formed under future high-temperature, high-pCO_2 and even under today's temperature/pCO_2 conditions. The fact that differences were reported for shells formed in all experimental conditions from 41 days suggests that they may be due to a long-term exposure to 29.2°C and 30.7°C.

Conclusion

This study enables the evaluation of *T. maxima*'s physiological responses to realistic temperature and pCO_2 predicted at the end of this century. We demonstrated that high temperature mimicking temperature encountered during the warmer months of the year has a significant negative impact on symbiont densities and photosynthetic capacities. This negative impact on the symbiont physiology induces a decrease in the net holobiont O_2 production.. Therefore, by influencing symbiont physiology, the temperature may affect the energetic needs of the giant clam host. The high pCO_2 has a negative impact on shell growth rate, symbiont densities and photosynthetic capacities. Shell microstructure is not affected by temperature nor by the pCO_2 in the first 29 days of exposure. However, for all temperature/pCO_2 conditions, a longer exposure (≥41 days) modified the shell ultrastructure. These observations support our hypothesis that 29.2°C is a temperature that already affects giant clam metabolism, at least over a long-term exposure. However, no synergetic effect was found between temperature and pCO_2 parameters. All these observations suggest that temperature and pCO_2 influence different physiological functions and that giant clam populations may dramatically suffer from the temperature and pCO_2 conditions predicted for the next decades. This is especially true for the temperature since the populations of giant clams (wild and farmed) of the Tuamotu Archipelago are already confronted with temperatures of ∼29.2°C every year. Additionally, the threshold of 30.7°C applied in our study and that will be encountered annually in the future corresponds to what is measured currently during abnormally warm years (Fig S1). During the heatwave event in 2016, 80% of the farmed clam populations have bleached resulting in a high level of mortality (personal communication). To complement these results on the effects of temperature on the giant clams, it is now essential to conduct integrative analyses that will take into account the acclimatization and adaptive potential of the whole holobiont. The tools of transcriptomic, genomic and epigenomic in association with ecologically relevant experiments both at the individual and population levels will be particularly relevant to address these questions (Torda *et al*., 2017). These will allow a better understanding of the fundamental physiological processes of the holobiont and its response to future changes. Results from these studies may help in adapting local policies and management to maintain sustainability of giant clam populations and their exploitation, especially in the Eastern Tuamotu islands where bleaching events have been observed at an increasing and alarming rate.

Funding

This work was supported by the Ifremer Institution (Politique de site program, GECO project) and the Université de la Polynésie française (MAPIKO and CLAMS projects).

Conflicts of interest

The authors declare no financial and personal conflict of interest.

Acknowledgments

We would like to acknowledge the two anonymous reviewers for their valuable comments. We also would like to thank Celine Lafabrie for fruitful discussions and Mickael Mege and Alexia Pihier for their technical assistance. Georges Remoissenet (Direction of Marine Resources of French Polynesia) is thanked for sharing information about bleaching events in Eastern Tuamotu islands. The Direction of Marine Resources and the Ministry of Economic Recovery, Blue Economy and Digital Policy of French Polynesia are also

thanked for the special permit to collect and hold small specimens of *T. maxima* species. This study is set within the framework of the 'Laboratoires d'Excellence (LabEX)' TULIP (ANR-10-LABX-41).

References

Addessi L (2001) Giant clam bleaching in the lagoon of Takapoto atoll (French Polynesia). *Coral Reefs* 19: 220.

Agbaje OBA, Wirth R, Morales LFG, Shirai K, Kosnik M, Watanabe T, Jacob DE (2017) Architecture of crossed-lamellar bivalve shells: the southern giant clam (*Tridacna derasa*, Röding, 1798). *R Soc Open Sci* 4: 170622. doi:10.1098/rsos.170622.

Agbaje OBA, Thomas DE, Dominguez JG, Mclnerney BV, Kosnik MA, Jacob DE (2019) Biomacromolecules in bivalve shells with crossed lamellar architecture. *J Mater Sci* 54: 4952–4969.

Aldridge DW, Payne BS, Miller AC (1995) Oxygen-consumption, nitrogenous excretion, and filtration-rates of *Dreissena polymorpha* at acclimation temperatures between 20 and 32 degrees. *Can J Fish Aquat Sci* 52: 1761–1767.

Allemand D, Ferrier-Pagès C, Furla P, Houlbrèque F, Puverel S, Reynaud S, Tambutté E, Tambutté S, Zoccola D (2004) Biomineralisation in reef-building corals: from molecular mechanisms to environmental control. *C R Palevol* 3: 453–467.

Allemand D, Tambutté E, Zoccola D, Tambutté S (2011) Coral calcification, cells to reefs. In Z Dubinsky, N Stambler, eds, *Coral Reefs: An Ecosystem in Transition*. Springer, Dordrecht, pp. 119–150

Andréfouët S, Van Wynsberge S, Gaertner-Mazouni N, Menkes C, Gilbert A, Remoissenet G (2013) Climate variability and massive mortalities challenge giant clam conservation and management efforts in French Polynesia atolls. *Biol Conserv* 160: 190–199.

Andréfouët S, Dutheil C, Menkes CE, Bador M, Lengaigne M (2015) Mass mortality events in atoll lagoons: environmental control and increased future vulnerability. *Glob Change Biol* 21: 95–205.

Andréfouët S, Van Wynsberge S, Kabbadj L, Wabnitz CCC, Menkes C, Tamata T, Pahuatini M, Tetairekie I, Teaka I, Ah Scha T *et al.* (2017) Adaptative management for the sustainable exploitation of lagoon resources in remote islands: lessons from a massive El Nino-induced giant clam bleaching event in the Tuamotu atolls (French Polynesia). *Environ Conserv* 45: 30–40.

Armstrong EJ, Dubousquet V, Mills SC, Stillman JH (2020) Elevated temperature, but not acidification, reduces fertilization success in the small giant clam. *Mar Biol* 167: 8. doi:10.1007/s00227-019-3615-0.

Avignon S, Auzoux-Bordenave S, Martin S, Dubois P, Badou A, Coheleach M, Richard N, Giglio S, Malet L, Servili A *et al.* (2020) An integrated investigation of the effects of ocean acidification on adult abalone (*Haliotis tuberculata*). *ICES J Mar Sci* 77: 757–772.

Baker AC (2003) Flexibility and specificity in coral-algal symbiosis: diversity, ecology. *Annu Rev Ecol Evol Syst* 34: 661–689.

Belda CA, Cuff C, Yellowlees D (1993) Modification of shell formation in the giant clam *Tridacna gigas* at elevated nutrient levels in sea water. *Mar Biol* 117: 251–257.

Blidberg E, Elfwing T, Planhnan P, Tedengren M (2000) Water temperature influences on physiological behaviour in three species of giant clams (Tridacnidae). In *Proceeding 9th International Coral Reef Symposium*, Bali, Indonesia, 23–27 October 2000

Bougrier S, Geairon P, Deslous-Paoli JM, Bacher C, Jonquières G (1995) Allometric relationships and effects of temperature on clearance and oxygen consumption rates of *Crassostrea gigas* (Thunberg). *Aquaculture* 134: 143–154.

Broeker WS, Takahashi T, Simpson HJ, Peng T-H (1979) Fate of fossil fuel carbon dioxide and the global carbon budget. *Science* 206: 409–418.

Buck BH, Rosenthal H, Saint-Paul U (2002) Effect of increased irradiance and thermal stress on the symbiosis of *Symbiodinium microadriaticum* and *Tridacna gigas*. *Aquat Living Resour* 15: 107–117.

Caldeira K, Wickett ME (2003) Anthropogenic carbon and ocean pH. *Nature* 425: 365.

Chalker BE, Taylor DL (1975) Light-enhanced calcification, and the role of oxidative phosphorylation in calcification of the coral *Acropora cervicornis*. *Proc R Soc Lond B* 190: 323–331.

Chew SF, Koh CZY, Hiong KC, Choob CYL, Wong WP, Neo ML, Ip Y (2019) Light-enhanced expression of Carbonic Anhydrase 4-like supports shell formation in the fluted giant clam *Tridacna squamosa*. *Gene* 683: 101–112.

Cuif J-P, Dauphin Y, Freiwald A, Gautret P, Zibrowius H (1999) Biochemical markers of zooxanthellae symbiosis in soluble matrices of skeleton of 24 Scleractinia species. *Comp Biochem Physiol A Mol Integr Physiol* 123: 269–278.

Cyronak T, Schulz KG, Jokiel PL (2016) The Omega myth: what really drives lower calcification rates in an acidifying ocean. *ICES J Mar Sci* 73: 558–562.

Downs CA, Fauth JE, Halas JC, Dustan P, Bemiss J, Woodley CM (2002) Oxidative stress and seasonal coral bleaching. *Free Radic Biol Med* 33: 533–543.

Dubousquet V, Gros E, Berteaux-Lecellier V, Viguier B, Raharivelomanana P, Bertrand C, Lecellier G (2016) Changes in fatty acid composition in the giant clam *Tridacna maxima* in response to thermal stress. *Biol Open* 5: 1400–1407.

Elfwing T, Plantman P, Tedengren WE (2001) Responses to temperature, heavy metal and sediment stress by the giant clam *Tridacna squamosa*. *Mar Freshw Behav Physiol* 34: 239–248.

Elfwing T, Blidberg E, Tedengren M (2002) Physiological responses to copper in giant clams: a comparison of two methods in revealing effects on photosynthesis in zooxanthellae. *Mar Environ Res* 54: 147–155.

Fautin D, Buddemeier R (2004) Adaptive bleaching: a general phenomenon. *Hydrobiologia* 530: 459–467.

Faylona MGPG, Lazareth CE, Sémah A-M, Caquineau S, Boucher H, Ronquillo WP (2011) Preliminary study on the preservation of giant clam (Tridacnidae) shells from the Balobok Rockshelter archaeological site. *Geoarchaeology* 26: 888–901.

Ferrier-Pagès C, Richard C, Forcioli D, Allemand D, Pichon M, Shick JM (2007) Effects of temperature and UV radiation increases on the photosynthetic efficiency in four scleractinian coral species. *Biol Bull* 213: 76–87.

Fitt WK, Brown BE, Warner ME, Dunne RP (2001) Coral bleaching: interpretation of thermal tolerance limits and thermal thresholds in tropical corals. *Coral Reefs* 20: 51–65.

Fitzer SC, Phoenix VR, Cusack M, Kamenos NA (2014) Ocean acidification impacts mussel control on biomineralisation. *Sci Rep* 4: 6218. doi:10.1038/srep06218.

Furla P, Galgani I, Durand I, Allemand D (2000) Sources and mechanisms of inorganic carbon transport for coral calcification and photosynthesis. *J Exp Biol* 203: 3445–3457.

Gannon ME, Pérez-Huerta A, Aharon P, Street SC (2017) A biomineralization study of the Indo-Pacific giant clam Tridacna gigas. *Coral Reefs* 36: 503–517.

Gazeau F, Gattuso J-P, Dawber C, Pronker A, Peene F, Peene J, Heip C, Middelburg J (2010) Effect of ocean acidification on the early life stages of the blue mussel *Mytilus edulis*. *Biogeosciences* 7: 2051–2060.

Gazeau F, Parker LM, Comeau S, Gattuso J-P, O'Connor W, Martin S, Portner H-O, Ross PM (2013) Impacts of ocean acidification on marine shelled molluscs. *Mar Biol* 160: 2207–2245.

Goreau TF (1959) The physiology of skeleton formation in corals. I. A method for measuring the rate of calcium deposition by corals under different conditions. *Biol Bull* 116: 59–75.

Hawkins AJS, Klumpp DW (1995) Nutrition of the giant clam *Tridacna gigas* (L.). II. Relative contributions of filter-feeding and the ammonium-nitrogen acquired and recycled by symbiotic alga towards total nitrogen requirements for tissue growth and metabolism. *J Exp Mar Biol Ecol* 190: 263–290.

Hoegh-Guldberg O, Mumby PJ, Hooten AJ, Steneck RS, Greenfield P, Gomez E, Harvell CD, Sale PF, Edwards AJ, Caldeira K *et al.* (2007) Coral reefs under rapid climate change and ocean acidification. *Science* 318: 1737–1742.

Holcomb M, Venn A, Tambutté E, Tambutté S, Allemand D, Trotter J, McCulloch M (2014) Coral calcifying fluid pH dictates response to ocean acidification. *Sci Rep* 4: 5207. doi: 10.1038/srep05207.

Holt AL, Vahidinia S, Gagnon YL, Morse DE, Sweeney AM (2014) Photosymbiotic giant clams are transformers of solar flux. *J R Soc Interface* 11: 20140678. doi:0.1098/rsif.2014.0678.

Ip YK, Loong AM, Hiong KC, Wong WP, Chew SF, Reddy K, Sivaloganathan B, Ballantyne JS (2006) Light induces an increase in the pH of and a decrease in the ammonia concentration in the extrapallial fluid of the giant clam *Tridacna squamosa*. *Physiol Biochem Zool* 79: 656–664.

Ip YK, Hiong KC, Goh EJK, Boo MV, Choo YL, Ching B, Wong WP, Chew SF (2017) The whitish inner mantle of the giant clam, *Tridacna squamosa*, expresses an apical Plasma Membrane Ca^{2+}-ATPase (PMCA) which displays light-dependent gene and protein expressions. *Front Physiol* 8: 781. doi:10.3389/fphys.2017.00781.

IPCC (2014) Summary for policymakers. In CB Field, VR Barros, DJ Dokken, KJ Mach, MD Mastrandrea, TE Bilir, M Chatterjee, KL Ebi, YO Estrada, RC Genova *et al.*, eds, *Climate Change 2014: Impacts, Adaptation, and Vulnerability. Part A: Global and Sectoral Aspects. Contribution of Working Group II to the Fifth Assessment Report of the Intergovernmental Panel on Climate Change*. Cambridge University Press, Cambridge, UK and New York, NY, USA, pp. 1–32

IPCC (2019) Summary for Policymakers. In H-O Pörtner, DC Roberts, V Masson-Delmotte, P Zhai, M Tignor, E Poloczanska, K Mintenbeck, M Nicolai, A Okem, J Petzold *et al.*, eds, *IPCC Special Report on the Ocean and Cryosphere in a Changing Climate*. In press.

Ishikura M, Adachi K, Maruyama T (1999) Zooxanthellae release glucose in the tissue of a giant clam, *Tridacna crocea*. *Mar Biol* 133: 665–673.

Jones RJ, Hoegh-Guldberg O (2001) Diurnal changes in the photochemical efficiency of the symbiotic dinoflagellates (*Dinophyceae*) of corals: photoprotection, photoinactivation and the relationship to coral bleaching. *Plant Cell Environ* 24: 89–99.

Junchompoo C, Sinrapasan N, Penpain C, Patsorn P (2013) Changing seawater temperature effects on giant clams bleaching, Mannai Island, Rayong province, Thailand. In *Proceedings of the Design Symposium on Conservation of Ecosystem (The 12th SEASTAR2000 workshop)*, pp. 71–76

Kleypas JA, Buddemeier RW, Archer D, Gattuso J-P, Langdon C, Opdyke BN (1999) Geochemical consequences of increased atmospheric carbon dioxide on coral reefs. *Science* 284: 118–120.

Klumpp DW, Griffiths CL (1994) Contributions of phototrophic and heterotrophic nutrition to the metabolic and growth requirements of four species of giant clam (*Tridacnidae*). *Mar Ecol Prog Ser* 115: 103–115.

Klumpp DW, Lucas JS (1994) Nutritional ecology of the giant clams *Tridacna tevoroa* and *T. derasa* from Tonga – Influence of light on filter-feeding and photosynthesis. *Mar Ecol Prog Ser* 107: 147–156.

Klumpp DW, Bayne BL, Hawkins AJS (1992) Nutrition of the giant clam *Tridacna gigas*. Contribution of filter feeding and photosynthates to respiration and growth. *J Exp Mar Biol Ecol* 155: 105–122.

Kroeker KJ, Kordas RL, Crim R, Hendriks IE, Ramajo L, Singh GS, Duarte CM, Gattuso J-P (2013) Impacts of ocean acidification on marine organisms: quantifying sensitivities and interaction with warming. *Glob Change Biol* 19: 1884–1896.

Kurihara H (2008) Effects of CO_2-driven ocean acidification on the early developmental stages of invertebrates. *Mar Ecol Prog Ser* 373: 275–284.

Kurihara H, Shikota T (2018) Impact of increased seawater pCO_2 on the host and symbiotic algae of juvenile giant clam *Tridacna crocea*. *Galaxea J Coral Reef Stud* 20: 19–28.

Kurihara T, Yamada H, Inoue K, Iwai K, Hatta M (2013) Impediment to symbiosis establishment between giant clams and *Symbiodinium* algae due to sterilization of seawater. *PLoS One* 8: 1–8. doi:10.1371/journal.pone.0061156.

LaJeunesse TC, Parkinson JE, Gabrielson PW, Jeong HJ, Reimer JD, Voolstra CR, Santos SR (2018) Systematic revision of Symbiodiniaceae highlights the antiquity and diversity of coral endosymbionts. *Curr Biol* 28: 2570–2580.e6.

Latchère O, Le Moullac G, Gaetner-Mazouni N, Fievet J, Magré K, Saulnier D (2017) Influence of preoperative food and temperature conditions on pearl biogenesis in *Pinctada margaritifera*. *Aquaculture* 479: 176–187.

Leggat W, Buck BH, Grice A, Yellowlees D (2003) The impact of bleaching on the metabolic contribution of dinoflagellate symbionts to their giant clam host. *Plant Cell Environ* 26: 1951–1961.

Le Moullac G, Soyez C, Latchère O, Vidal-Dupiol J, Fremery J, Saulnier D, Lo Yat A, Belliard C, Mazouni-Gaertner N, Gueguen Y (2016a) *Pinctada margaritifera* responses to temperature and pH: acclimation capabilities and physiological limits. *Estuar Coast Shelf Sci* 182: 261–269.

Le Moullac G, Soyez C, Vidal-Dupiol J, Belliard C, Fievet J, Sham-Koua M, Lo Yat A, Saulnier D, Gaertner-Mazouni N, Gueguen Y (2016b) Impact of pCO_2 on the energy, reproduction and growth of the shell of the pearl oyster *Pinctada margaritifera*. *Estuar Coast Shelf Sci* 182: 274–282.

Lesser MP (1996) Elevated temperatures and ultraviolet radiation cause oxidative stress and inhibit photosynthesis in symbiotic dinoflagellates. *Limnol Oceanogr* 41: 271–283.

Lesser MP, Stochaj WR, Tapley DW, Schick JM (1990) Bleaching in coral reef anthozoans: effects of irradiance, ultraviolet radiation and temperature on the activities of protective enzymes against active oxygen. *Coral Reefs* 8: 225–232.

Liu W, Huang X, Lin J, He M (2012) Seawater acidification and elevated temperature affect gene expression patterns of the pearl oyster *Pinctada fucata*. *PLoS One* 7: 1–7. doi:10.1371/journal.pone.0033679.

Marin F, Le Roy N, Marie B (2012) Formation and mineralization of mollusk shell. *Front Biosci* 4: 1099–1125.

McClintock JB, Angus RA, McDonald MR, Amsler CD, Catledge SA, Vohra YK (2009) Rapid dissolution of shells of weakly calcified Antarctic benthic macroorganisms indicates high vulnerability to ocean acidification. *Antarct Sci* 21: 449–456.

McCulloch M, Falter J, Trotter J, Montagna P (2012) Coral resilience to ocean acidification and global warming through pH up-regulation. *Nat Clim Change* 2: 623–627.

Melzner F, Stange P, Trübenbach K, Thomsen J, Casties I, Panknin U, Gorb S, Gutowska M (2011) Food supply and seawater pCO_2 impact calcification and internal shell dissolution in the blue mussel *Mytilus edulis*. *PLoS One* 6: 1–9. doi:10.1371/journal.pone.0024223.

Meng Y, Guo Z, Fitzer SC, Upadhyay A, Chan VBS, Li C, Cusack M, Yao H, Yeung KWK, Thiyagarajan V (2018) Ocean acidification reduces hardness and stiffness of the Portuguese oyster shell with impaired microstructure: a hierarchical analysis. *Biogeosciences* 15: 6833–6846.

Morse JW, Arvidson RD, Lüttge A (2007) Calcium carbonate formation and dissolution. *Chem Rev* 107: 342–381.

Muscatine L, Goiran C, Land L, Jaubert J, Cuif J-P, Allemand D (2005) Stable isotopes (delta C-13 and delta N-15) of organic matrix from coral skeleton. *Proc Natl Acad Sci U S A* 102: 1525–1530.

Norton JH, Shepherd MA, Long HM, Fitt WK (1992) The zooxanthellal tubular system in the giant clam. *Biol Bull* 183: 503–506.

Orr JC, Fabry VJ, Aumont O, Bopp L, Doney SC, Feely RA, Gnanadesikan A, Gruber N, Ishida A, Joos F *et al.* (2005) Anthropogenic ocean acidification over the twenty-first century and its impact on calcifying organisms. *Nature* 437: 681–686.

Palmer AR (1992) Calcification in marine molluscs: how costly is it? *Proc Natl Acad Sci U S A* 89: 1379–1382.

Parker LM, Ross PM, O'Connor WA, Pörtner HO, Scanes E, Wright JM (2013) Predicting the response of molluscs to the impact of ocean acidification. *Biology* 2: 651–692.

Pätzold J, Heinrichs JP, Wolschendorf K, Wefer G (1991) Correlation of stable oxygen isotope temperature record with light attenuation profiles in reef-dwelling *Tridacna* shells. *Coral Reefs* 10: 65–69.

Pearse VB, Muscatine L (1971) Role of symbiotic algae (zooxanthellae) in coral calcification. *Biol Bull* 141: 350–363.

Perez S, Weis V (2006) Nitric oxide and cnidarian bleaching: an eviction notice mediates breakdown of a symbiosis. *J Exp Biol* 209: 2804–2810.

Richier S, Sabourault C, Courtiade J, Zucchini N, Allemand D, Furla P (2006) Oxidative stress and apoptotic events during thermal stress in the symbiotic sea anemone. *FEBS J* 273: 4186–4198.

Richter C, Rühle W, Wild A (1990) Studies on the mechanisms of photosystem II photoinhibition II. The involvement of toxic oxygen species. *Photosynth Res* 24: 237–243.

Ries JB (2011) A physiochemical framework for interpreting the biological calcification response to CO_2-induced ocean acidification. *Geochim Cosmochim Acta* 75: 4053–4064.

Ries JB, Cohen AL, McCorkle DC (2009) Marine calcifiers exhibit mixed responses to CO_2-induced ocean acidification. *Geology* 37: 1131–1134.

Rodolfo-Metalpa R, Houlbreque F, Tambutte E, Boisson F, Baggini C, Patti FP, Jeffree R, Fine M, Foggo A, Gattuso J-P *et al.* (2011) Coral and mollusc resistance to ocean acidification adversely affected by warming. *Nat Clim Change* 1: 308–312.

Sabine CL, Feely RA, Gruber N, Key RM, Lee K, Bullister JL, Wanninkhof R, Wong CS, Wallace DWR, Tilbrook B *et al.* (2004) The oceanic sink for anthropogenic CO_2. *Science* 305: 367–371.

Schwartzmann C, Durrieu M, Sow M, Ciret P, Lazareth CE, Massabuau J-C (2011) In situ giant clam growth rate behavior in relation to temperature: a one-year couple study of high-frequency noninvasive valvometry and sclerochronology. *Limnol Oceanogr* 56: 1940–1951.

Smith DJ, Suggett DJ, Baker NR (2005) Is photoinhibition of zooxanthellae photosynthesis the primary cause of thermal bleaching in corals? *Glob Change Biol* 11: 1–11.

Soo P, Todd PA (2014) The behaviour of giant clams. *Mar Biol* 161: 2699–2717.

Talmage SC, Gobler CJ (2011) Effects of elevated temperature and carbon dioxide on the growth and survival of larvae and juveniles of three species of northwest Atlantic bivalves. *PLoS One* 6: 1–12. doi:10.1371/journal.pone.0026941.

Taylor AR, Brownlee C, Wheeler GL (2012) Proton channels in algae: reasons to be excited. *Trends Plant Sci* 17: 675–684.

Toonen RJ, Nakayama T, Ogawa T, Rossiter A, Delbeek JC (2012) Growth of cultured giant clams (*Tridacna spp.*) in low pH, high nutrient seawater: species-specific effects of substrate and supplemental feeding under acidification. *J Mar Biol Assoc UK* 92: 731–740.

Torda G, Donelson JM, Aranda M, Barshis DJ, Bay L, Berumen ML, Bourne DG, Cantin N, Foret S, Matz M *et al.* (2017) Rapid adaptive responses to climate change in corals. *Nat Clim Chang* 7: 627.

Vandermeulen JH, Davis ND, Muscatine L (1972) The effect of inhibitors of photosynthesis on zooxanthellae in corals and other marine invertebrates. *Mar Biol* 16: 185–191.

van Heuven S, Pierrot D, Lewis E, Wallace DWR (2009) MATLAB Program developed for CO2 system calculations, ORNL/CDIAC-105b, Carbon Dioxide Information Analysis Center, Oak Ridge National Laboratory, US Department of Energy, Oak Ridge, Tennessee.

Van Wynsberge S, Andréfouët S, Gaertner-Mazouni N, Wabnitz CCC, Gilbert A, Remoissenet G, Payri C, Fauvelot C (2016) Drivers of density for the exploited giant clam *Tridacna maxima*: a meta-analysis. *Fish Fish* 17: 567–584.

Venn A, Tambutté E, Holcomb M, Laurent J, Allemand D, Tambutté S (2013) Impact of seawater acidification on pH at the tissue-skeleton interface and calcification in reef corals. *Proc Natl Acad Sci U S A* 110: 1634–1639.

Vidal-Dupiol J, Zoccola D, Tambutté E, Grunau C, Cosseau C, Smith KM, Freitag M, Dheilly NM, Allemand D, Tambutté S (2013) Genes related to ion-transport and energy production are upregulated in response to CO_2-driven pH decrease in corals: new insights from transcriptome analysis. *PLoS One* 8: 1–11. doi: 10.1371/journal.pone.0058652.

Warner ME, Fitt WK, Schmidt GW (1999) Damage to photosystem II in symbiotic dinoflagellates: a determinant of coral bleaching. *Proc Natl Acad Sci U S A* 96: 8007–8012.

Watson S-A (2015) Giant clams and rising CO_2: Light may ameliorate effects of ocean acidification on a solar-powered animal. *PLoS One* 10: 1–18. doi: 10.1371/journal.pone.0128405.

Watson S-A, Southgate PC, Miller GM, Moorhead JA, Knauer J (2012) Ocean acidification and warming reduce juvenile survival of the fluted giant clam *Tridacna squamosa*. *Molluscan Res* 32: 177–180.

Welladsen HM, Southgate PC, Heimann K (2010) The effects of exposure to near-future levels of ocean acidification on shell characteristics of *Pinctada fucata* (Bivalvia: Pteriidae). *Molluscan Res* 30: 125–130.

Wessel N, Martin S, Badou A, Dubois P, Huchette S, Julia V, Nunes F, Harney E, Paillard C, Auzoux-Bordenave S (2018) Effect of CO_2-induced ocean acidification on the early development and shell mineralization of the European abalone (*Haliotis tuberculata*). *J Exp Mar Biol Ecol* 508: 52–63.

Yau AJY, Fan TY (2012) Size-dependent photosynthetic performance in the giant clam *Tridacna maxima*, a mixotrophic marine bivalve. *Mar Biol* 159: 65–75.

Zeebe RE, Zachos JC, Caldeira K, Tyrrell T (2008) Oceans-Carbon emissions and acidification. *Science* 321: 51–52.

Zhou Z, Liu Z, Wang L, Luo J, Li H (2019) Oxidative stress, apoptosis activation and symbiosis disruption in giant clam *Tridacna crocea* under high temperature. *Fish Shellfish Immunol* 84: 451–457.

ANNEXE 5

BMC Physiology

BioMed Central

Research article

Coral bleaching under thermal stress: putative involvement of host/symbiont recognition mechanisms

Jeremie Vidal-Dupiol[1], Mehdi Adjeroud[1], Emmanuel Roger[1], Laurent Foure[2], David Duval[1], Yves Mone[1], Christine Ferrier-Pages[3], Eric Tambutte[3], Sylvie Tambutte[3], Didier Zoccola[3], Denis Allemand[3] and Guillaume Mitta*[1]

Address: [1]UMR 5244, CNRS EPHE UPVD, Université de Perpignan, 52 Avenue Paul Alduy, 66860 Perpignan Cedex, France, [2]Aquarium du Cap d'Agde, 11 rue des 2 freres, 34300 Cap d'Agde, France and [3]Centre Scientifique de Monaco, Avenue Saint Martin, MC-98000 Monaco-Ville, Principality of Monaco

Email: Jeremie Vidal-Dupiol - jeremie.vidal-dupiol@univ-perp.fr; Mehdi Adjeroud - adjeroud@univ-perp.fr; Emmanuel Roger - emmanuel.roger@univ-perp.fr; Laurent Foure - lfoure@aquarium-agde.com; David Duval - david.duval@univ-perp.fr; Yves Mone - yves.mone@univ-perp.fr; Christine Ferrier-Pages - ferrier@centrescientifique.mc; Eric Tambutte - etambutte@centrescientifique.mc; Sylvie Tambutte - stambutte@centrescientifique.mc; Didier Zoccola - Zoccola@centrescientifique.mc; Denis Allemand - allemand@centrescientifique.mc; Guillaume Mitta* - mitta@univ-perp.fr

* Corresponding author

Published: 4 August 2009

BMC Physiology 2009, **9**:14 doi:10.1186/1472-6793-9-14

Received: 29 June 2009
Accepted: 4 August 2009

This article is available from: http://www.biomedcentral.com/1472-6793/9/14

Abstract

Background: Coral bleaching can be defined as the loss of symbiotic zooxanthellae and/or their photosynthetic pigments from their cnidarian host. This major disturbance of reef ecosystems is principally induced by increases in water temperature. Since the beginning of the 1980s and the onset of global climate change, this phenomenon has been occurring at increasing rates and scales, and with increasing severity. Several studies have been undertaken in the last few years to better understand the cellular and molecular mechanisms of coral bleaching but the jigsaw puzzle is far from being complete, especially concerning the early events leading to symbiosis breakdown. The aim of the present study was to find molecular actors involved early in the mechanism leading to symbiosis collapse.

Results: In our experimental procedure, one set of *Pocillopora damicornis* nubbins was subjected to a gradual increase of water temperature from 28°C to 32°C over 15 days. A second control set kept at constant temperature (28°C). The differentially expressed mRNA between the stressed states (sampled just before the onset of bleaching) and the non stressed states (control) were isolated by Suppression Subtractive Hybridization. Transcription rates of the most interesting genes (considering their putative function) were quantified by Q-RT-PCR, which revealed a significant decrease in transcription of two candidates six days before bleaching. RACE-PCR experiments showed that one of them (*PdC-Lectin*) contained a C-Type-Lectin domain specific for mannose. Immunolocalisation demonstrated that this host gene mediates molecular interactions between the host and the symbionts suggesting a putative role in zooxanthellae acquisition and/or sequestration. The second gene corresponds to a gene putatively involved in calcification processes (*Pdcyst-rich*). Its down-regulation could reflect a trade-off mechanism leading to the arrest of the mineralization process under stress.

Conclusion: Under thermal stress zooxanthellae photosynthesis leads to intense oxidative stress in the two partners. This endogenous stress can lead to the perception of the symbiont as a toxic partner for the host. Consequently, we propose that the bleaching process is due in part to a decrease in zooxanthellae acquisition and/or sequestration. In addition to a new hypothesis in coral bleaching mechanisms, this study provides promising biomarkers for monitoring coral health.

Background

Coral reefs are fascinating ecosystems, characterized by high levels of biodiversity and ecological complexity, high primary productivity and have significant aesthetic and commercial value, particularly in relation to fisheries, tourism and the aquarium industry. In recent decades coral reefs have been dramatically impacted by large-scale disturbances [1]. Natural disturbances are a routine part of coral reef community dynamics, but they have increased in frequency and severity during the last three decades [1,2]. In addition to providing multiple sources of anthropogenic disturbance that directly kill coral colonies [3], human activities have likely contributed to the increase in natural disturbances via global warming.

Of the broad range of natural and anthropogenic perturbations that affect coral reefs, coral bleaching is recognised as a major disturbance that has the potential to significantly alter the biological and ecological processes that maintain reef communities [4,5]. This phenomenon can occur from the colony scale to the geographical scale where it leads to "mass" coral bleaching with occasional high mortality rates. For example, in 1998 a global mass coral bleaching event led to the death of 16% of the worlds corals [6].

Physiologically, this phenomenon is due to the breakdown of the phototrophic mutualistic symbiosis between scleractinian corals and dinoflagellate endosymbionts (genus *Symbiodinium* spp.), commonly referred to as zooxanthellae. This symbiosis breakdown can be the consequence of a large variety of environmental stressors [7-9], but one of the most important for mass coral bleaching is abnormal high sea surface temperatures which can act synergistically with high solar irradiance [10-12]. At the cellular level, coral bleaching refers to a substantial or partial loss of the endosymbiotic algae from the coral tissues, and/or the loss or reduction of photosynthetic pigment concentrations within zooxanthellae [9].

At the molecular level, the first step of temperature or light induced coral bleaching is the photoinhibition mechanism experienced by the zooxanthellae [13-15]. This often results in the overproduction of reactive oxygen species (ROS) by transport chain electrons [16]. ROS are highly cytotoxic and some of them can easily cross biological membranes leading to severe oxidative stress in both host and symbiotic cells. This oxidative stress can result in the activation of cell necrosis and apoptosis [17,18], which represent two of the six identified ways of endosymbiotic loss during bleaching [18-23]. The four other ways of symbiont disappearance are: i) *in situ* digestion of zooxanthellae by the coral host [24,25], ii) expulsion by exocytosis or iii) by pinching off [24,26], and iv) host cell detachment [22].

The increase in the incidence and magnitude of coral bleaching episodes in recent decades [27] and the present context of global warming [5] strengthens the interest in this research field. Studies on early molecular mechanisms triggering and leading to these different ways of symbiotic loss are necessary to better understand the phenomenon and can provide early molecular markers to monitor coral health. In this context, several comparative molecular studies were undertaken. They compared healthy, semi-bleached and bleached corals or symbiotic *versus* aposymbiotic anemones. These studies revealed different genes involved in the response to the stress as well as genes putatively involved in bleaching mechanism or symbiosis breakdown/onset [28-35]. Some of the genes identified in these different studies are promising candidates to explain bleaching processes but studies on their expression and function are now necessary to validate their putative role. For example, a recent study of Desalvo et al. (2008) evidenced a putative calcium homeostasis disruption that could trigger different cellular processes leading to cell death via apoptosis and necrosis. Concerning symbiosis regulation, *Sym 32*, a fasciclin domain containing protein, was shown to be differentially expressed between symbiotic and aposymbiotic anemones, could be involved in host/symbiont interaction and symbiosis breakdown under cadmium exposure [34,36,37].

In the present study, the experiment was specifically designed to identify genes regulated in the early stages of the thermal stress process leading to bleaching. To achieve this aim, we developed a comparative transcriptomic approach (by Suppression Subtractive Hybridization) comparing stressed corals before bleaching symptoms appears *versus* controls. Because our aim was also to develop functional markers that could be used to monitor coral health, we choose *Pocillopora damicornis* as a model species due to its widespread distribution in the Indo-Pacific region [38] and its high sensitivity during mass bleaching events [39-42]. Our SSH approach led to the identification of two genes displaying an important down-regulation just before bleaching. Characterization of their precursors and immunolocalization experiments revealed their putative function and permitted the emergence of new hypotheses on coral bleaching mechanisms. In addition, these two genes constitute promising biomarkers for coral health monitoring.

Results

Bleaching monitoring

Zooxanthellae density and statistical tests (Figure 1) showed that bleaching occurred in the stressed set of corals at 32°C, 15 days after the beginning of the protocol and was complete by the 18th day. In the control set, no bleaching or paling was observed throughout the experiment. After 15 days at 32°C, bleaching induced a large

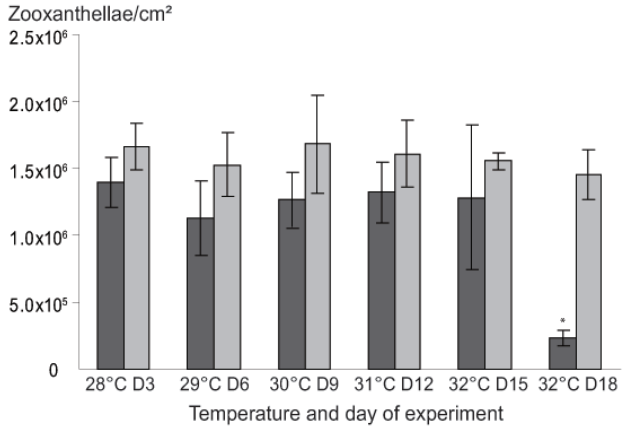

Figure 1
Zooxanthellae density measured during the temperature stress. Dark grey histograms refer to the stressed set, light grey histograms to the control set. The Kruskal-Wallis H-test shows significant differences in the stressed set ($P < 0.05$). The significant differences ($P < 0.05$) were identified using the Mann-Whitney U-test and indicated by a star.

increase in the standard deviation (SD) of zooxanthellae density in comparison to the other points of the kinetic, suggesting that symbiosis in some corals was starting to break. Bleaching was well-established 18 days after the beginning of the protocol with a 79.9% reduction in zooxanthellae density.

In order to select genes regulated early during bleaching, we performed the SSH with samples taken at day 12 and 15. This choice was also driven by an experimental constraint whereby stressed and control samples must have similar zooxanthellae densities to avoid false positive transcripts due to a differential representation of zooxanthellae between the two conditions.

EST sequencing, general characteristics of the BIG and BRG libraries, gene validation and selection

Two SSH experiments were performed resulting in the construction of four cDNA libraries. The first SSH experiment was the result of the subtractive hybridization between the 31°C (D12) and control sets, and the second experiment between the 32°C (D15) and control sets. One hundred clones from each library were sequenced. To simplify the analysis, putative induced clones and putative repressed clones of the SSH libraries were respectively pooled in two new libraries called "Bleaching Induced Genes" (BIG) and "Bleaching Repressed Genes" (BRG). After sequencing, 147 and 118 high quality cDNA sequences were obtained from the BIG and the BRG libraries, respectively. BIG library ESTs coalesced into 15 contigs and 96 singletons, suggesting that the overall redundancy of the library was about 10.2% (Table 1). The

Table 1: General characteristics of the BIG and BRG libraries.

	BIG library	BRG library
Sequenced clone	200	200
Analysed cDNA	147	118
Average insert size (bp)	360	429
Average EST size (bp)	310	308
EST contigs	15	17
Singletons	96	70
Redundancy* (%)	10.2	14.4

* R = nEST assembled in cluster/Total EST

BRG library coalesced into 17 contigs and 70 singletons for an overall redundancy of 14.4% (Table 1). In order to minimize redundancy in the EST database, sequences displaying 100% identity were submitted as a single sequence. ESTs aligning in the same contig but displaying differences in their nucleotidic sequence were submitted individually to the database. A total of 61 and 94 ESTs were submitted to the dbEST section of the NCBI/GenBank database for the BIG and BRG libraries respectively (GenBank: GH706795 to GH706855 and GH706856 to GH706949, for BIG and BRG library respectively). ESTs were subjected to BLASTN and BLASTX searches. Sequence similarities were considered to be significant when the expected value (e value) was less than 10^{-2}. Gene encoding proteins involved in photosynthesis, oxidative detoxification, intracellular signalling pathway, metabolism, cytoskeleton structure, conserved protein domains, calcium homeostasis, cell/cell or cell/ligand interactions, protein degradation, chaperone protein and protein synthesis were selected for further analysis [see additional file 1 for, Top blast, GeneBank accession number and specific primers used for Q-RT-PCR]. Among the tested clusters (data not shown), only clusters 12 and 27 showed a drastic regulation. They display 101 and 10.1 fold transcript decreases under stress, respectively.

Clusters 12 and 27 belong to the functional class of cell/cell or cell/ligand interaction and their putative functions make them promising candidates as key factors of symbiosis breakdown/maintenance. Consequently, we decided to focus the remainder of the present study on these genes.

Cluster 12 and 27 ORF characterization and protein structure

RACE-PCR experiments were performed to obtain the complete ORF of the two selected genes. The cDNA corre-

sponding to cluster 12 displayed significant similarities (E value = 3.10^{-7}) with a predicted protein of *Nematostella vectensis*. The precursor displays a cysteine array (InterProScan) shared by snake toxins and some proteins involved in cell adhesion (the uPAR/Ly6/CD59/Snake toxin domain super-family). This gene was named *Pdcyst-rich*, for *Pocillopora damicornis* cystein-rich. The second gene (cluster 27) displayed significant similarities (E value = 1.10^{-27}) for the Millectin protein, isolated from *Acropora millepora* [43]. Domain analysis using the InterProScan software showed that this protein contained a DC-SIGN domain characteristic for lectins of the C-type. Consequently, this gene was named *PdC-Lectin*.

cDNA corresponding to *Pdcyst-rich* (GenBank: FJ628421) displays an ORF of 441 base pairs corresponding to a precursor of 147 amino acids (AA). The analysis of the primary structure by PSORTII prediction software reveals that it has a secretory protein-like structure with a 23 peptide signal sequence. Between the residue 25 and 133 of the precursor a domain similar to the uPAR/Ly6/CD59/Snake toxin family was identified using the InterProScan software. The size range of this domain is comprised between 70 and 92 AA [44]. This type of domain is present in a large variety of proteins involved in different functions, including T-lymphocyte activation (Ly-6, [45,46]), fibrinogen formation (uPAR, [47,48]), inhibition of the complement mediating lysis (CD59, [44]) and snake venom [49]. The principal structural features of this domain are the presence of (i) 8 to 10 cysteine residues involved in di-sulphide bond formation, and (ii) a typical motif "CCXXDXCN" at the C-terminal end of the domain [50]. As the proteins sharing the uPAR/Ly6/CD59/Snake toxin domain are classically N-glycosylated and GPI anchored, the N-glycosylation and GPI anchored status of the *Pdcyst-rich* protein were investigated using NetGlyc and PSORT2 software [51,52]. The N-glycosilation site was predicted on the 75th residue of the precursor and a GPI anchored signal was found at the C-Terminal end of the protein (residues 144147).

cDNA corresponding to *PdC-Lectin* (GenBank: FJ628422) displayed an ORF of 486 base pairs corresponding to a precursor of 162 amino acids (AA; Figure 2A). The analysis of the primary structure by PSORTII prediction software revealed that it has a secretory protein-like structure with a 22 AA peptide signal sequence. The following 140 AA corresponded to a C-type lectin-like domain (CTLD) shared by a large group of extracellular Metazoan proteins [53]. This domain is involved in recognition and binding of carbohydrates in a Ca^{2+}-dependent manner [54]. The alignment of *PdC-Lectin* with the most similar CTLD (Millectin of *Acropora millepora*, Mermaid-1 of *Laxus oneistus*, CD 23 and DC-SIGN from *Homo sapiens*), showed the presence of highly conserved cysteine residues (Position: 52, 122, 146, and 158 on the precursor; Figure 2B). These residues are involved in the three dimensional structure by di-sulphide bond formation. C1 (position 52) and C4 (158) link β5 and α1 (the whole domain loop), and C2 (122) and C3 (146) link β3 and β5 (the long loop region, involved in Ca^{2+}-carbohydrate binding and domain-swapping dimerization) [53]. The "WIGL" motif present between the residues 63 and 68 is involved in the formation of all tree hydrophobic cores and contributes to structure stabilisation [53]. The presence of all conserved motif and key residues underlines the hypothesis that *PdC-Lectin* CTLD is functional [53]. The highly conserved motifs "EPN" and "WND" in the CTLD (Figure 2A) argue in favour of the specificity for mannose binding in a Ca^{2+}-dependent manner [53]. In addition, the MODWEB server [55] was used to perform the homology modelling of PdC-Lectin. It provides a molecular model based on the crystal structure of the human DC-SIGNR carbohydrate recognition domain (CRD) [56] and presented a model-score of 1.00 (a model is predicted to be good when the model score is higher than 0.7). The molecular model (Figure 2C) revealed that all residues involved in the binding of mannose in a Ca^{2+}-dependent manner (EPN and WND) are located in similar structures (a long loop region for EPN and a β strand for WND; Figure 2C). Moreover, the four conserved cysteines and the "WIGL" motif known to be involved in the maintenance of the CTLD fold have a conserved position in the 3D structure (see superimposition of Figure 2C). The differences (one loop and one β-strand) which can be observed between the template and the molecular model are located in regions of the molecule that are not considered as essential for function (see Figure 2C).

Expression rates of PdC-Lectin *and* Pdcyst-rich *in comparison to classical indicators of bleaching*

Q-RT-PCR were performed on RNA extracted from coral nubbins sampled at 28°C (D3), 31°C (D12) and 32°C (D15) of the kinetic to follow the transcript variations corresponding to *PdC-Lectin* and *Pdcyst-rich* during the stress protocol (Figure 3). Transcript amounts were expressed as a relative ratio to the control values obtained at 28°C (D3). For both genes, although zooxanthellae densities were stable until day 15 (Figure 3B), transcript decreases were observed after 12 days (Figure 3A). Indeed, 101 and 10.1 fold decreases were measured on the 12th day (D12) of the protocol for *Pdcyst-rich* and *PdC-Lectin* genes. At 32°C (D15), the zooxanthellae decrease was non-significant and the levels of *Pdcyst-rich* and *PdC-Lectin* transcripts remained low (25 and 11 fold decreases, respectively compared to control, Figure 3B).

In conclusion, these two genes were drastically down regulated at least six days before the first usual symptoms of

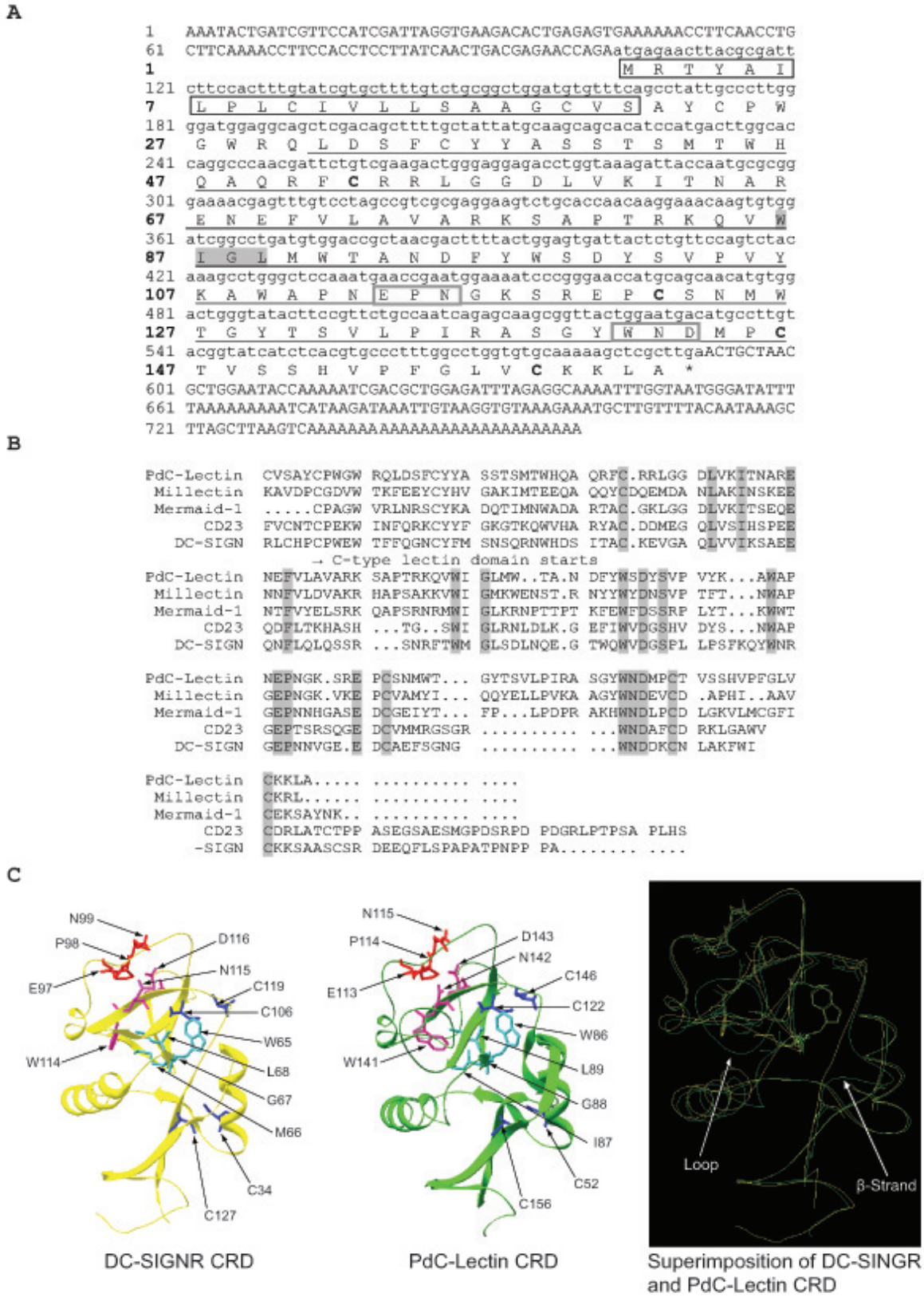

Figure 2 *(see legend on next page)*

Figure 2 *(see previous page)*
Sequence and structure analysis of PdC-Lectin gene and protein. A) cDNA and derived amino acid sequence of *PdC-Lectin*. Black boxes indicate a predicted signal peptide. Underlined area indicates the sequence span of an identified C-type lectin domain. Grey boxes denote conserved mannose binding motifs in a Ca^{2+}-dependent manner. Cysteines belonging to the C-type lectin conserved array are in bold. The WIGL motif is highlighted in grey. B) the alignment of C-type lectin domains of PdC-lectin with different C-type lectin domains contained in several similar proteins identified by Blast searches. Conserved amino acid positions are highlighted. Accession numbers: Millectin (GenBank: EU717895), human CD23 (GenBank: P06734), human DC-SIGN (GenBank: Q9NNX6), Mermaid-1 (GenBank: AY927371). C) the 3D structure of PdC-Lectin CRD. Crystal structure of DC-SIGNR CRD (yellow) and molecular model of PdC-Lectin CRD (green). Superposition of the crystal structure of DC-SIGNR CRD and molecular model of PdC-Lectin CRD (C). All conserved motifs are highlighted; "WIGL" is in clear blue, "EPN" in green, "WND" in pink. The four highly conserved cysteines are in dark blue.

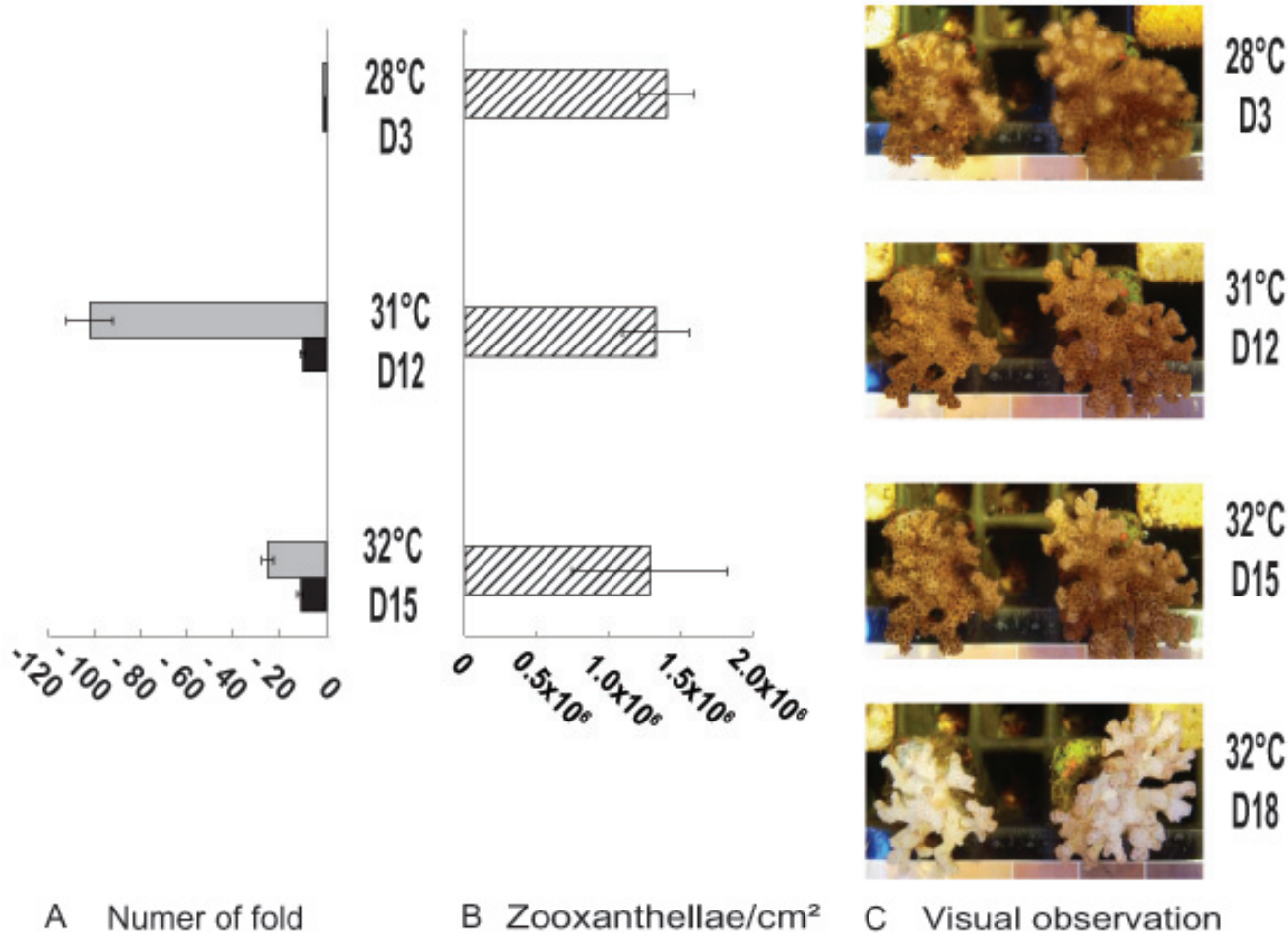

Figure 3
Transcription rates of *PdC-Lectin* and *Pdcyst-rich* in parallel with the classical indicator of bleaching. Expression rate (A) of *PdC-Lectin* (Black histogram) and *Pdcyst-rich* (Grey histogram) and the corresponding zooxanthellae density (B, Hatched histogram) at 28°C (day 3, D3), 31°C (D12) and 32°C (D15). Pictures of coral nubbins at the corresponding stages are shown (C).

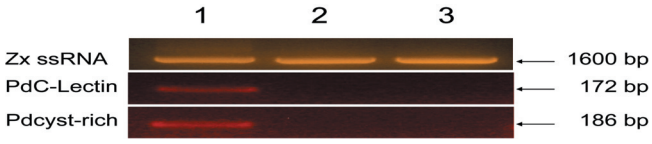

Figure 4
***PdC-Lectin* and *Pdcyst-rich* are expressed by the host.** Presence of *PdC-Lectin* and *Pdcyst-rich* genes and the zooxanthellae small ribosomal subunit RNA (Zx ssRNA) corresponding gene are investigated by PCR using specific primers on DNA extracted from holobionts (corals plus zooxanthellae, lane 1) or zooxanthellae isolated from *S. pistillata* and *G. fascicularis* (lanes 2 and 3, respectively).

bleaching (visual observation, Figure 3C and zooxanthellae density decreases, Figure 3B).

Genes corresponding to PdC-Lectin *and* Pdcyst-rich *are expressed by coral cells*

In order to determine the organism (host or symbiont) expressing each candidate gene we developed cross PCR experiments performed on DNA extracted from the holobiont (host plus symbiont, Figure 4, lane 1) and from pure cultured *Symbiodinium* spp. (isolated from *S. pistillata* and *G. fascicularis*, Figure 4, lane 2 and 3, respectively). These PCR were performed with oligonucleotides specifically amplifying both genes of interest and *Symbiodinium* spp. specific primers (ss5Z and ss3Z) identified in a previous study [57] and known to amplify small ribosomal subunit RNA. Whereas primers specific to genes encoding *PdC-Lectin* and *Pdcyst-rich* proteins only amplified DNA extracted from holobionts (Figure 4, lane 1), ss5Z and ss3Z primers amplified all DNA tested (Figure 4, lanes 1, 2 and 3). This last result demonstrated that PdC-Lectin and Pdcyst-rich protein corresponding genes are specific for corals and confirmed similarity results obtained after database comparisons (see above).

Immunolocalization of PdC-Lectin and Pdcyst-rich proteins

In order to further examine the location of PdC-Lectin and Pdcyst-rich proteins within coral tissues, antibodies were raised against synthetic peptides designed from PdC-Lectin and Pdcyst-rich primary structures. Initially, the specificity of the antibodies was tested by Western blot experiments on holobiont extracts which revealed a single band in both cases (data not shown).

In order to help the reader interpret immunolabeling observations, a schematic representation of the anatomy and histology of *P. damicornis* is provided in Figure 5. *P. damicornis* is a colonial coral characterized by the presence of numerous polyps, linked together by a common tissue usually referred to as the coenosarc (Figure 5). In the polyps, the tentacles are only composed of oral tissue (Figure 5A) whereas the coenosarc is composed of oral and the aboral tissues (Figure 5B). Each of these tissues is composed of an ectoderm separated from the endoderm by an acellular layer of mesoglea (Figure 5B). The oral endoderm faces the coelenteron (gastric cavity) and contains intracellular symbionts commonly called zooxanthellae. The aboral ectoderm faces the skeleton, is composed of calicoblastic cells and is referred to as the calicoblastic ectoderm or calicodermis.

Immunolabeling with anti-PdC-Lectin and anti-Pdcyst-rich protein antibodies is shown in Figure 6 (tentacles) and Figure 7 (coenosarc). Distinct tissues were immunolabeled: anti-PdC-Lectin antibodies labeled the oral endoderm containing intracellular zooxanthellae (Figure 6A) whereas anti-Pdcyst-rich antibody labeled the aboral ectoderm (Figure 7A). When tissues were observed at higher magnification, the immunolabeling with anti- PdC-Lectin antibodies showed a peripheral pattern adjacent to or in the cellular membrane of the endoderm in contact with the coelenteron (Figure 6B, E and 6F). Immunolabeling appeared clearly associated with the membranes (Figure 6B) and to granular structures located next to the membranes (Figure 6F). Additionally, in some cases the labeling was observed at the interface between free zooxanthellae and endodermal host coral cells (Figure 6C and 6G).

Anti-Pdcyst-rich antibodies labeled the calicoblastic ectoderm (Figure 7A) which faced the skeleton in calcified samples. At higher magnifications, it appeared that the immunolabeling of calicoblastic cells was granular and intracellular (Figure 7B, C).

The specificity of the immunolabeling was checked by pre-adsorption of anti-PdC-Lectin and anti-Pdcyst-rich protein IgG with the corresponding synthetic peptides used for immunizations. After this treatment, sections of tissues were no longer labeled (Figure 6D, H and Figure 7D, E) demonstrating the specificity of the immunolabeling.

Discussion

The aim of the present study was to identify molecular actors involved in the breakdown of the phototrophic mutualistic symbiosis between a scleractinian coral (*Pocillopora damicornis*) and its dinoflagellate endosymbiont (genus *Symbiodinium* spp.) during thermal stress. In contrast to some previous studies, thermal stress conditions used in the present work corresponded to natural conditions in terms of amplitude and rapidity of temperature increase. After SSH and validation steps, two genes belonging to the functional classes of cell/cell or cell/lig-

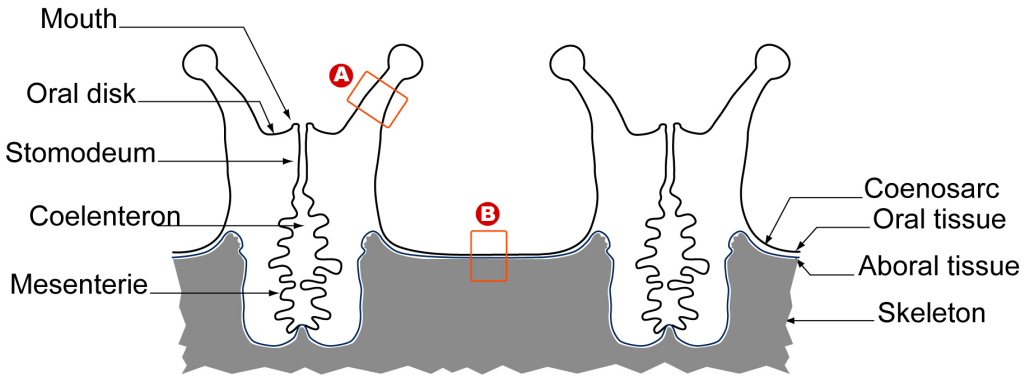

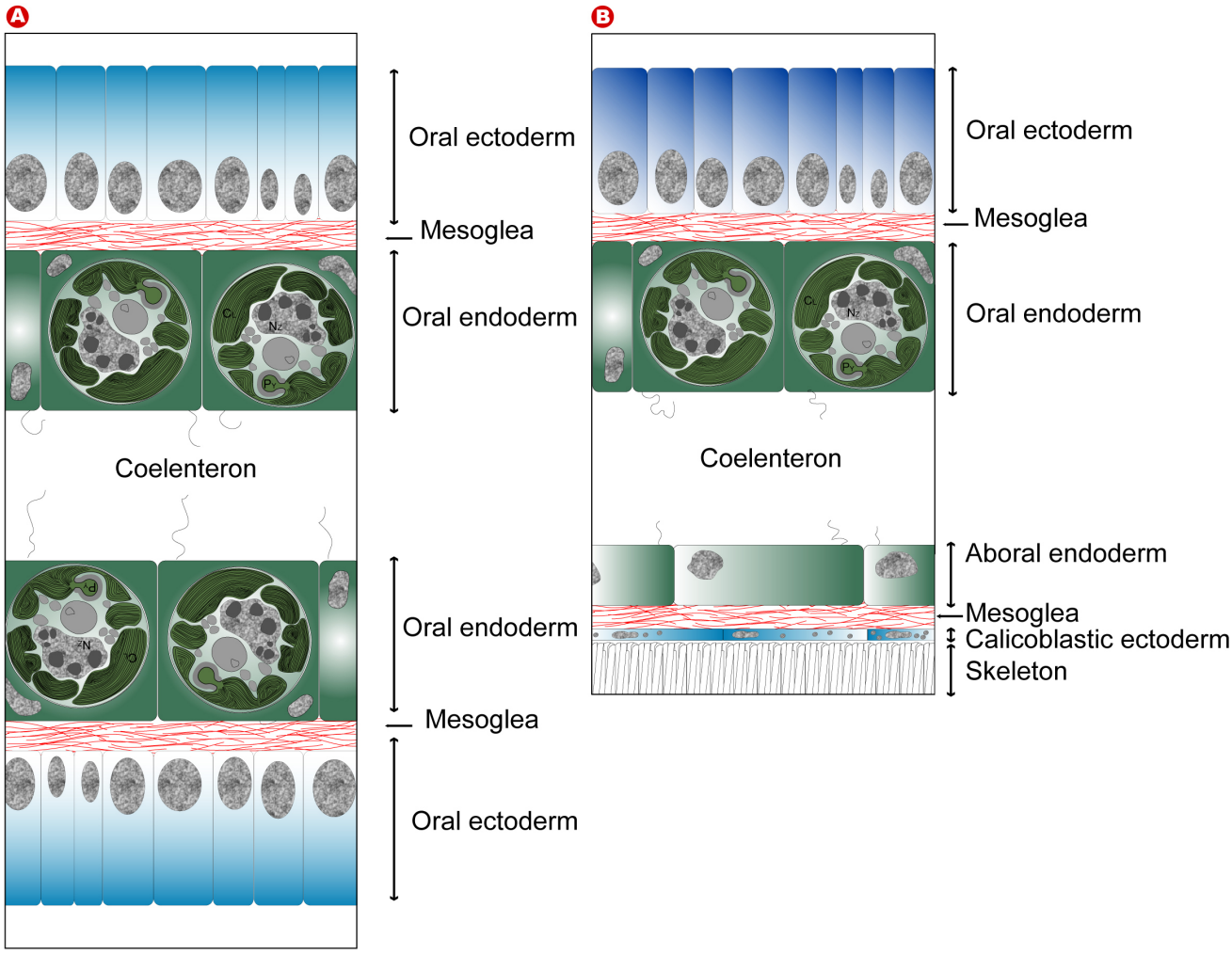

Figure 5
Schematic representation of the anatomy and histology of *P. damicornis*. (A) the histology of the tentacle composed of oral tissues and (B) the histology of the coenosarcs composed of oral and aboral tissue.

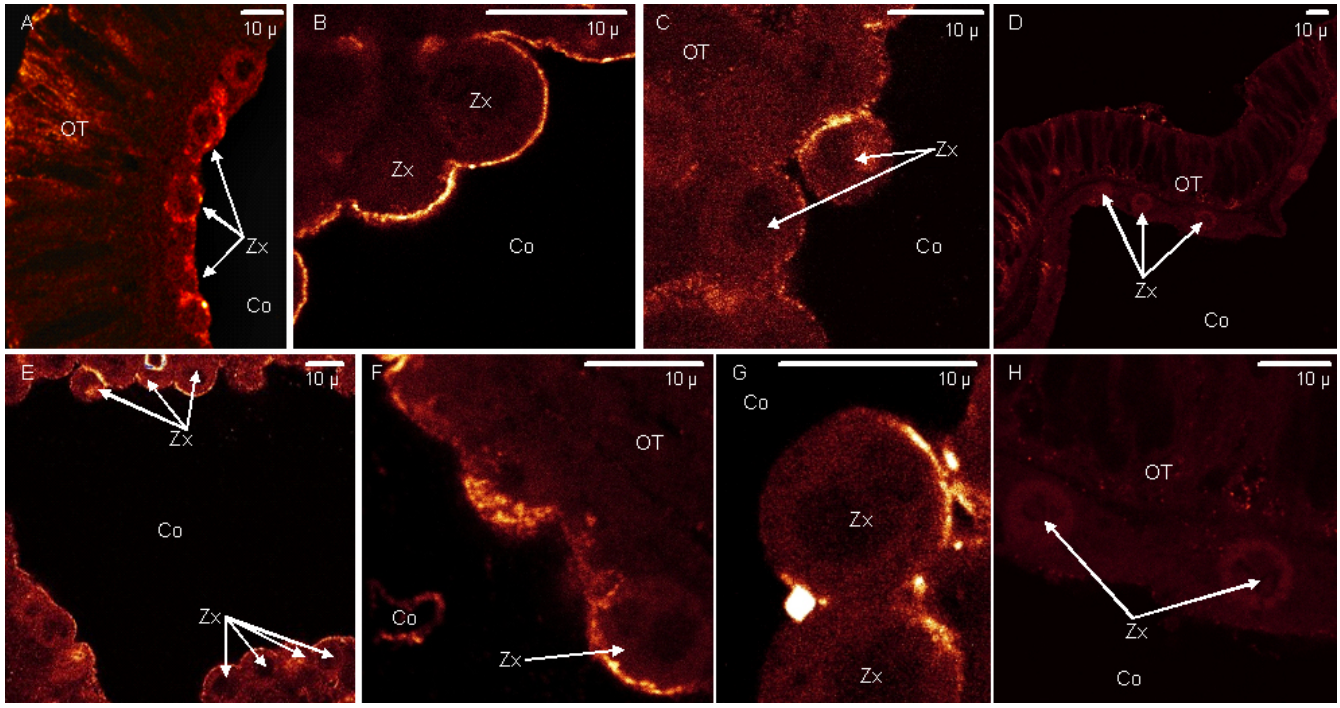

Figure 6

PdC-Lectin immunolabeling in endodermal cells of the oral tissue in tentacles. Anti-PdC-Lectin coupled to Alexafluor 568 is revealed in orange (A), (B), (C), (E), (F) and (G). (D) and (H) represent control experiments performed with anti-PdC-Lectin antibodies pre-adsorbed with the synthetic peptide used for immunization. (A), (D) and (E) are large views of the oral tissue (OT) facing the coelenteron (Co) of coral. (B), (C), (F), (G) and (H) correspond to magnifications of coral cells in contact with the coelenteron (Gastric cavity). Other abbreviations: Zx zooxanthellae.

and interaction present an important down-regulation. Their down-regulation and putative function make them very promising candidates as key indicators of symbiosis breakdown/onset. Consequently, we decided to focus the remainder of the present study on these genes.

The first gene, *Pdcyst-rich*, displayed significant similarities with a predicted protein of *Nematostella vectensis*. Their complete ORF characterization revealed that its precursor displays a putative signal of secretion and all key features shared by the uPAR/Ly6/CD59/Snake toxin family. As this domain is common to proteins involved in a large variety of functions, structural elements are not sufficient to provide hypotheses about the function of *Pdcyst-rich*. PCR experiments revealed that the corresponding gene is expressed in coral cells and complementary immunolocalization experiments showed that the protein displays a granular location in the calicoblastic ectoderm in contact with the skeleton. As *Pdcyst-rich* proteins are synthesized and stored in granules of this skeletogenic tissue, we investigated the suspected role of proteins of the uPAR/Ly6/CD59/Snake toxin family in mineralization process. Two proteins were interesting in this context: RoBo-1 [58] and HEP21 [59]. The function of these proteins remains elusive but their involvement in mineralization process of bones and eggs was hypothesized [58,59]. All these data taken together and in particular the granular location of Pdcyst-rich proteins in calicoblastic cells, suggests that Pdcyst-rich proteins could also play a role in the mineralization process. As it was shown that stress has an immediate effect triggering growth and calcification arrest in scleractinian corals [10,60-62], the strong decrease of the transcript corresponding to Pdcyst-rich protein could reflect the trade-off mechanism occurring during stress and leading to the arrest of the mineralization process. A recent transcriptomic study analyzing differential gene expression during thermal stress in *M. faveolata* also provides evidence of transcript decreases of genes involved in calcification [29].

The second gene identified in the present study was named *PdC-Lectin*. It contains a putative signal peptide and a C-type lectin-like domain shared by a large group of extracellular Metazoan proteins with diverse functions [53]. This domain is involved in recognition and binding of carbohydrates in a Ca^{2+}-dependent manner [54]. Alignments and diverse structural analyses revealed that PdC-Lectin is functional and shares the mannose binding spe-

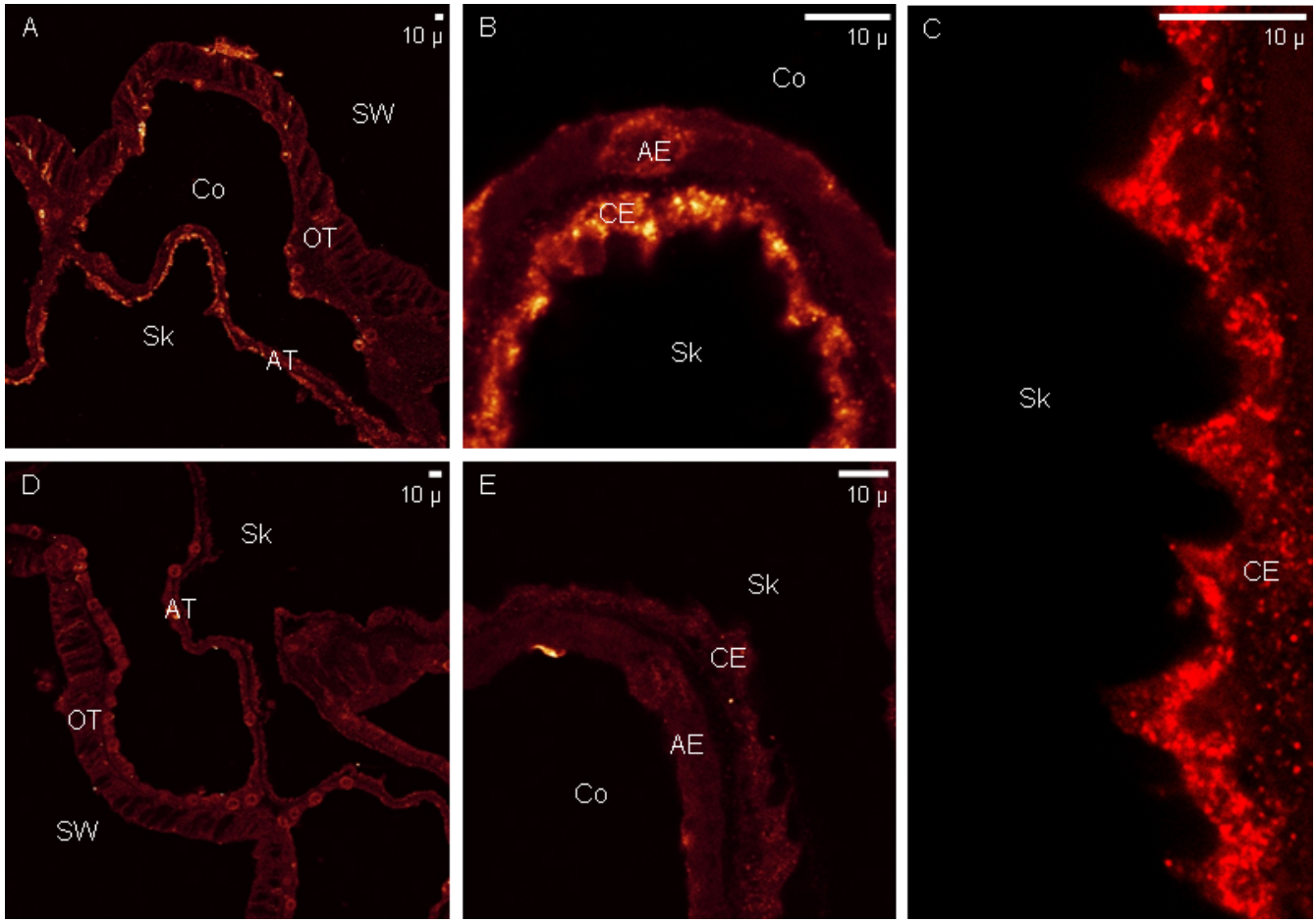

Figure 7
Pdcyst-rich protein immunolabeling in calicoblastic cells. Anti-Pdcyst-rich protein coupled to Alexafluor 568 is revealed in orange (A), (B) and (C). (D) and (E) represents control experiments performed with anti-Pdcyst-rich protein antibodies pre-adsorbed with the synthetic peptide used for immunization. (A) and (D) are large views of oral tissue (OT) and aboral tissues (AT) of the coenosarc. (B), (C) and (E) correspond to magnifications of the aboral tissue showing the aboral endoderm (AE), and the calicoblastic ectoderm (CE). Other abbreviations: Co coelenteron, Sk skeleton, SW seawater.

cificity characteristics of the human DC-SIGN CRD. The presence of the highly conserved motif "EPN" and "WND" in the CTLD of PdC-Lectin argues in favour of the specificity for mannose binding in a Ca^{2+}-dependent manner [53] and the molecular model obtained using the MODWEB server reveals that all residues involved in this binding specificity are located in similar predicted structures by comparison with the human DC-SIGNR CRD. Moreover, the differences observed between the template (human DC-SIGNR CRD) and the PdC-Lectin molecular model are located in regions of the molecule that are not considered as essential for function. In addition, PdC-Lectin displays high similarities (E value = 1.10^{-27} and see alignment Figure 2B) for lectins recently characterized from *Acropora millepora* [43]. These lectins, named Millectin, were isolated by mannose affinity chromatography and were shown to bind to bacterial pathogens as well as coral symbionts, dinoflagellates of the genus *Symbiodinium*. All these elements taken together strengthen the hypothesis that PdC-Lectin is functional and shares the mannose binding specificity of the human DC-SIGN CRD.

Recent work has highlighted the key role played by lectin/glycan interactions in symbiosis onset [63,64]. The Virginia Weis group provided evidence for a recognition mechanism involving lectin/glycan at the onset of symbiosis between aposymbiotic larvae of the coral *Fungia scutaria* and their endosymbiotic zooxanthellae [64]. They showed that algal cell surface glycan ligands, such as α-mannose/α-glucose and α-galactose play a role in recognition during initial contact at the onset of symbiosis [64]. A second study described the role of another lectin, called Mermaid-1 [63]. This protein displayed the same struc-

tural features as PdC-Lectin sharing the same DC-SIGN domain. Mermaid-1 mediates symbiotic bacteria acquisition by the marine nematode *Laxus oneistus*. In this thiotrophic symbiosis, a monolayer of symbiotic sulphur-oxidizing bacteria covers the cuticle of the nematode. The authors showed that this secreted Ca^{2+}-dependent mannose-specific lectin is capable of inducing symbiont aggregation and acquisition [63].

The different structural and bibliographic elements described here argue in favour of a putative role for PdC-Lectin in recognition and binding between the host and the symbionts. The putative signal of secretion, the structural similarities with these different proteins sharing the DC-SIGN domain and its mannose binding specificity suggest that PdC-Lectin could interact with zooxanthellae mannose ligands to mediate symbiont acquisition as it was described for the *F. scutaria*/*Symbiodinium* model [64]. In order to strengthen this hypothesis we performed expression analysis experiments. We confirmed the expression of *PdC-Lectin* in coral cells but the most interesting finding was obtained using immunolocalization experiments where we found evidence of PdC-Lectin immunoreactivity in coral cells belonging to endodermal tissue. This labeled tissue is in contact with free zooxanthellae that are transitorily present in the coelenteron (gastric cavity). We observed a peripheral immunostaining pattern adjacent to or in the cellular membrane in contact with the coelenteron. In addition, some free zooxanthellae were observed in contact with endodermal cells and interestingly, as shown in Figure 6C and 6G, the labeling appears at the interface between zooxanthellae and host coral cells. These data strongly suggest a putative role of PdC-Lectin in zooxanthellae interaction and acquisition.

Finally, our hypothesis is strengthened by the diminution of the *PdC-Lectin* transcript level during stress and during symbiosis breakdown. *PdC-Lectin* transcript concentration decreases just before bleaching occurs and remains low during bleaching process. This means that this gene could be regulated just before symbiosis breakdown. Consequently, and in agreement with the previous data obtained, we propose that bleaching is due in part to a decrease in zooxanthellae acquisition and/or sequestration.

Conclusion

This novel hypothetical mechanism could appear in conjunction with different cellular events reviewed in a recent paper [65]. In this review, the author examined the cellular events leading to the collapse of symbiosis during heat and light stress. Briefly, ROS is shown to play a central role in both injuries to the partners and to inter-partner communication of a stress response. This review also presented evidence that bleaching is a host innate immune response against symbionts. Finally, the different ways of elimination or removal of the symbiont tissues are described through a variety of mechanisms including exocytosis, host cell detachment and host cell apoptosis. Our work reveals another interesting hypothesis with the inhibition of zooxanthellae acquisition processes. During heat stress zooxanthellae could be considered as toxic due to the over-production of ROS and therefore eliminated by host immune responses.

Future work focusing on *PdC-Lectin* function has to be conducted to verify our hypothesis. We could study the mechanisms of zooxanthellae acquisition during the resilience process following experimental bleaching. Recombinant PdC-Lectin and antibodies directed against recombinant PdC-Lectin could be used to facilitate or inhibit the acquisition process of cultured and labeled zooxanthellae during resilience. This functional validation is necessary to be sure of having an early marker of thermal bleaching.

This marker could be used by coral reef managers to (i) distinguish between different stresses on corals, and (ii) precisely and accurately predict bleaching events in conjunction with temperature anomalies indices such as "Degree Heating Weeks" or "Hotspot" developed by the NOAA. This will help managers in the implementation of policy responses and compensatory measures. In addition, these functional biomarkers of thermal stress may be used to evaluate the health of coral transplants kept in public aquaria, in coral farms and for coral nubbins transplanted during restoration projects as these entities are key factors in coral reef conservation in a sustainable development and global warming context.

Methods

Biological material

The *Pocillopora damicornis* isolate used in the present study was harvested in Lombock (Indonesia, CITES number: 06832/VI/SATS/LN/2001) and maintained at the Cap d'Agde Aquarium (France). For our experimental stress, *P. damicornis* nubbins (10 g; 7 cm high; 6 cm in diameter) were propagated by cutting branches from parents and then fixing on a concrete support. To avoid toxicity and to facilitate fixation of the nubbins, the concrete supports were first rinsed and biologically stabilized by immersion in aquaria for two months. The nubbins were used after one month to allow complete cicatrisation and physiological stabilization [66]. During this cicatrisation step, nubbins were maintained at 27°C.

In order to determine which cells (host or symbiont) were expressing the candidate genes, two zooxanthellae isolates were used. The first corresponds to clonal cultures of

zooxanthellae (clade A [67]) originally isolated from a Red Sea colony of *Stylophora pistillata* [68]. The second corresponds to clonal cultures of zooxanthellae (clade B) originally isolated from a Red Sea colony of *Galaxea fascicularis* [69]. Both zooxanthellae clades were cultured in 250 mL screw-top polycarbonate Erlenmeyer flasks (Corning®) in modified ASP-8A medium [70] at pH 8.2. The zooxanthellae were grown in an incubator at 26 ± 1°C under a PAR irradiance of 150 µmol photon.$m^{-2}.s^{-1}$ (≈ 33 W m^{-2}) from Sylvania Gro Lux® and daylight fluorescent tubes, on a 12:12 h (light:dark) photoperiod. The stock cultures were transferred monthly. Cells were used in stationary phase.

Thermal stress protocol

Forty-six nubbins were randomly distributed between two sets (one stressed set and one control set) contained in two 200 L tanks (110 cm × 90 cm × 20 cm). These colonies were then acclimatized to a temperature of 28°C for two weeks [62]. This temperature corresponds to the sea surface temperature observed during the warmer months in most coral reefs around the world [11,60,71-76]. To create stress conditions triggering an *in situ* mass bleaching event, the temperature of the stressed set was increased by about 1°C every three days, until 32°C was achieved (D15). This last temperature corresponds to the maximal temperature observed in different coral reefs during mass bleaching events [11,60,71-76]. This temperature threshold was then maintained until bleaching occurred (D18) while the control set was maintained at 28°C (Figure 8). For each condition (stressed and control), three nubbins were randomly sampled at the end of each step (every three days). Three apexes of 0.5 cm were cut from each nubbin for zooxanthellae density measurements. Nubbins and apexes were frozen and stored in liquid nitrogen until analysed.

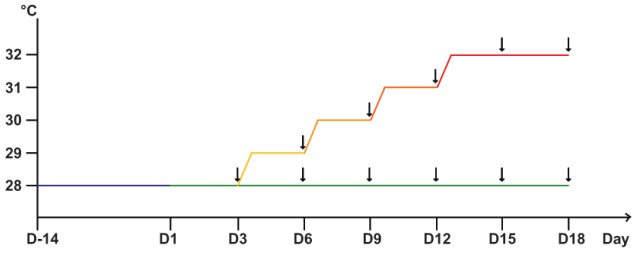

Figure 8
Schematic representation of the experimental design. After a 14 days-acclimatization step at 28°C (D-14 to D1, blue line), the stressed set (yellow to red line) was submitted to a gradual water temperature increase of one degree every 3 days until 32°C was reached (D3, D6, D9, D12, and D15). This last temperature was maintained until corals bleached (D18). In parallel, the control set (green line) was maintained at 28°C all along the experiment. Sampling times are indicated by arrows. Three nubbins were sampled for each time of the kinetic and each treatment.

Aquaria temperatures were controlled by connecting an aquarium heater (600 W, Schego) to an electronic thermostat (Hobby Biotherm Professional). Aquaria were illuminated by metal halide lamps (Osram Day Light 5200 K, 400 W) providing an irradiance of 350 µmol photon.$m^{-2}.s^{-1}$ (quantum meter: QMSW-SS; by Apogee Instruments Inc.) on a 12:12 h (light:dark) photoperiod. All other seawater characteristics (e.g., salinity 36 $g.L^{-1}$, pH 8.3) were maintained constant and equal for each set. A constant water flow was maintained in each tank using a water pump (Tunze Nanostream 6045, delivery 4500 $L.h^{-1}$). Seawater was continuously recycled at rate of 12 tank volumes per hour by coupling the action of a biological filter and an Aquavie protein skimmer (model: PS 1200), and refreshed by natural filtered Mediterranean seawater heated to 28°C at a renewal rate of 2.2 tank volumes per hour.

Bleaching monitoring

Zooxanthellae density was monitored during the whole experiment in order to follow the bleaching process. Coral tissues were extracted using a Water Pick [77] in 0.5 µ of filtered sea water. The slurry was homogenised using a Potter grinder and zooxanthellae were counted using an improved version of the Histolab 5.2.3 image analysis software (Microvision, Evry, France) [78]. Zooxanthellae number was then standardized per skeletal surface area, using the wax protocol described in [79].

The normality of the data set was assessed using the Kolmogorov-Smirnov test. As data was not normally distributed we used non-parametric statistical procedures. The Kruskal-Wallis H-test was used to compare the zooxanthellae density measures within each set. The Mann-Whitney U-test was used to compare the zooxanthellae density measures at each point on the kinetic between the stressed and control sets. All statistical analyses were conducted using GraphPad instat 3 (Kruskal-Wallis) and SPSS 10.0 (Kolmogorov-Smirnov and Man-Whitney). α was set at 0.05 for all analyses.

RNA extraction and mRNA purification

Tissues from three nubbins (sampled for each stress and control conditions) were harvested using a Water Pick in 800 ml of 0.5 µ filtered seawater refrigerated at 4°C. Extracts were pooled and centrifuged at 2000 g for 10 min at 4°C. Supernatant was discarded and pellets were homogenized in 15 ml of Trizol (Invitrogen). Total RNA was extracted following manufacturer instructions. mRNAs were purified using the NucleoTrap mRNA mini kit (Macherey-Nagel).

Subtractive cDNA library construction

Forward and reverse libraries were constructed by subtracting mRNA from stressed nubbins with mRNA from control nubbins. Two independent experiments were performed: D12 stressed *versus* control corals and D15 stressed *versus* control corals. SSH libraries were produced using the PCR-Select cDNA subtraction kit (Clontech). Tester and Driver cDNA were prepared using 2 μg of poly(A)+ RNA. Enzyme digestion, adapter ligation, hybridization, and PCR amplification were performed according to protocols provided by the manufacturer (Clontech). PCR products were cloned into pCR4-TOPO cloning vectors using the TOPO TA cloning kit (Invitrogen) and transformed into One Shot TOP10 chemically competent *Escherichia coli* cells (Invitrogen).

DNA Sequencing, sequence analysis and modelling

For each library, 100 clones were randomly selected and single pass sequenced using a dideoxy-dye-terminator method (CEQ™ DTCS-Quick Start Kit, Beckman coulter) and a CEQ™ 8000 apparatus (Beckman Coulter). Vector and adaptor sequences were trimmed from all sequences using Sequencher™ software (Gene Codes Corporation). High quality ESTs, longer than 150 bp in length, were assembled in clusters or unique sequences from singletons and submitted to database searches using BLASTX and BLASTN programs [80]. Specific domain searches were performed using InterProScan program [81]. EST sequences have been submitted to the dbEST database.

Homology modelling was performed on MODWEB [55] and the protein diagrams constructed on Swiss-PdbViewer 4.0.1 [82]. The three-dimensional (3D) structure comparison between the template and the molecular model was made using Superpose web server [83].

Real Time PCR

Gene encoding proteins involved in photosynthesis, oxidative detoxification, intracellular signalling pathway, metabolism, cytoskeleton structure, conserved protein domains, calcium homeostasis, cell/cell or cell/ligand interactions, protein degradation, chaperone protein and protein synthesis were selected for quantitative analysis of their transcripts. Real-Time RT-PCR was performed on total RNA extracted from the samples used for SSH. Reverse transcription was performed using the superscript III enzyme (Invitrogen). Specific primers for Q-RT-PCR were edited using the Light Cycler Probe Design Software version 1.0 (Roche Diagnostics) [see additional file 1, for primers sequences]. The following Light Cycler run protocol was used: denaturation program (95°C, 10 min), amplification and quantification programs repeated 40 times (95°C for 15 s, 60°C for 5 s, 72°C for 16 s), melting curve program (6095°C with a heating rate of 0.1°C per second and continuous fluorescence measurement), and a cooling step to 40°C. Amplification of single highly specific products was verified (melting curve analysis). For each reaction, the crossing point (CP) was determined using the "Fit Point Method" of the Light Cycler Software 3.3 (Roche Diagnostics). PCR reactions were performed in duplicate and the mean values of the CP were calculated.

For each candidate gene, the level of transcription of the target gene (Tg) was normalized using the transcription rate of the reference gene (Rg). The Rg used in the present study is the 28s ribosomal RNA from *Symbiodinium* spp. (GenBank: AJ830930). The transcription ratio (R) was calculated according to the formula:

$$R = (E_{Tg})^{CPTg} / (E_{Rg})^{CPRg}$$

Complete Open Reading Frame characterisation of the validated candidates

RACE PCR experiments were performed to characterize the complete Open Reading Frame (ORF) of the validated genes. Total RNA extraction and polyA+ purification were conducted on non stressed nubbin tissues (described above). RACE PCR experiments were performed using the SMART™ RACE cDNA Amplification Kit (Clontech). The final PCR amplification for the 5' and 3' ends was conducted using the Advantage 2 PCR Enzyme System (Clontech). PCR products were cloned, sequenced, and the sequences analysed as previously described.

Determination of the organism (host or symbiont) expressing the candidate genes

We developed cross PCR experiments performed on DNA extracted from the holobiont (host plus symbiont) and from pure cultured zooxanthellae to determine the organism (host or symbiont) expressing each candidate gene. Holobiont and zooxanthellae DNAs were extracted using DNAzol reagent (Invitrogen). Specific primers (see additional file 1) were designed for all the validated candidates and the zooxanthellae-specific primers ss5Z (5'-GCAGTTATAATTTATTTGATGGTCACTGCTAC-3') and ss3Z (5'-AGCACTGCGTCAGTCCGAATAATTCACCGG) identified in a previous study [57], were used in the present one. PCR reactions were performed using the Advantage 2 PCR Enzyme System (Clontech). PCR products were loaded on 1% agarose gels.

Peptide and antibodies

BSA-coupled peptides (Genpep, France) were used to immunize New Zealand rabbits as previously described [84]. Peptide sequences used were CAVARKSAPTRKQVWI and CFTMKFSTTPEVTFEM for PdC-Lectin and Pdcyst-rich proteins, respectively. Sera of immunized rabbits were collected and tested for the presence of specific Igs three months after the initial injection using ELISA [85] with uncoupled peptides adsorbed onto Maxisorp plates

(Nunc). IgG fraction was purified by affinity chromatography [86] and antibody specificity was tested by Western blot as previously described in [87].

Immunolocalization procedures

Tissues from unstressed colonies *Pocillopora damicornis* were processed following a procedure previously described in [88]. Tissues embedded in Paraplast were cut into thin section (7 μm), mounted on silane-coated glass slides stored at 4°C in a dry atmosphere.

Immunolocalization on tissue sections was performed according to a protocol previously described in [88]. Briefly, deparaffinized sections were incubated for 1 h at room temperature in saturating medium (1% BSA, 0.2% teleostean gelatine, 0.05% Tween20 in 0.05 mol.L^{-1} Phosphate-buffered saline [PBS] pH 7.4). The samples were then incubated overnight at 4°C in a moist chamber with the purified IgG at 20 μg.ml^{-1} in the preceding buffer. The primary antibodies surplus was discarded by multiple rinsing in the saturating medium and samples incubated for 1 h at room temperature with biotinylated anti-rabbit antibodies (secondary antibodies) diluted 1:250 in the saturating medium. After incubation, slides were rinsed with PBS pH 7.4, and samples finally stained for 15 min with streptavidin AlexaFluor 568 1:50 diluted (Molecular probes) and 4',6-diamino-2-phenylindole, DAPI (Sigma, 2 μg.ml^{-1}). Sections were mounted in Pro-Long antifade medium (Molecular Probes) and observed with a confocal laser-scanning microscope (Leica, TCS4D).

Authors' contributions

JVD and GM conceived and coordinated the study, participated in molecular genetic studies (SSH, Q-RT-PCR) and wrote the manuscript. MA and DA participated in the design and the coordination of the study, drafted the manuscript. ER and DD participated in RACE-PCR experiments and DNA sequencing. LF and JVD helped design and conduct the experimental procedures in the aquaria. YM participated in the molecular modelling of PdC-Lectin. CFP participated in the measurements of zooxanthellae density and drafted the manuscript. ST, ET and DZ performed immunolocalization experiments and drafted the manuscript. All authors read and approved the final manuscript.

Additional material

Additional file 1

Top blastx, annotation, GeneBank accession number and specific primers (Q-RT-PCR) of selected ESTs. *The data provided represents, Top blast, GeneBank accession number and specific primers used for Q-RT-PCR of selected ESTs.*

Click here for file

[http://www.biomedcentral.com/content/supplementary/1472-6793-9-14-S1.doc]

Acknowledgements

This work was supported by the Centre National pour la Recherche Scientifique (CNRS). The authors are indebted to Michel Pichon and Christoph Grunau for their help and many helpful discussions. We thank Alain Pigno from the Cap d'Agde Public Aquarium for his help in the project. We thank Severine Lotto, Jean-François Allienne, Cecile Rottier and Pierre Tisseyre for technical assistance, and Jérôme Bossier for his help in statistical procedure.

References

1. Hughes T, Baird A, Bellwood D, Card M, Connolly S, Folke C, Grosberg R, Guldberg H, Jackson J, Kleypas J, Lough J, Marshall P, Nyström M, Palumbi S, Pandolfi J, Rosen B, Roughgarden J: **Climate change, human impacts, and the resilience of coral reefs.** *Science* 2003, **301:**929-933.
2. Donner SD, Skirving WJ, Little CM, Oppenheimer M, Hoegh-Guldberg OVE: **Global assessment of coral bleaching and required rates of adaptation under climate change.** *Glob Chang Biol* 2005, **11:**2251-2265.
3. Chabanet P, Adjeroud M, Andréfouët A, Bozec Y, Ferraris J, Garcia-Charton J, Schrimm M: **Human-induced physical disturbances and their indicators on coral reef habitats: A multi-scale approach.** *Aquat Living Resour* 2005, **18:**215-230.
4. Hoegh-Guldberg O, Mumby PJ, Hooten AJ, Steneck RS, Greenfield P, Gomez E, Harvell CD, Sale PF, Edwards AJ, Caldeira K, Knowlton N, Eakin CM, Iglesias-Prieto R, Muthiga N, Bradbury RH, Dubi A, Hatziolos ME: **Coral reefs under rapid climate change and ocean acidification.** *Science* 2007, **318:**1737-1742.
5. Lesser MP: **Coral reef bleaching and global climate change: Can corals survive the next century?** *Proc Natl Acad Sci USA* 2007, **104:**5259-5260.
6. Wilkinson C: *Status of Coral Reefs of the world* Townsville: Australian Institute of Marine Science; 2000.
7. Brown BE: **Coral bleaching: causes and consequences.** *Coral Reefs* 1997, **16(supplement):**129-138.
8. Douglas AE: **Coral bleaching-how and why?** *Mar Pollut Bull* 2003, **46:**385-392.
9. Lesser MP: **Experimental biology of coral reef ecosystems.** *J Exp Mar Biol Ecol* 2004, **300:**217-252.
10. Coles SL, Jokiel PL: **Synergistic effects of temperature, salinity and light on the hermatypic Coral *Montipora verrucosa*.** *Mar Biol* 1978, **49:**187-195.
11. Glynn PW, D'croz L: **Experimental evidence for high temperature stress as the cause of El Niño-coincident coral mortality.** *Coral Reefs* 1990, **8:**181-191.
12. Richier S, Cottalorda J-M, Guillaume MMM, Fernandez C, Allemand D, Furla P: **Depth-dependant response to light of the reef building coral, *Pocillopora verrucosa*: Implication of oxidative stress.** *J Exp Mar Biol Ecol* 2008, **357:**48-56.
13. Bouchard JN, Yamasaki H: **Heat Stress Stimulates Nitric Oxide Production in *Symbiodinium microadriaticum*: A Possible Linkage between Nitric Oxide and the Coral Bleaching Phenomenon.** *Plant Cell Physiol* 2008, **49:**641-652.

14. Smith DJ, Suggett DJ, Baker NR: **Is photoinhibition of zooxanthellae photosynthesis the primary cause of thermal bleaching in corals?** *Glob Chang Biol* 2005, **11:**1-11.
15. Warner ME, Fitt WK, Schmidt GW: **The effects of elevated temperature on the photosynthetic efficiency of zooxanthellae *in hospite* from four different species of reef coral: a novel approach.** *Plant Cell Environ* 1996, **19:**291-299.
16. Lesser MP: **Oxidative stress in marine environments: Biochemistry and physiological ecology.** *Annu Rev Physiol* 2006, **68:**253-278.
17. Perez S, Weis V: **Nitric oxide and cnidarian bleaching: an eviction notice mediates breakdown of a symbiosis.** *J Exp Biol* 2006, **209:**2804-2810.
18. Richier S, Sabourault C, Courtiade J, Zucchini N, Allemand D, Furla P: **Oxidative stress and apoptotic events during thermal stress in the symbiotic sea anemone, *Anemonia viridis*.** *FEBS J* 2006, **273:**4186-4198.
19. Dunn SR, Bythell JC, Le Tissier MDA, Burnett WJ, Thomason JC: **Programmed cell death and cell necrosis activity during hyperthermic stress-induced bleaching of the symbiotic sea anemone *Aiptasia* sp.** *J Exp Mar Biol Ecol* 2002, **272:**29-53.
20. Dunn SR, Schnitzler CE, Weis VM: **Apoptosis and autophagy as mechanisms of dinoflagellate symbiont release during cnidarian bleaching: every which way you lose.** *Proc R Soc B Biol Sci* 2007, **274:**3079-3085.
21. Dunn SR, Thomason JC, Le Tissier MDA, Bythell JC: **Heat stress induces different forms of cell death in sea anemones and their endosymbiotic algae depending on temperature and duration.** *Cell Death Differ* 2004, **11:**1213-1222.
22. Gates RD, Baghdasarian G, Muscatine L: **Temperature stress caused host cell detachent in symbiotic cnidarians: implications for coral bleaching.** *Biol Bull* 1992, **182:**324-332.
23. Strychar KB, Coates M, Sammarco PW, Piva TJ: **Bleaching as a pathogenic response in scleractinian corals, evidenced by high concentrations of apoptotic and necrotic zooxanthellae.** *J Exp Mar Biol Ecol* 2004, **304:**99-121.
24. Brown BE, Le Tissier MDA, Bythell JC: **Mechanisms of bleaching deduced from histological studies of reef corals sampled during a natural bleaching event.** *Mar Biol* 1995, **122:**655-663.
25. Downs CA, Kramarsky-Winter E, Martinez J, Kushumaro A, Woodley CM, Loya Y, Ostrander GK: **Symbiophagy as a cellular mechanism for coral bleaching.** *Autophagy* 2009, **5:**211-216.
26. Steen RG, Muscatine L: **Low temperature evokes rapid exocytosis of symbiotic algae by a sea anemone.** *Biol Bull (Boston)* 1987, **172:**246-263.
27. Hoegh-Guldberg O: **Climate change, coral bleaching and the future of the world's coral reefs.** *Mar Freshw Res* 1999, **50:**839-866.
28. de Boer ML, Krupp DA, Weis VM: **Proteomic and transcriptional analyses of coral larvae newly engaged in symbiosis with dinoflagellates.** *Comp Biochem Physiol D Genomics Proteomics* 2007, **2:**63-73.
29. Desalvo MK, Voolstra CR, Sunagawa S, Schwarz JA, Stillman JH, Coffroth MA, Szmant AM, Medina M: **Differential gene expression during thermal stress and bleaching in the Caribbean coral *Montastraea faveolata*.** *Mol Ecol* 2008, **17:**3952-3971.
30. Edge SE, Morgan MB, Gleason DF, Snell TW: **Development of a coral cDNA array to examine gene expression profiles in *Montastraea faveolata* exposed to environmental stress.** *Mar Pollut Bull* 2005, **51:**507-523.
31. Gilbert AL, Guzmán HM: **Bioindication potential of carbonic anhydrase activity in anemones and corals.** *Mar Pollut Bull* 2001, **42:**742-744.
32. Harithsa S, Raghukumar C: **Stress response of two species in the Kavaratti atoll of the Lakshadweep Archipelago, India.** *Coral Reefs* 2005, **23:**463-474.
33. Hashimoto K, Shibuno T, Murayama-Kayano E, Tanaka H, Kayano T: **Isolation and characterization of stress-responsive genes from the scleractinian coral *Pocillopora damicornis*.** *Coral Reefs* 2004, **23:**485-491.
34. Reynolds WS, Schwarz JA, Weis VM: **Symbiosis-enhanced gene expression in cnidarian-algal associations: cloning and characterization of a cDNA, sym32, encoding a possible cell adhesion protein.** *Comp Biochem Physiol A Physiol* 2000, **126:**33-44.
35. Weis VM, Reynolds W: **Carbonic anhydrase expression and synthesis in the sea anemone *Anthopleura elegantissima* are enhanced by the presence of Dinoflagellate symbionts.** *Physiol Biochem Zool* 1999, **72:**307-316.
36. Mitchelmore CL, Schwarz JA, Weis VM: **Development of symbiosis-specific genes as biomarkers for the early detection of cnidarian-algal symbiosis breakdown.** *Mar Environ Res* 2002, **54:**345-349.
37. Schwarz JA, Weis VM: **Localization of a Symbiosis-Related Protein, Sym32, in the Anthopleura elegantissima-Symbiodinium muscatinei Association.** *Biol Bull (Boston)* 2003, **205:**339-350.
38. Veron JEN: *Corals of the World* Townsville: Australian Institute of Marine Science; 2000.
39. Drollet JH, Faucon M, Maritorena S, Martin PMV: **A survey of environmental physico-chemical parameters during a minor-massbleaching event in Tahiti in 1993.** *Aust J Mar Freshw Res* 1994, **45:**1149-1156.
40. Fisk DA, Done TJ: **Taxonomic and bathymetric patterns of bleaching in corals, Myrmidon Reef.** *Proceedings of the 5th International Coral Reef Congress; Tahiti* 1985:149-154.
41. Glynn PW: **Extensive 'bleaching' and death of reef corals on the pacific coast of Panama.** *Environ Conserv* 1983, **10:**149-154.
42. Salvat B: **Natural bleaching and mortality of scleractinian corals on Moorea Reefs (Society Archipelago) in 1991.** *C r Acad sci Sér 3 Sci vie* 1992, **314:**105-111.
43. Kvennefors ECE, Leggat W, Hoegh-Guldberg O, Degnan BM, Barnes AC: **An ancient and variable mannose-binding lectin from the coral *Acropora millepora* binds both pathogens and symbionts.** *Dev Comp Immunol* 2008, **32:**1582-1592.
44. Kieffer B, Driscoll PC, Campbell ID, Willis AC, Merwe PA van der, Davis SJ: **Three-dimensional solution structure of the extracellular region of the complement regulatory protein CD59, a new cell-surface protein domain related to snake venom neurotoxins.** *Biochemistry* 1994, **33:**4471-4482.
45. LeCler KP, Palfree RGE, Flood PM, Hämmerling U, Bothwell A: **Isolation of a murine Ly-6 cDNA reveals a new multigene family.** *EMBO J* 1986, **5:**3227-3234.
46. Palfree RG, Sirlin S, Dumont FJ, Hammerling U: **N-terminal and cDNA characterization of murine lymphocyte antigen Ly-6C.2.** *J Immunol* 1988, **140:**305-310.
47. Palfree RGE: **The urokinase-type plasminogen activator receptor is a member of the Ly-6 superfamily.** *Immunol Today* 1991, **12:**170-171.
48. Roldan AL, Cubellis MV, Masucci MT, Bhrendt N, Lund LR, Dano K, Appella E, Blasi F: **Cloning and expression of the receptor for human urokinase plasminogen activator, a central molecule in cell surface, plasmin dependent proteolysis.** *EMBO J* 1990, **9:**467-474.
49. Fleming TJ, O'HUigin C, Malek TR: **Characterization of two novel Ly-6 genes. Protein sequence and potential structural similarity to alpha-bungarotoxin and other neurotoxins.** *J Immunol* 1993, **150:**5379-5390.
50. Ploug M, Ellis V: **Structure-function relationships in the receptor for urokinase-type plasminogen activator Comparison to other members of the Ly-6 family and snake venom [alpha]-neurotoxins.** *FEBS Lett* 1994, **349:**163-168.
51. **PSORT II Prediction** [http://psort.ims.u-tokyo.ac.jp/form2.html]
52. **NetNGlyc** [http://www.cbs.dtu.dk/services/NetNGlyc/]
53. Zelensky AN, Gready JE: **The C-type lectin-like domain superfamily.** *FEBS J* 2005, **272:**6179-6217.
54. Zelensky AN, Gready JE: **Comparative analysis of structural properties of the C-type-lectin-like domain (CTLD).** *Proteins* 2003, **52:**466-477.
55. **ModWeb A Server for Protein Structure Modelling** [http://modbase.compbio.ucsf.edu/ModWeb20-html/modweb.html]
56. Feinberg H, Mitchell DA, Drickamer K, Weis WI: **Structural basis for selective recognition of oligosaccharides by DC-SIGN and DC-SIGNR.** *Science* 2001, **294:**2163-2166.
57. Rowan R, Powers DA: **Molecular genetic identification of symbiotics dinoflagellates (zooxanthellae).** *Mar Ecol Prog ser* 1991, **71:**65-73.
58. Noel LS, Champion BR, Holley CL, Simmons CJ, Morris DC, Payne JA, Lean JM, Chambers TJ, Zaman G, Lanyon LE, Suva LJ, Miller LR: **RoBo-1, a Novel Member of the Urokinase Plasminogen Activator Receptor/CD59/Ly-6/Snake Toxin Family Selectively Expressed in Rat Bone and Growth Plate Cartilage.** *J Biol Chem* 1998, **273:**3878-3883.

59. Nau F, Guerin-Dubiard C, Desert C, Gautron J, Bouton S, Gribonval J, Lagarrigue S: **Cloning and characterization of HEP21, a new member of the uPAR/Ly6 protein superfamily predominantly expressed in hen egg white.** *Poult Sci* 2003, **82:**242-250.
60. Hudson HJ: **Response of *Montastrea annularis* to environmental change in the Florida Keys.** *Proceeding of the fourth International Coral Reef Congress, Manila* 1981, **2:**229-239.
61. Jokiel PL, Coles SL: **Effects of temperature on the mortality and growth of hawaiian reef corals.** *Mar Biol* 1977, **43:**201-208.
62. Rodolpho-Metalpa R, Richard C, Allemand D, Ferrier-Pagès C: **Growth and photosynthesis of two Mediterranean corals, *Cladocora caespitosa* and *Oculina patagonica*, under normal and elevated temperatures.** *J Exp Biol* 2006, **209:**4546-4556.
63. Bulgheresi S, Schabussova I, Chen T, Mullin NP, Maizels RM, Ott JA: **A new C-Type Lectin similar to the human immunoreceptor DC-SIGN mediates symbiont acquisition by a marine nematode.** *Appl Environ Microbiol* 2006, **72:**2950-2956.
64. Wood-Charlson EM, Hollingsworth LL, Krupp DA, Weis VM: **Lectin/glycan interactions play a role in recognition in a coral/dinoflagellate symbiosis.** *Cell Microbiol* 2006, **8:**1985-1993.
65. Weis VM: **Cellular mechanisms of Cnidarian bleaching: stress causes the collapse of symbiosis.** *J Exp Biol* 2008, **211:**3059-3066.
66. Tambutté E, Allemand D, Bourge I, Gattuso JP, Jaubert J: **An improved 45Ca protocol for investigating physiological mechanisms in coral calcification.** *Mar Biol* 1995, **122:**453-459.
67. LaJeunesse TC: **Investigating the biodiversity, ecology, and phylogeny of endosymbiotic dinoflagellates in the genus *Symbiodinium* using the internal transcribed spacer region: in search of a "species" level marker.** *J Phycol* 2001, **37:**866-880.
68. Banaszak AT, LaJeunesse TC, Trench RK: **The synthesis of mycosporine-like amino acids (MAAs) by cultured, symbiotic dinoflagellates.** *J Exp Mar Biol Ecol* 2000, **249:**219-233.
69. Goiran C, Al-Moghrabi S, Allemand D, Jaubert J: **Inorganic carbon uptake for photosynthesis by the symbiotic coral/dinoflagellate association. Photosynthetic performances of symbionts and dependence on sea water bicarbonate.** *J Exp Mar Biol Ecol* 1996, **199:**207-225.
70. Blanck RJ: **Cell architecture of the dinoflagellate *Symbiodinium sp.* inhabiting the Hawaiian stony coral *Montipora verrucosa*.** *Mar Biol* 1987, **94:**143-155.
71. Brown BE, Suharsono : **Damage and recovery of coral reefs affected by El Niño related seawater warming in the Thousand Isand, Indonesia.** *Coral Reefs* 1990, **8:**163-170.
72. Glynn PW: **Widespread coral mortality and the 1982/83 El Niño warming event.** *Environ Conserv* 1984, **11:**133-146.
73. Glynn PW, Cortes J, Guzmán HM, Richmond RH: **El Nino (198283) associated coral mortality and relationship to sea surface temperature deviations in the tropical eastern Pacific.** *Proceeding of the 6th International Coral Reef Congress, Austrlia* 1988, **3:**237-243.
74. Jaap WC: **An epidemic zooxanthellae expulsion during 1983 in the lower florida keys reefs: hyperthermic etiology.** *Proceeding of the fifth International Coral Reef Congress, Tahiti* 1985, **6:**143-148.
75. Lang JC, Wicklund RI, Dill RF: **Depth- and habitat- related bleaching of reef corals near Lee Stocking Island, Bahamas.** *Proceedings of the 6th International Coral Reef Symposium; Townsville, Australia* 1988:269-274.
76. Lasker HR, Peters EC, Coffroth MA: **Bleaching of reef coelenterates in the San Blas islands, Panama.** *Coral Reefs* 1984, **3:**183-190.
77. Johannes RE, Wiebe WJ: **Method for determination of coral tissue biomass and composition.** *Limnol Oceanogr* 1970, **15:**822-824.
78. Rodolpho-Metalpa R, Richard C, Allemand D, Nike Bianchi C, Morri C, Ferrier-Pagès C: **Response of zooxanthellae in symbiosis with the Mediterranean corals *Cladocora caespitosa* and *Oculina patagonica* to elevated temperatures.** *Mar Biol* 2006, **150:**45-55.
79. Grover R, Maguer J, Allemand D, Ferrier-Pagès C: **Urea uptake by the scleractinian coral *Stylophora pistillata*.** *J Exp Mar Biol Ecol* 2006, **332:**216-225.
80. **Basic Local Alignment Search Tool** [http://blast.ncbi.nlm.nih.gov/Blast.cgi]
81. **InterProScan Sequence Search** [http://www.ebi.ac.uk/Tools/InterProScan/]
82. Eswar N, John B, Mirkovic N, Fiser A, Ilyin VA, Pieper U, Stuart AC, Marti-Renom MA, Madhusudhan MS, Yerkovich B, Sali A: **Tools for comparative protein structure modeling and analysis.** *Nucleic Acids Res* 2003, **31:**3375-3380.
83. Maiti R, Van Domselaar GH, Zhang H, Wishart DS: **SuperPose: a simple server for sophisticated structural superposition.** *Nucleic Acids Res* 2004, **32:**W590-594.
84. Vaitukaitis J, Robbins JB, Nieschlag E, Ross GT: **A method for producing specific antisera with small doses of immunogen.** *J Clin Endocrinol Metab* 1971, **33:**988-991.
85. Hancock CD, Evans GI: **Production and characterization of antibodies against synthetic peptides.** In *Methods in Molecular Biology: Immunochemical Protocols* Edited by: Manson M, Totowa NJ. USA: Humana Press; 1992:33-41.
86. Porath J, Olin B: **Immobilized metal ion affinity adsorption and immobilized metal ion affinity chromatography of biomaterials. Serum protein affinities for gel-immobilized iron and nickel ions.** *Biochemistry* 1983, **22:**1621-1630.
87. Roger E, Gourbal B, Grunau C, Pierce RJ, Galinier R, Mitta G: **Expression analysis of highly polymorphic mucin proteins (Sm PoMuc) from the parasite *Schistosoma mansoni*.** *Mol Biochem Parasitol* 2008, **157:**217-227.
88. Puverel S, Tambutte E, Zoccola D, Domart-Coulon I, Bouchot A, Lotto S, Allemand D, Tambutte S: **Antibodies against the organic matrix in scleractinians: a new tool to study coral biomineralization.** *Coral Reefs* 2005, **24:**149-156.

ANNEXE 6

OPEN ACCESS Freely available online

PLOS ONE

Thermal Stress Triggers Broad *Pocillopora damicornis* Transcriptomic Remodeling, while *Vibrio coralliilyticus* Infection Induces a More Targeted Immuno-Suppression Response

Jeremie Vidal-Dupiol[1,2]*, Nolwenn M. Dheilly[1,2], Rodolfo Rondon[3,2,1], Christoph Grunau[2,1], Céline Cosseau[2,1], Kristina M. Smith[4], Michael Freitag[4], Mehdi Adjeroud[5], Guillaume Mitta[2,1]

1 CNRS, Ecologie et Evolution des Interactions, UMR 5244, Perpignan, France, **2** Univ. Perpignan Via Domitia, Ecologie et Evolution des Interactions, UMR 5244, Perpignan, France, **3** Reponse Immunitaire des Macroorganismes et Environnement, Ecologie des Systèmes Marins côtiers, UMR 5119 CNRS-Ifremer-UM2, Montpellier, France, **4** Department of Biochemistry and Biophysics, Center for Genome Research and Biocomputing, Oregon State University, Corvallis, Oregon, United States of America, **5** Institut de Recherche pour le Développement, Unité 227 CoRéUs2 "Biocomplexité des écosystèmes coralliens de l'Indo-Pacifique", Laboratoire d'excellence CORAIL, Banyuls-sur-Mer, France

Abstract

Global change and its associated temperature increase has directly or indirectly changed the distributions of hosts and pathogens, and has affected host immunity, pathogen virulence and growth rates. This has resulted in increased disease in natural plant and animal populations worldwide, including scleractinian corals. While the effects of temperature increase on immunity and pathogen virulence have been clearly identified, their interaction, synergy and relative weight during pathogenesis remain poorly documented. We investigated these phenomena in the interaction between the coral *Pocillopora damicornis* and the bacterium *Vibrio coralliilyticus*, for which the infection process is temperature-dependent. We developed an experimental model that enabled unraveling the effects of thermal stress, and virulence *vs.* non-virulence of the bacterium. The physiological impacts of various treatments were quantified at the transcriptome level using a combination of RNA sequencing and targeted approaches. The results showed that thermal stress triggered a general weakening of the coral, making it more prone to infection, non-virulent bacterium induced an 'efficient' immune response, whereas virulent bacterium caused immuno-suppression in its host.

Citation: Vidal-Dupiol J, Dheilly NM, Rondon R, Grunau C, Cosseau C, et al. (2014) Thermal Stress Triggers Broad *Pocillopora damicornis* Transcriptomic Remodeling, while *Vibrio coralliilyticus* Infection Induces a More Targeted Immuno-Suppression Response. PLoS ONE 9(9): e107672. doi:10.1371/journal.pone.0107672

Editor: Pikul Jiravanichpaisal, Fish Vet Group, Thailand

Received May 16, 2014; **Accepted** August 13, 2014; **Published** September 26, 2014

Data Availability: The authors confirm that all data underlying the findings are fully available without restriction. The reference transcriptome used is accessible at http://2ei.univ-perp.fr/telechargement/transcriptomes/blast2go_fasta_Pdamv2.zip. The raw data (untreated reads) for all treatments are publicly available at http://www.ncbi.nlm.nih.gov/sra with the accession number SRP029998.

Funding: This study was supported by the Agence Nationale de la Recherche through the Program BIOADAPT (ADACNI ANR-12-ADAP-0016-03) and the French-Israeli High Council for Science and Technology (P2R n °29702YG). Work in the Freitag laboratory was supported by start-up funds from the OSU Computational and Genome Biology Initiative and Oregon State University. The funders had no role in the study design, data collection and analysis, decision to publish, or preparation of the manuscript.

Competing Interests: The co-author MF is a PLOS ONE editorial board member and this does not alter the authors' adherence to PLOS ONE editorial policies and criteria. In addition, the authors have declared that no competing interests exist.

* Email: jeremie.vidal-dupiol@univ-perp.fr

Introduction

Greenhouse gas emissions have increased since the industrial revolution, and the exceptionally high concentrations now reached have caused global climate change [1]. One of the major consequences of global climate change is that the overall seawater temperature has increased by a mean value of 0.6°C over the last 100 years [2]. The direct consequences of these changes are mass mortality of species having limited ability to adapt to temperature increase [2,3], but indirect consequences can include mortalities triggered by temperature-dependent epizootics [4].

Marine disease risk is clearly enhanced under global warming conditions [5,6], but the causes of the increase in the frequency and severity of epizootics are unclear and probably multi-factorial. It is known that global warming can change host and pathogen repartition to enhance the probability of host/pathogen encounters, or to facilitate new interactions. If some of these new host/pathogen interactions are compatible (susceptible host and/or virulent pathogen), a rapid spread of disease can occur [4–7], leading to massive terrestrial and marine vertebrate or invertebrate host die-offs [8–13]. In addition, an increase in temperature can diminish host immune abilities, leading to increased susceptibility to disease [14,15] or increased pathogen virulence [16–18]. Taken together, these data show that the emergence of epizootics under climate change conditions is probably a result of multiple factors, the relative contribution and synergy of which must be studied to better understand and predict the epizootic risk in the current context of climate change [5,19].

Among marine host/pathogen models, the interaction between the coral *Pocillopora damicornis* and the bacterium *Vibrio coralliilyticus* is useful for studying and unraveling the effects of temperature and bacterial virulence in pathogenesis. *P. damicornis* is widely distributed in the Indo-Pacific region [20,21] and is highly susceptible to a wide range of disturbances [22–25], including disease [26–29]. *V. coralliilyticus* is a common pathogen [30] whose virulence is temperature-dependent [26]. The genomes of two *V. coralliilyticus* strains were recently sequenced, and a proteomic study performed under a range of temperature conditions has revealed the thermo-dependent expression of several putative virulence factors [31,32], but their effects on coral physiology remain to be characterized. Recent data obtained using this infection model showed that the bacterium modulates the expression of several immune genes in *P. damicornis* [33], and that in its virulent state the *Vibrio* strongly decreases the expression of a gene encoding the antimicrobial peptide damicornin [34]. In this interaction the symptoms differ depending on the populations or strains involved. When *V. coralliilyticus* YB1 (isolated from Zanzibar) contacts its sympatric host, it triggers coral bleaching (i.e., substantial or partial loss of endosymbiotic dinoflagellate microalgae - commonly referred to as zooxanthellae - from coral tissues, and/or the loss or reduction of photosynthetic pigment concentrations within zooxanthellae) when the temperature reaches 29.5°C [22]. YB1 caused no pathogenicity in an allopatric coral from the Gulf of Eilat (Red Sea) at temperatures less than 24°C, triggered bleaching between 24 and 25°C, and caused tissue lysis at temperatures exceeding 25°C [35]. In another allopatric interaction involving a *P. damicornis* isolate from Lombok (Indonesia), no signs of infection were evident at temperatures up to 25°C, but at 28°C the bacteria penetrated the host tissues inducing rapid tissue lysis but no bleaching [33]. These results suggest that this bacterium has a high epizootic potential because of its ability to infect allopatric host populations and the various factors modulating its pathogenesis [32].

In this context, we used the infection model described above to investigate the relationship between temperature and bacteria (non-virulent and virulent), and their effects on coral physiology and pathogenesis. To this end, coral nubbins were exposed to stable or increasing temperature with or without bacterial addition, and the physiological changes caused at key stages of the interaction by the various treatments were assessed at the genome-wide scale using RNA sequencing (RNA-seq) approaches. We also used the quantitative reverse transcriptase polymerase chain reaction (q-RT-PCR) to study the response of 44 candidate immune genes during the stress response.

Methods

Biological material

The *P. damicornis* (Linnaeus, 1758) isolate used in this study was obtained from Lombok, Indonesia (Indonesian CITES Management Authority, CITES number 06832/VI/SATS/LN/2001-E; France Direction de l'Environnement, CITES number 06832/VI/SATS/LN/2001-I) and has been maintained in aquaria since the year 2001. Analysis of the first 600 bp of the mitochondrial ORF marker [36] showed that morphologically and genetically this *P. damicornis* isolate corresponds to the recently re-characterized *P. damicornis* clade [20,37,38]. For use in the experiments, coral explants (7 cm high, 6 cm diameter) were detached from the parent colony, and left to recover for a period of 1 month prior to use.

The coral pathogen *Vibrio coralliilyticus* strain YB1 [39]; CIP 107925, Institut Pasteur, Paris, France) was used to challenge or infect *P. damicornis* [22]. *V. coralliilyticus* was cultured as previously described [33].

Stress protocol

As the objective of the study was to detect stress effects and to avoid the potential influence of inter-individual variability and genetic background on these effects, the experiments were performed using clones of the same *P. damicornis* isolate and a unique bacterial strain (YB1). Coral nubbins were randomly placed in 120 L tanks (n = 27 per tank) and acclimatized at 25°C for a period of two weeks prior to initiating the treatments. To distinguish the effects of bacterial stress (exposure to *V. coralliilyticus* under non-virulence conditions), thermal stress and bacterial infection (*V. coralliilyticus* virulence activated by temperature increase) on the coral host, three independent treatments and a control were established as previously described [33]. For the non-virulent treatment, *V. coralliilyticus* was regularly added to coral nubbins held at 25°C, which is a sub-virulent temperature in this host/pathogen interaction. For the virulent treatment, *V. coralliilyticus* was regularly added to coral nubbins while the temperature was gradually increased from 25°C to 32.5°C, triggering activation of bacterial virulence and infection. For the control, the coral nubbins were held at 25°C without added bacteria. For the thermal stress treatment, the coral nubbins were subjected to a gradual increase in temperature without the addition of bacteria, triggering thermal stress that induces bleaching. For all treatments and the control, three nubbins were randomly sampled every three days and immediately frozen and stored in liquid nitrogen. Coral health and the stability/breakdown of the coral symbiosis were monitored over time in each experimental group by assessing the density of zooxanthellae and visual monitoring, as previously described [33].

cDNA library construction and high-throughput sequencing

Four cDNA libraries, corresponding to the control and treatment groups, were sequenced using Illumina GAIIx technology. One lane per library was used to generate an RNA-seq dataset of four 80-nucleotide paired-end short sequence reads. The samples for this analysis were collected at day 12, which was the last sampling occasion prior to the appearance of symptoms of bleaching or bacterial infection in the thermal stress and virulent treatments, respectively.

The total RNA from the 3 coral nubbins of each of the control and treatment groups was extracted using TRIzol reagent (Invitrogen), as previously described [40]. The cDNA libraries were then constructed following an established protocol [41]. Briefly, to obtain high quality mRNA, two cycles of oligo (dT) purification were performed using the Ambion Poly(A) Purification kit (Ambion). For the second round of purification, the mRNA purified in the first round was used in excess (4 μg mRNA per library). Subsequently, first strand cDNA synthesis was performed by combining 1 μg of the purified mRNA, 300 μg of random hexamer primers and the superscript III reverse transcription kit (Invitrogen) reagent. The excess of random primers enabled generation of first strand cDNA with an average length of 400 bp, and maximized coverage at the 5′ and 3′ ends of the mRNA. The second strand synthesis was performed using a combination of RNase H enzyme and DNA polymerase I (New England Biolabs). The resulting cDNA was purified using the QIAquick PCR purification kit (Qiagen). The amount and quality of nucleic acid obtained using this protocol was determined using a bioanalyzer and a nanodrop apparatus. The purified cDNA (1 μg) was used to generate each of the paired-end Illumina sequencing libraries. The

libraries were prepared using Illumina adapter and PCR primers, according to previously published protocols [42,43]. Libraries with an average insert size of 400–500 bp were isolated, and the concentration was adjusted to 10 nM. The samples (7 pM per sample) were loaded into separate channels of an Illumina GAIIx sequencer. The sequencing was performed at the Oregon State University Center for Genome Research and Biocomputing. The raw data (untreated reads) for all treatments are publicly available (http://www.ncbi.nlm.nih.gov/sra study accession number SRP029998).

Differential gene expression analysis

To assess changes in gene expression induced by the various treatments, reads from each library were mapped against a previously assembled reference transcriptome [44]. This transcriptome was assembled *de novo* from 80-nucleotide paired-end short sequence reads based on 6 lanes of Illumina sequencing, and contained 72,890 contigs. Among these contigs, 27.7% and 69.8% were predicted to belong to the symbiont and the host transcriptomes, respectively. Each sequencing lane contained cDNA prepared from coral nubbins of the same genotype. The sequencing lanes were loaded with cDNA from corals exposed to: 1) thermal stress (lane 1); 2) *V. coralliilyticus* in a non-virulent state (lane 2); 3) *V. coralliilyticus* in a virulent state (lane 3); 4) a constant temperature of 25°C (lane 4); 5) a pH of 7.4 for 3 weeks (lane 5); and 6) a pH of 8.1 for 3 weeks. This reference transcriptome is accessible at http://2ei.univ-perp.fr/telechargement/transcriptomes/blast2go_fasta_Pdamv2.zip.

The mapping was conducted using Burrows-Wheeler Aligner (BWA), using the default options: aln -n = 0.04; aln -o = 1; aln -e = -1; aln -d = 16; aln -i = 5; aln -l = -1; aln -k = 2; aln -M = 3; aln -O = 11; aln -E = 4 [45]. As RNA-seq data are a function of both the molar concentration and the transcript length, the results of the mapping step were corrected and expressed as reads per kilobase per million mapped reads (RPKM; [46]). To identify significantly different gene expressions among the control and treatment groups, the MARS method (MA plot-based methods using a random sampling model) of the R package in DEGseq was used [47].

q-RT-PCR

Quantitative real-time PCR (q-RT-PCR) was used to validate the expression profiles obtained from the MARS DEGseq analysis of the RNA-seq data. It was also used to measure expression levels of selected candidate genes during the non-virulent, thermal stress and virulent treatments. Total RNA was extracted and treated with DNase, and the poly(A) RNA was purified as described above. Approximately 50 ng of purified poly(A) RNA was reverse transcribed with hexamer random primers using ReverTAid H Minus Reverse Transcriptase (Fermentas). The q-RT-PCR experiments were performed using cDNA obtained from three coral nubbins per control and treatment group, as described previously [33]. For each candidate gene the level of transcription was normalized using the mean geometric transcription rate of three reference sequences encoding ribosomal protein genes from *P. damicornis* (60S ribosomal protein L22, GenBank accession number HO112261; 60S ribosomal protein L40A, accession number HO112283; and 60S acidic ribosomal phosphoprotein P0, accession number HO112666). The stable expression status of these three genes during biotic and abiotic stress has been demonstrated previously [33].

Statistical analysis

Differences in gene expression data obtained using the RNA-seq analyses were analyzed for statistical significance using the MARS method, as described above [47]. Differences in transcript levels among experimental groups were considered statistically significant at $p<0.0001$. The statistical analyses used to identify biological processes (Gene Ontology term) that were significantly up- or down-regulated [48] were performed using Blast2GO software (version 2.6.4). Increases in processes were considered statistically significant at $p<0.05$. The hierarchical clustering of q-RT-PCR data was performed using Multiple Array Viewer software (version 4.8.1), with average linkage clustering using the Pearson correlation as a default distance metric. The normality of the RPKM distribution was assessed using the Kolmogorov-Smirnov test. As the data were not normally distributed, we used non-parametric statistical procedures. The Mann-Whitney U-test was used to compare the expression level between the core set of up-regulated genes and the core set of down-regulated genes. These statistical analyses were conducted using SPSS 10.0 (Kolmogorov-Smirnov and Mann-Whitney), and were considered statistically significant at $p<0.05$.

Results

Gene expression analysis and validation

The global transcriptomic approach was conducted using RNA-seq methodology that was applied to samples collected 12 days following initiation of the various treatments. To distinguish the bacterial virulence effect from the thermal stress effect in the virulent treatment, in which corals were submitted to a combination of added bacteria and increased temperature, we used the same methods to compare the transcript content in the thermal stress and the virulent treatments. This comparison was called the virulence effect. For each treatments and comparison the results of the: i) Illumina sequencing, ii) quality control and filtering, iii) mapping to the reference transcriptome, and the iv) statistical approach (DEGseq) are summarized in the Table 1. To validate results from the RNA-seq analysis we used an alternative method (q-RT-PCR) for transcript quantification. For this analysis, 22 host transcripts were selected along the gradient of expression from highly up-regulated to highly down-regulated genes, based on RNA-seq data. A significant correlation between the log2-fold change in expression of the RNA-seq and the qRT-PCR data was obtained (log2-fold change qRT-PCR *vs.* log2-fold change RNA-seq: control *vs.* non-virulent, $r^2 = 0.87$ and $p<0.0001$; control *vs.* thermal stress, $r^2 = 0.89$ and $p<0.0001$; control *vs.* virulent, $r^2 = 0.875$ and $p<0.0001$; thermal stress *vs.* virulent, $r^2 = 0.64$ and $p<0.0001$; Fig. 1) and validated the results obtained through the RNA-seq analytical pipeline.

Specific biological processes modulated in the various experimental conditions

A Gene Ontology (GO) term enrichment analysis [48] was performed on the sets of transcripts showing a significant change in expression. The results showed that in response to the non-virulent treatment, 12 biological processes were significantly enriched in the set of up-regulated genes ($p<0.05$; Table 2), and 11 in the set of down-regulated genes ($p<0.05$; Table 3). In response to the thermal stress treatment 20 biological processes were significantly more represented in the set of up-regulated transcripts relative to the control ($p<0.05$; Table 2) and 20 from the set of down-regulated genes ($p<0.05$; Table 3). In response to the virulent treatment six biological processes were significantly enriched ($p<$

Table 1. Sequencing, filtering and gene expression analysis.

	Control	Non-virulent	Thermal stress	Virulent	Virulence (thermal stress vs virulent treatment)
Total reads (millions)	27.7	20.4	17.0	19.3	
Reads passing quality filter (millions)	7.0	6.8	8.7	9.4	
Predicted host transcriptome mapped reads		88.4%	85.2%	87.3%	81.6%
Predicted symbiont transcriptome mapped reads		79.9%	78.0%	79.5%	75.8%
Significantly up-regulated genes		5,810	8,179	2.696	4.702
Significantly down-regulated genes		3.543	13.342	14.166	11,299
Predicted host genes significantly up-regulated		4713	3126	1578	4089
Predicted symbiont genes significantly up-regulated		1097	5053	1118	613
Predicted host genes significantly down-regulated		2401	11735	11382	5272
Predicted symbiont genes significantly down-regulated		1142	1607	2784	6027

doi:10.1371/journal.pone.0107672.t001

0.05) from the set of up-regulated genes ($p<0.05$; Table 2) and 20 from the set of down-regulated genes ($p<0.05$; Table 3).

We then investigated whether there were conserved up- or down-regulated genes in response to all treatments. This analysis showed that 229 genes were significantly up-regulated in response to the non-virulent, thermal stress and virulent treatments, while 1372 were significantly down-regulated in all experimental groups. All the genes showing conserved regulation among groups are referred to as core response genes. Four biological processes were significantly enriched in the set of core up-regulated genes ($p<$ 0.05; Table 4), and 15 from the core down-regulated genes ($p<$ 0.05; Table 4). To distinguish the bacterial virulence effect in the virulent treatment, in which corals were submitted to a combination of added bacteria and increased temperature, the same enrichment analysis was performed comparing transcriptomic data obtained from the thermal stress and the virulent treatments. This enabled identification of six enriched biological processes from the set of genes up-regulated in the virulence treatment ($p<$ 0.05; Table 4) and nine in the set of genes down-regulated ($p<$ 0.05; Table 4).

The annotation and expression levels of the genes belonging to each enriched GO category are shown in Table S1 & S2.

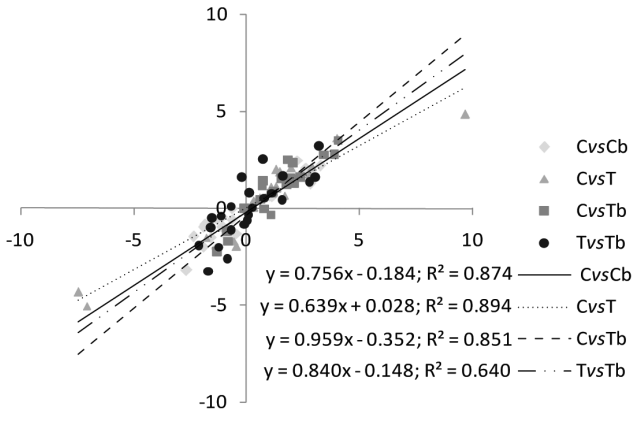

Figure 1. Validation of the RNA-seq approach using q-RT-PCR. Twenty-two genes were arbitrary selected, from highly up-regulated to highly down-regulated contigs. Their levels of expression were quantified by q-RT-PCR, and the results were compared with those obtained using the RNA-seq approach. The log2 changes in expression based on q-RT-PCR and RNA-seq analyses were closely correlated for all treatments, indicating the accuracy of the RNA-seq approach for quantification.
doi:10.1371/journal.pone.0107672.g001

Selection of immune candidate genes and expression analysis

As the enrichment analysis revealed a clear effect of the various treatments on the immune function, we investigated and compared the expression of putative *P. damicornis* immune genes, amongst the various treatments. These genes, annotated manually or using Blast2GO, corresponded to the immune toolbox of *P. damicornis*. They included genes encoding proteins involved in recognition (e.g. TLR and lectins), signaling pathways (e.g. NF-kB, AP1/ATF, c-Jun), complement system (e.g. C3, C-type lectin, and membrane attack complex), prophenoloxidase cascade (e.g. prophenoloxidase activating enzyme, laccase), leukotriene cascade (e.g. 5-lypoxigenase, leukotriene A4 hydrolase), antimicrobial molecules (e.g. LPBPI and antimicrobial peptides) and ROS scavengers (e.g. peroxidases, catalases, GFP-like molecules). The results supporting the annotation of these genes are presented in the Table S3.

To assess the impact of each treatment on the regulation of these genes, their expression was assessed every 3 days during the experimental period, using q-RT-PCR. To confirm that the observed regulation of gene expression was not because of physiological collapse of the coral or an experimental artifact, four housekeeping genes were also monitored during the experimental period. These genes were selected from amongst host genes that were not regulated in any treatment. As expected, the results showed that their expression remained stable in all treatments (Fig. 2; Table S4).

A hierarchical clustering approach was used to create sample and gene trees for the 24 samples (six for each treatment) and the 48 genes (44 immune genes and four housekeeping genes; Fig. 2). Three distinct clusters were identified. The first cluster mainly represented the response to thermal stress (cluster C1; Fig. 2), and contained two subgroups of genes that were highly modulated. The first subgroup comprised genes displaying a high level of down-regulation, including those encoding the antimicrobial peptide damicornin (average 40.0-fold decrease; Fig. 2), the mannose binding lectin PdC-Lectin (average 6.9-fold decrease; Figs 2 and 3), and two members of the membrane attack complex (Tx60A1 and A2; average 91.2-fold decrease; Fig. 2). The second

Table 2. Biological functions significantly ($p<0.05$) enriched in the sets of up-regulated genes.

Treatments	Non-virulent		Thermal stress		Virulent		Virulence	
GO Term	**Up-regulated**	**Not-regulated**	**Up-regulated**	**Not-regulated**	**Up-regulated**	**Not-regulated**	**Up-regulated**	**Not-regulated**
alcohol metabolic process			20	91				
aromatic compound biosynthetic process			6	9				
ATP synthesis coupled proton transport	10	43						
bioluminescence	6	10						
biosynthetic process							64	899
cellular amino acid biosynthetic process			18	60				
cellular aromatic compound metabolic process	10	46						
cellular component biogenesis			27	109				
Cellular metabolic process							190	2523
Cellular protein modification process	81	899						
cofactor metabolic process			24	58				
fatty acid metabolic process			7	15				
gene expression							57	481
generation of precursor metabolites and energy			88	95	68	113	45	187
heterocycle metabolic process			59	261				
innate immune response	10	45						
ion homeostasis	7	23						
ion transport			52	249				
macromolecular complex subunit organization			25	86				
metabolic process			726	3466	253	4022		
microtubule-based process			25	117				
nitrogen compound metabolic process			127	833				
nucleoside phosphate metabolic process			48	231				
nucleotide biosynthetic process	19	119						
organic acid metabolic process			43	202				
phosphorus metabolic process	68	871						
phosphorylation	57	411						
photosynthesis			67	47	65	54	39	74
protein stabilization			3	0				
proton transport	14	80						
regulation of gene expression			5	12				
response to chemical stimulus					7	39		
response to oxidative stress			10	24	7	29		
RNA processing	14	69						

Table 2. Cont.

Treatments	Non-virulent		Thermal stress		Virulent		Virulence	
GO Term	Up-regulated	Not-regulated	Up-regulated	Not-regulated	Up-regulated	Not-regulated	Up-regulated	Not-regulated
small molecule metabolic process			119	499				
translation							45	352
transmembrane transport	36	271			19	284		

doi:10.1371/journal.pone.0107672.t002

subgroup comprised genes displaying a high level of up-regulation, including those encoding a putative MASP1, putative C3 and Bf components of the complement pathway (average 26.4-fold increase; Figs 2 and 3), and two immune-related transcription factors ATF and AP1 (average 19.3-fold increase; Figs 2 and 3). The second cluster (cluster C2; Figs 2 and 3) corresponded to genes involved in the response to bacteria (non-virulent and virulent treatments). It included genes subject to down-regulation (e.g. a gene encoding a putative apextrin protein; average decrease 3.2-fold; Figs 2 and 3), and some showing up-regulation (e.g. genes encoding prophenoloxidase activating enzyme and laccase, which are two key elements of the prophenoloxidase pathway; average 8.1-fold increase; Figs 2 and 3). The third cluster (cluster C3; Fig. 2) corresponded to genes involved in the response to the virulence of the bacteria. This cluster was mainly characterized by general down-regulation of the innate immune recognition and signaling pathways; the genes encoding the LRR and TIR domains containing proteins, TAK1, IKK, NF-kB, MKK3/6, P38, IkBa, AP1/ATF and MKK4/7 were all down-regulated by an average factor of 4.1 (Figs 2 and 3).

In relation to specific biological functions, the q-RT-PCR experiments provided noteworthy results for several immune genes and the main ones are highlighted below. For antimicrobial effectors, we found that expression of the damicornin, mytimacin-like and LBP–BPI genes was decreased in the thermal stress and virulent treatments (Figs 2 and 3). The two genes of the prophenoloxidase pathway (prophenoloxidase activating enzyme and laccase) were co-up-regulated in the presence of bacteria (non-virulent and virulent treatments) whereas in response to bacterial virulence, there were strongly down-regulated at day 18. The complement pathway (PdC-lectin, MASP1 and 2, C3 and Bf) was mainly up-regulated by the presence of non-virulent bacteria and during the virulent treatment. Members of the membrane attack complex Tx60 A1 and A2, and apextrin (a downstream component of the complement pathway; Fig. 3) were strongly down-regulated under temperature stress conditions (thermal stress and virulent treatment). The expression of some key components of the backbone of the recognition and signaling pathways (LRR, TIR, Myd88 and TRAF6) was disturbed during the virulent, virulence and thermal stress treatments. The downstream pathways of this backbone (NF-kB, ATF/AP1 and JNK) showed a similar trend of regulation in response to the non-virulent bacteria, thermal stress and virulent bacteria. In response to bacterial virulence the NF-kB and ATF/AP1 pathways were completely down-regulated (Figs 2 and 3). The leukotriene cascade responded mainly to temperature stress by general up-regulation of its component. Among the genes encoding ROS scavengers, two groups could be clearly distinguished. The first group comprised 'classical' ROS scavengers (peroxidase, catalase, superoxide dismutase and nucleoredoxin), which showed strong up-regulation in response to thermal stress, non-virulent bacteria and virulent bacteria. The second group (encoding GFP-like protein); was initially up-regulated by thermal stress but then down-regulated at higher temperature (Figs 2 and 3). In response to the non-virulent bacterium these two genes were up-regulated, but were down-regulated immediately following initiation of virulence in the bacterium (virulent treatment, days 6–18; Figs 2 and 3).

Discussion

By combining the analysis of natural coral/*Vibrio* interaction, experimental exposures of corals to the bacteria, global transcriptomic studies (RNA-seq) confirmed by q-RT-PCR, we showed

Table 3. Biological functions significantly ($p<0.05$) enriched in the sets of down-regulated genes.

Treatments	Non-virulent		Thermal stress		Virulent		Virulence	
GO Term	**Down-regulated**	**Not-regulated**	**Down-regulated**	**Not-regulated**	**Down-regulated**	**Not-regulated**	**Down-regulated**	**Not-regulated**
apoptotic process			15	33				
biological regulation			162	646				
biosynthetic process	66	881			232	702		
cell surface receptor signaling pathway					38	114		
cellular biosynthetic process			186	662				
cellular component assembly at cellular level					27	74	33	79
cellular component organization or biogenesis			52	186	61	185		
cellular macromolecule biosynthetic process					165	394		
cellular macromolecule metabolic process							337	1456
cellular respiration			16	42				
cellular response to stress	7	68						
chromosome organization			18	29	21	26		
cofactor biosynthetic process			13	33				
cofactor metabolic process							25	59
gene expression	59	476	154	370	174	357		
generation of precursor metabolites and energy	56	128						
glutamine metabolic process					5	6		
hydrogen transport							31	63
immune response			19	49	20	47		
macromolecule metabolic process			407	1758				
metabolic process	220	4120						
microtubule-based process							40	115
neurotransmitter transport			11	9	10	13		
nitrogen compound metabolic process							60	178
nucleic acid metabolic process			77	306				
nucleobase-containing compound catabolic process					32	91		
organic acid transport					8	12		
peptidyl-amino acid modification			8	15				
phospholipid metabolic process			9	20				
phosphorylation			95	400				
photosynthesis	37	38						
primary metabolic process			524	2501	659	2422		
protein folding					47	108	46	113
protein metabolic process	93	1790	337	1477	422	1421		

Table 3. Cont.

Treatments	Non-virulent		Thermal stress		Virulent		Virulence	
GO Term	**Down-regulated**	**Not-regulated**	**Down-regulated**	**Not-regulated**	**Down-regulated**	**Not-regulated**	**Down-regulated**	**Not-regulated**
protein polymerization							30	36
protein targeting	7	8			7	8		
regulation of cell death					12	22		
regulation of metabolic process							25	65
regulation of phosphate metabolic process					12	21		
regulation of protein phosphorylation					11	21		
response to DNA damage stimulus	7	68						
response to stimulus			153	640				
S-adenosylmethionine metabolic process	2	9						
signaling			113	442				
translation	55	339	119	270	137	257		

doi:10.1371/journal.pone.0107672.t003

that thermal stress induces a general decrease in coral gene expression; this included decreased expression of immune genes, hence reducing the immune capacities of the coral. We also found that virulent bacteria triggered a marked suppression of host immunity. The RNA-seq approach unveiled a large range of transcripts expressed either by the coral host or by its dinoflagellate symbionts (entire holobiont response). A clear illustration of the response of the symbiont was the down-regulation of photosynthesis genes and for the host, the up-regulation of immune genes in response to the non-virulent treatment). In general it was possible to assign transcripts to either the host or the symbiont partner (as explained in the methods section), although for some genes the discrimination was not always obvious. Assembled genomes for the two partners in the symbiosis are lacking, and dinoflagellate genomes are known to contain numerous copies of orthologous genes, which can be divergent. The latter factor increases the complexity of the transcriptome [49–52] and can make assignment difficult. In addition, our transcriptome probably contained xenocontaminant sequences from bacteria, eukaryotic species and RNA viruses [53], which are part of the coral holobiont [54].

The sophisticated ancestral immune toolkit responds to experimental bacterial exposure

The immunity of scleractinian corals is an expanding field in basic research because of the basal position of cnidarians in the eumetazoan tree of life, and its relevance to understanding the evolution of defense systems against pathogens. It is also crucial to understand the immune capabilities of corals, because of the increase of coral epizootics. In this context, most past studies have focused on the identification of immune pathways and effectors, mainly through searches for orthologous genes in the expanding genome and transcriptome databases. These studies have revealed that the common ancestor of animal species contained several immune genes and pathways that are also present in higher invertebrate and vertebrate species (Table 5). This discovery led to the hypothesis that early eumetazoan species had an ancestral immune toolkit [61,81], which evolved to the more sophisticated systems found in higher lineage. This hypothesis remains to be proven because the functions of the putative immune genes and their involvement in immunity remain to be investigated [82]. Demonstration for this hypothesis was not trivial in our non-model organisms. Indeed, several immune genes are involved in a number of cellular processes (e.g. NF-kB transcription factor), but demonstrating their involvement in immunity will require knock-out or knock-down approaches that will have to be developed for non-model organisms, including corals. In this context, a targeted and organized response to a pathogen could be considered initial evidence that these genes and pathways are directly involved in the immune response. Some of the genes and proteins have been shown to respond to experimental infection or to pathogen elicitors (Table 5), but studies at the entire transcriptome level have not occurred. The present study partly addressed this shortcoming by showing that most of the known immune factors in the coral were modulated following a natural bacterial challenge. Indeed, we observed co-regulation of genes belonging to the same pathways, including genes for: (i) MASP1, C3 and Bf in the complement pathway; ii) the prophenoloxidase activating enzyme and laccase in the melanization pathway; and (iii) proteins involved in signaling pathways, including the transcription factors NF-kB and JNK (Fig. 3). In summary, the results of this study, and recent studies of *A. millepora* [83] and *Gorgonia ventalina* [84] indicate that corals are able to mount an immune response using an ancestral immune toolkit.

Table 4. Biological functions significantly ($p<0.05$) enriched in the sets of up-regulated and down-regulated core genes.

Regulation	Up-regulated		Down-regulated	
GO Term	**Up-regulated**	**Not-regulated**	**Down-regulated**	**Not-regulated**
transmembrane transport	7	299		
cellular biosynthetic process	7	865		
localization	7	873		
ATP biosynthetic process	5	78		
cellular process			66	4094
primary metabolic process			58	3079
protein metabolic process			38	1848
biosynthetic process			36	915
gene expression			32	503
macromolecule biosynthetic process			31	542
translation			30	364
nucleic acid metabolic process			11	417
protein localization			6	223
cellular respiration			4	54
developmental process			3	47
protein targeting			3	15
sulfur compound biosynthetic process			2	24
cellular modified amino acid metabolic process			2	29
nucleoside biosynthetic process			5	102

doi:10.1371/journal.pone.0107672.t004

The effect of non-virulent bacteria

In the presence of the non-virulent bacteria, we found that innate immune pathways (Table 2 and Fig. 2) were activated in the coral, which is consistent with previous data showing that non-virulent *V. coralliilyticus* triggers an immune response [33,34]. The absence of bacteria in host tissues during the non-virulent treatment [33] suggests that the coral either: (i) detected the presence of bacteria, and the coral cells developed an immune response directed against non-internalized bacteria; or (ii) was able to develop an efficient immune response that killed all bacteria on entry.

The mechanisms underlying the recognition of *V. coralliilyticus* by *P. damicornis* remain to be identified. However, in *Hydra* spp. (also a cnidarian) the unconventional pathogen sensors HyLRR, which are expressed at the surface of epithelial cells, interact with an intracellular HyTRR (a TIR domain-containing protein) during immune challenge [55], and this leads to the expression of an AMP (periculin-1). These LRR and TRR molecules were identified in the *P. damicornis* transcriptome, suggesting that *P. damicornis* can detect *V. coralliilyticus* using similar mechanisms. The ability to mount an immune response has been reported in numerous cnidarian species exposed to lipopolysaccharide (LPS) including *Montastraea faveolata*, *Stephanocoenia intersepta, Porites astreoides* and *Acropora millepora* [70,77]. However, our coral/pathogen model is the first to have enabled an association to be made between the absence of infection and an organized up-regulation of multiple and interlinked pathways that reflect the three key steps in the immune response: i) pathogen recognition; ii) signal transduction; and iii) effector responses (Figs 2 and 3).

The thermal stress effect

Consistent with several previous studies (for review, see; [85], we found that the response to thermal stress is characterized by up-regulation of several heat shock proteins (HSPs) and genes encoding ROS scavengers. However, we showed that this was accompanied by significant down-regulation of genes involved in innate immunity and apoptosis (Table 3). These observations support the hypothesis that high temperature favors infection because it impacts coral immune function [86–90]. However, this phenomenon may not occur with all immune genes. Indeed, our candidate gene approach showed that several immune genes were up-regulated in the thermal stress treatment (Fig. 2). Similar results have been reported in previous studies investigating the immune abilities of corals in response to thermal stress. Prophenoloxidase activity was shown to be higher in thermally stressed *M. faveolata* corals relative to healthy or diseased corals, whereas the opposite occurred for antibacterial and lysozyme-like activities [71]. Such results raise questions about the uniform nature of thermal stress effects on the coral immune response, and challenge the hypothesis that high temperature negatively impacts all coral immune functions and always favors infection [86–90]. Nevertheless, we showed that several encoding pattern recognition receptors (PRR; Toll-like, LBP–BP and mannose-binding lectin) followed a general trend of down-regulation, as did key factors in the downstream signaling pathway, including Myd88 (Figs 2 and 3). Other essential components of the immune response, and more particularly some effectors, were also down-regulated (damicornin, TX60A-1 and TX60A-2) during thermal stress, which may significantly alter the immune capabilities of the coral. Thus, the

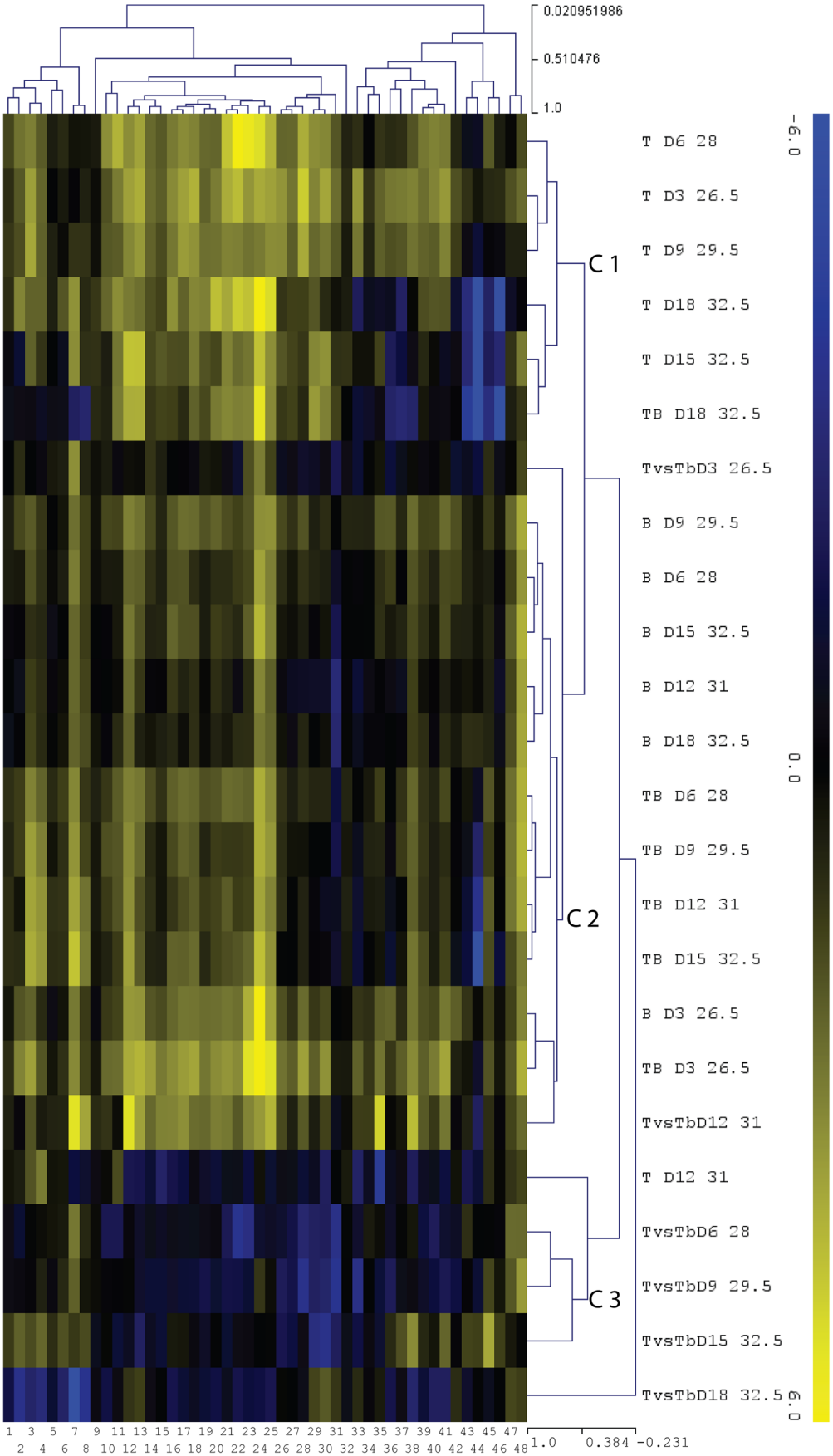
0.020951986
0.510476
1.0
T D6 28
T D3 26.5
T D9 29.5
T D18 32.5
T D15 32.5
TB D18 32.5
TvsTbD3 26.5
B D9 29.5
B D6 28
B D15 32.5
B D12 31
B D18 32.5
TB D6 28
TB D9 29.5
TB D12 31
TB D15 32.5
B D3 26.5
TB D3 26.5
TvsTbD12 31
T D12 31
TvsTbD6 28
TvsTbD9 29.5
TvsTbD15 32.5
TvsTbD18 32.5
C 1
C 2
C 3
6.0
0.0
-6.0
1 3 5 7 9 11 13 15 17 19 21 23 25 27 29 31 33 35 37 39 41 43 45 47
2 4 6 8 10 12 14 16 18 20 22 24 26 28 30 32 34 36 38 40 42 44 46 48
1.0
0.384
-0.231

Figure 2. Expression of innate immune candidate genes. The data included q-RT-PCR results for nubbins sampled during the non-virulent, thermal stress, virulent and bacterial virulence (thermal stress *vs.* virulent treatment) treatments (days 3, 6, 9, 12, 15 and 18). Quantification was normalized to the control conditions for the non-virulent, thermal stress and virulent treatment, and with results for colonies sampled at the same temperature as that for the thermal stress *vs.* virulent comparison (bacterial virulence effect only). The results are presented as a log2-fold change in expression. The hierarchical clustering of the q-RT-PCR data was done using Multiple Array Viewer software (version 4.8.1), with average linkage clustering based on the Pearson correlation as a default distance metric. Cluster C1 represents the response to thermal stress, cluster C2 represents the response to bacteria (non-virulent and virulent), and cluster C3 represents the response to the virulence of the bacteria. The numbers at the bottom of the figure correspond to the following genes: 1, epsilon isoform 1 (housekeeping control); 2, MASP3; 3, peroxidase2; 4, peroxidase1; 5, cyclin d2 (housekeeping control); 6, preprotein translocase SecY subunit (housekeeping control); 7, laccase; 8, prophenol oxidase activating enzyme; 9, ubiquitin-conjugating enzyme E2 (housekeeping control); 10, 5-lypoxigenase; 11, catalase1; 12, nucleoredoxin; 13, TAK1; 14, MKK7; 15, MKK4; 16, JNK; 17, TRAF6; 18, IKBa; 19, NF-kB; 20, TIR2; 21, AP1; 22, ATF; 23, Bf; 24, C3; 25, MASP1; 26, catalase2; 27, MKK3/6; 28, IKK; 29, p38; 30, LRR2; 31, apextrin; 32, SOD1; 33, leukotriene A4 hydrolase; 34,Leukotriene C4 synthase; 35, MyD88; 36, GFP-Like2; 37, TIR3; 38, SOD2; 39, MEKK1; 40, LPBPI; 41, LRR-TIR-IGG; 42, GFP-Like1; 43, Tx60A2; 44, Tx60A1; 45, PdC-Lectin; 46,damicornin; 47, phospholipase A2; 48, mytimacin-like.
doi:10.1371/journal.pone.0107672.g002

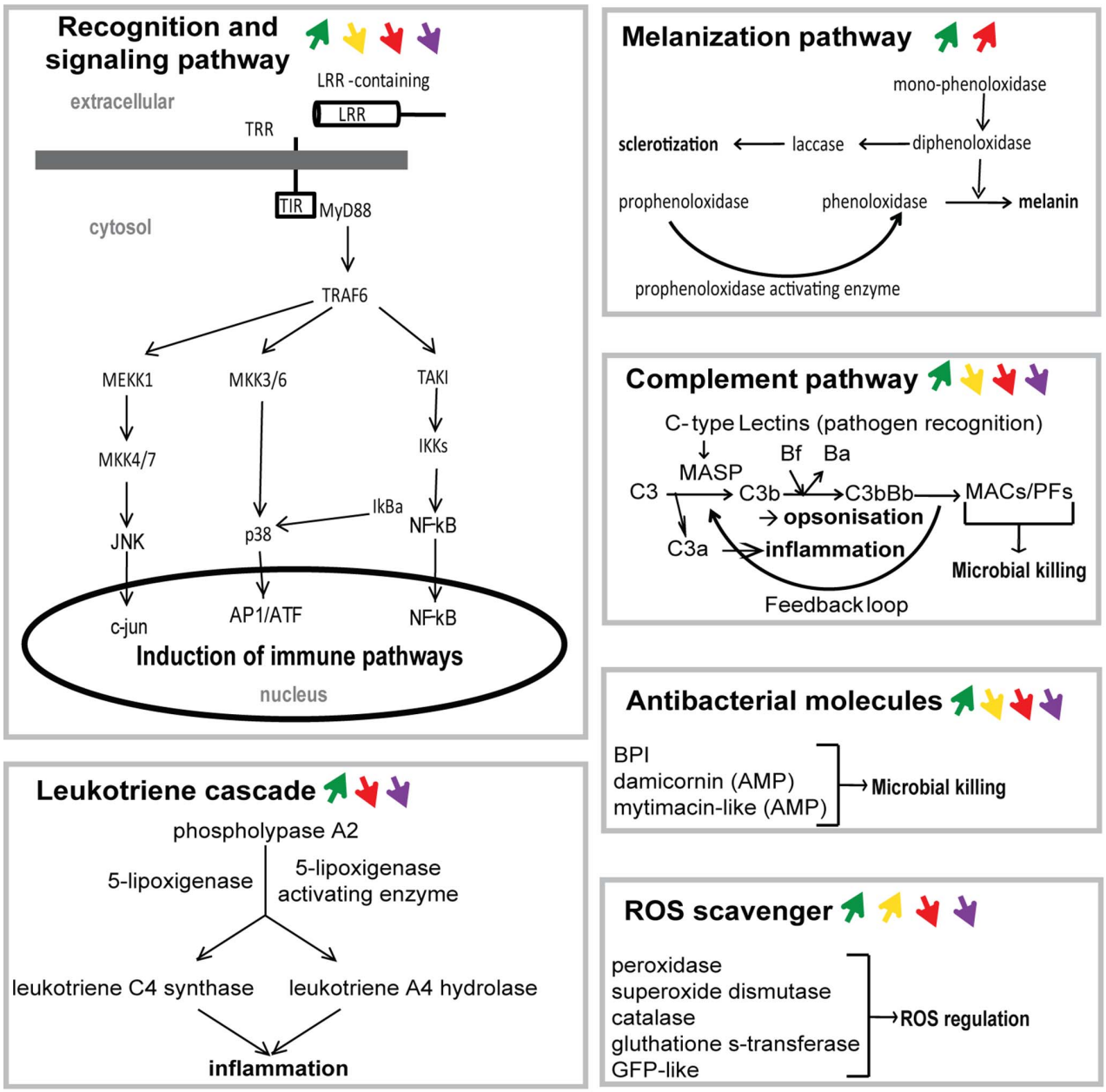

Figure 3. Schematic representation of the innate immune pathways monitored by q-RT-PCR, and their main response to each treatment. Reconstitution of the immune pathways identified in previous studies and from the present study (see Table 5 for references). Arrows highlight the average response (if any) of each pathway to each treatment or comparison. Green arrow: response to the non-virulent treatment; yellow arrow: response to the thermal stress treatment; red arrow: response to the virulent treatment; violet arrow: response to the virulence effect (the comparison between the thermal stress and the virulent treatment).
doi:10.1371/journal.pone.0107672.g003

Table 5. Summary of the cnidarian immune genes identified.

Immune function	Gene/protein	References
Recognition	Lectins, integrins, Toll-like receptors	[33,40,55–65]
Signaling	NF- k B, AP1/ATF, JNK, Myd88, MAPKs	[64,66,67]
Complement	C3, mannose binding lectins, MASPs	[40,60–62,68–70]
Melanization	Laccase, phenoloxidase, prophenoloxidase	[71–78]
Antimicrobial activity	Hydramacin-1, Periculin1, Aurelin, Damicornin, LBP-BPI, mytimacin-like	[34,55,79,80] this study
Leukotriene cascade	Phospholipase A2, 5-lipoxigenase, leukotriene C4-synthase, leukotriene A4-hydrolase	This study

doi:10.1371/journal.pone.0107672.t005

combination of our results and those reported previously suggest that, even if the immune abilities of *P. damicornis* are not completely inhibited by thermal stress, the changes induced by increased temperature reduce the capacity of the coral to mount an efficient immune response, thus facilitating pathogen colonization of host tissues.

The virulence +/− thermal stress effect

Analysis of the transcriptomic changes between the virulent treatment and the control (thermal stress+virulence effect) or the thermal stress (virulence effect) treatment indicated profound remodeling of the transcriptome. Coral immune function was highly affected by the infection process, and many genes were down-regulated, particularly following internalization of the bacteria. This finding is consistent with evidence from a previous study of *P. damicornis*, which showed down-regulation of the gene encoding the AMP damicornin during infection by *V. coralliilyticus* [34]. Nevertheless, this down-regulation response is not absolute, as revealed using the candidate gene approach, which demonstrated the up-regulation of some genes. This approach also highlights that the coral response to the virulent and non-virulent bacteria was very similar (Fig. 2; cluster C2). This suggests that the response is mediated following interaction with the bacteria, and is sufficient to neutralize the bacteria under non-virulent conditions, but not under virulent conditions. This shows that under virulent conditions the bacteria were able to circumvent the coral response and to establish the pathogenic intracellular and intra-vesicular form, which involves localization that facilitates protection of the bacteria from systemic immune attack [26,33]. This strategy is also used by the oyster (*Crassostrea gigas*) pathogen *V. splendidus*: following internalization in immune cells this bacterium manipulates and evades host defenses by preventing acidic vacuole formation and limiting ROS production [91]. At high temperature and at the same stage of infection, *V. coralliilyticus* has also been shown to be able to express a series of putative virulence factors involved in host degradation, secretion, antimicrobial resistance and transcriptional regulation, which may help this pathogen to survive and spread in the intracellular environment [31,32].

The greater the stress, the greater the transcriptomic disturbance: a trade-off mechanism?

Based on the symptoms evident in each treatment, exposure to the bacteria under high temperature conditions triggering virulence resulted in greater stress to the coral than exposure to thermal stress alone, which in turn was more stressful than exposure to the non-virulent bacteria. In the virulent treatment tissue lysis and death of the coral colonies occurred within 18 days, in the high temperature treatment the symbiosis broke down and coral bleaching occurred within 18 days, and no symptoms were observed in the treatment involving non-virulent bacteria [33]. Our RNA-seq results showed that 12 days following initiation of the treatments there was a clear correlation between the intensity of the stress and the number of down-regulated genes: the greater the stress, the greater the down-regulation (Table 1). Extensive down-regulation in response to environmental stressors is often reported in transcriptomic studies, but most research has focused on biological functions that are expected to be affected, rather than using the global analysis of the physiological status of the impacted organism. Indeed, it is easier and more straightforward to focus on down-regulated genes clearly associated with specific functions than to interpret the modulation of numerous genes associated with diverse, general biological processes. Nonetheless, the phenomenon of widespread down-regulation during stress responses has been verified through genome-wide transcriptomic studies in corals and other organisms exposed to various environmental stressors [44,92–97]. This suggests that down-regulation is a conserved phenomenon under stress conditions.

In this context, the coral stress response was recently compared with the environmental stress response (ESR) of a budding yeast [98], which involves a conserved, extreme, rapid, and genome-wide response to a broad set of environmental stressors that trigger a common response among a large set (approximately 900) of genes [99]. In corals the core stress response involves the up-regulation of HSP and ROS scavenger encoding genes, and disruption of the expression of genes involved in Ca^{2+} homeostasis, cytoskeleton organization, cell signaling and transcriptional regulation [98]. However, as was found in the yeast, in which approximately 66% of the genes of the ESR were down-regulated [99], the broad down-regulation observed in corals exposed to various stressors may also be a fundamental part of the coral stress response. This hypothesis is supported by parallels between the coral response in our study, and the main biological processes down-regulated in the yeast ESR. As in the yeast ESR [99], our GO enrichment analysis (Table 4) suggested a general down-regulation of what are usually considered to be housekeeping biological processes, including translation, nucleic acid metabolic processes, secretion, regulation of gene expression and others biosynthetic processes. These housekeeping functions are generally very costly, and monopolize most energy production and the cell's transcriptional and translational machinery [100]. Under stress conditions, down-regulation may help to minimize energetic expenditure, enabling rapid and efficient responses to the new environmental conditions [101]. In yeast, this energetic economy was shown to affect functions that are not essential for survival, but also involved the selective down-regulation of genes encoding high molecular weight and/or highly expressed proteins [101]. Demonstrating such phenomena in corals is difficult because of the lack of tools enabling complete transcriptome analysis. However, the results obtained in our study for the host core genes

were consistent with this hypothesis. Indeed, we found that under the control conditions the core coral genes were more represented among the down-regulated genes (RPKM average, 789.40 reads) than the up-regulated genes (RPKM average, 546.74 reads; Mann-Whitney U test, $p<0.01$).

Conclusion

Taken together, our results show that scleractinian corals have an immune system that is able to respond to pathogenic agents, and support the "sophisticated ancestral immune toolkit" hypothesis [61,81,102]. The results also have important implications for understanding the immune system of ancestral metazoans, and its evolution and conservation through the eumetazoan lineage. Our results demonstrate that thermal stress alters immune capacities, especially during recognition and antibacterial processes, and that this probably facilitates pathogenesis. However, bacterial virulence and the intracellular localization of the pathogen seem to be the major factors responsible for pathogenesis, especially through an immuno-suppressive effect that may decrease the efficiency of the immune response, and lead to bacterial proliferation and physiological collapse of the coral. In addition to effects on immunity, thermal stress induces a strong and energetically costly response that may weaken the coral and favor infection by specific or opportunistic pathogens, through a trade-off mechanism. In summary, the absolute effect of thermal stress on the coral is less than that of the virulent bacteria during pathogenesis, but is a clear facilitator of infection.

Supporting Information

Table S1 Detailed results of the GO term enrichment analysis for the up-regulated set of genes.
(XLS)

Table S2 Detailed results of the GO term enrichment analysis for the up-regulated set of genes.
(XLSX)

Table S3 Candidate innate immune genes, Annotation, Contig name, Sequence, Primer, BlastX results and protein domain.
(XLSX)

Table S4 Expression of innate immune candidate genes, numerical values.
(XLSX)

Acknowledgments

The facilities (bioinformatics and molecular biology) of the Tecnoviv platform were used for the study. The authors are indebted to Jérôme Bossier for his help in statistical procedures, and to Richard Galinier and Jean-François Allienne for technical assistance on the Tecnoviv platform.

Author Contributions

Conceived and designed the experiments: JVD CG CC MF GM. Performed the experiments: JVD RR CG CC KMS MF. Analyzed the data: JVD NMD RR CG KMS MA GM. Contributed reagents/materials/analysis tools: NMD RR MF MA. Contributed to the writing of the manuscript: JVD NMD RR CC CG KMS MA MF GM.

References

1. Pachauri RK (2007) Climate change 2007: Synthesis report. Geneva: IPCC Secreteria.
2. Hoegh-Guldberg O, Bruno JF (2010) The impact of climate change on the world's marine ecosystems. Science 328(5985): 1523–1528.
3. Walther GR, Post E, Convey P, Menzel A, Parmesan C et al. (2002) Ecological responses to recent climate change. Nature 416(6879): 389–395.
4. Harvell CD, Mitchell CE, Ward JR, Altizer S, Dobson AP et al. (2002) Climate warming and disease risks for terrestrial and marine biota. Science 296(5576): 2158–2162.
5. Harvell D, Altizer S, Cattadori IM, Harrington L, Weil E (2009) Climate change and wildlife diseases: When does the host matter the most? Ecology 90(4): 912–920.
6. Ward JR, Lafferty KD (2004) The elusive baseline of marine disease: Are diseases in ocean ecosystems increasing? PLoS Biol 2(4): e120.
7. Harvell CD, Kim K, Burkholder JM, Colwell RR, Epstein PR et al. (1999) Emerging marine diseases–climate links and anthropogenic factors. Science 285(5433): 1505–1510.
8. Burreson EM, Ragone Calvo LM (1996) Epizootiology of *Perkinsus marinus* disease of oysters in Chesapeake Bay, with emphasis on data since 1985. J Shellfish Res 15: 17–34.
9. Cook T, Folli M, Klinck J, Ford S, Miller J (2004) The relationship between increasing sea-surface temperature and the northward spread of *Perkinsus marinus* (Dermo) disease epizootics in oysters. Estuar Coast Shelf Sci 46(4): 587–597.
10. Devaux CA (2012) Emerging and re-emerging viruses: A global challenge illustrated by Chikungunya virus outbreaks. World J Virol 1(1): 11–22.
11. Pounds AJ, Bustamante MR, Coloma LA, Consuegra JA, Fogden MPL et al. (2006) Widespread amphibian extinctions from epidemic disease driven by global warming. Nature 439(7073): 161–167.
12. Scheibling RE, Hennigar AW (1997) Recurrent outbreaks of disease in sea urchins *Strongylocentrotus droebachiensis* in Nova Scotia: evidence for a link with large-scale meteorologic and oceanographic events. Mar Ecol-Prog Ser 152(1): 155–165.
13. Skerratt L, Berger L, Speare R, Cashins S, McDonald K et al. (2007) Spread of chytridiomycosis has caused the rapid global decline and extinction of frogs. EcoHealth 4(2): 125–134.
14. Campbell AH, Harder T, Nielsen S, Kjelleberg S, Steinberg PD (2011) Climate change and disease: bleaching of a chemically defended seaweed. Glob chang biol 17(9): 2958–2970.
15. Vargas-Albores F, Hinojosa-Baltazar P, Portillo-Clark G, Magallon-Barajas F (1998) Influence of temperature and salinity on the yellowleg shrimp, *Penaeus californieinsis* Holmes, prophenoloxidase system. Aquac Res 29(8): 549–553.
16. Case RJ, Longford SR, Campbell AH, Low A, Tujula N et al. (2011) Temperature induced bacterial virulence and bleaching disease in a chemically defended marine macroalga. Environ Microbiol 13(2): 529–537.
17. Decostere A, Haesebrouck F, Turnbull JF, Charlier G (1999) Influence of water quality and temperature on adhesion of high and low virulence *Flavobacterium columnare* strains to isolated gill arches. J Fish Dis 22(1): 1–11.
18. Kushmaro A, Rosenberg E, Fine M, Loya Y (1997) Bleaching of the coral *Oculina patagonica* by *Vibrio AK-1*. Mar Ecol-Prog Ser 147: 159–165.
19. Ellner SP, Jones LE, Mydlarz LD, Harvell CD (2007) Within-host disease ecology in the sea fan *Gorgonia ventalina*: Modeling the spatial immunodynamics of a coral-pathogen interaction. Am Nat 170(6): E143–E161.
20. Pinzon JH, LaJeunesse T (2011) Species delimitation of common reef corals in the genus *Pocillopora* using nucleotide sequence phylogenies, population genetics and symbiosis ecology. Mol Ecol 20(2): 311–325.
21. Veron JEN (2000) Corals of the World; Stafford-Smith M, editor. Townsville: Australian Institute of Marine Science. 463 p.
22. Ben-Haim Y, Rosenberg E (2002) A novel *Vibrio* sp. pathogen of the coral *Pocillopora damicornis*. Mar Biol 141: 47–55.
23. Hashimoto K, Shibuno T, Murayama-Kayano E, Tanaka H, Kayano T (2004) Isolation and characterization of stress-responsive genes from the scleractinian coral *Pocillopora damicornis*. Coral Reefs 23: 485–491.
24. Loya Y, Sakai K, Yamazato K, Nakano Y, Sambali R et al. (2001) Coral bleaching: the winners and the losers. Ecol Lett 4(2): 122–131.
25. Stimson J, Sakai K, Sembali H (2002) Interspecific comparison of the symbiotic relationship in corals with high and low rates of bleaching-induced mortality. Coral Reefs V21(4): 409–421.
26. Ben-Haim Rozenblat Y, Rosenberg E (2004) Temperature-regulated bleaching and tissue lysis of *Pocillopora damicornis* by the novel pathogen *Vibrio coralliilyticus*. In: Rosenberg E, Loya Y, editors. Coral health and disease. New-York: Spinger-Verlag. pp. 301–324.
27. Dinsdale EA. Abundance of black-band disease on corals from one location on the Great Barrier Reef: a comparison with abundance in the Caribbean region; 2002; Bali. pp. 1239–1243.
28. Luna GM, Biavasco F, Danovaro R (2007) Bacteria associated with the rapid tissue necrosis of stony corals. Environ Microbiol 9: 1851–1857.
29. Luna GM, Bongiorni L, Gili C, Biavasco F, Danovaro R (2010) *Vibrio harveyi* as a causative agent of the White Syndrome in tropical stony corals. Environ Microbiol Rep 2(1): 120–127.
30. Pollock FJ, Wilson B, Johnson WR, Morris PJ, Willis BL et al. (2010) Phylogeny of the coral pathogen *Vibrio coralliilyticus*. Environ Microbiol Rep 2(1): 172–178.

31. De O Santos E, Alves N, Jr., Dias GM, Mazotto AM, Vermelho A et al. (2011) Genomic and proteomic analyses of the coral pathogen *Vibrio coralliilyticus* reveal a diverse virulence repertoire. ISME J 5(9): 1471–1483.
32. Kimes NE, Grim CJ, Johnson WR, Hasan NA, Tall BD et al. (2012) Temperature regulation of virulence factors in the pathogen *Vibrio coralliilyticus*. ISME J 6: 835–846.
33. Vidal-Dupiol J, Ladrière O, Meistertzheim AL, Fouré L, Adjeroud M et al. (2011) Physiological responses of the scleractinian coral *Pocillopora damicornis* to bacterial stress from *Vibrio coralliilyticus*. J Exp Biol 214: 1533–1545.
34. Vidal-Dupiol J, Ladrière O, Destoumieux-Garzon D, Sautière P-E, Meistertzheim AL et al. (2011) Innate immune responses of a scleractinian coral to vibriosis. J Biol Chem 286(25): 22688–22698.
35. Ben-Haim Y, Zicherman-Keren M, Rosenberg E (2003) Temperature-regulated bleaching and lysis of the coral *Pocillopora damicornis* by the novel pathogen *Vibrio coralliilyticus*. Appl Environ Microbiol 69(7): 4236–4242.
36. Flot JF, Tillier S (2007) The mitochondrial genome of *Pocillopora* (Cnidaria: Scleractinia) contains two variable regions: the putative D-loop and a novel ORF of unknown function. Gene 401(1–2): 80–87.
37. Marti-Puig P, Forsman ZH, Haverkort-Yeh RD, Knapp ISS, Maragos JE et al. (2013) Extreme phenotypic polymorphism in the coral genus *Pocillopora*; micro-morphology corresponds to mitochondrial groups, while colony morphology does not. Bull Mar Sci 90(1): 1–21.
38. Pinzon JH, Sampayo E, Cox E, Chauka LJ, Chen CA et al. (2013) Blind to morphology: genetics identifies several widespread ecologically common species and few endemics among Indo-Pacific cauliflower corals (*Pocillopora*, Scleractinia). Journal of Biogeography 40(8): 1595–1608.
39. Ben-Haim Y, Thompson FL, Thompson CC, Cnockaert MC, Hoste B et al. (2003) *Vibrio coralliilyticus* sp. nov., a temperature-dependent pathogen of the coral *Pocillopora damicornis*. Int J Syst Evol Microbiol 53(1): 309–315.
40. Vidal-Dupiol J, Adjeroud M, Roger E, Foure L, Duval D et al. (2009) Coral bleaching under thermal stress: putative involvement of host/symbiont recognition mechanisms. BMC Physiol 9: 14.
41. Fox S, Sergei F, Mockler TC (2010) Applications of ultra-hignt-throughput sequencing. In: Belostotky DA, editor. Plant systems Biology. New York: Humana Press. pp. 79–108.
42. Pomraning KR, Smith KM, Bredeweg EL, Phatale PA, L.R C et al. (2012) Paired-end library preparation for rapid genome sequencing. Fungal Secondary Metabolism. New York: Humana Press.
43. Pomraning KR, Smith KM, Freitag M (2009) Genome-wide high throughput analysis of DNA methylation in eukaryotes. Methods 47: 142–150.
44. Vidal-Dupiol J, Zoccola D, Tambutté E, Grunau C, Cosseau C et al. (2013) Genes related to ion-transport and energy production are upregulated in response to CO_2-driven pH decrease in corals: New insights from transcriptome analysis. PloS ONE 8(3): e58652.
45. Li H, Durbin R (2009) Fast and accurate short read alignment with Burrows-Wheeler transform. Bioinformatics 25(14): 1754–1760.
46. Mortazavi A, Williams BA, McCue K, Schaeffer L, Wold B (2008) Mapping and quantifying mammalian transcriptomes by RNA-Seq. Nat Methods 5(7): 621–628.
47. Wang L, Feng Z, Wang X, Wang X, Zhang X (2010) DEGseq: an R package for identifying differentially expressed genes from RNA-seq data. Bioinformatics 26(1): 136–138.
48. Bluthgen N, Brand K, Cajavec B, Swat M, Herzel H et al. (2004) Biological profiling of gene groups utilizing Gene Ontology. Arxiv preprint q-bio/0407034.
49. Le QH, Markovic P, Hastings JW, Jovine RVM, Morse D (1997) Structure and organization of the peridinin-chlorophyll a-binding protein gene in *Gonyaulax polyedra*. Mol Gen Genet 255(6): 595–604.
50. Lee DH, Mittag M, Sczekan S, Morse D, Hastings JW (1993) Molecular cloning and genomic organization of a gene for luciferin-binding protein from the dinoflagellate *Gonyaulax polyedra*. J Biol Chem 268(12): 8842–8850.
51. Shoguchi E, Shinzato C, Kawashima T, Gyoja F, Mungpakdee S et al. (2013) Draft assembly of the Symbiodinium minutum nuclear genome reveals dinoflagellate gene structure. Curr Biol 23(15): 1399–1408.
52. Zhang H, Hou Y, Lin S (2006) Isolation and characterization of proliferating cell nuclear antigen from the Dinoflagellate *Pfiesteria piscicida*. J Eukaryot Microbiol 53(2): 142–150.
53. Rudd S (2003) Expressed sequence tags: alternative or complement to whole genome sequences? Trends in Plant Science 8(7): 321–329.
54. Rosenberg E, Koren O, Reshef L, Efrony R, Zilber-Rosenberg I (2007) The role of microorganisms in coral health, disease and evolution. Nature Review Microbiology 5(5): 355–362.
55. Bosch TCG, Augustin R, Anton-Erxleben F, Fraune S, Hemmrich G et al. (2009) Uncovering the evolutionary history of innate immunity: The simple metazoan *Hydra* uses epithelial cells for host defence. Dev Comp Immunol 33(4): 559–569.
56. Brower DL, Brower SM, Hayward DC, Ball EE (1997) Molecular evolution of integrins: Genes encoding integrin beta subunits from a coral and a sponge. Proc Natl Acad Sci U S A 94(17): 9182–9187.
57. Hayes ML, Eytan RI, Hellberg ME (2010) High amino acid diversity and positive selection at a putative coral immunity gene (tachylectin-2). BMC Evol Biol 10(1): 150.
58. Kazumitsu H, Masa-aki K (1983) The effects of lectins on the feeding response in *Hydra japonica*. Comp Biochem Physiol A-Mol Integr Physiol 76(2): 283–287.
59. Knack BA, Iguchi A, Shinzato C, Hayward DC, Ball EE et al. (2008) Unexpected diversity of cnidarian integrins: expression during coral gastrulation. BMC Evol Biol 8(1): 136.
60. Kvennefors ECE, Leggat W, Hoegh-Guldberg O, Degnan BM, Barnes AC (2008) An ancient and variable mannose-binding lectin from the coral *Acropora millepora* binds both pathogens and symbionts. Dev Comp Immunol 32(12): 1582–1592.
61. Miller D, Hemmrich G, Ball E, Hayward D, Khalturin K et al. (2007) The innate immune repertoire in Cnidaria - ancestral complexity and stochastic gene loss. Genome Biol 8(4): R59.
62. Reitzel AM, Sullivan JC, Traylor-Knowles N, Finnerty JR (2008) Genomic survey of candidate stress-response genes in the estuarine anemone *Nematostella vectensis*. Biol Bull 214(3): 233–254.
63. Schwarz J, Brokstein P, Voolstra C, Terry A, Miller D et al. (2008) Coral life history and symbiosis: Functional genomic resources for two reef building Caribbean corals, *Acropora palmata* and *Montastraea faveolata*. BMC Genomics 9(1): 97.
64. Shinzato C, Shoguchi E, Kawashima T, Hamada M, Hisata K et al. (2011) Using the *Acropora digitifera* genome to understand coral responses to environmental change. Nature 476: 320–323.
65. Wood-Charlson EM, Weis VM (2009) The diversity of C-type lectins in the genome of a basal metazoan, *Nematostella vectensis*. Dev Comp Immunol 33(8): 881–889.
66. Putnam NH, Srivastava M, Hellsten U, Dirks B, Chapman J et al. (2007) Sea anemone genome reveals ancestral eumetazoan gene repertoire and genomic organization. Science 317(5834): 86–94.
67. Souter P, Bay LK, Andreakis N, Csaszar N, Seneca FO et al. (2011) A multilocus, temperature stress-related gene expression profile assay in *Acropora millepora*, a dominant reef-building coral. Mol Ecol Resour 11(2): 328–334.
68. Dishaw L, Smith S, Bigger C (2005) Characterization of a C3-like cDNA in a coral: phylogenetic implications. Immunogenetics 57(7): 535–548.
69. Kimura A, Sakaguchi E, Nonaka M (2009) Multi-component complement system of Cnidaria: C3, Bf, and MASP genes expressed in the endodermal tissues of a sea anemone, *Nematostella vectensis*. Immunobiology 214(3): 165–178.
70. Kvennefors ECE, Leggat W, Kerr CC, Ainsworth TD, Hoegh-Guldberg O et al. (2010) Analysis of evolutionarily conserved innate immune components in coral links immunity and symbiosis. Dev Comp Immunol 34(11): 1219–1229.
71. Mydlarz LD, Couch CS, Weil E, Smith G, Harvell CD (2009) Immune defenses of healthy, bleached and diseased *Montastraea faveolata* during a natural bleaching event. Dis Aquat Org 87(1–2): 67–78.
72. Mydlarz LD, Holthouse SF, Peters EC, Harvell CD (2008) Cellular responses in sea fan corals: Granular amoebocytes react to pathogen and climate stressors. PloS ONE 3(3): e1811.
73. Mydlarz LD, Palmer CV (2011) The presence of multiple phenoloxidases in Caribbean reef-building corals. Comp Biochem Physiol A-Mol Integr Physiol 159(4): 372–378.
74. Palmer CV, Bythell JC, Willis BL (2010) Levels of immunity parameters underpin bleaching and disease susceptibility of reef corals. Faseb J 24(6): 1935–1946.
75. Palmer CV, Bythell JC, Willis BL (2011) A comparative study of phenoloxidase activity in diseased and bleached colonies of the coral *Acropora millepora*. Dev Comp Immunol 35(10): 1098–1101.
76. Palmer CV, Bythell JC, Willis BL (2012) Enzyme activity demonstrates multiple pathways of innate immunity in Indo-Pacific anthozoans. Proc R Soc B-Biol Sci 279(1743): 3879–3887.
77. Palmer CV, McGinty ES, Cummings DJ, Smith SM, Bartels E et al. (2011) Patterns of coral ecological immunology: variation in the responses of Caribbean corals to elevated temperature and a pathogen elicitor. J Exp Biol 214(24): 4240–4249.
78. Palmer CV, Mydlarz LD, Willis BL (2008) Evidence of an inflammatory-like response in non-normally pigmented tissues of two scleractinian corals. Proc R Soc B-Biol Sci 275(1652): 2687–2693.
79. Jung S, Dingley AJ, Augustin R, Anton-Erxleben F, Stanisak M et al. (2009) Hydramacin-1, Structure and Antibacterial Activity of a Protein from the Basal Metazoan Hydra. J Biol Chem 284(3): 1896–1905.
80. Ovchinnikova TV, Balandin SV, Aleshina GM, Tagaev AA, Leonova YF et al. (2006) Aurelin, a novel antimicrobial peptide from jellyfish *Aurelia aurita* with structural features of defensins and channel-blocking toxins. Biochem Biophys Res Commun 348(2): 514–523.
81. Hemmrich G, Miller DJ, Bosch TCG (2007) The evolution of immunity: a low-life perspective. Trends Immunol 28(10): 449–454.
82. Palmer CV, Traylor-Knowles N (2012) Towards an integrated network of coral immune mechanisms. Proc R Soc B-Biol Sci 279(1745): 4106–4114.
83. Weiss Y, Foret S, Hayward D, Ainsworth T, King R et al. (2013) The acute transcriptional response of the coral *Acropora millepora* to immune challenge: expression of GiMAP/IAN genes links the innate immune responses of corals with those of mammals and plants. BMC Genomics 14(1): 400.
84. Burge CA, Mouchka ME, Harvell CD, Roberts S (2013) Immune response of the Caribbean sea fan, *Gorgonia ventalina*, exposed to an *Aplanochytrium* parasite as revealed by transcriptome sequencing. Front Invert Physiol 4: 1–9.

85. Weis VM (2008) Cellular mechanisms of Cnidarian bleaching: stress causes the collapse of symbiosis. J Exp Biol 211: 3059–3066.
86. Bourne DG, Garren M, Work TM, Rosenberg E, Smith GW et al. (2009) Microbial disease and the coral holobiont. Trends Microbiol 17(12): 554–562.
87. Bruno JF, Selig ER, Casey KS, Page CA, Willis BL et al. (2007) Thermal stress and coral cover as drivers of coral disease outbreaks. PLoS Biol 5(6): e124.
88. Lesser MP, Bythell JC, Gates RD, Johnstone RW, Hoegh-Guldberg O (2007) Are infectious diseases really killing corals? Alternative interpretations of the experimental and ecological data. J Exp Mar Biol Ecol 346(1–2): 36–44.
89. Muller EM, van Woesik R (2012) Caribbean coral diseases: primary transmission or secondary infection? Glob chang biol 18(12): 3529–3535.
90. Mydlarz LD, McGinty ES, Harvell CD (2010) What are the physiological and immunological responses of coral to climate warming and disease? J Exp Biol 213(6): 934–945.
91. Duperthuy M, Schmitt P, Garzon E, Caro A, Rosa RD et al. (2011) Use of OmpU porins for attachment and invasion of *Crassostrea gigas* immune cells by the oyster pathogen *Vibrio splendidus*. Proc Natl Acad Sci USA 108(7): 2993–2998.
92. Kaniewska P, Campbell PR, Kline DI, Rodriguez-Lanetty M, Miller DJ et al. (2012) Major cellular and physiological impacts of ocean acidification on a reef-building coral. PloS ONE 7(4): e34659.
93. Meyer E, Aglyamova GV, Matz MV (2011) Profiling gene expression responses of coral larvae (*Acropora millepora*) to elevated temperature and settlement inducers using a novel RNA-Seq procedure. Mol Ecol 20(17): 3599–3616.
94. Moya A, Ganot P, Furla P, Sabourault C (2012) The transcriptomic response to thermal stress is immediate, transient and potentiated by ultraviolet radiation in the sea anemone Anemonia viridis. Mol Ecol 21: 1158–1174.
95. Moya A, Huisman L, Ball EE, Hayward DC, Grasso LC et al. (2012) Whole transcriptome analysis of the coral *Acropora millepora* reveals complex responses to CO_2-driven acidification during the initiation of calcification. Mol Ecol 21(10): 2440–2454.
96. Rodriguez-Lanetty M, Harii S, Hoegh-Guldberg O (2009) Early molecular responses of coral larvae to hyperthermal stress. Mol Ecol 18(24): 5101–5114.
97. Zhao X, Yu H, Kong L, Li Q (2012) Transcriptomic responses to salinity stress in the pacific oyster *Crassostrea gigas*. PloS ONE 7(9): e46244.
98. Barshis DJ, Ladner JT, Oliver TA, Seneca FoO, Traylor-Knowles N et al. (2013) Genomic basis for coral resilience to climate change. Proc Natl Acad Sci USA 110(4): 1387–1392.
99. Gasch AP, Spellman PT, Kao CM, Carmel-Harel O, Eisen MB et al. (2000) Genomic expression programs in the response of yeast cells to environmental changes. Mol Biol Cell 11(12): 4241–4257.
100. Warner JR (1999) The economics of ribosome biosynthesis in yeast. Trends Biochem Sci 24(11): 437–440.
101. Vilaprinyo E, Alves R, Sorribas A (2010) Minimization of biosynthetic costs in adaptive gene expression responses of yeast to environmental changes. PLoS Comput Biol 6(2): e1000674.
102. Irazoqui JE, Urbach JM, Ausubel FM (2010) Evolution of host innate defence: insights from Caenorhabditis elegans and primitive invertebrates. Nat Rev Immunol 10(1): 47–58.

ANNEXE 7

DR. JEREMY LE LUYER (Orcid ID : 0000-0001-9409-3196)

Article type : Primary Research Articles

Title

Molecular mechanisms of acclimation to long-term elevated temperature exposure in marine symbioses

Running head

Thermo-acclimation in symbiotic organisms

Authors

H. J. Alves Monteiro[1], C. Brahmi[2], A. B. Mayfield[3,4], J. Vidal-Dupiol[5], B. Lapeyre[6], J. Le Luyer[1*]

Affiliations

[1.] IFREMER, EIO UMR 241, Labex CORAIL, Unité RMPF, Centre Océanologique du Pacifique, Vairao - BP 49 Vairao, Tahiti, Polynésie française

[2.] Université de la Polynésie Française, EIO UMR 241, Labex CORAIL, BP 6570 Faa'a, Tahiti, Polynésie française

[3.] National Museum of Marine Biology and Aquarium, 2 Houwan Rd., Checheng, Pingtung 944, Taiwan

[4.] Atlantic Oceanographic and Meteorological Laboratory, National Oceanic and Atmospheric Administration, Miami, FL 33149 USA

[5.] IHPE, Univ. Montpellier, CNRS, Ifremer, Univ. Perpignan Via Domitia, Montpellier France

This article has been accepted for publication and undergone full peer review but has not been through the copyediting, typesetting, pagination and proofreading process, which may lead to differences between this version and the Version of Record. Please cite this article as doi: 10.1111/GCB.14907

[6.] EPHE-UPVD-CNRS, CRIOBE USR 3278, Labex CORAIL, Université de Perpignan, Perpignan, France

Keywords

co-expression network analysis; giant clams; metabarcoding; RNA-Seq; Symbiodiniaceae; thermo-acclimation;

Corresponding author (*)

J. Le Luyer; Email: Jeremy.le.luyer@ifremer.fr / Tel: +689 405 460 52

Paper type:

Primary research

Abstract

Seawater temperature rise in French Polynesia has repeatedly resulted in the bleaching of corals and giant clams. Because giant clams possess distinctive ectosymbiotic features, they represent a unique and powerful model for comparing molecular pathways involved in 1) maintenance of symbiosis and 2) acquisition of thermo-tolerance among coral reef organisms. Herein, we explored the physiological and transcriptomic responses of the clam hosts and their photosynthetically active symbionts over a 65-day experiment in which clams were exposed to either normal or environmentally relevant elevated seawater temperatures. Additionally, we used metabarcoding data coupled with *in situ* sampling/survey data to explore the relative importance of holobiont adaptation (i.e., a symbiont community shift) versus acclimation (i.e., physiological changes at the molecular level) in the clams' responses to environmental change. We finally compared transcriptomic data to publicly available genomic datasets for Symbiodiniaceae dinoflagellates (both cultured and *in hospite* with the coral *Pocillopora damicornis*) to better tease apart the responses of both hosts and specific symbiont genotypes in this mutualistic association. Gene module preservation analysis revealed that the function of the symbionts' photosystem II was impaired at high temperature, and this response was also found across all holobionts and Symbiodiniaceae lineages examined. Similarly, epigenetic modulation appeared to be a key response mechanism for symbionts *in hospite* with giant clams exposed to high temperatures, and such modulation was able to distinguish thermo-tolerant from thermo-sensitive *Cladocopium goreaui* ecotypes; epigenetic processes may, then, represent a promising research avenue for those interested in coral reef conservation in this era of changing global climate.

Introduction

The "small giant" clams (*Tridacna maxima*; hereafter referred to as simply "clams") are mixotrophic organisms living in obligatory symbiosis with photosynthetic dinoflagellates of the family Symbiodiniaceae (Holt, Vahidinia, Gagnon, Morse, & Sweeney, 2014; Jantzen et al., 2008; LaJeunesse et al., 2018). Symbiodiniaceae associate not only with clams, but with a diverse array of marine invertebrates, namely sponges, molluscs, and cnidarians; indeed, the coral-Symbiodiniaceae symbiosis is the functional basis of all coral reefs (Hughes et al., 2003). Whereas in scleractinian corals symbionts are located intracellularly, in clams they reside extracellularly inside a tubular system ("Z-tubules"), which is 1) found in the outer epithelium of the mantle and 2) connected to the stomach (Norton, Shepherd, Long, & Fitt, 1992). These *in hospite* dinoflagellates are known to provide nutrients to their clam hosts via photosynthesis and may account for a major part of the clams' energy needs (depending on the species and the life history stage) (Hawkins & Klumpp, 1995; Klumpp, Bayne, & Hawkins, 1992; Klumpp & Griffiths, 1994; Lucas, 1994; Soo & Todd, 2014).

The systematics of the family Symbiodiniaceae have recently been revised to include at least nine different genera (formerly referred to as "clades") with well characterized molecular and physiological differences (LaJeunesse et al., 2018). One Symbiodiniaceae genus, formerly known as clade A (which includes the species *Symbiodinium fitti, S. microadriaticum*, and *S. tridacnidorum*), has been recurrently found in symbiosis with *T. maxima*, though members of clades C (*Cladocopium*) and D (*Durusdinium*) have been found in clam tissues, as well (Baillie, Belda-Baillie, & Maruyama, 2000; DeBoer et al., 2012; Ikeda et al., 2017; LaJeunesse, 2001; Lee et al., 2015; Mies, Van Sluys, Metcalfe, & Sumida, 2017; Pinzón, Devlin-Durante, Weber, Baums, & LaJeunesse, 2011). Depending on the clam species, the symbiont assemblage has been found to vary with individual size (mostly observed in *T. squamosa*), as well as across environmental gradients (especially seawater temperatures) (DeBoer et al., 2012; Ikeda et al., 2017).

In French Polynesia, eastern Tuamotu's archipelagos were historically characterized by high densities of clams (Andréfouët et al., 2013; Gilbert et al., 2005; Gilbert, Remoissenet, Yan, & Andrefouet, 2006). Recent mortality episodes and/or "bleaching" events in the Tuamotu Islands have,

however, been reported, including 1) a massive mortality event in 2009 that reduced the clam population by 90% at Tatakoto Atoll (Andréfouët et al., 2013; Van Wynsberge, Andréfouët, Gaertner-Mazouni, & Remoissenet, 2018) and 2) a bleaching event in 2016 that affected 77 and 90% of the wild and cultured giant clam populations, respectively, at Reao Atoll (Andréfouët et al., 2017). An increase in surface seawater temperature over a prolonged period (approximately three months above 30°C) is suspected to have triggered such bleaching events (Andréfouët et al., 2013, 2017; Van Wynsberge et al., 2018).

As with corals, bleaching in clams corresponds to the loss of symbiotic Symbiodiniaceae from the hosts (Andréfouët et al., 2013; Buck, 2002; Fitt, Brown, Warner, & Dunne, 2001; Hoegh-Guldberg et al., 2007; Leggat, Buck, Grice, & Yellowlees, 2003). Symbiodiniaceae community variability and diversity (i.e., the collective assemblage of various genera and/or species) seems to be a determining factor in the sensitivity and resilience of both coral and clam hosts to increased temperatures (Barshis, Ladner, Oliver, & Palumbi, 2014; Barshis et al., 2013; Ladner, Barshis, & Palumbi, 2012; Rowan, Knowlton, Baker, & Jara, 1997). However, the cell physiology of the host and symbionts is likely to be as important, if not more so, than the Symbiodiniaceae assemblage, in terms of gauging the ability of the clam-Symbiodiniaceae symbiosis to acclimate to elevated temperature over prolonged durations.

To date, few studies have investigated the transcriptomic response of giant clams to elevated temperatures; lipid profiling analyses are more routinely undertaken (Dubousquet et al., 2016). The transcriptomic response to elevated temperature of several other taxa, mostly scleractinian coral species (Crowder, Meyer, Fan, & Weis, 2017; Hou et al., 2018; Kenkel & Matz, 2016; Pinzón et al., 2015) and cultured Symbiodiniaceae (Gierz, Forêt, & Leggat, 2017; Levin et al., 2016) have also been explored, yet few studies have looked at the mRNA level responses of multiple Symbiodiniaceae clades and host systems in the same study. Furthermore, few physiological data and even fewer transcriptomic data are available for the high-temperature responses of the giant clam *T. maxima* and its symbionts [but see (Dubousquet et al., 2016; Zhou, Liu, Wang, Luo, & Li, 2018)]; these two published studies, though, only considered the response to an abrupt, rapid increase in temperature (short-term stress response).

Consequently, our understanding of the possible key drivers in high-temperature acclimation remains largely incomplete, despite its importance in generating better predictions of the impact of climate change on wild populations of giant clams (Van Wynsberge et al., 2018). Given such knowledge deficiencies, we aimed herein to characterize the physiological and transcriptomic responses of clams and their symbionts to hypothetically sub-lethal elevated temperatures (~30.7°C over a two-month period) that aimed to mimic past episodes of anomalously high temperatures in French Polynesia. In addition to hypothesizing that the giant clams would ultimately acclimate to this experimentally elevated temperature, we further hypothesized that a "dual-compartmental" bioinformatic approach, similar to the one that has been used with corals (Mayfield, Wang, Chen, Lin, & Chen, 2014), would provide insight into the key molecular pathways underlying the ability of each member of this association to acclimate to an environmentally relevant, sub-lethal temperature.

Materials and Methods

Experimental design, tissue sampling, and physiological measurements

The experimental procedures were first described by Brahmi et al. (2019). Briefly, 24 individual clams (N=4/treatment) were sampled over a 65-day period (days 29, 53, and 65) in control (29.2°C; ambient at the time of experimentation) and elevated (30.7°C) temperature conditions. The temperatures employed and the duration of the experiment reflect conditions in normal and abnormally hot seasons, respectively [(correlated with mass clam bleaching events (Addessi, 2001)] reported in lagoons of French Polynesia's Tuamotu region (Brahmi et al., 2019).

Samples (approx. 1 cm^2) from each of the two treatments at each of the three sampling times were systematically collected from the same region of the mantle and stored in RNALater® (Life Technologies, USA) at -80°C until analysis (N=24). Furthermore, a single hermaphroditic individual (approximately two years old) was sampled for a total of seven different tissues (mantle, adductor muscle, gonads, gills, byssus, visceral mass, and kidney) for transcriptome assembly. Only one individual was used in an effort to reduce assembly polymorphism biases. For this individual, which was excluded from the quantification analysis outlined below, sexual status was confirmed by gonad biopsy and histology following a previously detailed procedure (Menoud et al., 2016). Additionally, 10 giant clams were collected *in situ* in October 2018 around Reao Atoll (Tuamotu Archipelago,

French Polynesia); tissues from each of these *in situ* individuals were collected from the same region of the mantle (approx. 1 cm^2) and stored in 95% ethanol at -20°C until later symbiont community analysis (described below).

As described in detail in Brahmi et al. (2019), a variety of physiological response variables were assessed in the 24 experimental replicates, in addition to the profiling of their transcriptomes: growth, Symbiodiniaceae density, and the maximum dark-adapted yield of photosystem II (Fv/Fm; as measured by an AquaPen pulse amplitude modulating fluorometer; APC-100m, Photon System Instruments, Czech Republic). Please see Brahmi *et al*. (2019) for details on these analyses. Physiological data were tested with two-way ANOVA (treatment x time) followed by Tukey's "honestly significant difference" (HSD) *post-hoc* tests ($p<0.05$), including the interaction between time and temperature, when data (raw or transformed) met the assumptions for ANOVA. For Symbiodiniaceae density and Fv/Fm, a non-parametric equivalent of the two-way ANOVA, the Scheirer-Ray-Hare test, was instead used (followed by Dunn's *post-hoc* tests).

DNA/RNA extractions and transcriptome sequencing

Total RNA was extracted from *T. maxima* mantles by lacerating tissues with a scalpel and rinsing with 1X PBS. Cellular lysis was induced by addition of 1.5 ml TRIzol (Invitrogen, USA) according to the manufacturer's recommendations. The supernatant was transferred into a 2-ml tube and incubated for 10 min on ice. Phase separation was achieved by addition of 300 µl of chloroform coupled with centrifugation at 12,000 *xg* for 12 min at 4°C. The upper aqueous layer contained the RNA, and the lower organic layer was stored at -20°C for later DNA extraction (according to the manufacturer's recommendations). Total RNA from each individual was subjected to a DNAse treatment using Qiagen's RNA cleanup kit (Germany). RNA and DNA were quantified using a NanoDrop ND-2000 spectrophotometer (Thermo-Fisher, USA), and RNA quality was further evaluated by a Bioanalyzer 2100 (Agilent, USA). High-quality RNA was sent to McGill University's "Genome Quebec Innovation Center" (Montréal, QC, Canada) for Nextera XT (Illumina; USA) library preparation and sequencing on an Illumina HiSeq4000 100-bp paired-end platform. Samples for transcriptome assembly (N=7) were sequenced on a single lane, while samples for expression level quantification analysis (N=24) were uniformly and randomly distributed over two sequencing lanes after barcoding.

Transcriptomes assembly

Raw reads provided by RNA-Seq were filtered for quality and length using Trimmomatic v.0.36 (Bolger, Lohse, & Usadel, 2014) with minimum length, trailing, and leading quality parameters set to 60 bp, 20, and 20, respectively. Illumina's adaptors and residual cloning vectors were removed via the UNIVEC database (https://www.ncbi.nlm.nih.gov/tools/vecscreen/univec/). Paired-end filtered reads were assembled *de novo* using Trinity v2.6.6 (Haas et al., 2013) with a default k-mer size of 25 bp and a minimum transcript length of 200 bp. Raw transcripts (n=726,689; 420 Gbp) were filtered for presence of open reading frames (ORFs) (length≥300 bp), longest isoform matches, and mapping rate (≥0.5 transcripts per million; TPM).

Transcripts matching Refseq entries from archaea, plasmids, viruses, and bacteria (BLASTn; *e*-value<10^{-10}), as well those transcripts that aligned significantly (*e*-value<10^{-4}) only to bacterial sequences in the NCBI nt database (max target seqs=5) were discarded in an effort to reduce putative contamination. To segregate between symbiont and host sources, the meta-transcriptome was blasted (BLASTn; *e*-value<10^{-4}) against a pool of Symbiodiniaceae genomes and transcriptomes including former clades A, C, and F [*sensu* (González-Pech, Ragan, & Chan, 2017)]. By default, all hits with no match were considered as originating from the host. For quality control, the *de novo* transcriptome's completeness was assessed with BUSCO's v2 metazoa and v2 eukaryotes databases for clam and Symbiodiniaceae, respectively (Simão, Waterhouse, Ioannidis, Kriventseva, & Zdobnov, 2015). Transcriptomes were annotated by BLAST search against the Uniprot-Swissprot database (BLASTx; *e*-value<10^{-4}). A schematic representation of the overall analysis pipeline has been provided in the Github repository (https://github.com/jleluyer/acclimabest).

Compartment-specific responses of the clam-dinoflagellate holobiont to long-term temperature exposure

Filtered reads were mapped against a combined host-symbiont transcriptome using GSNAP v2018.07.04 (Wu, Reeder, Lawrence, Becker, & Brauer, 2016) using the default parameters but allowing for a maximum mismatch value of 3 and a minimum coverage of 0.85. Only properly paired and uniquely mapped reads were conserved for downstream analysis ("concordant_uniq;" Wu, Reeder, Lawrence, Becker, & Brauer, 2016). Gene counts were conducted with HTSEQ v0.11.2 (Anders, Pyl, & Huber, 2015) using the default parameters. A filtering step including removal of

genes with residual expression >1 count per million (CPM) in 4 individuals was applied, and data were transformed using the *"rlog"* function (betaPriorVar=2) implemented in the DESeq2 v1.23.10 R package (Love, Huber, & Anders, 2014) for host and symbionts separately.

Signed co-expression networks were built for the host and symbiont datasets independently using the R package WGCNA with a filtering step for minimum overall variance (>10%) following the recommendations of Langfelder & Horvath (2008). The main goal of this analysis was to cluster genes in modules correlated with time, temperature, and relevant physiological responses (Figure 1). Briefly, we fixed "soft" threshold powers of 6 and 11 for the host and symbiont datasets, respectively, using the scale-free topology criterion to reach a model fit (|R|) of 0.90 and 0.80, respectively. The modules were defined using the "*cutreeDynamic*" function (minimum of 50 genes by module and default cutting-height=0.99) based on the topological overlap matrix, and an automatic merging step with the threshold fixed at 0.25 (default) allowed us to merge correlated modules. For each module, we defined the module membership (kME; Eigengene-based connectivity), and only statistically significant (p<0.05) modules were conserved for downstream functional analysis (Figure 1). Gene ontology (GO) enrichment analyses were conducted for each module using the GO_MWU R package (Wright, Aglyamova, Meyer, & Matz, 2015) based on the background gene dataset found in WGCNA. GO terms were considered enriched at Benjamini-Hochberg adj. p<0.05 (minimum of three genes for any individual GO term).

Meta-analysis of cultured and *in hospite* Symbiodiniaceae transcriptomes

We integrated publicly available datasets featuring similar experimental designs (i.e. control and elevated temperature conditions over a long-term timescale) to further unravel conserved symbiont responses across genera, holobionts, and culture environments (i.e., cultured vs. *in hospite*). Manuscript searches were conducted with the Web of Science platform using the search formula: «symbio* AND RNAseq* AND temperature» together with informal searches via other research engines (e.g., Google Scholar). A total of three studies met our criteria: Levin *et al*. (2016) and Gierz et al. (2017) for cultured Symbiodiniaceae (n=48 transcriptomes) and Mayfield *et al*. (2014) for the response of Symbiodiniaceae *in hospite* with the scleractinian coral *P. damicornis* (n=12 transcriptomes). Gierz et al. (2017) exposed cultured Symbiodiniaceae (*Fugacium kawagutii*; formerly clade F) to a 31°C heat stress (control temperature=24.5°C) over a 28-day period, while

Levin et al. (2016) exposed Symbiodiniaceae (*Cladocopium goreaui*; formerly type C1; including established thermo-tolerant and thermo-sensitive phenotypes) to a 32°C heat stress (control temperature=27°C) over a 13-day period. Finally, Mayfield *et al*. (2014) exposed corals housing Symbiodiniaceae (*Cladocopium* spp.; formerly a mixed assemblage of clade C individuals) to 30°C over a 9-month period (control temperature=27°C), and both the coral hosts and *in hospite* Symbiodiniaceae appeared to have acclimated to this temperature.

Raw data processing followed the same procedure as described above, though adapted for single-end reads for cultured Symbiodiniaceae datasets. To explore the convergence of Symbiodiniaceae responses despite large phylogenetic differences across the Symbiodiniaceae genera (*Symbiodinium*, *Cladocopium*, and *Fugacium*; LaJeunesse et al., 2018), we first searched for single-copy orthologs across the three genera using OrthoFinder v2.2.7 (Emms & Kelly, 2015) based on publicly available genomes (http://reefgenomics.org/; Liu et al., 2018). We found a total of 4,215 ortho-groups that were used for downstream analyses. The count matrix was filtered for low residual expression genes (>1 CPM in 40 individuals; 4,187 remaining genes), and raw count data were transformed using the "*vst*" function implemented in the DESeq2 R package (Love et al., 2014). We used the "*removeBatchEffect*" function implemented in the Limma R package (Ritchie *et al*., 2015) to remove experimental effects and fit the data prior the downstream analyses.

We then used a combination of redundant discriminant analysis (RDA) and partial dbRDAs approaches to assess the effect of temperature across Symbiodiniaceae clades and experiments. First, we computed a Euclidian distance matrix and performed a principal coordinates analysis (PCoA) on this Euclidian distance matrix using the "daisy" and "pcoa" functions, respectively, implemented in the "ape" R package (Paradis, Claude, & Strimmer, 2004). Only PCo axes explaining at least 2.5% of the total variance were kept for downstream analysis (Legendre & Gallagher, 2001; Legendre & legendre, 2012). To test for the effect of temperature and time, a distance-based redundancy analysis (db-RDA) was also produced with the retained PCo factors (n=8) as a response matrix and the variables temperature, experiment, and time as the explanatory factors. We first carried out stepwise model selection to identify relevant explanatory variables using the *"ordistep"* function implemented in the *vegan* R package (Oksanen et al., 2012) and ultimately retained only temperature and time (p<0.05). Partial db-RDAs were therefore produced to test for the effects of these two parameters

alone (no effect of experiment or genotype) after constraining the remaining variables. The effect of a given factor was considered significant when $p<0.05$. Finally, we used a weighted co-expression network analysis with WGCNA (similar thresholds as described above but with soft power fixed at 14) to reach a model fit (|R|) of 0.83, and subsequent module-wise GO enrichment analyses were undertaken using the GO_MWU R package (Wright et al., 2015).

Genomic basis of thermotolerance in Symbiodiniaceae dinoflagellates

We used an independent WGCNA co-expression network analysis to search for specific gene modules correlated with thermotolerance. For this purpose we focused on the dataset of Levin *et al*. (2016), with *Cladocopium goreaui* as the reference genome (Liu et al., 2018). Indeed, this is the only study to our knowledge featuring established thermotolerant phenotypes with transcriptomic data on long-term time series. The WGCNA analysis followed similar steps as described previously based, though based on rlog-transformed data (betaPrior=2). The soft threshold power was fixed at 20 to reach a model fit (|R|) of 0.85. The downstream, module-wise GO enrichment analyses followed the pipeline outlined above. Finally, we used the '*GO_deltaRanks_correlation'* function implemented in the GO_MWU R package (Wright et al., 2015) to assess similarity between response to stress in symbiont in hospite with clams in and specific mechanisms of thermotolerance for cultured Symbiodiniaceae.

Quantitative PCR- and meta-barcoding-based Symbiodiniaceae analysis

We evaluated the relative levels of various Symbiodiniaceae genera in our clam samples using a series of quantitative PCR (qPCR) assays. Amplifications were carried out on AriaMx real-time PCR System (Agilent, USA) using six primer sets optimized for the amplification of nuclear ribosomal 28S in Symbiodiniaceae of clades/genera A-F (Yamashita, Suzuki, Hayashibara, & Koike, 2011) following the protocol of Rouzé *et al.* (2017). The PCRs (25 µL) comprised 12.5 µL of 2X SYBR® Green master mix (Agilent, USA), 10 µL of DNA (previously diluted to 1 ng μL^{-1}), and 1.25 µL of each primer (forward and reverse; each at a stock concentration of 4 µM). PCR thermocycling included: 1 cycle of pre-incubation for 10 min at 95°C; 40 cycles of amplification (30 s at 95°C, 1 min at 64°C, and 1 min at 72°C), and a melting curve analysis that extended from 60°C to 95°C (30-s

incubations). All measurements were made in duplicate, and all analyses were based on the threshold cycle (Ct) values of the PCR products.

Ct values were averaged across duplicate samples when the variation was not exceeding 1; otherwise, samples were re-run until delta Ct<1. Similarity in relative clade abundance was assessed using PCA analysis of a Bray-Curtis similarity matrix with Hellinger-transformed data. Db-RDAs were conducted to identify whether either temperature or time had a significant impact on Symbiodiniaceae assemblage, and an alpha level of 0.05 was set *a priori*. To complement data from the experimental individuals, qPCRs were carried out with DNA isolated from mantle fragments from the 10 wild individuals described above collected from Reao Atoll [geographically proximal to the origin of the experimental individuals; see Brahmi *et al.*, (2019) for details.] in October 2018. Sample preparation and analyses were performed as described above and in Rouzé et al. (2017).

As a more detailed means of assessing Symbiodiniaceae diversity in the 24 clam samples, a meta-barcoding analysis was undertaken following the protocol of Cunning, Gates, & Edmunds (2017). Briefly, the ITS2 gene was PCR amplified using previously described primers (Cunning, Gates, and Edmunds, 2017) and sequenced at the facility listed above, albeit on a Illumina Miseq 250-bp paired-end platform. The Dada2 algorithm (Callahan et al., 2016) implemented in the QIIME2 software package (Bokulich et al., 2018) was used to infer exact sample sequences from amplicon data. The reference database was directly imported from the NCBI nt repository and trained on the basis of the ITS2 primers following Cunning, Gates, and Edmunds (2017). Detailed protocols and the corresponding scripts have been made available in a public Github repository (https://github.com/jleluyer/acclimabest).

Results

Physiology

We observed no mortality across the 65-day experiment, but some of the individuals exposed to elevated temperature showed signs of partial bleaching in the 30.7°C treatment by day 65. Symbiodiniaceae density and photosynthetic yield (Fv/Fm) were both lower in clams exposed to elevated temperatures (Scheirer-Ray-Hare; H=24.44, p<0.001 and H=22.88, p<0.001, respectively; Figure S1). There was no interaction between time and temperature for Symbiodiniaceae Fv/Fm

(Scheirer-Ray-Hare; H=1.26; p=0.53, Figure S1). Time had only a slight effect on Symbiodiniaceae density (Scheirer-Ray-Hare; H=6.07; p=0.048, Figure S1), though no *post-hoc* differences were detected between individual sampling times (Dunn's test; p>0.05).

Symbiodiniaceae communities *in hospite* with clams

The Symbiodiniaceae communities of all clam hosts (from both control and high temperature conditions) were primarily composed of *Symbiodinium* spp. (formerly clade A; Figure 1A). Four clams, however, were characterized by secondary populations of *Cladocopium* spp. (formerly clade C; with relative proportions reaching 1.8 to 32.8%), as well as residual quantities (<0.001%) of *Breviolum* (formerly clade B) and *Fugacium* (formerly clade F). There were no detectable effects of prolonged high-temperature exposure of the Symbiodiniaceae assemblages within the giant clam samples (Figure 1B). Similarly, *in situ* clam samples from Reao Atoll were also dominated by *Symbiodinium* spp. (mean 93.0%±10.7 SD), with smaller populations of *Breviolum* spp. and *Cladocopium* spp. Given the similarities in Symbiodiniaceae assemblages between the experimental and *in situ* specimens, we conclude that transport out of the ocean and into the aquarium husbandry facility did not result in community changes that could bias the results described below.

Metabarcoding of the internal transcribed spacer 2 (ITS2) sequence resulted in an average of 186.7k ± 25.7 PE sequences per sample. After sequence pre-processing, the Dada2 algorithm reported a total of 12 amplicon sequence variants matching to *Symbiodinium* spp. (N=9) and *Cladocopium* spp. (N=3) that paralleled results from qPCRs. *Symbiodinium* sequence variants mainly matched to *S. tridacnidorum* (formerly sub-clade A3; best-hit BLASTn e-value<10^{-6}). Neither cladal/genera representation based on UniFrac distance (PERMANOVA; pseudo-F=1.3; q-value=0.33) nor evenness values (Kruskall-Wallis; H=0.04; q-value=0.83) differed significantly between temperatures.

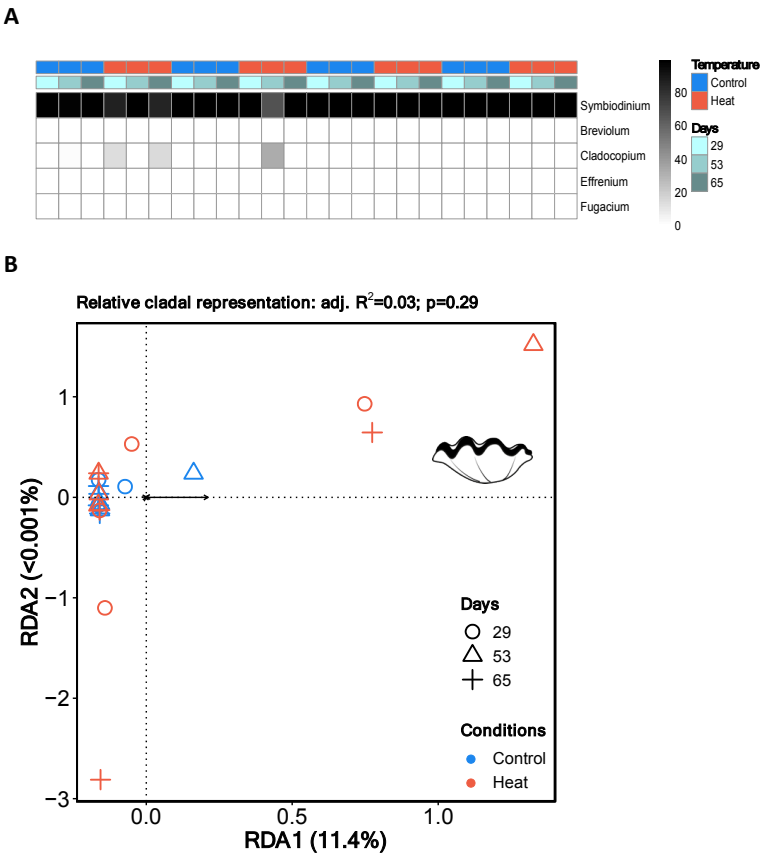

Figure 1: Symbiodiniaceae community representation assessed by qPCR, metabarcoding, and multivariate analysis. (A) Heatmap showing the median relative clade proportion by group (N=4 individuals/group), as determined by qPCR. (B) RDA representation based on PCoA of Euclidian distances.

Transcriptome assemblies

A total of 363.70 million 100-bp paired-end reads were used to assemble a raw meta-transcriptome (host + symbionts) of 726,689 transcripts (420.02 Gbp). After stringent filtering and segregation of host and Symbiodiniaceae sequences, the assemblies resulted in a transcriptome for *T. maxima* of 24,234 contigs (N50=1,011 bp; GC content=40.1%) and a meta-transcriptome for Symbiodiniaceae of 51,648 contigs (N50=1,027 bp; GC content=57.9%). High G-C content is

generally a hallmark of Symbiodiniaceae transcriptomes (González-Pech et al., 2017). Transcriptome statistics and annotations are provided in Figure 2 and Table S1, respectively.

A

Tridacna maxima	
Total number of transcripts	24,234
Average percent G-C	40.15
Contig N50	1,768
Median contig length (bp)	1,011
Average contig length (bp)	1,276.13
Total assembled bases	30,925,845

***Symbiodinium* spp.**	
Total number of transcripts	51,648
Average percent G-C	57.9
Contig N50	1,027
Median contig length (bp)	688
Average contig length (bp)	845.89
Total assembled bases	43,688,343

B

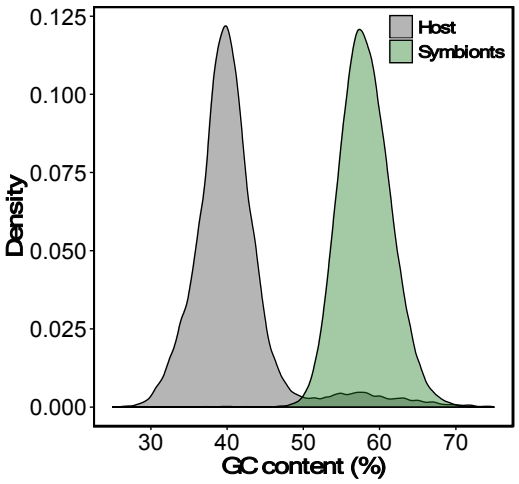

Figure 2: Transcriptome assembly statistics. (A) Table showing various assembly metrics for *Tridacna maxima* and Symbiodiniaceae. (B) Density plot of the relative G-C content (%) for Symbiodiniaceae and *Tridacna maxima* contigs.

Host clam acclimation response to prolonged high-temperature exposure

A gene co-expression network was built using the normalized RNA-Seq data from which low-expression genes had been eliminated, and three modules correlated significantly (p<0.05) with temperature and/or physiological data (including oxygen production, Symbiodiniaceae density and Fv/FM, and host dry weight; Figure S2). No module was correlated with sampling time, O_2 consumption, or shell extension. A single host module ($pink_{host}$) positively correlated with temperature (R=0.82) and negatively with photosynthetic rate and symbiont density (R=-0.52 and R=-0.48, respectively; Figure S2). The red_{host} module also correlated positively with Fv/Fm (R=0.59) but not significantly with temperature (R=-0.38; p=0.08). Among the most enriched GO terms in the $pink_{host}$ module were pituitary gland development (GO:0021983), L-ascorbic acid metabolic processes (GO:0019852), regulation of extrinsic apoptotic signaling pathways (GO:2001236), cholesterol efflux (GO:0033344), cilium movement (GO:0003341), and ommochrome biosynthetic processes (GO:0006727). Ommochromes are biological pigments and metabolites of tryptophan (Figon & Casas, 2019). The red_{host} module was enriched for cation transport (GO:0006812), neurotransmitter

uptake (GO:0001504), fructose 6-phosphate metabolic processes (GO:0006002), and reactive oxygen species metabolic processes (GO:0072593). Host module membership eigenvalues were also integrated with the symbiont network analysis (Figure 3), and a complete list of GO-enriched functions has been provided in Table S2.

Acclimation to prolonged high-temperature exposure in Symbiodiniaceae *in hospite* with clams

Co-expression network analysis of Symbiodiniaceae showed more modules correlated with temperature than for the clam host, either negatively [midnightblue$_{symbiont}$ (R=-0.94), blue$_{symbiont}$ (R=-0.45)] or positively [cyan$_{symbiont}$ (R=0.61), black$_{symbiont}$ (R=0.91), yellow$_{symbiont}$ (R=0.52), and pink$_{symbiont}$ (R=0.85); Figure 3]. Among the enriched GO terms in the black$_{symbiont}$ module were RNA processing (GO:0006396), methylation (GO:0043414), chloroplast-nucleus signaling pathways (GO:0031930), and glycerolipid metabolic processes (GO:0046486). For the cyan$_{symbiont}$ module, enriched GO terms included response to vitamins (GO:0033273), response to UV-C (GO:0071494), regulation of transferase activity (GO:0051338), intrinsic apoptotic signaling pathways (GO:0097193), and induced systemic resistance (GO:0009682). The yellow$_{symbiont}$ module featured RNA modification (GO:0009451) and aspartate family amino acid metabolic processes (GO:0009066). Finally, the blue$_{symbiont}$ module showed enrichment for movement of cellular or subcellular components (GO:0006928), reproduction (GO:0000003), regulation of cell shape (GO:0008360), oxidation-reduction processes (GO:0055114), and electron transport chain (GO:0022900) while the midnightblue$_{symbiont}$ module featured enrichment for regulation of BMP signaling pathways (GO:0030510), hormone biosynthetic processes (GO:0042446), peptidyl-lysine dimethylation (GO:0018027), short-term memory (GO:0007614), and response to red or far, red light (GO:0009639). The complete GO enrichment results can be found in Table S2.

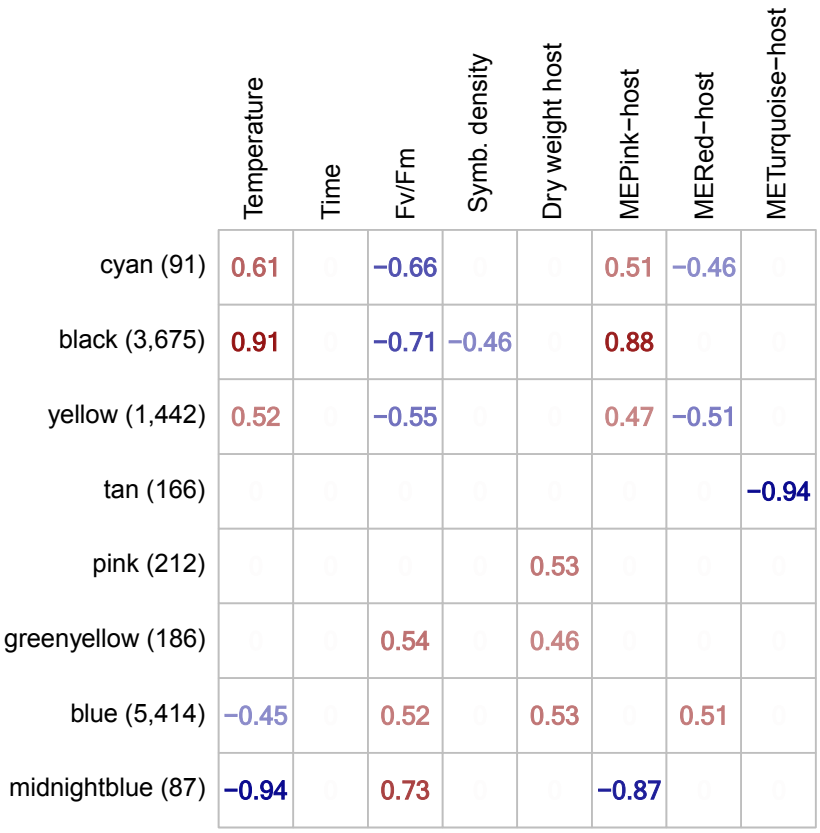

Figure 3: Correlation matrix of symbiont gene expression modules against experimental factors (temperature and time), quantitative physiological traits, and module membership (ME) for host modules. Genes have been clustered in modules (y–axis) according to their co-expression values. Values in cells indicate Pearson's correlation scores, and only statistically significant correlations (p<0.05) are depicted.

Multivariate analysis of public Symbiodiniaceae datasets

We used db-RDA to document gene expression variation in public Symbiodiniaceae datasets [in culture and *in hospite* with corals and clams (this study)], with temperature and time as the explanatory variables; there was a focus on single-copy orthologs from the genera *Cladocopium*, *Fugacium*, and *Symbiodinium*. The overall model was significant (p<0.001), and the adjusted R^2 was 0.12 (Figure 4). Partial db-RDAs showed that temperature also had a significant effect on total gene expression variation across genotypes and experiments (1000 permutations; F=9.07, p=0.001). A

WGCNA analysis was conducted to identify genes cluster correlated with temperature across all the orthologous genes (Figure S3).

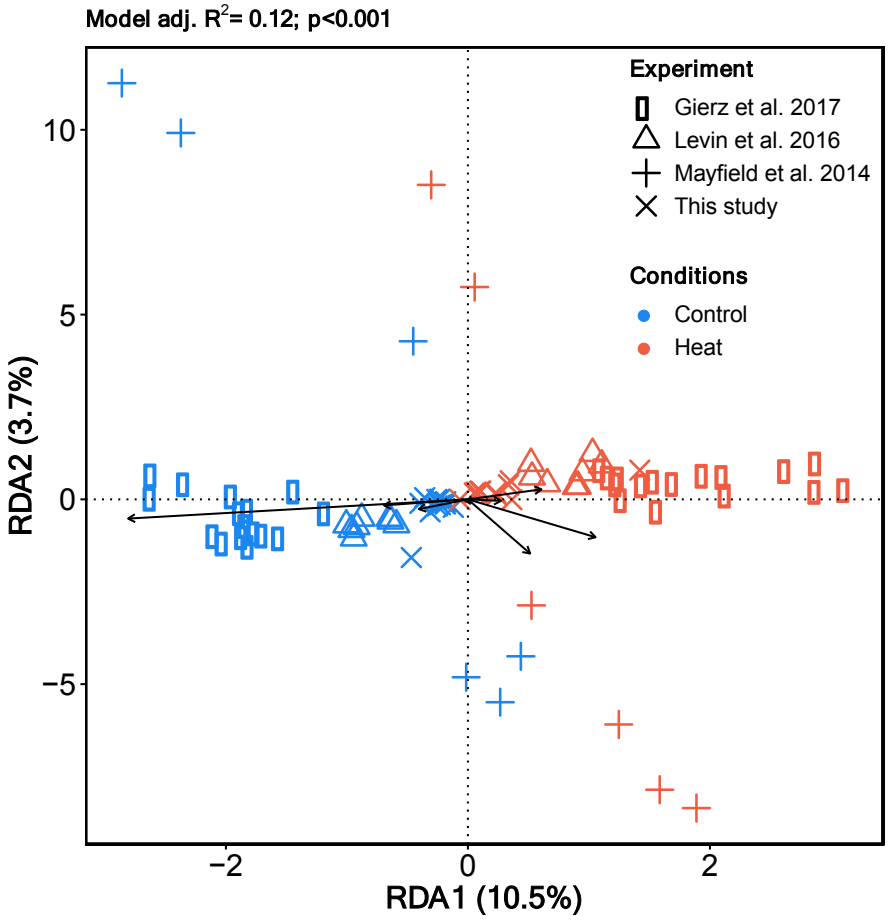

Figure 4: RDA of cultured Symbiodiniaceae (*Cladocopium* type C1 and *Fugacium kawagutii*) and *in hospite* with corals (*Cladocopium*) and giant clams (*Symbiodinium* spp.). The reference dataset only included the single-copy orthologous genes across the three genera (N=4,187 orthologs remaining after filtering for residual expression).

Search for thermotolerance-specific genes clusters

We also conducted independent WGCNA analyses to assess acclimatory responses in cultured Symbiodiniaceae based on the *Cladocopium goreaui* (formerly type C1) genome (Liu *et al*., 2018)

and compared them with thermotolerant phenotypes (Levin *et al*., 2016). No individual module correlated with time. Instead, we found the majority of the genes to be correlated with temperature, and three modules were uncovered: darkgrey$_{C1}$ (R=0.82), saddlebrown$_{C1}$ (R=-0.89; N=1,354), and orange$_{c1}$ (R=-0.87; N=378; Figure S4). We also found three modules (darkolivegreen$_{C1}$, lightgreen$_{C1}$, and white$_{C1}$) that were significantly correlated with thermotolerance (R=-0.74, -0.99, and 0.98, respectively; Figure S4) but not temperature. These modules effectively differentiated thermo-sensitive Symbiodiniaceae from thermotolerant C1 phenotypes described in Levin *et al*. (2016). Among the most enriched GO terms for lightgreen$_{c1}$ were cellular response to amino acid stimulus (GO:0071230), DNA methylation (GO:0006306), and genetic imprinting (GO:0071514; Figure S4 and Table S2). Furthermore, we found that impact on methylation-associated biological processes [methylation (GO:0032259) and macromolecule methylation (GO:0043414)] was conserved in the lightgreen$_{C1}$ module and the response to temperature of symbionts *in hospite* with clams (black$_{symb}$ module; Figure S5).

Discussion

Temperature increases are threatening marine invertebrate populations worldwide, especially for species already living at, or close to, their upper thermal tolerance limits (Hoffmann & Sgrò, 2011). Recent heat wave events have resulted in ~90% declines in *T. maxima* populations in some atolls of French Polynesia (Andréfouët et al., 2013, 2017). While several studies have investigated the invertebrate (mollusc and cnidarian) response to heat stress over short-term timescales, relatively few have investigated the prolonged response to elevated temperatures (e.g., Mayfield et al., 2014). Although our clam samples ultimately acclimated to an experimentally elevated temperatures of nearly 31°C, Symbiodiniaceae density was reduced in thermally challenged clams, and both host clams and their Symbiodiniaceae populations underwent gene expression changes over the course of this two-month experiment. Upon discussing such temperature-driven changes in gene expression, we

highlight some intrinsic responses of the symbionts (i.e., independent of the host species) and identify key mechanisms potentially underlying their thermal-tolerance.

Genus-specific fidelity in clam hosts might preclude symbiont community shifts/shuffling as a thermal acclimation strategy

A 1.5°C temperature elevation over a 65-day period was sufficient to induce a significant reduction in symbiont density in clams; no bleaching (even partial) was observed in control temperature clams. Our results support previous studies of corals and giant clams in which high-temperature exposure led to sub-lethal bleaching (Ainsworth, Hoegh-Guldberg, Heron, Skirving, & Leggat, 2008; Brahmi et al., 2019; Hoegh-Guldberg & Smith, 1989; Jones, Hoegh-Guldberg, Larkum, & Schreiber, 1998; Leggat et al., 2003; Warner, Fitt, & Schmidt, 1999; Zhou et al., 2018); whether the cellular mechanisms of bleaching are conserved between corals and giant clams remains to be determined (Mies et al., 2017; Zhou et al., 2018).

For some coral species, resilience to heat stress is associated with a more flexible symbiotic association (i.e., the capacity to shift from one dominant Symbiodiniaceae genus to another) (Hume et al., 2015; LaJeunesse et al., 2004; Putnam, Stat, Pochon, & Gates, 2012; Rowan, 2004; Silverstein, Correa, & Baker, 2012). Indeed, some bleaching events have largely been attributed to the thermal sensitivity of specific endosymbiotic Symbiodiniaceae residing in coral host tissues (Berkelmans & van Oppen, 2006; Oliver & Palumbi, 2011). Corals hosting *Cladocopium* spp. (formerly clade C) are typically more prone to bleaching, whereas those housing certain lineages of *Durusdinium* (formerly clade D) have demonstrated enhanced thermotolerance (Baker, 2003; Mieog, van Oppen, Cantin, Stam, & Olsen, 2007). Interestingly, *Cladocopium* spp. and/or *Durusdinium* spp. are more commonly found in giant clams inhabiting warmer environments while *Symbiodinium* spp. (formerly clade A) are more common in clams located in cooler waters (DeBoer et al., 2012). Herein, the Symbiodiniaceae communities were predominantly composed of *Symbiodinium* spp., even after two months of high-temperature exposure; this finding aligns with other studies in corals that found Symbiodiniaceae assemblages to be temporally stable, even as environmental conditions changed (Goulet, 2006; Sampayo, Ridgway, Bongaerts, & Hoegh-Guldberg, 2008; Thornhill, LaJeunesse, Kemp, Fitt, & Schmidt, 2006; Thornhill, Xiang, Fitt, & Santos, 2009). This was not an artifact due to

the experimental conditions enacted since individuals sampled from their original locations *in situ* also predominantly host *Symbiodinium* spp. (i.e., clade A).

Such a high proportion of *Symbiodinium* spp. in giant clams was expected, and it has also been reported in the sea anemone *Anemonia viridis*; however, it is in sharp contrast with other invertebrate hosts such as corals, which host a broader Symbiodiniaceae diversity (Manning & Gates, 2008; Rouzé et al., 2017; Stat, Carter, & Hoegh-Guldberg, 2006). This near-exclusive hosting of *Symbiodinium* spp. in clams, and the temporal stability of their association, suggests that some selection process favors this dinoflagellate lineage (or else impairs recruitment of others); lectin/glycan interactions were once thought to play a role, possibly in the primary recognition-related processes (Wood-Charlson, Hollingsworth, Krupp, & Weis, 2006), though this hypothesis has recently been called into question (Parkinson et al., 2018). Admittedly, broader *in situ* clam sampling, (e.g., encompassing different times of the year) will be necessary to verify the fidelity between *Symbiodinium* spp. and giant clams, and whether mixed-genera assemblages are common *in situ* (DeBoer et al., 2012; Parkinson, Banaszak, Altman, LaJeunesse, & Baums, 2015). The presumably low flexibility would appear to preclude community shifts as a strategy for these clams to cope with increased temperatures, at least in our experimental context. Rather than adaptation (i.e., a community shift resulting in a new "holobiont genomic landscape"), acclimation (i.e., physiological changes that initially manifested at the molecular level) appears to have played a larger role in this study.

Effect of prolonged exposure to elevated temperature on the clam transcriptome

Both host clam and Symbiodiniaceae gene expression were affected by elevated temperature exposure, with no significant effects of time from 29 days onwards; the temperature-related differences were from thenceforth sustained over time. We found one gene module positively impacted by temperature and negatively correlated with symbiont Fv/Fm and density. This module showed enrichment for ommochrome biosynthesis process and specifically included the tryptophan 2,3-dioxygenase coding gene (TDO), a pivotal regulator of systemic tryptophan levels also involved in the response to oxidative stress (Forrest et al., 2004; Thackray, Mowat, & Chapman, 2008). Tryptophan is the precursor of 5-hydroxytryptamine (5-HT), a bivalve serotonin transmitter that plays critical roles in numerous physiological functions [e.g., reproduction (Alavi, Nagasawa, Takahashi, & Osada, 2017)]. In larvae from the coral *Orbicella faveolata*, TDO (referred to as AGAP) was up-

regulated in response to ultraviolet radiation, and larval fitness (locomotion and settlement) went on to suffer (Aranda et al., 2011). A more thorough understanding, then, of ommochrome biosynthesis and, more generally, tryptophan regulation, is likely to be key to elucidating the molecular regulation of invertebrate-dinoflagellate symbioses, nearly all of which involve at least some degree of nitrogen transfer within holobionts (Chan et al., 2018).

A single module was 1) positively correlated with the maximum dark-adapted yield of photosystem II (Fv/Fm) and 2) enriched for genes encoding proteins involved in glyceraldehyde-3-phosphate metabolic processes. Glycerol excretion from dinoflagellate symbionts is largely influenced by the presence of host tissues (Muscatine, 1967). The glyceraldehyde-3-phosphate pathway, which culminates in glycerol production, was also significantly affected by sub-lethal elevated temperature (30°C) exposure in the reef coral *P. damicornis* (Mayfield et al., 2014). Pollutant exposure also altered the expression of genes involved in carbohydrate metabolism, albeit only in the coral host compartment (and not in Symbiodiniaceae) in another study (Gust *et al.*, 2014). Admittedly, we did not assess the proportion of energy derived from autotrophy herein, which ranges widely (from 25 to up to 100%) and is dependent on the species and/or life history stage in the *Tridacna* genus (Fisher, Fitt, & Trench, 1985; Klumpp et al., 1992; Klumpp & Griffiths, 1994); shifts from autotrophy to heterotrophy, and vice versa, are likely to affect host gene expression patterns. All that can be stated at present is that regulation of tryptophan levels and impairment of carbohydrate metabolism might be key elements in the long-term response to elevated temperature in clams; indeed, these two processes could be inter-linked. However, how these changes would affect fine-scale interactions between the host and symbionts remains to be explored and should be the focus of future studies of clam-Symbiodiniaceae symbioses.

The response of Symbiodiniaceae dinoflagellates *in hospite* with clams to prolonged elevated temperature exposure

Overall, gene clusters of Symbiodiniaceae showed positive correlation between expression levels and prolonged elevated temperature exposure, and some of the modules were also correlated with the lower Symbiodiniaceae Fv/Fm and cell densities documented at elevated temperatures. Other physiological studies have also shown that high temperatures lead to diminished photosynthetic yield in several clades of Symbiodiniaceae (Grégoire, Schmacka, Coffroth, & Karsten, 2017). In terms of

the RNA-Seq data, genes encoding proteins involved in nitrogen metabolism were significantly affected by high-temperature exposure, and this module correlated with host tryptophan dehydrogenase activity. Interestingly, this GO includes the salt- and drought-induced ring finger1 (SDIR 1)-coding gene known in plants to control abscisic acid (ABA) signal transduction (Zhang et al., 2007), a process that has never before been reported in Symbiodiniaceae. The phytohormone ABA and ROS regulating/modulating proteins are key molecular constituents involved in the capacity to acclimate to abiotic stressors, including oxidative stress tolerance in unicellular algae (Lu & Xu, 2015). Furthermore, up-regulation of ABA signaling genes is associated with a later increase in ABA biosynthesis in several plant species (Vishwakarma et al., 2017). The role of ABA signaling in the thermo-adaptation of Symbiodiniaceae dinoflagellates may consequently be a fruitful avenue for future research.

Herein we also found that expression of genes encoding certain components of the photosynthetic machinery, especially photosystem II (PSII), was dampened at elevated temperature. PSII integrity is vital for proper Symbiodiniaceae function, and PSII damage has been directly linked to bleaching in corals (Warner et al., 1999). It is noteworthy that the same gene module also included chloroplast thylakoid membrane rearrangement-related genes, which are used by Symbiodiniaceae and other photosynthetic organisms to cope with heat and high UV radiation (Sharkey, 2005; Slavov et al., 2016). Although the clam-dinoflagellate holobionts generally appeared to have acclimated to elevated temperatures over our two-month experiment (no large-scale bleaching), the Symbiodiniaceae communities, then, showed signs of intracellular stress given these gene expression changes, as well as the decreases in cell density and Fv/Fm. Whether or not these holobionts could have sustained an even longer exposure to ~31°C remains to be determined, though it is worth noting that, unlike *in situ*, clams were not fed in the aquaria. It is thus likely that clams allowed to feed both autotrophically *and* heterotrophically might, then, have an even superior capacity for high-temperature acclimation.

Conserved response to high temperatures across Symbiodiniaceae genera and molecular mechanisms linked to thermo-acclimation capacity

We documented a conserved response to long-term exposure to elevated temperature across Symbiodiniaceae genera based only on orthologous genes, which is noteworthy given the large evolutionary distance between genera (Correa & Baker, 2009; LaJeunesse, 2001). This common

response, which transcended the host effect, included genes involved in regulation of the DNA damage response, wound healing and low-temperature responses, chromatin remodeling, mRNA splicing, regulation of lipid biosynthetic processes, and motile cilium assembly. Our results, however, most likely underestimate the molecular complexity of thermo-acclimation given our use of exclusively "single-to-single" orthologous genes. It is also possible that there are holobiont-specific responses that were not explored or detected herein with our bioinformatics approach. For instance, recent studies have shown that the Symbiodiniaceae diverged, in part, in relation to their capacity for synthesizing UV-absorbing mycosporine-like amino acids (Shoguchi et al., 2013). Furthermore, while UV-B radiation in cultured Symbiodiniaceae drastically reduces photosynthetic output, such is not always observed for cells *in hospite* with clams since the clam hosts produce UV-absorbing proteins (Ishikura, Kato, & Maruyama, 1997).

We further explored basal differences within the *Cladocopium* genus that would differentiate the contrastingly thermotolerant phenotypes. We found that differences between thermotolerant phenotypes were driven by molecular pathways uncovered previously (Levin et al., 2016), including meiotic nuclear division and glutathione disulfide oxidoreductase activity; expression of genes involved in photosynthesis, cellular heat acclimation, and methylation programming also differed across gradients of thermotolerance. Regarding the latter, epigenetic landscape rearrangement has been shown to play a role in transgenerational inheritance of thermo-tolerance of various plant models (Bruce, Matthes, Napier, & Pickett, 2007). Here, thermotolerance-associated modules generally did not correlate with temperature, suggesting that phenotypes have intrinsic gene expression signatures that respond differentially to changes in temperature. It is known that in plants DNA methylation and histone modification are associated with the response to heat stress, and, more specifically, act to prevent heat-associated macromolecular damage (Liu, Feng, Li, & He, 2015). Such methylation changes might be inherited and account for, at least in part, the remarkable ability of plants to adapt and/or acclimate quickly to stressful environments (Ganguly, Crisp, Eichten, & Pogson, 2017; Lämke & Bäurle, 2017).

Conclusions

The co-expression network analysis proved to be a powerful tool for dissecting compartment-specific transcriptomic responses in symbiotic systems. This is especially true when looking for acclimatory signatures that, in contrast to short-term stress responses, are characterized by rather subtle changes over longer periods. Indeed, our data from a long-term high temperature study revealed that different cellular processes are impacted in the host clam and *in hospite* Symbiodiniaceae compartments; genes encoding key photosynthesis proteins were particularly temperature sensitive in not only Symbiodiniaceae *in hospite*, but also in culture. Future studies focusing on the range of optimal thermal conditions of the *T. maxima* species may improve our understanding on the thermal tolerance of the clams and their symbionts. Although the giant clams used in this study ultimately survived a two-month exposure to nearly 31°C, it is possible that slightly higher temperatures, or extended exposure times, might cause them to bleach to such a great extent that they would not survive. Regardless, our data show that novel mechanisms involving epigenetic landscape rearrangement are associated with elevated Symbiodiniaceae thermotolerance. How the impact of stressful environmental conditions might impact the subsequent generation's tolerance and/or physiological capacities (i.e., epigenetic effects) must consequently be addressed in the near future.

References

Addessi, L. (2001). Giant clam bleaching in the lagoon of Takapoto atoll (French Polynesia). *Coral Reefs*, *19*(3), 220–220. https://doi.org/10.1007/PL00006957

Ainsworth, T. D., Hoegh-Guldberg, O., Heron, S. F., Skirving, W. J., & Leggat, W. (2008). Early cellular changes are indicators of pre-bleaching thermal stress in the coral host. *Journal of Experimental Marine Biology and Ecology*, *364*(2), 63–71. https://doi.org/10.1016/j.jembe.2008.06.032

Alavi, S. M. H., Nagasawa, K., Takahashi, K. G., & Osada, M. (2017). Structure-function of serotonin in bivalve molluscs. In K. F. Shad (Ed.), *Serotonin - A Chemical Messenger Between All Types of Living Cells*. https://doi.org/10.5772/intechopen.69165

Anders, S., Pyl, P. T., & Huber, W. (2015). HTSeq—a Python framework to work with high-

throughput sequencing data. *Bioinformatics*, *31*(2), 166–169. https://doi.org/10.1093/bioinformatics/btu638

Andréfouët, S., Van Wynsberge, S., Gaertner-Mazouni, N., Menkes, C., Gilbert, A., & Remoissenet, G. (2013). Climate variability and massive mortalities challenge giant clam conservation and management efforts in French Polynesia atolls. *Biological Conservation*, *160*, 190–199. https://doi.org/10.1016/j.biocon.2013.01.017

Andréfouët, S., Wynsberge, S. V., Kabbadj, L., Wabnitz, C. C. C., Menkes, C., Tamata, T., … Remoissenet, G. (2017). Adaptive management for the sustainable exploitation of lagoon resources in remote islands: lessons from a massive El Niño-induced giant clam bleaching event in the Tuamotu atolls (French Polynesia). *Environmental Conservation*, 1–11. https://doi.org/10.1017/S0376892917000212

Aranda, M., Banaszak, A. T., Bayer, T., Luyten, J. R., Medina, M., & Voolstra, C. R. (2011). Differential sensitivity of coral larvae to natural levels of ultraviolet radiation during the onset of larval competence. *Molecular Ecology*, *20*(14), 2955–2972. https://doi.org/10.1111/j.1365-294X.2011.05153.x

Baillie, B. K., Belda-Baillie, C. A., & Maruyama, T. (2000). Conspecificity and Indo-Pacific distribution of *Symbiodinium* genotypes (Dinophyceae) from giant clams. *Journal of Phycology*, *36*(6), 1153–1161. https://doi.org/10.1046/j.1529-8817.2000.00010.x

Baker, A. C. (2003). Flexibility and Specificity in Coral-Algal Symbiosis: Diversity, Ecology, and Biogeography of *Symbiodinium*. *Annual Review of Ecology, Evolution, and Systematics*, *34*(1), 661–689. https://doi.org/10.1146/annurev.ecolsys.34.011802.132417

Barshis, D. J., Ladner, J. T., Oliver, T. A., & Palumbi, S. R. (2014). Lineage-Specific Transcriptional Profiles of *Symbiodinium spp.* Unaltered by Heat Stress in a Coral Host. *Molecular Biology and Evolution*, *31*(6), 1343–1352. https://doi.org/10.1093/molbev/msu107

Barshis, D. J., Ladner, J. T., Oliver, T. A., Seneca, F. O., Traylor-Knowles, N., & Palumbi, S. R. (2013). Genomic basis for coral resilience to climate change. *Proceedings of the National Academy of Sciences*, *110*(4), 1387–1392.

Berkelmans, R., & van Oppen, M. J. H. (2006). The role of zooxanthellae in the thermal tolerance of corals: a "nugget of hope" for coral reefs in an era of climate change. *Proceedings of the Royal*

Society B: Biological Sciences, *273*(1599), 2305–2312. https://doi.org/10.1098/rspb.2006.3567

Bokulich, N. A., Kaehler, B. D., Rideout, J. R., Dillon, M., Bolyen, E., Knight, R., … Gregory Caporaso, J. (2018). Optimizing taxonomic classification of marker-gene amplicon sequences with QIIME 2's q2-feature-classifier plugin. *Microbiome*, *6*(1). https://doi.org/10.1186/s40168-018-0470-z

Bolger, A. M., Lohse, M., & Usadel, B. (2014). Trimmomatic: a flexible trimmer for Illumina sequence data. *Bioinformatics*, *30*(15), 2114–2120. https://doi.org/10.1093/bioinformatics/btu170

Brahmi, Chloé, Le Moullac, G., Soyez, C., Beliaeff, B., Lazareth, C. E., Gaertner-Mazouni, N., & Vidal-Dupiol, J. (2019). *Effects of temperature and* p *CO* $_2$ *on the respiration, biomineralization and photophysiology of the giant clam* Tridacna maxima. https://doi.org/10.1101/672907

Brahmi, Chloe, Le Moullac, G., Soyez, C., Chapron, L., Gaertner-Mazouni, N., & Vidal-Dupiol, J. (2019). Effects of temperature and pH on the respiration, biomineralization and photophysiology of the giant clam *Tridacna maxima*. *BioRxiv*.

Bruce, T. J. A., Matthes, M. C., Napier, J. A., & Pickett, J. A. (2007). Stressful "memories" of plants: Evidence and possible mechanisms. *Plant Science*, *173*(6), 603–608. https://doi.org/10.1016/j.plantsci.2007.09.002

Buck, B. (2002). Effect of increased irradiance and thermal stress on the symbiosis of *Symbiodinium microadriaticum* and *Tridacna gigas*. *Aquatic Living Resources*, *15*(2), 107–117. https://doi.org/10.1016/S0990-7440(02)01159-2

Callahan, B. J., McMurdie, P. J., Rosen, M. J., Han, A. W., Johnson, A. J. A., & Holmes, S. P. (2016). DADA2: High resolution sample inference from Illumina amplicon data. *Nature Methods*, *13*(7), 581–583. https://doi.org/10.1038/nmeth.3869

Chan, C. Y. L., Hiong, K. C., Boo, M. V., Choo, C. Y. L., Wong, W. P., Chew, S. F., & Ip, Y. K. (2018). Light exposure enhances urea absorption in the fluted giant clam, *Tridacna squamosa*, and up-regulates the protein abundance of a light-dependent urea active transporter, DUR3-like, in its ctenidium. *Journal of Experimental Biology*, *221*(8), jeb176313. https://doi.org/10.1242/jeb.176313

Correa, A. M. S., & Baker, A. C. (2009). Understanding diversity in coral-algal symbiosis: a cluster-based approach to interpreting fine-scale genetic variation in the genus *Symbiodinium*. *Coral Reefs*, *28*(1), 81–93. https://doi.org/10.1007/s00338-008-0456-6

Crowder, C. M., Meyer, E., Fan, T.-Y., & Weis, V. M. (2017). Impacts of temperature and lunar day

on gene expression profiles during a monthly reproductive cycle in the brooding coral *Pocillopora damicornis*. *Molecular Ecology*, *26*(15), 3913–3925. https://doi.org/10.1111/mec.14162

Cunning, R., Gates, R. D., & Edmunds, P. J. (2017). *Using high-throughput sequencing of ITS2 to describe Symbiodinium metacommunities in St. John, U.S. Virgin Islands* (No. e2925v1). Retrieved from PeerJ Preprints website: https://peerj.com/preprints/2925

DeBoer, T., Baker, A., Erdmann, M., Ambariyanto, Jones, P., & Barber, P. (2012). Patterns of *Symbiodinium* distribution in three giant clam species across the biodiverse Bird's Head region of Indonesia. *Marine Ecology Progress Series*, *444*, 117–132. https://doi.org/10.3354/meps09413

Dubousquet, V., Gros, E., Berteaux-Lecellier, V., Viguier, B., Raharivelomanana, P., Bertrand, C., & Lecellier, G. J. (2016). Changes in fatty acid composition in the giant clam *Tridacna maxima* in response to thermal stress. *Biology Open*, *5*(10), 1400–1407. https://doi.org/10.1242/bio.017921

Emms, D. M., & Kelly, S. (2015). OrthoFinder: solving fundamental biases in whole genome comparisons dramatically improves orthogroup inference accuracy. *Genome Biology*, *16*(1), 157. https://doi.org/10.1186/s13059-015-0721-2

Figon, F., & Casas, J. (2019). Ommochromes in invertebrates: biochemistry and cell biology: Ommochromes in invertebrates. *Biological Reviews*, *94*(1), 156–183. https://doi.org/10.1111/brv.12441

Fisher, C. R., Fitt, W. K., & Trench, R. K. (1985). Photosynthesis and respiration in *Tridacna gigas* as a function of irradiance and size. *The Biological Bulletin*, *169*(1), 230–245. https://doi.org/10.2307/1541400

Fitt, W., Brown, B., Warner, M., & Dunne, R. (2001). Coral bleaching: interpretation of thermal tolerance limits and thermal thresholds in tropical corals. *Coral Reefs*, *20*(1), 51–65. https://doi.org/10.1007/s003380100146

Forrest, C. M., Mackay, G. M., Stoy, N., Egerton, M., Christofides, J., Stone, T. W., & Darlington, L. G. (2004). Tryptophan Loading Induces Oxidative Stress. *Free Radical Research*, *38*(11), 1167–1171. https://doi.org/10.1080/10715760400011437

Ganguly, D. R., Crisp, P. A., Eichten, S. R., & Pogson, B. J. (2017). The Arabidopsis DNA methylome is stable under transgenerational drought stress. *Plant Physiology*, *175*(4), 1893–1912. https://doi.org/10.1104/pp.17.00744

Gierz, S. L., Forêt, S., & Leggat, W. (2017). Transcriptomic analysis of thermally stressed *Symbiodinium* reveals differential expression of stress and metabolism genes. *Frontiers in Plant Science*, *8*. https://doi.org/10.3389/fpls.2017.00271

Gilbert, A., Yan, L., Remoissenet, G., Andréfouët, S., Payri, C., & Chancerelle, Y. (2005). Extraordinarily high giant clam density under protection in Tatakoto atoll (Eastern Tuamotu archipelago, French Polynesia). *Coral Reefs*, *24*(3), 495–495. https://doi.org/10.1007/s00338-005-0494-2

Gilbert, Antoine, Remoissenet, G., Yan, L., & Andrefouet, S. (2006). Special traits and promises of the giant clam (*Tridacna maxima*) in French Polynesia. *Fisheries Newsletter-South Pacific Commission*, *118*, 44.

González-Pech, R. A., Ragan, M. A., & Chan, C. X. (2017). Signatures of adaptation and symbiosis in genomes and transcriptomes of *Symbiodinium*. *Scientific Reports*, *7*(1). https://doi.org/10.1038/s41598-017-15029-w

Goulet, T. (2006). Most corals may not change their symbionts. *Marine Ecology Progress Series*, *321*, 1–7. https://doi.org/10.3354/meps321001

Grégoire, V., Schmacka, F., Coffroth, M. A., & Karsten, U. (2017). Photophysiological and thermal tolerance of various genotypes of the coral endosymbiont *Symbiodinium* sp. (Dinophyceae). *Journal of Applied Phycology*, *29*(4), 1893–1905. https://doi.org/10.1007/s10811-017-1127-1

Gust, K. A., Najar, F. Z., Habib, T., Lotufo, G. R., Piggot, A. M., Fouke, B. W., … Perkins, E. J. (2014). Coral-zooxanthellae meta-transcriptomics reveals integrated response to pollutant stress. *BMC Genomics*, *15*(1), 591. https://doi.org/10.1186/1471-2164-15-591

Haas, B. J., Papanicolaou, A., Yassour, M., Grabherr, M., Blood, P. D., Bowden, J., … Regev, A. (2013). De novo transcript sequence reconstruction from RNA-seq using the Trinity platform for reference generation and analysis. *Nature Protocols*, *8*(8), 1494–1512. https://doi.org/10.1038/nprot.2013.084

Hawkins, A. J. S., & Klumpp, D. W. (1995). Nutrition of the giant clam *Tridacna gigas* (L.). II. Relative contributions of filter-feeding and the ammonium-nitrogen acquired and recycled by symbiotic alga towards total nitrogen requirements for tissue growth and metabolism. *Journal of Experimental Marine Biology and Ecology*, *190*(2), 263–290. https://doi.org/10.1016/0022-

0981(95)00044-R

Hoegh-Guldberg, O., Mumby, P. J., Hooten, A. J., Steneck, R. S., Greenfield, P., Gomez, E., … Hatziolos, M. E. (2007). Coral Reefs Under Rapid Climate Change and Ocean Acidification. *Science*, *318*(5857), 1737–1742. https://doi.org/10.1126/science.1152509

Hoegh-Guldberg, Ove, & Smith, G. J. (1989). The effect of sudden changes in temperature, light and salinity on the population density and export of zooxanthellae from the reef corals *Stylophora pistillata Esper* and *Seriatopora hystrix Dana*. *Journal of Experimental Marine Biology and Ecology*, *129*(3), 279–303. https://doi.org/10.1016/0022-0981(89)90109-3

Hoffmann, A. A., & Sgrò, C. M. (2011). Climate change and evolutionary adaptation. *Nature*, *470*(7335), 479–485. https://doi.org/10.1038/nature09670

Holt, A. L., Vahidinia, S., Gagnon, Y. L., Morse, D. E., & Sweeney, A. M. (2014). Photosymbiotic giant clams are transformers of solar flux. *Journal of The Royal Society Interface*, *11*(101), 20140678. https://doi.org/10.1098/rsif.2014.0678

Hou, J., Xu, T., Su, D., Wu, Y., Cheng, L., Wang, J., … Wang, Y. (2018). RNA-Seq reveals extensive transcriptional response to heat stress in the stony coral *Galaxea fascicularis*. *Frontiers in Genetics*, *9*. https://doi.org/10.3389/fgene.2018.00037

Hughes, T. P., Baird, A. H., Bellwood, D. R., Card, M., Connolly, S. R., Folke, C., … Roughgarden, J. (2003). Climate change, human impacts, and the resilience of coral reefs. *Science*, *301*(5635), 929–933. https://doi.org/10.1126/science.1085046

Hume, B. C. C., D'Angelo, C., Smith, E. G., Stevens, J. R., Burt, J., & Wiedenmann, J. (2015). *Symbiodinium thermophilum* sp. nov., a thermotolerant symbiotic alga prevalent in corals of the world's hottest sea, the Persian/Arabian Gulf. *Scientific Reports*, *5*, 8562.

Ikeda, S., Yamashita, H., Kondo, S., Inoue, K., Morishima, S., & Koike, K. (2017). Zooxanthellal genetic varieties in giant clams are partially determined by species-intrinsic and growth-related characteristics. *PLOS ONE*, *12*(2), e0172285. https://doi.org/10.1371/journal.pone.0172285

Ishikura, M., Kato, C., & Maruyama, T. (1997). UV-absorbing substances in zooxanthellate and azooxanthellate clams. *Marine Biology*, *128*(4), 649–655. https://doi.org/10.1007/s002270050131

Jantzen, C., Wild, C., El-Zibdah, M., Roa-Quiaoit, H. A., Haacke, C., & Richter, C. (2008). Photosynthetic performance of giant clams, *Tridacna maxima* and *T. squamosa*, Red Sea. *Marine*

Biology, *155*(2), 211–221. https://doi.org/10.1007/s00227-008-1019-7

Jones, R. J., Hoegh-Guldberg, O., Larkum, A. W. D., & Schreiber, U. (1998). Temperature-induced bleaching of corals begins with impairment of the CO2 fixation mechanism in zooxanthellae. *Plant, Cell and Environment*, *21*(12), 1219–1230. https://doi.org/10.1046/j.1365-3040.1998.00345.x

Kenkel, C. D., & Matz, M. V. (2016). Gene expression plasticity as a mechanism of coral adaptation to a variable environment. *Nature Ecology & Evolution*, *1*(1), 0014. https://doi.org/10.1038/s41559-016-0014

Klumpp, D. W., Bayne, B. L., & Hawkins, A. J. S. (1992). Nutrition of the giant clam *Tridacna gigas* (L.) I. Contribution of filter feeding and photosynthates to respiration and growth. *Journal of Experimental Marine Biology and Ecology*, *155*(1), 105–122. https://doi.org/10.1016/0022-0981(92)90030-E

Klumpp, D. W., & Griffiths, C. L. (1994). Contributions of phototrophic and heterotrophic nutrition to the metabolic and growth requirements of four species of giant clam (Tridacnidae). *Marine Ecology Progress Series*, *115*(1/2), 103–115.

Ladner, J. T., Barshis, D. J., & Palumbi, S. R. (2012). Protein evolution in two co-occurring types of *Symbiodinium*: an exploration into the genetic basis of thermal tolerance in *Symbiodinium clade D*. *BMC Evolutionary Biology*, *12*(1), 217. https://doi.org/10.1186/1471-2148-12-217

LaJeunesse, T. C. (2001). Investigating the biodiversity, ecology, and phylogeny of endosymbiotic dinoflagellates in the genus *Symbiodinium* using the ITS region: in search of a "species" level marker. *Journal of Phycology*, *37*(5), 866–880. https://doi.org/10.1046/j.1529-8817.2001.01031.x

LaJeunesse, T. C., Parkinson, J. E., Gabrielson, P. W., Jeong, H. J., Reimer, J. D., Voolstra, C. R., & Santos, S. R. (2018). Systematic Revision of Symbiodiniaceae Highlights the Antiquity and Diversity of Coral Endosymbionts. *Current Biology*, *28*(16), 2570-2580.e6. https://doi.org/10.1016/j.cub.2018.07.008

LaJeunesse, ToddC., Thornhill, DanielJ., Cox, EvelynF., Stanton, FrankG., Fitt, WilliamK., & Schmidt, GregoryW. (2004). High diversity and host specificity observed among symbiotic dinoflagellates in reef coral communities from Hawaii. *Coral Reefs*, *23*(4), 596–603. https://doi.org/10.1007/s00338-004-0428-4

Lämke, J., & Bäurle, I. (2017). Epigenetic and chromatin-based mechanisms in environmental stress

adaptation and stress memory in plants. *Genome Biology*, *18*(1). https://doi.org/10.1186/s13059-017-1263-6

Langfelder, P., & Horvath, S. (2008). WGCNA: an R package for weighted correlation network analysis. *BMC Bioinformatics*, *9*, 559. https://doi.org/10.1186/1471-2105-9-559

Lee, S. Y., Jeong, H. J., Kang, N. S., Jang, T. Y., Jang, S. H., & Lajeunesse, T. C. (2015). *Symbiodinium tridacnidorum* sp. nov., a dinoflagellate common to Indo-Pacific giant clams, and a revised morphological description of *Symbiodinium microadriaticum* Freudenthal, emended Trench & Blank. *European Journal of Phycology*, *50*(2), 155–172. https://doi.org/10.1080/09670262.2015.1018336

Legendre, P., & Gallagher, E. D. (2001). Ecologically meaningful transformations for ordination of species data. *Oecologia*, *129*(2), 271–280. https://doi.org/10.1007/s004420100716

Legendre, P., & legendre, L. (2012). *Numerical Ecology, Volume 24 - 3rd Edition*. Elsevier.

Leggat, W., Buck, B. H., Grice, A., & Yellowlees, D. (2003). The impact of bleaching on the metabolic contribution of dinoflagellate symbionts to their giant clam host. *Plant, Cell and Environment*, *26*(12), 1951–1961. https://doi.org/10.1046/j.0016-8025.2003.01111.x

Levin, R. A., Beltran, V. H., Hill, R., Kjelleberg, S., McDougald, D., Steinberg, P. D., & van Oppen, M. J. H. (2016). Sex, scavengers, and chaperones: transcriptome secrets of divergent *Symbiodinium* thermal tolerances. *Molecular Biology and Evolution*, *33*(9), 2201–2215. https://doi.org/10.1093/molbev/msw119

Liu, H., Stephens, T. G., González-Pech, R. A., Beltran, V. H., Lapeyre, B., Bongaerts, P., … Chan, C. X. (2018). *Symbiodinium* genomes reveal adaptive evolution of functions related to coral-dinoflagellate symbiosis. *Communications Biology*, *1*(1). https://doi.org/10.1038/s42003-018-0098-3

Liu, J., Feng, L., Li, J., & He, Z. (2015). Genetic and epigenetic control of plant heat responses. *Frontiers in Plant Science*, *06*. https://doi.org/10.3389/fpls.2015.00267

Love, M. I., Huber, W., & Anders, S. (2014). Moderated estimation of fold change and dispersion for RNA-seq data with DESeq2. *Genome Biology*, *15*(12), 550. https://doi.org/10.1186/s13059-014-0550-8

Lu, Y., & Xu, J. (2015). Phytohormones in microalgae: a new opportunity for microalgal biotechnology? *Trends in Plant Science*, *20*(5), 273–282. https://doi.org/10.1016/j.tplants.2015.01.006

Lucas, J. S. (1994). The biology, exploitation, and mariculture of giant clams (Tridacnidae). *Reviews in Fisheries Science*, *2*(3), 181–223. https://doi.org/10.1080/10641269409388557

Manning, M. M., & Gates, R. D. (2008). Diversity in populations of free-living *Symbiodinium* from a Caribbean and Pacific reef. *Limnology and Oceanography*, *53*(5), 1853–1861. https://doi.org/10.4319/lo.2008.53.5.1853

Mayfield, A. B., Wang, Y.-B., Chen, C.-S., Lin, C.-Y., & Chen, S.-H. (2014). Compartment-specific transcriptomics in a reef-building coral exposed to elevated temperatures. *Molecular Ecology*, *23*(23), 5816–5830. https://doi.org/10.1111/mec.12982

Menoud, M., Van Wynsberge, S., Moullac, G. L., Levy, P., Andréfouët, S., Remoissenet, G., & Gaertner-Mazouni, N. (2016). Identifying robust proxies of gonad maturation for the protandrous hermaphrodite *Tridacna maxima* (Röding, 1798, Bivalvia) from individual to population scale. *Journal of Shellfish Research*, *35*(1), 51–61. https://doi.org/10.2983/035.035.0107

Mieog, J. C., van Oppen, M. J. H., Cantin, N. E., Stam, W. T., & Olsen, J. L. (2007). Real-time PCR reveals a high incidence of *Symbiodinium clade D* at low levels in four scleractinian corals across the Great Barrier Reef: implications for symbiont shuffling. *Coral Reefs*, *26*(3), 449–457. https://doi.org/10.1007/s00338-007-0244-8

Mies, M., Voolstra, C. R., Castro, C. B., Pires, D. O., Calderon, E. N., & Sumida, P. Y. G. (2017). Expression of a symbiosis-specific gene in *Symbiodinium* type A1 associated with coral, nudibranch and giant clam larvae. *Royal Society Open Science*, *4*(5), 170253. https://doi.org/10.1098/rsos.170253

Mies, Miguel, Van Sluys, M. A., Metcalfe, C. J., & Sumida, P. Y. G. (2017). Molecular evidence of symbiotic activity between *Symbiodinium* and *Tridacna maxima* larvae. *Symbiosis*, *72*(1), 13–22. https://doi.org/10.1007/s13199-016-0433-8

Muscatine, L. (1967). Glycerol excretion by symbiotic algae from corals and *Tridacna* and its control by the host. *Science*, *156*(3774), 516–519. https://doi.org/10.1126/science.156.3774.516

Norton, J. H., Shepherd, M. A., Long, H. M., & Fitt, W. K. (1992). The zooxanthellal tubular system in the Giant clam. *The Biological Bulletin*, *183*(3), 503–506. https://doi.org/10.2307/1542028

Oksanen, J., Blanchet, F. G., Kindt, R., Legendre, P., Minchin, P. R., Wagner, R. B. O., … Wagner, H. (2012). *Vegan: community ecology package*. R package. Version 2.0-3.

Oliver, T. A., & Palumbi, S. R. (2011). Many corals host thermally resistant symbionts in high-

temperature habitat. *Coral Reefs*, *30*(1), 241–250. https://doi.org/10.1007/s00338-010-0696-0

Paradis, E., Claude, J., & Strimmer, K. (2004). APE: Analyses of Phylogenetics and Evolution in R language. *Bioinformatics*, *20*(2), 289–290. https://doi.org/10.1093/bioinformatics/btg412

Parkinson, John E., Tivey, T. R., Mandelare, P. E., Adpressa, D. A., Loesgen, S., & Weis, V. M. (2018). Subtle Differences in Symbiont Cell Surface Glycan Profiles Do Not Explain Species-Specific Colonization Rates in a Model Cnidarian-Algal Symbiosis. *Frontiers in Microbiology*, *9*. https://doi.org/10.3389/fmicb.2018.00842

Parkinson, John Everett, Banaszak, A. T., Altman, N. S., LaJeunesse, T. C., & Baums, I. B. (2015). Intraspecific diversity among partners drives functional variation in coral symbioses. *Scientific Reports*, *5*. https://doi.org/10.1038/srep15667

Pinzón, J. H., Devlin-Durante, M. K., Weber, M. X., Baums, I. B., & LaJeunesse, T. C. (2011). Microsatellite loci for Symbiodinium A3 (*S. fitti*) a common algal symbiont among Caribbean Acropora (stony corals) and Indo-Pacific giant clams (Tridacna). *Conservation Genetics Resources*, *3*(1), 45–47. https://doi.org/10.1007/s12686-010-9283-5

Pinzón, J. H., Kamel, B., Burge, C. A., Harvell, C. D., Medina, M., Weil, E., & Mydlarz, L. D. (2015). Whole transcriptome analysis reveals changes in expression of immune-related genes during and after bleaching in a reef-building coral. *Royal Society Open Science*, *2*(4), 140214. https://doi.org/10.1098/rsos.140214

Putnam, H. M., Stat, M., Pochon, X., & Gates, R. D. (2012). Endosymbiotic flexibility associates with environmental sensitivity in scleractinian corals. *Proceedings of the Royal Society of London B: Biological Sciences*, *279*(1746), 4352–4361. https://doi.org/10.1098/rspb.2012.1454

Ritchie, M. E., Phipson, B., Wu, D., Hu, Y., Law, C. W., Shi, W., & Smyth, G. K. (2015). limma powers differential expression analyses for RNA-sequencing and microarray studies. *Nucleic Acids Research*, *43*(7), e47–e47. https://doi.org/10.1093/nar/gkv007

Rouzé, H., Lecellier, G. J., Saulnier, D., Planes, S., Gueguen, Y., Wirshing, H. H., & Berteaux-Lecellier, V. (2017). An updated assessment of *Symbiodinium* spp. that associate with common scleractinian corals from Moorea (French Polynesia) reveals high diversity among background symbionts and a novel finding of clade B. *PeerJ*, *5*, e2856. https://doi.org/10.7717/peerj.2856

Rowan, R. (2004). Thermal adaptation in reef coral symbionts. *Nature*, *430*, 742.

Rowan, R., Knowlton, N., Baker, A., & Jara, J. (1997). Landscape ecology of algal symbionts creates variation in episodes of coral bleaching. *Nature*, *388*(6639), 265–269. https://doi.org/10.1038/40843

Sampayo, E. M., Ridgway, T., Bongaerts, P., & Hoegh-Guldberg, O. (2008). Bleaching susceptibility and mortality of corals are determined by fine-scale differences in symbiont type. *Proceedings of the National Academy of Sciences*, *105*(30), 10444–10449. https://doi.org/10.1073/pnas.0708049105

Sharkey, T. D. (2005). Effects of moderate heat stress on photosynthesis: importance of thylakoid reactions, rubisco deactivation, reactive oxygen species, and thermotolerance provided by isoprene. *Plant, Cell and Environment*, *28*(3), 269–277. https://doi.org/10.1111/j.1365-3040.2005.01324.x

Shoguchi, E., Shinzato, C., Kawashima, T., Gyoja, F., Mungpakdee, S., Koyanagi, R., … Satoh, N. (2013). Draft assembly of the *Symbiodinium minutum* nuclear genome reveals dinoflagellate gene structure. *Current Biology: CB*, *23*(15), 1399–1408. https://doi.org/10.1016/j.cub.2013.05.062

Silverstein, R. N., Correa, A. M. S., & Baker, A. C. (2012). Specificity is rarely absolute in coral-algal symbiosis: implications for coral response to climate change. *Proceedings of the Royal Society B: Biological Sciences*, *279*(1738), 2609–2618. https://doi.org/10.1098/rspb.2012.0055

Simão, F. A., Waterhouse, R. M., Ioannidis, P., Kriventseva, E. V., & Zdobnov, E. M. (2015). BUSCO: assessing genome assembly and annotation completeness with single-copy orthologs. *Bioinformatics*, *31*(19), 3210–3212. https://doi.org/10.1093/bioinformatics/btv351

Slavov, C., Schrameyer, V., Reus, M., Ralph, P. J., Hill, R., Büchel, C., … Holzwarth, A. R. (2016). "Super-quenching" state protects *Symbiodinium* from thermal stress - Implications for coral bleaching. *Biochimica et Biophysica Acta (BBA) - Bioenergetics*, *1857*(6), 840–847. https://doi.org/10.1016/j.bbabio.2016.02.002

Soo, P., & Todd, P. A. (2014). The behaviour of giant clams (Bivalvia: Cardiidae: Tridacninae). *Marine Biology*, *161*(12), 2699–2717. https://doi.org/10.1007/s00227-014-2545-0

Stat, M., Carter, D., & Hoeghguldberg, O. (2006). The evolutionary history of *Symbiodinium* and scleractinian hosts—Symbiosis, diversity, and the effect of climate change. *Perspectives in Plant Ecology, Evolution and Systematics*, *8*(1), 23–43. https://doi.org/10.1016/j.ppees.2006.04.001

Thackray, S. J., Mowat, C. G., & Chapman, S. K. (2008). Exploring the mechanism of tryptophan 2,3-dioxygenase. *Biochemical Society Transactions*, *36*(Pt 6), 1120–1123. https://doi.org/10.1042/BST0361120

Thornhill, D. J., LaJeunesse, T. C., Kemp, D. W., Fitt, W. K., & Schmidt, G. W. (2006). Multi-year, seasonal genotypic surveys of coral-algal symbioses reveal prevalent stability or post-bleaching reversion. *Marine Biology*, *148*(4), 711–722. https://doi.org/10.1007/s00227-005-0114-2

Thornhill, D. J., Xiang, Y., Fitt, W. K., & Santos, S. R. (2009). Reef Endemism, Host Specificity and Temporal Stability in Populations of Symbiotic Dinoflagellates from Two Ecologically Dominant Caribbean Corals. *PLoS ONE*, *4*(7), e6262. https://doi.org/10.1371/journal.pone.0006262

Van Wynsberge, S., Andréfouët, S., Gaertner-Mazouni, N., & Remoissenet, G. (2018). Consequences of an uncertain mass mortality regime triggered by climate variability on giant clam population management in the Pacific Ocean. *Theoretical Population Biology*, *119*, 37–47. https://doi.org/10.1016/j.tpb.2017.10.005

Vishwakarma, K., Upadhyay, N., Kumar, N., Yadav, G., Singh, J., Mishra, R. K., … Sharma, S. (2017). Abscisic acid signaling and abiotic stress tolerance in plants: a review on current knowledge and future prospects. *Frontiers in Plant Science*, *8*, 161. https://doi.org/10.3389/fpls.2017.00161

Warner, M. E., Fitt, W. K., & Schmidt, G. W. (1999). Damage to photosystem II in symbiotic dinoflagellates: A determinant of coral bleaching. *Proceedings of the National Academy of Sciences*, *96*(14), 8007–8012. https://doi.org/10.1073/pnas.96.14.8007

Wood-Charlson, E. M., Hollingsworth, L. L., Krupp, D. A., & Weis, V. M. (2006). Lectin/glycan interactions play a role in recognition in a coral/dinoflagellate symbiosis. *Cellular Microbiology*, *8*(12), 1985–1993. https://doi.org/10.1111/j.1462-5822.2006.00765.x

Wright, R. M., Aglyamova, G. V., Meyer, E., & Matz, M. V. (2015). Gene expression associated with white syndromes in a reef building coral, *Acropora hyacinthus*. *BMC Genomics*, *16*(1), 371. https://doi.org/10.1186/s12864-015-1540-2

Wu, T. D., Reeder, J., Lawrence, M., Becker, G., & Brauer, M. J. (2016). GMAP and GSNAP for genomic sequence alignment: enhancements to speed, accuracy, and functionality. *Statistical Genomics: Methods and Protocols*, pp. 283–334.

Yamashita, H., Suzuki, G., Hayashibara, T., & Koike, K. (2011). Do corals select zooxanthellae by alternative discharge? *Marine Biology*, *158*(1), 87–100. https://doi.org/10.1007/s00227-010-1544-z

Zhang, Y., Yang, C., Li, Y., Zheng, N., Chen, H., Zhao, Q., … Xie, Q. (2007). SDIR1 Is a RING Finger E3 Ligase That Positively Regulates Stress-Responsive Abscisic Acid Signaling in

Arabidopsis. *The Plant Cell*, *19*(6), 1912–1929. https://doi.org/10.1105/tpc.106.048488

Zhou, Z., Liu, Z., Wang, L., Luo, J., & Li, H. (2018). Oxidative stress, apoptosis activation and symbiosis disruption in giant clam *Tridacna crocea* under high temperature. *Fish & Shellfish Immunology*, *84*, 451–457. https://doi.org/10.1016/j.fsi.2018.10.033

Acknowledgments

General: We are grateful to Michel Pahuatini for providing the "small giant" clams and seawater samples. We thank Claude Soyez and Leila Chapron for their help in animal rearing. We thank Dr. Laetitia Hédouin for valuable comments on prior versions of the manuscript, Corinne Belliard for help with DNA preparation, and Dr. Yu-Bin Wang for making the *P. damicornis*-Symbiodiniaceae transcriptomic resources openly accessible, as well as designing the afore-cited *P. damicornis*-Symbiodiniaceae transcriptome server. Finally, we thank O. Bichet for her help with the figures.

Funding: This experiment was made possible by a grant from Labex CORAIL (France), as well as an IFREMER grant (France; Master's internship to HAM).

Author contributions: CB and JVD conceived the experimental design, under which tissue samples featured herein were collected. CB and JLL conceived the transcriptomic study. HAM and JLL carried out the laboratory benchwork. HAM and JLL analyzed the data. HAM, CB, ABM, and JLL wrote the manuscript. All co-authors contributed substantially to revised drafts of the manuscript. We also thank two anonymous reviewers for their help in largely improving the manuscript.

Competing interests: We declare that we have no competing interests.

Data and materials availability: Raw sequencing RNA-Seq data for small giant clams featured herein have been made publicly available on the NCBI database (PRJNA579426), and all scripts discussed in the article can be found on Github (https://github.com/jleluyer/acclimabest). Raw meta-barcoding data are available here: (pending creation). Data for cultured Symbiodiniaceae have been previously deposited on the NCBI database: Levin *et al*. (2016)-BioProject NCBI: PRJNA295075, Gierz *et al*. (2017)-BioProject NCBI: PRJNA342240. Data for Symbiodiniaceae from the reef coral *P. damicornis* (Mayfield et al., 2014) can be found on the NCBI database (Sequence Read Archive: SRR1030692 and BioProject: PRJNA227785), as well as on this modular, interactive website: http://symbiont.iis.sinica.edu.tw/coral_pdltte/static/html/index.html#home.

ANNEXE 8

nature climate change

PERSPECTIVE

PUBLISHED ONLINE: 1 SEPTEMBER 2017 | DOI: 10.1038/NCLIMATE3374

Rapid adaptive responses to climate change in corals

Gergely Torda[1,2*], Jennifer M. Donelson[1], Manuel Aranda[3], Daniel J. Barshis[4], Line Bay[1,2], Michael L. Berumen[3], David G. Bourne[2,5], Neal Cantin[2], Sylvain Foret[1,6†], Mikhail Matz[7], David J. Miller[1,8], Aurelie Moya[1], Hollie M. Putnam[9], Timothy Ravasi[10], Madeleine J. H. van Oppen[1,2,11], Rebecca Vega Thurber[12], Jeremie Vidal-Dupiol[13,14], Christian R. Voolstra[3], Sue-Ann Watson[1], Emma Whitelaw[15], Bette L. Willis[1,5], Philip L. Munday[1]

Pivotal to projecting the fate of coral reefs is the capacity of reef-building corals to acclimatize and adapt to climate change. Transgenerational plasticity may enable some marine organisms to acclimatize over several generations and it has been hypothesized that epigenetic processes and microbial associations might facilitate adaptive responses. However, current evidence is equivocal and understanding of the underlying processes is limited. Here, we discuss prospects for observing transgenerational plasticity in corals and the mechanisms that could enable adaptive plasticity in the coral holobiont, including the potential role of epigenetics and coral-associated microbes. Well-designed and strictly controlled experiments are needed to distinguish transgenerational plasticity from other forms of plasticity, and to elucidate the underlying mechanisms and their relative importance compared with genetic adaptation.

The unprecedented rate of environmental change that characterizes the Anthropocene[1] has raised concerns over whether the pace of organismal adaptation will be sufficient to mitigate projected detrimental effects on populations, communities and ecosystems[2]. The appearance and fixation of new adaptive genetic mutations generally requires many generations, suggesting that only organisms with short generation times will be able to adapt at rates matching the pace of environmental change. However, genetic adaptation can sometimes occur remarkably rapidly — within just a few generations — when standing genetic variation and recombination rates are high[3] (Box 1). Furthermore, it is increasingly recognized that acclimatization through phenotypic plasticity may buffer populations against rapid environmental change, allowing genetic adaptation to catch up over the longer term[4].

The fate of tropical coral reefs is of particular concern due to their high social, ecological and economic value, and their sensitivity to environmental change[5]. Hermatypic scleractinians (reef-building corals), the ecosystem engineers of coral reefs, live close to their upper thermal limits, and elevated summer temperatures can cause mass coral bleaching and mortality[6]. Some reef-building corals are also sensitive to the declining saturation state of carbonate ions that accompanies ocean acidification[7], and declining water quality associated with altered land use and precipitation regimes[8]. Reef-building corals provide shelter, food and habitat, and therefore loss of live coral and associated structural complexity leads to declines in the diversity and abundance of other reef organisms[9,10]. The future of coral reefs will therefore depend on the capacity of these foundation species to respond adaptively to rapid environmental change.

Recent experiments indicate that some coral and reef fish species can, at least to some extent, acclimatize to warming and acidifying oceans via developmental and/or transgenerational plasticity (TGP)[11,12] (Box 2). However, there are profound limitations to our current understanding of the underlying mechanisms of TGP and how these might interact with genetic adaptation[13]. While it has been suggested that epigenetic processes may be involved[14], there are divergent opinions on the strength of evidence for transgenerational inheritance via epigenetic marks, even in some well-characterized model organisms[13,15]. Moreover, exact mechanisms and the extent to which they have an effect are still unclear and under discussion[15]. Understanding multigenerational effects in corals is further complicated by the intimate relationships that they form with diverse suites of microorganisms that may contribute to phenotypic plasticity[16,17]

[1]ARC Centre of Excellence for Coral Reef Studies, James Cook University, Townsville, Queensland 4811, Australia. [2]Australian Institute of Marine Science, PMB 3, Townsville, Queensland 4810, Australia. [3]Red Sea Research Center, Division of Biological and Environmental Science and Engineering Division (BESE), King Abdullah University of Science and Technology (KAUST), 23955-6900, Thuwal, Saudi Arabia. [4]Department of Biological Sciences, Old Dominion University, Norfolk, Viginia 23529, USA. [5]College of Science and Engineering, James Cook University, Townsville, Queensland 4811, Australia. [6]Evolution, Ecology and Genetics, Research School of Biology, Australian National University, Canberra, Australian Capital Territory 2601, Australia. [7]Department of Integrative Biology, University of Texas at Austin, Texas 78712, USA. [8]Department of Molecular and Cell Biology, James Cook University, Townsville, Queensland 4811, Australia. [9]Department of Biological Sciences, University of Rhode Island, Kingston, Rhode Island 02881, USA. [10]KAUST Environmental Epigenetic Program, Division of Biological and Environmental Science and Engineering, King Abdullah University of Science and Technology, 23955-6900, Thuwal, Saudi Arabia. [11]School of BioSciences, The University of Melbourne, Parkville, Victoria 3010, Australia. [12]Oregon State University, 454 Nash Hall, Corvallis, Oregon 97330, USA. [13]IFREMER, UMR 241 EIO, LabexCorail, BP 7004, 98719 Taravao, Tahiti, French Polynesia. [14]IFREMER, IHPE UMR 5244, University Perpignan Via Domitia, CNRS, University Montpellier, F-34095 Montpellier, France. [15]Department of Biochemistry and Genetics, La Trobe Institute for Molecular Science, Melbourne, Victoria 3000, Australia. †Deceased. *e-mail: gergely.torda@jcu.edu.au

Box 1 | The pace of genetic adaptation.

A common misconception is that genetic adaptation occurs slowly and cannot possibly match the rate of ongoing climate change. Genetic adaptation is the change in allele frequencies in a population between generations, leading to a shift in mean trait values. This process does not require the appearance of new beneficial mutations (which potentially requires many generations); instead, it recombines and redistributes existing genetic variants, termed 'standing genetic variation'. In genetically diverse populations, such redistribution can happen very rapidly, potentially leading to positive selection fuelling adaptation[111]. Metapopulations inhabiting broad environmental gradients can collectively harbour extensive standing genetic variation, creating an additional opportunity for genetic adaptation via the spread of adaptive alleles among populations through migration ('genetic rescue'; see the figure below)[112]. A major unknown is the relative importance of genetic adaptation versus phenotypic plasticity in responding to rapid environmental change and how the two may interact.

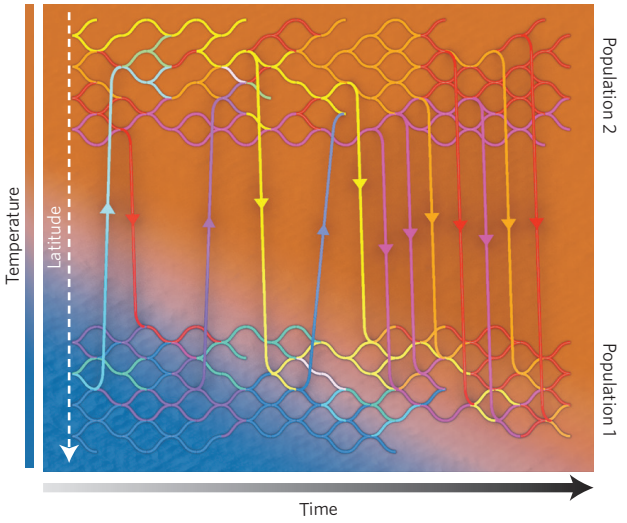

Rapid genetic adaptation to global warming in a metapopulation, based on standing genetic variation. Two populations are each represented by a network of genetically diverse genotypes, recombining through time. Occasional migration events (vertical lines) tie the two networks together and provide a way to share adaptive alleles. Warmer genotype colour indicates higher heat tolerance. In this example, the warm-adapted low-latitude population 'rescues' the cool-adapted high-latitude population by supplying heat-tolerant alleles.

Box 2 | Ecological and mechanistic context of TGP.

TGP occurs when the phenotype of a new generation is influenced by the environment experienced by the previous generation(s). TGP is adaptive when the exposure of parents to a particular environment leads to improved performance of offspring in the same environment[20], with classic examples of adaptive TGP including morphological defences in animals[19] and the shortening of lifecycles in plants[55]. Parents can influence the phenotype of their offspring through a range of mechanisms, including the transmission of nutrients or other cytoplasmic factors, such as hormones and proteins, or, in some cases, through epigenetic processes, such as CpG methylation, histone modifications and variants, or non-coding RNAs. The transmission of epigenetic marks between generations (transgenerational epigenetic inheritance via the gametes) is of particular interest because it has the potential to explain many examples of transgenerational phenotypic effects that are not easily accounted for by inherited genetic variation[113].

Distinguishing TGP from developmental plasticity is challenging. A number of recent studies have shown that negative effects of projected future climate change on marine organisms are greatly reduced if both parents and their offspring experience the same altered environmental condition[11,12,114]. These studies show that the parental environment can affect the offspring phenotype and may be examples of TGP. However, in all of the examples cited, the developing eggs or embryos (for example, in the mother) also experienced the altered environmental conditions, therefore it is not possible to rule out that the observed improvement in offspring performance is induced during early zygotic development rather than being TGP *sensu stricto*. While distinguishing between these possibilities is not critical if we simply want to know whether performance improves when multiple generations experience the same novel environmental conditions, it is important in terms of establishing the mechanistic basis of the changes observed. Future studies that aim to understand the mechanistic basis of TGP in marine organisms, while logistically challenging, will need to employ more complex experimental designs and spanning at least two to three generations (see Fig. 1). Research so far has generally assumed a simplistic situation where each generation is considered to be completely discrete (Case A, Fig. 1), and consequently phenotypic differences in F2 offspring between treatments are considered to be TGP by F1 parents. However, for most species it is unknown when the primordial germ cells develop, and consequently, TGP cannot be conclusively distinguished until the F3 generation (Case B). Ideally, the timing of germ cell development, or any effect on the developing reproductive cells is known before commencing TGP experiments, enabling divisions between treatments to be completed at the correct time (Case C).

and by their propensity for asexual reproduction. While the long lifespans and extensively overlapping generations typical of scleractinian corals might be expected to restrict the pace of genetic adaptation, this effect may be offset by other characteristics, particularly their close associations with a diverse range of microbes, high standing genetic variation (Box 1), colonial organization and high fecundity[18].

In this Perspective, we discuss mechanisms that could potentially enable plastic responses to climate change in reef corals. We provide a brief review of the available evidence (and the lack thereof) for the scope of transgenerational epigenetic inheritance to effect rapid phenotypic change in corals. We then predict the relative importance of TGP in various life-history traits, and strategies that are shared among, or unique to, foundation coral-reef species. Lastly, we discuss the potential of microbes to facilitate acclimatization in the coral holobiont.

Potential mechanisms for TGP

Phenotypic plasticity is a ubiquitous phenomenon that is increasingly gaining scientific attention as we focus on understanding the potential for organisms to respond to rapid changes in their environment. As global climate change is likely to occur on timescales that span multiple generations of corals (and many other multicellular organisms), attention has focussed on exploring the potential

for adaptive TGP (Box 2). While TGP has now been documented in a range of organisms at the phenotypic level[19–21], the underlying mechanisms are largely unknown.

Recent developments in omics technologies have enabled greater insight into the molecular pathways associated with plastic phenotypic responses and, in some cases, identified key genes whose altered expression may contribute to buffering against adverse environmental conditions within a generation[22,23] and across multiple generations[24,25]. Epigenetics, a term originally coined by Waddington in 1940, was intended to explain the phenomenon of cellular differentiation in multicellular organisms from a single genome[26]. More recently, the concept has evolved to include all mechanisms that potentially regulate gene expression, such as DNA methylation, histone modifications and variants, and noncoding and antisense RNAs. The discovery that some epigenetic marks are meiotically heritable (for example, the maternal DNA (CpG motif) methylation state of the *agouti* locus in mice[27,28]) led to an explosion of interest around epigenetic mechanisms driving transgenerational

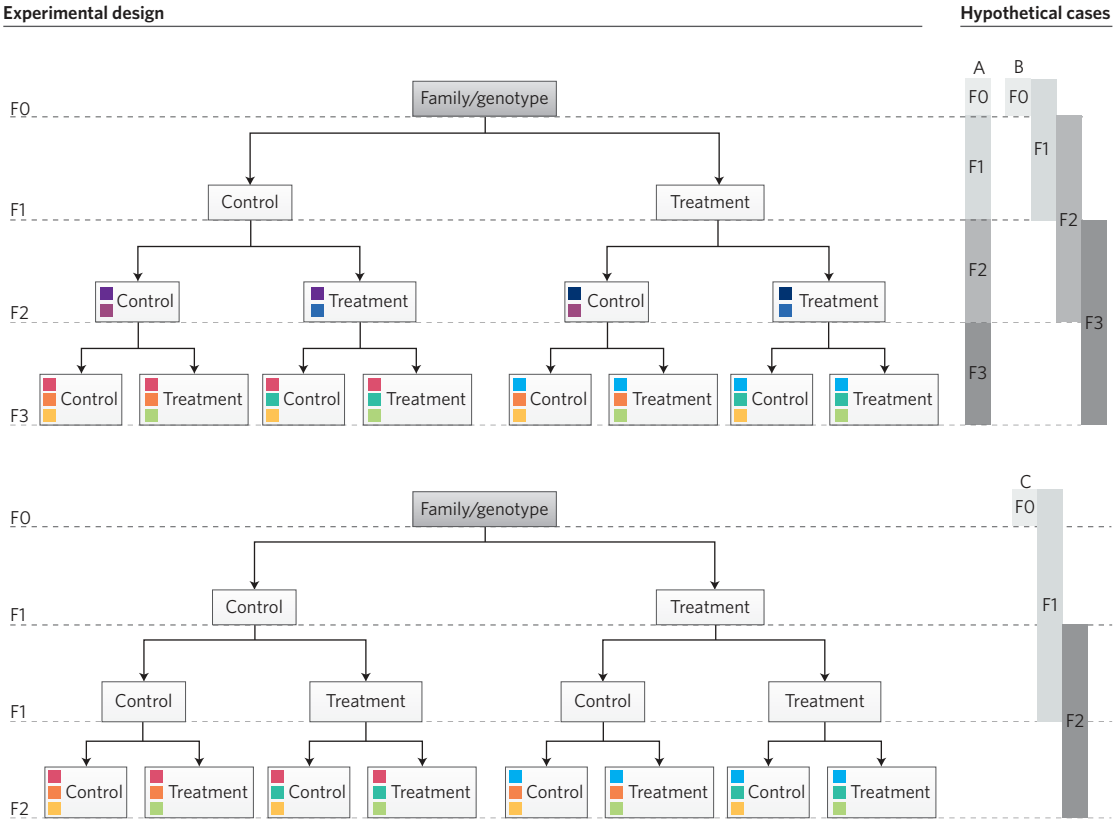

Comparisons of performance reaction norms between highlighted groups

	A	B	C
versus	F1 TGP	F1 TGP and/or F2 development	—
versus	F2 developmental	F2 developmental	—
versus	F1 TGP	F1 TGP and/or F2 TGP	F1 TGP
versus	F2 TGP	F2 TGP and/or F3 developmental	F1 TGP and/or F2 developmental
versus	F3 developmental	F3 developmental	F2 developmental

Figure 1 | Identifying TGP in offspring depending on generational overlap in exposure. Three hypothetical cases of overlap between generations (right) highlight the difficulties of determining TGP from developmental plasticity in a common experimental design (left). Phenotypic differences observed in the experiment could be due to transgenerational and/or developmental plasticity (as shown in the bottom table) depending on the overlap of environmental exposure between generations (Cases A–C). Case A depicts a situation where environmental treatments affect only one generation at a time; this is often assumed to be the case in TGP experiments. Case B depicts a situation where primordial germ cells are present at birth and thus the current and subsequent generations are exposed to the environmental treatment at the same time. Case C depicts a situation where the timing of effect on the subsequent generation is known, and division between treatments can be completed at the appropriate time. In all cases, critical to distinguishing phenotypic change due to TGP, or what may be a mixture of TGP and developmental plasticity, is the division of siblings (sexual) or clones (asexual) between the treatments at the commencement of the experiments (F1), and full orthogonal crossing of treatment conditions in each generation (or appropriate generational split). Interactions between exposures of generations, that is, TGP resulting from exposure of the parents versus grandparents to environmental change, can also be determined in the highlighted cases (when reared to the F3 generation) due to the orthogonal example experimental design displayed.

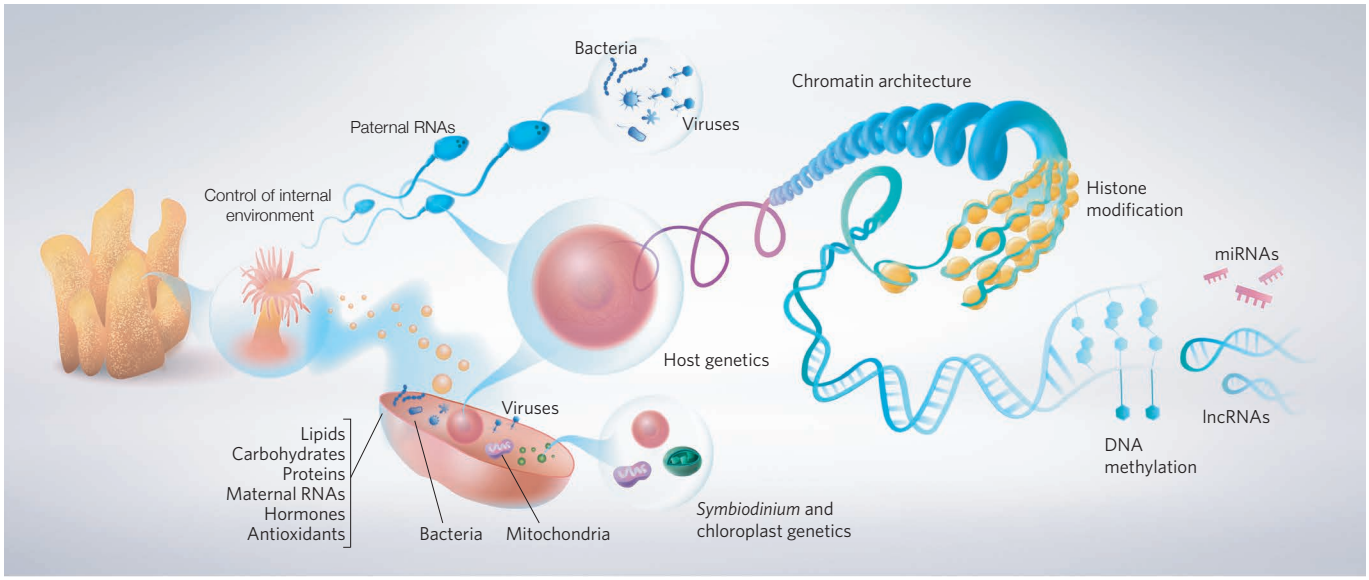

Figure 2 | Potential pathways that may enable TGP in corals include somatic, genetic and epigenetic factors of the coral gametes as well as their associated microbes transmitted vertically from one generation to the next. For details, see section 'Potential mechanisms for TGP'.

phenotypic plasticity across a wide range of organisms. While an increasing number of studies demonstrate association between epigenetic marks and overall phenotypes (including gene expression), causality remains to be established[29]. Moreover, the mechanisms involved seem to be highly variable across the tree of life, suggesting that there is no universal regulator of gene expression. For example, transgenerational inheritance linked to patterns of CpG methylation seems common in plants[20], but has been established in only a very limited number of cases in animals[28,30,31]. These examples mostly implicate atypical genomic regions, for example, retrotransposons that affect the transcription of neighbouring genes[13,30]. Furthermore, the low levels of correlation found between the transcriptome and the methylome of several multicellular organisms[32,33], combined with the lack of a CpG methylation system in some of the most widely studied model animals, including the fruit fly *Drosophila* and the roundworm *Caenorhabditis*[34,35], weakens the case for its significance as a universal regulator of gene expression[15,36], and hence a universal mediator of TGP. In corals, DNA methylation levels correlate strongly with gene function; broadly and uniformly expressed 'housekeeping' genes are strongly methylated, whereas genes responsible for inducible or cell-specific functions are weakly methylated[37,38] (Fig. 2). Nevertheless, it remains to be seen whether this divergent methylation causes or is caused by differences in gene expression, whether it responds to environmental cues[14], and whether it can be passed across generations. In summary, we do not dismiss a potential role for epigenetic inheritance in TGP of corals, but evidence is currently largely lacking, and mechanisms other than DNA methylation need increased attention.

Non-coding and antisense RNAs from the maternal cytoplasm can potentially affect zygotic transcriptional activity and provide short-term epigenetic memory that fades out with cell divisions[39] (Fig. 2). However, for some genes, transcriptional states established early in development can be maintained through mitotic divisions by epigenetic mechanisms[40]. Furthermore, epigenetic cross-talk[41,42], for example a positive feedback loop between chromatin and small RNAs, can promote long-term epigenetic memory in some organisms[40], but again this field remains highly understudied in corals.

Histone tail modifications and non-canonical histones modulate chromatin structure, and hence gene expression[43,44] (Fig. 2). In the cases where TGP is associated with histone modifications over multiple generations, it is likely that multiple epigenetic mechanisms affect target genomic regions. For example, temperature-induced changes in gene expression in *Caenorhabditis* last for over 14 generations, and are strongly associated with a histone modification that alters the chromatin structure and triggers a cascade that affects RNA-mediated gene silencing[31]. In corals, histone modifications are virtually unstudied, representing a major research gap that hinders our understanding of molecular mechanisms of TGP.

In addition to epigenetic mechanisms, parents can affect their offspring via a range of factors transmitted to the embryo through paternal and maternal germ cells[45] (Fig. 2). For example, nutritional factors passed through the oocyte's cytoplasm, such as lipids and carbohydrates, may directly influence the metabolic capacity of the early zygote and larva. Maternal provisioning of proteins can equip the oocyte and zygote with inaugural machinery for important functions before zygotic translation begins. Furthermore, the pool of maternal mRNA provides templates for early protein synthesis in the embryo, before zygotic transcription begins. In a range of plant species, hormones have been shown to play major roles in transgenerational environmental effects on offspring growth and development[20]. Transmission of mitochondria represents another potentially important pathway for maternal effects, especially in eukaryotic cells where cross-talk is assumed between the nuclear genome and mitochondria, with the organelle essentially acting as an interface between the environment and the epigenome[46] through metabolites[47–49].

Genetic information inherited from parents can contain copy number variations, repeat expansions or contractions, and the products of recombination events. Finally, gametes, embryos or larvae might undergo natural selection for alleles that provide advantage in the parental environment, particularly in highly fecund species. Such selection within full-sib larval families has been demonstrated experimentally in corals[50]. The resulting shift in the distribution of offspring phenotypes could be misinterpreted as TGP but is actually due purely to genetic adaptation.

These examples illustrate the diversity of mechanisms by which the parental environment could influence offspring phenotype, and warrant consideration in explaining TGP. Understanding the causal molecular mechanisms underlying adaptive phenotypes will be a major challenge, even in well-studied model organisms, but is needed to better predict the potential of these processes to enable organismal acclimatization to environmental changes.

In the next two sections, we first evaluate some of the common and unique life-history traits of corals that could enhance or hinder TGP. Secondly, given that oocytes could theoretically act as transgenerational vectors for the parental microbiome, we discuss the potential contributions that microbes, including bacteria, viruses and symbiotic protists, such as *Symbiodinium spp.*, could make to the phenotype and fitness of the coral host, as well as to the capacity for rapid adaptive responses in the holobiont.

Predictors of TGP in corals

Evidence of phenotypic plasticity across a range of coral life-history stages and traits is mounting, highlighting significant capacity for scleractinian corals to respond to altered environmental conditions. Within a lifetime, some corals can modulate their gross colony growth form to optimize light environments for photosynthesizing endosymbionts[51], physiologically acclimatize to elevated temperatures[22], and show signs of acclimatization under pH stress[14,23]. These examples suggest that corals may retain phenotypic plasticity in their adult life stage, which can itself be a trait affected by the corals' environment[52]. In tandem with high levels of intragenerational plasticity, multigenerational exposure of corals to altered environmental conditions can equip their offspring with enhanced stress tolerance[12]. In the brooding coral *Pocillopora damicornis*, the parental generation suffered metabolic depression under elevated temperature and CO_2 conditions, but the F1 larval offspring showed partial metabolic restoration to elevated conditions compared with offspring from un-exposed parents[12]. It is unclear, however, whether these beneficial parental effects last throughout the lifespan of the F1 generation and beyond. Furthermore, as explained in Box 2, it is difficult to disentangle TGP from developmental plasticity in this type of experiment, because the brooding larvae experienced the same environments as the parents. Regardless of the underlying mechanisms, these results highlight the importance of considering the ecological implications of multigenerational exposure to projected future environmental conditions when predicting the response of reef corals to climate change.

Corals vary enormously in their life-history traits, some of which may promote, and others impede, TGP. For example, adaptive TGP might be expected when the parental environment is a reliable predictor of environmental conditions that their offspring will experience[53,54]. Because short-range offspring dispersal typically enhances environmental predictability among generations[55], the benefits of TGP are expected to be inversely proportional to the dispersal capacity of the organism. The three main reproductive strategies that characterize coral-reef species — broadcast or pelagic spawning, benthic or demersal spawning, and brooding — represent a spectrum of dispersal potential, and hence differences between parental and offspring environmental conditions. Broadcast spawning, the most common mode of sexual reproduction in tropical reef corals[56], potentially provides greater offspring dispersal compared to demersal spawning; while brooding represents the least dispersive reproductive mode[57]. The high offspring-dispersal potential of broadcast spawners suggests that, in these cases, there may be limited correlation between the environmental conditions experienced by parents and offspring. Thus we predict TGP is least likely to be observed in broadcast spawners, as it should provide little selective advantage. Instead, broadcast spawners are predicted to produce offspring with a high capacity for developmental plasticity or offspring with a wide range of phenotypes (bet-hedging)[58,59]. TGP is more likely to be adaptive in brooding corals because the offspring are more likely to settle in a habitat that is similar to that of the parents. However, the relative importance of TGP across coral-reef species can only be understood via testing a range of species with robust experimental designs (see Fig. 1).

Longevity of some corals means that a genotype selected at the recruitment stage for an environment may be mismatched with changing environmental conditions as the sessile colony ages, so the selective advantages of TGP are likely to correlate with longevity. Modular organisms, such as scleractinians, octocorals, bryozoans and crustose coralline algae often not only have long lifespans but also reproduce asexually[60,61], which may result in exceptional lifespans of the genotype compared to other organisms[60,62], a feat only possible via substantial environmental tolerance or phenotypic plasticity[63]. Importantly, since such old colonies tend to be large and therefore highly fecund[64], they can potentially hinder genetic adaptation of the population by swamping the gamete pool with genotypes that are no longer a good match to the local environment. This can substantially reduce the rate of genetic adaptation in these organisms and may elevate the role of within-generation plasticity and TGP in helping the next cohort of recruits survive.

In long-lived corals, somatic mutations may accrue over the lifetime of modular colonies[18], highlighting another mechanism that could potentially aid phenotypic responses to environmental changes within the lifespan of the colony. Evolution through somatic mutations, as in the case of transgenerational epigenetic inheritance, is more likely to have a role in organisms that lack distinct segregation of the somatic and germ lines, such as fungi, plants and corals (but see ref. 65), or produce larvae asexually. Whether or not such mutations can be passed on to subsequent generations and hence contribute to genetic adaptation (Box 1) in corals remains controversial[65,66].

In summary, we predict that TGP is unlikely to be the main driver of plasticity in most coral species since the vast majority are broadcast spawners[56], for which the parental environment is a relatively poor predictor of the offspring environment. On the other hand, extended longevity in some corals could result in a mismatch between the genotype and present-day environmental conditions, and we predict that such species have evolved substantial capacity for plasticity in the offspring. Brooding corals are expected to benefit from both within-generation plasticity and TGP, because the developing embryo experiences the same environment as both its mother colony and subsequent juvenile and adult stages; and because many brooding corals have relatively short lifespans.

Potential involvement of microbes in coral acclimatization

Corals live in close association with a range of eukaryotic and prokaryotic microorganisms that may adapt or acclimatize faster than their metazoan host, potentially providing additional adaptive capacity to the holobiont. The coral holobiont[67] is an inter-domain community of complex and dynamic associations involving the photosynthetic alveolate *Symbiodinium* and a range of bacteria, fungi and viruses, some of which have been central to the success of the Scleractinia as the dominant contemporary tropical reef-builder[68] (Fig. 3). Although components of the holobiont have separate evolutionary trajectories[69], the intimate nature of some coral–microbial associations implies that their interactions may contribute to the overall fitness of the holobiont[68]. In comparison with the coral host, the orders of magnitude greater diversity, shorter generation times, and remarkable metabolic range of the coral microbiome suggest that some microbes could make contributions to adaptive responses of the holobiont. Here we consider the most prominent members of the coral microbiome and discuss how their evolution might affect coral performance under climate change. Such contributions are particularly relevant in the context of the long generation times of many corals and the rapid pace of current environmental change.

Symbiodinium. The well-studied coral–*Symbiodinium* association best illustrates the potential of microbial symbionts to effect rapid phenotypic change at the level of the coral holobiont, either through their own evolution[70] or changes in community composition (Fig. 3). The dinoflagellate genus *Symbiodinium* contains enormous genetic and functional diversity[71], and communities associated with corals vary among species, environments and host

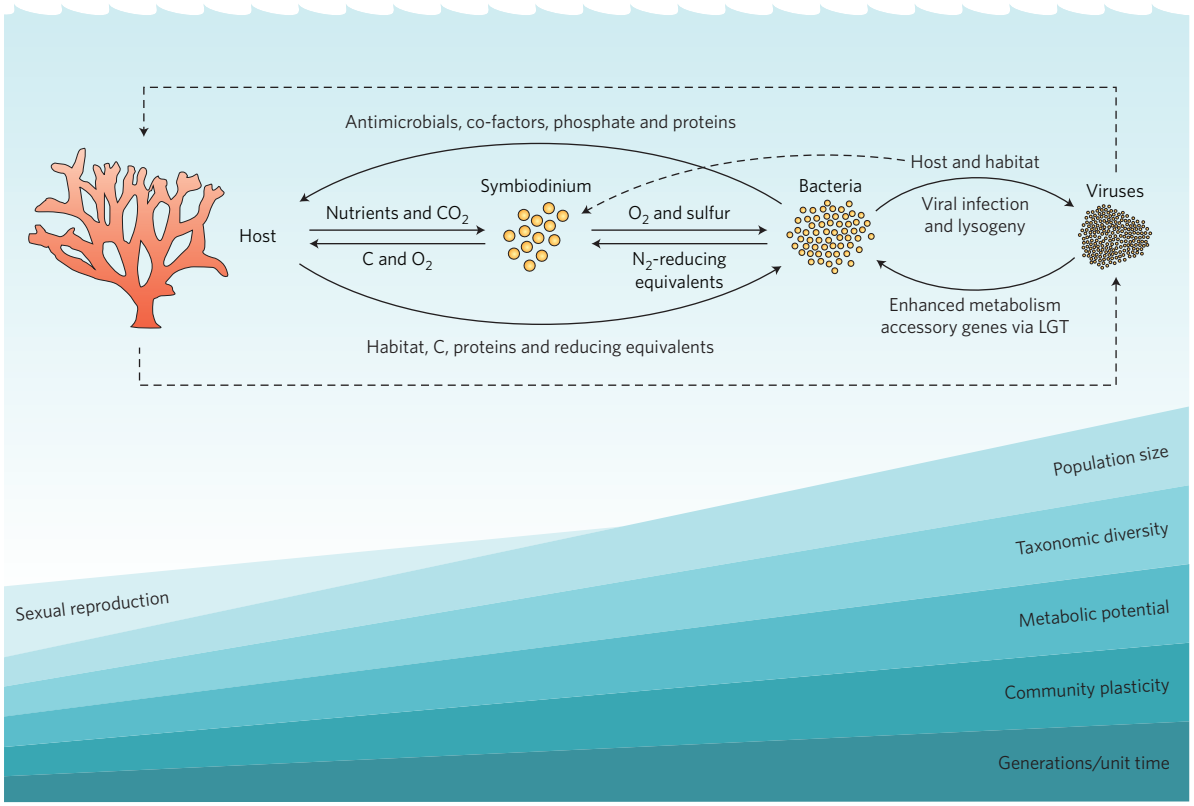

Figure 3 | Illustration showing members of the coral holobiont and their potential for contribution to adaptive holobiont responses. Member interactions are indicated with arrows (known interactions in solid lines, largely unknown interactions in dashed lines). Potential adaptive capacity increases in members of the holobiont, indicated by wedge height, reflected in population size, taxonomic diversity, metabolic potential, community plasticity, shortening intergenerational times, and potential for sexual reproduction.

microhabitats[72]. The short generation time of *Symbiodinium* means that its rate of mutation is much faster than for the coral host[18], and this, combined with its large within-host population sizes, potentially facilitates rapid responses to altered thermal environments, either through selection of existing genetic variants or through the evolution of novel adaptations[73,74]. Alternatively, the composition of host-associated *Symbiodinium* communities may vary temporally in response to environmental conditions or at different host life-history stages[75], either through shuffling of existing symbionts[76] or through acquisition of new *Symbiodinium* types from the environment (that is, switching)[16]. In particular, high genetic and phenotypic diversity among *Symbiodinium* taxa provides scope for some coral species to vary the composition of associated *Symbiodinium* communities, balancing photosynthetic activity (and hence growth) with stress tolerance, a type of acclimatory mechanism for responding to environmental extremes[76,77,78]. If associations enhance host health, they would also be likely to enhance the size and maternal provisioning of eggs and larvae, optimally positioning offspring within the natal environment through maternal effects[79]. Vertical transmission of *Symbiodinium* from maternal parent to gametes or brooded larvae by corals whose larvae typically settle in the parental habitat[59,80] could increase the likelihood that juvenile corals establish a symbiont community suited to ambient environmental conditions. Conversely, the acquisition of symbiotic communities from the environment (horizontally) in the case of broadcast spawning corals, whose larvae typically disperse more widely[79], may represent a strategy to ensure that juveniles settling under a range of environmental conditions acquire *Symbiodinium* types that are locally adapted (but see ref. 75). The generally greater diversity of *Symbiodinium* communities in early life-history stages compared to in adults[79] could be viewed as a bet-hedging strategy, providing juvenile corals with the opportunity to fine-tune endosymbiotic communities to suit ambient conditions. Finally, the retention of low-abundance background *Symbiodinium* types in adult stages of some corals[16,81] may provide further adaptive capacity to the holobiont (but see 82), facilitating future shuffling of dominant *Symbiodinium* types in response to changing environmental conditions[76,83].

Bacteria. Host-associated bacterial communities could also contribute to the adaptive capacity of their coral hosts, given the enormous breadth of their metabolic capabilities and of mechanisms that contribute to their rapid evolution[84]. Roles in immunity, nitrogen fixation, nutrient cycling, osmoregulation and oxidative stress responses have been suggested for bacteria associated with different microhabitats within the coral host[68]. The potential significance of specific bacterial groups is suggested by their vertical transmission[80] and common presence within the tissues of a wide range of corals[85,86]. In particular, whereas transient, highly variable communities are typically associated with external coral mucus layers, low and relatively stable numbers of 'core' types are more generally associated with host cells[85]. Bacterial community changes and resulting shifts in the holobiont metabolic network may provide further scope for maintaining holobiont functions in the face of environmental change. For example, transplantation of corals to a warmer environment resulted in shifts in the associated bacterial community that correlated with increased holobiont thermotolerance[87]. Additionally, higher bacterial diversity in deep compared to shallow water corals[88,89] suggests that some deep habitat-specific microbes may be involved in nutrient cycling specific to the low-irradiance environments. Both genetic and epigenetic processes contribute

to high phenotypic plasticity and rapid evolution in bacteria[90]. In addition, bacterial pathogens and mutualists are known to induce alterations in host epigenomes, leading to potentially long-lasting imprinting effects that provide a form of plasticity to their hosts[91]. Importantly, although all these examples illustrate how bacteria could, in principle, contribute to plastic responses of the holobiont and generally improve its function, direct experimental evidence of this is lacking, highlighting this area as a research priority[17].

Viruses and other microbiome components. The potential of other components of the holobiont to contribute to the adaptive capacity of corals is unknown. Although viral infections generally have negative consequences for the fitness of their hosts, there are examples from other symbiotic systems of viral infections enacting non-mutational alterations to the host that buffer environmental effects[92]. In addition, viruses of coral-associated eukaryotes and bacteria (bacteriophages) potentially contribute metabolic and functional diversity to the holobiont via several mechanisms. First, viral infection of animal hosts can prevent the invasion of foreign bacteria via signalling and immune system modulation[93]. Second, direct bacteriophage infection and lysis may regulate the abundance of specific bacteria within the holobiont, fulfilling an immunity-like function[94]. Third, phages may be agents of lateral gene transfer between microbial members of the holobiont[95]. Also, phage-induced and virus-induced mortality of bacterial and host cells may contribute to nutrient remineralization within the system, altering holobiont physiology and microbial ecology (the 'revolving door' hypothesis)[96]. Another mechanism by which viruses could influence coral-associated bacterial communities is through genetic rearrangement. For example, shuffling of bacterial genes may result in wider metabolic potential, with coincident beneficial consequences for the coral host, for example, a broader range of products produced by dimethylsulfoniopropionate (DMSP)-metabolizing bacteria might enhance bacteria-mediated production of sulfur-based antimicrobials[97]. Despite such possible beneficial roles, however, viruses more typically have negative effects on host fitness and, in the case of corals, have been implicated in bleaching[98,99] and disease[100].

In summary, the short generation times, large population sizes and high turnover of microbes, combined with their prodigious diversity, provide a range of potential mechanisms to enable the coral holobiont to respond to environmental change on ecologically relevant time-scales. Thus the emergent property of adaptive capacity of the holobiont could simply reflect 'selfish' evolution on the part of the symbiont. However, not all 'symbionts' are beneficial, for example, some *Symbiodinium* types are almost certainly opportunists that provide little or no benefit to their coral hosts[82,101]; a number of bacteria are pathogenic, causing a variety of diseases in corals[102]; and coral-associated bacteria may become pathogenic through the acquisition of prophages[103]. It is also conceivable that proviruses associated with bacteria or *Symbiodinium* could cause host-cell lysis upon emergence from the lysogenic state triggered by environmental stress. Thus, although evidence is accumulating that some host-associated microbes might facilitate adaptive responses in corals, the fitness consequences of climate-change-induced evolution of the coral microbiome are unclear. There is also uncertainty around the extent to which increased stress tolerance might involve physiological trade-offs that compromise host health and fitness[104], and whether selection occurs at the level of individuals or the holobiont.

Summary and future directions

The processes and pathways that could potentially facilitate rapid adaptive responses in reef-building corals are diverse, but there is a great deal of uncertainty around what contributions they will make to climate-change adaptation. Beneficial effects of parental exposure to offspring phenotype have been demonstrated in reef fishes and initial evidence has been presented for corals, however the extent to which TGP occurs in reef organisms can only be elucidated via experiments that tease apart developmental plasticity from TGP (Box 2 and Fig. 1). Understanding the relative contributions of parental provisioning, genetic and epigenetic mechanisms and changes in the microbiome to adaptive responses is paramount for predicting the fate of coral reefs as environmental conditions change. The revolution in omics approaches provides unparalleled opportunities for exploring the roles of the different components in coral adaptive responses if coupled with appropriate experimental design.

While reef-building corals present many challenges for genetic or epigenetic analyses, understanding the adaptive capacity of these critically important organisms requires the application of such molecular approaches within a rigorous experimental framework. Coral research can benefit enormously from advances made on the more tractable 'model' animals and better integration with the mainstream molecular genetics community. Recent technological advances allow transgenesis, gene knockdown, and a range of other methods to be applied to the sea anemone *Nematostella,* a 'near' relative of corals. The symbiotic sea anemone, *Exaiptasia*, holds similar promise as an experimental system of particular relevance to coral biology. However, empirical studies on classical model organisms cannot completely replace those on corals, because many cellular and molecular processes show substantial taxonomic variability. For example, CpG methylation appears to have quite different roles in vertebrates compared with insects, and the methylation patterns implied in corals differ from expectations based on either of these[105].

The potential for adaptive responses of the coral holobiont via its microbial partners is perhaps the most distinct, but also the most controversial, aspect of coral acclimatization. Rapid responses in the coral-associated microbiome do not need to rely on mutation, but may arise from changes in the relative abundance (or lifestyles, for example, pathogenic switch) of associated microorganisms, acquisition of novel microbes (with novel functions) from the environment, or horizontal gene transfer among microbes[106]. Importantly, most of these processes have not been tested or unequivocally proven in the coral holobiont system, highlighting an important research priority[87]. Furthermore, while changes in the genetic and community composition of coral-associated microbes may be fast, their evolution (including that of *Symbiodinium spp.*) is inherently selfish. The available (admittedly limited) evidence suggests that microbes may not coevolve with their coral hosts, and thus adaptation of coral-associated microbes may lead to host-switching,

Box 3 | Future research directions.

1. Demonstrate TGP in corals and other reef organisms via well-designed, strictly controlled experiments (for example, see Fig. 1).
2. Test causality between epigenetic mechanisms and phenotypes.
3. Demonstrate heritability of epigenetic marks in corals.
4. Understand the relative contributions of parental provisioning, genetic and epigenetic mechanisms, and changes in the microbiome to adaptive responses in corals.
5. Further develop model organisms closely related to scleractinian corals, such as the sea anemones *Nematostella* and *Exaiptasia*, on which advanced techniques, such as gene-knockdown and transgenesis are possible.
6. Understand flexibility of coral–microbial associations, including the control of microbial communities by the host and the microbes.
7. Improve models of the interaction of TGP and genetic adaptation.
8. Determine the pace of genetic adaptation in members of the coral holobiont.

non-symbiotic (that is, free-living) or even parasitic (pathogenic) strains, rather than the provision of benefits to their coral host. The likelihood of these alternative pathways will depend on the specificity and strength of coral–microbe associations.

Throughout this paper we have largely discussed TGP in relation to its potential to influence offspring phenotype in an adaptive capacity. However, TGP can also be maladaptive[107,108]. This increases the need to understand TGP in response to climate change for conservation and management, since it could potentially constrain evolutionary processes[109] and hinder future species persistence. Correlated effects also need to be explored, as the individual phenotype is comprised of a range of traits that are unlikely to be equally affected by the environment or exhibit the same capacity for plasticity. Different life stages may be oppositely affected[110]. This is further amplified in the coral holobiont where all components may not be plastically and/or adaptively shifting in the same direction or over the same timescales.

Given the enormous momentum in the climate system, the fate of coral reefs in the Anthropocene will largely depend on the rate at which reef-building corals can adapt or acclimatize to environmental change. There is an urgent need to fill important research gaps around TGP in corals (Box 3) to be able to inform conservation efforts and policymaking. This includes research into the cellular and molecular mechanisms, the temporal dynamics (for example, time frame for adaptive response), the strength and speed of host versus microbial plasticity, and the interaction between adaptive plasticity and evolution.

Received 21 December 2016; accepted 26 July 2017; published online 1 September 2017

References

1. IPCC *Climate Change 2014: Synthesis Report* (eds Core Writing Team, Pachauri, R. K. & Meyer L. A.) (IPCC, 2015).
2. Bell, G. Evolutionary rescue and the limits of adaptation. *Philos. Trans. R. Soc. B* **368,** 20120080 (2013).
3. Barrick, J. E. & Lenski, R. E. Genome dynamics during experimental evolution. *Nat. Rev. Genet*. **14,** 827–839 (2013).
4. Munday, P. L., Warner, R. R., Monro, K., Pandolfi, J. M. & Marshall, D. J. Predicting evolutionary responses to climate change in the sea. *Ecol. Lett*. **16,** 1488–1500 (2013).
5. Pandolfi, J. M., Connolly, S. R., Marshall, D. J. & Cohen, A. L. Projecting coral reef futures under global warming and ocean acidification. *Science* **333,** 418–422 (2011).
6. Hughes, T. P. *et al.* Global warming and recurrent mass bleaching of corals. *Nature* **543,** 373–377 (2017).
7. Albright, R. *et al.* Reversal of ocean acidification enhances net coral reef calcification. *Nature* **531,** 362–365 (2016).
8. Fabricius, K. E. Effects of terrestrial runoff on the ecology of corals and coral reefs: review and synthesis. *Mar. Pollut. Bull.* **50,** 125–146 (2005).
9. Graham, N. A. J. & Nash, K. L. The importance of structural complexity in coral reef ecosystems. *Coral Reefs* **32,** 315–326 (2013).
10. Fabricius, K. E., De'ath, G., Noonan, S. & Uthicke, S. Ecological effects of ocean acidification and habitat complexity on reef-associated macroinvertebrate communities. *Proc. R. Soc. B* **281,** 20132479 (2014).
11. Donelson, J. M., Munday, P. L., McCormick, M. I. & Pitcher, C. R. Rapid transgenerational acclimation of a tropical reef fish to climate change. *Nat. Clim. Change* **2,** 30–32 (2012).
Seminal study demonstrating adaptive transgenerational plasticity to climate change in a coral-reef fish.
12. Putnam, H. M. & Gates, R. D. Preconditioning in the reef-building coral Pocillopora damicornis and the potential for trans-generational acclimatization in coral larvae under future climate change conditions. *J. Exp. Biol*. **218,** 2365–2372 (2015).
13. Daxinger, L. & Whitelaw, E. Transgenerational epigenetic inheritance: more questions than answers. *Genome Res*. **20,** 1623–1628 (2010).
Critical review of evidence for transgenerational epigenetic inheritance.
14. Putnam, H. M., Davidson, J. M. & Gates, R. D. Ocean acidification influences host DNA methylation and phenotypic plasticity in environmentally susceptible corals. *Evol. Appl*. **9,** 1165–1178 (2016).
The only study to date that links environmental variation to epigenetic changes in corals.
15. Ptashne, M. Epigenetics: core misconcept. *Proc. Natl Acad. Sci. USA* **110,** 7101–7103 (2013).
16. Boulotte, N. M. *et al.* Exploring the Symbiodinium rare biosphere provides evidence for symbiont switching in reef-building corals. *ISME J.* **10,** 2693–2701 (2016).
17. Webster, N. S. & Reusch, T. B. H. Microbial contributions to the persistence of coral reefs. *ISME J*. http://dx.doi.org/10.1038/ismej.2017.66 (2017).
18. van Oppen, M. J. H., Souter, P., Howells, E. J., Heyward, A. & Berkelmans, R. Novel genetic diversity through somatic mutations: fuel for adaptation of reef corals? *Diversity* **3,** 405–423 (2011).
19. Agrawal, A. A., Laforsch, C. & Tollrian, R. Transgenerational induction of defences in animals and plants. *Nature* **401,** 60–63 (1999).
20. Herman, J. J. & Sultan, S. E. Adaptive transgenerational plasticity in plants: case studies, mechanisms, and implications for natural populations. *Front. Plant Sci*. **2,** 1–10 (2011).
21. Salinas, S., Brown, S. C., Mangel, M. & Munch, S. B. Non-genetic inheritance and changing environments. *Non-Genet. Inherit.* https://doi.org/10.2478/ngi-2013-0005 (2013).
22. Palumbi, S. R., Barshis, D. J., Traylor-Knowles, N. & Bay, R. A. Mechanisms of reef coral resistance to future climate change. *Science* **344,** 895–898 (2014).
Demonstrates the link between environmental change and gene expression levels, as well as rapid acclimatization in corals.
23. Moya, A. *et al.* Rapid acclimation of juvenile corals to CO_2-mediated acidification by upregulation of heat shock protein and Bcl-2 genes. *Mol. Ecol.* **24,** 438–452 (2015).
24. Veilleux, H. D. *et al.* Molecular processes of transgenerational acclimation to a warming ocean. *Nat. Clim. Change* **5,** 1074–1078 (2015).
25. Goncalves, P. *et al.* Rapid transcriptional acclimation following transgenerational exposure of oysters to ocean acidification. *Mol. Ecol.* **25,** 4836–4849 (2016).
26. Waddington, C. H. *Organisers and Genes* (Cambridge Univ. Press, 1940).
27. Wolff, G. L., Kodell, R. L., Moore, S. R. & Cooney, C. A. Maternal epigenetics and methyl supplements affect agouti gene expression in Avy/a mice. *FASEB J.* **12,** 949–957 (1998).
28. Morgan, H. D., Sutherland, H. G. E., Martin, D. I. K. & Whitelaw, E. Epigenetic inheritance at the agouti locus in the mouse. *Nat. Genet.* **23,** 314–318 (1999).
29. Metzger, D. C. H. & Schulte, P. M. Epigenomics in marine fishes. *Mar. Genomics* **30,** 43–54 (2016).
30. Rakyan, V. K. *et al.* Transgenerational inheritance of epigenetic states at the murine AxinFu allele occurs after maternal and paternal transmission. *Proc. Natl Acad. Sci. USA* **100,** 2538–2543 (2003).
31. Klosin, A., Casas, E., Hidalgo-Carcedo, C., Vavouri, T. & Lehner, B. Transgenerational transmission of environmental information in C. elegans. *Science* **356,** 320–323 (2017).
32. Libbrecht, R., Oxley, P. R., Keller, L. & Kronauer, D. J. C. Robust DNA methylation in the clonal raider ant brain. *Curr. Biol.* **26,** 391–395 (2016).
33. Meng, D. *et al.* Limited contribution of DNA methylation variation to expression regulation in Arabidopsis thaliana. *PLOS Genet*. **12,** e1006141 (2016).
34. Lyko, F., Ramsahoye, B. H. & Jaenisch, R. Development: DNA methylation in Drosophila melanogaster. *Nature* **408,** 538–540 (2000).
35. Suzuki, M. M. & Bird, A. DNA methylation landscapes: provocative insights from epigenomics. *Nat. Rev. Genet*. **9,** 465–476 (2008).
36. Bestor, T. H., Edwards, J. R. & Boulard, M. Notes on the role of dynamic DNA methylation in mammalian development. *Proc. Natl Acad. Sci. USA* **112,** 6796–6799 (2015).
37. Dimond, J. L. & Roberts, S. B. Germline DNA methylation in reef corals: patterns and potential roles in response to environmental change. *Mol. Ecol.* **25,** 1895–1904 (2016).
38. Dixon, G. B., Bay, L. K. & Matz, M. V. Evolutionary consequences of DNA methylation in a basal metazoan. *Mol. Biol. Evol*. **33,** 2285–2293 (2016).
39. Klosin, A. & Lehner, B. Mechanisms, timescales and principles of trans-generational epigenetic inheritance in animals. *Curr. Opin. Genet. Dev*. **36,** 41–49 (2016).
40. Holoch, D. & Moazed, D. RNA-mediated epigenetic regulation of gene expression. *Nat. Rev. Genet.* **16,** 71–84 (2015).
41. Cedar, H. & Bergman, Y. Linking DNA methylation and histone modification: patterns and paradigms. *Nat. Rev. Genet*. **10,** 295–304 (2009).
42. Rey, O., Danchin, E., Mirouze, M., Loot, C. & Blanchet, S. Adaptation to global change: a transposable element–epigenetics perspective. *Trends Ecol. Evol.* **31,** 514–526 (2016).
43. Jenuwein, T. & Allis, C. D. Translating the histone code. *Science* **293,** 1074–1080 (2001).
44. Karlić, R., Chung, H.-R., Lasserre, J., Vlahoviček, K. & Vingron, M. Histone modification levels are predictive for gene expression. *Proc. Natl Acad. Sci. USA* **107,** 2926–2931 (2010).
45. Hamdoun, A. & Epel, D. Embryo stability and vulnerability in an always changing world. *Proc. Natl Acad. Sci. USA* **104,** 1745–1750 (2007).

46. Wallace, D. C. & Fan, W. Energetics, epigenetics, mitochondrial genetics. *Mitochondrion* **10,** 12–31 (2010).
47. Marden, J. H. Nature's inordinate fondness for metabolic enzymes: why metabolic enzyme loci are so frequently targets of selection. *Mol. Ecol.* **22,** 5743–5764 (2013).
48. Shaughnessy, D. T. *et al.* Mitochondria, energetics, epigenetics, and cellular responses to stress. *Environ. Health Perspect.* **122,** 1271 (2014).
49. Gibbin, E. M. *et al.* Can multi-generational exposure to ocean warming and acidification lead to the adaptation of life history and physiology in a marine metazoan? *J. Exp. Biol.* **220,** 551–563 (2017).
50. Dixon, G. B. *et al.* Genomic determinants of coral heat tolerance across latitudes. *Science* **348,** 1460–1462 (2015).
51. Willis, B. L. Phenotypic plasticity versus phenotypic stability in the reef corals Turbinaria mesenterina and Pavona cactus. *Proc. Fifth Int. Coral Reef Symp.* **4,** 107–112 (1985).
52. Kenkel, C. D. & Matz, M. V. Gene expression plasticity as a mechanism of coral adaptation to a variable environment. *Nat. Ecol. Evol.* **1,** 0014 (2016).
53. Burton, T. & Metcalfe, N. B. Can environmental conditions experienced in early life influence future generations? *Proc. R. Soc. B* **281,** 20140311 (2014).
54. Burgess, S. C. & Marshall, D. J. Adaptive parental effects: the importance of estimating environmental predictability and offspring fitness appropriately. *Oikos* **123,** 769–776 (2014).
55. Galloway, L. F. & Etterson, J. R. Transgenerational plasticity is adaptive in the wild. *Science* **318,** 1134–1136 (2007).
56. Baird, A. H., Guest, J. R. & Willis, B. L. Systematic and biogeographical patterns in the reproductive biology of scleractinian corals. *Ann. Rev. Ecol. Evol. Syst.* **40,** 551–571 (2009).
57. Richmond, R. H. Competency and dispersal potential of planula larvae of a spawning versus a brooding coral. In *Proc. 6th Int. Coral Reef Symp.* **2,** 827–831 (1988).
58. Crean, A. J. & Marshall, D. J. Coping with environmental uncertainty: dynamic bet hedging as a maternal effect. *Philos. Trans. R. Soc. B* **364,** 1087–1096 (2009).
59. Padilla-Gamiño, J. L., Pochon, X., Bird, C., Concepcion, G. T. & Gates, R. D. From parent to gamete: vertical transmission of Symbiodinium (Dinophyceae) ITS2 sequence assemblages in the reef building coral Montipora capitata. *PLoS One* **7,** e38440 (2012).
60. Highsmith, R. C. Reproduction by fragmentation in corals. *Mar. Ecol. Prog. Ser.* **7,** 207–226 (1982).
61. Ayre, D. J. & Resing, J. M. Sexual and asexual production of planulae in reef corals. *Mar. Biol.* **90,** 187–190 (1986).
62. Devlin-Durante, M. K. & Miller, M. W., Caribbean Acropora Research Group, Precht, W. F. & Baums, I. B. How old are you? Genet age estimates in a clonal animal. *Mol. Ecol.* **25,** 5628–5646 (2016).
63. Reusch, T. B. H. Climate change in the oceans: evolutionary versus phenotypically plastic responses of marine animals and plants. *Evol. Appl.* **7,** 104–122 (2014).
64. Hall, V. R. & Hughes, T. P. Reproductive strategies of modular organisms: comparative studies of reef-building corals. *Ecology* **77,** 950–963 (1996).
65. Barfield, S., Aglyamova, G. V. & Matz, M. V. Evolutionary origins of germline segregation in Metazoa: evidence for a germ stem cell lineage in the coral Orbicella faveolata (Cnidaria, Anthozoa). *Proc. R. Soc. B* **283,** 20152128 (2016).
66. Schweinsberg, M., Pech, R. A. G., Tollrian, R. & Lampert, K. P. Transfer of intracolonial genetic variability through gametes in Acropora hyacinthus corals. *Coral Reefs* **33,** 77–87 (2013).
67. Rohwer, F. *et al.* Diversity and distribution of coral-associated bacteria. *Mar. Ecol. Prog. Ser.* **243,** 1–10 (2002).
68. Bourne, D. G., Morrow, K. M. & Webster, N. S. Insights into the coral microbiome: underpinning the health and resilience of reef ecosystems. *Annu. Rev. Microbiol.* **70,** 317–340 (2016).
69. Douglas, A. E. & Werren, J. H. Holes in the hologenome: why host-microbe symbioses are not holobionts. *mBio* **7,** e02099-15 (2016).
70. Chakravarti, L. J., Beltran, V. H. & van Oppen, M. J. H. Rapid thermal adaptation in photosymbionts of reef-building corals. *Glob. Change Biol.* http://dx.doi.org/10.1111/gcb.13702 (2017).
Experimental demonstration of rapid genetic adaptation of *Symbiodinium* to increased water temperatures.
71. van Oppen, M. J., Baker, A. C., Coffroth, M. A. & Willis, B. L. In *Coral Bleaching* 83–102 (Springer, 2009).
72. Rowan, R. Review—diversity and ecology of zooxanthellae on coral reefs. *J. Phycol.* **34,** 407–417 (1998).
73. Howells, E. J. *et al.* Coral thermal tolerance shaped by local adaptation of photosymbionts. *Nat. Clim. Change* **2,** 116–120 (2012).
74. Hume, B. C. C. *et al.* Ancestral genetic diversity associated with the rapid spread of stress-tolerant coral symbionts in response to Holocene climate change. *Proc. Natl Acad. Sci. USA* **113,** 4416–4421 (2016).
75. Poland, D. M. & Coffroth, M. A. Trans-generational specificity within a cnidarian–algal symbiosis. *Coral Reefs* **36,** 119–129 (2017).
76. Jones, A. M., Berkelmans, R., van Oppen, M. J. H., Mieog, J. C. & Sinclair, W. A community change in the algal endosymbionts of a scleractinian coral following a natural bleaching event: field evidence of acclimatization. *Proc. R. Soc. B* **275,** 1359–1365 (2008).
77. Ziegler, M. *et al.* Coral microbial community dynamics in response to anthropogenic impacts near a major city in the central Red Sea. *Mar. Pollut. Bull.* **105,** 629–640 (2016).
78. Howells, E. J., Abrego, D., Meyer, E., Kirk, N. L. & Burt, J. A. Host adaptation and unexpected symbiont partners enable reef-building corals to tolerate extreme temperatures. *Glob. Change Biol.* **22,** 2702–2714 (2016).
Demonstration of the role of *Symbiodinium* community composition on corals' thermal tolerance.
79. Quigley, K. M., Willis, B. L. & Bay, L. K. Maternal effects and Symbiodinium community composition drive differential patterns in juvenile survival in the coral Acropora tenuis. *R. Soc. Open Sci.* **3,** 160471 (2016).
80. Sharp, K. H., Distel, D. & Paul, V. J. Diversity and dynamics of bacterial communities in early life stages of the Caribbean coral Porites astreoides. *ISME J.* **6,** 790–801 (2012).
81. Quigley, K. M. *et al.* Deep-sequencing method for quantifying background abundances of Symbiodinium types: exploring the rare Symbiodinium biosphere in reef-building corals. *PLoS One* **9,** e94297 (2014).
82. Lee, M. J. *et al.* Most low-abundance "background" Symbiodinium spp. are transitory and have minimal functional significance for symbiotic corals. *Microb. Ecol.* **71,** 771–783 (2016).
83. Bay, L. K., Doyle, J., Logan, M. & Berkelmans, R. Recovery from bleaching is mediated by threshold densities of background thermo-tolerant symbiont types in a reef-building coral. *R. Soc. Open Sci.* **3,** 160322 (2016).
84. McFall-Ngai, M. *et al.* Animals in a bacterial world, a new imperative for the life sciences. *Proc. Natl Acad. Sci. USA* **110,** 3229–3236 (2013).
85. Ainsworth, T. D. *et al.* The coral core microbiome identifies rare bacterial taxa as ubiquitous endosymbionts. *ISME J.* **9,** 2261–2274 (2015).
86. Neave, M. J. *et al.* Differential specificity between closely related corals and abundant Endozoicomonas endosymbionts across global scales. *ISME J.* **11,** 186–200 (2017).
87. Ziegler, M., Seneca, F. O., Yum, L. K., Palumbi, S. R. & Voolstra, C. R. Bacterial community dynamics are linked to patterns of coral heat tolerance. *Nat. Commun.* **8,** 14213 (2017).
88. Hernandez-Agreda, A., Leggat, W., Bongaerts, P. & Ainsworth, T. D. The microbial signature provides insight into the mechanistic basis of coral success across reef habitats. *mBio* **7,** e00560-16 (2016).
89. Röthig, T., Yum, L. K., Kremb, S. G., Roik, A. & Voolstra, C. R. Microbial community composition of deep-sea corals from the Red Sea provides insight into functional adaption to a unique environment. *Sci. Rep.* **7,** 44714 (2017).
90. Casadesús, J. & Low, D. A. Programmed heterogeneity: epigenetic mechanisms in bacteria. *J. Biol. Chem.* **288,** 13929–13935 (2013).
91. Celluzzi, A. & Masotti, A. How our other genome controls our epi-genome. *Trends Microbiol.* **24,** 777–787 (2016).
92. Roossinck, M. J. The good viruses: viral mutualistic symbioses. *Nat. Rev. Microbiol.* **9,** 99–108 (2011).
93. Shui, J.-W. *et al.* HVEM signalling at mucosal barriers provides host defence against pathogenic bacteria. *Nature* **488,** 222–225 (2012).
94. Barr, J. J., Youle, M. & Rohwer, F. Innate and acquired bacteriophage-mediated immunity. *Bacteriophage* **3,** e25857 (2013).
95. Rohwer, F. & Vega Thurber, R. L. Viruses manipulate the marine environment. *Nature* **459,** 207–212 (2009).
96. Vega Thurber, R. L., Payet, J. P., Thurber, A. R. & Correa, A. M. S. Virus-host interactions and their roles in coral reef health and disease. *Nat. Rev. Microbiol.* **15,** 205–216 (2017).
Seminal review of the role of viruses in the phenotypic performance of the coral holobiont.
97. Raina, J. B. *et al.* DMSP biosynthesis by an animal and its role in coral thermal stress response. *Nature* **502,** 677–680 (2013).
98. Correa, A. M. S. *et al.* Viral outbreak in corals associated with an in situ bleaching event: atypical herpes-like viruses and a new megavirus infecting Symbiodinium. *Front. Microbiol.* **7,** 127 (2016).
99. Levin, R. A., Voolstra, C. R., Weynberg, K. D. & van Oppen, M. J. H. Evidence for a role of viruses in the thermal sensitivity of coral photosymbionts. *ISME J.* **11,** 808–812 (2017).
100. Soffer, N., Brandt, M. E., Correa, A. M., Smith, T. B. & Vega Thurber, R. L. Potential role of viruses in white plague coral disease. *ISME J.* **8,** 271–283 (2014).
101. LaJeunesse, T. C., Lee, S. Y., Gil-Agudelo, D. L., Knowlton, N. & Jeong, H. J. Symbiodinium necroappetens sp. nov. (Dinophyceae): an opportunist 'zooxanthella' found in bleached and diseased tissues of Caribbean reef corals. *Eur. J. Phycol.* **50,** 223–238 (2015).

102. Harvell, D. *et al.* Coral disease, environmental drivers, and the balance between coral and microbial associates. *Oceanography* **20,** 172–195 (2007).
103. van Oppen, M. J. H., Leong, J. A. & Gates, R. D. Coral-virus interactions: a double-edged sword? *Symbiosis* **47,** 1–8 (2009).
104. Sampayo, E. M. *et al.* Coral symbioses under prolonged environmental change: living near tolerance range limits. *Sci. Rep*. **6,** 36271 (2016).
105. Sarda, S., Zeng, J., Hunt, B. G. & Yi, S. V. The evolution of invertebrate gene body methylation. *Mol. Biol. Evol*. **29,** 1907–1916 (2012).
106. Theis, K. R. *et al.* Getting the hologenome concept right: an eco-evolutionary framework for hosts and their microbiomes. *mSystems* **1,** e00028-16 (2016).
107. Ghalambor, C. K. *et al.* Non-adaptive plasticity potentiates rapid adaptive evolution of gene expression in nature. *Nature* **525,** 372–375 (2015).
108. Kronholm, I. & Collins, S. Epigenetic mutations can both help and hinder adaptive evolution. *Mol. Ecol*. **25,** 1856–1868 (2016).
109. Ancel, L. W. Undermining the Baldwin expediting effect: does phenotypic plasticity accelerate evolution? *Theor. Popul. Biol*. **58,** 307–319 (2000).
110. Marshall, D. J. Transgenerational plasticity in the sea: context-dependent maternal effects across the life history. *Ecology* **89,** 418–427 (2008).
111. Messer, P. W. & Petrov, D. A. Population genomics of rapid adaptation by soft selective sweeps. *Trends Ecol. Evol*. **28,** 659–669 (2013).
Review of mechanisms that produce soft selective sweeps, with a case for soft sweeps dominating rapid adaptation in many species.
112. Whiteley, A. R., Fitzpatrick, S. W., Funk, W. C. & Tallmon, D. A. Genetic rescue to the rescue. *Trends Ecol. Evol*. **30,** 42–49 (2015).
113. Holeski, L. M., Jander, G. & Agrawal, A. A. Transgenerational defense induction and epigenetic inheritance in plants. *Trends Ecol. Evol.* **27,** 618–626 (2012).
114. Parker, L. M. *et al.* Adult exposure influences offspring response to ocean acidification in oysters. *Glob. Change Biol.* **18,** 82–92 (2012).

Acknowledgements

We dedicate this paper to our close friend and colleague, Dr. Sylvain Foret, a leader in coral genomics and invertebrate epigenetics who passed away unexpectedly days before this paper was submitted. The workshop where this paper was conceived was organized and funded by the ARC Centre of Excellence for Coral Reef Studies with additional support from the King Abdullah University of Science and Technology (KAUST) (M.A., M.L.B., T.R. and C.R.V.) and the KAUST Office of Competitive Research Funds award OCRF-2016-CRG4-25410101 (T.R. and M.L.B.). The authors would like to thank Xavier Pita for his help with Figs 1–3, Heno Hwang for his help with the figure in Box 1, and Hillary Smith for her help with Figs 2 and 3.

Author contributions

This paper is the result of a workshop organized by G.T., P.L.M., B.L.W. and J.M.D. All co-authors contributed to discussions. G.T. wrote the first draft of the manuscript with input from J.M.D., B.L.W. and P.L.M. All co-authors contributed to subsequent drafts. Figures conceived and designed by: Fig. 1, J.M.D; Fig. 2, H.P.; Fig. 3, L.B., D.G.B., R.V.T., C.R.V., S.-A.W. and B.L.W. Box 1 was written by M.V.M., Box 2 by P.L.M. The figure in Box 1 was conceived and designed by M.V.M.

Additional information

Competing financial interests

The authors declare no competing financial interests.

ANNEXE 9

Peer Community Journal

Section: Ecology

RESEARCH ARTICLE

Published
2022-02-02

Cite as
Kelly Brener-Raffalli, Jeremie Vidal-Dupiol, Mehdi Adjeroud, Olivier Rey, Pascal Romans, François Bonhomme, Marine Pratlong, Anne Haguenauer, Rémi Pillot, Lionel Feuillassier, Michel Claereboudt, Hélène Magalon, Pauline Gélin, Pierre Pontarotti, Didier Aurelle, Guillaume Mitta and Eve Toulza (2022) *Gene expression plasticity and frontloading promote thermotolerance in* Pocillopora *corals*, Peer Community Journal, 2: e13.

Correspondence
eve.toulza@univ-perp.fr

Peer-review
Peer reviewed and recommended by PCI Ecology, https://doi.org/10.24072/pci.ecology.100028

Gene expression plasticity and frontloading promote thermotolerance in *Pocillopora* corals

Kelly Brener-Raffalli[1], Jeremie Vidal-Dupiol[2], Mehdi Adjeroud[3,4,5], Olivier Rey[1], Pascal Romans[6], François Bonhomme[7], Marine Pratlong[8,9], Anne Haguenauer[10], Rémi Pillot[6], Lionel Feuillassier[6], Michel Claereboudt[11], Hélène Magalon[3,4,5], Pauline Gélin[3,4,5], Pierre Pontarotti[12,13], Didier Aurelle[9,10,14], Guillaume Mitta[1,15], and Eve Toulza[1]

Volume **2** (2022), article e13

https://doi.org/10.24072/pcjournal.79

Abstract

Ecosystems worldwide are suffering from climate change. Coral reef ecosystems are globally threatened by increasing sea surface temperatures. However, gene expression plasticity provides the potential for organisms to respond rapidly and effectively to environmental changes, and would be favored in variable environments. In this study, we investigated the thermal stress response in *Pocillopora* coral colonies from two contrasting environments by exposing them to heat stress. We compared the physiological state, bacterial and Symbiodiniaceae communities (using 16S and ITS2 metabarcoding), and gene expression levels (using RNA-Seq) between control conditions and heat stress (the temperature just below the first signs of compromised health). Colonies from both thermal regimes remained apparently normal and presented open and colored polyps during heat stress, with no change in bacterial and Symbiodiniaceae community composition. In contrast, they differed in their transcriptomic responses. The colonies from Oman displayed a more plastic transcriptome, but some genes had a higher basal expression level (frontloading) compared to the less thermotolerant colonies from New Caledonia. In terms of biological functions, we observed an increase in the expression of stress response genes (including induction of tumor necrosis factor receptors, heat shock proteins, and detoxification of reactive oxygen species), together with a decrease in the expression of genes involved in morpho-anatomical functions. Gene regulation (transcription factors, mobile elements, histone modifications and DNA methylation) appeared to be overrepresented in the Oman colonies, indicating possible epigenetic regulation. These results show that transcriptomic plasticity and frontloading can be co-occurring processes in corals confronted with highly variable thermal regimes.

[1]IHPE, Univ. Montpellier, CNRS, Ifremer, Univ. Perpignan via Domitia, Perpignan France, [2]IHPE, Univ. Montpellier, CNRS, Ifremer, Univ. Perpignan via Domitia, Montpellier France, [3]ENTROPIE, IRD, Université de la Réunion, CNRS, IFREMER, Université de la Nouvelle-Calédonie, Perpignan, France, [4]Laboratoire d'Excellence "CORAIL", Paris, France, [5]PSL Université Paris, USR 3278 CRIOBE EPHE-UPVD-CNRS, Perpignan, France, [6]Observatoire Océanologique de Banyuls, Sorbonne Université-CNRS, FR3724, Avenue Pierre Fabre, 66650 Banyuls-sur-Mer, France, [7]Institut des Sciences de l'Évolution, Univ. Montpellier, CNRS, IRD, EPHE, Montpellier, France. , [8]Aix Marseille Univ, CNRS, Centrale Marseille, I2M, Marseille, France, Equipe Evolution Biologique et Modélisation, Marseille, France, [9]Aix Marseille Univ, Université de Toulon, CNRS, IRD, MIO, Marseille, France, [10]Aix-Marseille Université, Avignon Université, CNRS, IRD, IMBE, Marseille, France, [11]Department of Marine Science and Fisheries, College of Agricultural and Marine Sciences, Sultan Qaboos University, Al-Khod, 123, Sultanate of Oman, [12]Aix Marseille Univ, IRD, APHM, Microbe, Evolution, PHylogénie, Infection, IHU Méditerranée Infection, Marseille France. Evolutionary Biology team, [13]CNRS SNC5039, [14]Institut de Systématique, Evolution, Biodiversité (ISYEB), Muséum National d'Histoire Naturelle, CNRS, Sorbonne Université, EPHE, 57 rue Cuvier, 75005 Paris, France, [15]Univ Polynesie Francaise, ILM, IRD, Ifremer, F-98719 Tahiti, French Polynesia, France

Peer Community Journal is a member of the Centre Mersenne for Open Scientific Publishing
http://www.centre-mersenne.org/

e-ISSN 2804-3871

Abstract

Ecosystems worldwide are suffering from climate change. Coral reef ecosystems are globally threatened by increasing sea surface temperatures. However, gene expression plasticity provides the potential for organisms to respond rapidly and effectively to environmental changes, and would be favored in variable environments. In this study, we investigated the thermal stress response in *Pocillopora* coral colonies from two contrasting environments by exposing them to heat stress. We compared the physiological state, bacterial and Symbiodiniaceae communities (using 16S and ITS2 metabarcoding), and gene expression levels (using RNA-Seq) between control conditions and heat stress (the temperature just below the first signs of compromised health). Colonies from both thermal regimes remained apparently normal and presented open and colored polyps during heat stress, with no change in bacterial and Symbiodiniaceae community composition. In contrast, they differed in their transcriptomic responses. The colonies from Oman displayed a more plastic transcriptome, but some genes had a higher basal expression level (frontloading) compared to the less thermotolerant colonies from New Caledonia. In terms of biological functions, we observed an increase in the expression of stress response genes (including induction of tumor necrosis factor receptors, heat shock proteins, and detoxification of reactive oxygen species), together with a decrease in the expression of genes involved in morpho-anatomical functions. Gene regulation (transcription factors, mobile elements, histone modifications and DNA methylation) appeared to be overrepresented in the Oman colonies, indicating possible epigenetic regulation. These results show that transcriptomic plasticity and frontloading can be co-occurring processes in corals confronted with highly variable thermal regimes.

Introduction

Earth is undergoing unprecedented global environmental changes with major effects on biodiversity (Barnosky *et al.* 2011). The ongoing erosion of the most vulnerable ecosystems due to current environmental degradation is particularly worrying and is only a premise to what scientists have called the sixth mass extinction (Barnosky *et al.* 2011). In particular, climate change, ocean acidification and extreme climatic events have already resulted in the irreversible degradation of more than 20% of coral reefs worldwide (Bellwood *et al.* 2004; Hoegh-Guldberg *et al.* 2007). Scleractinian corals constitute the biological and physical framework for a large diversity of marine organisms [c.a. ~600 coral, ~2000 fish, and ~5000 mollusk species (Veron & Stafford-Smith 2000; Reaka-Kudla 2005)]. Hence, the extinction or even major decrease of corals would have dramatic repercussions on the overall associated communities (Hughes *et al.* 2017a). Natural variation in thermal tolerance exists among coral populations (Oliver & Palumbi 2010; Palumbi *et al.* 2014), especially along a latitudinal gradient (Polato *et al.* 2010; Dixon *et al.* 2015), hence providing some hope for coral survival based on their capacity to cope with heat stress. More specifically, it has been shown that populations inhabiting in zones with more variable temperature regimes display better tolerance to heat stress from local (Kenkel *et al.* 2013) to geographical scales (Hughes *et al.* 2003; Riegl *et al.* 2011; Coles & Riegl 2013).

It nevertheless remains unclear whether thermo-tolerance is acquired via acclimation (i.e. intra-generational gene expression plasticity (Barnosky *et al.* 2011; Kenkel & Matz 2016)) and/or through genetic adaptation (i.e. inter-generational microevolution (Barnosky *et al.* 2011; Dixon *et al.* 2015)). Actually, some studies strongly suggest that both processes are likely to co-occur in wild coral populations (Hoegh-Guldberg *et al.* 2007; Reusch 2013; Palumbi *et al.* 2014; Hughes *et al.* 2017a; Torda *et al.* 2017).

With the recent advances of high throughput molecular methods, it is now possible to provide a more precise account of the molecular mechanisms underlying coral response to heat stress. In particular, recent studies clearly demonstrated that coral responses to heat stress involve the fine-tuned regulation of expression levels of some genes/proteins involved in several molecular pathways such as metabolism, stress-response and apoptosis (Brown *et al.* 2002; Weis 2008; Ainsworth *et al.* 2011; Barnosky *et al.* 2011; Bellantuono *et al.* 2012a; Barshis *et al.* 2013; Kenkel *et al.* 2013; Palumbi *et al.* 2014). In this regard, two main molecular patterns having different temporalities have been put forward: (1) “transcriptional plasticity”, i.e. extensive changes in gene expression levels according to the occurring thermal condition

and (2) “transcriptional frontloading”, i.e. the elevation of stress related genes baseline expression that preconditions organisms to subsequent (recurrent) stresses (Reaka-Kudla 2005; Mayfield *et al.* 2011; Barnosky *et al.* 2011; Barshis *et al.* 2013; Palumbi *et al.* 2014; Hughes *et al.* 2017a). While such elevated constitutive gene expression levels could reflect local adaptation (i.e. genetically fixed gene expression level (Bellwood *et al.* 2004; Hoegh-Guldberg *et al.* 2007; Oliver & Palumbi 2010; Palumbi *et al.* 2014), it could also reflect an acclimation via epigenetic processes leading to constitutive gene expression (Veron & Stafford-Smith 2000; Reaka-Kudla 2005; Torda *et al.* 2017). Epigenetic changes through environmental priming (i.e. translation of environmental cues) may be involved in adaptive evolution at such short timescales, eventually enabling transgenerational plasticity (Hughes *et al.* 2017a; Torda *et al.* 2017; Jablonka 2017).

Surprisingly, frontloading and gene expression plasticity were generally discussed as mutually exclusive patterns (Oliver & Palumbi 2010; Barshis *et al.* 2013; Palumbi *et al.* 2014; Dixon *et al.* 2015; Kenkel & Matz 2016) although these two molecular processes most likely co-occur during coral responses to heat stress. In particular, one might expect that the regulation strategy of genes (plasticity versus frontloading) will greatly depend on the molecular pathways in which they are involved and the energetic, physiological, and ultimately fitness cost associated with gene expression. So far, frontloading has been detected for stress response genes such as Heat Shock Proteins (HSPs), apoptosis and tumour suppression factors in resilient coral populations under experimentally simulated heat stress inducing bleaching in the common reef-building coral *Acropora hyacinthus* (Polato *et al.* 2010; Barshis *et al.* 2013; Dixon *et al.* 2015; Kenkel & Matz 2016) and for metabolic genes in populations pre-exposed to warm temperatures in response to long-term heat stress in *Porites astreoides* (Kenkel *et al.* 2013; Palumbi *et al.* 2014). Conversely, in the latter species, plasticity was observed in the expression of environmental stress response genes (Hughes *et al.* 2003; Riegl *et al.* 2011; Coles & Riegl 2013; Kenkel & Matz 2016), hence challenging the patterns observed in *A. hyacinthus* (Barnosky *et al.* 2011; Barshis *et al.* 2013; Coles & Riegl 2013; Kenkel & Matz 2016). Although both strategies (i.e. constitutive frontloading *versus* expression plasticity) undoubtedly exist in wild coral populations, the pre-exposure conditions that foster their induction and their relative effects on coral resistance to heat stress still remain unclear (but see (Hughes *et al.* 2003; Barnosky *et al.* 2011; Dixon *et al.* 2015; Kenkel & Matz 2016)).

Importantly, scleractinian corals are composed of several symbiotic organisms including the cnidarian host, the mutualist photosynthetic algae (formerly defined as belonging to the genus *Symbiodinium* but now considered as different genera within the family Symbiodiniaceae (Bellwood *et al.* 2004; Barnosky *et al.* 2011; Dixon *et al.* 2015; LaJeunesse *et al.* 2018)) and bacterial communities. All symbionts involved in a stable symbiosis effectively form the entire organism, and constitute what is referred to the holobiont (Margulis & Fester 1991; Hoegh-Guldberg *et al.* 2007; Reusch 2013; Palumbi *et al.* 2014; Torda *et al.* 2017). A decade after this term was defined, its use has been particularly popularized in reference to corals (Rohwer *et al.* 2002), and subsequent research has led to the hologenome theory of evolution (Rosenberg *et al.* 2007; Zilber-Rosenberg & Rosenberg 2008). In this context, the hologenome is defıned as the sum of the genetic information of the host and its symbiotic microorganisms. Phenotypes are thus the product of the collective genomes of the holobiont partners in interaction with the environment, which constitute the unit of biological organization and thus the object of natural selection (Zilber-Rosenberg & Rosenberg 2008; Guerrero *et al.* 2013; McFall-Ngai *et al.* 2013; Bordenstein & Theis 2015; Theis *et al.* 2016). Additionally to the cnidarian host response, the genotype -or association of genotypes- of the photosynthetic mutualist Symbiodiniaceae symbionts plays a key role in the thermotolerance of the holobiont (Hume *et al.* 2013; Mayfield *et al.* 2014; Suggett *et al.* 2017). There is less certainty about the importance of the coral bacterial community in participating to the fitness of the holobiont, although accruing evidences strongly suggest their implication in coral response to environmental conditions (Li *et al.* 2014; Pantos *et al.* 2015; Hernandez-Agreda *et al.* 2016), and in the resistance to diseases (Sato *et al.* 2009; Cróquer *et al.* 2013; Meyer *et al.* 2016). Finally, the role of the coral-associated microorganisms and their potential to modify holobiont response to stress remain so far overlooked (but see (Ziegler *et al.* 2017; Torda *et al.* 2017). Hence, studying how corals respond to stress implies an integrative approach to analyze the response of each symbiotic protagonist.

With this aim, we investigated the molecular mechanisms underlying thermo-tolerance of coral holobionts. We analyzed the holobiont response to stress of two coral populations originating from environments with contrasting thermal regimes. We used scleractinian corals from the genus *Pocillopora*

as model species because they have abroad spatial distribution throughout the Indo-Pacific (Veron & Stafford-Smith 2000). The genus *Pocillopora* is considered to be one of the most environmentally sensitive (van Woesik *et al.* 2011) but its widespread distribution clearly suggests potential for acclimation and/or adaptation which may be correlated to specific differences (i.e. different cryptic lineages may be adapted to different environmental conditions). In particular, we focused on *Pocillopora damicornis-like* colonies from two localities with contrasting thermal regimes: colonies from New Caledonia (NC) are exposed to temperate and stable temperatures over the year, while those from Oman are exposed to globally warmer and more seasonal fluctuating temperatures. As the *corallum* macromorphology is not a discriminant character in *Pocillopora* and as the taxonomic revision of this genus using molecular data reveals that some of the *Pocillopora* species (Schmidt-Roach *et al.* 2014; Gélin *et al.* 2017b) are actually species complexes, we identified *a posteriori* the species of the sampled colonies (mitochondrial ORF sequencing and individual clustering) in order to interpret the results in a precise evolutionary context. To avoid biases inherent in transplantation-based field experiments resulting from environmental factors other than temperature, we undertook our comparative study in a controlled environment in which we mimicked ecologically realistic heat stress to compare the responses of colonies from both localities. We combined a specific RNA-seq approach to study the cnidarian host response, and metabarcoding analyses using ITS-2 and 16S amplicon sequencing to study the dynamics of the associated algal (Symbiodiniaceae) and bacterial community compositions, respectively. According to the literature we first expected to detect changes in both symbiotic algal and bacterial communities in corals from both localities when exposed to heat stress. Moreover, since variable environments are expected to select for plasticity, we predicted that the cnidarian hosts from Oman may display more gene expression plasticity than those from New Caledonia. However, because frontloading was also found to be an alternative response to recurrent changing conditions, we might also expect some degrees of constitutive high levels of gene expression at least for some molecular pathways and more particularly in Oman corals.

Material and methods

Coral sampling and maintenance

Pocillopora damicornis-like colonies originating from environments characterized by contrasting thermal regimes were sampled during the warmer month in two different localities: (1) in Oman, Gulf of Oman, Northwestern Indian Ocean (Om; June 2014; local seawater temperature during sampling 30.8°C), where corals are exposed to a globally warmer and variable thermal environment, and (2) in New Caledonia, Southwestern Pacific Ocean (NC; November 2014; local seawater temperature during sampling 27.1°C), where corals are subject to more mitigate and stable temperatures (see Table 1 for the sampling sites and Table 2 for temperature regime of locality).

Table 1. Sampling sites

Locality	Colony	GPS
New Caledonia	NC1	22°18’919 S 166°26’333 E
	NC2	22°17’768 S 166°26’209 E
	NC3	22°20’886 S 166°21’952 E
Oman	Om1	23°30’806 N 58°45,340 E
	Om2	23°31’287 N 58°44’995 E
	Om3	23°37’258 N 058°36’003 E

Table 2. Sea Surface Temperatures (SST) to which the colonies sampled in this study are exposed in their natural environments. Thermal regime descriptors were compiled from weekly mean sea surface temperature data collected from the Integrated Global Ocean Services System Products Bulletin (IGOSS:

http://iridl.ldeo.columbia.edu/SOURCES/.IGOSS/) for quadrats of 1° longitude x 1° latitude from 1982 to the year of sampling (2014).

	New Caledonia	Oman
Mean SST (°C)	24.8	27.9
Variance (°C)	2.7	9.5
Min SST (°C)	22.6	22.1
Max SST (°C)	27.1	33.2
Mean SST of 3 warmer months (°C)	26.8	31.3
Mean SST of 3 cooler months (°C)	22.8	23.8

From each location, we thus sampled colonies morphologically similar and occupying the same water depth niche. To account for possible intra-population diversity, three colonies (>20 cm in diameter) were collected in each locality, and separated by at least 10 m to decrease the probability to collect members of the same genet, as some *Pocillopora* species are able to propagate by asexual reproduction (Adjeroud *et al.* 2013; Gélin *et al.* 2017a; 2018).

Immediately following collection, a 1 cm branch tip of each colony was excised, rinsed three times in filtered seawater (0.22 µm), and placed in RNAlater solution (Sigma Aldrich) for the *in situ* microbiota analysis. The rest of the colony was fragmented into 20 branches each of 10 cm length and physiologically stabilized in openwater system for one week before shipping (Al-Hail field stationof the Sultan Qaboos University and the Public aquarium of Noumea for OM and NC localities respectively). For shipping, individual branches were placed in plastic bags containing oxygenated seawater (800mL seawater and 1600mL of medical oxygen), and transported by aircraft to the research aquarium of the Banyuls-sur-Mer oceanographic observatory (France). The coral branches were maintained in artificial seawater (Seachem Reef Salt) at 26°C, and supplied daily with *Artemia* nauplii to satisfy their heterotrophic demand. The conditions in the maintenance tank were controlled to mimic the natural physicochemical parameters of coral reefs (pH:8.2; salinity: 36 psu; light intensity: 150 to 250 µmol of photons/m²/s; photoperiod: 12h night/12h day;kH: 6–7.5 dkH; calcium concentration: 410–450 mg/L; inorganic phosphate concentration: < 0.1 mg/L; magnesium concentration: 1300–1400 mg/L; nitrate concentration: < 5 mg/L). After 3 and 7 months of acclimatization to the laboratory condition (marked by growth resumption) for Om and NC colonies, respectively, corals were fragmented to produce a total of ~15 to 20 clones (nubbins) from each colony (~3 cm). These were individually fixed to a support (here a p1000 tip) using an epoxy adhesive. We waited for complete healing (evident as tissue extending to cover the epoxy adhesive) prior to run the experiment.

Ecologically realistic heat stress

The aim of this experiment was to compare the response to heat stress of colonies from two localities having the same physiological state, to investigate the patterns of expression of the molecular pathways involved during the stress exposure and the putative modifications of the coral microbiota.

The experimental design comprised four tanks of 53 L per locality in which the seawater was continuously recycled. The water was sterilized using UV (rate 3200 L/h) and renewed twice per hour in each tank (recirculation rate: 100L/h in each tank). The eight tanks shared the same seawater but their temperature was monitored individually (HOBBY BiothermPro, model 10892; 500W Aqua Medic titanium heater; HOBO TidbiT v2 logger) (Supplementary Figure S1). For each locality, 5 to 8 nubbins per mother colonies were randomly placed in each tank (four tanks per locality) for two weeks at the control temperature and the following protocol was applied: three tanks were then subjected to a gradual temperature increase (stress treatment) while the fourth (control) was maintained at the control temperature to verify that the stress observed in the stressful treatment was not due to other potential confounding effects or water cues (Figure 1). Both the control and stress temperatures were specific for each sampling locality to mimic their respective natural environment. In particular, we set the control temperature as the mean water temperature for the three warmer months measured at the coral sampling

site locality (Table 1): 31°C for the colonies from Om, and 27°C for the colonies from NC. The stress treatment was ecologically realistic, i.e. reflecting a naturally occurring warming anomaly, and consisted in increasing the temperature gradually by 1°C (over 5 consecutive hours) each week until physiological collapse of the corals became evident (polyps closure, bleaching or necrosis), as described by (Vidal-Dupiol *et al.* 2009). Sampling was performed in the three sampling tanks just before the first temperature increase (control condition) as well as each week before the next temperature increase. The beginning of polyp closure was consistently observed for the different colonies of the same locality at the same temperature threshold. Samples for subsequent genetic and transcriptomic analyses were chosen *a posteriori*. They corresponded to those sampled in each tank just before the first increase of temperature (control samples), and just before the temperature that produced the first signs of physiological collapse and before bleaching (stress temperature samples). Thus, for each condition (control and stress) we obtained three biological replicates of each colony from the three different tanks (three colonies per locality) to reach a total of 36 samples (2 localities × 3 colonies× 2 experimental conditions × 3 replicates/tanks). The general health of the nubbins was assessed via daily photographic monitoring (at noon prior to feeding) throughout the period of the experiment.

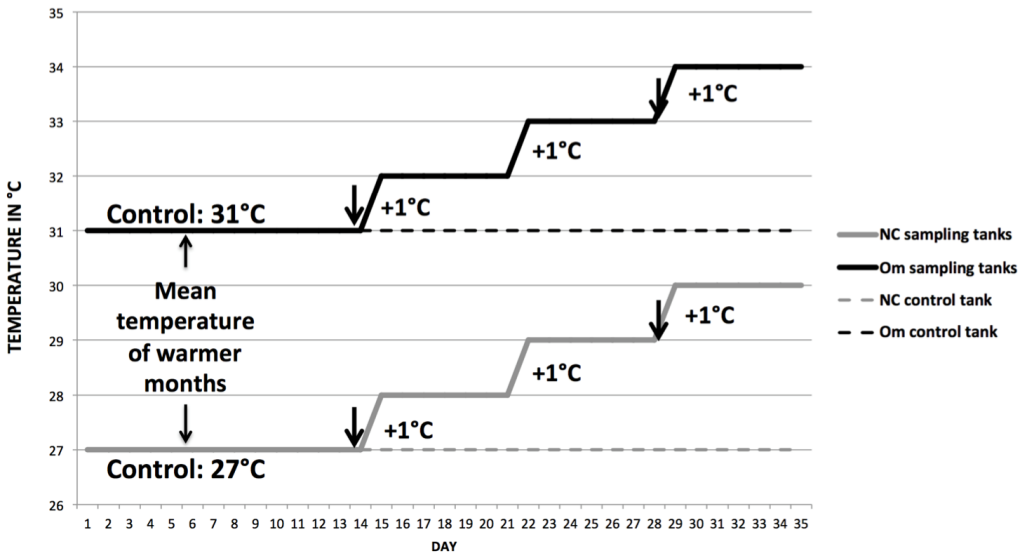

Figure 1. The ecologically realistic heat stress experiment: from mean temperatures of the warmer months in natura to a pre-bleaching physiological state. Nubbins were collected at each time point and arrows represent points at which nubbins were chosen for analyzing the microbial composition and the transcriptomic response of the host.

DNA extraction

DNA was extracted from each 36 samples as well as coral tips directly collected on the six colonies *in natura* for the *in situ* condition (three in Om, three in NC), using the DNeasy Blood and Tissue kit (Qiagen) following the manufacturer's instructions. DNA was quantified by spectrophotometry (NanoDrop).

Host species and clonemates identification

As the *corallum* macromorphology is not a diagnostic criterion in *Pocillopora* genus, the host species was thus identified molecularly. Thus each colony was sequenced for the mitochondrial variable open reading frame (ORF) and was genotyped using 13 specific microsatellites, as in Gélin *et al.* (Gélin *et al.* 2017b). Then each colony used in the experiment was assigned to Primary and Secondary Species Hypothesis (PSH and SSH; *sensu* Pante et al.) (Pante *et al.* 2015) following the nomenclature from Gélin *et al.* (Gélin *et al.* 2017b). Indeed, sampling *Pocillopora* colonies presenting various morphs from different locations from the Indo-Pacific, Gélin et al classified these colonies, without *a priori* based on *corallum* macromorphology, into Species Hypotheses (*sensu* Pante et al., i.e. the species are hypotheses that can be confirmed or refuted while new data are added) (Pante *et al.* 2015) using sequence-based species

delimitation methods, a first sorting allowed to define Primary Species Hypotheses (PSH) and then individual clustering based on microsatellite multilocus genotypes allowed a second sorting delimiting Secondary Species Hypotheses (SSH). Thus comparing the ORF sequences obtained in this study to those from (Gélin *et al.* 2017b), the sampled colonies were assigned to a PSH. Then, if relevant, the colonies were assigned to SSH performing clustering analysis using Structure 2.3.4 (Pritchard *et al.* 2000), as in (Gélin *et al.* 2017b). Meanwhile, the identical multi-locus genotypes (i.e. clonemates if any) were identified by microsatellite analysis using GenClone (Arnaud-Haond & Belkhir 2006) as in Gélin *et al.* (Gélin *et al.* 2017a).

Microbial community analysis using MiSeq 16S and ITS2 metabarcoding

The aim of this analysis was to investigate the composition and the dynamics of the two principal symbiotic coral communities (i.e. bacterial and algal) *in situ* and during heat stress.

Amplicon Sequencing

A bacterial 16S rDNA amplicon library was generated for each of the 42 samples (one *in situ* condition, three control conditions and three stress conditions per colony, three colonies per locality, two localities), using the 341F (CCTACGGGNGGCWGCAG) and 805R (GACTACHVGGGTATCTAATCC) primers, which target the variable V3/V4 loops (Klindworth *et al.* 2012). The Symbiodiniaceae assemblages were analyzed using ITS2 (internal transcribed spacer of the ribosomal RNA gene) amplicon libraries and specific primers targeting a sequence of approximately 350 bp (ITS2-F GTGAATTGCAGAACTCCGTG; ITS2-R CCTCCGCTTACTTATATGCTT) (Lajeunesse & Trench 2000; Quigley *et al.* 2014). For both markers, paired-end sequencing using a 250 bp read length was performed on the MiSeq system (Illumina) using the v2 chemistry, according to the manufacturer's protocol at the Centre d'Innovation Génome Québec and McGill University, Montreal, Canada.

Bioinformatic analysis

The FROGS pipeline (Find Rapidly OTU with Galaxy Solution) implemented on a Galaxy platform (http://sigenae-workbench.toulouse.inra.fr/galaxy/) was used for data processing (Escudié *et al.* 2017). In brief, paired reads were merged using FLASH (Magoč & Salzberg 2011). After cleaning and removal of primer/adapters using cutadapt (Martin 2011), *de novo* clustering was performed using SWARM (Mahé *et al.* 2014). This uses a local clustering threshold with an aggregation distance (d) of 3. Chimeras were removed using VSEARCH (Rognes *et al.* 2016). We filtered the dataset for singletons and performed affiliation using Blast+ against the Silva database (release 128, September 2016) for 16S amplicons (Altschul *et al.* 1990). For ITS2 metabarcoding, the Symbiodiniaceae type was assessed using Blast+ against an in-house database of Symbiodiniaceae reference sequences built from sequences publicly available. An OTU table in standard BIOM format with taxonomic affiliation was produced for subsequent analyses.

For community composition analysis we used the *phyloseq* R package (McMurdie & Holmes 2013) to infer alpha diversity metrics at the OTU level (i.e. Shannon and Chao indexes), and beta diversity (between sample similarity) from the OTU table. Community similarity was assessed by Principal Coordinate Analysis (PCoA) using the Bray-Curtis distance matrices.

To test for possible effect of corals' locality of origin and for temperature treatments on the two alpha diversity metrics (i.e. Shannon and Chao) we ran a series of four generalized mixed models including these two fixed factors and their interactions as explanatory variables. The four models consisted in considering all factors, the two fixed factors without accounting for their possible interactions, and the two factors independently. In all models, we also accounted for possible effect of genotypes that were considered as random factors nested within locality. All models were run using the lme4 package implemented in R (Bates *et al.* 2015) and considering a Gamma distribution. The best model for each alpha diversity metrics was identified based on the Akaike Information Criterion (AIC (Akaike 1974)). Concerning beta diversity, we performed MANOVAs to compare beta diversity metrics among the groups of samples by sampling locality, genotype or treatment.

Corrections based on multiple testing were performed using FDR (Benjamini & Hochberg 1995). For all analyses, the threshold significance level was set at 0.05.

Transcriptome analysis

The aim of this analysis was to study the transcriptomes of the sampled colonies in response to heat stress compared with controlled conditions.

RNA extraction

Total RNA was extracted from each coral sample using TRIzol reagent (Invitrogen), according to the manufacturer's protocol. The quantity and integrity of the total RNA extracted was checked using an Agilent 2100 Bioanalyzer (Agilent Technologies)(mean RIN =7.5). Paired-end fragment libraries (2 × 100 bp) were constructed and sequenced on an Illumina HiSeq 2000 platform at the Centre d'Innovation Génome Québec at McGill University, Montreal, Canada.

Bioinformatic analyses

Fastq read files were processed on the Galaxy instance of the IHPE (http://bioinfo.univ-perp.fr) (Giardine *et al.* 2005). Quality control and initial cleaning of the reads were performed using the filter by quality program (version 1.0.0) based on the FASTX-toolkit (Blankenberg *et al.* 2010). Reads having fewer than 90% of bases having a Phred quality score ≤ 26 were discarded (probability of 2.5 incorrect base call out of 1000, and a base call accuracy of 99.75%). Adaptors used for sequencing were removed using the cutadapt program version 1.6 (Martin 2011). All paired-end reads were aligned using RNAstar software under default parameters, with at least 66% of the bases being required to align to the reference, and a maximum of ten mismatches per read (Dobin *et al.* 2013). The *Pocillopora damicornis sensu lato* reference genome used in this study (Vidal-Dupiol *et al.* 2019) consisted of a draft assembly of 25,553 contigs (352 Mb total) and N50 = 171,375 bp. The resulting transcriptome served as the reference for reads mapping, and a GTF annotation file was constructed using cufflink/cuffmerge (Trapnell *et al.* 2010). HTseq was used to produce count files for genes (Anders *et al.* 2015). The DESeq2 package was used to estimate the normalized abundances of the transcripts, and to calculate differential gene expression for samples between the control temperature and the stress temperature for each locality (Love *et al.* 2014), considering the different genotypes (three biological replicates for each genotype) and using default parameters. We next analyzed genes according to their expression patterns among the different colonies and temperature treatments. Genes were clustered manually into six groups according to their differential expression levels: common over-expressed genes, NC-specific over-expressed genes, Om-specific over-expressed genes, common under-expressed genes, NC-specific under-expressed genes, and Om-specific under-expressed genes. Cluster 3.0 (de Hoon *et al.* 2004) and Treeview (Saldanha 2004) were used to build the heatmap.

Discriminant analysis of principal components (DAPC)

Our aim was to quantify and compare the level of genome-wide transcriptome plasticity between colonies from Om and NC in response to heat stress. To achieve this we performed a discriminant analysis of principal components (DAPC) based on a log-transformed transcript abundance matrix (containing 26,600 genes) obtained from the 36 samples (*i.e.* 9 control and 9 stressed replicates per locality), as described previously (Kenkel & Matz 2016). Specifically, we ran a DAPC analysis using the resulting log2 transformed dataset for the colonies from NC and Om reared in controlled conditions as predefined groups in the *adegenet* package implemented in R (Jombart *et al.* 2010). Two principal components and a single discriminant function were retained. We then predicted the position of stressed colonies from both localities (Om and NC) onto the unique discriminant function of the DAPC.

We next ran a general linear model (GLM) using the DAPC scores as dependent variable, and accounted for the locality of origin (NC and Om), the treatment (control and heat stress), and their interaction as explanatory variables. We also considered the effect of individual colonies nested within localities as random effects in the model. Our final objective was to test for a potential significant effect of the interaction between the locality and the treatment effects, as a proxy of significant differences in the genome-wide gene expression reaction norms (i.e. differences in DAPC scores between the control and the heat stress treatments) between Om and NC colonies.

GO enrichment of differentially expressed genes

The transcriptome was annotated *de novo* using a translated nucleotide query (blastx (Altschul *et al.* 1990)) against the non-redundant protein sequence database (nr). The 25 best hits were then used to search for gene ontology terms using the Blast2Go program (Conesa *et al.* 2016). To identify the biological functions significantly enriched within up or down-regulated genes, a Gene Ontology (GO) term enrichment analysis was performed. Lists of GO terms belonging to significantly up-regulated and down-regulated genes were compared to the GO terms of the whole expressed gene set using a Fischer exact test and a FDR value of 0.05. We used REVIGO to visualize the enriched biological processes (Supek *et al.* 2011).

Results

Host identification

Among the three colonies from New Caledonia, colonies NC2 and NC3 presented haplotype ORF18 and were assigned to Primary Species Hypothesis PSH05 and more precisely to Secondary Species Hypothesis SSH05a (Gélin *et al.* 2017b), corresponding to *P. damicornis* type *β* (Schmidt-Roach *et al.* 2014) or type 5a (Pinzón *et al.* 2013), while colony NC1 presented ORF09 and was assigned to PSH04, *P. damicornis* type *α*, *P. damicornis* or type 4a, respectively. As for colonies from Oman, they all presented ORF34 and were assigned to PSH12 (Gélin *et al.* 2017a) or type 7a (Pinzón *et al.* 2013) (Supplementary Table S2), that is not part of the *P. damicornis sensu lato* species complex. Thus NC colonies are phylogenetically closer from each other than from colonies from Oman. These three PSHs represent three different species.

Furthermore, NC2 and NC3 multi-locus genotypes (MLGs) differed only from one allele over 26 gene copies, and were thus part of the same clonal lineage (genet), i.e. the entity that groups together colonies whose multi-locus genotypes slightly differ due to somatic mutations or scoring errors. All the other colonies presented MLG that differed enough not to be considered as clonemates or members of the same clonal lineage (genet).

Ecologically realistic heat stress

Our goal was to ensure that our experimental heat stress faithfully reflects a realistic heat stress *in natura*. Following collection from the field, the corals from the different localities were first maintained in the same controlled conditions at 26°C prior to the experiment. During this period no mortality or signs of degradation/stress were observed for any of the coral colonies. Two weeks before the experiment, a first acclimatization to the control temperatures (27°C or 31°C for NC and Om respectively) was performed. During the experimental heat stress (i.e. gradual temperature increase), visual and photographic monitoring clearly indicated that the first sign of coral stress (i.e. the closure of polyps) occurred at day 30 for both sampling localities, corresponding to 30°C and 34°C for the NC and Om colonies, respectively. These temperatures perfectly match the warmest temperature experienced by these colonies in the field (Table 1). No sign of physiological collapse were observed in control corals throughout the experiment indicating that all the other parameters were maintained optimal for coral colonies.

Bacterial communities

Among the overall 42 samples analyzed, a total of 5,308,761 16S rDNA amplicon sequences were obtained after cleaning and singleton filtering corresponding to 15,211 OTUs. In all samples the class Gammaproteobacteria was dominant (77.7%), particularly the genus *Endozoicomonas* (44.7% of the sequences); this genus is known to be an endosymbiont of numerous scleractinians (Neave *et al.* 2016b) (See Supplementary Figure S3 for complete bacterial composition in each colony and replicate).

Concerning the two alpha diversity metrics (i.e. Shannon and Chao indexes), the best statistical models to explain the overall variance included the coral's locality of origin only (AIC = 101.9). According to these models, colonies from Oman displayed a higher Shannon index than those from New Caledonia ($P = 0.04$). Conversely, the effect of locality was not significant for the Chao index ($P > 0.05$). The PCoA of Bray-Curtis distances for all colonies showed no evident clusters based on the experimental treatments (Figure 2). We observed a loose grouping based on localities and colonies, except for colony NC1, which appeared to have a more specific microbiota composition, as it had a different grouping associated with the first axis, which explained 22.3% of the variance. This could be correlated with the different species hypotheses for NC1

compared to NC2 and NC3 (see above). These observations were confirmed by statistical analyses (MANOVA between localities: *P*=0.003; between genotypes: *P*=0.001; between temperature treatments: *P*=0.761; Supplementary Table S4). Thus, the bacterial composition appeared to be relatively specific to each colony within each locality, but no major shift was observed during the transition from the natural environment to artificial seawater, nor during heat stress exposure.

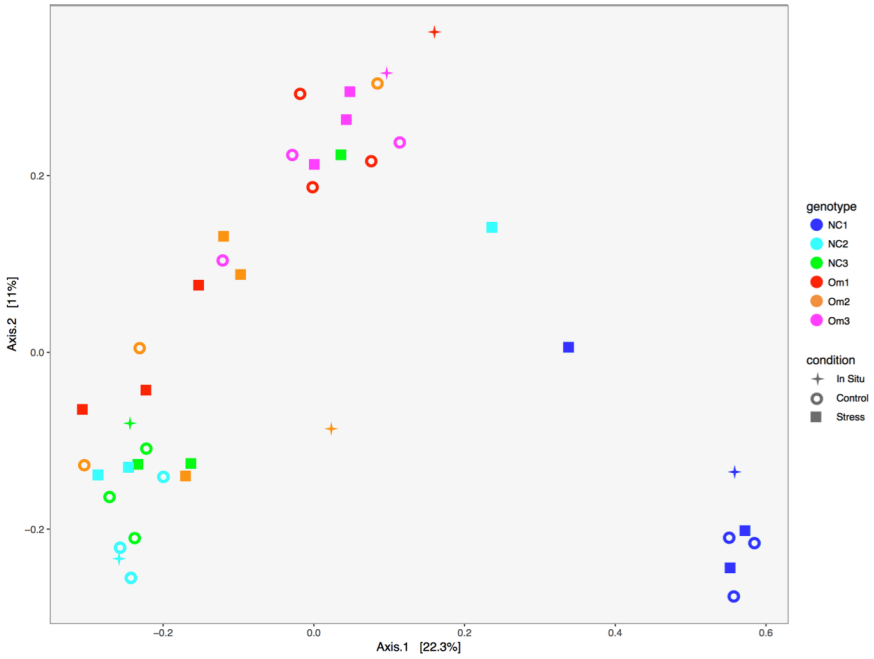

Figure 2. Principal coordinate analysis plot for Bray-Curtis distances of the bacterial composition of each colony in each experimental condition. Different colors represent different colonies, the stars represent the *in situ* conditions, the open circles represent the control conditions, and the squares represent the stress conditions.

Symbiodiniaceae assemblages

Analysis of the Symbiodiniaceae composition was performed based on an ITS2 metabarcoding, which allowed intra-clade resolution.

Removal of OTUs having an abundance of < 1% left only 4 OTUs among all samples. Two of these corresponded to type C1, while the other two corresponded to type D1a according to (Baker 2003). Type D1a was highly dominant in the colonies originating from Oman, whereas type C1 was almost exclusive to the corals from New Caledonia (Figure 3). The Symbiodiniaceae community composition was very specific to each locality, but remained stable during the transition from the natural environment to artificial seawater, and during heat stress exposure.

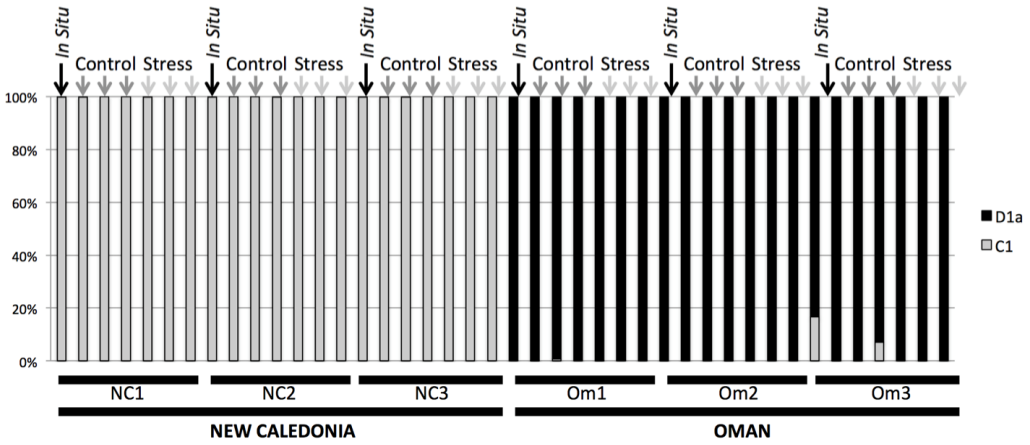

Figure 3. Composition of the Symbiodiniaceae community in each colony in situ and in controlled and stressful experimental conditions.

Host transcriptome analysis

We generated 36 transcriptomes corresponding to triplicate samples for three colonies of each locality exposed to the control (C) and stress (S) temperatures.

Overall, the transcriptome sequencing of these36 samples yielded 1,970,889,548 high quality Illumina paired reads of 100 bp. Globally, 40–64% of reads obtained for the Om colonies, and 59–70% of reads obtained for NC colonies successfully mapped to the *Pocillopora damicornis* (type β) reference genome. The apparently better alignment of samples from New Caledonia most likely relies on the fact that the New Caledonia colonies used in this study belong to *P. damicornis* types α or 4a (PSH04) and β or 5a (PSH05), which are phylogenetically close to each other and closer from the reference genome, than the Om colonies from type 7a (PSH12) that is phylogenetically more distant from the reference genome. The aligned reads were assembled in 99,571 unique transcripts (TCONS), representing putative splicing variants of 26,600 genes identified as "XLOC" in the genome (FASTA sequences available in Supplementary File S5).

The hierarchical clustering analyses clearly grouped together samples belonging to the same locality and species hypothesis according to their genome-wide gene expression patterns, in link with the phylogenetic differences between the NC and Om haplotypes (Figure 4). Within locality and species hypothesis, the transcriptomes also grouped by colony, indicating that the transcriptomes were genotype-specific. For each colony, the transcriptomes then grouped by condition (control or heat stress), except for New Caledonia colonies NC2 and NC3 (corresponding to the same clonal lineage) that clustered together when exposed to control and heat stress conditions.

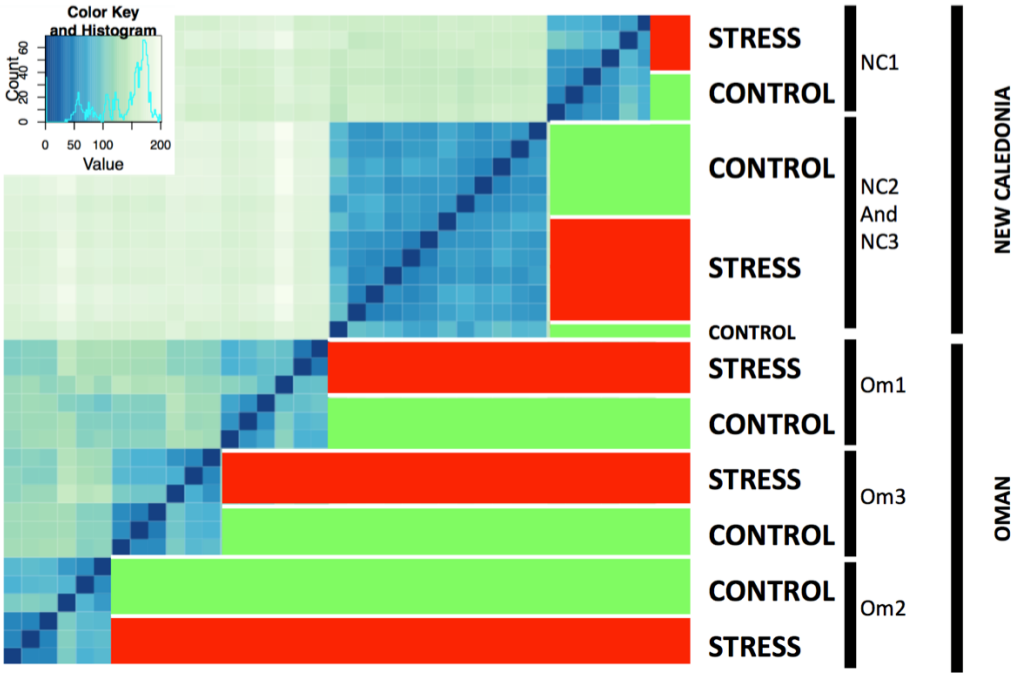

Figure 4. Hierarchical clustering analyses performed using DESeq2 rlog-normalized RNA-seq data for the 36 transcriptomes: two conditions (control and heat stress); three replicates per condition for each colony; three colonies per locality; and two localities [Oman (Om) and New Caledonia (NC)]. The color (from white to dark blue) indicates the distance metric used for clustering (dark blue corresponds to the maximum correlation values).

Despite clustering of the transcriptomes by locality, as the sampling of *Pocillopora damicornis*-like colonies actually corresponded to different species we performed differential gene expression analysis for each colony independently (comparing the biological triplicates for the control condition vs. triplicates for the heat stress conditions). For each locality, the different colonies displayed similar patterns of differential gene expression with in any case a higher number of differentially expressed genes and higher fold-changes between control and heat stress condition in Om compared to NC (Supplementary Figure S6). We detected 673, 479 and 265 differentially expressed genes for NC1, NC2 and NC3 respectively, vs. 2870, 2216 and 959 for Om1, Om2 and Om3. Samples were thus grouped for each locality (nine control nubbins + nine heat stress nubbins) for subsequent analyses (full results of the comparisons between stressed and controls (log2-foldchange and adjusted *p*-values) for each colony or between the two localities are provided in Supplementary File S7). For Om colonies, a total of 5,287 genes were differentially expressed between control and stress conditions (Figure 5). This number was much lower for NC colonies with 1,460 differentially expressed genes (adjusted $P < 0.05$).

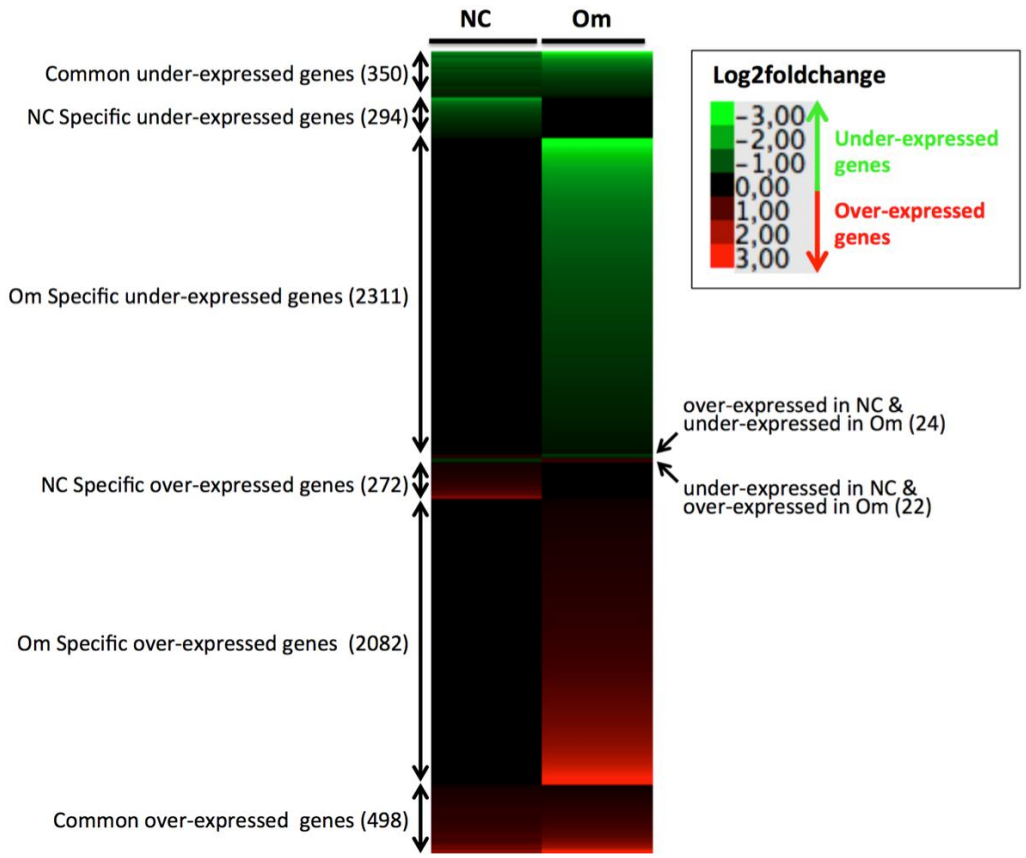

Figure 5. Heatmap and clustering of significantly differentially expressed genes between the control and the heat stress condition for colonies from each locality. Each gene is represented by a row.

Among differentially expressed genes, 848 were differentially expressed in the same direction in both localities (498 over-expressed and 350 under-expressed). In both cases, the differential expression level was significantly higher for the Om corals with a mean log2-fold change of 0.9 for shared over-expressed genes in Om *vs.* 0.6 in NC (Wilcoxon test; $P < 0.0001$), and -1.2 for the shared under-expressed genes in Om *vs*. -0.8 in NC (Wilcoxon test; $P < 0.0001$) (Figure 6 and Supplementary Table S8).

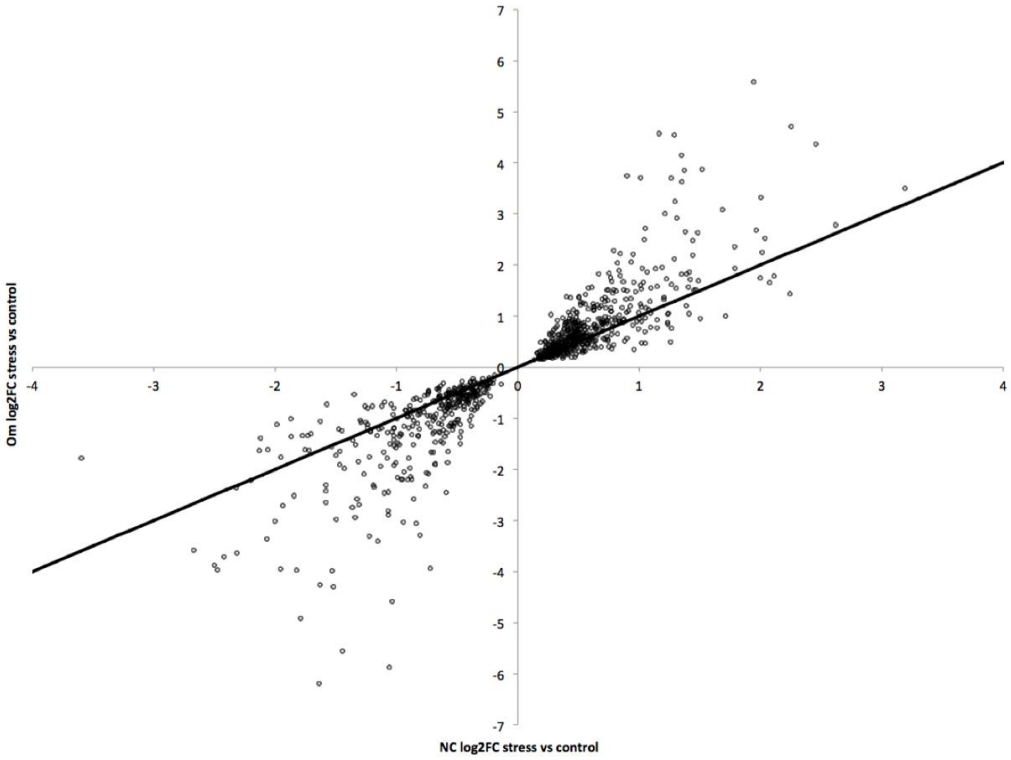

Figure 6. Scatterplot of the log2-fold changes in gene expression in response to heat stress in the Om colonies (y-axis) vs. the NC colonies (x-axis) for the 848 genes that were over-expressed (498 genes) or under-expressed (350 genes) in colonies from both localities. The line represents the y=x line depicting similar responses between colonies.

Additionally, colonies from the two localities also responded specifically to heat stress. In particular, 272 genes were over-expressed and 294 were under-expressed only in the NC corals, whereas 2,082 were over-expressed and 2,311 were under-expressed only in the Om ones when exposed to heat stress. Finally, the colonies from both localities displayed antagonistic transcriptomic responses to heat stress for a small subset of genes (24 over-expressed in NC but under-expressed in Om, and 22 under-expressed in NC but over-expressed in Om).

Altogether these results revealed a greater transcriptomic response to heat stress in colonies originating from Oman compared to those from New Caledonia (4,393 differentially expressed genes for the Om corals *vs.* 566 genes for the NC ones).

Discriminant Analysis of Principal Components (DAPC)

At the overall gene expression level, our DAPC analysis clearly discriminated the colonies from both localities (Figure 7). More interestingly, the GLM revealed a significant interaction term between the locality and condition (control or heat stress) effects (P = 0.04), hence indicating that the slope of the reaction norm was different between localities. More particularly, the Om colonies responded to a greater extent than the NC ones, and thus showed significantly higher gene expression plasticity in response to heat stress.

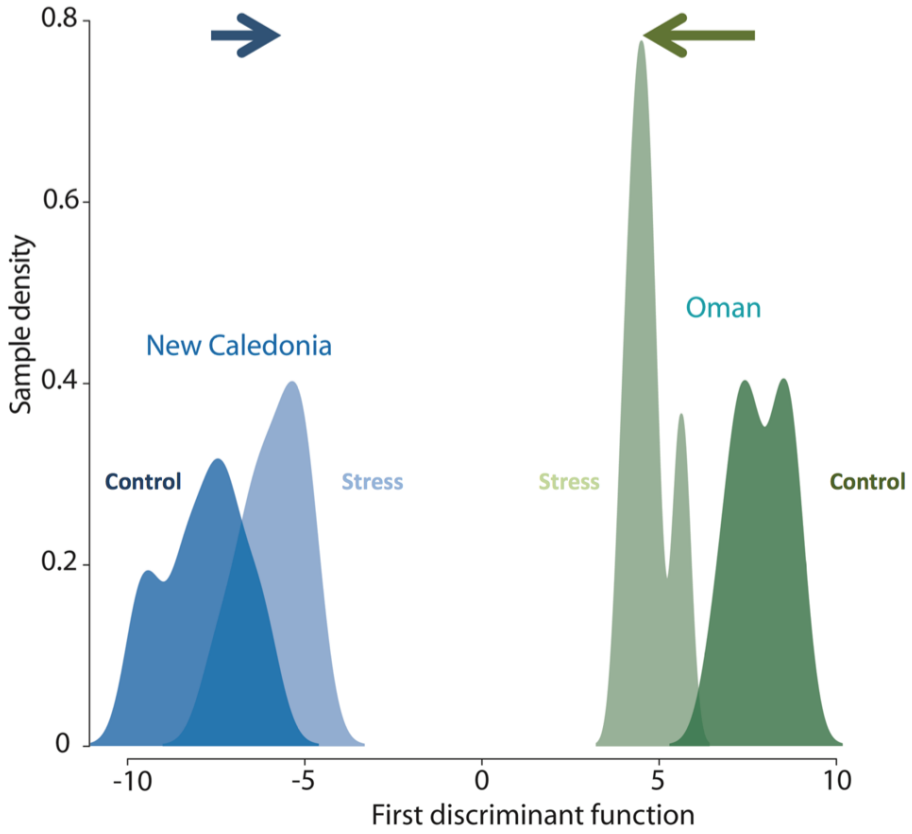

Figure 7. Colony level gene expression variation in response to heat stress, based on DAPC analysis. The x-axis is the first discriminant function of the DAPC along which the overall gene expression difference between colonies at both experimental conditions (stress and control) and from both localities (NC and Om) was maximized. This indicates the degree of similarity between the transcriptomes. The density plots obtained for NC and Om colonies are represented in blue and green, respectively. Dark and light density plots correspond to samples from the control and stress experimental conditions. The arrows above the density plots represent the direction of the mean change in the gene expression profiles.

It is worth stressing that colonies having experienced the heat stress displayed more similar genome-wide expression profiles than controlled colonies (Figure 7). Such pattern was also observed in colonies of mustard hill coral *P. astreoides* experiencing a heat stress compared to controls (Kenkel & Matz 2016). This apparent convergence in the functional response of colonies from different habitats to heat stress might be at least partly explain by the fact some common molecular pathways are turned-on when colonies are facing stressful conditions although the magnitude of such responses is different.

Analysis of gene function

To investigate the functions associated with the differentially expressed genes we performed a BLASTX annotation of transcripts followed by a Gene Ontology (GO) term (biological process, molecular function, and cell compartment) (Supplementary File S9).

For the 498 common over-expressed genes, 139 biological processes were enriched compared to the entire set of annotated genes. The most significant biological process identified in the REVIGO analysis (i.e. with lowest FDR= 2.1×10^{-68}) was response to stress (Figure 8). Following this sequentially, were cellular metabolism (FDR=3.7×10^{-49}), positive regulation of biological processes (FDR = 2.4×10^{-43}), cell death (FDR = 2.5×10^{-33}), cellular localization (FDR = 8.4×10^{-25}), and pigment metabolism (FDR = 2.1×10^{-21}). Among the 272 genes over-expressed in the NC but not in the Om colonies in response to heat stress, 38 biological processes were enriched: organic acid catabolism (FDR = 1.6×10^{-22}), protein transport (FDR = 1.8×10^{-16}),

stress response (FDR = 4.8×10^{-13}), and cellular metabolism (FDR = 3×10^{-12}) were the four most significantly enriched biological processes (Figure 8). Among the 2,082 genes over-expressed in the Om but not in the NC colonies in response to heat stress, 160 biological processes were enriched, the most significant being ncRNA metabolism (FDR = 8.9×10^{-303}), cellular metabolism (FDR = 4.4×10^{-70}), carbohydrate derivative biosynthesis (FDR = 5.9×10^{-64}), and organic substance transport (FDR = 2×10^{-44}).

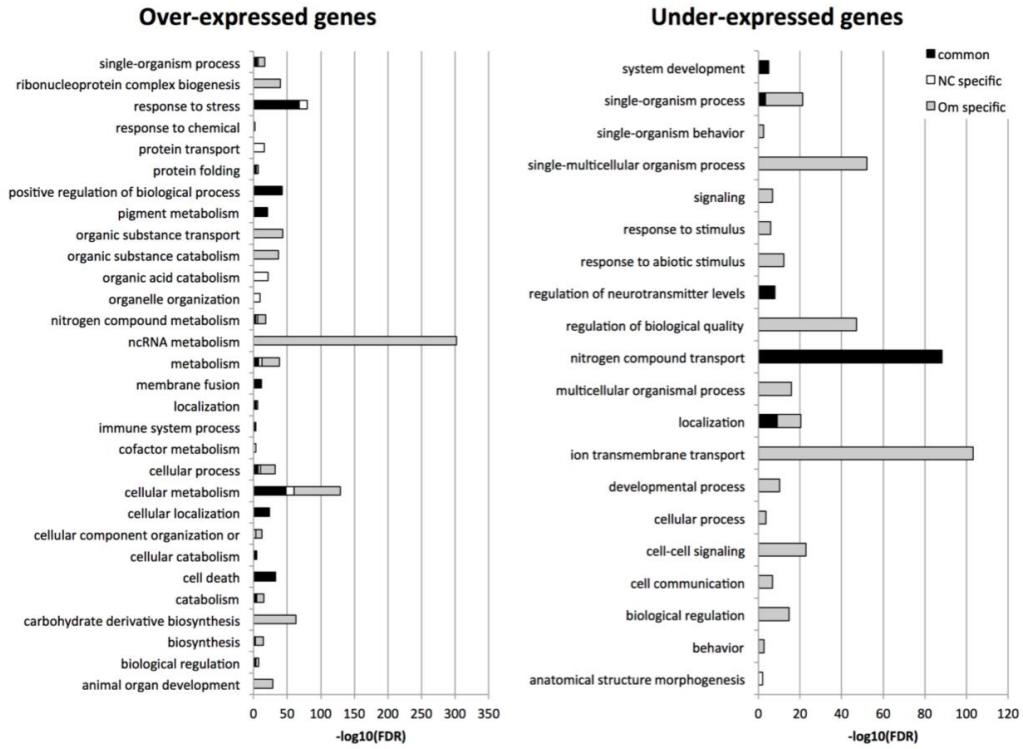

Figure 8. Summary of the GO enrichment analysis following REVIGO synthesis. Each enriched biological process is represented by a bar proportional to the log10(FDR). The colors correspond to the three categories of genes (common: black; Om-specific: grey; NC-specific: white) that were over-expressed (left panel) or under-expressed (right panel).

For the 350 genes that were under-expressed following heat stress irrespective to the locality of origin (Om or NC), 48 biological processes were enriched and grouped into five biological processes: nitrogen compound transport (FDR = 5.4×10^{-89}), localization (FDR = 8.1×10^{-10}), regulation of neurotransmitter levels (FDR = 1.2×10^{-8}), system development (FDR = 8.8×10^{-6}), and single organism process (FDR = 4×10^{-4}). Among the under-expressed genes in the NC colonies only, a single biological process (anatomical structure/morphogenesis) was found to be enriched (FDR = 9×10^{-3}). Among the under-expressed genes in the Om colonies, 139 biological processes were enriched, with the most significant being ion transmembrane transport (FDR = 7.6×10^{-104}), single multicellular organism process (FDR = 7.5×10^{-53}), regulation of biological quality (FDR = 6×10^{-48}), cell–cell signaling (FDR = 1.5×10^{-23}), single organism process (FDR = 1.1×10^{-18}), multicellular organism process (FDR = 1.5×10^{-16}), biological regulation (FDR = 2.3×10^{-15}), response to abiotic stimulus (FDR = 6.2×10^{-13}), and localization (FDR = 4.6×10^{-12}). The complete results for all GO term categories including molecular function are available in Supplementary File S9.

Regarding cellular compartments, the mitochondria was the most significantly enriched in the common over-expressed genes (FDR = 1.5×10^{-180}), as well as among genes over-expressed in NC (FDR = 2.5×10^{-82}) while in genes over-expressed in Om corals the intracellular organelle lumen was the most significantly enriched (FDR = 1×10^{-560}).

To investigate whether the presumably more thermotolerant colonies from Oman displayed a frontloading strategy (i.e. a higher expression for some genes compared to the colonies from NC) as previously described in scleractinian corals (Barshis *et al.* 2013), we compared the gene expression levels in control conditions between Om and NC colonies for those genes that were over-expressed in NC colonies (Supplementary File S10). This comparison revealed that the constitutive expression level was often greater in the Om colonies. Among the 770 genes that were over-expressed in NC colonies in response to thermal stress (272 specifically and 498 in common with Om), 484 were constitutively (i.e. in the control condition) more expressed in Om. Among these genes, 163 were not differentially expressed between the control and stress temperatures reflecting true frontloading based on the definition of Barshis et al. (2013), while 301 were over-expressed and only 20 were under-expressed during heat stress. These 484 genes with higher constitutive expression in Om were submitted to GO term enrichment analysis. No significant results were found for the under-expressed genes. The frontloaded genes were enriched in the biological processes cellular respiration (FDR = 4.4×10^{-23}), cellular component organization (FDR = 0.002), homeostatic process (FDR = 0.005), cellular component organization or biogenesis (FDR = 0.007), cofactor metabolism (FDR = 0.009), and stress response (FDR = 0.009), and in the mitochondrion for the most significant cellular compartment (FDR = 1.6×10^{-66}). Most interestingly, for genes associated with a higher basal expression level together with over-expression in the Om colonies, the most enriched biological processes were stress response (FDR = 1.2×10^{-26}), pigment metabolism (FDR = 5.1×10^{-24}), regulation of phosphate metabolism (FDR = 3.2×10^{-15}), cellular metabolism (FDR = 2.7×10^{-11}), and protein folding (FDR = 7.3×10^{-6}).

Discussion

Specific context of adaptation

Our aim was to compare the phenotypic plasticity in terms of transcriptomic response to heat stress of coral colonies originating from different localities displaying contrasted thermal regimes. As morphology can be misleading for species identification in scleractinians, notably in *Pocillopora* genus (Gélin et al., 2017a), we used a molecular approach to test the species relationships of our samples. The analysis of mitochondrial sequences and clustering analyses indicated that, despite similar morphologies, our samples corresponded to different species. This agrees well with previous works showing the importance of cryptic lineages and morphological plasticity in the *Pocillopora* genus (Gélin *et al.* 2017a and references herein). Oman colonies corresponded to species hypothesis PSH12 of (Gélin *et al.* 2017b), which is restricted to the Northwestern Indian Ocean. Regarding the two species hypotheses from NC, SSH05a (*P. damicornis* type *β* SSH05a or *P. acuta*) is found in the Pacific Ocean and PSH04 (*P. damicornis* type *α* or *P. damicornis sensu stricto*) is nearly exclusively found in the Pacific Ocean (very rare in the Indian Ocean, and not found yet in Red Sea) (Gélin *et al.* 2017b). It would be interesting to study whether inside each species hypothesis, different thermotolerance phenotypes are present. Conversely, the observation of a similar response to thermal stress in two different species in NC, as revealed by differential gene expression as well as DAPC analyses, could indicate either a conserved strategy or a convergence under the same ecological conditions.

An ecologically realistic heat stress

The heat stress applied in this study was ecologically realistic, since the first visual response (i.e. polyp closure) was observed for all colonies when the gradually increasing experimental temperature reached the upper temperature they are subjected to *in natura* (30°C and 34°C for NC and Om corals, respectively). From a biological point of view this first result hence clearly supports that these colonies from two localities that are experiencing two different thermal regimes *in natura* display differential ability to deal with heat stress. Moreover, the accurate control of all other seawater parameters allows us to consider that the holobiont response to the thermal treatment is specific to heat stress and not to other possible confounding effects. Last, as we analyzed the samples before the first visible signs of stress (polyp closure), any change in the holobiont would therefore reflect the response to the heat stress and not homeostasis breakdown after disruption of the coral integrity.

Symbiotic community: bacterial and Symbiodiniaceae composition

For the bacterial community, we identified significant differences between localities and colonies. The microbiota composition of all samples was consistent with previous studies, showing a high proportion of Gammaproteobacteria and dominance of the symbiotic *Endozoicomonas* genus (Bourne & Munn 2005; Neave *et al.* 2016a; Peixoto *et al.* 2017). However, our results clearly demonstrate that neither maintenance in the experimental structure nor experimental heat stress induced major bacterial community changes in coral colonies irrespective to their locality of origin. For the Symbiodiniaceae community, the ITS2 metabarcoding analysis enabled inter-clade resolution (Quigley *et al.* 2014). Two distinct types of D1a and C1 clades dominated, representing most of the sequences in the Om and NC corals, respectively. Nine ITS types (A to I) have been identified in the former genus *Symbiodinium* (Baker 2003). Some Symbiodiniaceae strains strongly participate to the overall holobiont fitness, with type D providing tolerance to higher temperatures (Berkelmans & van Oppen 2006) and C1 enhancing coral growth rates (Little *et al.* 2004). Interestingly, we found that the type D1a is dominant in the more thermotolerant Om corals, which is consistent with the results of previous works (Berkelmans & van Oppen 2006), however recent results shows that such an association is rather linked with minimal temperatures than annual amplitude of temperature changes (Brener-Raffalli *et al.* 2018).

Although the microbial community (both bacterial and Symbiodiniaceae) differed between the NC and Om corals, the composition did not change during transition from the field to the artificial seawater conditions, and remained similar during the experimental temperature increase. Thus, the coral holobiont assemblage remained similar after the course of the experiment. Such stability of the microbial community during experimental heat stress was previously observed in the scleractinian *Acropora millepora* (Bellantuono *et al.* 2012b) and *A. tenuis* (Littman *et al.* 2010). Thus, our study conforms to the idea that microbial communities associated with scleractinian corals remain unchanged when the holobionts are exposed to stressful temperatures (but see (Ziegler *et al.* 2017)) but further analyses of gene expression level would be needed to assess their functional responses. RNA-sequencing of eukaryotic poly-adenylated mRNA would allow in principle dual analysis of Symbiodiniaceae and coral host transcripts (Mayfield *et al.* 2014), but since our RNA extraction method resulted in very few algal transcripts, we only focused on the host transcriptomic response.

Based on these results, we investigated changes in host gene expression as the main mechanism of response to heat stress in our experimental design.

Host transcriptomic response

Given the observed stability of the microbial symbiotic community during heat stress, we focused more specifically on the responses attributable to the coral host. We thus compared gene expression patterns at the qualitative and quantitative levels in Om and NC colonies in response to heat stress compared to the control condition. Altogether, our results clearly highlight that the Oman colonies exposed to more variable thermal conditions *in natura* also display, in response to heat stress, a greater plasticity in gene expression levels than the NC colonies. In particular, the transcriptomic response of the Oman colonies involved a larger number of genes with 73% of commonly differentially expressed genes having higher fold changes compared to the NC colonies. These findings are consistent with the theoretical expectations that a more variable environment promotes the evolution of a greater plasticity (Lande 2009). Accordingly, a recent transplantation study conducted *in natura* also identified greater transcriptomic plasticity in a more thermotolerant (in-shore) population compared with an (off-shore) population inhabiting a more stable thermal habitat in the mustard hill coral *P. astreoides* (Kenkel & Matz 2016).

Importantly however, we also identified several genes whose expression is constitutively higher in the Om colonies compared to the NC colonies by comparing the expression levels in the control condition. This process recently called “frontloading” (Barshis *et al.* 2013) reflects the preemptive expression of stress-response genes, hence predisposing organisms to better respond to stress. It has been proposed that the occurrence of plasticity *vs*. frontloading strategies may depend on the frequency of stresses relative to the typical response time of organisms, with frequent stresses promoting frontloading strategies whereas less frequent perturbations would result in an increased plasticity (Kenkel & Matz 2016). Other conceptual considerations especially in regards to the predictability of environmental variation through generations should also be taken into account (Danchin 2013; Herman *et al.* 2014). The frontloading is by definition more costly than plasticity since it transforms a response to the environment in a constitutive function.

Frontloading is therefore a strategy that would be more efficient when offspring's habitat is highly predictable. On the contrary, an unpredictable or less predictable offspring environment may promote plasticity to enable the exploration of a wider phenotypic landscape at a lesser cost. Plasticity and frontloading are often discussed as mutually exclusive responses (Barshis *et al.* 2013; Kenkel & Matz 2016). However, corals are known to display a high level of variation in their reproduction strategies (brooder vs. broadcast spawner) (Whitaker 2006; Baird *et al.* 2009), timing (Fan *et al.* 2006) and pelagic larval duration (Harrison & Wallace 1990). Environmental predictability in terms of stress frequency and annual temperature variation should be therefore limited and we hypothesized that, rather than being exclusive, plasticity and frontloading often co-occur especially in the population experiencing extreme environments.

Our results clearly support that plasticity and frontloading indeed co-occur specifically in the thermotolerant Om colonies experiencing a more variable thermal environment *in natura*. To tease apart the biological processes that are regulated via plasticity or frontloading in *Pocillopora* response to heat stress, we conducted an enrichment analysis. Keeping in mind that congruency between gene expression and protein levels should be cautious (Mayfield *et al.* 2016), we propose a detailed discussion of the response of coral colonies at the molecular level for each main biological process identified (Supplementary File S11). Notably, we found differences in gene expression levels in response to temperature increase between the two localities for genes involved in response to heat stress (such as HSPs), detoxification of reactive oxygen species, apoptosis, mitochondria energetic functioning, and symbiont maintenance with higher number of differentially expressed genes for the Om corals associated to higher fold changes. In corals, Hsp70 which displayed more intense overexpression in Om colonies, is one of the most documented protein chaperones associated to heat stress response (Barshis *et al.* 2013; Haguenauer *et al.* 2013). Several genes involved in oxidative stress had greater differential expression levels in Om such as calmodulin, quinone oxidoreductases and thioredoxin (Supplementary File S11). Reactive oxygen species (ROS), generated in consequence to heat stress, play a central role in host-symbiont interactions ultimately leading to bleaching as a host innate immune response to a compromised symbiont (see (Weis 2008) for a review). We also identified many genes involved in apoptosis, a process that has been recurrently associated with coral responses to heat stress (Ainsworth *et al.* 2011; Barshis *et al.* 2013; Pratlong *et al.* 2015; Maor-Landaw & Levy 2016).

Our results also suggest that allocating energy in heat stress response is at the expense of other crucial biological processes such as growth and reproductive functions as already shown in *Pocillopora* (Vidal-Dupiol *et al.* 2009; 2014), even if we could not test experimentally fitness effect of the experimental heat stress. However, the molecular mechanisms underlying such overall response to heat stress are still partly unresolved. Interestingly, we also found specific gene expression patterns linked with epigenetic regulation such as histone modifying enzymes as well as enzymes involved in DNA methylation and dsRNA regulation (Supplementary File S11). We also identified expression of many retro-transposons in Om. These processes could be involved in rapid epigenome modifications and thus fuel rapid adaptive evolution (Maumus *et al.* 2009; Torda *et al.* 2017; Jablonka 2017) .

Conclusion

Comparison of the response to an ecologically realistic heat stress of corals from the same genus but pertaining to different species hypotheses thriving in two contrasting thermal environments sheds light on the molecular basis of thermotolerance. We found that after heat exposure, the symbiotic community composition remained similar in colonies from both localities, but we identified major differences in gene regulation processes in the coral, thereby underlining the role of the coral host in the response to heat stress. The colonies from the locality displaying the most variable environment displayed (i) a more plastic transcriptome response involving more differentially expressed genes and higher fold expression changes; as well as (ii) a constitutive higher level of expression for another set of genes (frontloading). In the context of climate change, which is predicted to cause abnormal and rapid temperature increase (IPCC 2014), phenotypic plasticity and the capacity for rapid adaptation through epigenetic regulation and/or genetic assimilation would increase the probability of coral survival. Previous studies highlighted the importance of reef managements measures (Rogers *et al.* 2015) and assisted evolution (van Oppen *et al.* 2015), but also underlined the importance of preserving standing genetic/epigenetic variation in wild coral populations (Matz *et al.* 2017). Although the molecular mechanisms we described are most likely largely

shared in this group of scleractinians, the question remains of the determinism of this thermotolerant phenotype and of the heritability of this character. It is however essential to keep in mind that even the most thermotolerant corals may bleach if they are exposed to temperature significantly higher to their own norm (Hughes *et al.* 2017b; Le Nohaïc *et al.* 2017).

Acknowledgements

We are thankful to Dr. Madjid Delghandi from the Center of Marine Biotechnology at Sultan Qaboos University, the Al-Hail field station and the central laboratory of the College of Agricultural and Marine Sciences for providing us with necessary equipment during field work in Oman. We acknowledge Dr. Gilles Le Moullac and Dr. Yannick Gueguen from the Centre Ifremer du Pacifique for providing us aquaculture facilities during sampling. We acknowledge the Plateforme Gentyane of the Institut National de la Recherche Agronomique (INRA, Clermont-Ferrand, France) for microsatellite genotyping. We also thank the Genotoul bioinformatics platform, and the Toulouse Midi-Pyrenees and Sigenae group for providing help and computing resources (Galaxy instance; http://sigenae-workbench.toulouse.inra.fr as well as the Bio-Environnement platform (University of Perpignan) for sequencing and bioinformatics service. We would like to thank Staffan Jacob, Xavier Pichon and Mar Sobral for their constructive and helpful comments. A preprint version of this article has been reviewed and recommended by Peer Community In Ecology (https://doi.org/10.24072/pci.ecology.100028).

Funding

This project was funded by the ADACNI program of the French national research agency (ANR) (project no. ANR-12-ADAP-0016; http://adacni.imbe.fr), the Campus France PHC program Maïmonide-Israel and the DHOF program of the UMR5244 IHPE. This work is a contribution to the Labex OT-Med (n° ANR-11-LABX-0061) funded by the ANR "Investissements d'Avenir" program through the A*MIDEX project (n° ANR-11-IDEX-0001-02). This study is set within the framework of the "Laboratoire d'Excellence (LABEX)" TULIP (ANR-10-LABX-41).

Conflict of interest disclosure

The authors of this preprint declare that they have no financial conflict of interest with the content of this article. GM is recommender for PCI Ecology.

Data, script and code availability

The datasets generated and analyzed during the current study have been submitted to the SRA repository under bioproject number PRJNA399069. R Scripts are available online: https://doi.org/10.5281/zenodo.5938252.

Supplementary information

The supplementary files are available online: https://doi.org/10.1101/398602.

Supplementary Figure S1. Experimental setup. Four tanks were used for each locality, 3 tanks containing the sampled colonies (one replicate per timepoint and per tank) and one additional tank as a control of coral health at the control temperature during the experiment.

Supplementary Table S2. Haplotype analysis of the six sampled colonies with microsatellite genotyping for the colonies from New Caledonia.

Supplementary Figure S3. Bacterial class composition (for the 24 most abundant) within each replicate for the Om and NC colonies, the three colonies of each locality, and three experimental conditions per colony. In situ (dark arrows); control temperature (green arrows); stress temperature (red arrows).

Supplementary Table S4. MANOVA results for beta diversity (Bray-Curtis distance) between localities, colonies, or experimental conditions.

Supplementary File S5. List and sequences of the 26,600 genes (XLOC) generated during RNAseq alignment.

Supplementary Figure S6. Heatmap and clustering of significantly differentially expressed genes between the control and the heat stress condition for each colony from the two localities. Each gene is represented by a line.

Supplementary File S7. DESeq2 results for the log2-fold changes, and adjusted p values between stress and control conditions for each locality (sheet 1) and for each colony (sheet 2).

Supplementary Table S8. Comparison between the log2-foldchange in Om and NC colonies for genes differentially under-expressed or over-expressed in the same way in colonies from both localities.

Supplementary File S9. GO enrichment results for biological processes, molecular functions, and cellular compartments for common, New Caledonia-specific, or Oman-specific over-expressed and under-expressed genes.

Supplementary File S10. Frontloaded genes in Oman corals among genes over-expressed in New Caledonia corals.

Supplementary File S11. Description of the functional analysis of genes, biological functions and cell compartment involved in the response to stress.

References

Adjeroud M, Guérécheau A, Vidal-Dupiol J et al. (2013) Genetic diversity, clonality and connectivity in the scleractinian coral Pocillopora damicornis: a multi-scale analysis in an insular, fragmented reef system. Marine Biology, 161, 531-541. https://doi.org/10.1007/s00227-013-2355-9

Ainsworth TD, Wasmund K, Ukani L et al. (2011) Defining the tipping point: a complex cellular life/death balance in corals in response to stress. Scientific Reports, 1, 160. https://doi.org/10.1038/srep00160

Akaike H (1974) A New Look at the Statistical Model Identification. IEEE Transactions on Automatic Control, 6, 716-723. https://doi.org/10.1109/TAC.1974.1100705

Altschul SF, Gish W, Miller W, Myers EW, Lipman DJ (1990) Basic local alignment search tool. Journal of molecular biology, 215, 403-410. https://doi.org/10.1016/S0022-2836(05)80360-2

Anders S, Pyl PT, Huber W (2015) HTSeq--a Python framework to work with high-throughput sequencing data. Bioinformatics, 31, 166-169. https://doi.org/10.1093/bioinformatics/btu638

Arnaud-Haond S, Belkhir K (2006) genclone: a computer program to analyse genotypic data, test for clonality and describe spatial clonal organization. Molecular Ecology Notes, 7, 15-17. https://doi.org/10.1111/j.1471-8286.2006.01522.x

Baird AH, Guest JR, Willis BL (2009) Systematic and Biogeographical Patterns in the Reproductive Biology of Scleractinian Corals. Annual Review of Ecology, Evolution, and Systematics, 40, 551-571. https://doi.org/10.1146/annurev.ecolsys.110308.120220

Baker AC (2003) Flexibility and Specificity in Coral-Algal Symbiosis: Diversity, Ecology, and Biogeography of Symbiodinium. Annual Review of Ecology, Evolution, and Systematics, 34, 661-689. https://doi.org/10.1146/annurev.ecolsys.34.011802.132417

Barnosky AD, Matzke N, Tomiya S et al. (2011) Has the Earth's sixth mass extinction already arrived? Nature, 471, 51-57. https://doi.org/10.1038/nature09678

Barshis DJ, Barshis DJ, Ladner JT et al. (2013) From the Cover: Genomic basis for coral resilience to climate change. Proceedings of the National Academy of Sciences, 110, 1387-1392. https://doi.org/10.1073/pnas.1210224110

Bates D, Mächler M, Bolker B, Walker S (2015) Fitting Linear Mixed-Effects Models Using lme4. Journal of Statistical Software, 67, 1-48. https://doi.org/10.18637/jss.v067.i01

Bellantuono AJ, Bellantuono AJ, Granados-Cifuentes C et al. (2012a) Coral Thermal Tolerance: Tuning Gene Expression to Resist Thermal Stress. PloS one, 7, e50685. https://doi.org/10.1371/journal.pone.0050685

Bellantuono AJ, Hoegh-Guldberg O, Rodriguez-Lanetty M (2012b) Resistance to thermal stress in corals without changes in symbiont composition. Proceedings. Biological sciences, 279, 1100-1107. https://doi.org/10.1098/rspb.2011.1780

Bellwood DR, Hughes TP, Folke C, Nyström M (2004) Confronting the coral reef crisis. Nature, 429, 827-833. https://doi.org/10.1038/nature02691

Benjamini Y, Hochberg Y (1995) Controlling the false discovery rate: a practical and powerful approach to multiple testing. Journal of the royal statistical society Series B, 57, 289-300. https://doi.org/10.1111/j.2517-6161.1995.tb02031.x

Berkelmans R, van Oppen MJH (2006) The role of zooxanthellae in the thermal tolerance of corals: a "nugget of hope" for coral reefs in an era of climate change. Proceedings of the Royal Society B-Biological Sciences, 273, 2305-2312. https://doi.org/10.1098/rspb.2006.3567

Blankenberg D, Gordon A, Kuster Von G et al. (2010) Manipulation of FASTQ data with Galaxy. Bioinformatics, 26, 1783-1785. https://doi.org/10.1093/bioinformatics/btq281

Bordenstein SR, Theis KR (2015) Host Biology in Light of the Microbiome: Ten Principles of Holobionts and Hologenomes (MK Waldor, Ed,). PLoS biology, 13, e1002226. https://doi.org/10.1371/journal.pbio.1002226

Bourne DG, Munn CB (2005) Diversity of bacteria associated with the coral Pocillopora damicornis from the Great Barrier Reef. Environmental microbiology, 7, 1162-1174. https://doi.org/10.1111/j.1462-2920.2005.00793.x

Brener-Raffalli K, Clerissi C, Vidal-Dupiol J et al. (2018) Thermal regime and host clade, rather than geography, drive Symbiodinium and bacterial assemblages in the scleractinian coral Pocillopora damicornis sensu lato. Microbiome, 6, 39. https://doi.org/10.1186/s40168-018-0423-6

Brown BE, Downs CA, Dunne RP, Gibb SW (2002) Exploring the basis of thermotolerance in the reef coral Goniastrea aspera. Marine Ecology Progress Series, 242, 119-129. https://doi.org/10.3354/meps242119

Coles SL, Riegl BM (2013) Thermal tolerances of reef corals in the Gulf: a review of the potential for increasing coral survival and adaptation to climate change through assisted translocation. Marine Pollution Bulletin, 72, 323-332. https://doi.org/10.1016/j.marpolbul.2012.09.006

Conesa A, Madrigal P, Tarazona S et al. (2016) A survey of best practices for RNA-seq data analysis. Genome biology, 17, 1. https://doi.org/10.1186/s13059-016-0881-8

Cróquer A, Bastidas C, Elliott A, Sweet M (2013) Bacterial assemblages shifts from healthy to yellow band disease states in the dominant reef coral Montastraea faveolata. Environmental Microbiology Reports, 5, 90-96. https://doi.org/10.1111/j.1758-2229.2012.00397.x

Danchin E (2013) Avatars of information: towards an inclusive evolutionary synthesis. Trends in Ecology & Evolution, 28, 351-358. https://doi.org/10.1016/j.tree.2013.02.010

Dixon GB, Davies SW, Aglyamova GA et al. (2015) CORAL REEFS. Genomic determinants of coral heat tolerance across latitudes. Science, 348, 1460-1462. https://doi.org/10.1126/science.1261224

Dobin A, Davis CA, Schlesinger F et al. (2013) STAR: ultrafast universal RNA-seq aligner. Bioinformatics, 29, 15-21. https://doi.org/10.1093/bioinformatics/bts635

Escudié F, Auer L, Bernard M et al. (2017) FROGS: Find, Rapidly, OTUs with Galaxy Solution. Bioinformatics, 34,1287-1294. https://doi.org/10.1093/bioinformatics/btx791

Fan TY, Lin KH, Kuo FW, Soong K, Liu LL (2006) Diel patterns of larval release by five brooding scleractinian corals. Marine Ecology Progress Series, 321, 133-142. https://doi.org/10.3354/meps321133

Gélin P, Fauvelot C, Mehn V et al. (2017a) Superclone Expansion, Long-Distance Clonal Dispersal and Local Genetic Structuring in the Coral Pocillopora damicornis Type β in Reunion Island, South Western Indian Ocean. PloS one, 12, e0169692. https://doi.org/10.1371/journal.pone.0169692

Gélin P, Pirog A, Fauvelot C, Magalon H (2018) High genetic differentiation and low connectivity in the coral Pocillopora damicornis type β at different spatial scales in the Southwestern Indian Ocean and the Tropical Southwestern Pacific. Marine Biology, 165, 167. https://doi.org/10.1007/s00227-018-3428-6

Gélin P, Postaire B, Fauvelot C, Magalon H (2017b) Reevaluating species number, distribution and endemism of the coral genus Pocillopora Lamarck, 1816 using species delimitation methods and microsatellites. Molecular Phylogenetics and Evolution, 109, 430-446. https://doi.org/10.1016/j.ympev.2017.01.018

Giardine B, Riemer C, Hardison RC, Burhans R, Elnitski L, Shah P, Zhang Y, Blankenberg D, Albert I, Taylor J, Miller W, Kent WJ, Nekrutenko A (2005) Galaxy: A platform for interactive large-scale genome analysis. Genome Research, 15, 1451–1455. https://doi.org/10.1101/gr.4086505

Guerrero R, Margulis L, Berlanga M (2013) Symbiogenesis: the holobiont as a unit of evolution. International Microbiology, 16, 133-143. https://doi.org/10.2436/20.1501.01.188

Haguenauer A, Zuberer F, Ledoux J-B, Aurelle D (2013) Adaptive abilities of the Mediterranean red coral Corallium rubrum in a heterogeneous and changing environment: from population to functional genetics. Journal of Experimental Marine Biology and Ecology, 449, 349-357. https://doi.org/10.1016/j.jembe.2013.10.010

Harrison PL, Wallace CC (1990) Reproduction, dispersal and recruitment of scleractinian corals. In: Ecosystems of the world , pp. 133–207. Elsevier Science Publishing Company, Amsterdam, The Netherlands.

Herman JJ, Spencer HG, Donohue K, Sultan SE (2014) How stable "should" epigenetic modifications be? Insights from adaptive plasticity and bet hedging. Evolution, 68, 632-643. https://doi.org/10.1111/evo.12324

Hernandez-Agreda A, Gates RD, Ainsworth TD (2017) Trends in Microbiology, 25, 125-140. https://doi.org/10.1016/j.tim.2016.11.003

Hoegh-Guldberg O, Mumby PJ, Hooten AJ et al. (2007) Coral reefs under rapid climate change and ocean acidification. Science, 318, 1737-1742. https://doi.org/10.1126/science.1152509

de Hoon MJL, Imoto S, Nolan J, Miyano S (2004) Open source clustering software. Bioinformatics, 20, 1453-1454. https://doi.org/10.1093/bioinformatics/bth078

Hughes TP, Baird AH, Bellwood DR et al. (2003) Climate change, human impacts, and the resilience of coral reefs. Science, 301, 929-933. https://doi.org/10.1126/science.1085046

Hughes TP, Barnes ML, Bellwood DR et al. (2017a) Coral reefs in the Anthropocene. Nature, 546, 82-90. https://doi.org/10.1038/nature22901

Hughes TP, Kerry JT, Álvarez-Noriega M et al. (2017b) Global warming and recurrent mass bleaching of corals. Nature, 543, 373-377. https://doi.org/10.1038/nature21707

Hume B, D'Angelo C, Burt J et al. (2013) Corals from the Persian/Arabian Gulf as models for thermotolerant reef-builders: Prevalence of clade C3 Symbiodinium, host fluorescence and ex situ temperature tolerance. Marine Pollution Bulletin, 72, 313-322. https://doi.org/10.1016/j.marpolbul.2012.11.032

Jablonka E (2017) The evolutionary implications of epigenetic inheritance. Interface focus, 7, 20160135. https://doi.org/10.1098/rsfs.2016.0135

Jombart T, Devillard S, Balloux F (2010) Discriminant analysis of principal components: a new method for the analysis of genetically structured populations. BMC genetics, 11, 94. https://doi.org/10.1186/1471-2156-11-94

Kenkel CD, Matz MV (2016) Gene expression plasticity as a mechanism of coral adaptation to a variable environment. Nature Ecology & Evolution, 1, 0014. https://doi.org/10.1038/s41559-016-0014

Kenkel CD, Meyer E, Matz MV (2013) Gene expression under chronic heat stress in populations of the mustard hill coral (Porites astreoides) from different thermal environments. Molecular Ecology, 22, 4322-4334. https://doi.org/10.1111/mec.12390

Klindworth A, Pruesse E, Schweer T et al. (2012) Evaluation of general 16S ribosomal RNA gene PCR primers for classical and next-generation sequencing-based diversity studies. Nucleic Acids Research, 41, e1. https://doi.org/10.1093/nar/gks808

Lajeunesse TC, Trench RK (2000) Biogeography of two species of Symbiodinium (Freudenthal) inhabiting the intertidal sea anemone Anthopleura elegantissima (Brandt). The Biological bulletin, 199, 126-134. https://doi.org/10.2307/1542872

LaJeunesse TC, Parkinson JE, Gabrielson PW et al. (2018) Systematic Revision of Symbiodiniaceae Highlights the Antiquity and Diversity of Coral Endosymbionts. Current Biology, 28, 2570-2580. https://doi.org/10.1016/j.cub.2018.07.008

Lande R (2009) Adaptation to an extraordinary environment by evolution of phenotypic plasticity and genetic assimilation. Journal of Evolutionary Biology, 22, 1435-1446. https://doi.org/10.1111/j.1420-9101.2009.01754.x

Le Nohaïc M, Ross CL, Cornwall CE et al. (2017) Marine heatwave causes unprecedented regional mass bleaching of thermally resistant corals in northwestern Australia. Scientific Reports, 7, 14999. https://doi.org/10.1038/s41598-017-14794-y

Li J, Chen Q, Long L-J et al. (2014) Bacterial dynamics within the mucus, tissue and skeleton of the coral Porites lutea during different seasons. Scientific Reports, 4, 7320. https://doi.org/10.1038/srep07320

Little AF, van Oppen MJH, Willis BL (2004) Flexibility in algal endosymbioses shapes growth in reef corals. Science, 304, 1492-1494. https://doi.org/10.1126/science.1095733

Littman R, Bourne DG, Willis BL (2010) Responses of coral-associated bacterial communities to heat stress differ with Symbiodinium type on the same coral host. Molecular Ecology, 19, 1978-1990. https://doi.org/10.1111/j.1365-294X.2010.04620.x

Love MI, Huber W, Anders S (2014) Moderated estimation of fold change and dispersion for RNA-seq data with DESeq2. Genome biology, 15, 31. https://doi.org/10.1186/s13059-014-0550-8

Magoč T, Salzberg SL (2011) FLASH: fast length adjustment of short reads to improve genome assemblies. Bioinformatics, 27, 2957-63. https://doi.org/10.1093/bioinformatics/btr507

Mahé F, Rognes T, Quince C, De Vargas C, Dunthorn M (2014) Swarm: robust and fast clustering method for amplicon-based studies. PeerJ, 2, e593. https://doi.org/10.7717/peerj.593

Maor-Landaw K, Levy O (2016) Gene expression profiles during short-term heat stress; branching vs. massive Scleractinian corals of the Red Sea. PeerJ, 4, e1814. https://doi.org/10.7717/peerj.1814

Margulis L, Fester R (Eds.) (1991) Symbiosis as a Source of Evolutionary Innovation: Speciation and Morphogenesis. MIT Press, Cambridge, MA, USA.

Martin M (2011) Cutadapt removes adapter sequences from high-throughput sequencing reads. EMBnet journal, 17, 10. https://doi.org/10.14806/ej.17.1.200

Matz MV, Treml EA, Aglyamova GA, van Oppen MJH, Bay LK (2017) Potential for rapid genetic adaptation to warming in a Great Barrier Reef coral. PLoS Genet., 19, e1007220. https://doi.org/10.1101/114173

Maumus F, Allen AE, Mhiri C et al. (2009) Potential impact of stress activated retrotransposons on genome evolution in a marine diatom. BMC Genomics, 10, 624. https://doi.org/10.1186/1471-2164-10-624

Mayfield AB, Wang L-H, Tang P-C et al. (2011) Assessing the impacts of experimentally elevated temperature on the biological composition and molecular chaperone gene expression of a reef coral. PloS one, 6, e26529. https://doi.org/10.1371/journal.pone.0026529

Mayfield AB, Wang Y-B, Chen C-S, Chen S-H, Lin C-Y (2016) Dual-compartmental transcriptomic + proteomic analysis of a marine endosymbiosis exposed to environmental change. Molecular Ecology, 25, 5944-5958. https://doi.org/10.1111/mec.13896

Mayfield AB, Wang Y-B, Chen C-S, Lin C-Y, Chen S-H (2014) Compartment-specific transcriptomics in a reef-building coral exposed to elevated temperatures. Molecular Ecology, 23, 5816-5830. https://doi.org/10.1111/mec.12982

McFall-Ngai M, Hadfield MG, Bosch TC et al. (2013) Animals in a bacterial world, a new imperative for the life sciences. Proceedings of the National Academy of Sciences of the United States of America, 110, 3229-3236. https://doi.org/10.1073/pnas.1218525110

McMurdie PJ, Holmes S (2013) phyloseq: An R Package for Reproducible Interactive Analysis and Graphics of Microbiome Census Data (M Watson, Ed,). PloS one, 8, e61217. https://doi.org/10.1371/journal.pone.0061217

Meyer JL, Rodgers JM, Dillard BA, Paul VJ, Teplitski M (2016) Epimicrobiota Associated with the Decay and Recovery of Orbicella Corals Exhibiting Dark Spot Syndrome. Frontiers in Microbiology, 7, 893. https://doi.org/10.3389/fmicb.2016.00893

Neave MJ, Apprill A, Ferrier-Pages C, Voolstra CR (2016a) Diversity and function of prevalent symbiotic marine bacteria in the genus Endozoicomonas. Applied Microbiology and Biotechnology, 100, 8315-8324. https://doi.org/10.1007/s00253-016-7777-0

Neave MJ, Rachmawati R, Xun L et al. (2016b) Differential specificity between closely related corals and abundant Endozoicomonas endosymbionts across global scales. The ISME Journal, 11, 186-200. https://doi.org/10.1038/ismej.2016.95

Oliver TA, Palumbi SR (2010) Many corals host thermally resistant symbionts in high-temperature habitat. Coral Reefs, 30, 241-250. https://doi.org/10.1007/s00338-010-0696-0

Palumbi SR, Barshis DJ, Traylor-Knowles N, Bay RA (2014) Mechanisms of reef coral resistance to future climate change. Science, 344, 895-898. https://doi.org/10.1126/science.1251336

Pante E, Puillandre N, Viricel A et al. (2015) Species are hypotheses: avoid connectivity assessments based on pillars of sand. Molecular Ecology, 24, 525-544. https://doi.org/10.1111/mec.13048

Pantos O, Bongaerts P, Dennis PG, Tyson GW, Hoegh-Guldberg O (2015) Habitat-specific environmental conditions primarily control the microbiomes of the coral Seriatopora hystrix. The ISME Journal, 9, 1916-1927. https://doi.org/10.1038/ismej.2015.3

Peixoto RS, Rosado PM, Leite DC de A, Rosado AS, Bourne DG (2017) Beneficial Microorganisms for Corals (BMC): Proposed Mechanisms for Coral Health and Resilience. Frontiers in Microbiology, 8, 100. https://doi.org/10.3389/fmicb.2017.00341

Pinzón JH, Sampayo E, Cox E et al. (2013) Blind to morphology: genetics identifies several widespread ecologically common species and few endemics among Indo-Pacific cauliflower corals (Pocillopora, Scleractinia). Journal of Biogeography, 40, 1595-1608. https://doi.org/10.1111/jbi.12110

Polato NR, Voolstra CR, Schnetzer J et al. (2010) Location-specific responses to thermal stress in larvae of the reef-building coral Montastraea faveolata. PloS one, 5, e11221. https://doi.org/10.1371/journal.pone.0011221

Pratlong M, Haguenauer A, Chabrol O et al. (2015) The red coral (Corallium rubrum) transcriptome: a new resource for population genetics and local adaptation studies. Molecular ecology resources, 15, 1205-1215. https://doi.org/10.1111/1755-0998.12383

Pritchard JK, Stephens M, Donnelly P (2000) Inference of population structure using multilocus genotype data. Genetics, 155, 945-959. https://doi.org/10.1093/genetics/155.2.945

Quigley KM, Quigley KM, Davies SW et al. (2014) Deep-Sequencing Method for Quantifying Background Abundances of Symbiodinium Types: Exploring the Rare Symbiodinium Biosphere in Reef-Building Corals. PloS one, 9, e94297. https://doi.org/10.1371/journal.pone.0094297

Reaka-Kudla ML (1997) The global biodiversity of coral reefs: a comparison with rain forests. In: Biodiversity II: Understanding and protecting our biological resources (eds Solis MA., Reaka-Kudla ML, Wilson DE, & Wilson EO) pp 83-108. Joseph Henry Press, Washington, DC. https://doi.org/10.17226/4901

Reusch TBH (2013) Climate change in the oceans: evolutionary versus phenotypically plastic responses of marine animals and plants. Evolutionary Applications, 7, 104-122. https://doi.org/10.1111/eva.12109

Riegl BM, Purkis SJ, Al-Cibahy AS, Abdel-Moati MA, Hoegh-Guldberg O (2011) Present Limits to Heat-Adaptability in Corals and Population-Level Responses to Climate Extremes. PloS one, 6, e24802. https://doi.org/10.1371/journal.pone.0024802

Rogers A, Harborne AR, Brown CJ et al. (2015) Anticipative management for coral reef ecosystem services in the 21st century. Global Change Biology, 21, 504-514. https://doi.org/10.1111/gcb.12725

Rognes T, Flouri T, Nichols B, Quince C, Mahé F (2016) VSEARCH: a versatile open source tool for metagenomics. PeerJ, 4, e2584. https://doi.org/10.7717/peerj.2584

Rohwer F, Seguritan V, Azam F (2002) Diversity and distribution of coral-associated bacteria. Marine Ecology Progress Series, 243, 1-10. https://doi.org/10.3354/meps243001

Rosenberg E, Koren O, Reshef L, Efrony R, Zilber-Rosenberg I (2007) The role of microorganisms in coral health, disease and evolution. Nature Reviews Microbiology, 5, 355-362. https://doi.org/10.1038/nrmicro1635

Saldanha AJ (2004) Java Treeview--extensible visualization of microarray data. Bioinformatics, 20, 3246-3248. https://doi.org/10.1093/bioinformatics/bth349

Sato Y, Willis BL, Bourne DG (2009) Successional changes in bacterial communities during the development of black band disease on the reef coral, Montipora hispida. The ISME Journal, 4, 203-214. https://doi.org/10.1038/ismej.2009.103

Schmidt-Roach S, Miller KJ, Lundgren P, Andreakis N (2014) With eyes wide open: a revision of species within and closely related to the Pocillopora damicornis species complex (Scleractinia; Pocilloporidae) using morphology and genetics. Zoological Journal of the Linnean Society, 170, 1-33. https://doi.org/10.1111/zoj.12092

Suggett DJ, Warner ME, Leggat W (2017) Symbiotic Dinoflagellate Functional Diversity Mediates Coral Survival under Ecological Crisis. Trends in Ecology & Evolution, 32, 735-745. https://doi.org/10.1016/j.tree.2017.07.013

Supek F, Bošnjak M, Škunca N, Šmuc T (2011) REVIGO summarizes and visualizes long lists of gene ontology terms. PloS one, 6, e21800. https://doi.org/10.1371/journal.pone.0021800

Theis KR, Dheilly NM, Klassen JL, Brucker RM, Baines JF, Bosch TCG, Cryan JF, Gilbert SF, Goodnight CJ, Lloyd EA, Sapp J, Vandenkoornhuyse P, Zilber-Rosenberg I, Rosenberg E, Bordenstein SR (2016) Getting the Hologenome Concept Right: an Eco-Evolutionary Framework for Hosts and Their Microbiomes. mSystems1, e00028-16. https://doi.org/10.1128/mSystems.00028-16

Torda G, Donelson JM, Aranda M et al. (2017) Rapid adaptive responses to climate change in corals. Nature Climate Change, 7, 627-636. https://doi.org/10.1038/nclimate3374

Trapnell C, Williams BA, Pertea G et al. (2010) Transcript assembly and quantification by RNA-Seq reveals unannotated transcripts and isoform switching during cell differentiation. Nature Biotechnology, 28, 511-515. https://doi.org/10.1038/nbt.1621

van Oppen MJH, Oliver JK, Putnam HM, Gates RD (2015) Building coral reef resilience through assisted evolution. Proceedings of the National Academy of Sciences, 112, 2307-2313. https://doi.org/10.1073/pnas.1422301112

van Woesik R, Sakai K, Ganase A, Loya Y (2011) Revisiting the winners and the losers a decade after coral bleaching. Marine Ecology Progress Series, 434, 67-76. https://doi.org/10.3354/meps09203

Veron JEN, Stafford-Smith M (2000) Corals of the world. Australian Institute of Marine Science, Townsville MC, Qld, Australia.

Vidal-Dupiol, J., Chaparro, C., Pratlong, M., Pontaroti, P., Grunau, C., & Mitta, G. (2019). Sequencing, de novo assembly and annotation of the genome of the scleractinian coral, Pocillopora acuta. bioRxiv, 698688. https://doi.org/10.1101/698688

Vidal-Dupiol J, Dheilly NM, Rondon R et al. (2014) Thermal stress triggers broad Pocillopora damicornis transcriptomic remodeling, while Vibrio coralliilyticus infection induces a more targeted immuno-suppression response. PloS one, 9, e107672. https://doi.org/10.1371/journal.pone.0107672

Vidal-Dupiol J, Adjeroud M et al. (2009) Coral bleaching under thermal stress: putative involvement of host/symbiont recognition mechanisms. BMC physiology, 9, 14. https://doi.org/10.1186/1472-6793-9-14

Weis VM (2008) Cellular mechanisms of Cnidarian bleaching: stress causes the collapse of symbiosis. The Journal of experimental biology, 211, 3059-3066. https://doi.org/10.1242/jeb.009597

Whitaker K (2006) Genetic evidence for mixed modes of reproduction in the coral Pocillopora damicornis and its effect on population structure. Marine Ecology Progress Series, 306, 115-124. https://doi.org/10.3354/meps306115

Ziegler M, Seneca FO, Yum LK, Palumbi SR, Voolstra CR (2017) Bacterial community dynamics are linked to patterns of coral heat tolerance. Nature Communications, 8, 14213. https://doi.org/10.1038/ncomms14213

Zilber-Rosenberg I, Rosenberg E (2008) Role of microorganisms in the evolution of animals and plants: the hologenome theory of evolution. FEMS Microbiology Reviews, 32, 723-735. https://doi.org/10.1111/j.1574-6976.2008.00123.x

ANNEXE 10

Science Advances
AAAS
Manuscript Template

Genetic and epigenetic changes can mediate rapid acclimatization of a tropical coral to global warming

Short title: Acclimatization to heat in corals

J. Vidal-Dupiol,[1*] E. Toulza,[2] C. Grunau,[2] O. Rey,[2] D. Roquis,[2] C. Chaparro,[2] C. Cosseau,[2] A. Picart-Picolo,[2,3] L. Fouré,[4] P. Romans,[5] M. Pratlong,[6,7] K. Brener-Raffalli,[2] S. Nidelet,[8] P. Pontarotti,[6,9] M. Adjeroud,[10,11,12] G. Mitta[2]

[1] IHPE, Univ. Montpellier, CNRS, Ifremer, Univ. Perpignan Via Domitia, Montpellier, France.
[2] IHPE, Univ. Montpellier, CNRS, Ifremer, Univ. Perpignan Via Domitia, Perpignan, France.
[3] Laboratoire Génome et Développement des Plantes, UMR 5096: CNRS - Université de Perpignan Via Domitia, 58 Avenue P. Alduy, 66860 Perpignan, France.
[4] Aquarium du Cap d'Agde, 11 rue des 2 frères, 34300 Cap d'Agde, France.
[5] Sorbonne Université, CNRS – FR 3724 – Observatoire Océanologique de Banyuls sur Mer, Service Mutualisé d'Aquariologie, Avenue Pierre Fabre, 66650 Banyuls/Mer, France.
[6] Aix Marseille Univ, IRD, APHM, Microbe, Evolution, PHylogénie, Infection IHU Méditerranée, Evolutionary Biology team, Marseille, France. [7] Aix-Marseille Université, Avignon Université, CNRS, IRD, IMBE, Marseille, France.
[8] SNC5039 CNRS 19-21 Boulevard Jean Moulin 13005 Marseille, France.
[9] MGX, BCM, Univ Montpellier, CNRS, INSERM, Montpellier, France
[10] ENTROPIE, IRD, Université de La Réunion, CNRS, Perpignan, France.
[11] PSL Université Paris, EPHE, UPVD, CNRS, USR 3278 CRIOBE, Perpignan, France.
[12] Laboratoire d'Excellence "CORAIL", Paris, France.

*Corresponding author: jeremie.vidal.dupiol@ifremer.fr

Abstract

Coral reefs are declining worldwide under the pressure of global warming but field observations suggest that thermotolerance of some corals may increase in response to recurrent heat stresses. Initial evidence indicates that this response relies on transcriptomic plasticity. However, the molecular determinants of this phenotypic variation remain to be elucidated. Here, we addressed this issue by training colonies of the coral *Pocillopora acuta* with ecologically relevant recurrent heat stresses that clearly improved thermotolerance. To understand the molecular bases of these induced phenotypic changes, we combine genome-wide transcriptomics, (meta)genomics and epigenomics methods. We showed that stress response genes become constitutively expressed in thermotolerant corals and showed that the acquisition of thermotolerance was strongly associated with changes in the host's DNA methylation and, to a lesser degree, to intra-colonial genetic variation.

Introduction

The Anthropocene is defined as the epoch during which human activities have induced significant changes in the Earth's geology and ecosystems. These unprecedented changes have jeopardized some species and, by domino effects, entire ecosystems such as coral reefs (*1*). Scleractinian corals, the primary framework builders and key to reef health and biodiversity, live very close to their upper thermal limit (*1*). Beyond this limit, corals suffer bleaching (*i.e.*, loss of their obligate algae endosymbionts, the Symbiodiniaceae), which can lead to coral death. Since the 1980s, several abnormal warming episodes have led to recurrent mass bleaching events. These phenomena have devastated numerous coral reefs and constitute the major drivers of the worldwide coral reef crisis (*1*).

Nevertheless, several indications of rapid thermotolerance increase in response to recurrent heat stresses were recently observed in the field (*2*, *3*), thus providing hope concerning the fate of corals in a warming world. Because of its life traits (long-living, sessile, stenotherm, colonial and symbiotic), the coral holobiont may rely on a variety of mechanisms to acclimatize and/or adapt to stressful environmental conditions (*4*). These could rely on phenotypic changes heritable through mitosis and/or meiosis resulting from modifications at the genomic, epigenomic or symbiotic scales (*4*). Considering gene expression phenotypes, recent results have provided evidence for transcriptomic plasticity (*5*), 'frontloading'(*6*) (*i.e.* higher constitutive expression of stress response genes), or both (*7*) as mechanisms of coral acclimatization or adaptation. However, the mechanisms promoting these transcriptomic changes remained to be elucidated. Here, we aim at addressing this issue through an integrative omic approach (genome-wide transcriptomics, (meta)genomics and epigenomics) applied to the coral *Pocillopora acuta* displaying an improved thermotolerance induced by a training with ecologically relevant recurrent heat stresses.

Results and Discussion

Training induces increased coral thermotolerance

To study the mechanisms underpinning rapid intra-generationnal (mitotic inheritance) thermotolerance increases, we trained nubbins obtained from a single wild coral colony of *Pocillopora acuta* with recurrent heat stresses inducing bleaching over a 2-year period (trained corals, Fig. 1.a); nubbins from the same mother colony were kept in a non-stressful environment and used as controls (naive corals, Fig. 1a). Our results shows that recurrent stresses significantly increased thermotolerance, since trained corals bleached (chi-square=22.688; $p < 0.01$), and showed partial colony death (chi-square=24.039; $p < 0.01$) or total colony death (chi-square=24.125; $p < 0.01$) significantly later than naive corals (Fig. 2a). Although beneficial effects of pre-exposure to stressful environment has already been investigated (*8*, *9*), such long lasting effects through several years have never been tested and/or reported. The procedure applied can be considered as ecologically realistic since the two stressful events inducing bleaching were separated by a full year of recovery, hence mimicking annual temperature variation in the field. These results mirror recent field observations (*2*, *3*) and suggest that the same mechanisms occur under natural condition.

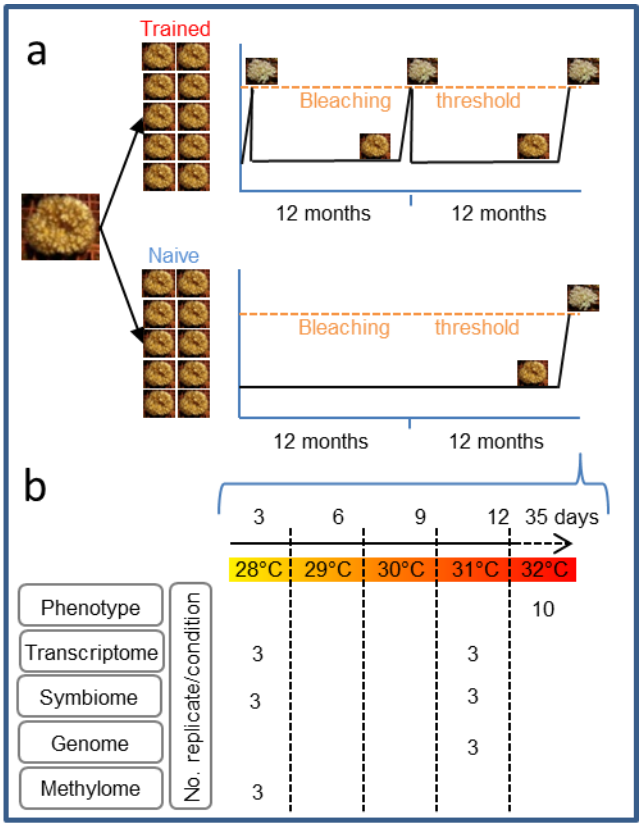

Fig. 1. Experimental design. a. Two sets of nubbins were obtained from the same mother colony, naives nubbins were maintained under optimal temperature, trained nubbins were subjected to 2 successive heat stresses (*i.e* once a year) inducing bleaching followed by one year of recovery. Coral thermotolerance assessment and tissue sampling used for molecular analyses were conducted during the last increase in temperature.

Trained corals constitutively express stress responding genes

To better understand the molecular changes underlying such differences in phenotype, we next studied the transcriptomic response of trained *vs.* naive corals. This comparison was done between three fragments sampled at 28°C (control temperature) and three at 31°C, a time point for which corals respond to thermal stress without reaching physiological collapse (*10*) (Fig. 1b). Sequencing produced 44 to 63 million high-quality clusters. After cleaning, paired reads were mapped and counted against the gene repertoire of a reference genome (Supplementary file 1). Finally, 31,562,006 paired mapped reads per sample were used for quantification. The discriminant analysis of principal components (DAPC) performed at the whole transcriptomic level revealed that trained corals displayed a weaker transcriptomic reprogramming under heat stress by comparison with naive corals (Fig. 2b and Fig. S1). In addition, enrichment analysis revealed a classical Coral Stress Response (CSR) in naive corals (Fig. S2). This CSR was characterized by the overexpression of pathways associated with responses to oxidative stress (over-representation of a catalase and a peroxidase), calcium homeostasis (over-representation of a calreticulin and an EGF domain-containing protein), heat shock proteins (over-representation of several HSP70s, HSP90s, a HSP105, a HSP60 and a small HSP), cell death (over-representation of several TRAFs and a caspase 3), immune function (over-representation of a MAPK, a NF-kappa-B-inhibitor, NF-kappa-B, three complement component C3 precursors and a complement factor b precursor), energy and protein metabolism (over-representation of a succinate

dehydrogenase and ubiquitin ligases), and the under-expression of genes associated with non-vital functions (*6*, *11*).

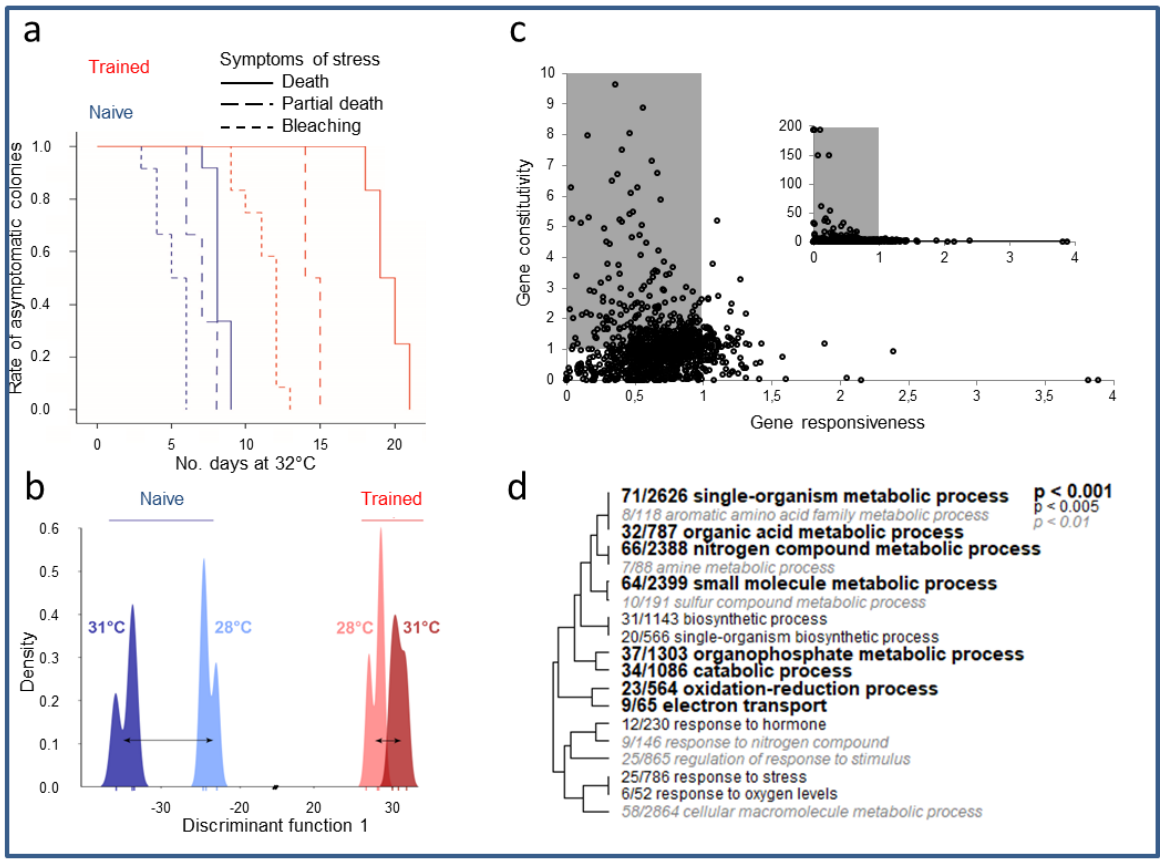

Fig. 2. Thermotolerance characterization. a. Kaplan-Meier thermotolerance curve analysis for naive and trained corals (n=10). **b.** Quantification of the genome-wide transcriptomic plasticity in naive and trained corals by discriminant analysis of principal components (DAPC). **c.** Evolution of gene expression between naive and trained corals by plotting gene constitutively (Y axis = RPKM ratio of trained *vs.* naive at control temperature) against the change in gene responsiveness (X axis = fold change ratio of the response to heat in the trained *vs.* naive corals). Grey box show the genes that gained in constitutive expression and loose in responsiveness in the trained corals (frontloaded gene). The small inset graph displays the un-truncated Y axis. **d.** GO categories from the biological process roots that are significantly enriched (Fisher exact test; FDR<0.01), in the frontloaded genes.

We therefore studied how the expression of genes differentially expressed in naive corals (differentially expressed genes, DEGs) had changed over time, in trained corals. Consistent with previous work (*6*, *7*), trained corals showed frontloading and were thus already prepared to respond when the stress arrived. Plotting the change in the constitutive expression of genes (RPKM ratio of trained *vs.* naive at the control temperature) against the change in gene responsiveness (fold change ratio of trained *vs.* naive in response to heat stress) showed that 1,040 of the 1,143 induced DEGs in naive corals were not overexpressed in trained colonies. However, 500 of these genes were expressed with higher basal expression levels in trained corals (Fig. 2c, grey box), many of which being involved in the CSR according to our GO term enrichment analysis (Fisher exact test procedure; Fig. 2d). In particular, they participate to the oxidative stress response (*i.e.* a catalase, a glutathione peroxidase, a thioredoxin, two allene oxide synthase 8r-lipoxygenase fusion proteins), the heat shock responses (*i.e.* three HSP90s, two HSP70s, one HSP60, one small HSP) and in cell death regulation and immunity–(*i.e.* four genes members of

the TRAF family, a NF-kappa-B, three complement component C3 precursors, and one complement factor b precursor). In summary, the increase of thermotolerance induced by recurrent heat stresses in trained corals is associated with the constitutive expression of genes belonging to the CSR.

These transcriptomic adjustments resulting in corals adaptive responses can originate from genetic or non-genetic modifications (*4*). In corals, non-genetic avatars include epigenetic marks and symbiotic associations (*4*); all of these factors being interrelated elements of an inclusive system (*12*). Since it was not possible to attribute *a priori* the observed phenotypic changes to one or the other elements, we decided to study these three elements (Fig. 1b).

No significant change in the composition of *Symbiodiniaceae* communities

It has long been hypothesized that changes in *Symbiodiniaceae* community composition could influence the adaptation of scleractinian corals to heat stress (*4*). We thus hypothesized that the recurrent bleaching experienced by trained corals may have led to changes in the *Symbiodiniaceae* community structure. Relative abundances of *Symbiodiniaceae* species in trained and naive corals before (28°C) and during the heat stress (31°C; Fig. 1b) were studied using a metabarcoding approach. ITS2 amplicon sequencing with MiSeq yielded 679,326 informative clusters, *i.e.*, 56,600 per sample on average (range: 21,797–85,396). After clustering and filtering for operational taxonomic unit (OTUs) containing less than 0.1% of sequence tags, four OTUs of ITS2 were obtained (Table S1A and B). Taxonomic affiliation showed that the four OTUs identified and differing by 4 nucleotides are all affiliated to *Cladocopium* sp. (type C1; Table S1). Comparisons of the relative abundances of each clade between samples did not reveal any significant changes in dominance between the different clusters of *Cladocopium* sp.. On the contrary, the main differences lie in the increasing dominance of the cluster 1 in trained corals and a general decrease in the representation of the three other clusters. *Cladocopium* is not a genus generally recognized as thermotolerant but variation among this genera can be huge (*13*). In Swain et al. 2017 (*13*), the type C1 was ranked 69 over 110 for its thermotolerance (thermotolerance score 21.72/100). It is therefore unlikely that this subtle change of proportion among the same *Cladocopium* type would have significantly modified the thermotolerance of the entire holobiont, and we conclude that the thermotolerance increase observed was mainly host-dependent. However, we cannot rule out the hypothesis that these symbionts were also subjected to acclimatization or adaptive epigenetic and genetic modifications (*14*). Molecular analysis with complementary molecular markers would be used to provide a deeper analysis of the taxonomic diversity present among the *Cladocopium* C1 species and the (epi)genomic modifications potentially induced by the recurrent stresses.

Temporal intracolonial genetic variation

Historically, a coral colony was considered a group of individuals sharing the same genome. However, it is now acknowledged that intra-colonial genetic variability originating from mosaicism (the accumulation of somatic mutations through time) and/or chimerism (the fusion of two or more genets) is common in corals and can provide fitness advantages (*15, 16*). By merging the data of our whole genome sequencing (WGS; corals sampled at 31°C, Fig. 1b) and whole genome bisulfite sequencing (WGBS; corals sampled at 28°C, Fig. 1b), we show that intra-colonial genetic variability increased in the course of recurrent stresses in trained corals (Fig. 3).

As a first approach, we calculated the kinship coefficient of Manichaikul (Fig. 3a) and showed that at the end of the experiment naive colonies remained genetically close (KCM>0.47) while trained ones presented more genetic variation (0.06<KCM<0.49). Tajima's D indices calculated over 1-kb sliding windows (Fig. 3b) illustrate that naive corals presented rare alleles occurring at a low frequency (positive D; Fig. 3b), whereas the shift towards the left of the D distribution and the occurrence of negative D in trained colonies reflected a shift of rare alleles from low to high frequency (Fig. 3b). This increased genetic diversity was confirmed by the nucleotide diversity index *Pi*, which reached 0.9% in trained *vs.* 0.7% in naive corals. To better characterize these intra-colonial genetic variations, we investigated for small (single-nucleotide polymorphisms, SNPs) and large (copy number variation, CNV) structural genomic variations that significantly differed between naive and trained corals. We used a genome-wide scan based on pairwise F_{ST} (fixation index) comparison over 200 kb sliding windows for the former and a read depth analysis for the latter genomic repertoire (Fig. S3). Intersect between these two bearers of genetic diversity revealed that CNVs are likely the main triggers of SNPs in our dataset. Indeed, among the 6,026 genes presenting SNPs, 97% are also affected by CNVs (Fig. S4). These CNVs could arise from various non-exclusive mechanisms, including the (potentially stress-induced) mobilization of transposable elements and errors during replication and recombination events (*17, 18*). In this context, we found that 63% of the identified CNVs contained traces of transposable elements (Supplementary Table S2). The mechanisms underlying the increase of intra-colonial genetic diversity could also be linked to mosaicism, to chimerism or both. Indeed, abiotic stress is a well-known inducer of small (SNP) and large (CNV) somatic mutations (*19*). Corals are naturally living under a high level of oxidative stress because of the photosynthetic activity of its endocellular phototrophic symbionts (*20*). However, in addition to this daily stress the trained corals were further more subjected to periodic intense oxidative stresses because of the recurrent bleaching events they have endured (*21*). From a chimerism point of view, we suggest that stress recurrence favor changes in the proportion of genotypes cohabiting in a colony (through selective processes). Theoretical and experimental considerations suggest that chimerism can result in complementarity but also in competition between genotypes living together (*22*). Under a long-lasting ecological stability, genotype/genotype interactions can drive the relative representation of each entity within the colony. Strong ecological modifications such as recurrent bleaching events can however modify this genotype/genotype equilibrium and lead to a change of the intracolonial genetic variability within the same colony (*15*). From a mosaicism point of view, the induction of mechanisms producing genetic diversity was already reported in corals especially in response to stress (*23*). Given the colonial nature of this organisms, the lethal risk associated to this hyper mutability is buffered by the number of individuals available for the maintenance and the rebuilding of the colony (*24*). These organisms are therefore prone to produce genetic diversity and to get adaptive benefits from it.

To test if these small and large genomic structural variations were associated with the observed transcriptomic changes, genes' functions of the affected regions were studied. In the regions displaying the top 1% F_{ST} values, 223 genes were found and a GO term enrichment analysis revealed that genes of the "amino acid transmembrane transport" function were over-represented. However, we were not able to identify obvious links between such functions and the increase in corals' thermotolerance. In total, 9,871 genes showed CNV in their sequence, with

5,859 and 4,012 of these displaying a higher copy number in trained and naive colonies, respectively. No biological function was enriched in the set of genes that had higher copy numbers in naive corals. Conversely,14 functions were found to be enriched among genes that displayed higher copy numbers in the trained compared to naive colonies (Fig. 3c). Three of these functions, including “immune system process”, “regulation of response to stimulus” and “positive regulation of response to stimulus” are classically associated with the CSR. Interestingly, these functions contain 22 genes of the tnf/tnf receptor-associated factors family (two tnf and 20 TRAF) that are crucial in the heat stress response of corals (*25*). More particularly, two of these genes were overexpressed in the response of naive and one in trained and none were frontloaded. Even if the genetic variation induced by the training is significant, few specific genetic changes were directly associated with changes in the molecular phenotype. It is worth noting that our approach focused on possible *cis* regulation only and we thus cannot rule out a contribution of undetected genetic variation associated with *trans* regulation that might underlie the emergence thermotolerance in trained nubbins. Still, these results strengthen the emerging vision that intra-colonial genetic diversity might provide a mechanism of rapid acclimatization and adaptation to stress. However, we anticipate that identifying whether such genetic variation is promoted by mosaicism or by chimerism will be a real challenge, in particular when using unphased genetic markers. In this regard, methods that produce phased reads (*e.g.* reads that start at the same position of the genome, such as RAD-seq) allows reconstructing haplotype sequences better than shotgun approaches and constitute interesting alternatives to differentiate the signal of a polyploid colony (chimerism) from a colony rich in somatic mutations (mosaicism).

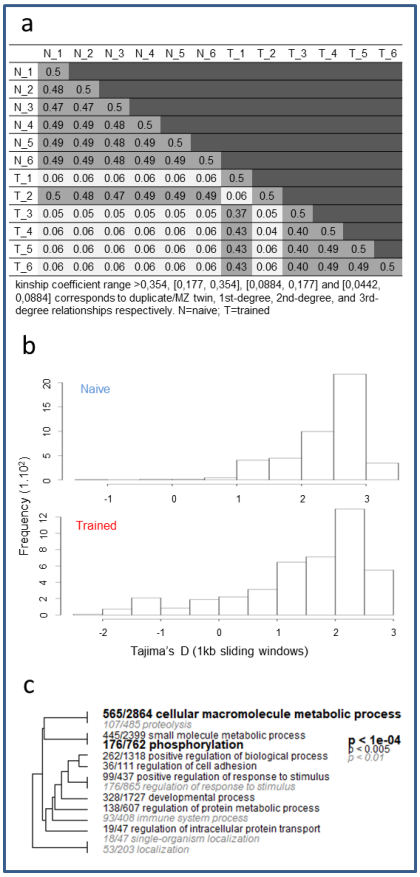

Fig. 3.Genetic differences between naive and trained corals. a. Kinship coefficient of Manichaikul (KCM), KCM>0.354 for duplicate/mono-zygotic twin, 0.354>KCM>0.177 for 1st-degree, 0.>KCM>0.0884 for 2nd-degree and 0.0884>KCM>0.0442 for 3rd-degree relationships. **b.** Frequency distribution of Tajima’s D indices calculated over 1kb sliding windows. **c.** GO categories from the biological process roots that are significantly enriched (Fisher exact test; FDR<0.01) in genes displaying more CNV in trained corals.

DNA methylation changes associated to the constitutive expression of the CSR

Changes in DNA methylation patterns constitute a molecular mechanisms allowing rapid acclimatization and adaptive responses to environmental stress, thus providing the time needed for adaptive genetic mutations to be selected and spread throughout populations (*4*). To test if such a mechanism was involved in the thermotolerance increase of trained corals, Whole Genome Bisulfite Sequencing (WGBS) was performed on samples sampled just before the beginning of the last stress at a temperature of 28°C. We deliberately chose this sampling time point based on the assumption that potential epimutations underlying the increase of thermotolerance result from the overall training process rather than emerging only during the stress period. (Fig 1a &b).

On average, WGBS resulted in the mapping of 56.4 ± 0.1% (77,509,870 paired reads) and 31.7 ± 5.4% (53,780,284 paired reads) of the filtered paired reads obtained for naive and trained corals, respectively. Methylation calling and analysis shows that, *P. acuta* presented a mosaic DNA methylation pattern (Fig. 4a and Fig. S5) and that gene body methylation rate (GBMR) is associated to transcript abundance, two general patterns that were found in other scleractinian species (*26-28*). In *P. acuta,* gene expression maxima are reach for GBMR values of 19.6% on average (mean obtained based on the methylation status of the 1,000 most expressed genes; Fig. 4b).

Differential methylation analyses indicated that 8,708 and 1,940 regions of 500 bp were hypo- or hypermethylated in trained corals, respectively. Among these regions, 4,942 hypomethylations and 1,184 hypermethylations were located in gene bodies. A GO term enrichment analysis conducted on these targeted genomic regions and synthesized with REVIGO showed that biological functions of the CSR (Fig. S6) were enriched with both hypo- and hypermethylated genes (Fig. 4c). Among these differently methylated genes, 998 (17.6%) displayed both genetic (SNPs and/or CNVs) and epigenetic variation (Fig. S4). To which extent the methylation level at these genes is influenced by the genomic composition of gene sequences is unknown, but we argue that the expression of these genes likely result from a regulation driven by both the genetic and epigenetic components. However, further enrichment analyses (against all genes with DNA methylation changes) indicated that no biological functions were enriched when accounting for those genes that display both genetic and epigenetic variation, making these candidates poorly relevant to explain the clear association found between differently methylated genes and the CSR.

Since gene body methylation is associated with transcript abundance with a maximum abundance for a GBMR of 19.6%, we might expect that the transcriptional effect of hypo- / hyper-methylation of genes that are initially methylated above / below this 19.6% threshold, converge toward the same optimal transcriptomic profile. In other words, lowly (environmental responsive genes) and highly (housekeeping genes) methylated genes can respectively become constitutively express at a high level through a hyper- or a hypo- methylation bringing back their GBMR close to the 19-20% threshold. To test this hypothesis, we focused on genes contained in the stress related GO categories (*i.e.*, 236 and 96 genes in the hypo- and the hyper- methylated groups, respectively) and plotted their GBMRs independently for naive and trained corals (Fig. 4d). Methylation changes that occurred in trained corals maximized the quantity of genes located in the GBMR window corresponding to maximal transcription status and therefore favored higher abundance of stress-associated gene transcripts under basal conditions (Fig. 4d). This result is consistent with the frontloading strategy identified at the transcriptomic level. Although causality

still remains to be demonstrated, our data provide strong evidence that DNA methylation changes at some targeted genes at least partly contribute to the increase of coral thermotolerance in response to recurrent heat stresses. This result shows that corals can rely on DNA methylation changes to acclimatize to global warming as it was shown for ocean acidification (*28, 29*).

In addition to its significance for the field of coral epigenetic, our results and methods used to interpret DNA methylation changes strengthen and deepen the emerging understanding of the role of DNA methylation in invertebrate's ecology and evolution. Indeed, it was proposed that DNA methylation changes reflect a shifting balance between the expression of environmentally responsive and housekeeping genes (*27*), highlighting its role for intragenerational acclimatization. The recent demonstration that DNA methylation is transmitted from adults to their sperm and larvae at the CpG level further confirm a role for CpG methylation in invertebrate's intergenerational acclimatization (*30*). Although the consequences of intragenic DNA methylation changes are still poorly understood, we provide here evidences for a link between frontloading and methylation changes, and we strengthen with experimental data the hypothesis recently proposed and stating that "*transcription and GBMR can influence each other through a negative feedback loop where an increasing transcription induces the methylation of the gene while a heavy methylation reduces its transcription*" (*27*). This model predicts that genes which require a high and constitutive expression should display a GBMR close to the value associated to the maximum of transcription. This prediction is indeed confirmed in our controlled experiment where the main environmental force inducing acclimatization is the recurrence of heat stresses and the frontloading of stress-responding genes.

Conclusion

This study confirms that coral colonies facing recurrent heat stress can train and better acquire thermotolerance to cope with new (predictable) heat waves. We also provide some evidence that coral training is achieved in parallel with an increase of intra-colonial genetic and epigenetic variations. If there is no doubt about the inheritance of genetic information, the role of epigenetics in evolution is still challenged because of the soft nature of its inheritance. However, an increasing number of studies show that epigenetic modifications can be transmitted and mediate transgenerational plasticity (*30*). The present work does not address the meiotic inheritance of epigenetic marks, and this will be an important point to investigate in future work. Corals use both sexual and asexual reproduction modes (parthenogenesis, fragmentation, polyp bail out, etc.), from which the quantity of descendant can significantly vary (*31*). Mitotic inheritance (asexual reproduction) has been clearly established in our study and such mechanisms can therefore rapidly enhance local adaptation of natural populations displaying asexual reproduction such as those of the *Pocillopora damicornis* clade (including *P. acuta*) of the Central Pacific (*31*).

The identification of genetic or/and epigenetic markers of coral adaptation to global changes would open the door to a new era of reef management. Indeed, it would not only inform the use of assisted evolution in restoration programs (*32*), but would also help prioritizing reef areas that must be protected by identifying reefs undergoing acclimatization and/or adaptation (*33*). Such local actions must be maintained and strengthened together with global action aiming to reduce CO_2 emissions, because, even if corals can rapidly acclimatize, they will continue to

bleach under extreme heat stress events such as those encountered in 2016, 2017(*1*) or encountered in 2020 while we are writing these lines.

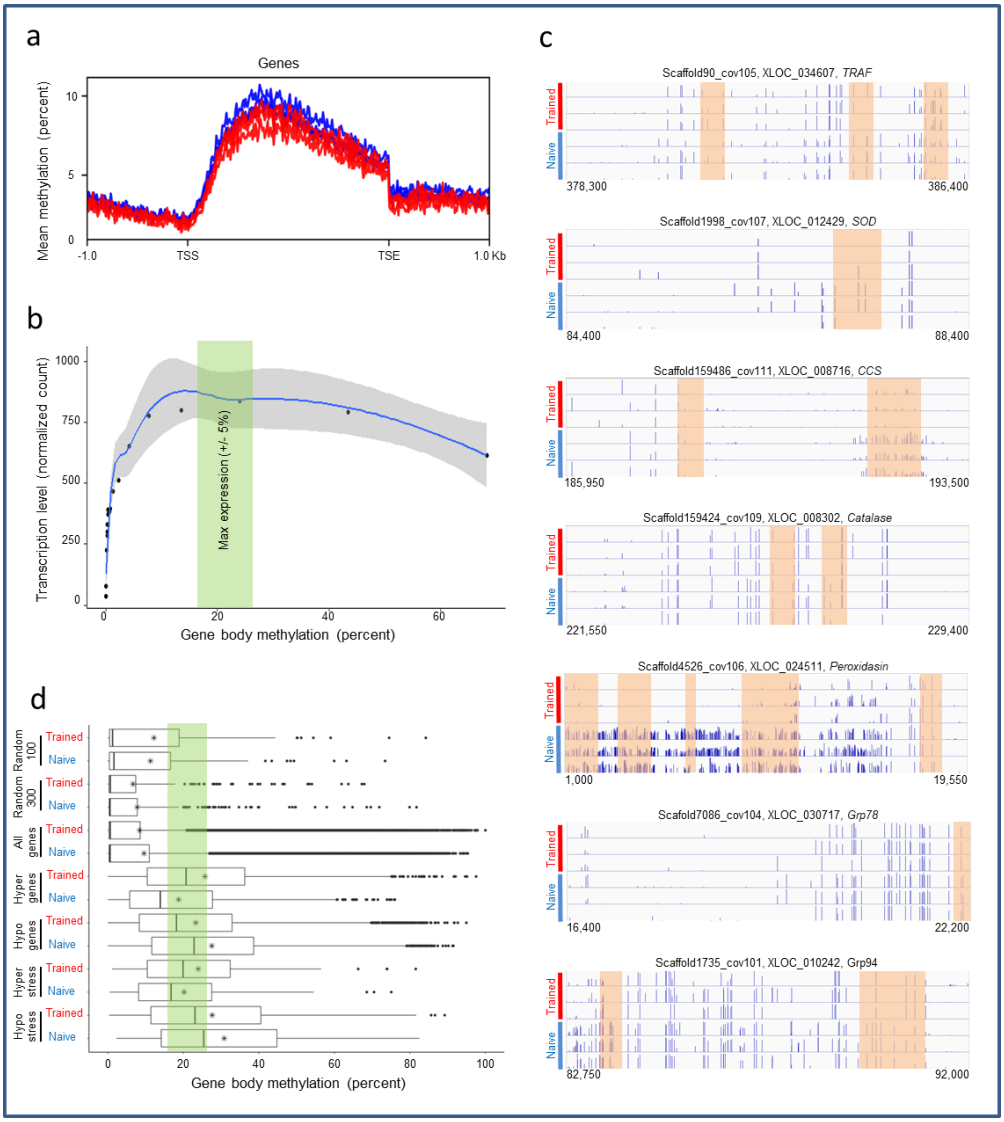

Fig. 4. Epigenetic differences between naive and trained corals. a. Methylation profiles in the CpG context deduced from WGBS in six replicates. b. average transcription level (Y axis) in function of gene body methylation rate divided in 20 quantiles scored by gene body methylation rate (X axis). The green box highlights the methylation rate (+/-5%) associated to the maximum of transcript abundance (calculated from the 1000 most abundant transcripts). c. DNA methylation differences (orange box) in candidate genes belonging to the CSR: cell death regulation, a tnf receptor-associated factors (TRAF); oxidative stress, a superoxide dismutase (SOD), a copper chaperone for superoxide dismutase (CCS), a catalase, a peroxidasin; Protein folding of the HSP family, 78 kD glucose regulated protein (Grp78), 94 kD glucose regulated protein (Grp94).d. Box plot of the gene body methylation rate in trained and naive corals for: significantly hyper or hypomethylated genes that belong to the stress related GO term; the entire set of genes showing significant hyper or hypomethylation; all the genes of the genome and random selection of 100 or 300 genes as a reference. The green box highlights the methylation rate (+/-5%) associated to the maximum of transcript abundance (calculated from the 1000 most abundant transcripts).

Materials and Methods

Experimental Design

Coral maintenance

Twenty-one initial fragments (~10 g; 7 cm high; 6 cm in diameter) from the same mother colony of *Pocillopora acuta* (Indonesian CITES Management Authority, CITES number 06832/VI/SATS/LN/2001-E; France Direction de l'Environnement, CITES number 06832/VI/SATS/LN/2001-I) were produced as previously described (*10*) and randomly assigned to two sets: the naive and the trained sets. They were equally distributed in three 300L tanks (seven fragments per set) that are part of the aquarium facility. They were maintained in these common garden conditions at a temperature ranging between 25 and 28°C and were in contact with ~30 different coral species (no other *P. acuta*) hosted at the Cap d'Agde Aquarium coral's husbandry. Since the size of a colony is known to induce micro environments that can influence bleaching response, all initial fragments were fragmented twice a year to limit size variations and avoid size effects. These fragmentations were done in the same time for all the individuals of the trained and the control sets. The new fragments (same number per initial fragments) were kept to increase the number of samples in each set.

The temperature in the facility was controlled by connecting an aquarium heater (600 W, Schego) to an electronic thermostat (Hobby Biotherm Professional). Aquaria were illuminated by metal halide lamps (Osram Day Light 5200 K, 400 W) providing an irradiance of 350 µmol photon.m^{-2}.s^{-1} (quantum meter: QMSW-SS; by Apogee Instruments Inc.) on a 12:12h (light:dark) photoperiod. Coral were fed twice a week with *Artemia salina* nauplii to reach a natural heterotrophic rate. All other seawater characteristics (*e.g.*, salinity 36 g.L^{-1}, pH 8.3) were maintained constant and equal. A constant water flow was maintained in each tank using a water pump (Tunze Nanostream 6045, delivery 4500 L.h^{-1}). Seawater was continuously recycled at rate of 12 tank volumes per hour by coupling the action of a biological filter and an Aquavie protein skimmer (model: PS 1200), and refreshed by filtered and preheated Mediterranean seawater at a renewal rate of one tank volume per hour.

Training protocol

In January, all fragments were transferred in 100L experimental tanks (3 control tanks and 3 heat stress tanks) for experimental heat stress accordingly to a previously published protocol (*10*). This was done two times in order to exposed the trained set to two consecutive thermal stress treatments (inducing bleaching) separated by one year of recovery (Fig. 1a). To enable coral recovery, the temperature was decreased to 28°C for two weeks immediately after bleaching. Then, corals were moved back to the aquarium facility and let to recover for a year. The naive set was maintained at a control temperature of 28°C during heat stress and moved between the aquarium facility and the experimental tanks in the same time than the trained set.

Thermotolerance quantification and biological material for integrative Omics

After the two years of training, a third heat stress was performed in order to quantify the thermotolerance of each set and to produce the samples needed to understand thermotolerance modifications at the molecular level. For this purpose, naive and trained corals were exposed simultaneously to a heat stress inducing bleaching (the same as for the training period). During this last heat stress three fragments from each set (one per 100L tank) were sampled at 28°C (Day

3), 29°C (Day 6), 30°C (Day 9), 31°C (Day 12) and 32°C (Days 15, 18 and 21). They were flash frozen and stored in liquid nitrogen until analysis.

The remaining fragments were used to quantify the thermotolerance of naive and trained corals. To do so, the 32°C temperature was maintained and the occurrence of phenotypes that are classically used to quantify corals response to heat stress were visually monitored through time and until 100% of mortality was reach: (i) bleached coral, (ii) partial mortality (bleached with some parts of the colony dead), or (ii) complete mortality. To monitor the bleaching response in a nondestructive manner, we used the Coral Health Chart of the Coral Watch program (*34*). A colony was considered "bleached" when the color dropped from D4 scale (healthy coral) to D2-D1 scale. A colony was classified as "displaying partial mortality" when it displayed >10% of bare skeleton and as "totally dead" when no trace of tissue could be observed anymore.

Nucleic acid extraction

When an identical time point was studied using different omic approach (transcriptomic, epigenomic, genetic and metabarcoding) the nucleic acids were extracted from the same fragment (Fig. 1b). RNA and DNA extraction were done using a previously published protocol. DNA for Whole Genome Bisulfite Sequencing was extracted using a protocol designed to reduce *Symbiodiniacea* DNA representation in order to maximize cnidarian host representation (*35*).

RNA-seq

Library construction and sequencing

RNA-seq libraries were prepared using TrueSeq Stranded mRNA Sample Preparation kit (Illumina) accordingly to the manufacturer's instructions. Libraries were sequenced with an IlluminaHiSeq 2000. Library constructions and sequencing were performed by the Montpellier GenomiXplateforme (Montpellier, France). Sequence data have been made available through the SRA database (BioProject PRJNA553143).

Gene expression quantification

The bioinformatic pipeline used in the present study was adapted from Rondon et al. (*36*). Briefly, after demultiplexing, raw data were filtered to keep reads with a Phred score above Q26 for at least 95% of the sequence using the filter by quality of the FASTX toolkit suite and adapters were removed with cutadapt. To optimize the mapping step, the scaffolds with a size below 5 kb were removed from the reference genome (Supplementary material and methods). Paired reads were mapped using TopHat2 with the following parameters; minimum intron length = 70 bp, maximum intron length = 62,000 bp, mismatch allowed = 2. Unmapped reads were removed using samtools. To produce mapping libraries with an identical mapping efficiency, 31,562,006 paired mapped reads were randomly selected using a custom Perl script and sorted according to their position on scaffolds. Remove duplicates V1.0.0 (samtools) was used to remove PCR duplicates, allowing four exact matches. Because the quantity of duplicates was not the same between each mapping library, a second random selection of reads was performed (23,059,925 read pairs) to have the same number of reads between libraries. Htseq-count was used to count aligned reads that overlapped genes annotated by the experimental approach (Supplementary material).

Whole Genome Sequencing

Library construction and sequencing

DNA-seq library were prepared using the illumine Truseq DNA kit accordingly to manufacturers instruction. Libraries were sequenced with an Illumina HiSeq 2000. Library constructions and sequencing were performed by Genome Quebec (Montreal, Canada). Sequence data have been made available through the SRA database (BioProject PRJNA553143).

Quality control and cleaning

Initial quality control and cleaning of reads was performed using FASTX-toolkit version 0.0.13. Reads were then groomed and filtered based on their quality score (Q30 over 90% of the length of the read). This step allows us to retain reads for which at least 90% of their bases have a minimum Phred quality score of 30, corresponding to less than 1 incorrect base call out of a 1000 and a precision of 99.9% accuracy in the base calling. Finally, adapters used for sequencing were removed using cutadapt software.

Read Mapping

High quality reads were mapped to the *Pocillopora acuta* reference genome (filtered for scaffolds > 5 kb; Supplementary material and methods) using Bowtie 2 software v 0.6 in single-end mode to increase coverage of the genome, and thus optimize the detection of variants thereafter. To avoid false positives in subsequent detection of variants, we eliminated the reads mapping to several locations. Simple descriptive statistics were then performed on the BAM mapping files using samtools.

SNP calling

SNP calling was performed with Varscan 2 software to search for sequence variations in the genome with each sample. The minimum coverage used for detection was set to 8 reads, the minimum alternative allele frequency to 0.1, and the number of reads supporting the variant allele was set to 2.

Transposable element detection

The identification of transposable elements (TE) in the regions displaying CNVs was done using RepeatMasker (http://repeatmasker.org) and using the TE database produced from the reference genome (Supplementary material and methods).

Whole Genome Bisulfite Sequencing analysis

Library construction and sequencing

Purified DNA was sent for bisulfite conversion, library construction and sequencing to GATC biotech (www.gatc-biotech.com). Libraries with fragment sizes ranging from 150 to 500 bp were paired-end sequenced (100 bp on each extremity) on an Illumina HiSeq 2000. Sequence data have been made available through the SRA database (BioProject PRJNA553143).

Quality control and cleaning

All data processing was carried out under a local galaxy instance (http://bioinfo.univ-perp.fr). Fastq Groomer v1.0 was used for verification of the fastq sanger format, and the

FASTX-Toolkit v0.0.13 (Compute quality statistics, Draw quality score boxplot, Draw nucleotides distribution chart) was used for initial quality control. The first and last five nucleotides of all reads were removed using the TRIM tool from the FASTX-Toolkit because of lower quality. Overall, read quality was judged sufficiently good (the majority of reads showed a quality score above 26 for the non-trimmed position) and no further quality filter was applied.

Read Mapping

Read alignment on the *P. acuta* reference genome (Supplementary material and methods) was done in paired-end using Bismark v2.74 and Bowtie2 with default parameters. We only kept alignments for which both read mates were successfully aligned and fragment size was between 150 and 500 bp.

Methylation calling

BAM files output from Bismark were sorted and converted to SAM format using Samtools v0.1.19. SAM files were loaded into the R package methylKit v0.5.6 using the read.bismark() command and specifying the cytosine context (CpG, CHG or CHH, respectively). Afterwards, we used the getMethylationStats() command to obtain the percentage of methylated cytosines per context. Visualization of the methylated regions was done by converting alignment BED files into bigWig format with the Wig/Bedgraph-to-bigWig converter v1.1.1 included in Galaxy. BigWig files were then uploaded into Trackster, the visual analysis environment embed in Galaxy.

Metabarcoding

MiSeqamplicon sequencing

Symbiodiniaceae communities in symbiosis with naive and trained corals were analyzed using ITS2 (internal transcribed spacer of the ribosomal RNA gene) amplicon libraries with specific primers targeting a ~350 bp sequence (ITS2-F GTGAATTGCAGAACTCCGTG ; ITS2-R CCTCCGCTTACTTATATGCTT) (*37*). Paired-end sequencing with 250 bp read length was performed on the MiSeq system (Illumina) using the v2 chemistry according to the manufacturer's protocol. Sequence data have been made available through the SRA database (BioProject PRJNA553143).

Sequence analysis

The FROGS pipeline (Find Rapidly OTU with Galaxy Solution) implemented in a Galaxy instance (http://sigenae-workbench.toulouse.inra.fr/galaxy/) was used for data processing. In brief, paired reads were merged using FLASH. After denoising and primer/adapter removal with cutadapt, *de novo* clustering was done using SWARM with a local clustering threshold, with aggregation distance d=3. Chimeras were removed using VSEARCH. The dataset was filtered for singletons and affiliation performed using blastn against the nr/nt database of the NCBI. Finally, an operational taxonomic unit (OTU) table in standard BIOM format was produced for subsequent analysis. To confirm blast identification, we performed phylogenetic analysis using MAFFT to produce sequence alignment and FastTree (GTR+CAT model) to compute tree with the approximately maximum likelihood method.

Statistical Analysis

Phenotyping

The occurrence of heat stress symptoms monitored through time to characterize the thermotolerance of the trained and the naive corals were analyzed with a Kaplan-Meier analysis. This statistically compares the shape of phenotypic curves of naive and trained coral sets. Differences were tested with the Log-Rank test (Mantel-Cox) and were considered significant under the level of 5% error.

Differential gene expression

The R package DEseq2 was used to test if gene expression differences between two conditions were significant (adjusted *p*-value (*p*adj) for multiple testing with the Benjamini-Hochberg procedure FDR <0.01).

Quantification of molecular phenotypic plasticity

To compare levels of genome-wide transcriptomic plasticity between trained and naive corals in response to heat stress, we performed a Discriminant Analysis of Principal Components (DAPC for transcriptome; (*5, 38*)). We based our DAPC analysis on $\log_2$ transformed abundance matrices obtained from the 12 coral samples studied, including three individuals from both the naive and trained treatment sampled at 28°C (*i.e.,* control temperature) and sampled at 31°C (*i.e.,* heat stress temperature). These matrices contained a total of 36,140 genes and $\log_2$ transformation was performed using DESeq2. Specifically, we first ran a DAPC analysis considering the naive and trained samples from the 28°C treatment as predefined groups using the Adegenet package implemented in R. This first step allowed us to differentiate these two experimental groups based on their overall gene expression profiles. Next, we projected the coordinates of the stressed samples (*i.e.,* 31°C) from both treatments (naive and trained) into the unique discriminant function of the DAPC.

Enrichment analysis

To identify the biological functions over or under represented in a set of genes by comparison to another the R package RBGOA was used. Scripts we used in this work were published in (*39*) and can be downloaded here (https://github.com/z0on/GO_MWU). For gene expression data, the Mann-Whitney U-test procedure (continuous value) was used using the a signed log(p-value) as the continuous value. This strategy enables to take into account the level of expression and the significance of the differential expression. For genetic and epigenetic data, a unweighted approach was undertaken and use the Fisher exact test procedure. For our study, the following parameters were used for adaptive clustering: largest=0.1; smallest=10; clusterCutHeight=0.5. A category was considered enriched under an FDR of 0.5%. When needed, REVIGO (http://revigo.irb.hr/) was used to synthetized and graphically (NMDS) represent RGOA results.

Genetic variation, SNP analysis

Mpileup files with the coverage and quality information from the BAM alignment files were produced for each population using SAMtools. The kinship coefficient of Manichaikul was

calculated with VCFtools (--relatedness). Tajima's D and Tajima's Pi indexes were calculated within and between each population using PoPoolation2. Analyses were performed on 10 and 200 kb windows with two reads supporting the allelic variant for Pi indexes and a minimum coverage of 8 reads for D indexes. Differentiation levels (or fixation index Fst) between treatments were also calculated based on SNP information using PoPoolation2 on 200 kb windows. A synchronized file was generated from the mpileup files, which contains the allele frequencies for each condition at each position in the reference genome. The parameters used were the same as for the previously calculated indices in PoPoolation2.

Genetic variation, CNV analysis

The identification of copy number variation (CNV) was performed using CNV-seq and the R software CNV package. Comparing the changes in sequence coverage between the two conditions, this algorithm detects changes in copy number of a region defined by a sliding window, allowing the detection of CNVs across the entire genome.

The cnv-seq.pl Perl script was used to calculate the size of the sliding window, the number of reads aligned in each window, the ratios ($\log_2$) and the p-values associated with each CNV. The naive corals mapping file was provided as the reference genome, and the trained corals mapping file as the test. The settings for algorithm calculation were Log2ratio at 0.6, and *p*-value at 10^{-6}.

DNA methylation variation analysis

Differential methylation between conditions was tested using the R package methylKit v0.5.6. For this purpose, methylated cytosines with coverage above 10 were kept and differentially methylated regions (DMRs) were identified using windows of 500 bp, q <0.01 and difference of ≥25%. Gene body methylation rate were calculated for each sample using MapBed from bedtools. Two bed files were used as input, one referencing genes in the reference genome and a second referencing methylation levels for each CpG of the genome (Methylkit output).

Symbiodiniaceae community analysis

The phyloseq R package was used for community composition analysis to infer alpha diversity metrics at the OTU level, as well as beta diversity (between sample distance) from the OTU table. Community similarity was assessed by nonmetric multidimensional scaling using the Bray-Curtis distance matrices.

Acknowledgments:

General: We thank the Bio-Environnement platform (University of Perpignan) for bioinformatics service as well as the GenoToul bioinformatics platform, and the Toulouse Midi-Pyrenees and Sigenae group for providing help and computing resources (Galaxy instance; http://sigenae-workbench.toulouse.inra.fr).We thank François Bonhomme, Pierre-Alexandre Gagnaire and Sophie Arnaud-Haond for fruitful discussions. The authors acknowledge Life Science Editors for editing services.

Funding: This project was funded by the ADACNI program of the French national research agency (Agence Nationale pour la Recherche, ANR) (project no. ANR-12-ADAP-0016;

http://adacni.imbe.fr), the Campus France PHC program Maïmonide-Israel, the DHOF (http://ihpe.univ-perp.fr/en/ihpe-transversal-holobiont/), and the DGE program (http://ihpe.univ-perp.fr/en/ihpe-transversal-epigenetics/) of the UMR 5244 IHPE (http://ihpe.univ-perp.fr/en/ihpe-transversal-holobiont/). This study is set within the framework of the "Laboratoire d'Excellence (LABEX)" TULIP (ANR-10-LABX-41). SN acknowledges financial support from France Génomique National infrastructure, funded as part of the "Investissement d'avenir" program managed by Agence Nationale pour la Recherche (contract ANR-10-INBS-09).

Author contributions

JVD, GM and MA conceived the study; JVD, LF, PR and KBR performed experiments in mesocosm; JVD, ET, CG, OR, DR, CC, CC, APP, MP, KBR, SN and PP were involved in data acquisition. All authors were involved in data analysis. JVD wrote the manuscript with contributions from all other authors.

Competing interests

The authors declare no competing interests.

Data and materials availability

ANNEXE 11

SCIENTIFIC REPORTS

OPEN

Colour plasticity in the shells and pearls of animal graft model *Pinctada margaritifera* assessed by HSV colour quantification

Received: 29 October 2018
Accepted: 1 May 2019
Published online: 17 May 2019

Pierre-Louis Stenger[1], Jérémie Vidal-Dupiol[2], Céline Reisser[1], Serge Planes[3] & Chin-Long Ky[1]

The bivalve *Pinctada margaritifera* has the capacity to produce the most varied and colourful pearls in the world. Colour expression in the inner shell is under combined genetic and environmental control and is correlated with the colour of pearls produced when the same individual is used as a graft donor. One major limitation when studying colour phenotypes is grader subjectivity, which leads to inconsistent colour qualification and quantification. Through the use of HSV (Hue Saturation Value) colour space, we created an R package named '*ImaginR*' to characterise inner shell colour variations in *P. margaritifera*. Using a machine-learning protocol with a training dataset, *ImaginR* was able to reassign individual oysters and pearls to predefined human-based phenotype categories. We then tested the package on samples obtained in an experiment testing the effects of donor conditioning depth on the colour of the donor inner shell and colour of the pearls harvested from recipients following grafting and 20 months of culture *in situ*. These analyses successfully detected donor shell colour modifications due to depth-related plasticity and the maintenance of these modifications through to the harvested pearls. Besides its potential interest for standardization in the pearl industry, this new method is relevant to other research projects using biological models.

The marvellous diversity of colours among molluscan shells has been widely esteemed for hundreds of years by collectors and scientists[1]. Colour is a well-known naturally plastic trait that varies due to inter-individual genetic differences, crystalline structure of exoskeletons or appendages, variable diet or other environmental conditions[1–6]. Colour phenotype has been the centre of interest in many biological studies since it is involved in some evolutionary processes (natural selection for camouflage or defence, sexual selection for fitness in a partner, etc.) and can be exploited for industrial purposes (dyes, jewellery)[1,7–10]. For the pearl industry, this trait has been selected to create commercially specific strains such as golden Pacific oysters *Magallana gigas* (Thunberg, 1793)[11–13], "ivory" strains of the Japanese scallop *Patinopecten yessoensis* (Jay, 1987)[6,14] and "gold" pearl production from the silver- or gold-lipped pearl oyster *Pinctada maxima* (Jameson, 1901)[15]. The black-lipped pearl oyster, *Pinctada margaritifera* (Linnaeus, 1758), is the top aquaculture species in French Polynesia. The species is cultivated for pearl production and the associated industry is the second greatest source of revenue for French Polynesia after tourism[16]. *P. margaritifera* has the ability to produce cultured pearls with a very wide range of colours[17,18], derived from the donor oysters used to provide grafting tissue[19–22]. The pearl production process depends upon a grafting operation requiring a donor pearl oyster, a recipient pearl oyster and a skilled technician to perform the surgery[23]. A piece of tissue from the edge of the mantle of a donor oyster (the "saibo", also known as the graft), selected based on the quality of the donor's shell colour, is inserted together with a nucleus (made of mollusc shell or synthetic material) into a recipient oyster chosen for its vigor[23,24]. The external shell of *P. margaritifera* is commonly black, sometimes with white dotted lines arranged in lateral bands. However, some individuals are red in colour over the entire surface of their shells[18], while others are yellow just at the base of the external shell surface. A very rare white albino shell morphotype (named "pupure") also exists[25]. The inner side of the shell has a larger colour

[1]IFREMER, UMR 241 Écosystèmes Insulaires Océaniens, Labex Corail, Centre Ifremer du Pacifique, BP 49, 98725, Tahiti, French Polynesia. [2]IFREMER, UMR 5244 IHPE, University Perpignan Via Domitia, CNRS, University Montpellier, F-34095, Montpellier, France. [3]PSL Research University, EPHE-UPVD-CNRS, USR 3278 CRIOBE, Labex Corail, Université de Perpignan, 52 Avenue Paul Alduy, 66860, Perpignan Cedex, France. Correspondence and requests for materials should be addressed to C.-L.K. (email: chinky@ifremer.fr)

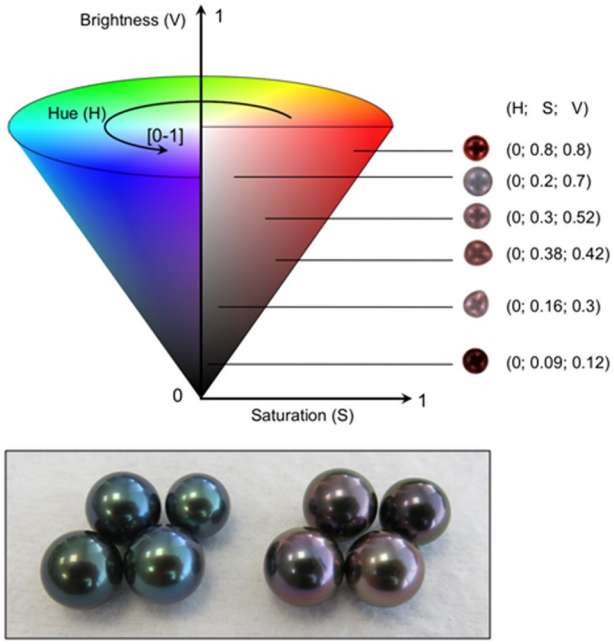

Figure 1. The Hue Saturation Value (HSV) colour code system used to quantify colour in *Pinctada margaritifera* shells and cultured pearls. For a determined hue (H), saturation (S) range (from 0, white, to 1), and brightness (V) range (from 0, black, to 1) were measured, as illustrated here by red pearl samples, with HSV values shown in brackets. Red and green pearl samples are illustrated above the conical representation of the HSV system.

gamut, ranging from red to yellow, green to blue or peacock to white, with all possible intermediate nuances[21,26]. Pigments are primarily visible on the peripheral parts of the shell[27]. Indeed, because the nacreous layer covers the prismatic layer, this may make the pigments opaque[27–29]. According to Ky *et al.*[19], the factors contributing to the colour of a pearl include the phenotype of the donor oyster (partial genetic inheritance), geographical location, and the environmental conditions in which the recipient oyster is reared during pearl development[30].

The assessment of colour nonetheless remains a subjective trait in which human quantification and qualification can be strongly biased, as visual perception of colours differs between individuals[31]. For this reason, efforts are currently being made to develop accurate and reproducible computational methods for automatic objective colour qualification and quantification[10]. In this study, based our approach on the HSV (Hue Saturation Value) colour space to characterize the colour variation in our biological model (Fig. 1).

The objective of the present study is the qualification and quantification of colour with a new standardized and reproducible method. We used HSV colour space to characterise colour variation in the inner shell of black-lipped oysters and pearls produced by the pearl industry. Finally, to enable a wider use of this method in scientific and private programmes, we developed an R package, *ImaginR*[32] and made this publicly available.

Results

Shell and pearl materials issued from an experimental graft. To validate our newly developed method for qualifying and quantifying colours, we first used material issued from a basic experimental graft on which we assessed the colour of donors and of pearls produced with the grafts of these donors. For this graft, the mantle (the biomineralizing tissue) from each of the donors selected for their colours was cut into 30 pieces, which were then grafted into the gonads of 30 recipient oysters in order to produce pearls.

Colours were then analysed in a total of 669 pearls issued from grafts made with two donor colour phenotypes (green and red) and cultured at two depths (4 or 30 m) to create a baseline for measuring colour determination stability using the new colour assessment method. The average nucleus retention rate of the experimental graft was 93.0% (N = 749) at 42 days post-grafting. After 20 months of culture, pearls were successfully harvested from 89.9% of the individuals initially grafted (N = 669). The difference (3.1%) corresponded to nucleus rejection after day 42, and oyster mortalities. The numbers of pearls harvested per donor colour class and per depth group were: 363 pearls formed by grafts from the green donor phenotype (197 for the group at 4 m and 166 for the group at 30 m) and 306 pearls formed by grafts from the red donor phenotype (143 for the group at 4 m and 163 for the group at 30 m).

Hue values for inner shells and cultured pearls. The hue distributions for the shell phenotypes and rearing conditions revealed four dominant hues for green donors reared at 4 m depth (GS) (0.500; 0.555; 0.444; 0.4166), three for green donors reared at 30 m (GD) (0.500; 0.583; 0.416), three for red donors reared at 4 m (RS) (0.000; 0.066; 0.100) and three for red donors reared at 30 m (RD) (0.000; 0.055; 0.04) (Fig. 2a).

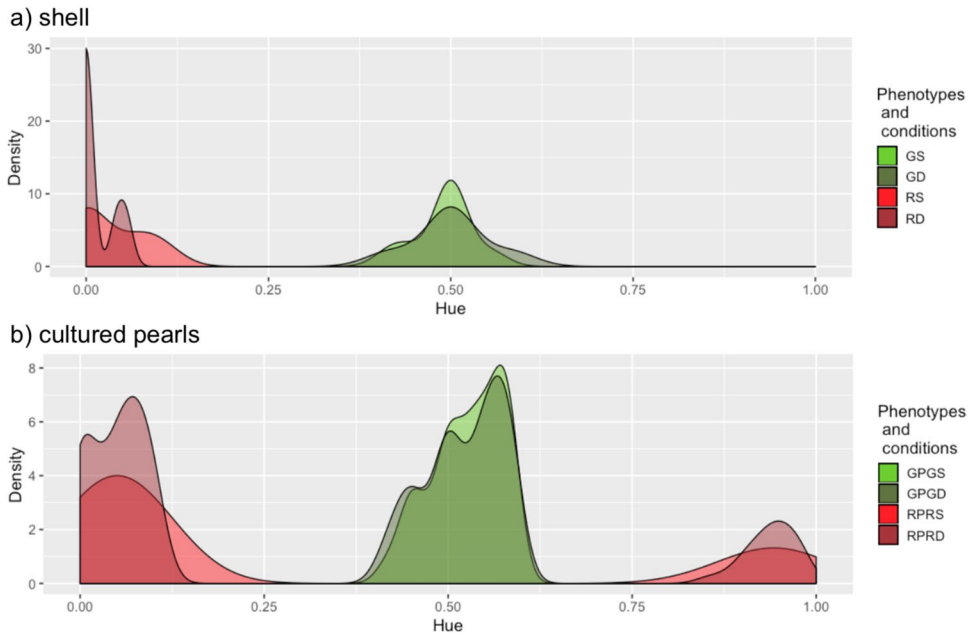

Figure 2. Hue density plot distribution of *P. margaritifera* for: (**a**) donor oyster shells from: GS (green donors reared at 4 m; N = 9), GD (green donors reared at 30 m; N = 6); RS (red donors reared at 4 m; N = 5), and RD (red donors reared at 30 m; N = 7), (**b**) cultured pearls associated with the donors illustrated in (**a**), with GPGS (green pearls from green donors reared at 4 m; N = 132), GPGD (green pearls from green donors reared at 30 m; N = 66), RPRS (red pearls from red donors reared at 4 m; N = 84) and RPRD (red pearls from red donors reared at 30 m; N = 118). Light green (or red) and dark green (or red) distributions correspond to donor conditioning in subsurface (4 m) or deep (30 m) culture, respectively, prior to graft operations.

	Green donors			Red donors		
Donor conditioning depth	**4 m**	**30 m**	**Total**	**4 m**	**30 m**	**Total**
Number of pearls	197	166	363	143	163	306
Number of green (or red) pearls from green (or red) donors	132	66	198	84	118	202
Rate (%) of green (or red) pearls from green (or red) donors	67.0	39.6	53.3	58.7	72.4	65.55
Number of hues	84	98	138	103	112	185
Diversity index	0.43	0.59	0.38	0.72	0.69	0.60

Table 1. Number of pearls and pearl hues categorized by phenotype and culture treatment. The percentages (line number 4) represent the proportion of pearls with same colour phenotype as their donors. Comparisons of this rate were all significant: 1) between conditioning depth (4 m vs. 30 m), within green ($p < 0.001$) and red donors ($p < 0.05$); and 2) between green and red donors for the 30 m conditioning depth ($p < 0.001$) and for both depths together ($p < 0.005$). All p-values were obtained from Pearson's Chi-squared test with Yates continuity correction test. The diversity index was obtained by calculating the ratio of the number of hues to the number of pearls.

Overall, 138 different hues were found among the 363 pearls produced with grafts from green donors and 185 hues for the 306 pearls produced with grafts from red donors (Table 1). Some of the pearls produced with grafts from green donors reared at 4 m (PGDS) and 30 m (PGDD) shared the same hues, as the diversity index (ratio of the hue number and pearl number) for PGD total (0.38) was lower than both the PGDS (0.43) and PGDD (0.59) diversity indices. The hue diversity index was greater for the red phenotype (0.60 in total) than the green, even though the red donor phenotype also shared hues between pearls from grafts of the donors conditioned at 4 m (PRDS) (0.72) and pearls from grafts of the donors conditioned at 30 m (PRDD) (0.69) (Table 1). Statistically, we observed more green pearls from the grafts of green donors when these donors had been reared at 4 m than at 30 m (67% at 4 m and 39.6% at 30 m, Chi^2 test $p < 0.001$) (Table 1). However we observed the opposite phenomenon for the red phenotype. Indeed, we observed more red pearls from the graft of red donors when these had been reared at 30 m than at 4 m (58.7% at 4 m and 72.4% at 30 m, Chi^2 test $p < 0.05$) (Table 1). Among the pearls produced with grafts from donors grown at 4 m, there were more green pearls from the green donor grafts (67%) than red pearls from the red donor grafts (58.7%). At 30 m, the opposite phenomenon was shown, with more red pearls from the red donor grafts (72.4%) than green pearls from the green donor grafts (39.6%) (Chi^2 test $p < 0.001$). When the pearls from the two depths were considered together, the same pattern was found overall,

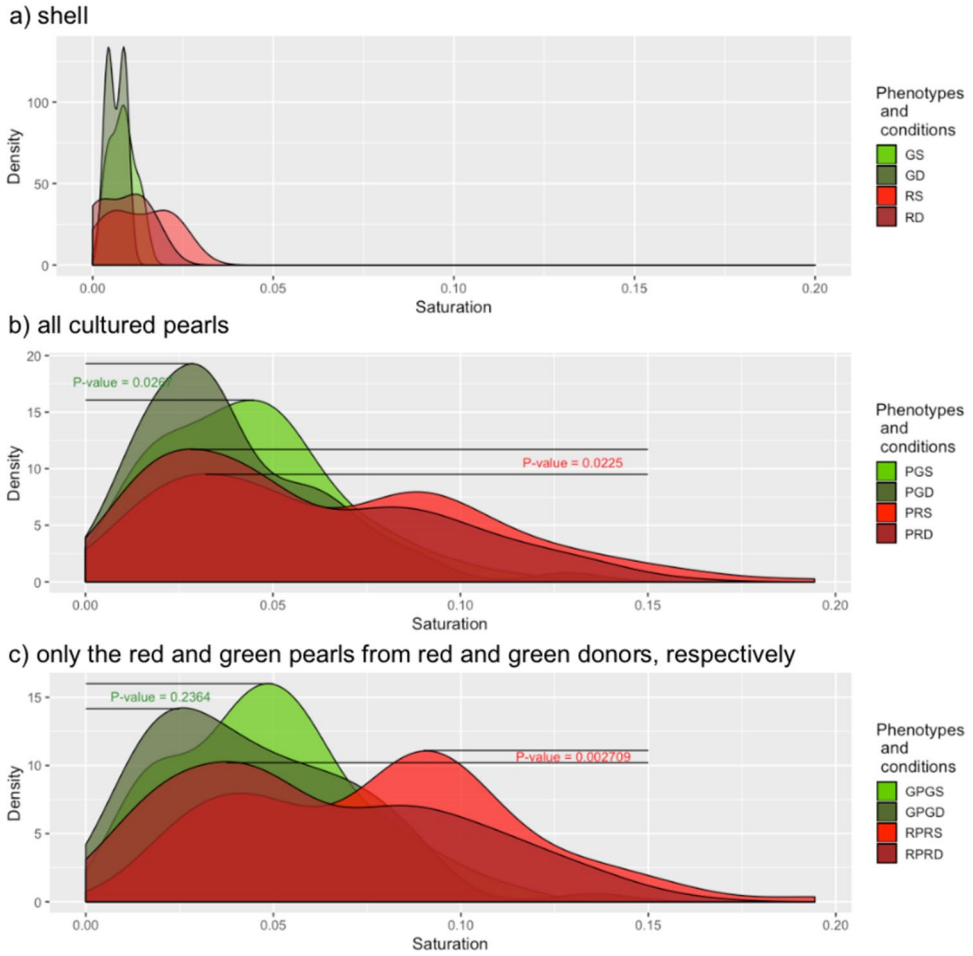

Figure 3. Saturation density plot distribution of *P. margaritifera* for: (**a**) shells of donor oysters from: GS (green donors reared at 4 m; N = 9), GD (green donors reared at depth of 30 m; N = 6), RS (red donors reared at 4 m; N = 5), and RD (red donors reared at 30 m; N = 7), (**b**) multicoloured cultured pearls associated with the donors in (**a**), with PGDS (pearls from green donors reared at 4 m; N = 197) and PGDD (pearls from green donors reared at 30 m; N = 166); PRDS (pearls from red donors reared at 4 m; N = 143) and PRDD (pearls from red donors reared at 30 m; N = 163), (**c**) associated cultured pearls that show the same colour hue as their corresponding donors, GPGS (green pearls from green donors reared at 4 m; N = 132), GPGD (green pearls from green donors reared at 30 m; N = 66), RPRS (red pearls from red donors reared at 4 m; N = 84), and RPRD (red pearls from red donors reared at 30 m; N = 118). Light green (or red) and dark green (or red) distributions correspond to donor conditioning in subsurface (4 m) or deep (30 m) culture, respectively, prior to graft operations.

with again more red pearls from red donors than green pearls from green ones (65.55% for red and 53.3% for green; Chi^2 test $p < 0.005$; Table 1).

The analysis of saturation for inner shell colour and cultured pearls. The distributions of donor inner shell colour shifted closer towards low saturation for the 30 m depth group than for the 4 m group (Fig. 3a).

When all cultured pearls were considered, samples from both green ($p < 0.05$) and red ($p < 0.05$) donors showed a significant shift of saturation towards lower levels following deep conditioning (30 m) compared with sub-surface (4 m) conditioning (Fig. 3b).

When only red pearls from grafts of red donors and green pearls from grafts of green donors were considered, the saturation distribution also significantly shifted towards lower saturation, with greater depth for RPRD only ($p < 0.005$ and $p = 0.2364$, respectively). These results are similar when all cultured pearls were considered, but the differences between the depths were 140.8 times stronger for the red phenotype (Fig. 3c). In terms of saturation, the inner shell colour therefore became less intense and less bright with depth.

Brightness (V) of donor oyster inner shells and cultured pearls. Regarding the inner shell colour, the brightness (V) of the distributions shifted to higher levels in the samples conditioned at 30 m depth compared with those conditioned at 4 m depth (Fig. 4a).

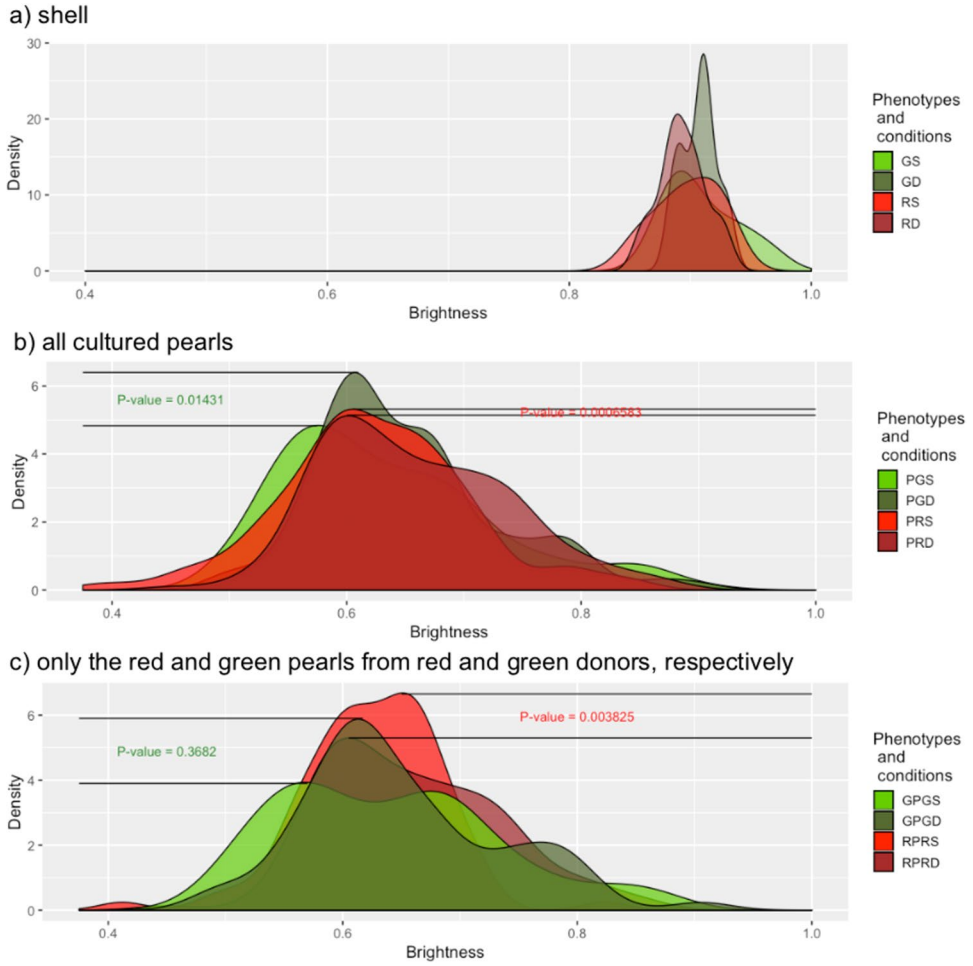

Figure 4. Brightness density plot distribution of *P. margaritifera* for: (**a**) shells of donor oysters from GS (green donors reared at 4 m; N = 9), GD (green donors reared at 30 m; N = 6), RS (red donors reared at 4 m; N = 5), and RD (red donors reared at 30 m; N = 7), (**b**) associated cultured pearls that can have different colours, PGDS (pearls from green donors reared at 4 m; N = 197), PGDD (pearls from green donors reared at 30 m; N = 166), PRD4 (pearls from red donors reared at 4 m; N = 143), and PPDD (pearls from red donors reared at 30 m; N = 163), and (**c**) associated cultured pearls that have the same colour hue as their donors, GPGS (green pearls from green donors reared at 4 m; N = 132), GPGD (green pearls from green donors reared at 30 m; N = 66), RPRS (red pearls from red donors reared at 4 m; N = 84), and RPRD (red pearls from red donors reared at 30 m; N = 118). Light green (or red) and dark green (or red) distributions correspond respectively to donor conditioning in subsurface (4 m depth) or depth culture (30 m depth), prior to graft operations.

When all cultured pearls were considered, samples from both green ($p < 0.001$) and red ($p = 0.014$) donors had a significant shift to higher values of V following the deeper conditioning (30 m) compared with sub-surface (4 m) (Fig. 4b).

When red pearls from grafts of red donors ($p < 0.005$) and green pearls from grafts of green donors ($p = 0.3682$) were considered separately, the distribution of V values shifted significantly to greater darkness with depth, but this difference was not significant for the green pearls (Fig. 4c). The differences between the depths were 5.07 times greater for the red phenotype considered alone. In terms of darkness, the inner shell colour became more grey, dull and drab at greater conditioning depth.

Discussion

Our R package, based on image analysis with HSV colour space and machine-learning approaches, validated the method used through the analysis of the influence of depth on the colour of two economically important pearl donor phenotypes: the green and the red inner shell phenotypes. Our results show that (i) the R package successfully categorized the pearl phenotypes used in this study, that (ii) cultivation environment of the donor oysters (here depth) heavily influences the brightness V and the saturation S of the colour, and (iii) that the colour variation related to depth was transmitted from donors to pearls. The *ImaginR* package is thus suitable for indicating colour variations in oysters and could now be used in other biological models of animal or plant origin. The package was deposited in CRAN under the name *ImaginR* V2.0 (https://cran.r-project.org/web/packages/ImaginR/index.html)[32].

We developed this tool in the form of an R package to reduce the subjectivity in quantifying and qualifying colour in the pearl oyster *P. margaritifera*. Marchais *et al.*[33] were the first to develop a new method based on digital colour analysis, using HSL colour space, to highlight the link between shell colour and algal pigments under experimental conditions. However, the HSL colour space has an unfortunate interaction between brightness and saturation during image processing[34]. Thus, for a maximum lightness value, with HSL, the saturation always gives white data, while this problem does not arise with HSV colour space[34], which gives values closer to human vision[35,36]. Trinkler *et al.*[37] already attempted to measure and quantify colour in juvenile *P. margaritifera* with an International Commission on illumination (ISI) chromaticity diagram, but did not find any differences of colour trend in the shells. We therefore decided to create our own R package adapted to our biological model (*P. margaritifera*), using HSV colour space. To our knowledge, there is no other free software with these characteristics.

Interestingly, we observed that the differences induced by depth in the red donor phenotype were higher overall than those in the green phenotype. This could provide some first clues on how colour is genetically controlled in *P. margaritifera*. Indeed, we could hypothesize that by being more "stable" in terms of colouration change, the green phenotype could be controlled by more genes than the red phenotype. Multifactorial genetic control of a trait is often synonymous with a continuous phenotype, in which variations might be more subtle[38,39]. This could mean that the molecular pathways leading to the expression of the colour of these two phenotypes differ. It would be interesting to work towards a better understanding of the molecular control of expression of the colour phenotypes of *P. margaritifera*, to see if our suppositions are correct.

The effects of depth on the colouration of marine animals have been little described so far, but there are nonetheless some reports[40–42]. Change in colour correlated with depth can be explained by many other environmental factors linked to depth, such as diet composition[40,43], temperature[44], light levels[42], or even pressure[45], which complicates its study. Southgate & Lucas[41] report absolutely no influence of hydrostatic pressure on *P. margaritifera*, but other environmental parameters associated with depth are known to have significant influences. Light decreases with depth and, according to Gervis and Sims[42], so does pearl quality and colour. Indeed, *Pinctada fucata martensii* (Gould, 1850) produces high quality pinkish pearls below 5 metres, but nacre deposition is maximized under blue light like that found in deeper water. Food intake can also influence nacre deposition. Indeed, according to Joubert *et al.*[43], when trophic levels are high (microalgal concentration), there is a decrease in aragonite tablet thickness, but a strong increase in the speed of nacreous deposit. However, Latchère *et al.*[46] demonstrated that food level had no effects on quality traits of *P. margaritifera* mineralization. It is also well known that water temperature strongly influences bivalve metabolism and physiological processes[47–49]. Indeed, temperature influences the relative expression of genes involved in biomineralization[43,46]. So there can me multiple environmental reasons for such changes. Furthermore, Rousseau & Rollion-Bard[45] found variation in the shape of nacre tablets as a function of depth, in relation to the shell growth direction. The shape of the tablets changed from hexagonal to rhomboid at a depth of 39 m. With this modification in shape, the tablets become larger, but also thinner, so that the new pigments laid down are more visible by transparency. According to these authors, the iridescent colours are affected by the thickness of the layers. Pigment concentration also depends on their final location in the shell layers[43,46]. The shell of the black-lipped pearl oyster has four layers, from exterior to interior: (i) the periostracum, (ii) the prismatic layer, (iii) the fibrous layer, and (iv) the nacreous layer[28,50]. These layers show progressive changes in their crystalline structure and associated organic matrix structure[28]. The precise location, kinds of pigments and the relative quantities of these pigments in each of these different layers are not yet well known.

Our results indicate that depth can change the expression of colour and it was already well known that the environment can influence the expression of biomineralizing genes[43,46]. We hypothesize that a thickness gradient of the aragonite layer could explain why colour pigmentation only appears at the top of the inner shell. Indeed, a dorso-ventral section of a valve of *P. margaritifera* shows that the nacreous layer is thinner closer to the ventral side than to the dorsal side[43] a phenomenon that would enable the pigments to be more visible here due to higher transparency in this part of the shell. As the aragonite tablets elongate faster with depth[45], this layer could therefore act to slightly darken the pigments at the top of the inner shell.

Donor oysters conditioned at 30 m depth were used as donors to produce pearls, as were counterparts conditioned at 4 m. Interestingly, the pearls produced and harvested 20 months after grafting displayed colour variations corresponding to those expressed by the donors. The maintenance of this phenotype expression by the donor tissues suggests epigenetic regulation of the colour intensity. Indeed, environmental changes can modify individual phenotypes[51,52] and such modifications can persist in a transplanted organ grafted into another individual[53,54]. So the graft has a memory, but we do not yet know how reversible this (memory of these modifications) is and over how much time. It would be interesting to study this level of regulation in the expression of colour in *P. margaritifera*.

Our results on the impact of depth on the colour of *P. margaritifera*, although they do not provide a description of the mechanisms, is of great importance for the Polynesian pearl industry that is still recovering from the 2008 crisis, when pearl price per gram plummeted. To ensure a sustainable future for the industry, there is a growing interest in producing fewer pearls, of better quality[23], particularly pearls of more contrasting colours. Indeed, pearls presenting a colour with high saturation and less darkness are of great value on most markets. However, in past years, spat collection has become increasingly unreliable, and problems such as vandalism (or theft of grafted and non-grafted oysters in marine concession areas) have increased. In addition, the increase in the length and number of exceptionally warm climatic conditions (lagoon surface waters over 30 °C) has forced producers to install their lines at 30 m depth to avoid theft, or mortality due to high temperatures. In the light of our findings this could be problematic if non-grafted oysters stocked at 30 meters were subsequently used as donors. Indeed, we showed that the inner shell colour and associated pearls from donors that had spent one month at 30 m depth were darker and duller than those from source-cultivated oysters, despite the fact that, during the post-graft culture period, the recipient oysters were cultured at 4 m depth for 20 months. It would be interesting to do other

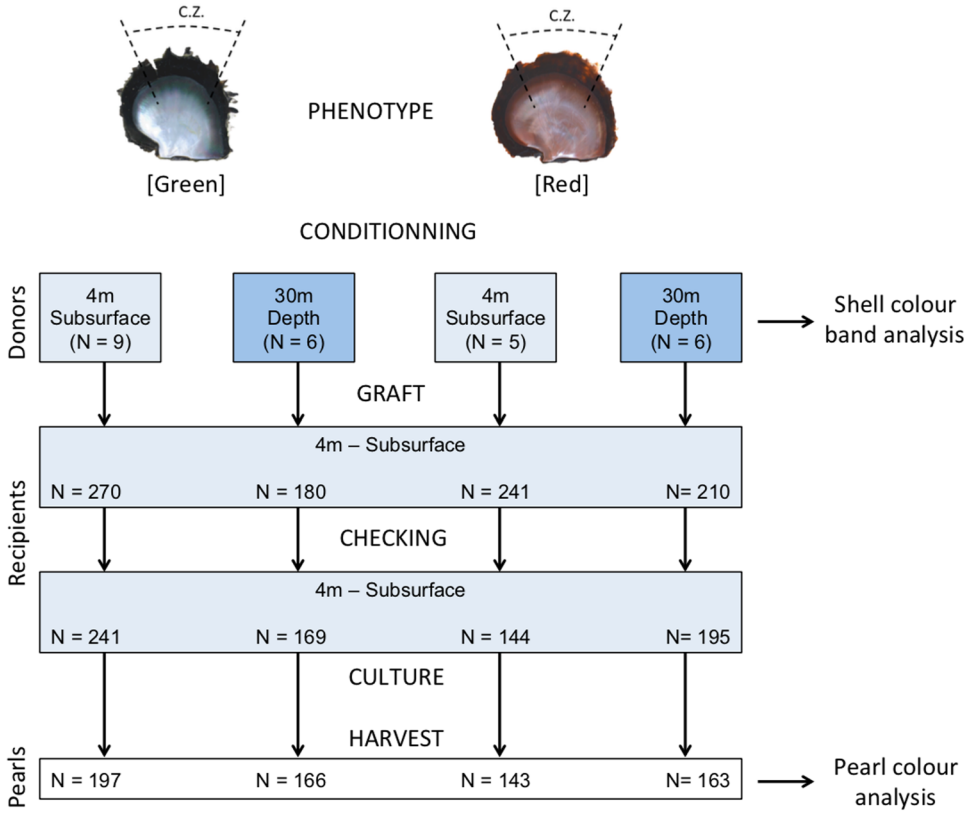

Figure 5. Experimental design of the experimental *Pinctada margaritifera* grafting procedure using two donor oyster phenotypes, green and red. Each phenotype was conditioned for one month prior to the graft operation, either in subsurface (4 m) or deep culture (30 m). The commercial zone (C.Z.), indicated by the dotted lines, is the section of the donor mantle from which grafts are usually cut. Thirty grafts were made from each donor. A check for nucleus retention was made 42 days post-graft and the pearls were harvested 20 months post-graft. Numbers in brackets correspond to the frequencies of donors, recipients or pearls.

similar experiments, but with more depths tested (e.g. 4 m, 10 m, 20 m and 30 m) in order to see the behaviour of colour expression variation at these different depths.

Our exploration of colour plasticity in response to an environmental difference was made with a new tool using HSV colour space. The emergence of this type of analysis could be useful not only for the pearl industry, but also in other domains and for other biological models. This method was not only able to confirm and characterize variation in the colouration of black-lipped pearl oysters but also the persistence of this phenotypic difference in pearls harvested 20 months after exposure.

Materials and Methods

An experimental graft was performed in 2013 with two colour phenotypes of *P. margaritifera* donors (red and green) reared at 4 and 30 m depth. Visually, colour differences were observed in both green and red donors between the two depth groups. These four groups were used as donors in an experimental graft. After harvesting, colour differences were again found visually in the different groups of pearls. We decided to analyse these variations using a suitable colour space in an automated manner.

Animal conditioning and experimental graft. Two *P. margaritifera* phenotypes, with either a green or a red inner shell, were selected as donors for an experimental graft (Fig. 5). The green individuals originated from Mangareva Island lagoon (Gambier archipelago, French Polynesia) and the red phenotype came from the Takaroa atoll (Tuamotu archipelago, French Polynesia). The red oysters were transferred by plane to Mangareva one month before grafting to allow acclimation. After a month, future donors of each phenotype were separated into two groups. One group was then reared at 4 m depth (N = 9 for green; N = 5 for red) and the other at 30 m depth (N = 6 for green; N = 7 for red) for one additional month in order to obtain a colour change (final donors). After the second month, the oysters were collected and used in the experimental graft operation. *P. margaritifera* of about two years were used to serve as recipients were collected as spat in the Mangareva Island lagoon (Gambier Archipelago, French Polynesia). Passive spat catching techniques were used with commercial collectors.

The experimental graft using these donors was performed in Regahiga Pearl Farm (Gambier archipelago, French Polynesia) in December 2013 (Fig. 5). For this graft, the mantle (the biomineralizing tissue) from donors selected for their colours (i.e. red and green) were cut into 30 small pieces known as "saibo". These pieces of

mantle were grafted into 30 recipient oysters together with a nucleus (nucleus weight: 0.2337 g; nucleus diameter: 0.56425 mm). Cells of the "saibo" (from the donor) produce nacre that builds up on the nucleus to form a pearl in the recipient oyster. Recipient and donor oysters measured approximately 12 cm in height from the bottom to the top of their shells. The shells of the donor oysters were kept for chromatic analysis.

All recipient oysters were individually labelled (with numbered colour coded plastic labels) so as to maintain traceability between donor identity, and corresponding harvested pearls. All the grafted recipient oysters were then cultured at 4 m depth. As is normal aquaculture practice, the oysters were regularly cleaned in order to remove biofouling (epibiota), which can hinder healthy oyster growth and pearl production. After 42 days, nucleus retention was checked. Finally, the pearls were harvested 20 months later and cleaned by ultrasonication in soapy water with a LEO 801 laboratory cleaner (2-L capacity, 80 W, 46 kHz). They were then rinsed with distilled water and assessed by chromatic analysis.

Choice of colour space. According to Vezhnevets *et al.*[35], when developing a project that uses colour as the main feature of interest, one usually faces three main issues: the choice of the relevant colour space for the project, the means to obtain and model a colour distribution for your biological model, and the choice of how to process the colour segmentation results in order to obtain a valid and reproducible characterization and quantification of the colour. To reduce the subjectivity of this trait, different colour spaces can be used[55,56] to shift from qualitative to quantitative data. Among colour space landscapes, the HSL space (Hue Saturation Lightness) is beginning to be used in the biological sciences because it can provide a solution by describing colour components separately[33]. HSV is a colour space similar to HSL and both are used as a convenient way to represent the colour variation. HSL and HSV are both conical geometries, with hue (H) describing the colour spectrum on a chromatic wheel. However, saturation (S) is calculated differently between these two spaces (with a possible conversion between the two values) and lightness (L) and value (V) (referred to here as "brightness" for clearer understanding) represent different aspects of colour. Fairchild[36] describes brightness (V) as the perception of the amount of light, and the lightness (L) as the perception of the amount of white. V and L are both given in percentages or in [0–1] format. The intuitiveness of this two-colour space and the explicit discrimination between S and L or S and V properties have made these approaches popular in studies on colour segmentation[35]. However, these colour spaces are not perfect. The HSL space, for instance, has an unfortunate interaction between brightness and saturation during image processing. Indeed, for a maximum lightness value, the saturation always gives white data, while this problem does not appear with HSV colour space, which gives a value closer to human vision[34]. We therefore chose the HSV space to analyse shell and pearl chromatic variations resulting from environmental pressure.

Chromatic analysis of shells and pearls. The shells of the donor oysters and harvested pearls were cleaned, conserved and protected from light. The pearls were put in boxes that classified them by their donor oysters. Both the donors and the boxed pearls were photographed with a Canon® PowerShot G9, with a maximal resolution of 12.1 megapixels and using the same parameters for each picture. Images were taken into a Packshot Creator™ (v. 3.0.3.8) to prevent dark shadows and light reflection. The pictures of the donor's inner shells were clipped to extract the peripheral coloured zone, which was pasted onto a white background. Similarly, the backgrounds of the pearl pictures were clipped to retain only the coloured sphere and these were pasted onto a white background. We selected one side of each pearl (at random) to be photographed and used this to represent the colour of the pearl. To select the colour area, the free GNU Image Manipulation Program (version 2.8.22) was used (selection with lasso, copy, paste like image, export as.jpeg). R software v 3.2.3 (R foundation for Statistical Computing) was used to develop and run an image analysis package, which we named ImaginR. For the remainder of the analysis, the working directory is set and the folder containing all the pictures is placed inside it. After loading the *ImaginR* (V2) package, the only function needed to run the analysis is called OutPutResult(). Simply by typing OutPutResult(), R will then recognize the picture folder and automatically perform the analysis. *ImaginR* will import all pictures with the.jpeg extension and list the file names into an R object. Thus, the picture's name (which corresponds to one sample) is stocked into this object. The analysis will therefore be made on a picture-by-picture basis. The picture is imported through the load.image() function of the *ImaginR* package[57]. Then, each pixel is given an RGB (Red Green Blue channels) coding, which will be converted into hex triplet code (all conversions are realized with the *grDevices* package[58]) and compared to a white hex triplet database. The white hex triplet values of the pictures are thus deleted in order to remove any information derived from the background of the picture. The remaining pixels are converted back into an RGB matrix, and an average is calculated for each channel (R, G and B). The average colour of the chromatic zone of each sample is then obtained. The hex triplet code is also calculated from this average. The average RGB is converted into HSV code with the rgb2hsv() function from the *grDevices* package. Thus, for each image, the hue (H), saturation (S) and brightness (V) provide a synthesis of the colour status. The hue variable is compared to a reference hue range that delimits colours to classify the sample into a known phenotype. The reference hue range was delimited with a machine learning procedure using pictures of individuals with the coloured peripheral zones of the two valves extracted as described above. These *ImaginR* database individuals were obtained from a colour breeding selection programme at SCA Regahiga Pearls (Mangareva island, Gambier archipelago, French Polynesia). Approximately 200 individuals of each colour phenotype with a size between 10 and 12 cm were produced. Among these, five individuals per colour phenotype group were selected for their particularly colourful phenotypes and according to colour characteristics sought by pearl farmers. These five individuals per phenotype were then used for the machine learning in order to delimit the phenotype by hue. Following this approach, the hue range for the red phenotype ranged from 0 to 0.1625770; and the hue range for the green phenotype ranged from 0.3215928 to 0.5637775. Finally, the *ImaginR* package provided the hue (H), saturation (S), brightness (V), average hex triplet code and interpreted colour phenotype of each sample ("green", "red" or "other") based on the machine learning of that hue. In the procedure, this task is looped over all the samples/pictures in the folder, and the package produces a final tabular file summarizing all the information detailed above, along with the name of the sample. The text file is

saved in. csv format. For subsequent statistical analysis, the grouping of the harvested pearl dataset was made in two ways: (i) all the pearls were grouped according to the colour of the donor colour inner shell phenotype characterized in *ImaginR* (since the trait is only partially genetically inherited, pearls with different colour phenotypes were pooled into the same category); (ii) only the green pearls from green donors and red pearls from red donors were analysed.

Statistical analysis. For the experimental study, we performed several pairwise comparisons to answer two main biological questions: (i) For each colour phenotype, is there a significant difference between the colour of the shells of the donor oysters cultivated at 4 m versus 30 m depth? and (ii) For each phenotype, is there a colour difference between the pearls coming from donors cultivated at 4 m, versus 30 m? A Shapiro test (*stats v3.5.0* R package) was used to check the normal distribution of the data. To test for the presence of a difference in the brightness and saturation between groups, we used a Wilcoxon test (*stats v3.5.0* R package based on Hollander and Wolfe[59] and Patrick Royston[60]) and a confidence interval based on Bauer[61]. Chi^2 tests were performed (*stats v3.5.0* R package) on the number of green (or red) pearls obtained from green (or red) oyster donors by donor rearing depth divided by the total number of pearls by rearing depth so as to see which colour phenotype had produced the most pearls of the same colour.

Data Availability

The authors declare that all data are available.

References

1. Williams, S. T. Molluscan shell colour. *Biol. Rev*., https://doi.org/10.1111/brv.12268 (2016).
2. Bradshaw, A. D. Evolutionary significance of phenotypic plasticity in plants. *Advances in genetics* **13** (Elsevier, 1965).
3. Moore, H. B. The Biology of *Purpura Lapillus*. I. Shell Variation in Relation to Environment. *J. Mar. Biol. Assoc. United Kingdom* **21**, 61–89 (1936).
4. Manríquez, P. H., Lagos, N. A., Jara, M. E. & Castilla, J. C. Adaptive shell color plasticity during the early ontogeny of an intertidal keystone snail. *PNAS* **106**, 16298–16303 (2009).
5. Kawaii, K. Shell-color polymorphism of intertidal gastropods in Chuuk State, Federated States of Micronesia. *Occas. Pap*. 19–22, at http://hdl.handle.net/10232/17204 (2013).
6. Ding, J. *et al*. Transcriptome sequencing and characterization of Japanese scallop Patinopecten yessoensis from different shell color lines. *PLoS One* **10**, 1–18 (2015).
7. Ramirez Boehme, J. New Chilean species of Lucapina, Fissurella and Collisella (Molusca: Archaeogastropoda). *Boletin-Museo Nac. Hist. Nat*., at http://agris.fao.org/agris-search/search.do?recordID=XL7610034 (1974).
8. Espoz, C., Guzman, G. & Castilla, J. C. The lichen *Thelidium litorale* on shells of intertidal limpets: a case of lichen-mediated cryptic mimicry. *Mar. Ecol. Prog. Ser.* **119**, 191–197 (1995).
9. Williams, S. T. *et al*. Colorful seashells: Identification of haem pathway genes associated with the synthesis of porphyrin shell color in marine snails. *Ecol. Evol.* **7**, 10379–10397 (2017).
10. Cuthill, I. C. *et al*. The biology of color. *Science (80-.)*. **357** (2017).
11. Ge, J., Li, Q., Yu, H. & Kong, L. Mendelian inheritance of golden shell color in the Pacific oyster Crassostrea gigas. *Aquaculture* **441**, 21–24 (2015).
12. Feng, D., Li, Q., Yu, H., Zhao, X. & Kong, L. Comparative transcriptome analysis of the pacific oyster Crassostrea gigas characterized by shell colors: Identification of genetic bases potentially involved in pigmentation. *PLoS One* **10**, 1–17 (2015).
13. Feng, D., Li, Q., Yu, H., Kong, L. & Du, S. Transcriptional profiling of long non-coding RNAs in mantle of *Crassostrea gigas* and their association with shell pigmentation. *Sci. Rep.* **8**, 1–10 (2018).
14. Chang, Y. Q. *et al*. Genetic diversity in five scallop populations of the Japanese scallop (Patinopecten yessoensis). *Acta Ecol. Sin.* **27**, 1145–1152 (2007).
15. Evans, B. S., Knauer, J., Taylor, J. J. U. & Jerry, D. R. Development and characterization of six new microsatellite markers for the silver- or gold-lipped pearl oyster, Pinctada maxima (Pteriidae). *Mol. Ecol. Notes* **6**, 835–837 (2006).
16. Ky, C.-L., Lau, C., Koua, M. S. & Lo, C. Growth Performance Comparison of *Pinctada margaritifera* Juveniles Produced by Thermal Shock or Gonad Scarification Spawning Procedures. *J. Shellfish Res.* **34**, 811–817 (2015).
17. Blay, C. *et al*. Influence of nacre deposition rate on cultured pearl grade and colour in the black-lipped pearl oyster *Pinctada margaritifera* using farmed donor families. *Aquac. Int.* **22**, 937–953 (2014).
18. Ky, C.-L. *et al*. Is pearl colour produced from *Pinctada margaritifera* predictable through shell phenotypes and rearing environments selections? *Aquac. Res.* **48**, 1041–1057 (2017).
19. Ky, C.-L., Demmer, J., Blay, C. & Lo, C. Age-dependence of cultured pearl grade and colour in the black-lipped pearl oyster *Pinctada margaritifera*. *Aquac. Res*. 1–14, https://doi.org/10.1111/are.12938 (2015).
20. Ky, C.-L. *et al*. Family effect on cultured pearl quality in black-lipped pearl oyster *Pinctada margaritifera* and insights for genetic improvement. *Aquat. Living Resour.* **26**, 133–145 (2013).
21. Ky, C.-L., Lo, C. & Planes, S. Mono- and polychromatic inner shell phenotype diversity in *Pinctada margaritifera* donor pearl oysters and its relation with cultured pearl colour. *Aquaculture* **468**, 199–205 (2017).
22. Ky, C.-L., Sham Koua, M. & Le Moullac, G. Impact of spat shell colour selection in hatchery-produced *Pinctada margaritifera* on cultured pearl colour. *Aquac. Reports* **9**, 62–67 (2018).
23. Ky, C.-L., Nakasai, S., Molinari, N. & Devaux, D. Influence of grafter skill and season on cultured pearl shape, circles and rejects in *Pinctada margaritifera* aquaculture in Mangareva lagoon. *Aquaculture* **435**, 361–370 (2014).
24. Haws, M. *The basic methods of pearl farming: a layman's manual*, at http://nsgl.gso.uri.edu/hawau/hawauh02001.pdf (Center for Tropical and Subtropical Aquaculture, 2002).
25. Ky, C.-L., Nakasai, S., Pommier, S., Sham Koua, M. & Devaux, D. The Mendelian inheritance of rare flesh and shell colour variants in the black-lipped pearl oyster (*Pinctada margaritifera*). *Anim. Genet.* **47**, 610–614 (2016).
26. Ky, C.-L., Quillien, V., Broustal, F., Soyez, C. & Devaux, D. Phenome of pearl quality traits in the mollusc transplant model *Pinctada margaritifera*. *Sci. Rep*. 1–11, https://doi.org/10.1038/s41598-018-20564-1 (2018).
27. Cuif, J.-P. *et al*. Evidence of a Biological Control over Origin, Growth and End of the Calcite Prisms in the Shells of *Pinctada margaritifera* (Pelecypod, Pterioidea). *Minerals* **4**, 815–834 (2014).
28. Dauphin, Y. *et al*. Structure and composition of the nacre-prisms transition in the shell of *Pinctada margaritifera* (Mollusca, Bivalvia). *Anal. Bioanal. Chem.* **390**, 1659–1669 (2008).
29. Marie, B., Joubert, C., Tayalé, A. & Zanella-cléon, I. Different secretory repertoires control the biomineralization processes of prism and nacre deposition of the pearl oyster shell. *Proc. Natl. Acad. Sci. USA* **109**, 20986–20991 (2013).
30. Snow, M. R., Pring, A., Self, P., Losic, D. & Shapter, J. The origin of the color of pearls in iridescence from nano-composite structures of the nacre. *Am. Mineral.* **89**, 1353–1358 (2004).

31. Kuriki, I. *et al*. The modern Japanese color lexicon. *J. Vis.* **17**, 1 (2017).
32. Stenger, P.-L. Package ImaginR, at https://cran.r-project.org/web/packages/ImaginR/ImaginR.pdf (2017).
33. Marchais, V. *et al*. New tool to elucidate the diet of the ormer *Haliotis tuberculata* (L.): Digital shell color analysis. *Mar. Biol.* **164** (2017).
34. Poynton, C. A. *Frequently asked questions about colour*, at http://poynton.ca/PDFs/ColorFAQ.pdf (1995).
35. Vezhnevets, V., Sazonov, V. & Andreeva, A. A Survey on Pixel-Based Skin Color Detection Techniques. *Proc. Graph. 2003* **85**, 85–92 (2003).
36. Fairchild, M. D. *Color appearance models* (John Wiley & Sons, 2013).
37. Trinkler, N., Le Moullac, G., Cuif, J.-P., Cochennec-Laureau, N. & Dauphin, Y. Colour or no colour in the juvenile shell of the black lip pearl oyster, *Pinctada margaritifera*? *Aquat. Living Resour.* **25**, 83–91 (2012).
38. Boyle, C. R. & Elston, R. C. Multifactorial genetic models for quantitative traits in humans. *Biometrics* 55–68 (1979).
39. Bonney, G. E. On the statistical determination of major gene mechanisms in continuous human traits: Regressive models. *Am. J. Med. Genet.* **18**, 731–749 (1984).
40. Chandrapavan, A., Gardner, C., Linnane, A. & Hobday, D. Colour variation in the southern rock lobster *Jasus edwardsii* and its economic impact on the commercial industry. *New Zeal. J. Mar. Freshw. Res.* **43**, 537–545 (2009).
41. Southgate, P. & Lucas, J. *The pearl oyster* (Elsevier, 2011).
42. Gervis, M. H. & Sims, N. A. *The biology and culture of pearl oysters (Bivalvia pteriidae)*. **21** (WorldFish, 1992).
43. Joubert, C. *et al*. Temperature and food influence shell growth and mantle gene expression of shell matrix proteins in the pearl oyster *Pinctada margaritifera*. *PLoS One* **9**, 1–9 (2014).
44. Pouvreau, S. Etude et modélisation des mécanismes impliqués dans la croissance de l'huître perlière, *Pinctada margaritifera*, au sein de l'écosystème conchylicole du lagon de l'atoll de Takapoto (Polynésie Française) (1999).
45. Rousseau, M. & Rollion-Bard, C. Influence of the Depth on the Shape and Thickness of Nacre Tablets of *Pinctada margaritifera* Pearl Oyster, and on Oxygen Isotopic Composition. *Minerals* **2**, 55–64 (2012).
46. Latchere, O. *et al*. Influence of preoperative food and temperature conditions on pearl biogenesis in *Pinctada margaritifera*. *Aquaculture* **479**, 176–187 (2017).
47. Brown, J. R. & Hartwick, E. B. Influences of temperature, salinity and available food upon suspended culture of the Pacific oyster, *Crassostrea gigas*. I. Absolute and allometric growth. *Aquaculture* **70**, 231–251 (1988).
48. Kanazawa, T. & Sato, S. Environmental and physiological controls on shell microgrowth pattern of *Ruditapes philippinarum* (Bivalvia: Veneridae) from Japan. *J. Molluscan Stud.* **74**, 89–95 (2008).
49. Thébault, J., Thouzeau, G., Chauvaud, L., Cantillánez, M. & Avendaño, M. Growth of *Argopecten purpuratus* (Mollusca: Bivalvia) on a natural bank in Northern Chile: sclerochronological record and environmental controls. *Aquat. Living Resour.* **21**, 45–55 (2008).
50. Farre, B. *et al*. Shell layers of the black-lip pearl oyster *Pinctada margaritifera*: Matching microstructure and composition. *Comp. Biochem. Physiol. - B Biochem. Mol. Biol.* **159**, 131–139 (2011).
51. Jaenisch, R. & Bird, A. Epigenetic regulation of gene expression: How the genome integrates intrinsic and environmental signals. *Nat. Genet.* **33**, 245–254 (2003).
52. Feil, R. & Fraga, M. F. Epigenetics and the environment: Emerging patterns and implications. *Nat. Rev. Genet.* **13**, 97–109 (2012).
53. Hagmann, C. A., Schildberg, F. A. & Tolba, R. H. Epigenetics and transplantation: clinical applications of chromatin regulation. *Discov. Med.* **10**, 511–520 (2010).
54. McCaughan, J. A., McKnight, A. J., Courtney, A. E. & Maxwell, A. P. Epigenetics: Time to translate into transplantation. *Transplantation* **94**, 1–7 (2012).
55. Clydesdale, F. M. & Ahmed, E. M. Colorimetry — methodology and applications. *Crit. Rev. Food Sci. Nutr.* **10**, 243–301 (2009).
56. Hunter, R. S. & Harold, R. W. *The measurement of appearance* (John Wiley & Sons, 1987).
57. Simon, A., Tschumperle, D. & Wijffels, J. Package imager. 1–126, at https://cran.r-project.org/web/packages/imager/imager.pdf (2018).
58. R Core Team. grDevices package, at http://www.r-project.org/ (2013).
59. Hollander, M., A Wolfe, D. & Chicken, E. The one-way layout. *Nonparametric Stat. Methods*, Third Ed. 202–288 (1973).
60. Royston, P. Remark AS R94: A remark on algorithm AS 181: The W-test for normality. *J. R. Stat. Soc. Ser. C (Applied Stat.* **44**, 547–551 (1995).
61. Bauer, D. F. Constructing confidence sets using rank statistics. *J. Am. Stat. Assoc.* **67**, 687–690 (1972).

Acknowledgements

This study was supported by grants from the "Direction des Ressources Marines", through the AmeliGEN project (2016–2019). The authors would especially like to thank the team of the host site, SCA Regahiga Pearls (Mangareva island, Gambier archipelago, French Polynesia) for their generous support.

Author Contributions

C.L.K. conceived, designed and conducted the graft experiments. P.L.S. analysed the data, wrote the R package and drafted the manuscript. J.V.D., C.R. and S.P. corrected the main manuscript text. All authors read and approved the final manuscript.

Additional Information

Competing Interests: The authors declare no competing interests.

Publisher's note: Springer Nature remains neutral with regard to jurisdictional claims in published maps and institutional affiliations.

ANNEXE 12

genes

MDPI

Article

Molecular Pathways and Pigments Underlying the Colors of the Pearl Oyster *Pinctada margaritifera* var. *cumingii* (Linnaeus 1758)

Pierre-Louis Stenger [1,2], Chin-Long Ky [1,2], Céline Reisser [1,3], Julien Duboisset [4], Hamadou Dicko [4], Patrick Durand [5], Laure Quintric [5], Serge Planes [6] and Jeremie Vidal-Dupiol [1,2,*]

1 IFREMER, UMR 241 Écosystèmes Insulaires Océaniens, Labex Corail, Centre Ifremer du Pacifique, BP 49, 98725 Tahiti, France; Pierrelouis.stenger@gmail.com (P.-L.S.); chinky@ifremer.fr (C.-L.K.); Celine.Reisser@ifremer.fr (C.R.)
2 IHPE, Univ Montpellier, CNRS, IFREMER, Univ Perpignan Via Domitia, Montpellier, France
3 MARBEC, Univ Montpellier, CNRS, IFREMER, IRD, Montpellier, France
4 Aix Marseille Univ, CNRS, Centrale Marseille, Institut Fresnel, Marseille, France; julien.duboisset@fresnel.fr (J.D.); hamadou.dicko@fresnel.fr (H.D.)
5 Service de Bioinformatique, Département IRSI, IFREMER, ZI de la Pointe du Diable, 29280 Plouzané, France; Patrick.Guido.Durand@ifremer.fr (P.D.); Laure.Quintric@ifremer.fr (L.Q.)
6 EPHE-UPVD-CNRS, USR 3278 CRIOBE, Labex Corail, PSL Research University, Université de Perpignan, Perpignan, France; planes@univ-perp.fr
* Correspondence: jeremie.vidal.dupiol@ifremer.fr

Abstract: The shell color of the Mollusca has attracted naturalists and collectors for hundreds of years, while the molecular pathways regulating pigment production and the pigments themselves remain poorly described. In this study, our aim was to identify the main pigments and their molecular pathways in the pearl oyster *Pinctada margaritifera*—the species displaying the broadest range of colors. Three inner shell colors were investigated—red, yellow, and green. To maximize phenotypic homogeneity, a controlled population approach combined with common garden conditioning was used. Comparative analysis of transcriptomes (RNA-seq) of *P. margaritifera* with different shell colors revealed the central role of the heme pathway, which is involved in the production of red (uroporphyrin and derivates), yellow (bilirubin), and green (biliverdin and cobalamin forms) pigments. In addition, the Raper–Mason, and purine metabolism pathways were shown to produce yellow pigments (pheomelanin and xanthine) and the black pigment eumelanin. The presence of these pigments in pigmented shell was validated by Raman spectroscopy. This method also highlighted that all the identified pathways and pigments are expressed ubiquitously and that the dominant color of the shell is due to the preferential expression of one pathway compared with another. These pathways could likely be extrapolated to many other organisms presenting broad chromatic variation.

Keywords: *Pinctada margaritifera*; color; pigment; transcriptomics; Raman spectroscopy

Citation: Stenger, P.-L.; Ky, C.-L.; Reisser, C.; Duboisset, J.; Dicko, H.; Durand, P.; Quintric, L.; Planes, S.; Vidal-Dupiol, J. Molecular Pathways and Pigments Underlying the Colors of the Pearl Oyster *Pinctada margaritifera* var. *cumingii* (Linnaeus 1758). *Genes* **2021**, *12*, 421. https://doi.org/10.3390/genes12030421

Academic Editor: Antonio Figueras

Received: 5 February 2021
Accepted: 5 March 2021
Published: 15 March 2021

1. Introduction

Color is a well-known trait involved in many biological interactions in nature, but the eye-catching color range of some gem-producing Mollusca such as pearl oysters and abalones has also attracted human interest. Mollusca is the largest marine phylum when considering the number of species [1]. Most of these animals have a shell displaying incredible colors and patterns of pigmentation. However, much remains to be discovered about the nature of these pigments and the molecular pathways that produce these colors [2]. Such knowledge could have widespread implications from evolutionary biology to economics [2,3].

Shell color can have a broad range of origins, ranging from a pure genetic basis to a pure environmental one [4–6]. Abalones are a textbook illustration of such a panel of

drivers. In *Haliotis discus hannai* (Ino, 1953), the bluish and greenish colors are determined genetically by the combination between a recessive and a dominant allele [4]. However, in *Haliotis rufescens* (Swainson, 1822), diet determines the color expressed [6,7]—the reddish coloration is due to the uptake of red algae [8]. The phycoerythrin pigment contained in red algae is metabolized (tetrapyrrole synthesis in plants pathway) by the abalone into the red bile pigment rufescine [9]. Carotenoid pigments (astaxanthin, β-carotene, and cantaxanthin) are also known to contribute to this coloration, although the drivers controlling the expression of these additional pigments are unknown [6]. The mechanisms behind the characteristic reddish color of *H. rufescens* are therefore convoluted, highlighting the complexity of identifying both the pigments involved and the pathways by which they are produced.

To address this challenge, analytical chemistry [10–12] and transcriptomic analyses [13–16] can offer complementary approaches to identify pigments and pigment-producing pathways. Lemer et al., 2015 [17] performed a comparative transcriptomic analysis of black and albino pearl oysters *P. margaritifera* (Linnaeus, 1758) and identified putative pigmentation-related genes (*shem 4*, *mp8*, *krmp*, *chit*, and *serp*) involved in the synthesis of black eumelanin, the dominant color in this species. Analytical chemistry techniques were used to study the pigments responsible for its broad range of color. Chromatography and spectroscopic analyses revealed the important role of porphyrins (a group of heterocyclic macrocycle organic compounds) in the pigmentation of several species of the *Pinctada* genus. Uroporphyrin, which can lead to red or purple coloration [10,12], was present in black cultured pearls, as well as in the nacre (inner shell) and the prismatic layer (outer shell) of *P. margaritifera* [18]. Its presence was also confirmed more recently using Raman spectroscopy [19]. The use of Ultraviolet Visible (UV-Vis) spectrophotometry and physicochemical approaches has indicated that red, yellow, brown, and black coloration of *P. margaritifera* may result from an "unusual" melanin [20], or from a combination of eumelanin and pheomelanin [21]. While these results are essential starting points in understanding shell coloration, the joint identification of pigments and molecular pathways involved in the production of color is now necessary in order to improve our understanding of these complex mechanisms and provide innovative tools for commercial pearl production.

In this study, our aim was to identify the main pigments and pigment-producing pathways likely responsible for three economically major inner shell colors in *P. margaritifera*: red [22], yellow [22], and green [23] (Figure 1). Color-specific populations were farmed and reared in a common garden to limit confounding environmental effects. Their transcriptomes were compared by an RNA-seq approach to reveal differential gene expression among different pigment-producing pathways. The presence of the hypothetic pigments we identified from this transcriptomic approach was tested using Raman spectroscopy on the shells, which permits a direct and specific chemical characterization method. The joint use of these two methods led us to confidently identify both the pigments and the pathways underlying pearl oyster inner shell color phenotypes.

Figure 1. Different colors of *P. margaritifera* inner shell: (**A**): red, (**B**): yellow, (**C**): green, (**D**): albino, (**E**): black.

2. Materials and Methods

2.1. Biological Material

To obtain homogeneous phenotypes with red, green, and yellow shells, three multi-parental reproduction (10 males and 10 females each) were made at the Regahiga Pearl farm (23°06′56.6″ S 134°59′08.4″ W, Mangareva island, Gambier archipelago, French Polynesia) following a previously described procedure [24,25]. After two years of growth (corresponding to the stage of maximum pigmentation expression [22]), 200 individuals of each population (with a dorsal to ventral shell measurement between 10 and 12 cm) were selected for their color and transferred to Ifremer's experimental concession (Tahiti island, Society archipelago, French Polynesia: concession No. 8120/MLD: 17°48′39.0″ S 149°18′03.8″ W) following regulations of the Ministry of Marine Resources of French Polynesia (transfer authorization No. 3605). To reduce transcriptomic variability linked to environmental influences, all 600 individuals were maintained in a common garden (i.e., in the same area) for two months (October–November 2016, optimal growth season [26,27]). Finally, four individuals of each population displaying the strongest inner shell color were selected and immediately dissected. A piece of mantle corresponding to the part use for grafting was sampled as previously described [28] and stored in RNAlater™ (4 °C for 24 h then −80 °C).

2.2. RNA Extraction, Purification, and Sequencing

Mantle tissue samples were individually ground in liquid nitrogen in a Retsh® MM400 grinder (grinding speed = 30 oscillations/sec for 20 s) (Retsh, Haan, Germany). RNA extraction was performed using TRIZOL® Reagent (Life Technologies™, Carlsbad, CA, USA) according to the manufacturer's recommendations. After RNA precipitation, the pellets were suspended in RNA secure reagent® (ThermoFisher Scientific, Waltham, MA, USA) and heated to 65 °C for 10 min to inactivate the RNase. DNA contamination was removed with the DNA-free kit (Ambion® RNA Life Technologies™, Carlsbad, CA, USA) according to the manufacturer's instructions. Finally, RNAs were cleaned with the PureLink™ RNA Mini Kit (Ambion® RNA Life Technologies™™, Carlsbad, CA, USA) according to the manufacturer's protocol. RNA quality and quantity were verified with a NanoDrop 1000© and an Agilent 2100 Bioanalyzer® (Agilent Technologies™, Santa Clara, CA, USA). RNA sequencing libraries were produced using the Truseq3 kit. Sequencing was performed on an Illumina® HiSeq® 4000 (Illumina, San Diego, CA, USA), with 100 bp stranded paired-end

reads. Library construction and sequencing were done by Génome Québec (Montreal, Québec, QC, Canada) (MPS Canada).

2.3. Bioinformatics Analysis

Analyses were performed at the ABIMS Roscoff Galaxy facility (galaxy3.sb-roscoff.fr; accessed on 22 January 2019). Raw data are available through the NCBI Sequence Read Archive (SRA, BioProject PRJNA521849, BioSample SUB5166470). Read quality was assessed using the FastQC program (V0.11.5) (www.bioinformatics.babraham.ac.uk/projects/fastqc; accessed on 22 January 2019). Raw reads were filtered with Trimmomatic V0.36.4 [29] to remove Illumina adapters (for Truseq3) and reads with an average Q-value below 26 for 95% of their length. To characterize and quantify the transcriptome of each sample, the filtered reads were paired-mapped against a *P. margaritifera* draft genome [30] with TopHat (V1.4.0). Cufflinks (V2.2.1.0) and Cuffmerge (V2.2.1.0) were used to assemble and merge the transcriptome produced for each library, respectively [31]. HTSeq-count (V0.6.1) [32] was used to obtain read count per transcript. All codes and parameters used for bioinformatics analysis are given in Supplementary Materials Table S1.

2.4. Transcriptome Functional Annotation

The transcriptome produced was annotated by sequence comparison against worldwide databases. First, an initial annotation with PLASTX [33] was made against NR data base (*e*-value at 1×10^{-3}) [34] and Uniprot-Swissprot (*e*-value at 1×10^{-3}) [35]. A protein domain search was then performed with InterProscan [36]. Finally, Gene Ontology terms were assigned with Blast2GO [37]. Scripts are provided in Supplementary Materials Table S1.

2.5. Differential Molecular Function and Gene Expression

To analyze our data, we followed a two-step strategy. The first step was transcriptome-wide, considering the entire transcriptome for each color, and using RBGOA tool [38] to identify significantly over-, or under-represented molecular function. To weigh the analysis, the -Log(*p*-value) method was used to take into account the strength and significance of the regulation of each gene of the transcriptome (https://github.com/z0on/GO_MWU; accessed on 22 January 2019). The second step of the strategy was more targeted and aimed to identify candidate genes directly from significantly Differentially Expressed Genes (DEGs). For each approach, we performed the same pairwise comparisons (red vs. yellow, red vs. green, and yellow vs. green) using the DESeq2 R package (v. 3.7) [39]. The three color phenotypes were used at the same factor level (green individuals compared against yellow individuals compared against red individuals). The collective gene expression differences between phenotypes were examined with a Principal Component Analysis (PCA) from the tool set of the *DESeq2* R package (v. 3.7) [39]. Gene expression differences between color phenotypes obtained with DEseq2, were considered significant below the 5% level (adjusted *p*-value (Padj) for multiple testing with the Benjamini-Hochberg procedure FDR < 0.05). The online version of KAAS (http://www.genome.jp/tools/kaas/; accessed on 23 June 2018) was used to find the functional pathways in which significant DEGs were involved [40]. Pathview (https://bioconductor.org/packages/release/bioc/html/pathview.html; accessed on 27 July 2018) was used to link differential expression with the KEGG Automatic Annotation Server (KAAS) pathways.

2.6. Enzymatic Structure Analysis by Homology Modeling

Three-dimensional homology modeling of the protein structures (longest ORF) was performed on the PDB (Protein Data Bank) file obtained with I-TASSER (https://zhanglab.ccmb.med.umich.edu/I-TASSER/; accessed on 30 March 2019) for the four PBGD sequences found in the DEGs analysis (named PBGD_1 to PBGD_D). The secondary structures are results from the I-TASSER analysis. Modeling was done with UCSF Chimera software [41]. Hinge residues were determined with the HingProt server link in Song et al. 2009 [42]. Superimposition of our candidate proteins on a reference protein with

a known structure was performed in SuperPose [43] (Version 1, http://wishart.biology.ualberta.ca/SuperPose/; accessed on 2 July 2019). Only the longest PBGD (A) is shown. Detailed parameters are given in Supplementary Materials Table S2.

2.7. Raman Spectroscopy

Three individuals from the red, the yellow, and the green population were studied. Additionally, three black and three albino individuals were also studied and used as control. Raman spectra were acquired using a Raman spectrometer in reflection mode (LabRAM Evolution spectrometer, Horiba, Kyoto, Tokyo) with a 10× air objective (NA 0.4, Carl Zeiss, Oberkochen, Germany). The laser (632.8 nm) was focused on the colored border of the inner shell. The power delivered at the sample level was 1 mW on average. Three spectral windows, from 300 cm^{-1} to 1800 cm^{-1} (380–880 mm; 880–1380 mm; 1380–1880 mm), were recorded using an array of 1200 lines/mm. The acquisition time for each window was three hours.

2.8. Raman Spectra Analysis

Vibrational spectra of pearl oyster shell molecules were produced and analyzed by principal component analysis following the techniques described in Bonnier and Byrne, 2012 [44] directly on raw spectra. Then, subtraction of the baseline and a lightweight smoothing (5 points) were added to the raw spectra data. To improve data accuracy, spectra from each of the three windows were mathematically calibrated against referential inorganic components found in molluscan shell. Thus, calcite at 703 cm^{-1} was used for the 380–880 mm window [19], aragonite at 1085 cm^{-1} was used for the 880–1380 window [19], and carbonate at 1547 cm^{-1} was used for the 1380–1880 window [45]. The stat_peaks function from the *ggspectra* [46] R package (V. 0.3.5) was used to identify the exact peak position from the raw data to perform these calibrations. A manual verification was then made.

In order to associate peaks with pigments, all peaks from all spectra were extracted with the stat_peaks function from the *ggspectra* [46] R package (V. 0.3.5) and compared with a homemade bibliographic database (897 peaks obtained from 36 marine molluscan pigments extracted from 65 species in 32 studies, see Supplementary Materials Table S3). Since biological materials are known to produce noisy spectra, three different methods were used to compare peaks between the different shells analyzed [19,44,47]. First, a visual screening was operated to identify peaks matching or not expected signals. They were classified as: (*i*) *clear peak*, (*ii*) *putative peak*, and (*iii*) *no* peak. Second, the intensity of each selected peak was measured (the value of the lowest point of the peak minus the value of the peak). Third, a ratio was calculated between the intensity of the selected peak (calculated as previously described) and the peak of the referential calcite for each spectrum.

3. Results

3.1. Sequencing Results

Based on Illumina sequencing and after cleaning, 61,663,289 (±2,597,015; n = 4), 60,153,015 (±1,598,914; n = 4), and 68,500,895 (±2,535,550; n = 4) sequence reads were kept from red, yellow, and green individuals, respectively. Filtered reads mapped with similar rates of 84.01% (±0.95%), 84.2% (±0.69%), and 82.04% (±2.39%) for red, yellow and green individuals, respectively. These data are provided for each individual in Supplementary Materials Table S4. Transcriptome annotation is given in Supplementary Materials Table S5.

3.2. Transcriptome-Wide Functional Analysis

PCA based on gene expression profiles of the 12 sequenced transcriptomes (4 individuals per color) shows that individuals are randomly distributed across the graph rather than clustered according to their color, suggesting that if transcriptomic regulation supports color phenotypes, it only involves a few genes and/or subtle differences in regulation (Figure 2).

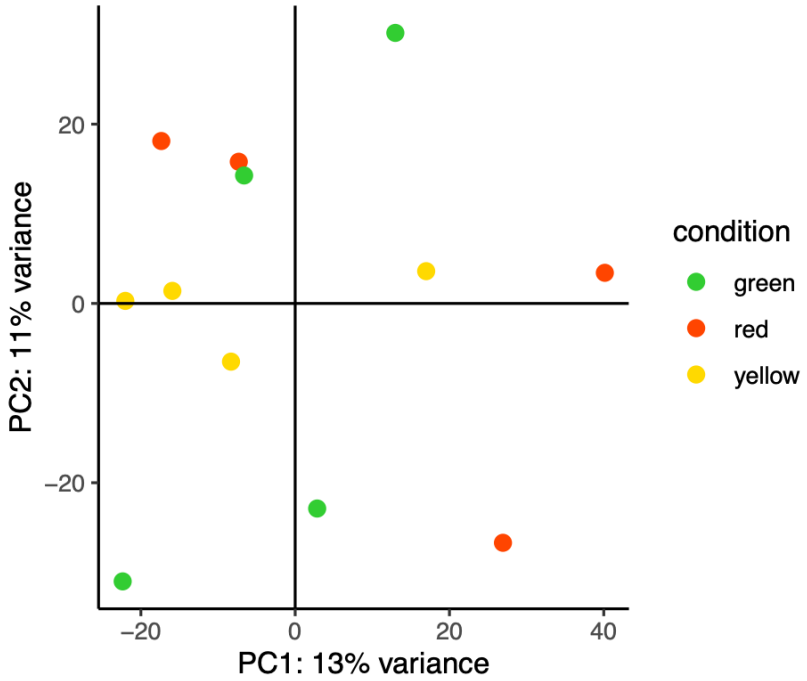

Figure 2. Principal component analysis (PCA) of genome-wide gene expression based on the negative binomial distribution of gene expression for all phenotypes. Each green, red or yellow dots represent an individual of the corresponding color.

Three RBGOA analysis were performed: (i) red vs. yellow (Figure 3A), (ii) red vs. green (Figure 3B), and (iii) yellow vs. green (Figure 3C). Significantly enriched GO terms (p value < 0.01) were identified for each paired color combination: 45 GO terms for the comparison of red vs. yellow (27 over-represented and 18 under-represented), 16 GO terms for red vs. green, (7 over-represented and 9 under-represented), and 89 GO terms for yellow vs. green (36 over-represented and 53 under-represented). Among these enriched molecular functions, several belonged to pathways already known to be involved in pigmentation or biomineralization in various organisms [48–50]: "hydroxymethylbilane synthase activity" [48] (GO:0004418; under-represented in red vs. yellow), "oxidoreductases, acting on the CH-CH group of donors" [49,50] (GO:0016627; under-represented in red vs. yellow, but over-represented in yellow vs. green), "UDP-glycosyltransferase activity" [49] (GO:0008194; under-represented in yellow vs. green), and "UDP-glucosyltransferase activity" [49] (UGTs) (GO:0035251; under-represented in red vs. green and in yellow vs. green). The pterin and Raper–Mason pathways are also known to produce pigments [51–53], and molecular functions characteristic of these pathways were also significantly enriched. These included "GTPase activity" (GO:0003924) and "oxidoreductase, acting on NAD(P)H" (GO:0016651), both of which had a higher amount of transcripts in red vs. yellow and yellow vs. green; "monooxygenase activity" (GO:0004497), "tetrapyrrole binding" (GO:0046906), and "quinone binding" (GO:0048038), all over-represented in yellow vs. green; "phosphotransferase, alcohol group as acceptor" (GO:0016773), under-represented in yellow vs. green; "transferase activity, transferring alkyl or aryl (other than methyl) groups" (GO:0016765) and "glutathione transferase activity" (GO:0004364), both over-represented in yellow vs. green.

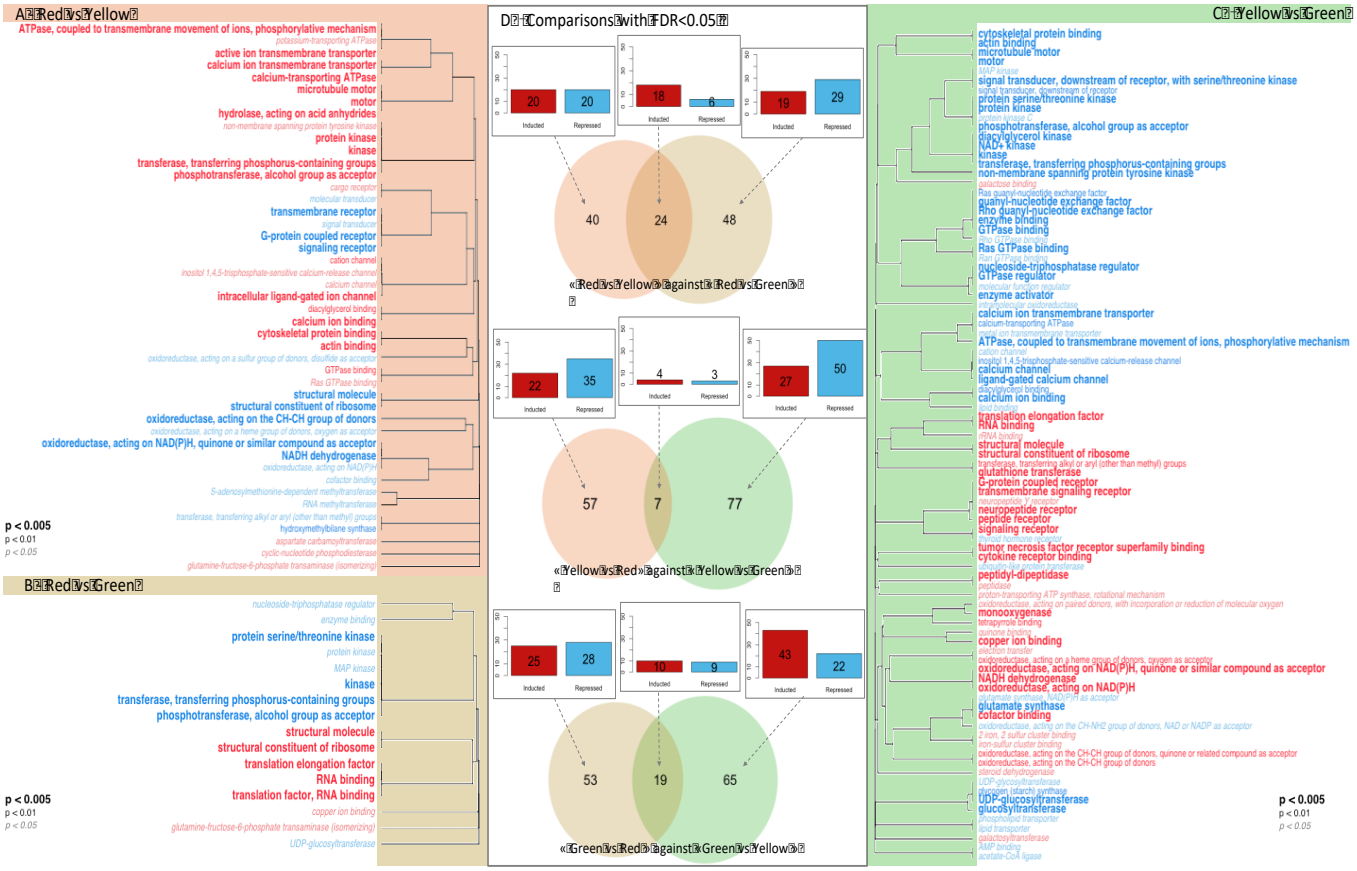

Figure 3. Enrichment analysis and differential expression. (**A**–**C**), Molecular functions significantly enriched by either over- (in red) or under- (in blue) expressed genes (**A**)—the red phenotype compared to the yellow, (**B**)—the red phenotype compared to the green, (**C**)—the yellow phenotype compared to the green. (**D**) Venn diagrams representing shared and specific genes differentially expressed (FDR < 0.05) between phenotypes. Histograms show the number of over- (red) or under-represented (blue) genes.

Two categories involved in purine metabolism, "oxidoreductase activity, acting on CH or CH2 groups" (GO:0016727) and "oxidoreductase activity" (GO:0016491) had lesser and greater amounts of transcripts in yellow vs. green, respectively. These categories included 21 genes coding for xanthine dehydrogenase, an enzyme known to degrade the yellow pigment xanthine into uric acid [51,54]. According to the literature and present knowledge, the other enriched GO terms identified in this study are not directly related to pigmentation or biomineralization but could still affect color expression directly or indirectly. These genes would make an interesting subject for future analyses.

3.3. DEG Functional Analysis

Differences in gene expression were analyzed by pairwise comparison of color phenotypes using DESeq2. In total, 71,059 genes were expressed with at least one read counted. Among these expressed genes, 64, 72 and 84 DEGs were identified (False Discovery Rate, FDR < 0.05) for the red vs. yellow, red vs. green, and yellow vs. green pairwise comparisons, respectively (DEGs for all pairwise comparisons are given in Supplementary Materials Tables S6–S8. With this approach, we hypothesized that a DEG present in two pairwise comparisons would be more likely to be associated with the phenotype present in both of these pairwise comparisons. We, therefore, drew Venn diagrams that identified 24 DEGs (18 over-represented, 6 under-represented) shared between the red vs. yellow and between red vs. green, 7 DEGs (4 over-represented 3 under-represented) shared between the red vs. yellow and yellow vs. green, and 19 DEGs (10 over-represented, 9 under-represented) shared between the red vs. green and yellow vs. green comparisons (Figure 3D). Among these DEGs,

16 red-associated, 3 yellow-associated, and 11 green-associated genes encode proteins of unknown function.

Several genes associated with the red phenotype are good candidates for explaining the red color. Among them, four genes encoding a porphobilinogen deaminase (PBGD) protein were under-represented (Log2FCs: (−2.91; −2.39) in red vs. green and Log2FCs: (−3.54; −2.77) in red vs. yellow). These genes had already been identified by the RBGOA analysis, and belong to "hydroxymethylbilane synthase activity" (GO:0004418). Porphobilinogen deaminase (KEGG entry K01749) can be involved in four pathways referenced in KEGG: "porphyrin and chlorophyll metabolism" (ko00860), "metabolic pathways" (ko01100), "biosynthesis of secondary metabolites" (ko01110), and "microbial metabolism in diverse environments" (ko1120). In addition, three DEGs belonging to the glycosyltransferase family were found under-represented in the red phenotype: (i) one glycosyltransferase family 8 protein, also found in the "transferase activity, transferring glycosyl groups" (GO:0016757; Log2FC: −2.63, for red vs. green and Log2FC: −2.61, for red vs. yellow); (ii) one glycosyltransferase-like protein LARGE also found in "transferase activity, transferring glycosyl groups" (GO:0016757) and "glucuronosyltransferase activity" (GO:0015020; Log2FC: −2.45 for red vs. green and Log2FC: −3.07 for red vs. yellow); and *iii*) one xylosyl- and glucuronyltransferase 1-like also found in the "transferase activity, transferring glycosyl groups" (GO:0016757), and "glucuronosyltransferase activity" (GO:0015020) molecular functions (Log2FC: −1.95 for red vs. green and Log2FC: −2.42 for red vs. yellow). The glycosyltransferase family 8 protein was found in "starch and sucrose metabolism" (tre00500). The glycosyltransferase-like protein LARGE and xylosyl- and glucuronyltransferase 1-like could both be involved in two pathways: "mannose type O-glycan biosynthesis" (ko00515) and "metabolic pathways" (ko01100). Finally, the under-represented decaprenyl-diphosphate synthase subunit 2-like was also found in the "transferase activity" (GO:0016740) molecular function by RBGOA (Log2FC: −2.88 for red vs. green and Log2FC: 3.006 for red vs. yellow). The "terpenoid backbone biosynthesis pathway" (ec00900) was found to be associated with the red phenotype. Finally, although we cannot exclude their involvement in color expression, none of the yellow- and green-associated DEGs had sufficient background literature or sequence similarity to a gene of known function for us to draw a direct link to pigmentation.

Among the DEGs present in only one pairwise comparison, we identified four interesting candidate genes linked to the green phenotype. The first two of these candidates, which were found under-represented in the green vs. yellow comparison and encode two glutathione-S-transferase (GST) enzymes (Log2FC: −1.02 and −1.27), were also found in the "glutathione transferase activity" (GO:0004364) molecular function in RBGOA and are involved in "glutathione metabolism" (ec00480), "metabolism of xenobiotics by cytochrome P450" (ec00980), and in "drug metabolism–cytochrome P450" (ec00982). Interestingly, GST has been shown to balance the production of eumelanin and pheomelanin [55]. The two other candidates encoded transcobalamin-2 found in the "copper ion binding" (GO:0005507) molecular function in RBGOA and were present in lesser quantities in green vs. red (Log2FC: −3.02) and green vs. yellow (Log2FC: −2.70). According to KEGG classification, transcobalamin-2 (K14619) is involved in the vitamin digestion and absorption pathway (mmu04977). Interestingly, vitamins such as the B12 (cobalamin) could also be related to pigment synthesis. Detailed information on DEGs is given in Supplementary Materials Tables S6–S8.

3.4. Enzymatic Structure Analysis with Homology Modeling

In our DEGs results, four genes encoding for a porphobilinogen deaminase (PBGD) were found in the red-associated analysis and this gene is known to be involved in red coloration in some Mollusca [56]. Since we have very strong evidence for the involvement of PBGDs in the expression of red color, we checked whether these enzymes displayed sufficient structural and biochemical similarities with a reference PBGD to be considered active. We did so by comparing their primary, secondary and tertiary structure to human

PBGD, which has been studied by crystallography (chain A of the 3ECR) [42]. K98, D99, R149, R150, R173, R195, Q217, and C261 are key residues for catalysis with the cofactor [42]; S96, H120, and L238 enable the movement of the protein domains; and R116, R225, D228, and L278 ensure the stability of movement. R167 is involved in the release of the final product [42].

At the primary structure level, the sequences were 306, 217, 95, 161, and 122 amino acids long for human PBGD and the four *P. margaritifera* PBGD (A to D), respectively (Figure 4). *P. margaritifera* PBGD_A to _D displayed 54.3%, 30.3%, 37.4%, and 42.6% of similarity with human PBGD, respectively. Alignment with human PBGD produced scores of 273, 69, 120, and 122 and coverage of 66%, 21%, 32%, and 33% (*e*-value 5e-91, 2e-14, 2e-32, and 2e-33) for PBGD_A to D, respectively. Based on these results, the four *P. margaritifera* PBGD can be considered as homologous to human PBGD [57].

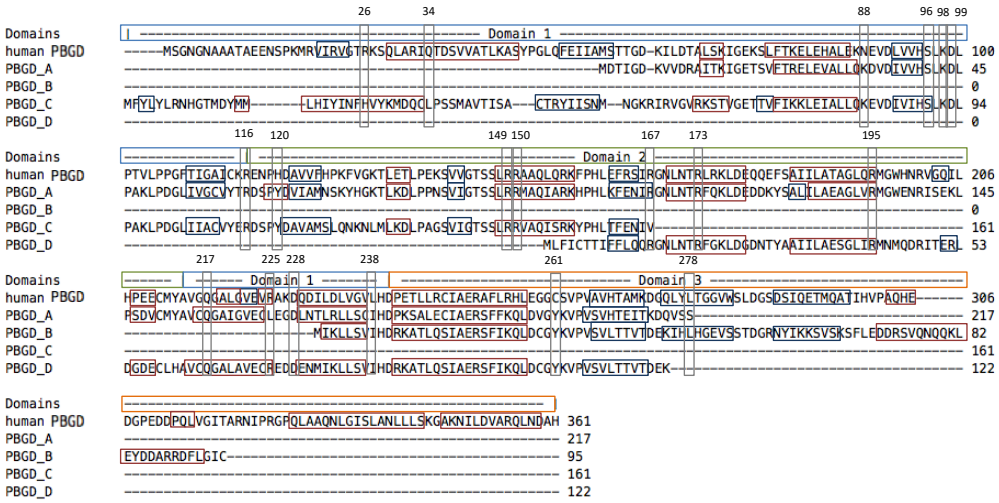

Figure 4. Alignments of the four *P. margaritifera* porphobilinogen deaminase (PBGD) (PBGD_A to PBGD_D) against the human PBGD (Song et al. 2009). The pale blue boxes correspond to domain 1, the green to domain 2 and the orange to domain 3. Red boxes show α helix (H) and dark blue boxes β strands (S). Grey boxes correspond to key residues (amino acids).

At the secondary and tertiary structure levels, the succession of α helix and β strands is mainly conserved, although some differences can be observed (Figure 4). Most importantly, the key amino acids for enzymatic processing (Figure 4, Table 1) were retrieved in the *P. margaritifera* PBGDs, especially isoform A, which appeared to be the most conserved. In this PBGD_A, the binding and the interaction with the dipyrromethane cofactor may be performed by residues K43, D44, R94, R95, R118, R140, Q162, and Y206 (Figures 4 and 5, Table 1). Hinge residues that enable the movement (S41, Y65, and I183) and stability (R61, L170, D173, and S223) of the protein domains were also identified (Figures 4 and 5, Table 1). Finally, R112, an essential residue for the release of the substrate was also present (Figures 4 and 5, Table 1). In addition to this biochemical conservation, these key residues occupy a similar position in PBGD_A and human PBGD (Figure 5).

Table 1. Conservation of key residues between *P. margaritifera* PBGDs and human PBGD. Amino acid numbering is based on the alignment given in Figure 5.

Human's_PBGD	PBGD_A	PBGD_B	PBGD_C	PBGD_D
R26	NA	NA	H23	NA
Q34	NA	NA	L32	NA
N88	K33	NA	K82	NA
S96	S41	NA	S90	NA
K98	K43	NA	K92	NA
D99	D44	NA	D93	NA
R116	R61	NA	R110	NA
H120	Y65	NA	Y114	NA
R149	R94	NA	R143	NA
R150	R95	NA	R144	NA
R167	R112	NA	V161	R14
R173	R118	NA	NA	R20
R195	R140	NA	NA	R42
Q217	Q162	NA	NA	Q64
R225	L170	NA	NA	R72
D228	D173	NA	NA	D75
L238	I183	I8	NA	Y85
C261	Y206	Y31	NA	Y108
L278	S223	L48	NA	NA

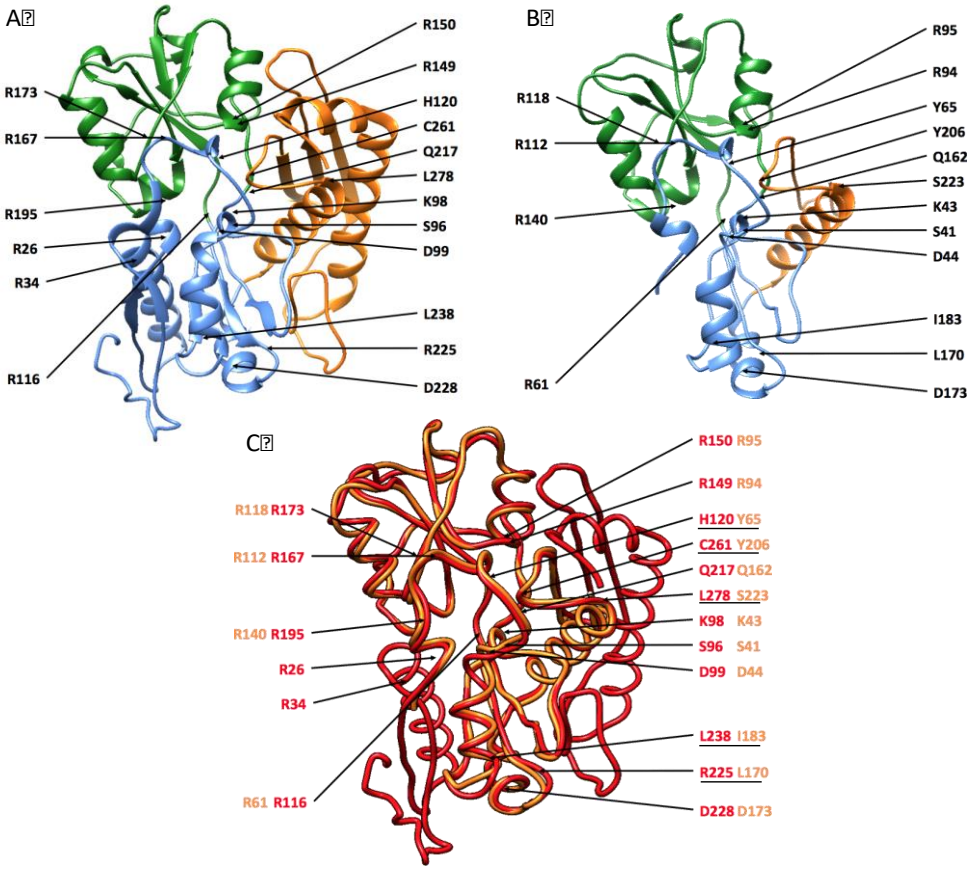

Figure 5. Enzymatic structure and homology modeling for human PBGD (**A**) and *P. margaritifera* PBDG_A (**B**). Domain one is shown in blue, domain two in green, and domain three in orange. Key residues are labeled, as are their positions in the primary structure. (**C**) Superimposition of *P. margaritifera* PBGD_A (in orange) on human PBGD (in red). Positions of key residues for each enzyme are indicated, and amino acid substitutions are underlined.

Overall, the enzymatic structure analyses demonstrated conserved general biochemical and structural properties of protein domains, despite variations in some amino acid sequences. We can therefore hypothesize that PBGD_A is active in *P. margaritifera*, which would be expected since even PBGDs displaying high structural variation have been reported several times as being active [42,58–60].

3.5. Raman Spectra Analysis

The transcriptomic approach identified molecular pathways that were differentially regulated between phenotypes. To test the involvement of these pathways in the expression of the red, yellow, or green colors, we performed Raman spectra analysis on five different phenotypes: the red, yellow, and green. Albino (no color) and black (in which a mix of colors are expressed to a lesser degree among different individuals) phenotypes were used as controls. PCA analysis performed on raw Raman spectra (Figure 6) reveals two distinct clusters, one including the yellow and albino phenotypes and the red, the second including black and green phenotypes. In this last cluster, the variability in Raman spectra is lower for the green phenotypes, for which individuals grouped together more closely, compared with the black and red, which show a wider distribution (Figure 6).

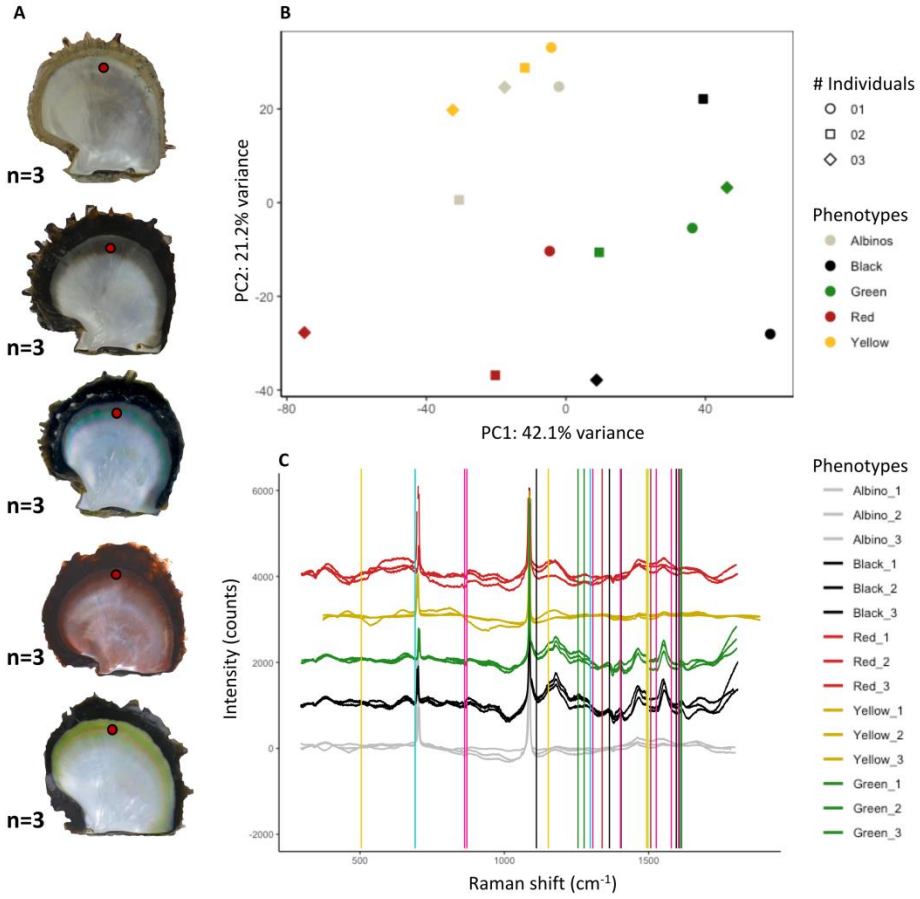

Figure 6. Raman spectroscopy results. (**A**): Experimental design of RAMAN validation. Three individuals per phenotype were studied. Red dots show s where on the inner shell Raman spectra were produced. (**B**): Principal component analysis of raw Raman spectra obtained for the 5 inner shell colors analyzed (3 individuals per color). (**C**): calibrated spectra presenting the intensity (counts) of the signal as a function of the Raman shift (cm^{-1}). Colored vertical lines mark the positions of peaks constituting a Raman signature specific to one of the identified pigments: forest green, biliverdin; dark sea green, cobalamin; red, uroporphyrin I; dark turquoise, bilirubin; gold, phaeomelanin; black, melanin; and deep pink, xanthine. Enlargements of the spectra for each signature are provided in the Supplementary Materials Figure S1.

Individual spectra display the characteristic peaks of high intensity corresponding to the $CaCO_3$ biomineral in its aragonitic and calcitic forms. This high intensity reflects that the shell is essentially composed of these two polymorphs [61]. At a lower intensity, dozens of peaks are present and illustrate the high chemical complexity of this biomaterial, with more than 78 different Shell Matrix Proteins (90% of the organic matrix [61,62]), at least 4 different lipid's family (fatty acids, cholesterol, phytadienes, and ketones; 0.15 to 0.29% of the organic matrix [61]); 10 different traces of heavy metals [63], polysaccharides, and secondary metabolites [61].

Among the 174 peaks included in our homemade database (see Supplementary Materials Table S3), 40 peaks were found in the spectra obtained from our red, yellow, and green individuals (Table 2 and Supplementary Materials Figure S1). The combination of these peaks represents the signatures corresponding to nine pigments previously proposed by the transcriptomic approach: uroporphyrin I or III (three peaks), copper-uroporphyrin (six peaks), FeIII-uroporphyrin (six peaks), biliverdin (four peaks), cobalamin (two peaks), pheomelanin (four peaks), eumelanin (five peaks), xanthine (eight peaks), and bilirubin (two peaks). The complete set of peaks characteristic of each molecule were not identified and/or were not present in all individuals of the same phenotype. This phenomenon is classically observed in Raman spectroscopy, where the absence of a peak does not demonstrate the absence of a molecule, whereas the presence of a peak can be considered as evidence, a phenomenon also reported for pure pigments such as the pheomelanin [64].

Table 2. Pigment validation by Raman spectroscopy, synthetic results. Raman signatures characteristic of each pigment found in the literature; Peak characterization (identify peaks matching or not expected signals), peak intensity (the value of the lowest point of the peak minus the value of the peak) and ratio relative to the intensity of the calcite reference peak (ratio was calculated between the intensity of the selected peak (calculated as previously described) and the peak of the referential calcite for each spectrum). Each red, yellow, green, black or white background/text color are corresponding to the phenotype color. The full table is presented in Supplementary Materials Table S9.

Pigment	Peaks	Publication	Red Individual 1			Red Individual 2			Red Individual 3			Yellow Individual 1			Yellow Individual 2			Yellow Individual 3			Green Individual 1			Green Individual 2			Green Individual 3			Black Individual 1			Black Individual 2			Black Individual 3			Albino Individual 1			Albino Individual 2			Albino Individual 3		
			Peak	Intensity	Ratio	Peak	Intensity	Ratio	Peak	Intensity	Ratio	Peak	Intensity	Ratio	Peak	Intensity	Ratio	Peak	Intensity	Ratio	Peak	Intensity	Ratio	Peak	Intensity	Ratio	Peak	Intensity	Ratio	Peak	Intensity	Ratio	Peak	Intensity	Ratio	Peak	Intensity	Ratio	Peak	Intensity	Ratio	Peak	Intensity	Ratio	Peak	Intensity	Ratio
Uropor–phyrin I	1335	Williams et al. 2017	yes	29.26	0.66	yes	19.70	0.49																yes	16.05	0.50																				
	1445		yes	44.39	0.83	yes	29.10	0.72													yes	120.49	0.77				yes	46.51	0.64																	
	1556														yes	13.18	0.57																														
Coproporphyrin	1310	Shelnutt 1981, 1982, et al. 1984	yes	6.52	0.66	yes	5.63	0.46	yes	5.37	0.22																																				
	1379								yes	35.73	0.25																																				
	1403								yes	11.34	0.27																					yes	106.76	0.51	yes	99.57	0.41	yes	62.13	0.43								
	1499		yes	27.21	0.73	yes	19.07	0.74	yes	8.45	0.31																																				
	1582					yes	17.18	0.71																																							
	1637					yes	10.28	0.66																																							
FeIII uroporphyrin	1307	Shelnutt 1982	yes	5.48	0.66	yes	11.81	0.45																																						
	1376		yes	9.29	0.62	yes	29.43	0.51	yes	21.71	0.23																			yes	59.22	0.49														
	1402		yes	11.29	0.67	yes	16.37	0.54	yes	11.34	0.26																					yes	114.98	0.51												
	1489		yes	12.80	0.76	yes	16.93	0.74	yes	8.04	0.31																					yes	111.01	0.73	yes	42.97	0.51								
	1581		yes	15.64	0.70				yes	4.23	0.30																																				
	1627		yes	16.99	0.72																																								
Biliverdin	1252	Margulies and Toporowicz 1984, Holt et al. 1989																											yes	40.58	0.81																
	1273																								yes	24.18	0.56																		
	1606																				yes	11.07	0.73	yes	20.05	0.56	yes	12.97	0.60																
	1608																				yes	38.36	0.73	yes	7.60	0.56	yes	21.08	0.60																
Cobala–min	1495	Puckett et al 1996, Galluzzi et al. 1974																			yes	16.70	0.72	yes	14.17	0.57																				
	1502					yes	19.50	0.75													yes	18.87	0.72	yes	15.99	0.56	yes	24.57	0.53																
Xanthine	862	Muniz-Miranda et al. 2018																yes	25.06	0.48	yes	29.51	0.71				yes	17.56	0.60																
	870		yes	79.86	0.71	yes	35.32	0.57	yes	81.36	0.21									yes	30.95	0.72	yes	38.01	0.53	yes	111.64	0.66							yes	45.10	0.51						
	1303											yes	7.64	0.54	yes	9.09	0.53																												
	1398																				yes	5.58	0.68	yes	2.73	0.57	yes	7.76	0.55																
	1521					yes	25.67	0.75										yes	8.88	0.48							yes	41.97	0.51																
	1573																							yes	28.38	0.56	yes	6.44	0.55	yes	42.71	0.60												
	1593																																													
	1598																	yes	9.26	0.53																											
Pheomelanin	507	Galvan et al. 2013										yes	3.67	0.54				yes	26.49	0.48																											
	1150																	yes	17.71	0.56											yes	42.43	1.00												
	1488											yes	2.08	0.53	yes	2.69	0.55	yes	0.43	0.48																											
	1490											yes	1.11	0.53	yes	1.92	0.55	yes	1.48	0.47											yes	92.35	0.72				yes	70.77	0.63						
Bilirubin	692	Dybas et al. 2018										yes	22.07	0.55	yes	13.70	0.56																												
	1294														yes	5.46	0.53	yes	4.40	0.51	yes	32.05	0.70				yes	23.52	0.66																
Melanin	1109	Centeno and Shamir 2008, Williams et al. 2016				yes	27.08	0.71	yes	34.65	0.24										yes	20.82	0.79																								
	1360																	yes	12.87	0.49	yes	12.00	0.67																								
	1400																				yes	71.58	0.67	yes	54.95	0.57	yes	27.01	0.54				yes	39.33	0.43	yes	44.05	0.46						
	1590																							yes	13.25	0.52																		
	1600																							yes	23.14	0.53																		

Likewise, most of the pigments corresponding to a specific color displayed some of their signature peaks in individuals of different phenotype, but with variation in their intensity (Table 2). These results are validated by the absence of detection of peaks characteristic of each pigments in the albino control, a phenotype displaying an absence of coloration.

Red phenotypes were mainly characterized by peaks corresponding to uroporphyrin I or III or its derivatives, copper or FeIII-uroporphyrin (Table 2). Red individuals also displayed Raman signatures characteristic of the green cobalamin, yellow xanthine, and black eumelanin, although this non-red signature was shown to a lesser degree (Table 2, Supplementary Materials Table S9). None of these peaks were retrieved in the albino control.

Green phenotypes were mainly characterized by peaks corresponding to the green pigments biliverdin and cobalamin (Table 2, Supplementary Materials Table S9). Green phenotypes also had a strong signal for the yellow pigment xanthine and the black pigment eumelanin (Table 2). Signatures of uroporphyrin I (red) and bilirubin (yellow) were also present but minor. These results, showing a large diversity of pigments in the green phenotypes, confirm that it is the most complex. None of these peaks were retrieved in the albino control.

Yellow phenotypes were mainly characterized by the two yellow pigments pheomelanin and bilirubin. At a lesser proportion, they also showed signatures characteristic of xanthine (yellow pigments), uroporphyrin I (red), and eumelanin (black), also in minor proportions. None of these peaks were retrieved in the albino control.

The black and albino phenotypes had served as controls. As expected, the black phenotype did not have a signature for one particular color and presented an average proportion of all the identified pigments (except green). The albino did not show any peaks, which confirmed the absence of pigmentation from these samples.

4. Discussion

P. margaritifera is known for its ability to express the broadest range of internal shell and pearl colors of all pearl oyster species [65]. To characterize pathways and pigments underlying these colors, we developed an integrated approach combining experimental strategy to minimize the impact of phenotypic diversity and environmental effects, genome-wide transcriptomics, and Raman spectroscopy. The combination of these two last methods has first revealed that monochrome shell does not exist in this species, except in the particular case of albino. Indeed, all the identified pathways and pigments are transcribed ubiquitously, and the Raman signatures of red, yellow, and green pigments were retrieved in varying proportions in all phenotypes (except albino). The dominant color of an inner shell is, therefore, due to the preferential expression of one pathway relative to another. Second, the analyses revealed the central role played by the heme pathway, involved at different levels in the production of red (uroporphyrin and derivates), yellow (bilirubin), and green (biliverdin and forms of cobalamin) pigments. Additionally, but to a lesser extent, the Raper–Mason, and purine metabolism pathways were also shown to produce the yellow pigments pheomelanin and xanthine and the black pigment eumelanin.

4.1. The Inner Shell of P. margaritifera: Chemically Complex, Polychromic, but Containing Dominant Pigments

Mollusca shell is a biomaterial constituted by two distinct types of component—the mineral and the organic layer. The former has a composition of $CaCO_3$ that can take different form (aragonite, calcite etc.). The organic layer is much more complex and harbor dozens of different proteins, polysaccharides, lipids, traces of metals, and secondary metabolite [61,62]. This cocktail of molecules forms a highly complex assemblage where only a very small fraction will determine the inner shell pigmentation, making it a challenge to detect them. This challenge is even increased by the diffuse and unstable nature of the inner shell color of *P. margaritifera* [66,67], which all together explains the complexity and the low intensity of the Raman spectra we obtained, highlighting the need to combine several methods to tackle the same question from different angles. This combined approach revealed differences in gene expression levels between phenotypes rather than a binary

pattern of expression (expressed/unexpressed), highlighting the polychromic nature of the inner shell. This was further confirmed by the Raman spectra, bringing another set of evidence by the detection of the same pigments in various phenotypes, but with different intensities. This concomitant analysis raises the conclusion that all oysters express all pigments but in various proportions, which gives rise to the dominant color. This is further confirmed by the absence of Raman's signature for the unpigmented albino specimens, but also visually (Figure 1) where a reddish band can be observed on the green shell and a greenish and reddish band on the yellow shell. This polychromic nature of the black-lipped pearl oyster is an original characteristic of the species and is incidentally exploited in pearl farming [65].

4.2. Dysfunctions of Porphobilinogen Deaminase in the Heme Pathways Produce Red Uroporphyrin and its Derivates in Red Individuals

Among the candidate pathways identified, the heme biosynthesis and degradation pathways appear to be central (Figure 7). Hemes are most commonly recognized as components of hemoproteins such as hemoglobin, cytochromes, or catalases [68] and are excreted after their degradation [68]. We identified four DEGs encoding a porphobilinogen deaminase (PBGD), one of the main enzymes in the heme pathway. All of these genes were under-represented in the red phenotype according to the DEG functional analysis. Homology modeling illustrates that at least PBGD_A is functional since it displays the key biochemical and structural characteristics needed to catalyze its enzymatic reaction (Figure 5). PBGD is the third enzyme of the heme pathway and catalyzes the production of hydroxymethylbilane from four molecules of porphobilinogen in the presence of dipyrromethane as a cofactor [69]. In humans, deficiency of PBGD is characteristic of Acute Intermittent Porphyria (AIP), a genetic disease in which the main symptom is red urine coloration due to uroporphyrin overproduction [70,71]. The molecules of hydroxymethylbilane that are produced are converted to uroporphyrinogen I and then to uroporphyrin I by a non-enzymatic process and oxidation (Figure 7), respectively [48,71,72]. Uroporphyrin I is a well-known pigment in Mollusca: it has been previously identified by spectrophotometry and HPLC techniques in yellow-brown snail [2,48] and in the inner and outer shells and cultured pearls of *P. margaritifera* [18,19]. The color variation of the shells of *P. margaritifera* may be associated to variation in the concentration of the pigments, or more probably, to the proportion of the different derivate of uroporphyrin that are associated with metal ion [48,73]. Our Raman spectroscopy analysis strengthens this last hypothesis since it highlights the presence of derivatives of uroporphyrin: copper and FeIII uroporphyrin. Because of its toxicity, uroporphyrin I is usually excreted, which is mainly achieved through urine in mammals [74] and, putatively, through deposition in the shell in Mollusca (the shell is well known to bio-accumulate toxic compounds in Mollusca [75]). In this context and based on actual knowledge, we propose that the red color in *P. margaritifera* originates from deregulation of the heme pathway at the level of PBDG. Interestingly, the crossing of red individuals produces a dominant red F1 [24], which argues in favor of an oligogenic basis for the red phenotype as is the case for human AIP [76]. This overproduction of uroporphyrin does not appear to be detrimental for the pearl oysters since this phenotype occurs naturally in wild populations, sometimes at a non-negligible frequency [65].

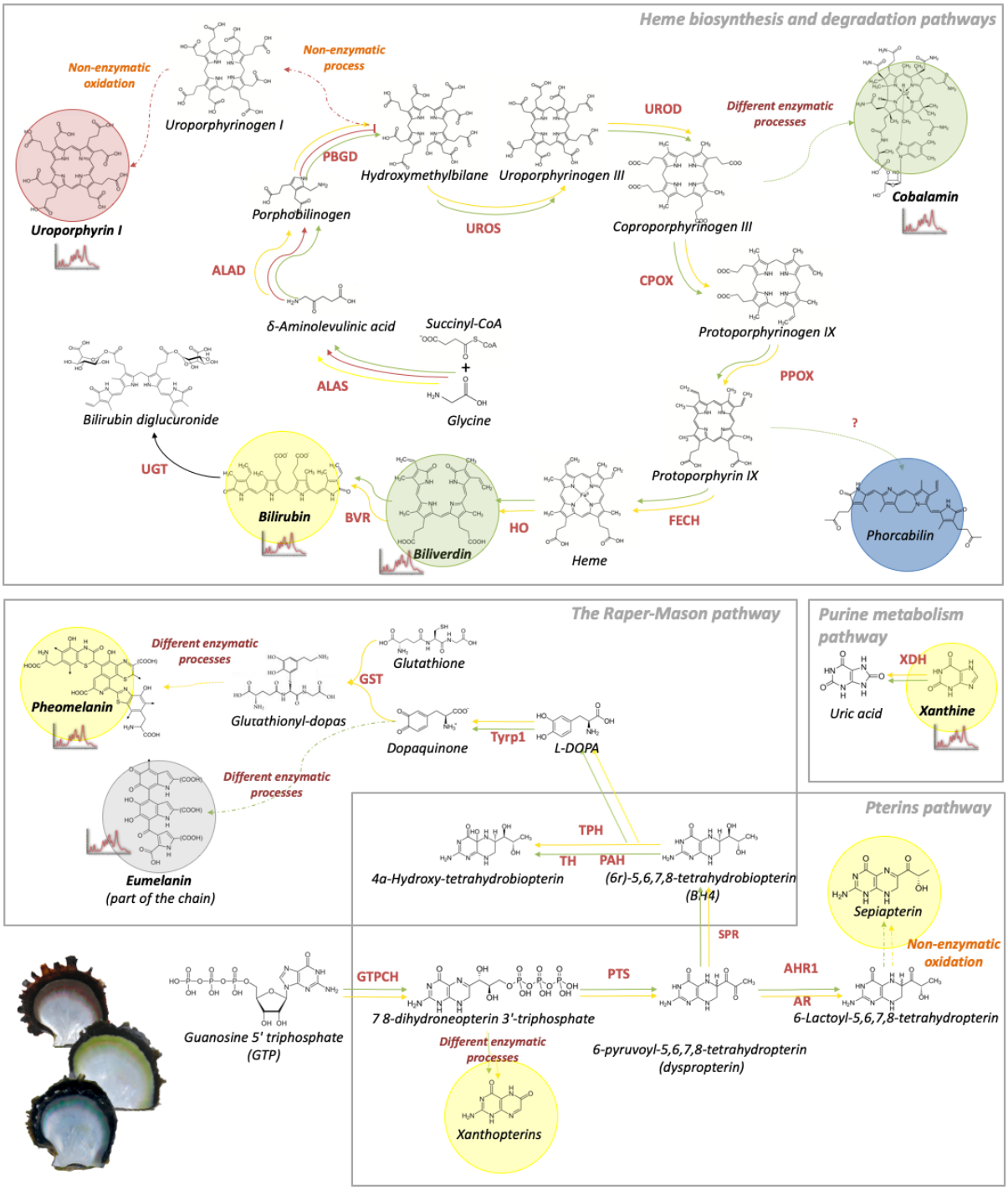

Figure 7. The four identified pathways responsible for *P. margaritifera* inner shell color: the heme biosynthesis and degradation pathways, the pterins pathway, the Raper–Mason pathway, and the purine metabolism pathway. The putative pigments are shown with colored circles; those validated by Raman spectroscopy have a Raman graph symbol. The red, yellow, and green arrows refer to the synthesis of red, yellow, and green pigments, respectively. ALAS: aminolevulinic acid synthase; ALAD: delta-aminolevulinic acid dehydratase; PBGD: porphibilinogen deaminase; UROS: uroporphyrinogen III synthase; UROD: uroporphyrinogen decarboxylase; CPOX: coproporphyrinogen oxidase; PPOX: protoporphyrinogen oxidase; FECH: ferrochelatase; HO: heme oxygenase; BVR: biliverdin reductase; UGT: UDP-glucuronyltransferase; GTPH: GTP cyclohydrolyase I; PTS: 6-pyruvoyltetrahydropterin/6-carboxytetrahydropterin synthase; AR: aldose reductase; AHR1: aldehyde reductase 1; SPR: sepiapterin reductase; PAH: phenylalanine-4-hydroxylase; TPH: tryptophan 5-monooxygenase; TH: tyrosine 3-monooxygenase; Tyrp1: tyrosinase-related protein 1; GST: gluthathione-S-transferase; XDH: xanthine dehydrogenase.

4.3. Heme, Raper–Mason, and Purine Metabolism Pathways Produce Bilirubin, Pheomelanin, and Xanthine Pigments Underlying the Yellow Phenotype

The first yellow pigment identified in the present analysis, bilirubin, was also related to the heme pathway. In the downstream part of the heme degradation pathway, heme oxygenase (HO) converts heme into biliverdin [77], which is then transformed into bilirubin (a well-known yellow pigment in animals [77–79]) through the action of biliverdin reductase (BVR; Figure 7). Although HO and BVR genes were already found expressed in Mollusca species [56,80], these two genes were not found in our analysis. However, the gene encoding a UDP-glucuronosyltransferase (UGT), the enzyme that degrades bilirubin into bilirubin diglucuronide [81,82] (a colorless compound) was found under-represented in the yellow phenotype compared with the green and red, suggesting a possible accumulation of bilirubin in the animal, later excreted and deposited into the shell. In addition, other genes belonging to the UGT family were found in high numbers in the GO categories "UDP-glycosyltransferase" and "UDP-glucosyltransferase", two molecular functions expressed at a lesser degree in the yellow compared with the green phenotype. The involvement of the bilirubin in the yellow phenotype was also confirmed by Raman spectroscopy results, showing specific signatures of the bilirubin mainly in the yellow individuals. The bilirubin is a well-known pigment in vertebrates but was not yet detected in invertebrates. Our study provides a first line of evidence of its synthesis in invertebrates as well, but this should be further confirmed by additional analyses enabling the chemical purification of this compound to provide a definitive confirmation.

The second identified pathway that may lead to the production of yellow pigment was the purine metabolism pathway, ending with the production of xanthine (Figure 7). RB-GOA analysis revealed the over-representation of categories that contain at least 21 genes coding for xanthine dehydrogenase, an enzyme known to degrade the yellow pigment xanthine into uric acid [51,54]. Some of these 21 genes were more expressed in the yellow phenotype, while others were more expressed in the green phenotype, suggesting a generalized production of this pigment. Raman spectroscopy revealed the specific signatures of 7/16 referential peaks of xanthine in all phenotypes except in albino (0/16). All these results strengthen the possibility that xanthine synthesis through the purine metabolism pathway is involved in the expression of the yellow phenotype.

The third identified pathway leading to the production of yellow pigments for which we obtained transcriptomic and Raman evidence is the Raper-Mason pathway that leads to the yellow pheomelanin [53]. The Raper–Mason pathway starts with the L-DOPA, which is transformed into dopaquinone by the activity of tyrosinase-related protein 1 (Tyrp1). Dopaquinone could either become the black pigment eumelanin [83], through a non-enzymatic process, or the yellow pigment pheomelanin [83] by the successive action of glutathione-S-transferase (GST) and glutamine γ-glutamyltransferase [55]. Both of these pigments have already been described in Mollusca [84]. The molecular function "glutathione transferase activity" (GO:0004364), as well as two GST genes, were over-represented in the yellow phenotype (relative to the green phenotype). Since the ratio between the production of pheomelanin and eumelanin is a fine balance regulated by GST [55] activity, it is probable that yellow shells are enriched in yellow pheomelanin in comparison to green ones. This hypothesis was validated by the Raman spectroscopy results confirming the presence of the 4/4 specific peaks for the pheomelanin only in the yellow individuals and 2/4 in some black individuals. In addition, Raman spectroscopy results also indicated the presence of black eumelanin with a strong degree of confidence in the green phenotype (several signatures), while this was almost undetected in the yellow shells. This result confirms the proposed regulation pathway whereby the production of pheomelanin or eumelanin is controlled by fine-tuning regulation of GST activity.

In summary, we can conclude that the yellow phenotype results from the production and accumulation of several pigments, mainly bilirubin, xanthine, and pheomelanin (Figure 7). These three pigments come from three different pathways, which increase the potential for high phenotypic variation among individuals of this color phenotype but also

of the others. Indeed, it is not rare to observe shades of yellow in green, black, or even red shells as well as different sheds of yellow among yellow individuals [65,83].

4.4. Heme Pathways Are Central to the Green Phenotype through the Production of Biliverdin and Green Forms of Cobalamin

Green pigments are uncommon in animals [84,85] and usually originate from three non-exclusive sources: a mixture of black and yellow pigments, a mixture of blue and yellow pigments, or, more rarely, from an actual green pigment [86]. The mixture of black and yellow pigments to create a green color is interesting in our case, since the yellow and green phenotypes appear to be transcriptionally very similar to each other. The green pearl oyster phenotype could result from the mixture of yellow pigments (i.e., Pheomelanin, xanthine and bilirubin) with the black pigment eumelanin produced by the Raper–Mason pathway as described above.

The mixture of blue and yellow pigments is also a plausible scenario. Although blue color phenotypes are rare in pearl oyster and no blue pigment has been clearly identified to date, *P. margaritifera* is known to produce blue internal shells and pearls. In some butterflies, the blue pigment phorcabilin [87,88] is mixed with yellow pigments to produce a green color [87,88]. The biosynthesis of phorcabilin takes place in the heme biosynthesis pathway, resulting from the oxidation of protoporphyrin IX into pterobilin, followed by its conversion into phorcabilin by a non-enzymatic process [88]. This pathway remains underexplored: several of its steps are not completely understood, and the oxygenase catalyzing the conversion of protoporphyrin IX in pterobilin is still unknown. However, in our RBGOA comparison of yellow and green phenotypes, some oxygenase-like genes were identified and observed to be over-represented in the green phenotype. Since no reference Raman signatures of phorcabilin are yet available, we were not able to either confirm or deny its presence in the green shells. Validation of this hypothesis will therefore require further experiments.

Considering the third possible source of green color, the direct synthesis of a green pigment, biliverdin, is a good candidate. This pigment has already been identified in Mollusca [89] and is produced in the heme degradation pathway [90]. Although we did not identify genes encoding the heme oxygenase and biliverdin reductase enzymes that are necessary for the production and the degradation of biliverdin, our Raman spectroscopy results showed its presence in the green shells. Since the heme pathway is well conserved in the animal kingdom [56], the absence of these genes in *P. margaritifera* is unlikely and is here probably due to assembly or annotation errors in the reference genome. The heme degradation pathway can also produce another green pigment, cobalamin. Cobalamin is a hemic molecule derived from coproporphyrinogen III [91] and some of its forms can be green [73,91,92]. Another interesting feature of cobalamin is its bacterial-dependent synthesis [93–95] that often relies on a symbiotic interaction between a host and bacteria [96–99]. Alternatively, cobalamin can be directly acquired by food uptake [96]. In our data, the next two enzymes after coproporphyrinogen III (the cobalamin precursor), coproporphyrinogen oxidase (CPOX), and protoporphyrinogen oxidase (PPOX), were under-expressed in the green phenotype than the yellow according to our RBGOA results. In addition, two genes encoding a transcobalamin-2 were significantly under-expressed in the green phenotype compared with the yellow or red phenotypes. Transcobalamins are proteins involved in the transport and excretion of cobalamins [100]. This transcriptomic evidence is strengthened by the Raman spectroscopy results which indicated the presence of specific signatures of cobalamin in green individuals. At the species level, this result suggests symbiotic interaction between the oyster and some of the bacteria composing their microbiome. This bacterium would be involved in the production of cobalamin, and the green phenotype would be due to a less efficient transport and excretion of this pigment in comparison to other phenotypes.

In summary, the green phenotype in pearl oysters appears to arise in two different ways: the direct production of green pigments biliverdin and green cobalamin forms by the

heme pathway, and the indirect production of a green color through the mixing of black eumelanin and yellow pigments from the Raper–Mason pathway.

5. Conclusions

To conclude, we demonstrated that the heme pathways appear to be central in the inner shell coloration of *P. margaritifera*. The red phenotype is clearly linked to the reduced expression of an enzyme, PBGD, likely originating from a genetic mutation. The yellow and green phenotypes appear to be more interlinked and share several pathways. Interestingly, the Raman spectra obtained highlighted that any of the studied phenotypes could be characterized as pure or monochromatic even among populations produced to be monochromatic such as the three populations used in this study. This indicates that all these pathways and pigments are probably expressed universally in all individuals and that the dominant color comes from gene expression variations between individuals, a phenomenon that can probably be extended to many other organisms with large chromatic variation.

In the wild, the inner shell color of most *P. margaritifera* individuals is either grey/black or is highly polychromic. This characteristic leads to a high level of uncertainty in the future color of the pearls produced by the farming process based on wild-collected pearl oysters [65]. Producing pearls with saturated monochromatic colors is a promising way to "produce fewer, but better" pearls [22]. Our results show that reaching this goal through selective breeding will be challenging given the natural tendency toward polychromy and the diversity of pigments, genes, and pathways involved in this phenotypic trait. However, this work constitutes a significant step in the understanding of the molecular mechanisms underlying the color of *P. margaritifera* and pearls produced through its culture. This work also built solid foundations for the development of future research that will contribute to a sustainable pearl industry. Indeed, our results will be used to develop marker-assisted selection [101,102] to strengthen genetic selection programs for elite donor pearl oysters [25].

Supplementary Materials: The following are available online at https://www.mdpi.com/2073-4425/12/3/421/s1, Figure S1: Raman spectra and enlargement corresponding to Raman signatures of interest, Table S1: Detailed parameters of the bioinformatic pipelines, Table S2: Detailed protocol of the homology modeling, Table S3: Homemade bibliographic database referencing Raman peaks specific to pigments, Table S4: a) Detailed results of FastQC for each individual (R1 = Reverse & R2 = Forward) before and after Trimmomatic (X16–X19 = red individuals; X21–X25 = yellow individuals; X26–X30 = green individuals). b) FlagStat results for the mapping of each individual (X16–X19 = red individuals; X21–X25 = yellow individuals; X26–X30 = green individuals), Table S5: Transcriptome annotation, Table S6: DEGs and corresponding BlastX results for the comparison "Red versus Yellow". The colored cells correspond to the color-specific DEGs that can be found in two comparisons, Table S7: DEGs and corresponding BlastX results for the comparison "Red versus Green". The colored cells correspond to the color-specific DEGs that can be found in two comparisons, Table S8: DEGs and corresponding BlastX results for the comparison "Yellow versus Green". The colored cells correspond to the color-specific DEGs that can be found in two comparisons, Table S9: Pigment validation by Raman spectroscopy, full results table.

Author Contributions: J.V.-D., C.-L.K. and S.P. designed and supervised the study. J.D. and H.D. performed the Raman. P.-L.S. analyzed the data. P.-L.S. and J.V.-D. draft the manuscript. P.D. and L.Q. annotated the transcriptome. Funding was obtained by C.-L.K., S.P. and J.V.-D., J.V.-D., J.D., C.-L.K., S.P., C.R. corrected the main manuscript. All authors have read and agreed to the published version of the manuscript.

Funding: This research was funded by grants from the Direction des Ressources Marines, through the AmeliGEN project (# 10065/MEI/DRMM). Pierre-Louis Stenger's PhD was funded by AmeliGEN and the doctoral school of the Pacific (ED 469). This study is set within the framework of the Laboratoire d'Excellence (LABEX) TULIP (ANR-10-LABX-41) and CORAIL (ANR-10-LABEX).

Institutional Review Board Statement: Animal Ethics approval was not required for Mollusca species living in pearl farms. All the experimental procedures were conducted in accordance with standard commercial practices and regulations of the local government. All procedures were approved by the Institut français de recherche pour l'exploitation de la mer (IFREMER) and the Ministry of Marine Resources of French Polynesia (transfer authorization No. 3605).

Informed Consent Statement: Not applicable.

Data Availability Statement: Data can be found in Supplementary Materials section.

Acknowledgments: The authors would like to thank the Regahiga Pearl Farm (Mangareva island, Gambier archipelago, French Polynesia) for providing the pearl oysters used in this study. The authors would also like to acknowledge Virginie Chamard for her support and advice during the Raman experiments.

Conflicts of Interest: The authors declare no conflict of interest.

References

1. Rosenberg, G. A New Critical Estimate of Named Species-Level Diversity of the Recent Mollusca. *Am. Malacol. Bull.* **2014**, *32*, 308–322. [CrossRef]
2. Williams, S.T. Molluscan shell colour. *Biol. Rev.* **2016**. [CrossRef] [PubMed]
3. Cuthill, I.C.; Allen, W.L.; Arbuckle, K.; Caspers, B.; Chaplin, G.; Hauber, M.E.; Hill, G.E.; Jablonski, N.G.; Jiggins, C.D.; Kelber, A.; et al. The biology of color. *Science (80-)* **2017**, *357*. [CrossRef]
4. Kobayashi, T.; Kawahara, I.; Hasekura, O.; Kijima, A. Genetic control of bluish shell color variation in the Pacific abalone, Haliotis discus hannai. *J. Shellfish Res.* **2004**, *23*, 1153–1157.
5. Liu, X.; Wu, F.; Zhao, H.; Zhang, G.; Guo, X. A Novel Shell Color Variant of the Pacific Abalone *Haliotis Discus Hannai* Ino Subject to Genetic Control and Dietary Influence. *J. Shellfish Res.* **2009**, *28*, 419–424. [CrossRef]
6. Canales-Gómez, E.; Correa, G.; Viana, M.T. Effect of commercial carotene pigments (astaxanthin, cantaxanthin and β-carotene) in juvenile abalone *Haliotis rufescens* diets on the color of the shell or nacre. *Vet. Mex.* **2010**, *41*, 191–200.
7. Creese, R.G.; Underwood, A.J. Observations on the biology of the trochid gastropod *Austrocochlea constricta* (Lamarck) (Prosobranchia). I. Factors affecting shell-banding pattern. *J. Exp. Mar. Biol. Ecol.* **1976**, *23*, 211–228. [CrossRef]
8. Leighton, D.L. Observations on the effect of diet on shell coloration on the red abalone *Haliotis rufescens* Swainson. *Veliger* **1961**, *4*, 29–32.
9. Fox, D.L. *Biochromy, Natural Coloration of Living Things*; University of California Press: Berkeley, CA, USA, 1979.
10. Comfort, A. Acid-soluble pigments of shells; the distribution of porphyrin fluorescence in molluscan shells. *Biochem. J.* **1949**, *44*, 111–117. [CrossRef] [PubMed]
11. Comfort, A. Acid-soluble Pigments of Molluscan Shells. *Biochem. J.* **1947**, *45*, 199–204. [CrossRef]
12. Comfort, A. The pigmentation of molluscan shells. *Biochem. J.* **1950**, *45*, 208. [CrossRef]
13. Feng, D.; Li, Q.; Yu, H.; Zhao, X.; Kong, L. Comparative transcriptome analysis of the pacific oyster *Crassostrea gigas* characterized by shell colors: Identification of genetic bases potentially involved in pigmentation. *PLoS ONE* **2015**, *10*, 1–17. [CrossRef] [PubMed]
14. Yue, X.; Nie, Q.; Xiao, G.; Liu, B. Transcriptome Analysis of Shell Color-Related Genes in the Clam *Meretrix meretrix*. *Mar. Biotechnol.* **2015**, *17*, 364–374. [CrossRef] [PubMed]
15. Ding, J.; Zhao, L.; Chang, Y.; Zhao, W.; Du, Z.; Hao, Z. Transcriptome sequencing and characterization of Japanese scallop *Patinopecten yessoensis* from different shell color lines. *PLoS ONE* **2015**, *10*, 1–18. [CrossRef] [PubMed]
16. Shinohara, M.; Kinoshita, S.; Tang, E.; Funabara, D.; Kakinuma, M. Comparison of two pearl sacs formed in the same recipient oyster with different genetic background Involved in yellow pigmentation in *Pinctada fucata*. *Mar. Biotechnol.* **2018**, *20*, 594–602. [CrossRef] [PubMed]
17. Lemer, S.; Saulnier, D.; Gueguen, Y.; Planes, S. Identification of genes associated with shell color in the black-lipped pearl oyster, *Pinctada margaritifera*. *BMC Genomics* **2015**, *16*, 568. [CrossRef] [PubMed]
18. Iwahashi, Y.; Akamatsu, S. Porphyrin pigment in Black-Lip pearls and Its application to pearl identification. *Fish. Sci.* **1994**, *60*, 69–71. [CrossRef]
19. Karampelas, S.; Fritsch, E.; Makhlooq, F.; Mohamed, F.; Al-Alawi, A. Raman spectroscopy of natural and cultured pearls and pearl producing mollusc shells. *J. Raman Spectrosc.* **2019**, 1–9. [CrossRef]
20. Elen, S. Identification of yellow cultured pearls from the Black-lipped oyster *Pinctada margaritifera*. *Gems Gemol.* **2002**, *38*, 66–72. [CrossRef]
21. Caseiro, J. L'huître Perlière de Polynésie: Biominéralisation, Paramètres et Processus de Croissance, Effets Chromatiques Dans la Coquille et la Perle de *Pinctada margaritifera*. Ph.D. Thesis, Claude Bernard University Lyon 1, Lyon, France, 1993.
22. Ky, C.L.; Demmer, J.; Blay, C.; Lo, C. Age-dependence of cultured pearl grade and colour in the black-lipped pearl oyster *Pinctada margaritifera*. *Aquac. Res.* **2015**, *48*, 955–968. [CrossRef]

23. Ky, C.-L.; Le Pabic, L.; Sham Koua, M.; Nicolas, M.; Seiji, N.; Devaux, D. Is pearl colour produced from *Pinctada margaritifera* predictable through shell phenotypes and rearing environments selections? *Aquaculture* **2017**, *48*, 1041–1057. [CrossRef]
24. Ky, C.-L.; Nakasai, S.; Pommier, S.; Sham Koua, M.; Devaux, D. The Mendelian inheritance of rare flesh and shell colour variants in the black-lipped pearl oyster (*Pinctada margaritifera*). *Anim. Genet.* **2016**, *47*, 610–614. [CrossRef]
25. Ky, C.-L.; Blay, C.; Sham-Koua, M.; Vanaa, V.; Lo, C.; Cabral, P. Family effect on cultured pearl quality in black-lipped pearl oyster *Pinctada margaritifera* and insights for genetic improvement. *Aquat. Living Resour.* **2013**, *26*, 133–145. [CrossRef]
26. Le Moullac, G.; Soyez, C.; Vidal-Dupiol, J.; Belliard, C.; Fievet, J.; Sham-Koua, M.; Lo-Yat, A.; Saulnier, D.; Gaertner-Mazouni, N.; Gueguen, Y. Impact of pCO2 on the energy, reproduction and growth of the shell of the pearl oyster *Pinctada margaritifera*. *Estuar. Coast. Shelf Sci.* **2016**, *182*, 274–282. [CrossRef]
27. Ky, C.-L.; Nakasai, S.; Molinari, N.; Devaux, D. Influence of grafter skill and season on cultured pearl shape, circles and rejects in *Pinctada margaritifera* aquaculture in Mangareva lagoon. *Aquaculture* **2014**, *435*, 361–370. [CrossRef]
28. Le Moullac, G.; Soyez, C.; Latchere, O.; Vidal-Dupiol, J.; Fremery, J.; Saulnier, D.; Lo Yat, A.; Belliard, C.; Mazouni-Gaertner, N.; Gueguen, Y. *Pinctada margaritifera* responses to temperature and pH: Acclimation capabilities and physiological limits. *Estuar. Coast. Shelf Sci.* **2016**, *182*, 261–269. [CrossRef]
29. Bolger, A.M.; Lohse, M.; Usadel, B. Genome analysis Trimmomatic: A flexible trimmer for Illumina sequence data. *Bioinformatics* **2014**, *30*, 2114–2120. [CrossRef] [PubMed]
30. Le Luyer, J.; Auffret, P.; Quillien, V.; Leclerc, N.; Reisser, C.; Ky, C. Whole transcriptome sequencing and biomineralization gene architecture associated with cultured pearl quality traits in the pearl oyster, *Pinctada margaritifera*. *BMC Genom.* **2019**, *20*, 1–11. [CrossRef]
31. Trapnell, C.; Roberts, A.; Goff, L.; Pertea, G.; Kim, D.; Kelley, D.R.; Pimentel, H.; Salzberg, S.L.; Rinn, J.L.; Pachter, L. Differential gene and transcript expression analysis of RNA-seq experiments with TopHat and Cufflinks. *Nat. Protoc.* **2012**, *7*, 562–578. [CrossRef]
32. Anders, S.; Pyl, P.T.; Huber, W. Genome analysis HTSeq—A Python framework to work with high-throughput sequencing data. *Bioinformatics* **2015**, *31*, 166–169. [CrossRef]
33. Nguyen, V.H.; Lavenier, D. PLAST: Parallel local alignment search tool for database comparison. *BMC Bioinformatics* **2009**, *10*, 329. [CrossRef] [PubMed]
34. Altschul, S.F.; Madden, T.L.; Alejandro, S.A.; Zhang, J.; Zhang, Z.; Miller, W.; Lipman, D.J. Gapped BLAST and PSI-BLAST: A new generation of protein database search programs. *Nucleic Acids Res.* **1997**, *25*, 3389–3402. [CrossRef]
35. Bairoch, A.; Apweiler, R. The SWISS-PROT protein sequence database and its supplement TrEMBL in 2000. *Nucleic Acids Res.* **2000**, *28*, 45–48. [CrossRef]
36. Zdobnov, E.M.; Apweiler, R. InterProScan—An integration platform for the signature-recognition methods in InterPro. *Bioinformatics* **2001**, *17*, 847–848. [CrossRef]
37. Conesa, A.; Götz, S.; García-gómez, J.M.; Terol, J.; Talón, M.; Genómica, D.; Valenciano, I.; Agrarias, D.I.; Valencia, U.P. De Blast2GO: A universal tool for annotation, visualization and analysis in functional genomics research. *BMC Bioinform.* **2005**, *21*, 3674–3676. [CrossRef]
38. Wright, R.M.; Aglyamova, G.V.; Meyer, E.; Matz, M. V Gene expression associated with white syndromes in a reef building coral, *Acropora hyacinthus*. *BMC Genom.* **2015**, *16*, 371. [CrossRef]
39. Love, M.I.; Huber, W.; Anders, S. Moderated estimation of fold change and dispersion for RNA-seq data with DESeq2. *Genome Biol.* **2014**, *15*, 550. [CrossRef] [PubMed]
40. Kanehisa, M.; Goto, S. KEGG: Kyoto Encyclopedia of Genes and Genomes. *Nucleic Acids Res.* **2000**, *28*, 27–30. [CrossRef]
41. Pettersen, E.F.; Goddard, T.D.; Huang, C.C.; Couch, G.S.; Greenblatt, D.M.; Meng, E.C.; Ferrin, T.E. UCSF Chimera—A visualization system for exploratory research and analysis. *J. Struct. Biol.* **2004**, *157*, 281–287. [CrossRef]
42. Song, G.; Li, Y.; Cheng, C.; Zhao, Y.; Gao, A.; Zhang, R.; Joachimiak, A.; Shaw, N.; Liu, Z. Structural insight into acute intermittent porphyria. *FASEB J.* **2009**, *23*, 396–404. [CrossRef]
43. Maiti, R.; Van Domselaar, G.H.; Zhang, H.; Wishart, D.S. SuperPose: A simple server for sophisticated structural superposition. *Nucleic Acids Res.* **2004**, *32*, 590–594. [CrossRef]
44. Bonnier, F.; Byrne, H.J. Understanding the molecular information contained in principal component analysis of vibrational spectra of biological systems. *Analyst* **2012**, *137*, 322–332. [CrossRef]
45. Buzgar, N.; Ionut Apopei, A. The Raman study of certain carbonates. *Geologie* **2009**, *55*, 97–112.
46. Aphalo, P.J. *The r4photobiology Suite: Spectral Irradiance*; Package 'ggspectra'; CRAN: Auckland, New-Zealand, 2015. [CrossRef]
47. Barnard, W.; De Waal, D. Raman investigation of pigmentary molecules in the molluscan biogenic matrix. *J. Raman Spectrosc.* **2006**, *37*, 342–352. [CrossRef]
48. Williams, S.T.; Lockyer, A.E.; Dyal, P.; Nakano, T.; Churchill, C.K.C.; Speiser, D.I. Colorful seashells: Identification of haem pathway genes associated with the synthesis of porphyrin shell color in marine snails. *Ecol. Evol.* **2017**, *7*, 10379–10397. [CrossRef]
49. Pirone, C.; Quirke, J.M.E.; Priestap, H.A.; Lee, D.W. Animal pigment bilirubin discovered in plants. *J. Am. Chem. Soc.* **2009**, *131*, 2830. [CrossRef]
50. Kikuchi, G.; Yoshida, T.; Noguchi, M. Heme oxygenase and heme degradation. *Biochem. Biophys. Res. Commun.* **2005**, *338*, 558–567. [CrossRef]

51. Shamim, G.; Ranjan, S.K.; Pandey, D.M.; Ramani, R. Biochemistry and biosynthesis of insect pigments. *Eur. J. Entomol.* **2014**, *111*, 149–164. [CrossRef]
52. Schallreuter, K.U.; Schulz-Douglas, V.; Bünz, A.; Beazley, W.; Körner, C. Pteridines in the control of pigmentation. *J. Invest. Dermatol.* **1997**, *109*, 31–35. [CrossRef]
53. Siracusa, L.D. The agouti gene: Turned on to yellow. *Trends Genet.* **1994**, *10*, 423–428. [CrossRef]
54. Bagnara, J.T.; Matsumoto, J.; Ferris, W.; Frost, S.K.; William, A.; Tchen, T.T.; Taylor, J.D. Common origin of pigment cells. *Science* **1979**, *203*, 410–415. [CrossRef]
55. Sonthalia, S.; Daulatabad, D.; Sarkar, R. Glutathione as a skin whitening agent: Facts, myths, evidence and controversies. *Indian J. Dermatol.* **2016**, *82*, 262. [CrossRef]
56. Williams, S.T.; Ito, S.; Wakamatsu, K.; Goral, T.; Edwards, N.P.; Wogelius, R.A. Identification of shell colour pigments in marine snails *Clanculus pharaonius* and *C. margaritarius* (Trochoidea; Gastropoda). *PLoS ONE* **2016**, *11*, 1–25. [CrossRef]
57. Pearson, W.R. An introduction to sequence similarity ("homology") searching. *Curr. Protoc. Bioinform.* **2013**, *42*, 1–8. [CrossRef] [PubMed]
58. Furuichi, T.; Yoshikawa, S.; Miyawakft, A.; Wadat, K.; Maedat, N.; Mikoshiba, K. Primary structure and functional expression of the inositol 1, 4, 5-trisphosphate-binding protein P 400. *Nature* **1989**, *342*, 714–716. [CrossRef] [PubMed]
59. Wek, R.C.; Cannon, J.F.; Dever, T.E.; Hinnebuschl, A.G. Truncated protein phosphatase GLC7 restores translational activation of GCN4 expression in yeast mutants defective for the eIF-2a kinase GCN2. *Mol. Cell. Biol.* **1992**, *12*, 5700–5710. [CrossRef]
60. Ma, C.H.E.; Marassi, F.M.; Jones, D.H.; Straus, S.K.; Bour, S.; Strebel, K.; Schubert, U.; Oblatt-montal, M.; Montal, M.; Opella, S.J. Expression, purification, and activities of full-length and truncated versions of the integral membrane protein Vpu from HIV-1. *Protein Sci.* **2002**, *11*, 546–557. [CrossRef]
61. Farre, B.; Dauphin, Y. Lipids from the nacreous and prismatic layers of two Pteriomorpha Mollusc shells. *Comp. Biochem. Physiol. B Biochem. Mol. Biol.* **2009**, *152*, 103–109. [CrossRef]
62. Marie, B.; Joubert, C.; Tayalé, A.; Zanella-cléon, I. Different secretory repertoires control the biomineralization processes of prism and nacre deposition of the pearl oyster shell. *Proc. Natl. Acad. Sci. USA* **2013**, *109*, 20986–20991. [CrossRef] [PubMed]
63. Chang, F.; Li, G.; Haws, M.; Niu, T. Element concentrations in shell of *Pinctada margaritifera* from French Polynesia and evaluation for using as a food supplement. *Food Chem.* **2007**, *104*, 1171–1176. [CrossRef]
64. Wang, H.; Osseiran, S.; Igras, V.; Nichols, A.J.; Roider, E.M.; Pruessner, J.; Tsao, H.; Fisher, D.E.; Evans, C.L. In vivo coherent Raman imaging of the melanomagenesis-associated pigment pheomelanin. *Sci. Rep.* **2016**, *6*, 1–10. [CrossRef] [PubMed]
65. Ky, C.L.; Lo, C.; Planes, S. Mono- and polychromatic inner shell phenotype diversity in *Pinctada margaritifera* donor pearl oysters and its relation with cultured pearl colour. *Aquaculture* **2017**, *468*, 199–205. [CrossRef]
66. Stenger, P.-L.; Vidal-Dupiol, J.; Reisser, C.; Planes, S.; Ky, C. Colour plasticity in the shells and pearls of animal graft model *Pinctada margaritifera* through colour quantification with the HSV system. *Sci. Rep.* **2019**, *75*, 20. [CrossRef]
67. Ky, C.L.; Quillien, V.; Broustal, F.; Soyez, C.; Devaux, D. Phenome of pearl quality traits in the mollusc transplant model *Pinctada margaritifera*. *Sci. Rep.* **2018**, *8*, 1–11. [CrossRef]
68. Paoli, M.; Marles-wright, J.O.N.; Smith, A.N.N. Structure—Function relationships in heme-proteins. *DNA Cell Biol.* **2002**, *21*. [CrossRef]
69. Jordan, P.M.; Warren, M.J. Evidence for a dipyrromethane cofactor at the catalytic of E. coli porphobilinogen deaminase. *FEBS Lett.* **1987**, *225*, 87–92. [CrossRef]
70. Lim, C.K.; Peters, T.J. Urine and faecal porphyrin profiles by reversed-phase high-performance liquid chromatography in the porphyrias. *Clin. Chim. Acta* **1984**, *139*, 55–63. [CrossRef]
71. Doss, M.O. Dual porphyria in double heterozygotes with porphobilinogen deaminase and uroporphyrinogen decarboxylase deficiencies. *Clin. Genet.* **1989**, *35*, 146–151. [CrossRef] [PubMed]
72. Shoolingin-Jordan, P.M. Porphobilinogen deaminase and uroporphyrinogen III synthase: Structure, molecular biology, and mechanism. *J. Bioenerg. Biomembr.* **1995**, *27*, 181–195. [CrossRef]
73. Kainrath, S.; Stadler, M.; Reichhart, E.; Distel, M.; Janovjak, H. Green-light-induced inactivation of receptor signaling using cobalamin-binding domains. *Angew. Chem. Int. Ed.* **2017**, *56*, 4608–4611. [CrossRef]
74. Ajioka, R.S.; Phillips, J.D.; Kushner, J.P. Biosynthesis of heme in mammals. *Biochim. Biophys. Acta (BBA) Mol. Cell Res.* **2006**, *1763*, 723–736. [CrossRef] [PubMed]
75. Ravera, O.; Cenci, R.; Beone, G.M.; Dantas, M.; Lodigiani, P. Trace element concentrations in freshwater mussels and macrophytes as related to those in their environment. *J. Limnol.* **2003**, *62*, 61–70. [CrossRef]
76. Meyer, U.A.; Strand, L.J.; Doss, M.; Rees, A.C.; Marver, H.S. Intermittent acute porphyria—demonstration of a genetic defect in porphobilinogen metabolism. *N. Engl. J. Med.* **1972**, *286*, 1277–1282. [CrossRef]
77. Fox, D.L. *Animal Biochromes and Structural Colours: Physical, Chemical, Distributional & Physiological Features of Coloured Bodies in the Animal World*; University of California: Oakland, CA, USA, 1976.
78. Tenhunen, R.; Marver, H.S.; Schmid, R. The enzymatic conversion of heme to bilirubin by microsomal heme oxygenase. *Proc. Natl. Acad. Sci. USA* **1968**, *61*, 748–755. [CrossRef] [PubMed]
79. Singleton, J.W.; Laster, L. Biliverdin reductase of guinea pig liver. *J. Biol. Chem.* **1965**, *240*, 4780–4789. [CrossRef]

80. Bouétard, A.; Noirot, C.; Besnard, A.L.; Bouchez, O.; Choisne, D.; Robe, E.; Klopp, C.; Lagadic, L.; Coutellec, M.A. Pyrosequencing-based transcriptomic resources in the pond snail *Lymnaea stagnalis*, with a focus on genes involved in molecular response to diquat-induced stress. *Ecotoxicology* **2012**, *21*, 2222–2234. [CrossRef]
81. Jansen, P. The enzyme-catalyzed formation of bilirubin diglucuronide by a solubilized preparation from cat liver microsomes. *Biochim. Biophys. Acta (BBA) General Subj.* **1974**, *338*, 170–182. [CrossRef]
82. Nawa, S. The Structure of the Yellow Pigment from *Drosophila*. *Bull. Chem. Soc. Jpn.* **1960**, *33*, 1555–1560. [CrossRef]
83. Blay, C.; Planes, S.; Ky, C.L. Donor and recipient contribution to phenotypic traits and the expression of biomineralisation genes in the pearl oyster model *Pinctada margaritifera*. *Sci. Rep.* **2017**, *7*, 1–12. [CrossRef]
84. McGraw, K.J. Mechanics of uncommon colors: Pterins, porphyrins, and psittacofulvins. In *Bird Coloration*; Harvard University Press: Cambridge, MA, USA, 2006; pp. 354–398.
85. Grant, H.E.; Williams, S.T. Phylogenetic distribution of shell colour in Bivalvia (Mollusca). *Biol. J. Linn. Soc.* **2018**, *125*, 377–391. [CrossRef]
86. Mills, M.G.; Patterson, L.B. Not just black and white: Pigment pattern development and evolution in vertebrates. *Semin. Cell Dev. Biol.* **2009**, *20*, 72–81. [CrossRef] [PubMed]
87. Petrier, C.; Dupuy, C.; Jardon, P.; Gautron, R. The configurations in solution of the biliverdin TXγ phorcabilin and isophorcabilin dimethyl esters. *Tetrahedron Lett.* **1981**, *22*, 855–858. [CrossRef]
88. Choussy, M.; Barbier, M. Photo-oxidation and photoprotection in the IXγ bile pigment series: A comparison of the photoprotective roles of pterobilin, phorcabilin and sarpedobilin in vitro. *Tetrahedron* **1983**, *39*, 1915–1918. [CrossRef]
89. Ju, Z.Y.; Viljoen, C.; Hutchinson, P.; Reinicke, J.; Horgen, F.D.; Howard, L.; Lee, C. Effects of diets on the growth performance and shell pigmentation of Pacific abalone. *Aquac. Res.* **2016**, *47*, 4004–4014. [CrossRef]
90. Sassa, S. Why heme needs to be degraded to iron, biliverdin IX, and carbon monoxide? *Antioxid. Redox Signal.* **2004**, *6*, 819–824. [CrossRef] [PubMed]
91. Kikkawa, H.; Fujito, S. Nature of pigments derived from tyrosine and tryptophan in Animals. *Science* **1955**, *121*, 43–47. [CrossRef] [PubMed]
92. Kumudha, A.; Sarada, R. Effect of different extraction methods on vitamin B12 from blue green algae, *Spirulina platensis*. *Pharm. Anal. Acta* **2015**, *6*, 2–7. [CrossRef]
93. Roper, J.M.; Raux, E.; Brindley, A.A.; Schubert, H.L.; Gharbia, S.E.; Shah, H.N.; Warren, M.J. The enigma of cobalamin (vitamin B12) biosynthesis in *Porphyromonas gingivalis*: Identification and characterization of a functional corrin pathway. *J. Biol. Chem.* **2000**, *275*, 40316–40323. [CrossRef]
94. Kondo, H.; Kolhouse, J.F.; Allen, R.H. Presence of cobalamin analogues in animal tissues. *Proc. Natl. Acad. Sci. USA* **1980**, *77*, 817–821. [CrossRef] [PubMed]
95. Roth, J.; Lawrence, J.; Bobik, T. Cobalamin (Coenzyme B12): Synthesis and Biological Significance. *Ann. Rev. Microbiol.* **1996**, *50*, 137–181. [CrossRef] [PubMed]
96. Croft, M.T.; Lawrence, A.D.; Raux-Deery, E.; Warren, M.J.; Smith, A.G. Algae acquire vitamin B12 through a symbiotic relationship with bacteria. *Nature* **2005**, *438*, 90–93. [CrossRef]
97. Xie, B.; Bishop, S.; Stessman, D.; Wright, D.; Spalding, M.H.; Halverson, L.J. *Chlamydomonas reinhardtii* thermal tolerance enhancement mediated by a mutualistic interaction with vitamin B12-producing bacteria. *ISME J.* **2013**, *7*, 1544–1555. [CrossRef]
98. Ruaux, C.G. Cobalamin in companion animals: Diagnostic marker, deficiency states and therapeutic implications. *Vet. J.* **2013**, *196*, 145–152. [CrossRef]
99. LeBlanc, J.G.; Milani, C.; de Giori, G.S.; Sesma, F.; van Sinderen, D.; Ventura, M. Bacteria as vitamin suppliers to their host: A gut microbiota perspective. *Curr. Opin. Biotechnol.* **2013**, *24*, 160–168. [CrossRef]
100. Pathare, P.M.; Wilbur, D.S.; Heusser, S.; Quadros, E.V.; Mcloughlin, P.; Morgan, A.C. Synthesis of Cobalamin—Biotin Conjugates That Vary in the Position of Cobalamin Coupling. Evaluation of Cobalamin Derivative Binding to Transcobalamin II. *Bioconjug. Chem.* **1996**, *7*, 217–232. [CrossRef] [PubMed]
101. Villanueva, B.; Pong-Wong, R.; Woolliams, J.A. Marker assisted selection with optimised contributions of the candidates to selection. *Genet. Sel. Evol.* **2002**, *34*, 679–703. [CrossRef] [PubMed]
102. Dekkers, J.C.M. Marker-assisted selection for commercial crossbred performance. *J. Anim. Sci.* **2007**, *85*, 2104–2114. [CrossRef]

ANNEXE 13

frontiers in Genetics

ORIGINAL RESEARCH
published: 19 March 2021
doi: 10.3389/fgene.2021.630290

Environmentally Driven Color Variation in the Pearl Oyster *Pinctada margaritifera* var. *cumingii* (Linnaeus, 1758) Is Associated With Differential Methylation of CpGs in Pigment- and Biomineralization-Related Genes

*Pierre-Louis Stenger[1,2], Chin-Long Ky[1,2], Céline M. O. Reisser[1,3], Céline Cosseau[4], Christoph Grunau[4], Mickaël Mege[1,5], Serge Planes[6] and Jeremie Vidal-Dupiol[2]**

[1] IFREMER, UMR 241 Écosystèmes Insulaires Océaniens, Labex Corail, Centre du Pacifique, Tahiti, French Polynesia, [2] IHPE, Université de Montpellier, CNRS, IFREMER, Université de Perpignan Via Domitia, Montpellier, France, [3] MARBEC, Université de Montpellier, CNRS, IFREMER, IRD, Montpellier, France, [4] IHPE, Université de Montpellier, CNRS, IFREMER, Université de Perpignan Via Domitia, Perpignan, France, [5] IFREMER, PDG-RBE-SGMM-LGPMM, La Tremblade, France, [6] EPHE-UPVD-CNRS, USR 3278 CRIOBE, Labex Corail, PSL Research University, Université de Perpignan, Perpignan, France

OPEN ACCESS

Edited by:
Stephanie McKay,
University of Vermont, United States

Reviewed by:
Silvio Zaina,
University of Guanajuato, Mexico
Yu Jiao,
Guangdong Ocean University, China

***Correspondence:**
Jeremie Vidal-Dupiol
jeremie.vidal.dupiol@ifremer.fr

Specialty section:
This article was submitted to Epigenomics and Epigenetics, a section of the journal Frontiers in Genetics

Received: 17 November 2020
Accepted: 19 February 2021
Published: 19 March 2021

Citation:
Stenger P-L, Ky C-L, Reisser CMO, Cosseau C, Grunau C, Mege M, Planes S and Vidal-Dupiol J (2021) Environmentally Driven Color Variation in the Pearl Oyster Pinctada margaritifera var. cumingii (Linnaeus, 1758) Is Associated With Differential Methylation of CpGs in Pigment- and Biomineralization-Related Genes. Front. Genet. 12:630290. doi: 10.3389/fgene.2021.630290

Today, it is common knowledge that environmental factors can change the color of many animals. Studies have shown that the molecular mechanisms underlying such modifications could involve epigenetic factors. Since 2013, the pearl oyster *Pinctada margaritifera* var. *cumingii* has become a biological model for questions on color expression and variation in Mollusca. A previous study reported color plasticity in response to water depth variation, specifically a general darkening of the nacre color at greater depth. However, the molecular mechanisms behind this plasticity are still unknown. In this paper, we investigate the possible implication of epigenetic factors controlling shell color variation through a depth variation experiment associated with a DNA methylation study performed at the whole genome level with a constant genetic background. Our results revealed six genes presenting differentially methylated CpGs in response to the environmental change, among which four are linked to pigmentation processes or regulations (*GART*, *ABCC1*, *MAPKAP1*, and *GRL101*), especially those leading to darker phenotypes. Interestingly, the genes *perlucin* and *MGAT1*, both involved in the biomineralization process (deposition of aragonite and calcite crystals), also showed differential methylation, suggesting that a possible difference in the physical/spatial organization of the crystals could cause darkening (iridescence or transparency modification of the biomineral). These findings are of great interest for the pearl production industry, since wholly black pearls and their opposite, the palest pearls, command a higher value on several markets. They also open the route of epigenetic improvement as a new means for pearl production improvement.

Keywords: pearl oyster, environmental pressure, depth, color change, pigmentation, DNA methylation, methylome characterization

INTRODUCTION

Pearls have captivated and amazed human civilization since 7500 BP (Charpentier et al., 2012) and have formed the basis for economic development of several tropical countries. French Polynesia started to trade pearls with Europeans at the end of the 18th century (Southgate and Lucas, 2011) and has been an industrial producer since 1964 (Le Pennec, 2010). Today, cultured pearl farming represents the second economic resource of the country, just behind tourism (Ky et al., 2019). However, since 2001, an unprecedented economic crisis has endangered the French Polynesian pearl farming sector due to the overproduction of low quality pearls (Bouzerand, 2018). To remediate to this socio-economic crisis, the policy of producing "less but better" was adopted in 2013 (Ky et al., 2013). Since then, production has focused on obtaining cultured pearls with high market value, by selecting traits such as pearl color.

Two individuals are needed to produce a pearl, a donor and a recipient oyster. The sacrificed donor is used to provide a piece of mantle (the biomineralizing graft) which is placed, together with a small marble of nacre, into the gonad of the recipient oyster. Donor oysters are selected for their inner-shell color, since the color of a cultured pearl is determined by that of the donor oyster (Ky et al., 2013). Recipient oysters are selected for their vigor. The Polynesian black-lipped pearl oyster, *Pinctada margaritifera* var. *cumingii* (Linnaeus, 1758) is the pearl oyster species showing the largest range of inner shell color (Ky et al., 2013, 2017), therefore offering a wide range of pearl colors and shades, like dark, pastel, silver, peacock, red, golden, green, blue, and even rainbow (Ky et al., 2014; Stenger et al., 2019). Moreover, the color of this bivalve has both a structural (iridescence; Liu et al., 1999) and a biological (pigments; Iwahashi and Akamatsu, 1994) basis. While the genetic determination of this color has been partly demonstrated (Ky et al., 2013, 2017), several environmental factors are also known to affect the shell color (Joubert et al., 2014; Le Pabic et al., 2016; Le Moullac et al., 2018), such as the depth at which an oyster is grown (Stenger et al., 2019). In this latter work, authors demonstrated that the transplantation of oysters from the sub-surface (−4 m) to the bottom of the lagoon (−30 m) significantly darkens the inner shell color compared with oysters maintained at the sub-surface. This induced phenotype was persistent through time ("enduring"), even after the oysters were returned to shallow water, which would seem to indicate an epigenetic control mechanism rather than a direct environmental influence acting on the darkening of the shell color (Stenger et al., 2019).

Since the first definition of epigenetic by Waddington in the late 1930s, epigenetic received many definitions (Nicoglou and Merlin, 2017). In this work we have selected the definition proposed by Russo et al. (1996), e.g., *"epigenetic is the study of mitotically and/or meiotically heritable changes in gene function that cannot be explained by changes in DNA sequence"* (Russo et al., 1996). Mechanistically, this memory function is based on changes in chromatin structure, such as non-coding RNA and/or histone modifications and/or DNA methylation. Here, we use the term epigenetics to describe any changes in DNA methylation that occur upon environmental cues. Coloration mediates an organism's relationship with their environment in important ways including anti-predator defenses, social signaling, thermoregulation, or protection (Cuthill et al., 2017). Several species are known to change their coloration more than once in their lifetime in response to environmental triggers to reach an optimal phenotype in a new environment. To increase their camouflage the arctic hare *Lepus arcticus* (Ross, 1819), the ermine *Mustela erminea* (Linnaeus, 1758), and the ptarmigan *Lagopus muta* (Montin, 1776) changed their coat color from brown or gray in the summer to white in the winter (Zimova et al., 2018). These changes are known to be induced by temperature, photoperiod, and/or food rarefaction (Zimova et al., 2018). The corresponding changes in color expression could be brought by epigenetic processes (Hu and Barrett, 2017) like in mouses (Dolinoy, 2008). Indeed, the most striking example of color change in mammals rely on the environmentally induced differential DNA methylation of the intracisternal A-particle gene located upstream of the agouti locus (Dolinoy et al., 2006; Dolinoy, 2008). In Mollusca, a few epigenetic studies have been made, especially on color expression and variation. To date, Feng et al. (2018) provided a catalog of long non-coding RNA (lncRNA) expressed in the mantle of the Pacific oyster *Crassostrea gigas* (Thunberg, 1793). These authors suggested that these lncRNAs may affect the expression of pigment-related genes such as tyrosinase-like proteins, dopamine, beta-monooxygenase, chorion peroxidase, or cytochrome P450 2U1, thus leading to different shell color phenotypes. More recently, the same group (Feng et al., 2020) have studied the role of microRNAs in the regulation of the shell color of *Crassostrea gigas*. In this study, four miRNAs (lgi-miR-315, lgi-miR-96b, lgi-miR-317, and lgi-miR-153) were found closely associated with shell color along with the regulation of Cytochrome P450 2U1, Tyrosinase-like protein 2 and 3. The authors concluded that lgi-miR-317, its targeted mRNA encoding peroxidase, and the lncRNA TCONS_00951105 might play a key role in shell melanin synthesis.

Because color phenotype is important for the pearl market and the phenotypic plasticity of this trait is associated with the putative involvement of epigenetic mechanisms, the study of these mechanisms opens a new avenue for improvement in the pearl industry with, for example, the development of epi-markers for environmentally induced color variation testing. As a first step in exploring a possible interaction between epigenetic mechanisms and color variation, we designed a depth variation experiment to induce environmentally driven color variation. In order to disentangle the genetic factors from the epigenetic ones influencing color variation, a non-lethal sampling design was used enabling us to monitor changes in DNA methylation over time and depth within the same individuals (constant genotypes). DNA methylation was studied at the whole genome scale by whole-genome bisulfite sequencing and provided evidence for an epigenetic control of pearl oyster color variation. This approach enabled us to find any differences in DNA methylation in pearl oysters after a period at increased depth and, when this occurred, to examine whether genes related to pigmentation and/or biomineralization processes were affected by such changes. Results of this kind could allow the pearl industry to turn to more sustainable production strategies.

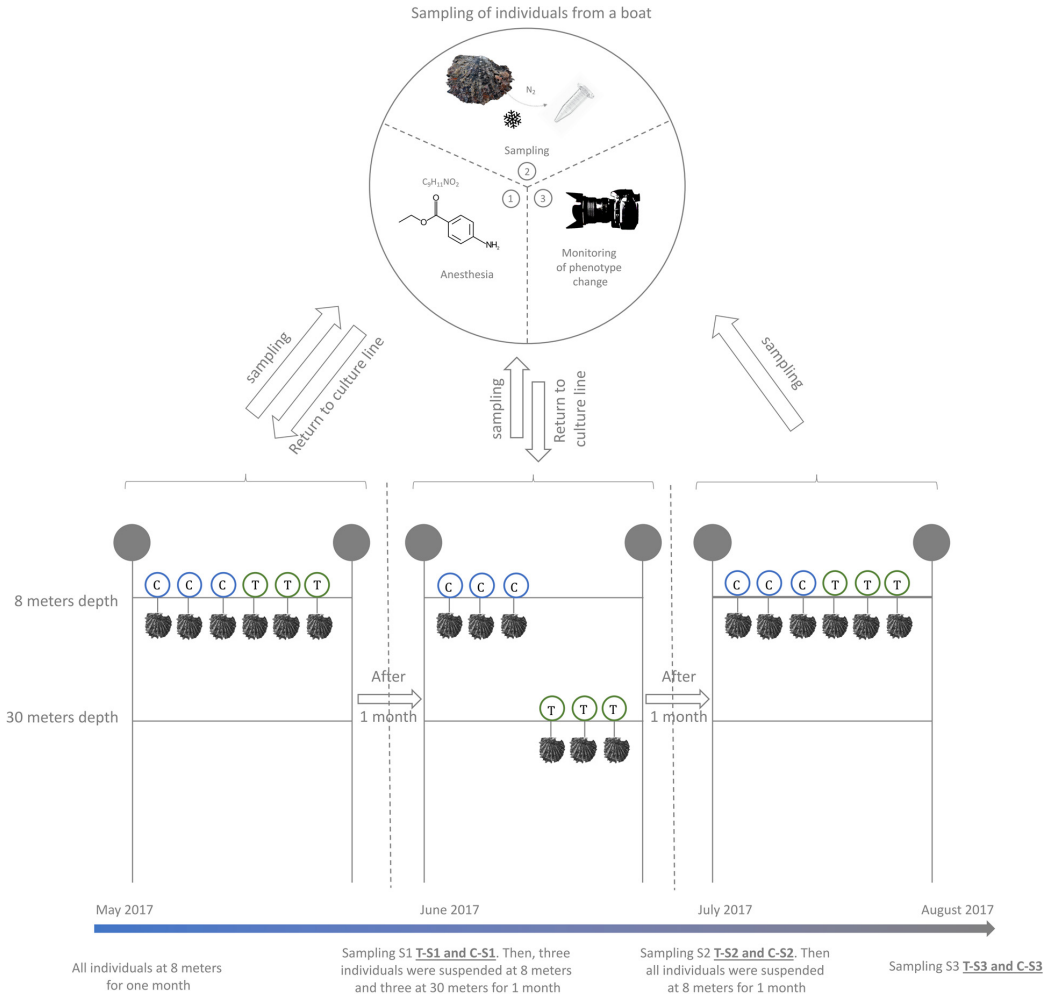

FIGURE 1 | Design of the Yo-Yo experiment. Six *P. margaritifera* individuals were used for this experiment. Three individuals were maintained at a depth of 8 m during the whole experiment and were used as a control (C – in blue circles). The three other individuals were subjected to depth variation treatment (T – in green circles). A non-lethal sampling of mantle tissue was made every month at the time of the depth change.

MATERIALS AND METHODS

Biological Material and the Yo-Yo Experiment

In order to trigger an environmentally driven color change of the inner shell of *P. margaritifera*, we set up an *in situ* "yo-yo" experiment (May to August 2017) (**Figure 1**). Six individuals of 4 years of age (approximately 14 cm height) originating from three different families (two individuals per family Stenger et al., in press) were used. These six individuals were first maintained at 8 m depth for 1 month (May 2017). Then, three of them (1 from each family) were selected and transferred to 30 m depth (treatment) for environmental pressure while the three others were left at 8 m (control). This exposure was maintained for 1 month (June 2017). Then, the three pearl oysters that had been placed at 30 m were transferred back to 8 m depth for a final month of exposure (July 2017). During each transfer, a piece of mantle (the biomineralizing tissue responsible for the inner shell coloration) was sampled by a non-lethal method: (i) oysters were anesthetized in 20 L seawater containing 200 mL benzocaine at 120 g/L 96° ethanol under air aeration; (ii) they opened their valves under the effect of the benzocaine, a 5 mm^3 fragment of the mantle was carefully sampled with tweezers and scissors; (iii) the sample was flash frozen in liquid nitrogen. Alongside the sampling of the mantle, the color of the inner shell of each individual (control and treatment) was filmed with a mini photo studio for color variation analysis. This mini standardized photo studio was composed of a tripod supporting a Nikon D3100 reflex camera equipped with a Nikon 18-55VR lens. This set up was used to film the reflection of the inner shell color on a small mirror (spatula). To assess constant exposition to light, all films were made under a blackout drape with three white LED lamps.

Color Variation Analysis

For each sample, ten screenshots from the films were randomly captured and analyzed for color variation. Color was quantified

and qualified using the R package *ImaginR* V.2 (Stenger, 2017) as previously described (Stenger et al., 2019). A Shapiro test (stats v3.5.0 R package) was used to assess the normal distribution of the data. The average saturation and darkness for each sample were calculated from all ten screenshots, and a Wilcoxon test (*stats v3.5.0* R package based on Hollander et al., 1973 and Royston, 1995) was used to test for any difference between the groups.

DNA Extraction and BS-seq

DNA was extracted with the QIAamp DNA Mini Kit (QIAGEN®, Cat No./ID: 51306) following manufacturer's recommendations, with the addition of two steps: (i) a RNase A treatment to remove RNA and (ii) after overnight digestion the addition of 50 µL of a saturated KCl solution (34 g KCl/100 g H_2O) and a centrifugation at 14,000*g* for 15 min to remove the mucopolysaccharides (Sokolov, 2000). DNA quality and quantity were assessed with a NanoDrop™ 2000 and 1.2% agarose gel electrophoresis. Bisulfite-conversion, library construction, and sequencing (2 × 150 bp) were performed by Genome Québec (MPS Canada) on an Illumina HiSeq X.

Bioinformatics Pipeline

Analyses were performed on the Ifremer Datarmor cluster[1]. Raw read quality was assessed with FastQC (Andrews, 2010; **Supplementary Table 1**). Reads were cleaned and adaptors removed with Trimmomatic (Bolger et al., 2014) (V. 0.36 – illuminaclip 2:30:10; leading 28, trailing 28, and minlen 40). Bismark aligner (Krueger and Andrews, 2011) (V. 0.19) was used to map reads on the draft genome of *P. margaritifera* (Reisser et al., 2020) using the following parameters: multi-seed length of 30 bp, 0 mismatches, default minimum alignment score function. Deduplication was done with Deduplicate_bismark (Krueger and Andrews, 2011). Bed files for methylome characterization were obtained with Bismark_methylation_extractor (Krueger and Andrews, 2011). All scripts are provided on GitHub (PLStenger/Pearl_Oyster_Colour_BS_Seq/00_scripts). Raw reads are available through the NCBI Sequence Read Archive (SRA, BioProject PRJNA663978, BioSample SAMN16191417 to SAMN16191446).

Methylation Calling, Methylome Characterization, and Differential Methylation Analysis

The R package *Methylkit* (Akalin et al., 2012) (V. 1.11.0) was used for methylation calling in CpG, CHH, and CHG contexts using a minimum coverage of 10, directly from BAM files with *processBismarkAln*. *Methylkit* was also used for methylation characterization in the CpG, CHH, and CHG contexts, as well as for the coverage calculation and clustering analysis (ward clustering correlation distance method). The average gene methylation was calculated with DeepTools V. 3.3.0 (Ramírez et al., 2014). The gene body methylation rate (GBMR), corresponding to the CpG methylation rate, was calculated with the map function from bedtools V. 2.27.1 (Quinlan and Hall, 2010).

[1]https://wwz.ifremer.fr/pcdm/Equipement

The mantle' gene expression data used for methylation/gene expression correlation analysis came from individuals studied in Stenger et al., in press (SRA BioProject PRJNA521849). Briefly, RNA sequencing was done using high quality RNA extracted from twelve individuals. Library construction and sequencing was performed (Paired–end 100-bp; Illumina® HiSeq® 4000) by Génome Québec (MPS Canada). Read quality check and trimming were done as described in the section "Bioinformatics Pipeline." Cleaned reads were paired-mapped against the *P. margaritifera* draft genome with TopHat (V1.4.0) (Trapnell et al., 2012). Cufflinks (V2.2.1.0) and Cuffmerge (V2.2.1.0) were used to assemble and merge the transcriptome produced for each library, respectively (Trapnell et al., 2012). HTSeq-count (V0.6.1) (Anders et al., 2015) was used to count read-mapped per transcript. The average of the twelve count files was computed and the RPKM method was used for gene expression data normalization as previously done in Wang et al., 2014.

To identify the effect of the depth treatment, differentially methylated CpGs (DMCpGs) were identified with the *getMethylDiff* function of the R package *Methylkit*, with difference >25% and q value < 0.05 for CpG positions between depth treatment and control oysters at each sampling time.

Functional Analysis of Differentially Methylated Genes

An annotation file was obtained following the first three steps of https://github.com/enormandeau/go_enrichment, completed with PLASTX (Nguyen and Lavenier, 2009) against UniProt-Swiss-Prot and TrEMBL (e-value at 1×10^{-3}). A protein domain search was then performed with InterProScan. Finally, Gene Ontology terms were assigned with Blast2GO by combining information from the two annotation files (Conesa et al., 2005).

GOATOOLS (Klopfenstein et al., 2018) was used to test for enrichment of GO terms in a selected set of genes (significantly differentially methylated, lowly and highly methylated), using a Fisher's exact test. Histograms showing the GO terms enrichment of were generated with the *ggplot2* R package (Wickham and Chang, 2019) (V. 2.2.1).

RESULTS

Depth Variation Induces Significant Darkening

The color variation analysis with the *ImaginR* package detected no significant modification of hue, saturation or darkness among the controls during the 3 months of the "yo-yo" experiment (pairwise Wilcoxon tests with P values > 0.05). Among the samples subjected to the treatment, no significant change occurred for hue or saturation during the 3 months of the experiment. However, a significant difference in darkness (pairwise Wilcoxon tests with P values < $1.10e^{-5}$) was detected, with an increase in the darkness value during the month at 30 m depth. This increase was still visible and significant after the oysters were returned to 8 m depth for 1 month (pairwise Wilcoxon tests with P values < $1.10e^{-5}$; **Table 1**).

Raw data are available for download using the following links (screenshots: https://figshare.com/articles/dataset/ImaginR_raw_data_screenshots_zip/14049983; videos: https://figshare.com/articles/dataset/ImaginR_raw_data_videos_zip/14049986).

Read Processing and Read Mapping to the Reference Genome

For the control, Illumina sequencing produced averages of 105,505,318 (±1,514,514; n = 3), 103,770,226 (±5,087,254; n = 3), and 103,490,158 (±5,509,306; n = 3) raw sequence reads for sampling times 1, 2, and 3, respectively. For the depth treatment, averages of 98,184,541 (±6,186,502; n = 3), 104,727,236 (±6,141,350; n = 3), and 113,132,278 (±4,306,828; n = 3) raw sequence reads were produced for sampling times 1, 2, and 3, respectively. After cleaning and filtering, averages of 101,575,689 (±1,584,202), 100,159,677 (±5,076,306), and 100,073,964 (±5,415,409) reads were kept for the control, and 94,669,211 (±5,877,099), 101,048,705 (±6,094,775), and 109,246,931 (±4,195,331) for the depth treatment, for the three successive sampling times, respectively. Filtered reads were mapped on the reference genome with Bismark and showed similar mapping rates for all samples (∼32.1%) (**Supplementary Table 2**). PCR duplicates were removed and represented, on average, 0.059% (±0.002) of the total reads.

Characterization of the *P. margaritifera* Mantle Methylome

Methylation in the *P. margaritifera* mantle displayed a mosaic pattern with an enrichment in the gene showing a CpG methylation rate of 22.81% in introns, 17.32% in exons, and an average of 18.26% in gene body (**Figures 2A,B**). A slight enrichment in the 3 kbps upstream (12.67%) and downstream (16.58%) of genes (**Figures 2A,B**) is also found. The whole genome CpG methylation rate is equal to 11.53% on average.

The fractionation of gene body methylation rate (**Figure 2C**) shows a bimodal distribution characterized by two peaks. This distribution enables the classification of genes into two sets: the "lowly" methylated genes (0.00–0.19% methylation – rank 0–0.2 and marked as "1" **Figure 2C**) and the "highly" methylated genes (0.50–40.12% of methylation; 40.12% is the maximum methylation found in a gene in these data – rank 0.5–1 and marked as "2" **Figure 2C**). The enrichment analysis performed on the lowly methylated genes showed an overrepresentation of GO terms involved in reproductive process functions, such as "oocyte maturation" (GO:0001556), "primary sex determination" (GO:0007539), "male meiosis I" (GO:0007141), etc., cellular signaling, such as "negative regulation or cellular response to drug" (GO:0048523), "negative regulation of phospholipid metabolic process" (GO:0071072), etc., and "androgen receptor signaling pathway" (GO:0030521). In the highly methylated genes set, the enrichment analysis showed an overrepresentation of GO terms involved in housekeeping functions, such as "mRNA regulation" (GO:0043488), "mRNA splice site regulation" (GO:0006376), "ribosomal small unit assembly" (GO:0000028), "transcription-dependent tethering of RNA polymerase II" (GO:0000972), "DNA amplification" (GO:0006277), etc (**Supplementary Figure 1**).

To test for a correlation between the GBMR and the level of gene expression, the distribution of gene body methylation levels was represented according to gene expression rank (in RPKM). This distribution revealed that moderately expressed genes (100–1000 RPKM) have higher methylation levels than lowly (>100 RPKM) or highly (<1000) expressed ones in *P. margaritifera* (**Figure 2D**).

TABLE 1 | Darkness values obtained with the *ImaginR* R package analysis.

Conditions	Individual	Time 1	Time 2	Time 3
Control	#1	0.600000	0.596078	0.629804
	#2	0.646275	0.653595	0.650000
	#3	0.455462	0.522876	0.455556
Depth treatment	#4	0.775686	0.387451	0.375686
	#5	0.866231	0.437909	0.513726
	#6	0.845378	0.326797	0.419608
		P values<1.10e^{-5}		
		P values<1.10e^{-5}		

*Only P. margaritifera individuals from the depth treatment group showed significant differences (pairwise Wilcoxon tests with P values < 1.10e^{-5} ***) between sampling times 1 and 2, and sampling times 1 and 3. Sampling times 1, 2, and 3 correspond to June, July and August 2017, respectively, as explained in* ***Figure 1****.*

Methylation Calling and Differential Methylation Analysis

Methylation calling showed that the Cytosine methylation level was in average of 16.5% [12.0% in the CpG context, 0.9% in the CHG context, 1.0% in the CHH context, and 2.6% in another context (CN or CHN); **Supplementary Figure 2**]. Similarities between the methylation patterns of each sample were analyzed by a clustering approach (ward clustering correlation distance method). This showed that samples clustered first by treatment (depth vs. control), then by genotype (i.e., individuals) and, for the control only, by sampling time (**Figure 3**).

For the differential methylation analysis, triplicates were made according to treatment (depth and control), and nine pairwise comparisons were made in order to identify and disentangle the different effects (**Figure 4**). Time effect was quantified by the differential methylation analysis performed among the control individuals (C; three different genotypes), but between the sampling times (S; three samples per genotype). This led us to perform three comparisons (C-S1 vs. C-S2, C-S2 vs. C-S3, and C-S1 vs. C-S3). Overall, time effect was associated with non-redundant (not visible in other conditions) hyper- or hypomethylations of 60 and 111 CpGs, respectively. Neither hyper- nor hypomethylation were detected in CHG or CHH contexts.

The cumulative effect of depth variation and time was quantified by differential methylation analysis performed among the individuals in the depth treatment (T; three different genotypes), but between the sampling times (S; three samples per genotype). As previously, this led us to make three pairwise comparisons (T-S1 vs. T-S2, T-S2 vs. T-S3, and T-S1 vs. T-S3).

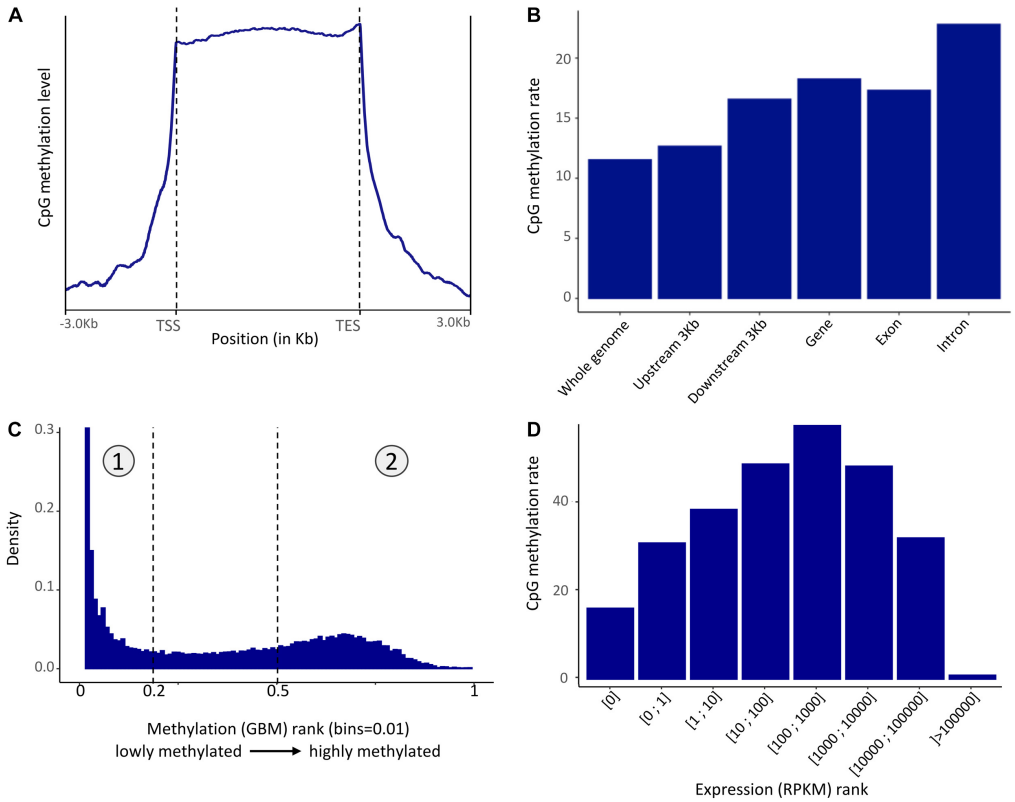

FIGURE 2 | (A) Pattern of methylation level in the mantle of *P. margaritifera* (TSS, Transcription Start Site; TES, Transcription End Site) reported on a metagene. **(B)** Distribution of methylated CpG in different genomic regions. **(C)** Distribution of methylated CpG across genes ranked according to methylation level. The left part (1) is composed of lowly methylated genes while the right part (2) is composed of highly methylated genes. **(D)** CpG methylation rate averaged across rank of gene expression.

In total, 71 non-redundant hyper- and 76 non-redundant hypomethylations were identified, all in the CpG context.

The cumulative effect of depth variation and genotype was quantified by differential methylation analysis performed between treatments (depth treatment vs. control; three genotypes per condition) at the three-sampling times (T-S1 vs. C-S1, T-S2 vs. C-S2, and T-S3 vs. C-S3). These analyses revealed that: (i) in the CpG context, 2087 non-redundant cytosines were hypermethylated while 2935 non-redundant cytosines were hypomethylated; (ii) in the CHG context, 12 non-redundant cytosines were hypermethylated and 16 were hypomethylated; (iii) in the CHH context, three non-redundant cytosines were hypermethylated and three were hypomethylated.

Finally, to extract the effect of the depth variation only, we subtracted the time effect from the cumulative effect of depth and time (comparison among treatments, but between the sampling times). To do so, positions presenting differential methylation in response to the time effect were considered as non-significant when they were also differentially methylated in the cumulative effect of depth and time. None of the CpGs that were differentially methylated for the time effect were also differentially methylated for the depth variation and time effect. All the 71 hyper- and 76 hypomethylations previously identified were therefore kept for subsequent analysis.

Enrichment Analysis and Exploration of Genes With Differentially Methylated Positions

To correlate changes in DNA methylation with changes in pigmentation, we first performed an enrichment analysis and looked for biological processes and molecular functions linked to pigmentation. As a second step, we then individually screened the genes displaying DMCpGs and searched the literature for their putative involvement in pigmentation. DMCpG that were located outside of the gene body were not considered (92 DMCpGs). Genes encoding proteins of unknown function were present in the set of genes containing DMCpGs, but the lack of functional annotation prevented us from proposing a mechanism that could explain their involvement in the phenotypic changes that occurred, although we cannot exclude that they may have a role in this phenomenon.

C-S1 vs. C-S2 vs. C-S3 Comparison

The GO categories significantly enriched in control conditions in relation to time were not associated with pigmentation. They were, however, associated with a seasonal effect, shown by an enrichment in GO terms linked to growth and reproduction (**Supplementary Figure 2**). The methylation information for

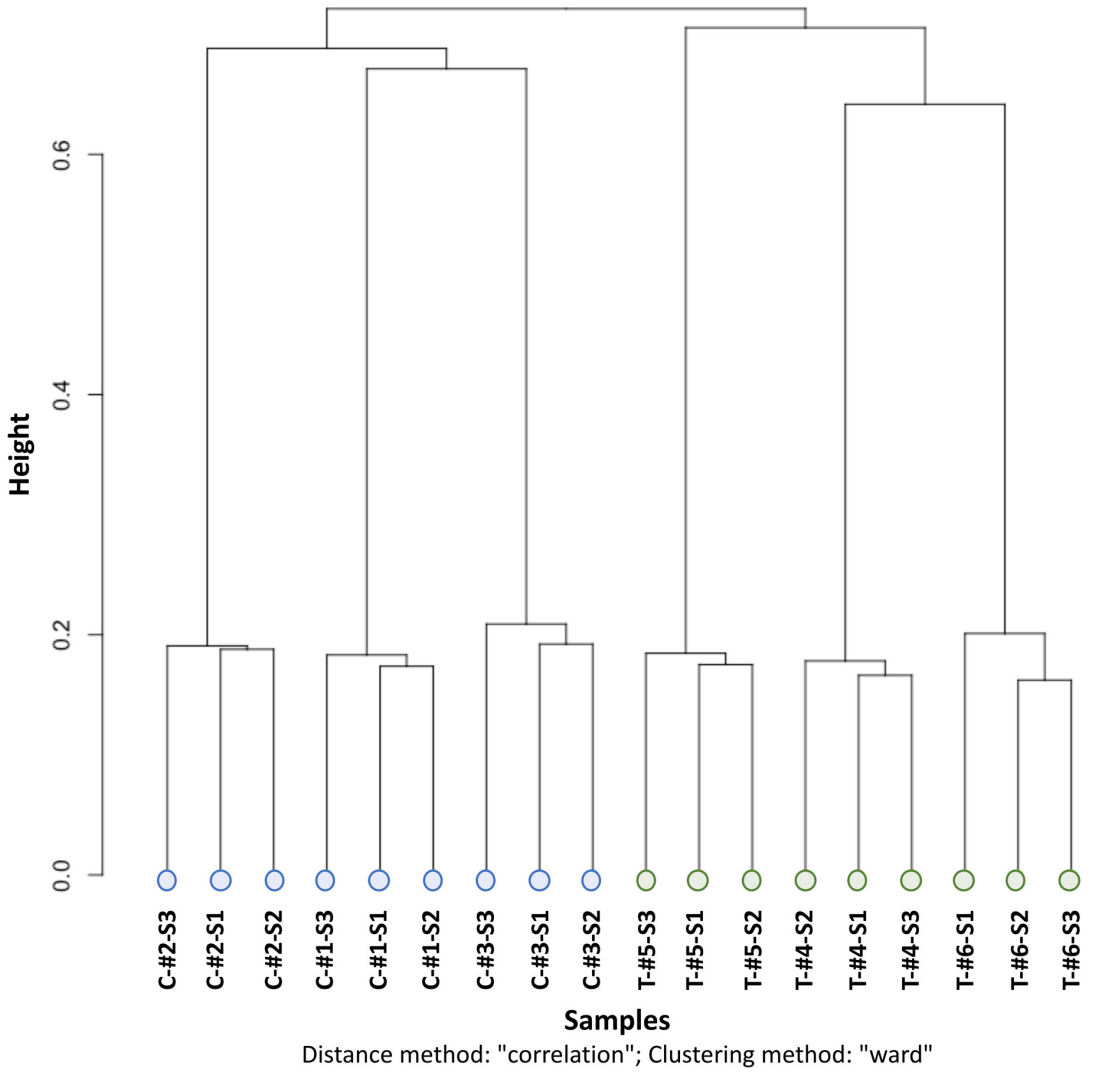

FIGURE 3 | CpG methylation clustering with the distance method "correlation" and clustering method "ward" from the clusterSamples function of the R package *Methylkit*. C, control individual (in blue); T, depth treatment individual (in green); #, label of the individual number; S1, sampling time 1; S2, sampling time 2; S3, sampling time 3.

all these genes and for all comparisons are provided in **Supplementary Table 3**.

T-S1 (1 Month at 8 m Depth) vs. T-S2 (1 Month at 8 m Depth Followed by 1 Month at 30 m Depth)

Gene ontology (GO) terms enrichment analysis performed for biological process category showed an enrichment of several GO terms associated with pigmentation (**Figure 5**): "pigment metabolic process" (GO:0042440), "pteridine-containing compound metabolic process" (GO:0042558, Frost and Malacinski, 1979), and "folic acid-containing compound biosynthetic process" (GO:0009396, Katz et al., 1987). For the molecular function category, additional GO terms linked to pigmentation processes were enriched: "UDP-glycosyltransferase activity" (GO:0008194, Vajro et al., 1995), "hydroxymethyl-formyl- and related transferase activity" (GO:0016742, Moreau et al., 2012), "alpha-1,3-mannosyl-glycoprotein 2-beta-N-acetylglucosaminyltransferase activity" (GO:0003827, Zhai et al., 2016), "phosphoribosylglycinamide formyltransferase activity" (GO:0004644), and "acetylglucosaminyltransferase activity" (GO:0016262, Chakraborty et al., 1999; Shin et al., 2015).

At the gene level (**Table 2**), three candidate genes were identified that had hypermethylated CpGs after the month at −30 m. The first encodes a trifunctional purine biosynthetic protein adenosine-3 (*GART*), the second an alpha-1,3-mannosyl-glycoprotein-2-beta-n-acetylglucosaminyltransferase (*MGAT1*), and the third a multidrug resistance-associated protein (*ABCC1*). *GART* is known to be involved in the synthesis of purines (purine synthesis pathway) and expression disturbances of this gene can modify the production of two pigments: melanin and pheomelanin (Amsterdam et al., 2004; Ng et al., 2009).

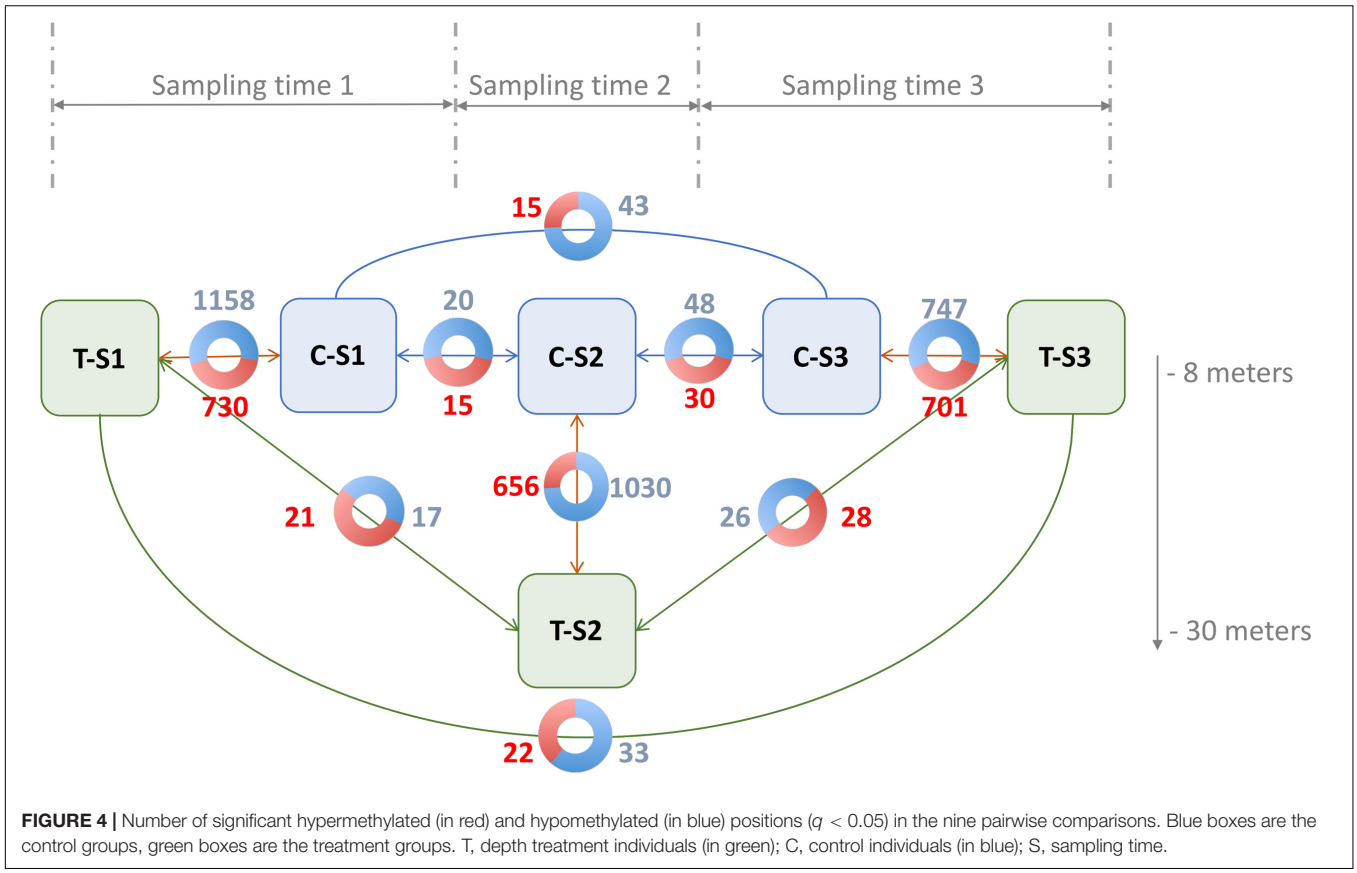

FIGURE 4 | Number of significant hypermethylated (in red) and hypomethylated (in blue) positions ($q < 0.05$) in the nine pairwise comparisons. Blue boxes are the control groups, green boxes are the treatment groups. T, depth treatment individuals (in green); C, control individuals (in blue); S, sampling time.

MGAT1 is involved in the glycan synthesis pathway, and is known to be essential for shell formation in the *Pinctada* genus (Takakura et al., 2008). Finally, the *ABBC1* gene encodes an active transporter of glutathione-S-transferase (Homolya et al., 2003; Fernandes and Gattass, 2009; Rocha et al., 2014), an enzyme regulating the balance of eumelanin/pheomelanin production (Sonthalia et al., 2016).

T-S2 (1 Month at 8 m Depth Followed by 1 Month at 30 m Depth) vs. T-S3 (1 Month at 8 m, 1 Month at 30 m, and 1 Month Back at 8 m)

GO term enrichment analysis highlighted enrichment for several GO terms associated with pigmentation (**Figure 6**): "L-ornithine transmembrane transporter" (GO:0000064) for the biological process category; and "ornithine transport" (GO:0015822), "lysine transport" (GO:0015819), "L-amino acid transport" (GO:0015807), "basic amino acid transmembrane transporter activity" (GO:0015171), "L-amino acid transmembrane transporter activity" (GO:0015179), and "xenobiotic transporter activity" (GO:0015238) for the molecular function category.

At the gene level, 15 genes displaying DMCpGs were deemed good candidates to partly explain the phenotypic changes observed. Among the hypomethylated genes, we found those for a cationic amino acid transporter 2 (*SLC7A2*), a multidrug-associated protein (also present in the T-S1 vs. T-S2 comparison), and a coiled-coil domain-containing protein 79 (*CCDC79*). SLC7A2 is involved in the transport of arginine, lysine, and ornithine. A high number of the proteins found in the mineralized structure of *P. margaritifera* are known to be enriched in arginine and lysine, such as MSP-1, MSP-2, Aspein, Prismlain-14, and MSI60 (Addadi et al., 2006; Joubert et al., 2010; Gueguen et al., 2013). According to the NCBI GenPept database, CCDC79 can bind ion calcium, like the product of the *MGAT1* gene (see above). Among the hypermethylated genes, we found those for a G-protein coupled receptor (*GRL101*), a target of rapamycin complex 2 subunit (*MAPKAP1*), an enolase (*enolase-4*), sodium/potassium/calcium exchanger 1 and a perlucin-like protein. MAPKAP1 (TOR signaling pathway) promotes dark epithelial pigmentation (Liu et al., 2017), GRL101 (rhodopsin signaling pathway) is an ortholog of the pigment dispersing factor (Tanaka et al., 2014), and enolase (glycolysis/gluconeogenesis pathway) is a biomarker of vitiligo, a human pigmentation disorder affecting melanocytes (Hamid et al., 2015). Perlucin is a well-known matrix protein found in the nacreous layer of the pearl oyster shell (Joubert et al., 2010) with a function in the biomineralization process.

We also identified several GO terms with a less important role in pigmentation, like "TOR signaling" (GO:0031929), "TORC2 signaling" (GO:0038203), "glycolytic process" (GO:0006096), and "compound eye development" (GO:0048749) for the biological process GO category; and "calcium, potassium: sodium antiporter activity" (GO:0005432), "alkali metal ion binding" (GO:0031420), and "mannose binding" (GO:0005537) for the molecular function GO category.

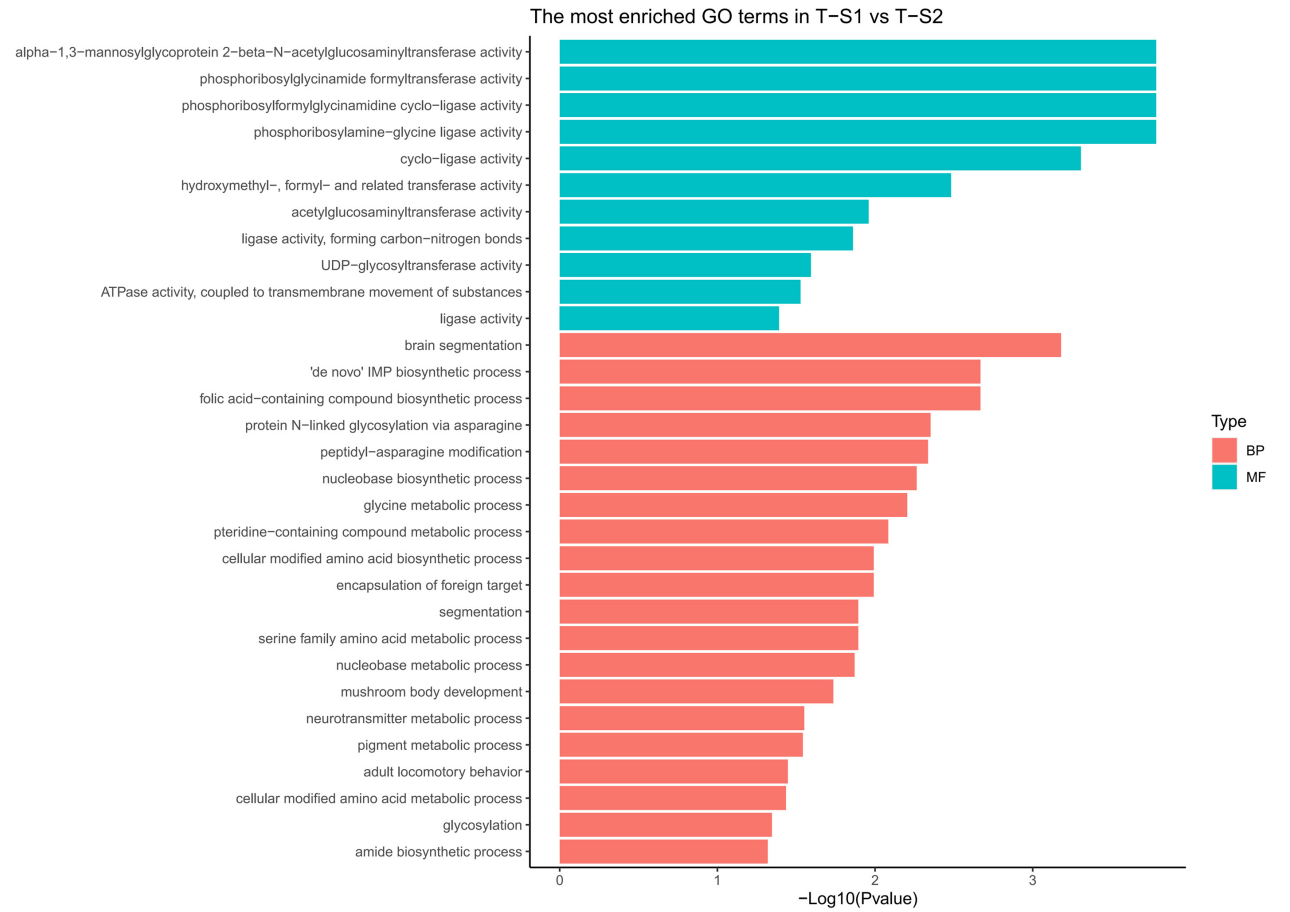

FIGURE 5 | Histograms of the enriched biological processes (BP) and molecular functions (MF) from the genes with differentially methylated positions in individuals from the depth treatment samplings in T-S1 vs. T-S2 (T-S1, T-S2 = depth treatment at sampling times 1 and 2, respectively).

T-S1 (1 Month at 8 m Depth) vs. T-S3 (1 Month at 8 m, 1 Month at 30 m, and 1 Month Back at 8 m)

As the previous enrichment analyses revealed, significant enrichment of several GO categories correlated with pigmentation were identified like in the T-S2 vs. T-S3 pairwise comparison (**Figure 7**): "L-ornithine transmembrane transporter" (GO:0000064) for the biological process GO category; and "ornithine transport" (GO:0015822), "lysine transport" (GO:0015819), "L-amino acid transport" (GO:0015807), "basic amino acid transmembrane transporter activity" (GO:0015171), "L-amino acid transmembrane transporter activity" (GO:0015179), and "xenobiotic transporter activity" (GO:0015238) for molecular function GO category.

At the gene level, only the *GPI-anchor transamidase gene* could be linked to the pigmentation process (among other pathways) since it is involved in a human disorder characterized by altered dermal pigmentation (Ng and Freeze, 2014).

We also identified several GO terms with a less important role in pigmentation, such as the "drug transmembrane transport" (GO:0006855) for the biological process GO category; and "attachment of GPI anchor to protein" (GO:0016255), "regulation of TOR signaling" (GO:0032006), and "protein glycosylation" (GO:0006486) for the molecular function GO category.

DISCUSSION

Pearl farming, the second economic resource of French Polynesia, has been suffering a major economic crisis since 2001. To address this problem, stakeholders, together with pearl farmers and scientists, are developing an ambitious plan to reduce the volume of pearl production, but to increase pearl quality. This objective could be reached through one of the most economically interesting traits of *Pinctada margaritifera*: its ability to express the largest range of inner shell color (and thus pearl color) of any pearl-producing species worldwide (Ky et al., 2014; Stenger et al., 2019). Indeed, producing unique, highly valuable, pearls displaying a palette of phenotypes ranging from very dark to very pale colors constitutes an efficient way to diversify the production and appeal to different markets. Selection of donor oysters based on color phenotype was started a few years ago (Ky et al., 2013). However, the possibility of acting directly on the selected

TABLE 2 | All significantly differentially methylated positions (q value < 0.05) for treatment comparisons.

Scaffold name	Scaffold size	Position	Genomic element	*q*value	Diff_M	Gene annotation name	
scaffold11	453194	35819	UPSTREAM	0.0282	−17.46	—NA—	Depth treatment: time 1 *vs* time 2
scaffold11	453194	35847	UPSTREAM	0.0282	−21.46		
scaffold11282	54383	4058	GENE_mRNA	0.0354	31.90	trifunctional purine biosynthetic protein adenosine-3-like isoform X1	
scaffold1133	336669	153064	UPSTREAM	0.0133	24.13	—NA—	
scaffold1625	401360	350179	GENE_mRNA	0.0284	20.83	alpha-1,3-mannosyl-glycoprotein 2-beta-N-acetylglucosaminyltransferase isoform X3	
scaffold2357	95418	29644	GENE_mRNA	0.0284	29.22	multidrug resistance-associated protein 1-like isoform X1	
scaffold2357	95418	29691	GENE_mRNA	0.0284	31.77		
scaffold3816	161365	94615	UPSTREAM	0.0284	−31.61	—NA—	
scaffold4468	144975	29587	DOWNSTREAM	0.0470	20.43	PREDICTED: uncharacterized protein LOC109618538	
scaffold4716	65370	6520	EXON_CDS	0.0284	27.45	—NA—	
scaffold5609	111224	54055	UPSTREAM	0.0257	−24.59	—NA—	
scaffold10	363274	309202	EXON_CDS	0.0201	−15.97	—NA—	Depth treatment: time 2 *vs* time 3
scaffold10423	31023	17485	GENE_mRNA	0.0406	−14.58	cationic amino acid transporter 2-like isoform X1	
scaffold11822	47775	21990	GENE_mRNA	0.0186	27.95	uncharacterized protein LOC111108810	
scaffold1371	144177	54477	GENE_mRNA	0.0433	16.39	G-protein coupled receptor GRL101-like	
scaffold18	585035	250513	GENE_mRNA	0.0361	30.71	target of rapamycin complex 2 subunit MAPKAP1-like	
scaffold2163	271214	87225	DOWNSTREAM	0.0433	28.72	PREDICTED: uncharacterized protein LOC105344672	
scaffold2357	95418	29691	GENE_mRNA	0.0261	−29.94	multidrug resistance-associated protein 1-like isoform X1	
scaffold236	195829	77424	GENE_mRNA	0.0216	25.97	enolase 4-like isoform X3	
scaffold2576	104445	84826	GENE_mRNA	0.0026	−38.55	Coiled-coil domain-containing protein 79	
scaffold2582	91290	78204	GENE_mRNA	0.0133	41.28	sodium/potassium/calcium exchanger 1-like	
scaffold2582	91290	78245	GENE_mRNA	0.0099	43.74		
scaffold381	319941	276927	DOWNSTREAM	0.0433	17.94	—NA—	
scaffold5757	154693	48096	GENE_mRNA	0.0406	15.15	perlucin-like protein	
scaffold5757	154693	48114	GENE_mRNA	0.0336	19.65		
scaffold592	283515	144263	GENE_mRNA	0.0261	31.63	PREDICTED: uncharacterized protein LOC105317977 isoform X11	
scaffold6243	82815	59659	GENE_mRNA	0.0409	38.89	RNA polymerase II-associated protein 3-like isoform X2	
scaffold720	228729	148045	GENE_mRNA	0.0186	−28.81	DNA-directed RNA polymerase I subunit RPA2-like	
scaffold10423	31023	17485	GENE_mRNA	0.0318	−15.74	cationic amino acid transporter 2-like isoform X1	Depth treatment: time 1 *vs* time 3
scaffold10423	31023	17511	GENE_mRNA	0.0199	−19.43		
scaffold10423	31023	17518	GENE_mRNA	0.0326	−17.08		
scaffold10423	31023	17520	GENE_mRNA	0.0129	−19.70		
scaffold11	453194	35819	UPSTREAM	0.0198	−17.46	—NA—	
scaffold1133	336669	153064	UPSTREAM	0.0320	19.98	—NA—	
scaffold1657	298101	43346	GENE_mRNA	0.0127	−24.93	kinesin-like protein KIF2A	
scaffold2163	271214	87184	DOWNSTREAM	0.0207	−26.20	PREDICTED: uncharacterized protein LOC105344672	
scaffold2163	271214	87224	DOWNSTREAM	0.0153	−27.03		
scaffold273	459813	427122	GENE_mRNA	0.0334	−16.66	NACHT and WD repeat domain-containing protein 2-like isoform X2	
scaffold273	459813	427125	GENE_mRNA	0.0326	−16.14		

(Continued)

TABLE 2 | Continued

Scaffold name	Scaffold size	Position	Genomic element	*q*value	Diff_M	Gene annotation name
scaffold273	459813	427294	GENE_mRNA	0.0256	−20.97	
scaffold3199	215908	10021	UPSTREAM	0.0318	30.03	—NA—
scaffold4848	64103	14806	GENE_mRNA	0.0261	−35.91	GPI-anchor transamidase-like
scaffold6242	215376	126991	GENE_mRNA	0.0164	−22.59	SH3 and cysteine-rich domain-containing protein 3
scaffold734	224438	4180	UPSTREAM	0.0079	16.63	polypeptide N-acetylgalactosaminyltransferase 5-like
scaffold734	224438	4185	UPSTREAM	0.0153	14.74	

Scaffold name: scaffold number; Scaffold size: scaffold size; Position: position of the significantly differentially methylated positions on this scaffold; Genomic element: the genomic feature containing the DNA methylation change; q value: q value; Diff-M: the differential methylation level obtained using the Methylkit R package; Gene annotation name: Gene annotation according to the nr and swiss-prot blast top hit. Blue shading (negative values) indicates hypomethylation of the position and red shading (positive values) hypermethylation; darker shading indicates a stronger degree of hypomethylation of hypermethylation, respectively. The last column indicates in which comparison the significantly different methylated positions were found.

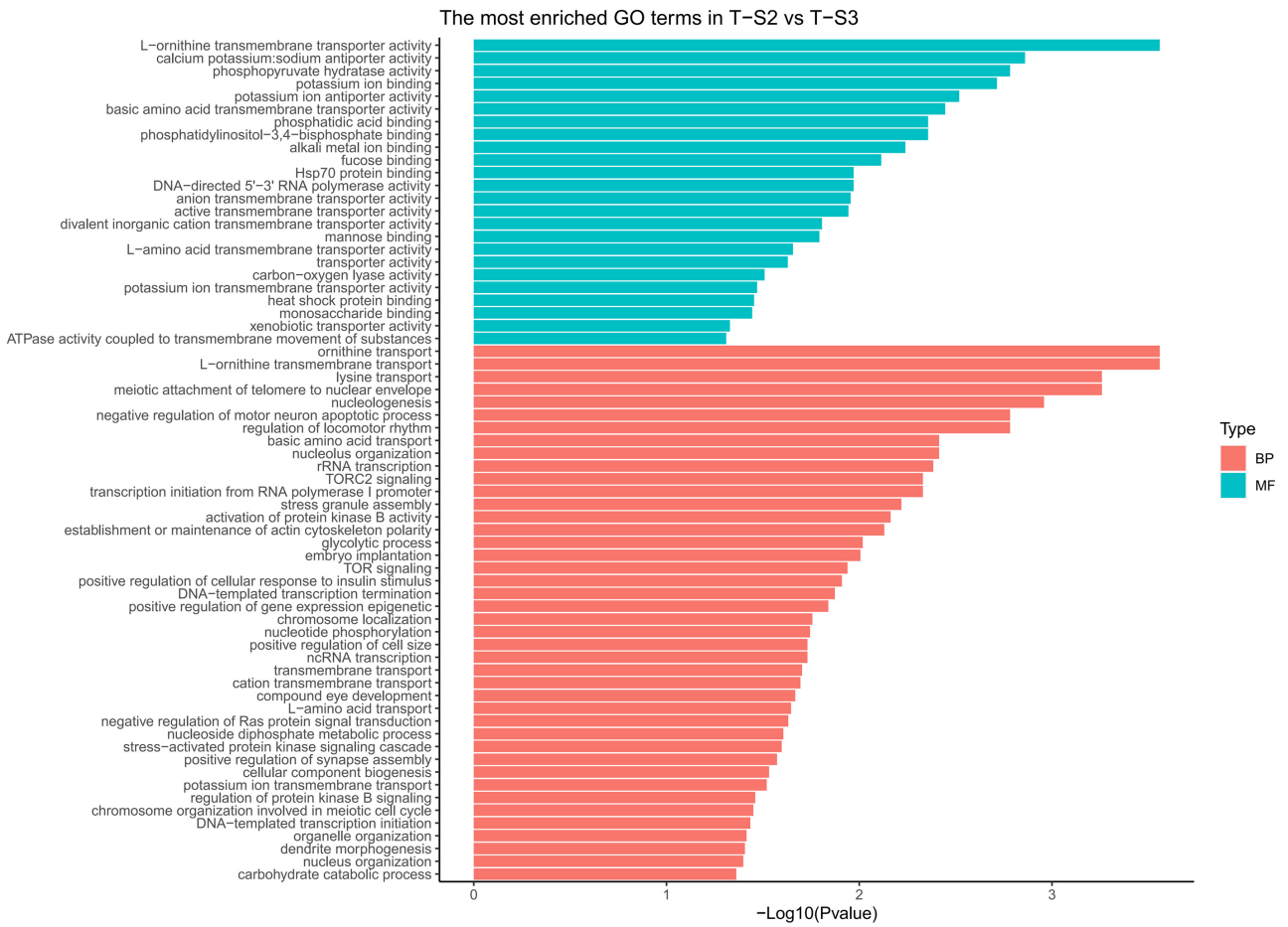

FIGURE 6 | Histograms of the enriched biological processes (BP) and molecular functions (MF) from the genes with differentially methylated positions in individuals from the depth treatment samplings in T-S2 vs. T-S3 (T-S2, T-S3 = depth treatment at sampling times 2 and 3, respectively).

oysters to enhance their color and quality as donors is also an attractive method for improving pearl quality. For this, a better understanding of the interactions between the phenotype and gene expression correlated with environmental conditions is essential (Gavery and Roberts, 2017), and would allow the development of epigenetic marker-assisted selection or, more generally, epigenetics-assisted cultural practices.

As a first step to understanding the mechanisms behind this environmentally induced color variation, we applied an environmental forcing (culture-depth variation) known to affect

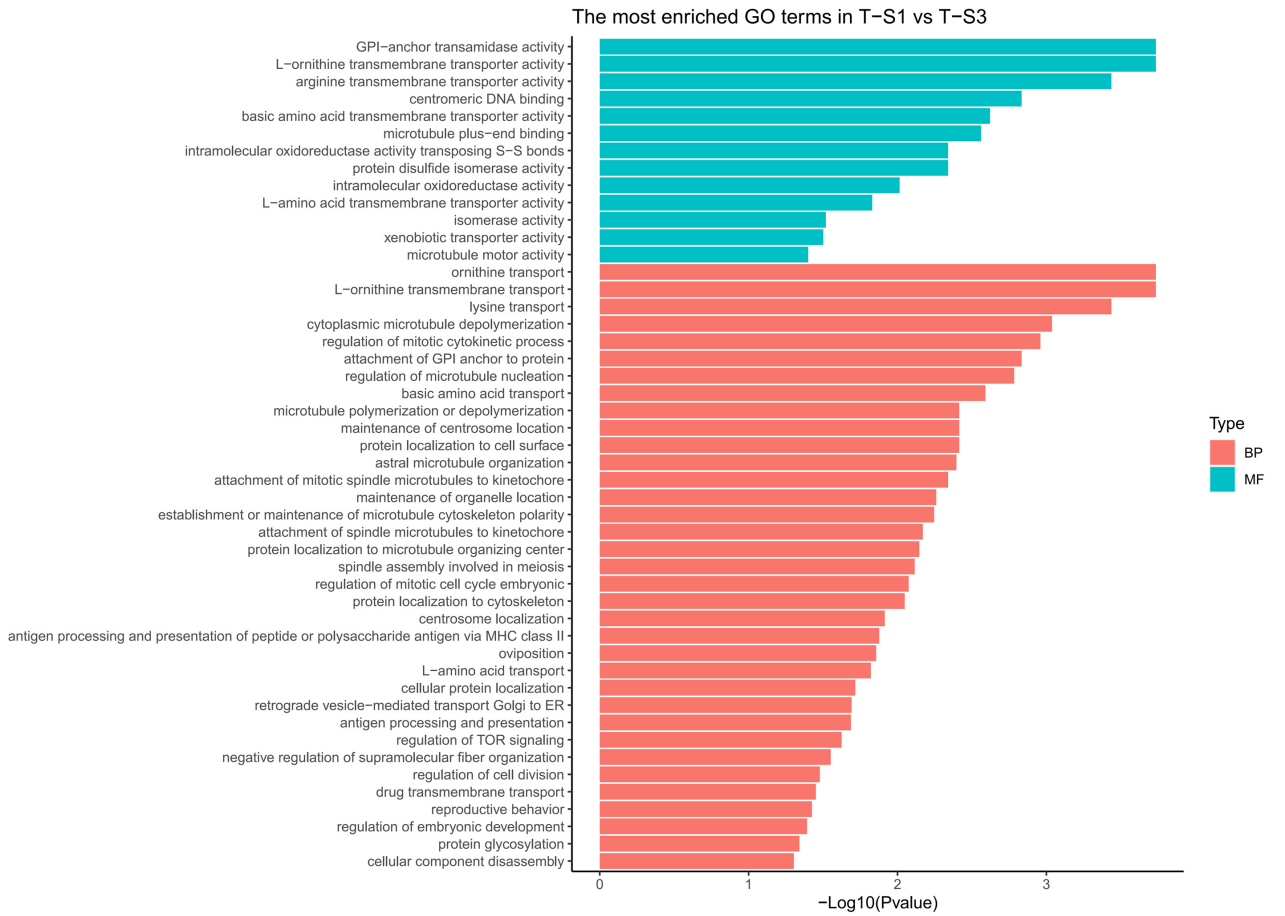

FIGURE 7 | Histograms of the enriched biological processes (BP) and molecular functions (MF) from the genes with differentially methylated positions in individuals from the depth treatment samplings in T-S1 vs. T-S3 (T-S1, T-S3 = depth treatment at sampling times 1 and 3, respectively).

pearl and inner-shell darkness (Stenger et al., 2019), and studied, under constant genotype, the DNA methylation changes induced. In addition to providing the first description of a pearl oyster methylome, our analyses identified specific methylation changes that affected candidate genes involved in the expression of shell and pearl color darkness. These genes were involved in both pigmentation (biological coloring mechanisms) and iridescence (physical coloring mechanisms based on the differential organization of biomineral crystals).

The First Methylome of the *Pterioidea* Super-Family Shows Similar Characteristics to Other Invertebrate Methylomes

The present study provides to our knowledge the first methylome of a member of the *Pterioidea* super-family. The whole-genome bisulfite sequencing (WGBS-seq) of the pearl oyster mantle tissues revealed that its methylome is of the mosaic type and similar in many ways to what is classically described in some other invertebrates. Indeed, *P. margaritifera* mainly displays cytosine methylation in the CpG context, as already described in *Crassostrea gigas* (Thunberg, 1793) by Gavery and Roberts (2013) and in *Biomphalaria glabrata* (Say, 1818) by Adema et al. (2017). Likewise, differential methylation was also mainly identified in the CpG context, as in Wang et al. (2014) who reported that more than 99% of DNA methylation changes were restricted to the CpG context in *C. gigas*. The pattern of methylation we obtained occurred essentially in the gene bodies, with some accretion upstream and downstream of the gene, as described for mosaic methylation in other mollusks (Sarda et al., 2012; Wang et al., 2014; Rondon et al., 2017). These features of a short, but densely methylated region (corresponding to the genes), interspersed by long unmethylated regions (intergenic) are characteristic of the mosaic pattern of DNA methylation (Gavery and Roberts, 2013), which shows the typical bimodal distribution generally met in invertebrates. The lowly methylated genes were involved in the reproductive process, cellular signaling, and environmentally responsive functions. The low methylation of genes involved in the response to environmental changes is something reported in many different invertebrates (Sarda et al., 2012), but the presence of functions associated with reproduction is less common. It may be explained by the tissue used to produce this methylome, the mantle, which is a tissue not involved in reproduction

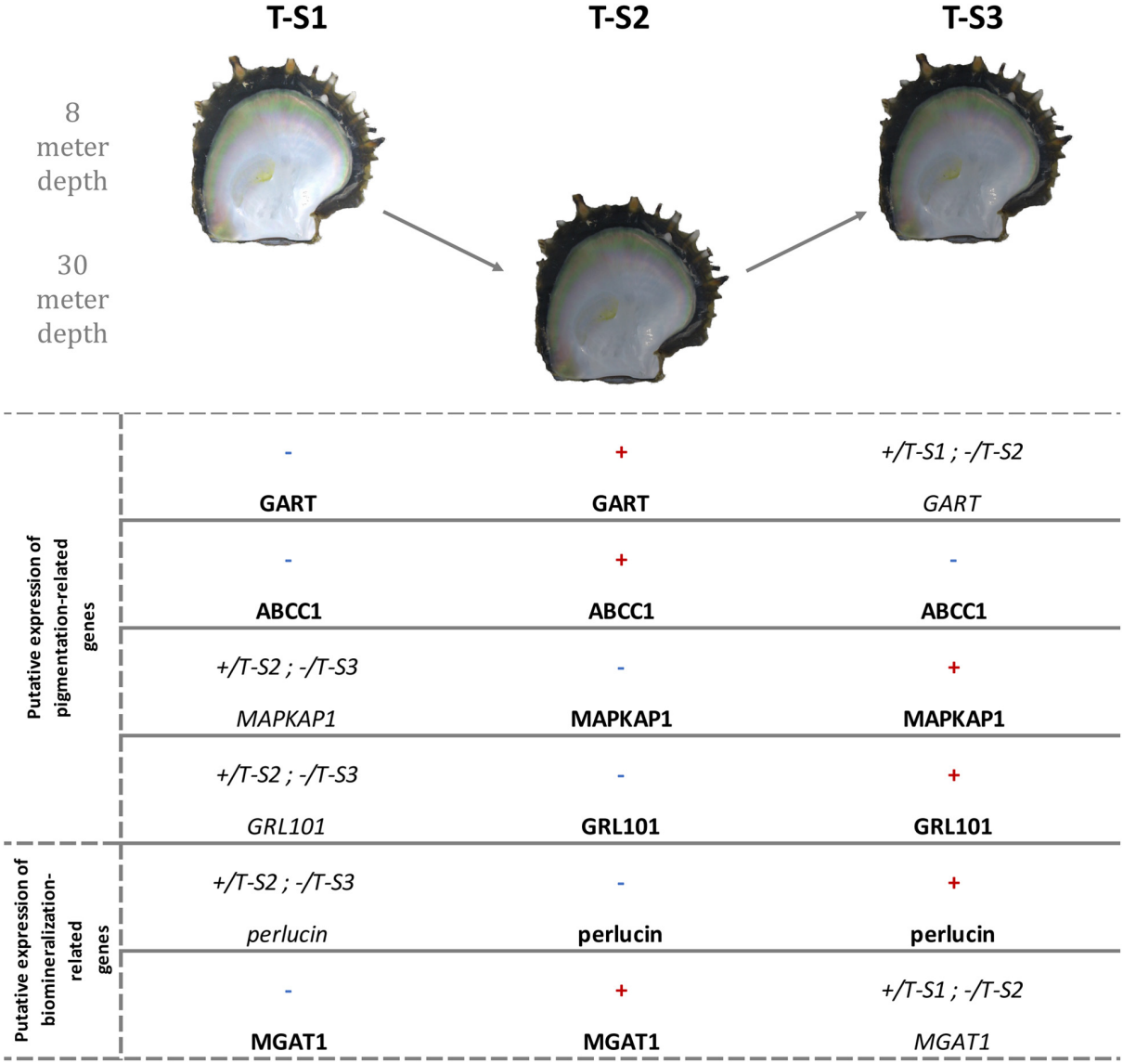

FIGURE 8 | Methylation direction changes in candidate genes linked to inner shell color darkening in the depth treatment individuals at the three successive sampling times (T-S1, T-S2, and T-S3). The first four genes are involved in pigmentation processes, and the last two in biomineralization processes. Red "+" illustrates a significant hypermethylation of at least one CpG and blue "-" illustrates a significant hypomethylation of at least one CpG. +/T-S(a) and -/T-S(b) mean that the methylation in the present sampling time is more methylated than in the T-S(a) and less than in the T-S(b). *GART*, trifunctional purine biosynthetic protein adenosine-3; *ABCC1*, multidrug resistance-associated protein 1; *MAPKAP1*, target of rapamycin complex 2 subunit *MAPKAP1*; *GRL101*, G-protein coupled receptor *GRL101*; *MGAT1*, alpha-1,3-mannosyl-glycoprotein-2-beta-n-acetylglucosaminyltransferase. Pictures showed are illustrative.

(see correlation between methylation levels and gene expression **Figure 2D**). The genes identified in highly methylated regions were essentially involved in housekeeping functions (Gavery and Roberts, 2013; Olson and Roberts, 2014; Wang et al., 2014). When comparing the gene body methylation rate with the gene expression level, we demonstrated that moderately methylated genes have higher expression levels than lowly or highly methylated ones. This result is consistent with other studies (Feng et al., 2010; Xiang et al., 2010; Zemach et al., 2010) and strengthens the emerging hypothesis that, in invertebrates, gene expression and gene body methylation functions as a negative feedback loop in which gene expression increases with gene methylation until reaching a tipping point where additional methylation decreases transcription (Dixon et al., 2018).

Environmentally Induced DNA Methylation Changes and Their Link With Pigmentation

Among the DNA methylation changes that occurred during our experiment, several occurred in genes known to be involved in pigmentation pathways. Among these, the pteridine pathway

was recently identified as a key player in the expression of the yellow color phenotype in *P. margaritifera* (Stenger et al., in press). Indeed, different derivates of pteridine can lead to the production of sepiapterin and xanthopterins, two yellow pigments (Ng et al., 2009). The folic acid pathway is also significantly affected by DNA methylation changes. Although its involvement in molluscan pigmentation is unknown, folic acid deficiency is linked to melanosis (e.g., melanin overproduction) in mammals, which results in a black pigmentation (Sharp et al., 1980). Since the implication of melanin in pearl oyster pigmentation has previously been identified (Lemer et al., 2015), an epigenetically driven modification of gene expression in the folic-acid pathway could be associated with the darkening color phenotypes expressed in response to an increase in depth.

At the gene level, *GART*, a hypermethylated gene included in three enriched GO categories (**Figure 8**), encodes a trifunctional purine biosynthetic protein, adenosine-3. This protein is involved in the *de novo* purine synthesis pathway (Amsterdam et al., 2004) and is composed of three subunits (a phosphoribosylglycinamide formyltransferase, a phosphoribosylglycinamide synthetase, and a phosphoribosylaminoimidazole synthetase). Biochemically, it catalyzes steps 2, 3, and 5 of inosine monophosphate (IMP) synthesis (Amsterdam et al., 2004; Ng et al., 2009). IMP is one of the precursors initiating the pterin and the Raper-Manson pathways, two pathways leading to pigmentation in *P. margaritifera* (Stenger et al., in press). Ng et al. (2009) have shown that mutations in *GART* are associated with pigmentation defects in juvenile zebrafish *Danio rerio* (Buchanan-Hamilton, 1822) due to disturbances of the pterin and Rapper-Mason pathways. Wild-type zebrafish are mainly yellow with black spots, while Δ-GART juveniles are entirely black (Ng et al., 2009). We can, therefore, hypothesize that methylation changes in the *GART* gene may affect its expression, subsequently affecting the pterin and Rapper-Mason pathways and leading to a darkening of the shell.

The gene for multidrug resistance-associated protein 1 (*ABCC1*) presented two hypermethylated positions after the period at 30 m, a methylation state that reverted after the return to 8 m. *ABCC1* is known to mediate ATP-dependent transport of glutathione and glutathione conjugates (Homolya et al., 2003). In a previous study it was proposed that glutathione plays an essential role in the expression of the yellow and black pigments (Stenger et al., in press). Glutathione-S-transferase (GST) activity is central in regulating the production of the yellow pheomelanin and black eumelanin pigments through the Raper-Manson pathway (Sonthalia et al., 2016). Methylation changes in the *ABCC1* gene could therefore promote variation in the quantity of glutathione available and modify the regulation of the production of pheomelanin and eumelanin. An overproduction of eumelanin may explain the observed darkening of the shell.

GRL101 presented a hypermethylated response to the return to 8 m. According to Tanaka et al. (2014), this gene is an ortholog of the pigment dispersing factor, a gene responsible for changes in the concentration of chromatophoral pigment in response to darkness (Rao and Riehm, 1993). In crustaceans, it was proposed that color variation due to changing light conditions was caused by the dispersion of retinal chromatophore pigments linked with the activation of *GRL101* (Rao and Riehm, 1993; Auerswald et al., 2008). The methylation change of *GRL101*, the similarities between the environmental triggers (a decrease of light) activating *GRL101* in other organisms, and the phenotypes resulting from this activation argue in favor of the involvement of *GRL101* in *P. margaritifera* color variation.

The *GPI-anchor transamidase-like* gene was hypomethylated after the return to 8 m depth. According to Ng and Freeze (2014), a mutation of the *GPI-anchor transamidase* genes is involved in a human disorder characterized by an altered dermal pigmentation (Ng and Freeze, 2014). This was later confirmed by RNAi experiments targeting GPI-anchor transamidase transcripts and resulting in a hyper-pigmented dark swellings in the maize anthracnose fungus *Colletotrichum graminicola* (G.W. Wilson 1914) (Oliveira-Garcia and Deising, 2016).

Enolase-4 is another candidate gene displaying hypomethylation at 30 m. Enolases are metalloenzymes involved in glycolysis and glycogen storage. One study reported a correlation between enolase activity and pigmentation: Hamid et al. (2015) showed that patients with vitiligo (a pigmentation disorder affecting melanocytes and inhibiting pigment synthesis) synthesize antibodies directed against enolases. Since their discovery, enolases have been used as biomarkers for the diagnosis, treatment, and monitoring of vitiligo (Hamid et al., 2015). The causes of this pathology are still unclear, although both genetic and environmental factors seem to be involved (Hamid et al., 2015). In the case of the pearl oyster, the hypomethylation of the enolase gene at 30 m may be associated with a change of expression inducing a darker phenotype.

The last of the genes subject to methylation change (hypermethylation after the last period at 8 m) and displaying a functional link with pigmentation is the target of rapamycin complex 2 subunit (*MAPKAP1*). This gene is involved in the TORC2 and TOR signaling pathways. The activation of these signaling pathways is known to promote a dark epithelial pigmentation due to the proliferation and the migration of retinal pigmentation epithelial cells (RPE cells) (Liu et al., 2017).

Among the six genes displaying a functional link with the pigmentation process or its regulation, four (*GART*, *ABCC1*, *MAPKAP1*, and *GRL101*) were associated with the expression of darker phenotypes, while the two others were associated with pigmentation disorders. Further experiments will be necessary to confirm and define their role, such as gene expression quantification, RNAi, and, once possible, genome editing, and epigenetic engineering. Thus, our results provide the first step toward this new research field.

Biomineralization and Pearl Darkness

In addition to a darkening of the coloration (Stenger et al., 2019), previous experiments have shown that a variation in depth also affects the shape and size of the aragonite tablets of the shell of *P. margaritifera* (Rousseau and Rollion-Bard, 2012). Aragonite tablets are the structural unit of nacre, the $CaCO_3$ polymorph that constitutes the inner-shell of pearl oyster and the pearl itself (Rousseau and Rollion-Bard, 2012). Variation in the organization of these aragonite tablets can induce a change in color and luster (brightness) due to a change in the physical iridescence

(Liu et al., 1999; Wang et al., 2008). Although not yet demonstrated, it is suspected that pigments contributing to nacre color are constituents of the intra-lamellar silk-fibroin gel that is localized between aragonite tablets (Addadi et al., 2006). Variation in the size of these tablets could therefore lead to a variation in the quantity of pigments that can be viewed through the last biomineralized aragonite layers. Interestingly, among the genes displaying methylation changes in response to a variation in water depth, two are well-known actors of the biomineralization processes of the nacreous layer: *perlucin* (Joubert et al., 2010) and *MGAT1* (Takakura et al., 2008).

Perlucin is a protein found in the shell organic matrix of several Mollusca, including *P. margaritifera* (Weiss et al., 2000; Blank et al., 2003; Marie et al., 2013; Joubert et al., 2014). Experiments with purified Mollusca perlucin have suggested its involvement in calcium carbonate precipitation by favoring nucleation, crystallization and crystal growth control (Weiss et al., 2000). A variation in its expression can therefore have a huge effect on aragonite tablet size and organization (Rousseau and Rollion-Bard, 2012) and may thus modify the iridescence and transparency properties of the top aragonite layers (Rousseau and Rollion-Bard, 2012).

MGAT1 is a gene whose product initiates carbohydrate formation and is essential for the conversion of high-mannose to hybrid and complex N-glycans. This protein is involved in the protein glycosylation pathway, which is part of Protein modification. Interestingly, Takakura et al. (2008) identified an acidic N-glycan post-translationally attached to nacrein in *Pinctada fucata* that allows calcium binding. Moreover, nacrein is one of the main proteins found in the nacreous part of the shell (Rousseau and Rollion-Bard, 2012). So, although the *MGAT1* gene plays no role in crystal formation, a possible link affecting nacrein formation can still be found. Future proteomics studies will be necessary to better uncover the role of *MGAT1* in *P. margaritifera* shell coloration.

Epigenetics and Pearl Culture

As previously reported, the yo-yo experiment resulted in a general darkening of the inner shell of *P. margaritifera* in response to an increase in depth (Stenger et al., 2019), an environmentally induced phenotype that was maintained even after a return to the control depth (8 m). Such an enduring phenotypic response could be considered as good evidence of the involvement of epigenetic control (Sutherland and Costa, 2003; Harris et al., 2012; Bräutigam et al., 2013). The maintenance of this phenotype was previously documented in this species cultured for pearl production, and can last for over 18 months (Stenger et al., 2019). In another biological model, maize, stress-induced hypermethylation of *P-pr* (Richards, 2006; Lukens and Zhan, 2007) was associated with a reduced pigmentation that lasted in some cases for the entire life of an individual, and could even be transmitted to the next generation (Richards, 2006; Bossdorf et al., 2008). Such effects could offer huge benefits for pearl farming. First, this long-lasting effect suggests that farmers could better control their production through dedicated conditioning of recipient and/or donor oysters. Additionally, the transgenerational effect described for maize, although not yet tested for pearl oysters, suggests that epigenetic marker-assisted selection could be envisioned. Such an approach may offer the possibility of selecting phenotypes of interest without the associated risk of eroding genetic diversity and/or the integration into natural populations of spat produced by farmed oysters (Reisser et al., 2020).

DATA AVAILABILITY STATEMENT

The datasets generated for this study can be found on the NCBI (BioProject PRJNA663978). Scripts used are provided on GitHub (PLStenger/Pearl_Oyster_Colour_BS_Seq/00_scripts).

AUTHOR CONTRIBUTIONS

JV-D, P-LS, SP, and C-LK designed the study. P-LS and MM performed the experiments. P-LS, CC, and CG analyzed the data. P-LS and JV-D drafted the manuscript. Funding was obtained by CL-K, SP, and JV-D. All authors approved the manuscript.

FUNDING

This study was supported by grants from the "Direction des Ressources Marines," through the AmeliGEN project (# 10065/MEI/DRMM). P-LS's Ph.D. was funded by AmeliGEN and the Pacific Doctoral School (EDP) (ED 469). This study was performed within the framework of the "Laboratoire d'Excellence (LABEX)" TULIP (ANR-10-LABX-41) and CORAIL (ANR-10-LABEX).

ACKNOWLEDGMENTS

The authors would like to thank the Regahiga Pearl Farm (Mangareva Island, Gambier Archipelago, French Polynesia) for providing the pearl oysters used in this study.

SUPPLEMENTARY MATERIAL

The Supplementary Material for this article can be found online at: https://www.frontiersin.org/articles/10.3389/fgene.2021.630290/full#supplementary-material

Supplementary Figure 1 | Treemaps of biological processes obtained from the GO terms significantly enriched from the lowly methylated genes **(A)** (data from **Figure 2C** – "1" part) and the highly methylated genes **(B)** (data from **Figure 2C** – "2" part).

Supplementary Figure 2 | Treemaps of biological processes and molecular functions obtained from the GO terms significantly enriched from the genes with differentially methylated positions in control individuals (C-S1, control in time 1; C-S2, control in time 2; C-S3, control in time 3).

Supplementary Table 1 | FastQC results for raw and trimmed data.

Supplementary Table 2 | Average values by category (control/depth treatment) and sampling time for: the number of read pairs, paired-end alignments, mapping efficiency, number of duplicated alignments removed after mapping, the number of C in sequences, the number of C in percentage in CpG,

CHG, CHH or in unknown contexts, and the basic statistics of the gene body methylation rate (GBM – on the 54408 genes of the reference genome).

Supplementary Table 3 | All significantly differentially methylated positions (*q* value < 0.05) for the controls. Scaffold name: scaffold number; Scaffold size: scaffold size; Position: position of the significantly differentially methylated positions on this scaffold; Genomic element: the genomic feature containing the DNA methylation change; *q* value: *q* value; Diff-M: the differential methylation level obtained using the *Methylkit R* package; Gene annotation name: Gene annotation according to the nr and swiss-prot blast top hit. Blue shading (negative values) indicates hypomethylation of the position and red shading (positive values) hypermethylation; darker shading indicates a stronger degree of hypomethylation of hypermethylation, respectively. The last column indicates in which comparison the significantly different methylated positions were found.

REFERENCES

Addadi, L., Joester, D., Nudelman, F., and Weiner, S. (2006). Mollusk shell formation: a source of new concepts for understanding biomineralization processes. *Chemistry* 12, 980–987. doi: 10.1002/chem.200500980

Adema, C. M., Hillier, L. D. W., Jones, C. S., Loker, E. S., Knight, M., Minx, P., et al. (2017). Whole genome analysis of a schistosomiasis-transmitting freshwater snail. *Nat. Commun.* 8:15451. doi: 10.1038/ncomms15451

Akalin, A., Kormaksson, M., Li, S., Garrett-Bakelman, F. E., Figueroa, M. E., Melnick, A., et al. (2012). MethylKit: a comprehensive R package for the analysis of genome-wide DNA methylation profiles. *Genome Biol.* 13:R87. doi: 10.1186/gb-2012-13-10-R87

Amsterdam, A., Nissen, R. M., Sun, Z., Swindell, E. C., Farrington, S., and Hopkins, N. (2004). Identification of 315 genes essential for early zebrafish development. *Proc. Natl. Acad. Sci. U.S.A.* 101, 12792–12797. doi: 10.1073/pnas.0403929101

Anders, S., Pyl, P. T., and Huber, W. (2015). Genome analysis HTSeq — a Python framework to work with high-throughput sequencing data. *Bioinformatics* 31, 166–169. doi: 10.1093/bioinformatics/btu638

Andrews, S. (2010). *FastQC: A Quality Control Tool for High Throughput Sequence Data*. Cambridge: Babraham Bioinforma.

Auerswald, L., Freier, U., Lopata, A., and Meyer, B. (2008). Physiological and morphological colour change in Antarctic krill, *Euphausia superba*: a field study in the Lazarev Sea. *J. Exp. Biol.* 211, 3850–3858. doi: 10.1242/jeb.024232

Blank, S., Arnoldi, M., Khoshnavaz, S., Treccani, L., Kuntz, M., Mann, K., et al. (2003). The nacre protein perlucin nucleates growth of calcium carbonate crystals. *J. Microsc.* 212(Pt 3), 280–291. doi: 10.1111/j.1365-2818.2003.01263.x

Bolger, A. M., Lohse, M., and Usadel, B. (2014). Genome analysis trimmomatic: a flexible trimmer for illumina sequence data. *Bioinformatics* 30, 2114–2120. doi: 10.1093/bioinformatics/btu170

Bossdorf, O., Richards, C. L., and Pigliucci, M. (2008). Epigenetics for ecologists. *Ecol. Lett.* 11, 106–115. doi: 10.1111/j.1461-0248.2007.01130.x

Bouzerand, E. (2018). *Points Forts de la Polynésie Française – Bilan – La Perle en 2016*. Papeete: Institu de la Statistique de la Polynésia française.

Bräutigam, K., Vining, K. J., Lafon-Placette, C., Fossdal, C. G., Mirouze, M., Marcos, J. G., et al. (2013). Epigenetic regulation of adaptive responses of forest tree species to the environment. *Ecol. Evol.* 3, 399–415. doi: 10.1002/ece3.461

Chakraborty, A. K., Funasaka, Y., Ichihashi, M., Sodi, S., Bhattacharya, M., and Pawelek, J. (1999). Upregulation of mRNA for the melanocortin-1 receptor but not for melanogenic proteins in macrophage x melanoma fusion hybrids exhibiting increased melanogenic and metastatic potential. *Pigment Cell Res.* 12, 355–366. doi: 10.1111/j.1600-0749.1999.tb00519.x

Charpentier, V., Phillips, C. S., and Méry, S. (2012). Pearl fishing in the ancient world: 7500 BP. *Arab. Archaeol. Epigr.* 23, 1–6. doi: 10.1111/j.1600-0471.2011.00351.x

Conesa, A., Götz, S., García-gómez, J. M., Terol, J., Talón, M., Genómica, D., et al. (2005). Blast2GO: a universal tool for annotation, visualization and analysis in functional genomics research. *BMC Bioinformatics* 21:3674–3676. doi: 10.1093/bioinformatics/bti610

Cuthill, I. C., Allen, W. L., Arbuckle, K., Caspers, B., Chaplin, G., Hauber, M. E., et al. (2017). The biology of color. *Science* 357:eaan0221. doi: 10.1126/science.aan0221

Dixon, G., Liao, Y., Bay, L. K., and Matz, M. V. (2018). Role of gene body methylation in acclimatization and adaptation in a basal metazoan. *Proc. Natl. Acad. Sci. U.S.A.* 115, 13342–13346. doi: 10.1073/pnas.1813749115

Dolinoy, D. C. (2008). The agouti mouse model: an epigenetic biosensor for nutritional and environmental alterations on the fetal epigenome. *Nutr. Rev.* 66, 7–11. doi: 10.1111/j.1753-4887.2008.00056.x

Dolinoy, D. C., Weidman, J. R., Waterland, R. A., and Jirtle, R. L. (2006). Maternal genistein alters coat color and protects Avy mouse offspring from obesity by modifying the fetal epigenome. *Environ. Health Perspect.* 114, 567–572. doi: 10.1289/ehp.8700

Feng, D., Li, Q., Yu, H., Kong, L., and Du, S. (2018). Transcriptional profiling of long non-coding RNAs in mantle of *Crassostrea gigas* and their association with shell pigmentation. *Sci. Rep.* 8:1436. doi: 10.1038/s41598-018-19950-6

Feng, D., Li, Q., Yu, H., Liu, S., Kong, L., and Du, S. (2020). Integrated analysis of microRNA and mRNA expression profiles in *Crassostrea gigas* to reveal functional miRNA and miRNA-targets regulating shell pigmentation. *Sci. Rep.* 10:20238. doi: 10.1038/s41598-020-77181-0

Feng, S., Cokus, S. J., Zhang, X., Chen, P. Y., Bostick, M., Goll, M. G., et al. (2010). Conservation and divergence of methylation patterning in plants and animals. *Proc. Natl. Acad. Sci. U.S.A.* 107, 8689–8694. doi: 10.1073/pnas.1002720107

Fernandes, J., and Gattass, C. R. (2009). Topological polar surface area defines substrate transport by multidrug resistance associated protein 1 (MRP1/ABCC1). *J. Med. Chem.* 52, 1214–1218. doi: 10.1021/jm801389m

Frost, S. K., and Malacinski, G. M. (1979). The developmental genetics of pigment mutants in the Mexican axolotl. *Dev. Genet.* 1, 271–294. doi: 10.1002/dvg.1020010402

Gavery, M. R., and Roberts, S. B. (2013). Predominant intragenic methylation is associated with gene expression characteristics in a bivalve mollusc. *PeerJ* 2013, 1–15. doi: 10.7717/peerj.215

Gavery, M. R., and Roberts, S. B. (2017). Epigenetic considerations in aquaculture. *PeerJ* 5:e4147. doi: 10.7717/peerj.4147

Gueguen, Y., Montagnani, C., Joubert, C., Marie, B., Belliard, C., Tayale, A., et al. (2013). "Characterization of molecular processes involved in the pearl formation in *Pinctada margaritifera* for the sustainable development of pearl farming industry in French Polynesia," in *Recent Advances in Pearl Research–Proceedings of the International Symposium on Pearl Research 2011*, eds S. Watabe, K. Maeyama, and H. Nagasawa (Setagaya: TERRAPUB), 183–193.

Hamid, K. M., Bitsue, Z. K., and Mirshafiey, A. (2015). Autoantibodies profile in vitiligo. *J. Pigment. Disord.* 2, 1–5. doi: 10.4172/2376-0427.1000187

Harris, K. D. M., Bartlett, N. J., and Lloyd, V. K. (2012). *Daphnia* as an emerging epigenetic model organism. *Genet. Res. Int.* 2012, 1–8. doi: 10.1155/2012/147892

Hollander, M., Wolfe, D. A., and Chicken, E. (1973). "The one-way layout," in *Nonparametric Statistical Methods*, 3rd Edn, eds John Wiley & sons (New York, NY: John Wiley and Sons), 202–288.

Homolya, L., Váradi, A., and Sarkadi, B. (2003). Multidrug resistance-associated proteins: export pumps for conjugates with glutathione, glucuronate or sulfate. *BioFactors* 17, 103–114. doi: 10.1002/biof.5520170111

Hu, J., and Barrett, R. D. H. (2017). Epigenetics in natural animal populations. *J. Evol. Biol.* 30, 1612–1632. doi: 10.1111/jeb.13130

Iwahashi, Y., and Akamatsu, S. (1994). Porphyrin pigment in Black-Lip pearls and Its application to pearl identification. *Fish. Sci.* 60, 69–71. doi: 10.2331/fishsci.60.69

Joubert, C., Linard, C., Le Moullac, G., Soyez, C., Saulnier, D., Teaniniuraitemoana, V., et al. (2014). Temperature and food influence shell growth and mantle gene expression of shell matrix proteins in the pearl oyster *Pinctada margaritifera*. *PLoS One* 9:e103944. doi: 10.1371/journal.pone.0103944

Joubert, C., Piquemal, D., Marie, B., Manchon, L., Pierrat, F., Zanella-Cléon, I., et al. (2010). Transcriptome and proteome analysis of *Pinctada margaritifera* calcifying mantle and shell: focus on biomineralization. *BMC Genomics* 11:613. doi: 10.1186/1471-2164-11-613

Katz, M. L., Drea, C. M., and Robison, W. G. Jr. (1987). Dietary vitamins A and E influence retinyl ester composition and content of the retinal pigment epithelium. *Biochim. Biophys. Acta* 924, 432–441.

Klopfenstein, D. V., Zhang, L., Pedersen, B. S., Ramírez, F., Vesztrocy, A. W., Naldi, A., et al. (2018). GOATOOLS: a python library for gene ontology analyses. *Sci. Rep.* 8:10872. doi: 10.1038/s41598-018-28948-z

Krueger, F., and Andrews, S. R. (2011). Bismark: a flexible aligner and methylation caller for Bisulfite-Seq applications. *Bioinformatics* 27, 1571–1572. doi: 10.1093/bioinformatics/btr167

Ky, C. L., Broustal, F., Potin, D., and Lo, C. (2019). The pearl oyster (*Pinctada margaritifera*) aquaculture in French Polynesia and the indirect impact of long-distance transfers and collection-culture site combinations on pearl quality traits. *Aquac. Rep.* 13:100182. doi: 10.1016/j.aqrep.2019.100182

Ky, C.-L., Blay, C., Sham-Koua, M., Lo, C., and Cabral, P. (2014). Indirect improvement of pearl grade and shape in farmed *Pinctada margaritifera* by donor "oyster" selection for green pearls. *Aquaculture* 432, 154–162. doi: 10.1016/j.aquaculture.2014.05.002

Ky, C.-L., Blay, C., Sham-Koua, M., Vanaa, V., Lo, C., and Cabral, P. (2013). Family effect on cultured pearl quality in black-lipped pearl oyster *Pinctada margaritifera* and insights for genetic improvement. *Aquat. Living Resour.* 26, 133–145. doi: 10.1051/alr/2013055

Ky, C.-L., Le Pabic, L., Sham Koua, M., Nicolas, M., Seiji, N., and Devaux, D. (2017). Is pearl colour produced from *Pinctada margaritifera* predictable through shell phenotypes and rearing environments selections? *Aquaculture* 48, 1041–1057. doi: 10.1111/are.12947

Le Moullac, G., Schuck, L., Chabrier, S., Belliard, C., Lyonnard, P., Broustal, F., et al. (2018). Influence of temperature and pearl rotation on biomineralization in the pearl oyster, *Pinctada margaritifera*. *J. Exp. Biol.* 221:jeb186858. doi: 10.1242/jeb.186858

Le Pabic, L., Parrad, S., Sham Koua, M., Nakasai, S., Saulnier, D., Devaux, D., et al. (2016). Culture site dependence on pearl size realization in *Pinctada margaritifera* in relation to recipient oyster growth and mantle graft biomineralization gene expression using the same donor phenotype. *Estuar. Coast. Shelf Sci.* 182, 294–303. doi: 10.1016/j.ecss.2016.03.009

Le Pennec, M. (2010). *Huître Perlière et Perle de Tahiti*. Puna'auia: Université de la Polynésie française.

Lemer, S., Saulnier, D., Gueguen, Y., and Planes, S. (2015). Identification of genes associated with shell color in the black-lipped pearl oyster, *Pinctada margaritifera*. *BMC Genomics* 16:568. doi: 10.1186/s12864-015-1776-x

Liu, Y., Chen, Z., Cheng, H., Chen, J., and Qian, J. (2017). Gremlin promotes retinal pigmentation epithelial (RPE) cellproliferation, migration and VEGF production via activating VEGFR2-Akt-mTORC2 signaling. *Oncotarget* 8, 979–987.

Liu, Y., Shigley, J., and Hurwit, K. (1999). Iridescent color of a shell of the mollusk *Pinctada margaritifera* caused by diffraction. *Opt. Express* 4, 177–182. doi: 10.1364/OE.4.000177

Lukens, L. N., and Zhan, S. (2007). The plant genome's methylation status and response to stress: implications for plant improvement. *Curr. Opin. Plant Biol.* 10, 317–322. doi: 10.1016/j.pbi.2007.04.012

Marie, B., Joubert, C., Tayalé, A., and Zanella-cléon, I. (2013). Different secretory repertoires control the biomineralization processes of prism and nacre deposition of the pearl oyster shell. *Proc. Natl. Acad. Sci. U.S.A.* 109, 20986–20991. doi: 10.1073/pnas.1210552109

Moreau, C., Ambrose, M. J., Turner, L., Hill, L., Noel Ellis, T. H., and Hofer, J. M. I. (2012). The b gene of pea encodes a defective flavonoid 3',5'-hydroxylase, and confers pink flower color. *Plant Physiol.* 159, 759–768. doi: 10.1104/pp.112.197517

Ng, A., Uribe, R. A., Yieh, L., Nuckels, R., and Gross, J. M. (2009). Zebrafish mutations in gart and paics identify crucial roles for de novo purine synthesis in vertebrate pigmentation and ocular development. *Development* 136, 2601–2611. doi: 10.1242/dev.038315

Ng, B. G., and Freeze, H. H. (2014). Human genetic disorders involving glycosylphosphatidylinositol (GPI) anchors and glycosphingolipids (GSL). *J. Inherit. Metab. Dis.* 38, 171–178. doi: 10.1007/s10545-014-9752-1

Nguyen, V. H., and Lavenier, D. (2009). PLAST: parallel local alignment search tool for database comparison. *BMC Bioinformatics* 10:329. doi: 10.1186/1471-2105-10-329

Nicoglou, A., and Merlin, F. (2017). Epigenetics: a way to bridge the gap between biological fields. *Stud. Hist. Philos. Sci. Part C Stud. Hist. Philos. Biol. Biomed. Sci.* 66, 73–82. doi: 10.1016/j.shpsc.2017.10.002

Oliveira-Garcia, E., and Deising, H. B. (2016). The glycosylphosphatidylinositol anchor biosynthesis genes GPI12, GAA1, and GPI8 are essential for cell-wall integrity and pathogenicity of the maize anthracnose fungus *Colletotrichum graminicola*. *Mol. Plant Microbe Interact.* 29, 889–901. doi: 10.1094/MPMI-09-16-0175-R

Olson, C. E., and Roberts, S. B. (2014). Genome-wide profiling of DNA methylation and gene expression in *Crassostrea gigas* male gametes. *Front. Physiol.* 5:224. doi: 10.3389/fphys.2014.00224

Quinlan, A. R., and Hall, I. M. (2010). BEDTools: a flexible suite of utilities for comparing genomic features. *Bioinformatics* 26, 841–842. doi: 10.1093/bioinformatics/btq033

Ramírez, F., Dündar, F., Diehl, S., Grüning, B. A., and Manke, T. (2014). DeepTools: a flexible platform for exploring deep-sequencing data. *Nucleic Acids Res.* 42, W187–W191. doi: 10.1093/nar/gku365

Rao, K. R., and Riehm, J. P. (1993). Pigment-dispersing hormones. *Ann. N. Y. Acad. Sci.* 680, 78–88.

Reisser, C. M. O., Gendre, R., Le, Chupeau, C., Lo-Yat, A., Planes, S., et al. (2020). Population connectivity and genetic assessment of exploited and natural populations of pearl oysters within a French polynesian atoll lagoon. *Genes (Basel).* 11, 1–16. doi: 10.3390/genes11040426

Richards, E. J. (2006). Inherited epigenetic variation—revisiting soft inheritance. *Nat. Rev. Genet.* 7, 395–402. doi: 10.1038/nrg1834

Rocha, G. D. G., Oliveira, R. R., Kaplan, M. A. C., and Gattass, C. R. (2014). 3β-Acetyl tormentic acid reverts MRP1/ABCC1 mediated cancer resistance through modulation of intracellular levels of GSH and inhibition of GST activity. *Eur. J. Pharmacol.* 741, 140–149. doi: 10.1016/j.ejphar.2014.07.054

Rondon, R., Grunau, C., Fallet, M., Charlemagne, N., Sussarellu, R., Chaparro, C., et al. (2017). Effects of a parental exposure to diuron on Pacific oyster spat methylome. *Environ. Epigenetics* 3, 1–13. doi: 10.1093/eep/dvx004

Rousseau, M., and Rollion-Bard, C. (2012). Influence of the depth on the shape and thickness of nacre tablets of *Pinctada margaritifera* pearl oyster, and on oxygen isotopic composition. *Minerals* 2, 55–64. doi: 10.3390/min2010055

Royston, P. (1995). Remark AS R94: a remark on algorithm AS 181: the W-test for normality. *J. R. Stat. Soc. Ser. C Appl. Stat.* 44, 547–551. doi: 10.2307/2986146

Russo, V. E., Martienssen, R. A., and Riggs, A. D. (1996). *Epigenetic Mechanisms of Gene Regulation*. Cold Spring Harbor, NY: Cold Spring Harbor Laboratory Press.

Sarda, S., Zeng, J., Hunt, B. G., and Yi, S. V. (2012). The evolution of invertebrate gene body methylation. *Mol. Biol. Evol.* 29, 1907–1916. doi: 10.1093/molbev/mss062

Sharp, J. R., Insalaco, S. J., and Johnson, L. F. (1980). "Melanosis" of the duodenum associated with a gastric ulcer and folic acid deficiency. *Gastroenterology* 78, 366–369. doi: 10.1016/0016-5085(80)90590-9

Shin, D. H., Cho, M., Choi, M. G., Das, P. K., Lee, S. K., Choi, S. B., et al. (2015). Identification of genes that may regulate the expression of the transcription factor production of anthocyanin pigment 1 (PAP1)/MYB75 involved in *Arabidopsis* anthocyanin biosynthesis. *Plant Cell Rep.* 34, 805–815. doi: 10.1007/s00299-015-1743-7

Sokolov, E. P. (2000). An improved method for DNA isolation from mucopolysaccharide-rich molluscan tissues. *J. Molluscan Stud.* 66, 573–575. doi: 10.1093/mollus/66.4.573

Sonthalia, S., Daulatabad, D., and Sarkar, R. (2016). Glutathione as a skin whitening agent: facts, myths, evidence and controversies. *Indian J. Dermatol.* 82, 262. doi: 10.4103/0378-6323.179088

Southgate, P., and Lucas, J. (2011). *The Pearl Oyster*. Amsterdam: Elsevier.

Stenger, P.-L. (2017). *Package ImaginR*. Available online at: https://cran.r-project.org/web/packages/ImaginR/ImaginR.pdf (accessed May 29, 2017).

Stenger, P.-L., Ky, C.-L., Reisser, C., Duboisset, J., and Dicko, H. (in press). Molecular pathways and pigments behind the colors of the pearl oyster *Pinctada margaritifera* var. *cumingii* (Linnaeus 1758). *Genes*.

Stenger, P.-L., Vidal-Dupiol, J., Reisser, C., Planes, S., and Ky, C. (2019). Colour plasticity in the shells and pearls of animal graft model *Pinctada margaritifera* through colour quantification with the HSV system. *Sci. Rep.* 75:20. doi: 10.1038/s41598-019-43777-4

Sutherland, J. E., and Costa, M. A. X. (2003). Epigenetics and the environment. *Ann. N. Y. Acad. Sci.* 983, 151–160.

Takakura, D., Norizuki, M., Ishikawa, F., and Samata, T. (2008). Isolation and characterization of the N-linked oligosaccharides in nacrein from

Pinctada fucata. *Mar. Biotechnol.* 10, 290–296. doi: 10.1007/s10126-007-9063-8

Tanaka, Y., Suetsugu, Y., Yamamoto, K., Noda, H., and Shinoda, T. (2014). Transcriptome analysis of neuropeptides and G-protein coupled receptors (GPCRs) for neuropeptides in the brown planthopper *Nilaparvata lugens*. *Peptides* 53, 125–133. doi: 10.1016/j.peptides.2013.07.027

Trapnell, C., Roberts, A., Goff, L., Pertea, G., Kim, D., Kelley, D. R., et al. (2012). Differential gene and transcript expression analysis of RNA-seq experiments with TopHat and Cufflinks. *Nat. Protoc.* 7, 562–578. doi: 10.1038/nprot.2012.016

Vajro, P., Thaler, M. M., and Blanckaert, N. (1995). Bile pigment composition and bilirubin esterification in the developing chick. *Pediatr. Res.* 38, 349–355. doi: 10.1203/00006450-199509000-00013

Wang, N., Lee, Y. H., and Lee, J. (2008). Recombinant perlucin nucleates the growth of calcium carbonate crystals: molecular cloning and characterization of perlucin from disk abalone, *Haliotis discus discus*. *Comp. Biochem. Physiol. B Biochem. Mol. Biol.* 149, 354–361. doi: 10.1016/j.cbpb.2007.10.007

Wang, X., Li, Q., Lian, J., Li, L., Jin, L., Cai, H., et al. (2014). Genome-wide and single-base resolution DNA methylomes of the Pacific oyster *Crassostrea gigas* provide insight into the evolution of invertebrate CpG methylation. *BMC Genomics* 15:1119. doi: 10.1186/1471-2164-15-1119

Weiss, I. M., Kaufmann, S., Mann, K., and Fritz, M. (2000). Purification and characterization of perlucin and perlustrin, two new proteins from the shell of the mollusc *Haliotis laevigata*. *Biochem. Biophys. Res. Commun.* 267, 17–21. doi: 10.1006/bbrc.1999.1907

Wickham, H., and Chang, W. (2019). *Package 'ggplot2.'*.

Xiang, H., Zhu, J., Chen, Q., Dai, F., Li, X., Li, M., et al. (2010). Single base-resolution methylome of the silkworm reveals a sparse epigenomic map. *Nat. Biotechnol.* 28, 516–520. doi: 10.1038/nbt.1626

Zemach, A., McDaniel, I. E., Silva, P., and Zilberman, D. (2010). Genome-wide evolutionary analysis of eukaryotic DNA methylation. *Science* 328, 916–919. doi: 10.1126/science.1186366

Zhai, S., Xia, X., and He, Z. (2016). Carotenoids in staple cereals: metabolism, regulation, and genetic manipulation. *Front. Plant Sci.* 7:1197. doi: 10.3389/fpls.2016.01197

Zimova, M., Hackländer, K., Good, J. M., Melo-Ferreira, J., Alves, P. C., and Mills, L. S. (2018). Function and underlying mechanisms of seasonal colour moulting in mammals and birds: what keeps them changing in a warming world? *Biol. Rev.* 93, 1478–1498. doi: 10.1111/brv.12405

Conflict of Interest: The authors declare that the research was conducted in the absence of any commercial or financial relationships that could be construed as a potential conflict of interest.

Résumé administratif

Situation actuelle :
Chargé de Recherche Ifremer au Laboratoire Interaction Hôtes Pathogènes Environnements, UMR 5244. Directeur d'Unité Christoph Grunau
Thème de recherche actuel :
Mécanismes d'adaptation/acclimatation rapides aux changements environnementaux
Production scientifique :
34 publications dans des revues internationales à comité de lecture.
Direction de recherche :
-2 Post-doctorants taux d'encadrement de 50%
- 4 thèses, taux d'encadrement de 20 à 100%
- 5 Master 2 recherche taux d'encadrement de 100%
- 5 Master 1 à DUT taux d'encadrement de 100%
Responsabilités :
- Equipe Microévolution des Interactions dans l'Anthropocène. Projet IHPE 2021-2026
- Thème Adaptabilité des hôtes. Projet IHPE 2015-2020
- Membre du conseil scientifique du Labex TULIP depuis Janvier 2020

Résumé scientifique

Pour de très nombreuses populations d'organismes, l'aire anthropocène est synonyme de perturbations croissantes et diversifiées. Ces changements peuvent donc impliquer des modifications environnementales biotiques, telle que l'émergence de pathogène, ou abiotiques telle que l'augmentation des températures. Quelle que soit leur origine et leur nature, ces perturbations conduiront dans un premier temps au développement d'une réponse de stress puis d'un processus éventuel d'acclimatation et enfin à l'échelle populationnelle et transgénérationnelle à l'adaptation.

C'est à l'étude et la compréhension de ces mécanismes de réponse, d'acclimatation et enfin d'adaptation rapides que je me suis intéressé depuis le début de ma carrière. Cette recherche s'est focalisée sur deux grands modèles d'étude : i) les coraux constructeurs de récifs et ii) les bivalves marins confrontés à des pressions de sélection fortes et soudaines induites par l'émergence de pathogènes, le réchauffement climatique ou encore l'acidification des océans.

Afin d'appréhender ces mécanismes j'ai développé des approches expérimentales écologiquement réalistes aussi bien en milieu contrôlé qu'en milieu naturel et à différentes échelles spatiales et temporelles. Par la suite, j'ai étudié les réponses, les processus d'acclimatation et d'adaptation de ces populations et organismes par des approches d'omics intégratives et pluridisciplinaires en appréhendant notamment le triptyque génome, épigénome, phénome et leurs interactions avec l'environnement.

L'objectif finalisé de ma recherche est de transformer cette compréhension des mécanismes d'adaptation (*sensus lato*) rapides en des outils de gestion des changements en cours que ce soit dans un contexte d'aquaculture ou de protection et de restauration des écosystèmes.